APOLLO

Final Report

ER 12007-1 JUNE 1961

Guidance and Control System I

[redacted]

MARTIN

[redacted]

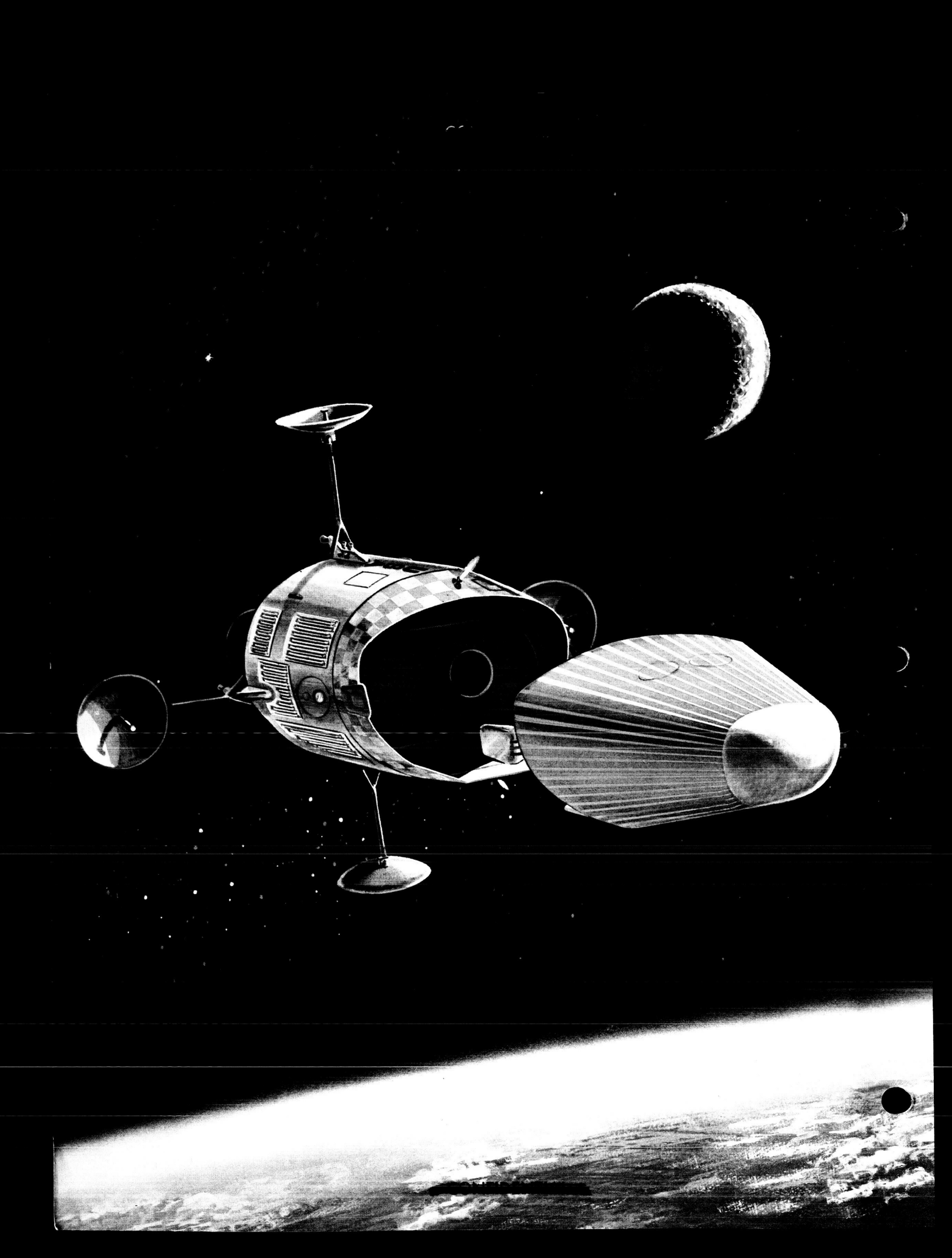

APOLLO

Final Report

Guidance and Controls

I

(ER 12007-1) JUNE 1961

Submitted to: NASA Space Task Group.
(NASA) Contract NAS 5-303, Exhibit A, Item 1.2

Copy June 1961 416 p

[redacted] FROM THE GDS

5524004 MARTIN Co. Baltimore, Md.

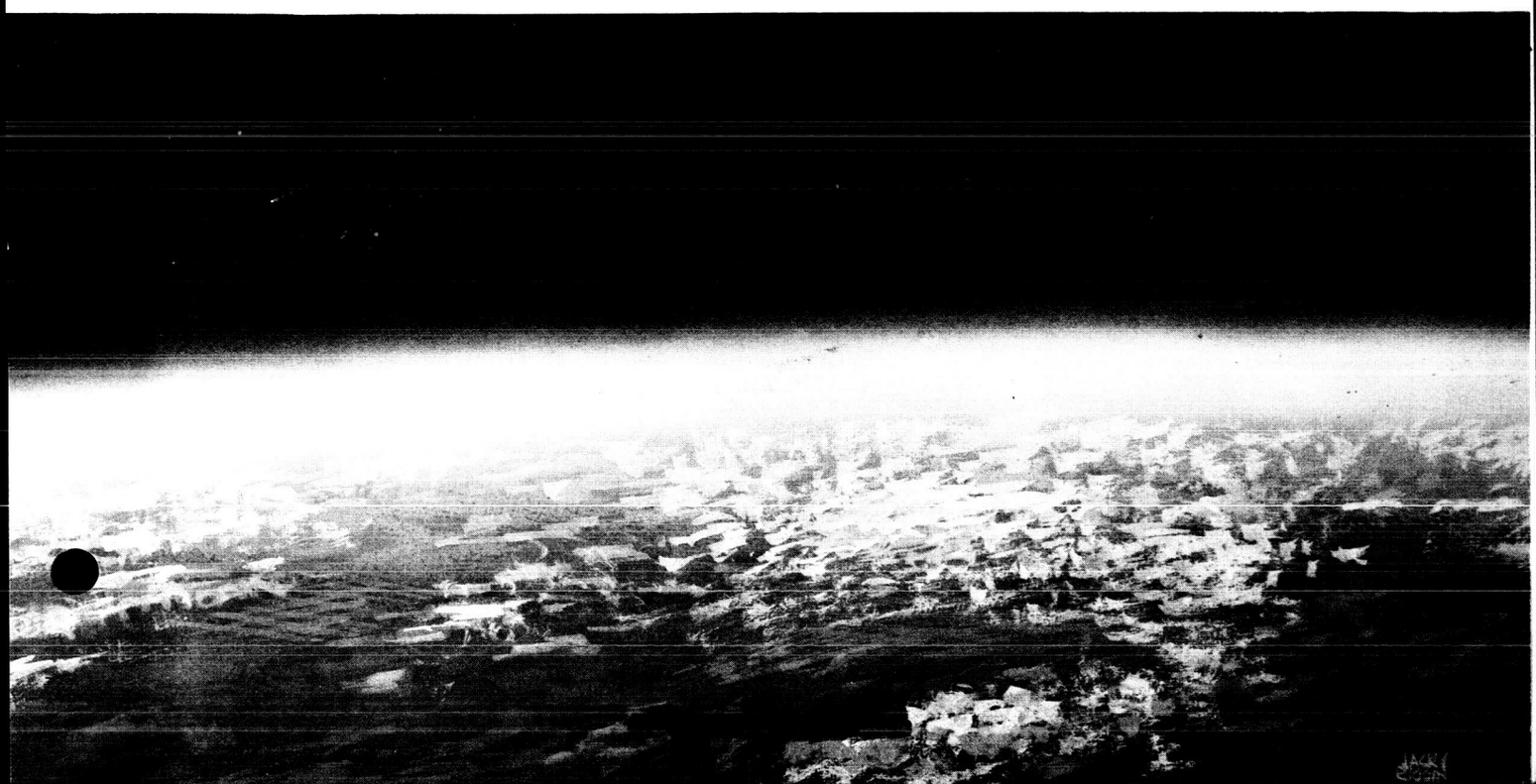

MODEL 410 — THE SYSTEM AND ITS OPERATION

*A BRIEF DESCRIPTION**

Model 410 is the spacecraft system recommended by Martin for the Apollo mission. Its design satisfies the guidelines stated in NASA RFP–302, as well as a more detailed set of guidelines developed by Martin during the Apollo design feasibility study.

We conceive the ultimate Apollo mission to be a manned journey to the lunar surface, arrived at by the preliminary steps of earth orbit, circumlunar and lunar orbit flights. Operational procedures proved out in the early steps will be carried over into the advanced steps, thus establishing a high level of confidence in the success of the lunar flights. With the recommended system, manned lunar orbit missions can be made as early as 1966.

Operational Features

For a circumlunar flight when the moon is at its most southerly declination (Fig. p–1) the launch operation proceeds southeast from Cape Canaveral and down the Atlantic Missile Range. The Saturn C–2 third stage shuts down when orbital velocity is reached at an altitude of 650,000 feet. What follows is a coasting orbit passing over the southern tip of Africa, the Indian Ocean and up the Pacific Missile Range. In this interval the crew checks out all onboard equipment, which has just passed through the accelerations, noise and vibration of the boost phase. If the pilot-commander is satisfied that all systems are working properly, the third stage is restarted and the spacecraft is injected at parabolic velocity northwest of Hawaii. If the pilot-commander is dissatisfied with the condition of the vehicle or crew, he separates from the Saturn S–IV, starts the mission abort engine, re-enters at the point shown in Fig. p–1 and lands at Edwards AFB.

Continuing translunar flight from the point of injection, the trajectory trace swings down over the Caribbean and then west over South America. This particular trajectory passes within 240 naut mi of the moon, then turns back for a direct re-entry some six days after launch. Re-entry occurs southwest of Hawaii some 3300 naut mi from the Edwards AFB landing site.

Tracking. The range coverage provided by present and planned facilities is shown in Fig. p–1 for this trajectory and for a second return trace representing the case when the moon is at the most northerly declination. This second trajectory establishes the 10000-naut mi re-entry range requirement for Apollo to meet the guidelines of operation on every day of the lunar month and of operation into a single landing site.

*For more complete descriptions, see ER 12000 or ER 12001.

[redacted]

Abort. During the critical launch and checkout phase, abort will be possible at any time : at the crew's discretion, automatically or by ground command. Up to nine minutes after launch (from Canaveral), the abort landing is restricted to the AMR for a circumlunar flight. Beyond this point the pilot has the option of continuing to any point along the AMR, PMR or into Edwards AFB through the use of the mission abort propulsion system and the inherent downrange maneuverability of the Model–410.

The Selected Spacecraft

The Apollo space vehicle (Model 410 spacecraft plus launching vehicle) is shown in Fig. p–2. The spacecraft—that portion of the space vehicle which makes the flight to the moon—consists of these three modules:

(1) Command module, housing the three crew members during all thrusting periods, e.g., launch from earth, any corrections to the flight path during flight in space, during re-entry and, ultimately, during landing and launch from the moon. It is the operating center from which all control of the flight is made.

(2) Propulsion and equipment module, containing all the propulsion units which operate between the point of final booster separation and re-entry after the lunar flight. It is separated from the command module at 200 naut mi from the earth on the return trip. It is designed with tankage for lunar takeoff and will be offloaded for less ambitious missions.

(3) Mission module—contained within the outer frame of the propulsion and equipment module—providing space during the lunar voyage for scientific observations and crew living functions.

Command Module

With its lifting capability, the Apollo command module represents a step forward in technology over ballistic vehicles, Mercury and (to the best of our knowledge the *Boctók* (*Vostok*). The lift results from the capsule's shape—a blunted cone flattened on the top (see Fig. p–3).

Heating and radiation protection. The Model 410 is shaped conservatively for aerodynamic heating in addition to its relatively high L/D (0.77). By accepting the large convective heat load of a nose radius smaller than that of the Mercury type, the Model 410 shape tends to minimize radiative heat transfer which is less well understood and harder to protect against. The thermal protection system provides excellent protection for the crew from the large aerodynamic heat loads, from space radiation (including solar flares) and from meteorites.

The normal mission radiation dose will not exceed the five rem limit defined by NASA. If the crew should encounter a solar event as severe as that following the May 10, 1959 flare, they would receive a dose of only 67 rem—well within the 100 rem dose limit set by Martin as tolerable during an emergency.

[redacted]

Thermal protection for re-entry is provided by a composite shield of deep charring ablator (nylon phenolic) bonded to superalloy honeycomb panels which are set off and insulated from the water-cooled pressure shell. The control flaps are protected from the high initial heat rate by an ablator bonded directly to the flap. The long-time, lower heating rates are handled by re-radiation from the backside. The aft bulkhead is protected by a fiberglas phenolic honeycomb panel with a foamed polyurethane insulation.

Crew provisions. The crew has access to all electronic and electrical equipment in the command module for maintenance and replacement. Both pilots have two-axis sidestick and foot controllers as well as a manual guidance mode used with the computers inoperative for deep space and re-entry operations.

Cabin pressure is maintained at the equivalent of 5000 feet altitude ("shirt sleeve" environment). Protective suiting is donned only for launching and landing, but need not be inflated except in emergency.

Guidance. The guidance system consists of both automatic and manual star tracking equipment, as well as two inertial platforms and two general purpose digital computers. Two windows, with ablative heat shield covers, are provided for use with tracking instruments.

Flight control. Pitch and yaw attitude control within the atmosphere is provided by flaps driven by hot gas servos. Outside the atmosphere dual reaction controls are used. Roll is controlled at all times by a dual reaction system.

Communications. Communications equipment includes a K$_u$ band for re-entry, a C-band for the pre-reentry and both HF and VHF rescue beacons for landing and recovery.

Landing system. The landing system consists of a steerable parachute, retrorocket combination, enabling the M–410 to avoid local obstacles, trim out wind drift and reduce sinking speed to a nominal three feet per second—low enough for safe landing on any kind of terrain or in very rough seas. In the event of retrorocket failure, accelerations on the crew will not exceed 20 G.

Launch escape propulsion system (LEPS). LEPS is a thrust-vector-controlled, solid rocket system which separates the command module from the rest of the space vehicle in the event of an emergency during launch pad operations or during boost through the atmosphere. In an off-the-pad abort, it lifts the command module to an altitude of more than 4000 feet. During a normal boost trajectory, LEPS is jettisoned at 300,000 feet.

Propulsion and Equipment Module

The propulsion and equipment module (shown in Fig. p–3) contains propulsion devices and equipment which are not necessary for re-entry. Its outer skin serves both as a load carrying structure and as a meteorite shield for the propellant tanks, mission module and other equipment.

Propulsion devices. The mission engine, used for trajectory correction and abort, is a high preformance, modified LR–115 (Pratt & Whitney), developing 15,600 pounds of thrust. A total of 10,450 pounds of liquid hydrogen and liquid oxygen propellants may be carried, sufficient for lunar takeoff.

[redacted]

Four vernier engines, with 300 pounds of thrust each, are used for midcourse correction, ullage impulse to settle the mission engine propellants and for thrust vector control during operation of the mission engine. In addition there are two sets of six control jets which provide 30 pounds of thrust for roll, pitch and yaw control.

Power sources. Spacecraft equipment is powered by fuel cells (2 kw) which under normal conditions, use the boiloff from the mission propulsion system. A supply of independent reactants is provided for emergencies. Battery power is used during re-entry.

Communications. Four large antennas fold out to provide S-band communications and X-band radar altimeter information. VHF communications gear is also provided.

Mission Module

The mission module provides 400 cubic feet of living space during the lunar voyage. It serves as a midcourse work-rest area, providing freedom of movement and privacy. For operations on the lunar surface it will be a base of scientific investigations, and will serve as an airlock. The same "shirt sleeve" environment at 12.2 psi is maintained as in the command module.

The mission module provides the space and flexibility required for effective lunar reconnaissance and scientific experimentation. An Eastman-Kodak camera-telescope has been selected, for example, which has one-meter resolution at lunar orbit altitude of 50 naut mi.

MODEL 410 WEIGHT SUMMARY

Mission	Circumlunar	Lunar Orbit	Lunar Takeoff
Command Module	6954	6954	6954
Propulsion and Equipment Module	7372	13,192	15,618
Launch Escape Propulsion System	185	185	0
Adapter	489	489	0
Effective Launch Weight	15,000	20,820	22,572

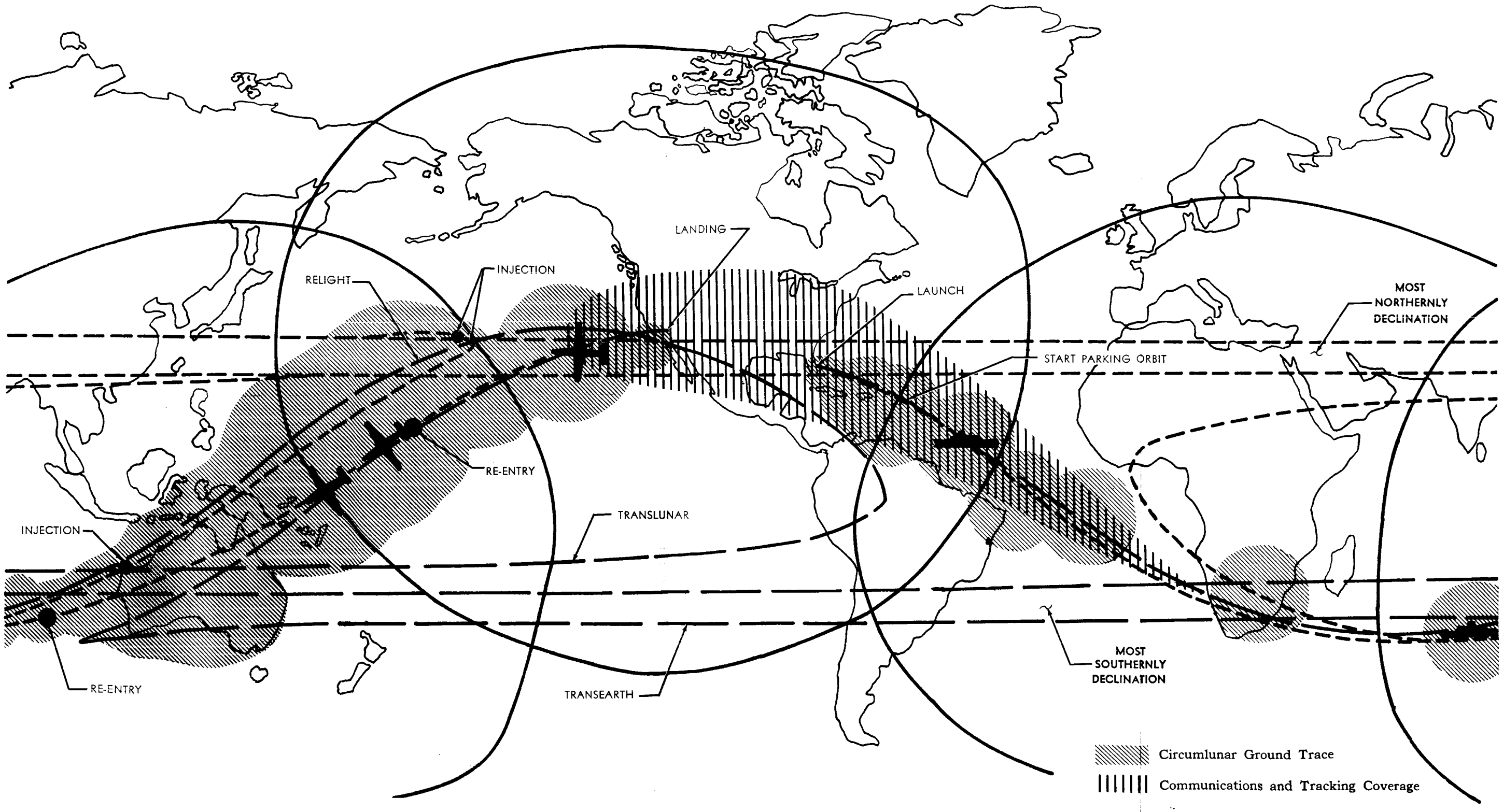

Fig. p–1 Model 410 Circumlunar Trajectory and Range Coverage

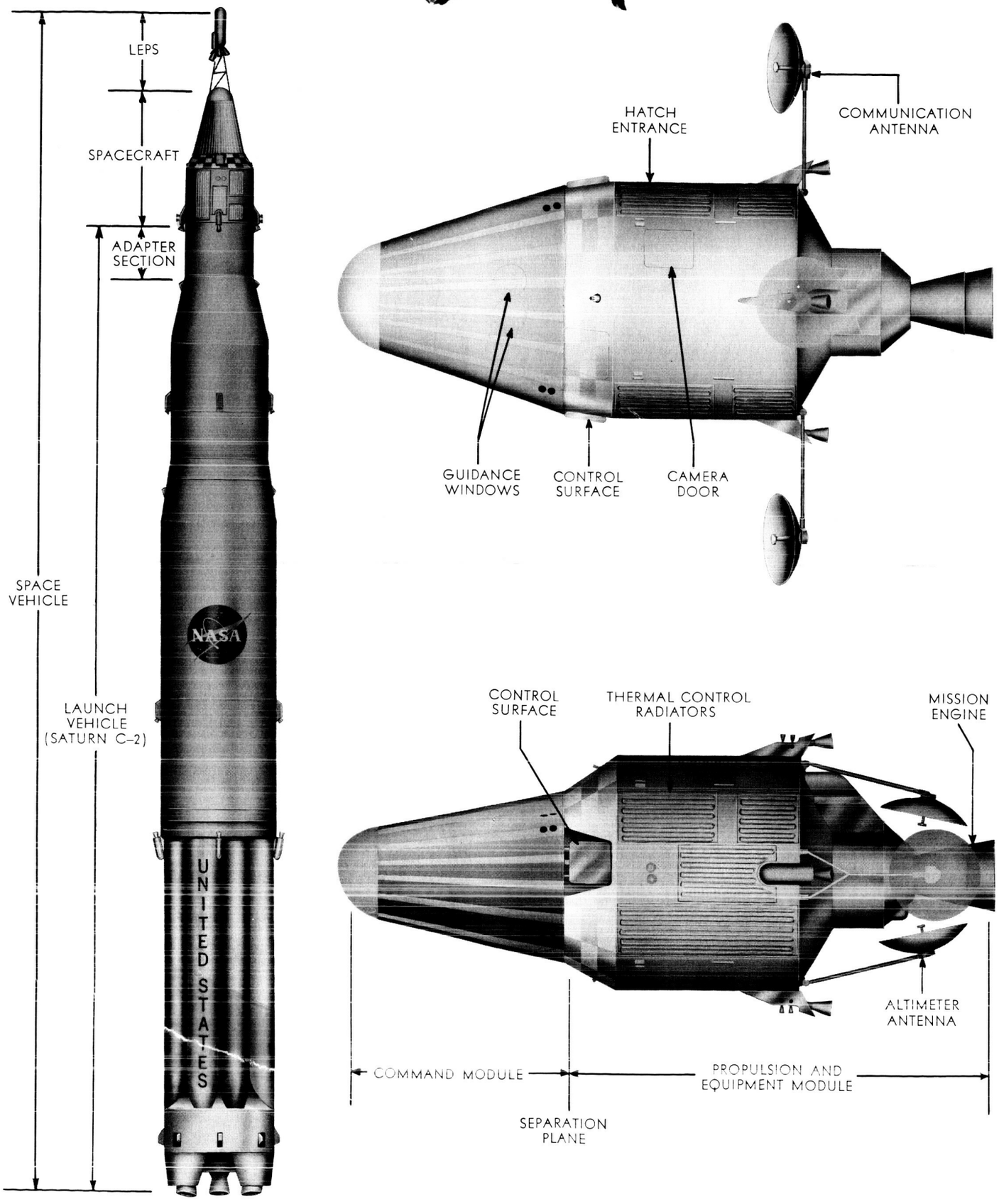

Fig. p-2. Model 410 Apollo Space Vehicle

MISSION	EFFECTIVE GROSS WEIGHT (lb)	PROPULSION ΔV CAPABILITY (fps)	
		MISSION	VERNIER
CIRCUMLUNAR	15000	1830	525
LUNAR ORBIT	20820	6100	525
LUNAR TAKEOFF	22572	8600	200

VOLUMES (cu ft)	
COMMAND MODULE	350
MISSION MODULE	400
MISSION H_2 TANK	400
MISSION O_2 TANK	122

PROPULSION SYSTEM DATA

PURPOSE	TYPE	ISP. (sec)	THRUST (lb)
MISSION (1)	H_2—O_2 (ADV. LR115)	427	15600
VERNIER (4)	N_2H_4/UDMH–N_2O_4	315	300 EACH
ATTITUDE CONTROL (14+BACKUP)	N_2H_4/UDMH–N_2O_4	250–315	15 TO 50

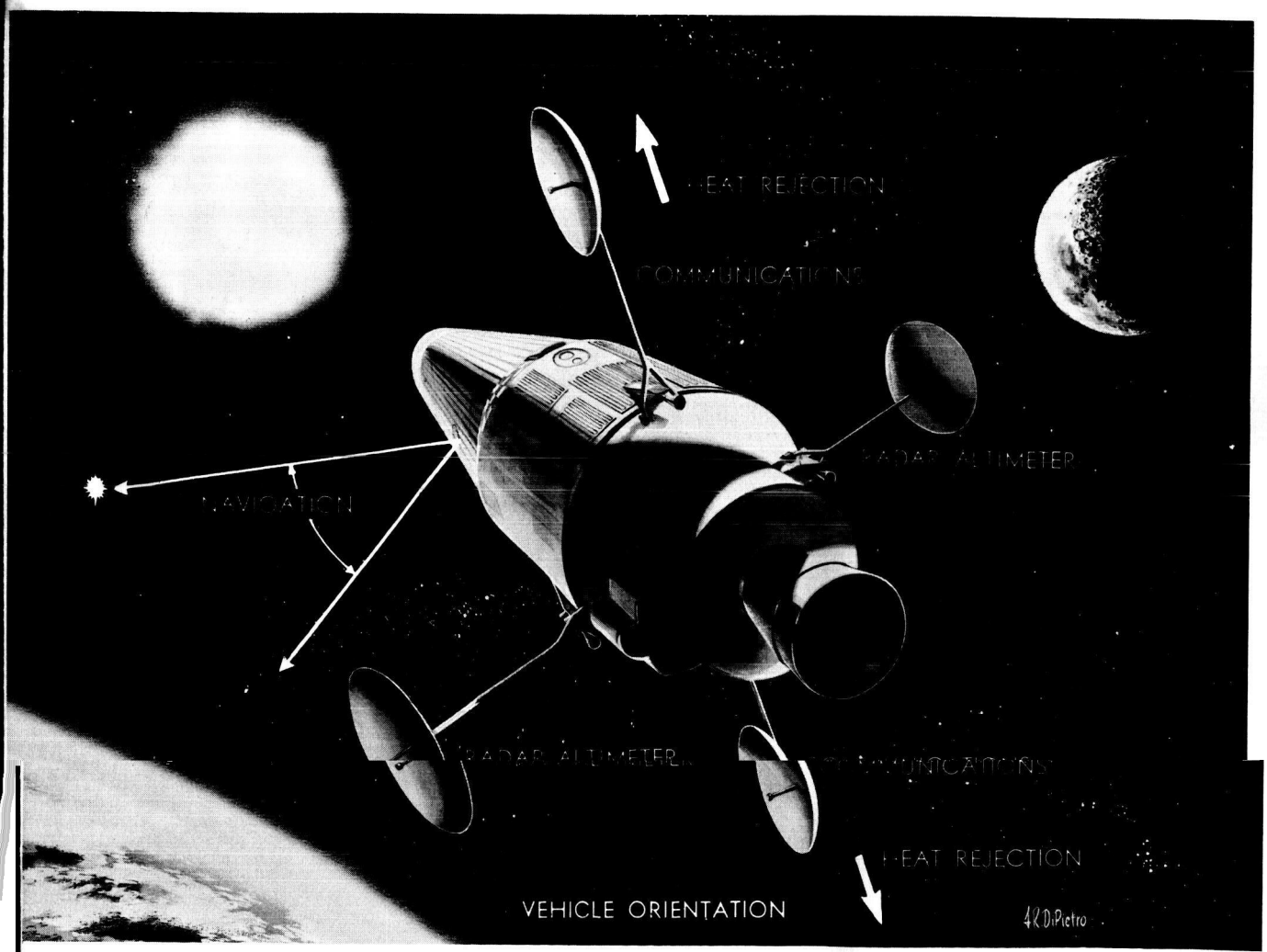

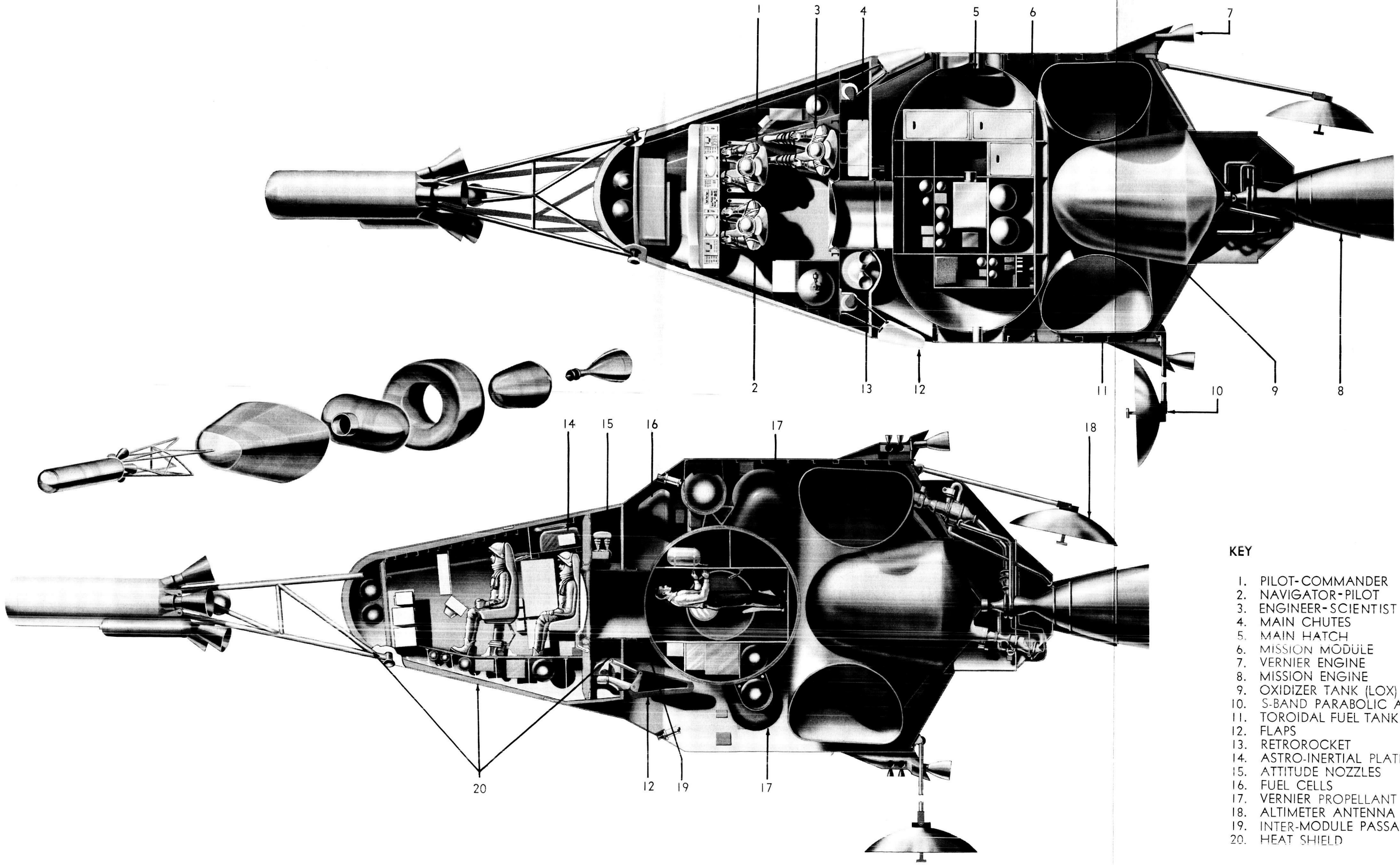

KEY

1. PILOT-COMMANDER
2. NAVIGATOR-PILOT
3. ENGINEER-SCIENTIST
4. MAIN CHUTES
5. MAIN HATCH
6. MISSION MODULE
7. VERNIER ENGINE
8. MISSION ENGINE
9. OXIDIZER TANK (LOX)
10. S-BAND PARABOLIC ANTENNA
11. TOROIDAL FUEL TANK (LH)
12. FLAPS
13. RETROROCKET
14. ASTRO-INERTIAL PLATFORM
15. ATTITUDE NOZZLES
16. FUEL CELLS
17. VERNIER PROPELLANT TANK
18. ALTIMETER ANTENNA
19. INTER-MODULE PASSAGE
20. HEAT SHIELD

Fig. p-3. Model 410 **Apollo Inboard Profile**

CONTENTS

The overall Table of Contents is included in all volumes of this Report for the reader's convenience, and to aid him in his review.

VOLUME I

CONTENTS (cont)

CONTENTS (cont)

CONTENTS (cont)

CONTENTS (cont)

I INTRODUCTION

A. GENERAL

The Apollo guidance system is used to direct the vehicle throughout the entire mission, from launch at Cape Canaveral to touchdown at Edwards Air Force Base. This is accomplished by performing two tasks, namely, position and velocity determination and generation of steering and thrust control signals. In designing a guidance system to perform the Apollo mission, a number of design objectives must be kept in mind. First, the system must be reliable and safe: It is of primary importance that the mission be successfully concluded and the crew returned safely. Next in the order of importance is the incorporation of simplicity in design and operation. Simplicity greatly aids in realizing the reliability goals, and integrating the navigator in the system. A third objective entails the optimum utilization of the navigator. His functions, as controller of the guidance system, include those that reduce complexity of the system, improve reliability, and increase accuracy. Further objectives in the guidance system are lightweight, small components possessing low power requirements so that the overall configuration is not penalized. Finally, with the specified schedule, only proven techniques and components, or at least those currently under development, should be used. How these objectives have been met is delineated in the succeeding discussion.

B. UTILIZATION

The Martin concept involves complete on-board guidance capability during all phases of the mission. Data provided by ground radio tracking stations will in some instances be more accurate than that generated onboard. The guidance system will therefore be capable of using such data at the discretion of the human navigator.

Although the system is designed around a human crew, it is felt that a certain amount of automaticity should be included. This portion of the system would take over during incapacitation of the crew--sickness, space suit restrictions, etc. It is also believed that redundancy in function and equipment is desired to obtain the required reliability and confidence for the relatively long period manned mission. These two goals, and maximizing the crew's utility, are fulfilled by providing two systems: one in which the inputs are primarily automatic, the other in which the inputs are primarily manual. A further increase in reliability is achieved by judicious interconnection between these systems, thereby periodically "resting" various portions of both systems.

C. MATHEMATICAL MODEL

The equations which constitute the mathematical model describing the physical motion of the Apollo spacecraft play an important function in the guidance system design. Near Earth or the moon, the equations of motion can be

formulated considering only the gravitational field of the respective body: This comprises the restricted two-body model. Such is current practice when dealing with ICBM's and earth satellites. The ballistic equations of motion in such a gravitational field are analytic, facilitating easy curve-fitting and steering computations. In fact, in situations when time is not critical, such as coast or parking orbit, trajectory determination and steering computations can be accomplished by hand. Even when the vehicle is under the influence of external forces (thrust or aerodynamic), acceleration data can be processed and the appropriate differential equation integrated numerically quite rapidly.

However, during the midcourse phases of flights to the moon, the spacecraft passes through a very complex gravitational field composed of significant effects from the earth, moon and sun. Including the vehicle (but ignoring its gravitation), this environment requires what is normally referred to as the restricted four-body model to simulate vehicle motion. For the restricted two-body model to be utilized during such phases of flight, appropriate bias terms must be selected, and the inefficiency of operation in obtaining the desired accuracy must be evaluated in terms of fuel consumption. Unfortunately, general solutions to the restricted four-body equations of motion for the spacecraft's flight through the cislunar environment are not available. The differential equations, though complex, can of course be numerically integrated, and present trends in the design of miniaturized digital computers have indicated feasibility for solving four-body equations with the speed required for timely and effective trajectory determination and steering computations onboard the Apollo spacecraft.

Hence, in selecting a computational model to be used in the Apollo guidance system, studies have proceeded along two lines, both of which seek answers to the following questions:

(1) Can the restricted four-body equations of motion be adequately mechanized for guidance in a computer made sufficiently small for use in the overall Apollo system?

(2) Knowing that the restricted two-body equation can be mechanized, do these equations--with appropriate bias terms--result in a reasonably efficient midcourse guidance system?

Regarding question (1), our studies in conjunction with guidance system companies such as Arma and Autonetics show that the computer required for midcourse guidance utilizing the four-body equation of motion can be accomplished in a state of the art digital computer weighing approximately 20 pounds. However, guidance programs utilizing the restricted two-body formulation are still required for thrusting, possible abort, and the re-entry and aerodynamic phases of flight.

Regarding question (2), our studies have shown that the restricted two-body formulation, with appropriate bias terms, is feasible for midcourse guidance

and that such guidance can be accomplished in an efficient and very flexible manner. The computer size required will be less than that for the restricted four-body formulation. However, at the 20-pound level, a weight-saving factor is not considered significant, particularly in view although of the fact that there would likely be some improvement in reliability.

Martin's studies show that the selection of a mathematical model is not critical in sizing the computer. Therefore, current hardware selection is based upon a general-purpose digital computer capable of solving either the restricted two-body or four-body equations. Rather than being a basic problem, then, the mathematical model selection involves a system-design problem requiring only system analysis. Further study is required with both formulations in which complete guidance schemes are mechanized, including all measurement and system errors. The restricted four-body formulation provides greater accuracy, but such refined accuracy may not be required. The restricted two-body formulation provides greater simplicity, and simplicity is always desirable. Also, if for no other reason, the two-body work must proceed in its development aimed toward the end of perfecting the purely manual guidance technique to be used by the crew in emergency situations.

D. EQUIPMENT DESIGN

The automatic system consists of an astro-inertial platform similar to a 55-pound platform under development at Autonectics, and a digital computer. The astro-inertial platform is a four-gimbaled unit with a pair of two-axes gas bearing gyros and three orthogonally mounted accelerometers. A star tracker mounted on the inner gimbal looks out a window in the top of the vehicle. This subsystem is capable of automatically searching, acquiring and tracking stars to update the gyro stabilized inertial reference. The star tracker also has the capability of rim tracking a celestial body to determine its center and apparent diameter. These angular data, as well as platform outputs, are fed to the digital computer which determines the vehicle's orbit and required correction signals and supplys inputs to the displays. The computer, similar to a 15-pound computer under development at Arma, is of the general-purpose class with core storage and microminiaturized packaging.

The manual input system consists of a telesextant, a miniature inertial platform and a digital computer similar to the one in the automatic system. The telesextant, similar to optical equipment built by Kollsman and others, is a manually operated combined telescope and sextant. This unit tracks stars, determines body centers, takes sextant readings (angles between star and landmark and included angle of body), observes occultations and measures lunar latitude of occultations. A second direct-viewing window in the top of the vehicle is provided for the telesextant. This window is also available to the astronaut for general observation of the heavens and other purposes such as photography. The miniature platform, similar to 15-pound platform under development at Litton, is also a four-gimbaled unit with a pair of gas bearing gyros and three

orthogenally mounted accelerometers. The digital computer accepts angular data and platform outputs, computes the present orbit and steering signals and feeds information to the displays. This computer is identical to the one described for the automatic system.

It must be emphasized that, although two seemingly separate systems have been discussed, they actually operate on an interdependent bais: they comprise an integrated system during normal operation, and subsystems of both work in conjunction to combat emergency situations. The advantages provided by such system integration will become more apparent in the following discussion on operation and with reference to the block diagram in Fig. I-1.

The process of trajectory determination during midcourse is extremely flexible. At the discretion of the navigator, appropriate combinations of readings from the astro-tracker and/or the telesextant can be processed in the digital computer to compute the orbit. The readings can be (but need not be) all of the same type. A mixture of sextant, stadiametric, occultation, body center, or rim track readings is permissible.

All components have been developed or are currently under development by leading guidance component manufacturers. Typical components that can accomplish the Apollo guidance system tasks are shown in Fig I-2.

Another important feature of the guidance system is its flexible display system utilizing cathode ray tubes (CRT). The electronics associated with these tubes enables them to display graphic or alphanumeric information, depending on the nature of the information involved. Many different kinds of information can be displayed simultaneously and each crew member can be selective in choosing the subject he wants to view.

E. OPERATION

During ascent, the accelerometers mounted on the astro-inertial platform measure vehicle accelerations. Resulting data are fed to the digital computer which calculates and acts to generate velocity, position and steering signals which command the control system. The computer also commands propulsion cutoff to initiate coast, re-ignites propulsion at the end of coast and finally cuts off the thrust at injection into translunar orbit.

After injection, one hour is utilized to allow ground tracking operation to check out equipment and to assess the overall situation. At the end of this time various on-board measurements will be taken for the next 1-1/2 hours. These measurements include:

(1) Star tracking by astro-inertial platform for angular reference updating.

(2) Ranging by rim tracking from astro-inertial platform.

(3) Sextant reading-star on landmark-earth-by telesextant.

(4) Sextant reading-star on landmark-moon-by telesextant.

(5) Sextant reading for ranging-earth-by telesextant.

(6) Line-of-position to center of moon by astro-inertial platform and telesextant.

(7) Lines-of-position to the moon edge by occultations--telesextant.

(8) Lines-of-position to landmarks-earth-by telesextant.

The data obtained from these measurements are fed directly to the computer which uses them to calculate a smoothed orbit. Based on the deviation from a reference trajectory, the computer also calculates the correction required at three hours after injection. This correction takes the form of an incremental velocity in a given direction. Therefore, the vehicle is rotated to the proper attitude and at the correction time, thrust is applied. The accelerometers and computer monitor and calculate the velocity gained and when the appropriate correction velocity is attained the computer commands thrust termination.

The vehicle is now on a new trajectory aimed at arriving at a given point on the reference trajectory at a given time--i.e., 50 hours after launch. Before midrange (25-hour point), however, another set of observations (de-emphasizing ranging) is made to determine whether additional correction is required to hit the 50-hour point. Periodic observations made between the 25- and 50-hour points further refine orbital knowledge. At the 50-hour point, a correction is made to match the velocity of the vehicle to the reference trajectory.

The vehicle then will arrive at the prescribed periselenium within tolerance; however, before this time (10,000 miles to the moon) further correction is made, if required, to trim the periselenium altitude. Observations preceding this correction will emphasize moon ranging and moon landmarks. In any mission calling for lunar orbit, injection would occur at periselenium. Observations would then be referenced primarily to lunar landmarks.

After ejection, which would also occur near the original periselenium point, any trimming correction necessary for aiming at a specific perigee would be made. Again, observations preceding this correction would emphasize moon ranging and moon landmarks. On the return leg, required observations and corrections, would be made at times corresponding to the outgoing leg. From 10,000 to 40,000 miles out from Earth, a series of observations and a final correction are made to trim the corridor entrance accuracy. Also, initial conditions are established in the inertial system from observations from 40,000 to 80,000 miles. During this period, final alignment of the astro-inertial platform is performed preparatory to re-entry.

The vehicle is trimmed at an angle of attack corresponding to the maximum lift coefficient and maintained in this attitude until aerodynamic control is initiated. At this point the re-entry range prediction steering system uses inputs from the inertial platform to determine the desired angle of attack necessary for arrival at the desired landing area.

F. RE-ENTRY

Re-entry guidance, though in a way similar, is more complex than ascent guidance. For example, during most of the ascent phase, the thrust force is fairly constant and the performance reasonably predictable. Also, most of the required maneuvering is accomplished outside the atmosphere. For re-entry, however, all steering is accomplished within the atmosphere, whose properties are not known too precisely, and the aerodynamic forces are varying over a very wide range. In steering to arrive at a target at a specified range, aerodynamic heat loads and acceleration limits must be monitored. Five re-entry steering techniques have been studied, some in more depth than others, in a search for the best compromise between simplicity, flexibility, overall system compatibility and feasibility. These techniques are:

(1) Explicit hit point steering (with heating and load factor control overrides)

(2) Explicit hit point steering plus equilibrium glide

(3) Equilibrium glide steering

(4) Re-entry range prediction steering (similar to mechanizing the equations of motion)

(5) Re-entry optimum trajectory steering

The explicit hit point steering is the same as the ascent guidance technique. More study is required to establish the best re-entry steering method. Were it not for the extreme complexity of the Re-entry Optimum Trajectory Steering technique (as a completely on-board system) and the accompanying large computer (100 pounds), this method would look very attractive. At present, however, sufficient study has been accomplished with the re-entry range prediction steering (utilizing Chapman's formulation), including simulation work at The Martin Company to demonstrate the feasibility of this technique for re-entries including skip re-entry where ranges up to 10,000 nautical miles and more are required. Associated with establishing the feasibility of this technique is the fact that it has been shown that the digital computer selected for the ascent and midcourse guidance can easily accommodate this technique. The explicit hit point and the equilibrium glide methods are simple techniques and studies should continue in these areas.

The inertial platform is a necessary and extremely important part of the re-entry guidance problem. In fact, Apollo guidance studies have shown that it is the re-entry acceleration histories that stipulate platform requirements.

In other words, the re-entry requirements necessitate an inertial capability more than adequate to handle the ascent and injection guidance.

G. SYSTEM ERRORS

The errors in the system are primarily induced by gyros, accelerometers and the optical equipment. Typical error values for these instruments are $0.01°/hr$ for the gyros, 5×10^{-5} g for the accelerometers, and 5 to 10 arc secs for the optics.

Accuracy at injection is approximately one mile and 4 ft/sec rms. In mid-course, position errors of up to 10 miles exist but with smoothing the error reduces to 3 to 5 miles. In the vicinity of the moon, position is known to 1 to 3 miles. Smoothing of the pre-re-entry measurements causes the vehicle to arrive at the re-entry corridor with an accuracy of better than 1.7 miles. The accuracy of the re-entry system allows the vehicle to land in a 3.5-mile radius circle for long range reentry and 2.0-mile for the short range case.

H. SUMMARY

It has been made apparent that the design objectives for the guidance system have been met. These objectives encompass reliability, optimum use of the crew, utilization only of proven techniques, simplicity of design, and use of development components and lightweight equipment. Finally, it has been seen the system possesses the accuracy needed to perform the mission and to safely return the vehicle and crew to Earth.

II. GUIDANCE CONCEPT STUDIES

A. GENERAL GUIDELINES

In order to ascertain the overall feasibility of the Apollo mission it is necessary to assess what development is required in three major technical areas:

(1) Large launch booster.

(2) Parabolic re-entry vehicle.

(3) Accurate onboard guidance.

The first two areas clearly will involve the development of hardware which this country does not currently possess. The third area may involve hardware development in the sense of some improvement in system reliability and in packaging techniques; it will most certainly require the development of techniques beyond the present state of the art. This section is devoted to reporting results derived from the Martin Company study of the feasibility of various techniques for accomplishing guidance of the Apollo spacecraft.

The most significant factor influencing our study of guidance concepts is that there is a human crew on board; this means that the Apollo spacecraft is a manned space vehicle and not merely a guided missile. Accordingly, two primary guidelines have exerted large influence in establishing Apollo guidance concepts. These guidelines were based upon assumptions that:

(1) The primary guidance system is on-board the spacecraft. Information will be transmitted to the vehicle from the ground; however, the decision to use this information rests with the crew.

(2) The crew must be an integral part of the guidance system, especially in areas where a contribution to improved reliability, simplicity, or flexibility can be realized.

Thus, the crew members are considered, in a complete sense, to be "captain of their ship." This is particularly desirable in the face of possible mission-abort situations.

Now what contributions can we except this human crew to make?

The environment is so foreign to man, and the space navigation and steering problems are so complicated, that his intuition and experience alone will not be adequate. He must rely explicitly upon the analytical aid of an electronic digital computer. Specifically, this computer must have the capability of processing measured data to determine the appropriate guidance commands for any particular phase of the flight problems. However, since man can make very

accurate optical measurements in midcourse, he can provide the computer with many input data. Also, the task of telling the computer with which specific phase of the flight problem it is confronted, and of preparing it for solving this particular phase, is essentially a programming task: this, man can do better than machine.

Thus, we see that the guide for studying guidance concepts has been to tailor them to man's peculiar capabilities of making accurate optical measurements and of providing some types of complicated program logic. These attributes, together with appropriate inertial and optical elements and a flexible digital computer, will result in a guidance system possessing optimum adaptability and reliability.

The guidance programs, and the equipment required to mechanize these programs, often can be "optimized" for each individual phase of the mission. If care is not exercised, however, such an approach could result in a conglomerate system which may be incompatible and hence inefficient from the standpoint of overall requirements. Accordingly, the primary guidance system (including the role of man) for Apollo should be regulated and judged on the basis of the following overall criteria:

(1) Suitability of the system to do the job for each particular phase of the mission.

(2) Compatibility of the system requirements for the various phases.

B. PHASES

1. Ascent Phase

No comparative study of various ascent guidance techniques has been conducted since this phase is conceptually well within the present state of the art. A technique possessing some unique aspects is suggested here mainly to ensure compatibility with the cislunar portion of the trajectory.

The extreme sensitivity characteristic of cislunar trajectories to injection conditions requires high injection-guidance accuracy to minimize the inevitable deviation from the intended path. However, more than plain and simple accuracy is required. Operationally it is highly desirable to achieve the correct:

(1) Outgoing and return inclinations for the particular time of launch.

(2) Periselenium and perigee altitude.

(3) Total flight time.

As demonstrated in the trajectory analysis later in this section, these constraints minimize Van Allen radiation dosage, satisfy range safety, provide for AMR-PMR tracking, and reduce lateral maneuver requirements for landing at Edwards AFB to simple nulling around nominal zero. In order to honor all of these constraints, within the limits of reasonable midcourse fuel expenditures, it is necessary to fly closely to the trajectory uniquely satisfying these constraints. Accordingly, the guidance objective during ascent should be to rendezvous, simultaneously nulling relative range and range rate, with a "phantom" traversing this unique trajectory. This would impose no operational limitation, since an appropriate phantom ephemeris within the booster capability could be programmed for whatever launch time actually is achieved.

The ascent trajectory would be flown essentially in the phantom orbital plane in a two-part sequence. First, there would be the phase from launch through a coasting period which in reality would be a low altitude parking orbit. The steering objective during powered flight in this phase would be to intercept ballistically (after thrust termination) an aim point fixed in space and time at a judicious displacement ahead of the phantom. The second phase of the ascent would begin approximately at the time of arrival at this aim point. It would comprise the injection into the cislunar orbit, and would achieve rendezvous with the phantom.

To minimize prelaunch guidance computation for ascent, it is recommended that an explicit computation be employed for the aim point steering and thrust termination. It would be necessary to precompute only the aim point and time; but no sensitivity parameters, such as those required by perturbative guidance schemes, would be required. The explicit technique described is also noniterative, thus facilitating rapid data processing during the thrust period.

[redacted]

We limit ourselves to a two-dimensional consideration of the problem in the guidance plane and assume a Keplerian free-fall trajectory. In a cartesian frame centered at the center of the earth, the vehicle position and velocity will be denoted x_1, z_1 and $\dot{x}_1, \dot{z}_1$ at time t_1. The aim point position and time are x_f, z_f and t_f.

The equation of a Kepler ellipse with focus at the origin can be written

$$ax + bz + c = (x^2 + z^2)^{\frac{1}{2}} \equiv r \tag{1}$$

where a, b, c are the in-plane "orbital elements" and can be related to the more familiar ones. This expression together with its derivative

$$a\dot{x} + b\dot{z} = \frac{x\dot{x} + z\dot{z}}{r} \tag{2}$$

tells all there is to say about the kinematics. A third relation depends upon the dynamics and is called Kepler's Second Law:

$$c = \frac{(\dot{x}z - x\dot{z})^2}{K} \tag{3}$$

where K is the product of the universal gravitational constant and the mass of the earth. For given $x_1, z_1, \dot{x}_1, \dot{z}_1$ these three equations set forth above completely define a, b, c and hence the free-fall trajectory.

Our problem, however, is to determine $\dot{x}_1, \dot{z}_1$ so that the resulting path goes from x_1, z_1 at time t_1 to x_f, z_f at time t_f. The relations

$$\begin{aligned} ax_1 + bz_1 + c &= r_1 \\ a\dot{x}_1 + b\dot{z}_1 &= \frac{x_1\dot{x}_1 + z_1\dot{z}_1}{r_1} \\ c &= \frac{(\dot{x}_1 z_1 - x_1 \dot{z}_1)^2}{K} \\ ax_f + bz_f + c &= r_f \end{aligned} \tag{4}$$

constitute four equations in the five unknowns a, b, c, $\dot{x}_1, \dot{z}_1$.

[redacted]

At this point, the usual procedure for explicit guidance is to introduce the expression for the free-fall time as the fifth relation. This system cannot be solved in closed form for $\dot{x}_1, \dot{z}_1$, because of the transcendental nature of the time equation; hence an iteration technique is employed. A "guessed" trajectory passing through the two points is selected. The initial velocity and the flight time then can be computed. The flight time is checked against $t_f - t_1$ and the trajectory guess is modified in successive steps until a match is obtained.

The objections to this procedure are as follows:

(1) The expression for time is complicated, hence iterating it is undesirable.

(2) Even after the perfect or correlated velocity is computed, the vehicle can only steer to null one component or else to establish a preferred ratio of components. Then, as the non-zero components are driven to zero by the acceleration, rocket thrust is terminated.

An obvious alternative suggests itself at this point; i. e., to redefine the correlated velocity. We therefore take whatever speed we happen to have and steer to hit the target point, regardless of the time of arrival there. In this manner, the troublesome expression for time is eliminated from the steering computation, thereby permitting a solution in closed form. The procedure then would be to monitor the flight time resulting from this steering and, when it matches the time remaining, to terminate the thrust.

If $\dot{x}, \dot{z}$ in (4) are replaced with

$$\left.\begin{aligned} \dot{x}_1 &= V \cos \Gamma_D \\ \dot{z}_1 &= V \sin \Gamma_D \end{aligned}\right\} \qquad (5)$$

and a, b, c are eliminated, a single equation in tan Γ_D can be obtained (V is assumed known). It was anticipated, from physical considerations, that this equation should be a quadratic. When the speed is less than minimum energy, there should be no real root; and when the speed is greater, there should be only two roots. The equation turned out to be a cubic, but a linear factor was found: it corresponded to the degenerate case of two straight lines from the center of the earth to the points x_1, z_1 and x_f, z_f. The resulting quadratic is

$$A \tan^2 \Gamma_D - 2B \tan \Gamma_D + C = 0 \qquad (6)$$

where

$$A = x_1(x_f - x_1) - D$$
$$B = \frac{z_1 x_f + x_1 z_f - 2 x_1 z_1}{2} \qquad (7)$$
$$C = z_1(z_f - z_1) - D$$
$$D = \frac{K}{r_1 V^2}(z_1 z_f - r_1 r_f + x_1 x_f)$$

The solution for tan Γ_D is

$$\tan \Gamma_D = \frac{B \pm (B^2 - AC)^{\frac{1}{2}}}{A} \qquad (8)$$

Since we want the smallest tan Γ_D , the sign ambiguity is easily settled. The steering law can then be written as

$$\tan \Gamma_D - \frac{\dot{z}_1}{\dot{x}_1} = \dot{\theta}_\varepsilon \qquad (9)$$

a commanded pitch rate. When the radicand in (8) is negative, minimum energy velocity has not been attained and it is impossible to reach the target. Under these conditions the real part B/A could be used. This poses no problem since, from performance considerations, a shaping function normally is added to (9) in order to ensure that the trajectory flown is close to a nominal one.

The expression for the time of flight as a function of the rectangular form orbital elements is derived in Appendix A.1. This time t_{1-f} when compared with the desired time $t_f - t_1$ generates the cutoff signal

$$t_{1-f} + t_1 - t_f = E \qquad (10)$$

Here, E is a specified constant which accounts for the nominal thrust decay time.

Simply, then, the procedure is to compute (7), (8), to steer by (9), and to cutoff by (10). The time computation could be slowed down compared with the necessarily very rapid steering calculation. The cutoff expression would then require some extrapolation.

After the ascent thrust phase, the vehicle would coast, in the parking orbit, toward the aim point. During this time, the inertial navigation system would continuously integrate the motion, keeping track of position and velocity. This running assessment would be more accurate than the Keplerian prediction of the steering law since gross gravitational anomalies such as the oblateness can be accounted for. The difference between this inertially measured position and velocity, and the stored position and velocity of the phantom, would constitute the relative range and range rate data for the rendezvous injection guidance scheme described next.

The coasting, or parking orbit, and the aim point would be chosen for the particular phantom orbit so that essentially the vehicle and the phantom would be flying colinearly in the vicinity of the aim point. Two functions must be performed during the primary injection rocket burning. First, the pitch and yaw attitudes must be controlled to constrain the flight along the phantom orbit. Secondly, ignition and thrust termination must be controlled to approximate a rendezvous with the phantom.

Theoretically, an exact rendezvous can be achieved only with continuously throttleable thrust. The technique suggested involves a two impulse on-off approximation. The first impulse, delivered by the Saturn S-IV, would constitute the primary injection. The second impulse would be metered by the Apollo spacecraft midcourse or vernier engines; this comprises the injection vernier.

The procedure during primary injection would be to ignite the S-IV on the basis of its expected nominal performance and to terminate the thrust to ensure at least an intercept with the phantom at low relative velocity. The assumption of colinearity reduces the problem to a one-dimensional rocket problem along the flight path. Range R, measured along the path from the vehicle to the phantom, is considered positive in the direction of inertial motion of the vehicle. With this convention

$$\dot{R} = V_p - V_v$$

$$\ddot{R} = -\dot{V}_v = -\frac{T}{M} \qquad (11)$$

assuming constant thrust T and fuel mass rate $\dot{M}$, this can be written

$$\ddot{R} = - \frac{T}{M_o - \dot{M} t} \qquad (12)$$

where t is time from injection initiation (taken as zero). Integrating (12) once for range rate, and again for range from

$$t = 0 \qquad \begin{cases} R(0) = R_o \\ \dot{R}(0) = \dot{R}_o \end{cases}$$

to the desired rendezvous condition

$$t = t_c \qquad \begin{cases} R(t_c) = 0 \\ \dot{R}(t_c) = 0 \end{cases}$$

gives

$$\dot{R}_o = - \frac{T}{\dot{M}} \log \left(\frac{M_o - \dot{M} t_c}{M_o} \right)$$

$$R_o = - \dot{R}_o \frac{M_o}{\dot{M}} + \frac{T t_c}{\dot{M}}$$

Eliminating t_c gives initial range as a function of initial range rate:

$$R_o^* = \frac{M_o}{\dot{M}} \left\{ \frac{T}{\dot{M}} \left[1 - \exp\left(- \frac{\dot{R}_o \dot{M}}{T} \right) \right] - \dot{R}_o \right\} \qquad (13)$$

$$= \frac{W_o}{\dot{W}} \left\{ I_{sp} g \left[1 - \exp\left(- \frac{\dot{R}_o}{I_{sp} g} \right) \right] - \dot{R}_o \right\}$$

The asterisk (*) is used to indicate that (13) is considered as an equation giving the value of R_0 required for a specified $\dot{R}_o$ to achieve a rendezvous in the time t_c. The primary injection ignition criterion therefore requires that

$$\delta = R_o^* - R_o$$

$$= \frac{W_o}{\dot{W}} \left\{ I_{sp} g \left[1 - \exp\left(- \frac{\dot{R}_o}{I_{sp} g} \right) \right] - \dot{R}_o \right\} - R_o \qquad (14)$$

vanishes. Actually, some anticipation is required to account for the thrust buildup time lag.

R_o^* should remain relatively constant in the vicinity of the aim point, since the coasting velocities of the vehicle and the phantom are only slowly changing, making $\dot{R}_o$ and R_o^* nearly constant. Thus, as the sketch below shows, the differences between the actual and the desired range would close to zero, giving the injection initiation signal. In mechanizing this scheme in the inertial guidance system, it may prove desirable to program a curve representing nominal injection stage performance more realistically than Eq (13).

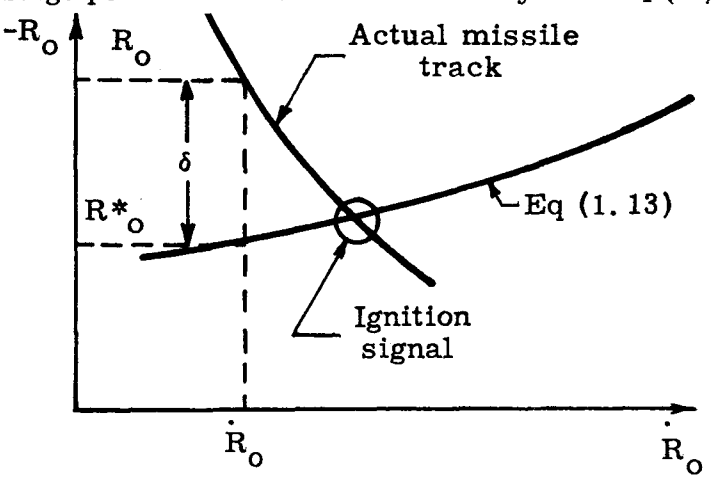

In particular, if experimental or semi-empirical determination of the nominal thrust and fuel flow rates are made, these could be substituted into Eq (12) and the result twice integrated numerically to arrive at a more accurate curve than that given by Eq (13).

Whichever of these schemes is used, the burning time t_c is predicated upon nominal performance. It makes sense to ignite this rocket on the basis of the expected nominal performance, but it is not possible to rely explicitly upon this stage performing nominally and hence to precalculate the cutoff time. The variation of R versus $\dot{R}$ during injection burning appears as sketched below. The slopes

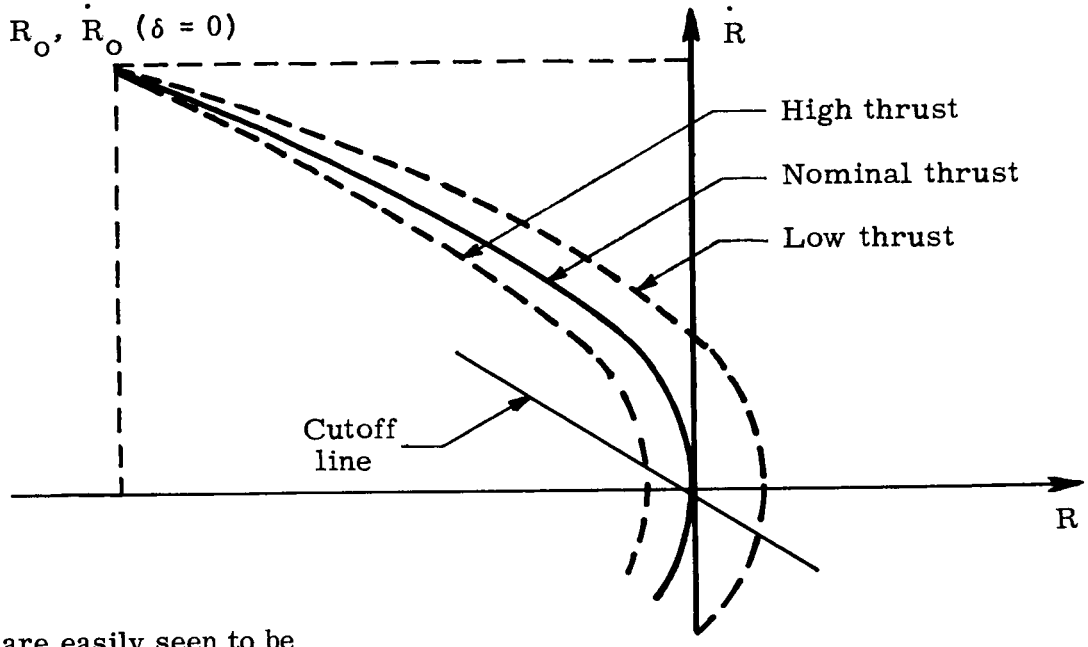

are easily seen to be

$$\frac{d\dot{R}}{dR} = \frac{\ddot{R}}{\dot{R}} \qquad \begin{cases} <0 & \text{for } \dot{R}>0 \\ >0 & \text{for } \dot{R}<0 \end{cases}$$

and, of course,

$$\frac{d\dot{R}}{dR} \to \infty \qquad \text{as } \dot{R} \to 0$$

The nominal curve obviously passes through the origin; off-nominal curves may not. Thus, if the injection stage does not perform as expected, a true rendezvous ($R = \dot{R} = 0$) is not possible.

The phase plane switching line technique will salvage at least an intercept situation ($R=0$) out of any off-nominal case. If the vehicle should happen to accelerate rapidly and tend to outrun the phantom, then thrust should be terminated before $\dot{R}=0$. If, on the other hand, the phantom should overtake the vehicle before the range rate is nulled, then the rocket should be allowed to burn until the range rate changes sign and the vehicle starts catching up. As the phase plane sketch shows, the straight line

$$t_v \dot{R} + R = \Delta \to 0 \qquad (15)$$

through the origin accomplishes just this. The slope t_v assures the proper combination of R, $\dot{R}$ for cutoff so that the range will be nulled in the time t_v. The vernier engine then must null the cutoff rate $\dot{R}(\Delta \approx 0)$. Whether the required vernier impulse is either forward or backward, it will just reduce the residual $\dot{R}$ to zero. Obviously the velocity will not be added truly impulsively, hence a small position error theoretically will exist after final shutdown. However, variations from nominal performance of the primary injection stage should be small. This means that the residual velocities to be verniered out will be small; hence, the theoretical error will be small indeed: certainly well within the expected accuracy of the instrumentation.

2. Cislunar or Midcourse Phases

a. General

In this section the descriptions of the steering objectives in the various cislunar phases of the Apollo mission are separated from the descriptions of the means studied for accomplishing these objectives. The reason for this separation lies in the fact that the objectives really are determined on the basis of flight mechanics aspects of the trajectories satisfying the operational concepts selected, and are independent of the means of implementation. The next three paragraphs (b, c, d) are devoted to describing the objectives in the various phases. Paragraph e describes the geometric ramifications of the various types of onboard optical measurements, and tells how these data are utilized in the navigation or trajectory determination process. Paragraphs f, g, h and i describe the studies of the 4-body, 3-body series approximation, and 2-body mechanizations for cislunar steering and navigation. Finally, in paragraph j, the various studies are evaluated and compared, and an indication is given of the guidance computer requirements. An indication is also given of the further studies which must be done.

b. Translunar steering objectives

The translunar phase, at least for all early Apollo fights, should be flown as the outgoing leg of a circumlunar trajectory with appropriate return characteristics. This operational concept has been selected so that, if the mission engine should fail on lunar injection, a "free return" to earth would be assured. All the arguments previously given for rendezvous guidance in the ascent phase, therefore, are just as valid for the early part of the translunar phase. Of course, the vehicle would be essentially in free-fall; hence, the rendezvous could be achieved by a two-impulse correction technique.

A study of this technique has been conducted (see Trajectory Analysis Section in Volume I, Report 3) to ascertain the optimum translunar aim point location for rendezvous from the standpoint of propulsive efficiency. Perfect

guidance was assumed and the reference was a typical circumlunar trajectory involving an 84-hour (3.5 day) flight from earth injection to periselenium. Making the first correction 3 hours after injection (the earliest time felt practicable), this study revealed that the 50-hour point was the best aim point. This requires a minimal total of two impulsive velocities. This result is a quantitative expression of the intuitive fact that, because of the sensitivity characteristics, the trajectory had better be right before entering the sphere of influence of the moon, or else large penalties must be paid to make it right.

Accordingly, the steering objective in the first part of the translunar phase should be to rendezvous with the phantom again. As soon as a trajectory determination can be made - - perhaps 3 hours after injection - - a correction should be made, aimed at intercepting a fixed point in space and time corresponding to the phantom position prior to entry into the moon's sphere of influence. For a 3.5-day trajectory to periselenium, this point would be 50 hours after injection. Upon reaching this point at the corresponding time, the velocity discrepancy should be nulled.

During approach to the moon there is insufficient time to permit a series of readings and corrections aimed at maintaining the rendezvous. The same goal can be achieved, for all practical purposes, in a simpler fashion. The orbit relative to the moon is hyperbolic; hence very large energy changes would be required to alter the major axis orientation. Since the periselenium angular location in effect cannot be moved, then no control of this parameter is necessary. Thus, the guidance objective during this phase should be to control the orbital inclination relative to the moon, the periselenium altitude, and the time to periselenium. This would place the vehicle in a good position for the next phase.

c. Lunar orbit steering objectives

Because of the performance limitation of the vehicle, due in turn to the booster limitations, the lunar orbit must be essentially in the plane of the translunar orbit relative to the moon; this would involve a minimal velocity change to establish the lunar orbit. The translunar orbit could therefore be viewed as a transfer, or parking, orbit from the earth to the desired orbit around the moon. Thus the lunar injection guidance would be the same as the cislunar injection back at earth, except that now the vehicle velocity would be decreased to rendezvous with the lunar-orbiting phantom.

Once injection into moon orbit has been accomplished, steering would involve the same type of rendezvous maintenance described for the early translunar phase.

Ejection to a transearth orbit would, of course, be a repetition of the translunar injection procedure - - and the inverse of the lunar orbit injection.

If a simple circumlunar trajectory is flown, steering would proceed directly from the translunar phase; the subsequent transearth phase would follow without involving the procedures described here.

d. Transearth steering objectives

On this phase of the journey, many of the constraints would be past history, and the flight mechanics of the trajectory would indicate the same type of relaxation of rendezvous maintenance as that allowed during the moon-approach portion of the outgoing phase. Again, the orbital energy would be high; hence, the stability of perigee angular location would be assured. The earth-approach phase would therefore entail identical objectives: control of orbital inclination relative to earth plus control of perigee altitude and time.

The first correction would not be made until after leaving the moon's sphere of influence. At this time the greatest control should be exercised over the return inclination and perigee time, for the cost of changing these parameters later quickly becomes very dear. Finally, at some point on the earth approach, the sole objective would be to maintain the perigee altitude to ensure accurate threading of the re-entry corridor.

e. Optical measurement and cislunar navigation

All onboard optical observations will be classified into one of three fundamental types:

(1) Occultation

(2) Stadiametric

(3) Sextant.

Occultations simply involve timing the disappearance of identifiable stars behind the limb of the moon, with no attempt being made to measure the winkout point on the limb. Since they necessitate only the measurement of time, such readings are extremely accurate. This places the observer at a precise time somewhere on the surface of an infinite cylinder of precisely known direction, diameter and location in space.

A stadiametric reading of course is a means of inferring radial distance from a body of known size from the subtended angle. Such readings are inherently inaccurate at long range since, in addition to time, small angles must be measured with great precision. This type reading tells the observer that, at the reading time, he is somewhere on the surface of a sphere which is accurately centered in space but whose radius is less accurately known.

Sextant-type readings involve the measurement of the angle between the line of sight from the observer to a known point in space and a known reference direction (a star line). This very general type of reading can be made in many ways. First, there is the well-known technique of optically superimposing images of the point and a star to measure the angle directly. This can be done quite accurately to place the observer somewhere on the surface of a cone having its apex at the known point, and with its axis precisely oriented in space. The angle of the cone is known with fairly high accuracy.

The second method amounts to making two readings between a given point and two different stars simultaneously. It is accomplished by mounting a telescope on an inertial platform, aligning the platform to the star reference, aligning the telescope to the known point, and reading the angles between the telescope and the inertial axes—two plus the sign of the third are sufficient. Such a procedure would have obvious accuracy limitations, but enjoys the advantage wherein the observer is placed along a single line in space (which is the intersection of two cones having the same apex) passing through the known point but with some inaccuracy of direction.

The third method is inherently accurate in that it involves the degenerate case of zero angle, or an occultation of a star by the known point. This method, consisting of identifying the occulted star winkout point on the limb of the moon, also locates the observer along a single line in space.

The geometry involved in these three types of readings is illustrated by the accompanying sketch. The X, Y, Z axes constitute an inertial reference frame to which all ephemeris data are referred. The vectors shown in the sketch are defined as:

$\vec{R}_c$ - Position vector of center of body being observed. Known ephemeris

$\vec{R}_P$ - Position vector from center of observed body to specific point being observed. Known ephemeris.

$\vec{R}_v$ - Position vector of vehicle.

$\vec{R}_R$ - Relative position or line-of-sight vector from vehicle to observed point.

$\vec{R}_S$ - Star line from specific star through observed point to point closest to vehicle position. Direction known from star catalog.

$\vec{R}_n$ - Minimum or orthogonal distance from vehicle to $\vec{R}_S$.

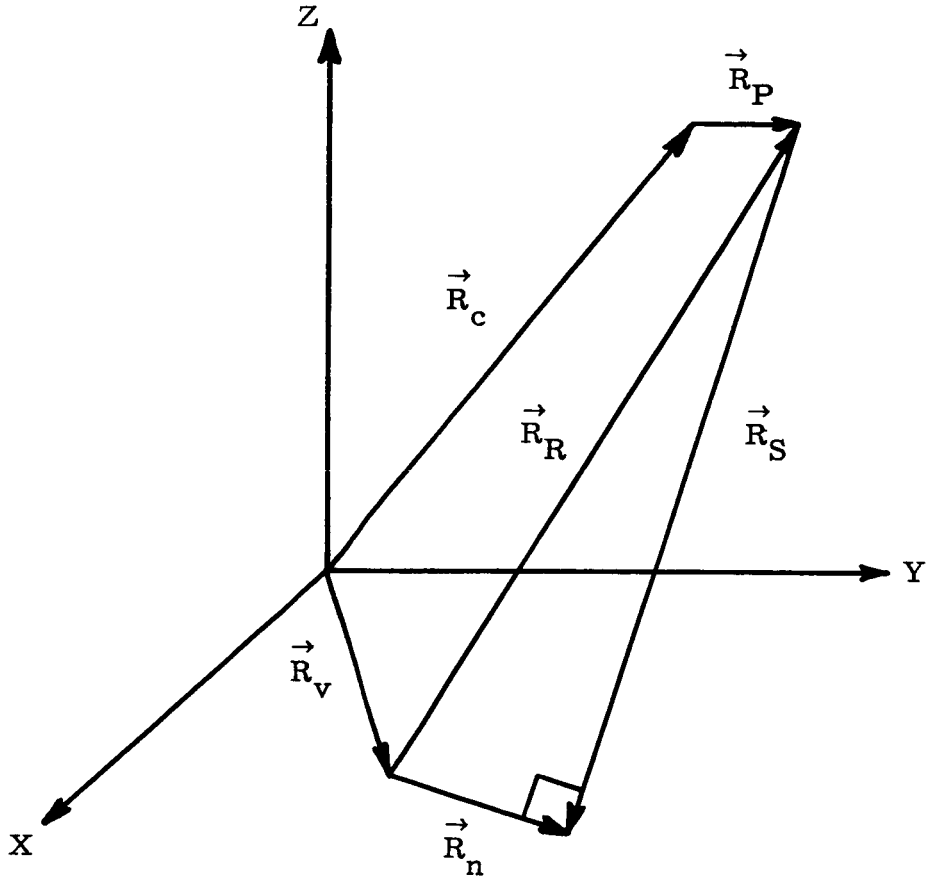

First, let us assume that the vehicle position is known, and then determine the distance D from the vehicle to the center of the observed body by the law of cosines:

$$D^2 = R_c^2 + R_v^2 - 2\vec{R}_c \cdot \vec{R}_v \qquad (16)$$

From this, we can find the distance from the vehicle to the observed point similarly as

$$R_R^2 = D^2 + R_P^2 - 2\vec{R}_P \cdot (\vec{R}_v - \vec{R}_c) \qquad (17)$$

Furthermore, if R_S were known, R_n could be found from

$$R_n^2 = R_R^2 - R_S^2 \qquad (18)$$

We now proceed to solve for R_S. The vector $\vec{R}_R$ can be written as two different vector sums which obviously must be equal.

$$\vec{R}_R = \vec{R}_c + \vec{R}_p - \vec{R}_v = \vec{R}_n - \vec{R}_s \equiv \vec{R}_n - R_s \vec{r}_s \qquad (19)$$

Here we have defined $\vec{R}_S$ as

$$\vec{R}_s = R_s \vec{r}_s = R_s(\alpha_s \vec{i} + \beta_s \vec{j} + \gamma_s \vec{k}) \qquad (20)$$

where $\vec{r}_S$ is the unit vector of the star direction as given by the catalog. The stipulated condition of orthogonality of $\vec{R}_n$, $\vec{R}_S$ is written

$$\vec{R}_n \cdot \vec{R}_s = 0 = X_n \alpha_s + Y_n \beta_s + Z_n \gamma_s \qquad (21)$$

We then solve the four equations (20), (21) for the four unknowns X_n, Y_n, Z_n, R_s. Solving Eq (20) explicity for the components of $\vec{R}_n$:

$$X_n = R_s \alpha_s + X_c + X_p - X_v$$
$$Y_n = R_s \beta_s + Y_c + Y_p - Y_v$$
$$Z_n = R_s \gamma_s + Z_c + Z_p - Z_v$$

and substituting into (21), we can solve for R_S

$$R_s = \alpha_s(X_v - X_c - X_p) + \beta_s(Y_v - Y_c - Y_p) + \gamma_s(Z_v - Z_c - Z_p) \qquad (22)$$

Recapitulating, (16), (17), (22) could be solved if the vehicle position were known, giving D, R_R, R_S. This would permit solution for R_n by (18). The quantity D can be related to the stadiametric readings σ_T as

$$\frac{\rho}{D} = \sin \frac{\sigma_T}{2} \qquad (23)$$

where ρ is the radius of the observed body. R_n at the time of an occultation must be

$$R_n = \rho \qquad (24)$$

where ρ is the same as before. Finally, the sextant readings σ_S relate R_n, R_R according to

$$\frac{R_n}{R_R} = \sin \sigma_S \qquad (25)$$

In writing these relationships, we assumed that the vehicle position is known; in fact, however, this really is what we are trying to find. Thus, we ask: How can readings such as these be utilized to solve for the orbital position? and how many readings are required?

Of course, the equations of motion of the vehicle in three-dimensional space are a system of second order differential equations. Accordingly, a set of six independent parameters, which satisfy compatibility conditions, is necessary to specify a solution. Thus, at least six readings are required for an orbit determination. Geometrically stated, we seek a curve which is an integral of the equations of motion and which pierces six surfaces (cones, cylinders and/or spheres) at the times appropriate to the surfaces. Stated this way, it is clear that in general there may be many possible solutions. In practical application we know grossly what parts of these surfaces we are on and hence can pick out the particular solution of interest in all but unusual cases.

Two fundamentally different types of approaches can be taken to fitting the orbit to the data observations. One technique makes no attempt to treat separately the geometries of the observed data and of the trajectory. An estimate of the trajectory is made by guessing the initial position R and velocity V at some reference time. Then, at times corresponding to the observation times,

calculations are made of the "readings" according to equations (23), (24), and (25) derived above. The deviation of these "readings" from the actual observations and the linearized sensitivities of the "readings" to perturbations of the initial conditions can be utilized to improve the estimate of the initial conditions and hence the trajectory. If just six readings are taken, there are just enough equations for determining the components of the corrections $\Delta\vec{R}$, $\Delta\vec{V}$ to the initial conditions. If redundant data are taken, there will be more equations than unknowns and a least squares technique can be used to find the corrections. In effect, then, this procedure starts with distorted geometries of the observation cones, cylinders and/or spheres and of the trajectory itself and improves the shapes iteratively. The trajectory determination and the data smoothing are done together.

The second technique treats separately the geometries of the observed data and of the trajectory. In the discussion of the types of readings, mention was made of simultaneous sextant readings of a single landmark and two stars. The intersection of these two cones with common apex was remarked to be a straight line. More generally, if any two types of readings on any landmarks can be taken simultaneously, the vehicle must obviously lie on the space curve which is the intersection of these two observation surfaces. We know that three "lines of position" (six readings) and the times are sufficient to determine an orbit (see Moulton), and this would mean three pairs of simultaneous readings. However, if yet a third reading were made simultaneously with the pair mentioned above, the vehicle would now be pin-pointed at the intersection point of the space curve (intersection of first two surfaces) and the third observation surface.

This is simply a more general type of triangulation and is easily visualized in terms of the special case of a body center (2 sextant readings) determination plus a stadiametric reading on the body. We know in this case that two points (again six readings) and the elapsed time are sufficient to determine an orbit. This procedure means a pair of three simultaneous readings.

Now how do we make simultaneous readings, solve for the surface intersections and smooth redundant data? This is all accomplished in the handling of the observation geometry so that the final triangulated points marking position at the initial and final observation "times" are smoothed and non-redundant data points. Then the trajectory fit is a straightforward process.

On the basis of previous knowledge of the trajectory characteristics relative to the earth and the moon, a judicious choice can be made of the types of three readings which should comprise the best geometry at a given point. Then repetitious readings would be taken of these three basic readings over a time span bracketing the observation time t* of interest. Now a least squares technique can be utilized to fit an appropriate time curve (quadratic or higher if necessary) to these data points for each individual type of reading.

The points on these curves at time t* represent the smoothed "simultaneous" readings, defining the three geometric surfaces (cones, cylinders and/or spheres). These equations can be solved simultaneously for the common point of intersection to yield the triangulated point. If this is repeated at a subsequent time t**, the two points will be determined, specifying the trajectory. Note that sextant (conical) and stadiametric (spherical) readings can be processed in this fashion, but occultation (cylindrical) readings cannot for the obvious reason that they occur discretely. Thus, there can be no smoothing of an occultation reading, but none really is required since it is inherently extremely accurate. Therefore, if we desire to use an occultation reading, the actual time of the observed occultation must comprise the value t*. This imposes no limitation because the other types of readings can easily be taken to bracket the occultation.

The latter approach of separating the geometries in the orbit determination has some important advantages.

(1) An assessment of position is available to the navigator shortly after the first observation time and before the new trajectory is computed. It is not necessary to wait for all observations to be processed together at the end.

(2) Storage requirements in the computer can be reduced since the first series of observations can be processed down to the single triangulated point before the next series is taken.

(3) It will be easier to separate out instrumentation errors from those caused by uncertainties in physical constants.

f. Approaches to mechanization

The gravitation field of cislunar space is a composite of the relatively moving fields of the earth, moon and sun. The influence of the sun is small in comparison with that of the earth and moon, but its perturbative effect at large distances from the earth is comparable to the perturbing effect of earth oblateness close to the earth.

This complex nature of the physical problem presents a dilemma in choosing an appropriate mathematical model. On the one horn is a complicated but highly accurate n-body (n = 3 or larger) model, and on the other is a simple but somewhat inaccurate 2-body model. The two basic approaches, therefore, are to mechanize (in the sense of a conceptual mechanization):

(1) The complicated model, accepting the fact that closed form solutions are not possible, and ascertain what computer is required (taking advantage of microminiaturized packaging techniques).

(2) The closed form solutions of the simple model and ascertain the cost, if any, of achieving the ultimate objectives with the requisite accuracies.

A philosophical question arises at this point. Should we be able to compute, aboard the vehicle, an extremely high precision orbit even if it should not be required from the standpoint of vehicle guidance alone? The argument for such a capability is that instrumentation errors and uncertainties in physical constants can be reduced only when the computing accuracy is much better by comparison. The counter argument says that instrumentation improvement and uncertainty reduction should be accomplished by means of refined ground calculations--the on-board computation should be adequate to solve the guidance problem reliably, with sufficient accuracy and within the limits of allowable fuel. The navigator really does not care about the absolute precision of his present position and velocity other than to know that it is adequate and that the relative precision is high in the vicinity of his objective.

The Martin Apollo study has pursued both of the basic approaches. Three investigations of the n-body model were conducted. Arma and Autonetics looked at mechanizing the four-body problem from the standpoint of detailed computer requirements since the computer is the principal question regarding the feasibility of this approach. Martin-Orlando looked into the feasibility of utilizing approximate series solutions to the three-body problem and took a cursory look at computer requirements. One investigation of the simple two-body problem was conducted at Martin-Baltimore. Here the emphasis was laid upon casting the equations in simple form and upon ascertaining the applicability of the two-body representation. These studies are reported in the following three paragraphs.

g. Two-body study

In Paragraph IIB-2b, a study was reported of the best aim point from the standpoint of propulsive efficiency for the translunar phase of the mission. For a 3.5-day flight from earth injection to periselenium, and making the first correction 3 hours after injection, the minimum fuel was expended aiming at the 50-hour point.

Accordingly, it was decided to measure the applicability of the two-body representation over this same range. Starting at the 3-hour point with precisely the reference trajectory position and velocity relative to earth, one finds that corresponding time points on the Kepler orbit relative to the earth depart from the reference as shown in Fig. II-1. The distances and velocities are the magnitudes of the relative vectors. This picture is encouraging as far as navigation at the 3-hour point is concerned. Two hours after the exact match point, the position and velocity errors are less than 0.25 nautical miles and knots respectively. Actually the deviation before the 3-hour point would be even less, making the match very good indeed.

The very rapid growth of the errors with increasing time, however, is discouraging from the standpoint of steering. By the time the 50-hour point is reached, the position error amounts to some 485 nautical miles. In fact, if Kepler orbits are computed to the 50-hour time for a series of subsequent starting time points along the reference trajectory, one finds a disappointingly slow decay of this 485 nautical miles error to zero at 50 hours. One would guess from these results that we simply cannot afford the luxury of making midcourse corrections on this basis in terms of mid-course fuel required. That this indeed is true has been shown in an example case reported in the trajectory analysis set forth in ER 12003.

It is evident that in this situation, where the sensitivities are extremely high initially but very rapidly decreasing thereafter, it is mandatory that a fairly accurate correction be made as early as possible; therefore some form of biasing is required for the steering calculation.

It is obviously possible to bias off the aim point physically to account for the deviation of the reference trajectory from the Kepler orbit. This technique is satisfactory but would require storing the unique biased aim points as a function of correction time for each trajectory. Such a procedure is simpler than determining a set of sensitivity coefficients versus correction time.

A second alternative exists, however, which shows promise of somewhat greater universality. Basically, the method consists in separating the problem into two parts.

The orbital plane defined by the initial position and velocity at some point on the reference trajectory is the plane to which the entire Kepler motion obviously is constrained. In the actual situation, of course, the attraction of the moon distorts the reference trajectory out of this plane, hence the aim point has a normal displacement. Therefore, we treat separately the problems of drift out of the initial orbital plane and of deviations of the Kepler orbit from the in-plane projection of the reference trajectory. Further, we assume that the in-plane characteristics are relatively uninfluenced by the inclination of this plane to the earth-moon orbital plane and are primarily functions of flight time. The out-of-plane drift, on the other hand, is primarily a function of the inclination and of the flight time from the correction point to the aim point.

Let us consider the normal drift correction first. The gravitational acceleration of one body by a second (called the gravitating body) is

$$\ddot{y} = -\frac{K}{D^2} \qquad (26)$$

where

K = product of universal gravitation constant and mass of gravitating body (as in Section II-B1)

D = distance of accelerated body from gravitating body.

Therefore, we can write the difference in the acceleration of the vehicle and the earth by the moon as

$$\Delta \ddot{y} = \left(D_v^{-2} - D_e^{-2}\right) K_m \tag{27}$$

The component of this differential acceleration normal to the trajectory plane inclined i_{VM} to the earth-moon orbital plane is approximately

$$\Delta \ddot{y}_N = \left(D_v^{-2} - D_e^{-2}\right) K_m \sin i_{VM} \tag{28}$$

This is only approximately true because the vehicle actually is displaced out of the earth-moon plane, hence its acceleration vector has a different angularity. The average value of this normal differential acceleration over some time period is

$$\Delta \ddot{y}_{N_{av}} = \left(D_{V_{av}}^{-2} - D_e^{-2}\right) K_m \sin i_{VM} \tag{29}$$

where $D_{V_{av}}$ is evaluated at an appropriate time, in the sense of the mean value theorem, within the interval of interest. Therefore, the normal displacement over the time t is approximately

$$\Delta y_N = \frac{1}{2} \Delta \ddot{y}_{N_{av}} t^2 \tag{30}$$

Figure II-2 shows the out-of-plane drift accumulated at the 50-hour point as measured from the Kepler planes defined at various initial points along the reference trajectory. This 3.5-day reference trajectory is inclined roughly 21° to the earth-moon orbital plane. A calculation made according to equations (29) and (30) for the 3-hour initial point gave 207 nautical miles as contrasted

to the exact value of 189 nautical miles shown. This value was computed taking the $D_{V_{av}}$ roughly half-way in time between 3 and 50 hours (26.5 hours) from the reference trajectory. A more accurate method of selecting the appropriate $D_{V_{av}}$ undoubtedly is possible.

The value of this method lies in the fact that it enables the calculation of this component of the bias in flight and requires only the knowledge of the vehicle present position $\vec{R}_1$ and the true aim point position $\vec{R}_f$ and time. The procedure is as follows:

(1) Calculate unit normal to plane of $\vec{R}_1$, $\vec{R}_f$ as

$$\vec{n}_t = \frac{\vec{R}_1 \times \vec{R}_f}{|\vec{R}_1 \times \vec{R}_f|}$$

(2) Dot this into the unit normal of earth-moon orbital plane to give

$$\cos i_{VM} = \vec{n}_t \cdot \vec{n}_{EM}$$

(3) Calculate Δy_N by equations (29) and (30), using $D_{V_{av}}$ from middle time point of reference trajectory.

(4) Bias aim point to account for drift:

$$\vec{R}_{f_b} = \vec{R}_f - \Delta y_N \vec{n}_t$$

Turning now to the in-plane problem, the Kepler orbit defined at any initial point along the reference trajectory will deviate from the projection of the reference onto that plane. This Kepler orbit can be "biased" in a somewhat unusual manner to pass through the projected aim point.

The following equations describing a Kepler orbit

$$\left.\begin{aligned} ax + bz + c &= (x^2+z^2)^{1/2} \equiv r \\ a\dot{x} + b\dot{z} &= \frac{x\dot{x}+z\dot{z}}{r} \\ c &= \frac{(x\dot{z}-z\dot{x})^2}{K} \end{aligned}\right\} \qquad (31)$$

were introduced in Section B-1 of this chapter. As remarked there, given the values x_1, z_1, $\dot{x}_1$, $\dot{z}_1$, it is possible to solve this system for the in-plane orbital elements a, b, c, completely defining the orbit. However, we would like to specify not only x_1, z_1, $\dot{x}_1$, $\dot{z}_1$, but also the point x_f, z_f.

The problem obviously would be over-determined if K were given, hence we allow it to be variable and ask what K is required. Solving the system

$$\left.\begin{aligned} ax_1 + bz_1 + c &= r_1 \\ ax_f + bz_f + c &= r_f \\ a\dot{x}_1 + b\dot{z}_1 &= \frac{x_1\dot{x}_1 + z_1\dot{z}_1}{r_1} \\ c &= \frac{(x_1\dot{z}_1 - z_1\dot{x}_1)^2}{K} \end{aligned}\right\} \qquad (32)$$

explicitly for K yields

$$K = \frac{A\dot{z}_1^2 + B\dot{x}_1\dot{z}_1 + C\dot{x}_1^2}{D} \qquad (33)$$

where

$$A = X_1(X_f - X_1)$$

$$B = 2X_1Z_1 - Z_1X_f - X_1Z_f$$

$$C = Z_1(Z_f - Z_1)$$

$$D = \frac{Z_1Z_f - r_1r_f + X_1X_f}{r_1}$$

This technique of "biasing" the gravitation constant means that the flight time from point 1 to point F will be changed also. The K values given by (33) and the corresponding times to the in-plane projections of the true aim point were computed for the same reference trajectory as described above. The departure of K from the nominal value is plotted in Fig. II-3, and the corresponding excess of the final point time over 50 hours is plotted in Fig. II-4.

To assess the validity of the original assumptions that the problem could be separated into two independent parts--one in the plane, the other normal--the technique was applied to a different trajectory. The flight time to periselenium was roughly the same, but the trajectory inclination to the earth-moon plane was slightly over 9° instead of 21°. An intentional representative injection error was allowed to propagate for 3 hours, and then the techniques developed here were used to compute the correction at 3 hours. This corrected path showed an error of about 35 nautical miles at 50 hours. This path was again corrected at the 25-hour point, reducing the error to 18 nautical miles, at the aim point. The magnitude of this second correction was on the order of 1 knot. This is reported in the trajectory analysis set forth in ER 12003.

These results are very encouraging and certainly suggest that additional work in the area is warranted. In particular, the technique described for calculating the out-of-plane drift, indicates that perhaps we should be looking at barycentric, rather than geocentric, Kepler orbits. Such an approach may even improve the in-plane representation.

So much for the discussion of the applicability of the two-body representation. Let us examine now just what forms the two-body solutions take for various phases of the mission. We have already seen in discussing the ascent phase, Section B-1 of this chapter, the simple equations for guiding to hit ballistically a specified point. Rather than proceed with the derivation of complete sets of equations specifically for each phase, we will illustrate the simplicity of the two-body approach to the complete mission requirements.

First we will describe a few simple sub-routines designed to do certain

basic jobs. Then we will show how the guidance programs for the various phases of the mission are all comprised of appropriate combinations of these sub-routines.

The sub-routines (SR) are listed below in order to associate a convenient letter identification system with the titles:

A. Kepler orbit to specified point

B. Tangent Kepler orbits

C. Orbital elements for specified position and velocity

D. Pericenter determination

E. Kepler orbit time of flight

F. Velocity at specified point on given Kepler orbit

G. Rendezvous thrust initiation

H. Rendezvous thrust termination

SR-A computes the in-plane flight path angle required for given present position and speed (magnitude of velocity) to yield a Kepler orbit passing through a specified aim point. In the case where V is less than the minimum energy speed, this is indicated and the program gives the real part of the answer.

SR-B computes the flight path angle required for given present position and speed to yield a Kepler orbit tangent to another specified Kepler orbit.

SR-C computes, for given position and velocity, the in-plane orbital elements for the Kepler orbit in the form

$$ax + bz + c = (x^2 + z^2)^{1/2}$$

SR-D computes the coordinates of pericenter for given orbital elements.

SR-E computes the time of flight along a Kepler orbit, given by its elements, between two specified points.

SR-F calculates the in-plane velocity components at a given point on a Kepler orbit specified by its elements.

SR-G assumes the rendezvous vehicle is moving essentially colinearly with a known target. The rendezvous vehicle thrust initiation time is computed on the basis of the relative range and range rate so that, for nominal performance, relative range and range rate will be nulled simultaneously.

SR-H accounts for deviations from nominal performance in determining

the rendezvous vehicle thrust termination time so that an intercept at low relative velocity is achieved in a desired time. The relative velocity is also computed for final vernier correction.

The equations comprising these sub-routines are listed in the following tables and their derivations are referenced. Observe that all of the Keplerian orbit equations are derived in rectangular coordinates in the plane of the orbit with origin at the force center. The advantage of the use of these coordinates is apparent in the simplicity of the equations. The only occurrence of a bothersome trigonometric function is in the time computation.

The equations listed in Table II-2 for SR-B are valid only for tangency with a circular orbit. This special case is the only one of concern in the Apollo application. However, the derivation in Appendix A is general.

[redacted]

TABLE II-1

Equations for SR-A: Kepler Orbit to Specified Point

Given data:

K - product of universal gravitation constant G and mass of central body

x_1, z_1 - present position in inertial coordinates in plane of $\vec{R}_1$, $\vec{R}_F$

x_F, z_F - target point in inertial coordinates in plane of $\vec{R}_1$, $\vec{R}_F$

V^2 - square of present speed

Equations:

$$r_1 = (x_1^2 + z_1^2)^{1/2}$$

$$r_F = (x_F^2 + z_F^2)^{1/2}$$

$$D = \frac{K}{r_1 V^2}(z_1 z_F - r_1 r_F + x_1 x_F)$$

$$A = x_1(x_F - x_1) - D$$

$$B = \frac{-2x_1 z_1 + z_1 x_F + x_1 z_F}{2}$$

$$C = z_1(z_F - z_1) - D$$

$$\tan \Gamma_D = \frac{B \pm (B^2 - AC)^{1/2}}{A} \qquad (\text{when } B^2 - AC \geq 0)$$

$$= \frac{B}{A} \qquad (\text{when } B^2 - AC < 0)$$

This flight path angle is referenced to the inertial x axis.
Derivation: Section II-B1 --Ascent Guidance

[redacted]

TABLE II-2

Equations for SR-B: Tangent Kepler Orbits

Given data:

- K - product of universal gravitation constant G and mass m of central body
- x_1, z_1 - present position in inertial coordinates in a plane containing $\vec{R}$
- V^2 - square of present speed
- r_c - radius of target orbit

Equations:

Flight path angle referenced to the inertial x axis:

$$r_1 = (x_1^2 + z_1^2)^{1/2}$$

$$A = \frac{V^2}{K}(r_c^2 - x_1^2) + 2r_c\left(1 - \frac{r_c}{r_1}\right)$$

$$B = -\,x_1 z_1 \frac{V^2}{K}$$

$$C = \frac{V^2}{K}(r_c^2 - z_1^2) + 2r_c\left(1 - \frac{r_c}{r_1}\right)$$

$$\tan \Gamma_D = \frac{B \pm (B^2 - AC)^{1/2}}{A}$$

Derivation: Appendix A. II

TABLE II-3

Equations for SR-C: Orbital Elements for Specified Position and Velocity

Given data:

K

x, z

$\dot{x}, \dot{z}$

Equations:

$$r = (x^2 + z^2)^{1/2}$$

$$a = \frac{x}{r} - \frac{\dot{z}(x\dot{z} - \dot{x}z)}{K}$$

$$b = \frac{z}{r} + \frac{\dot{x}(x\dot{z} - \dot{x}z)}{K}$$

$$c = \frac{(x\dot{z} - \dot{x}z)^2}{K}$$

$$e = (a^2 + b^2)^{1/2}$$

$$\ell = \frac{a}{e}$$

$$m = \frac{b}{e}$$

Derivation: Appendix A. III

TABLE II-4

Equations for SR-D: Pericenter Determination

Given data:

c, e, l, m

Equations:

$$x_p = -\frac{lc}{1+e}$$

$$z_p = -\frac{mc}{1+e}$$

Derivation: Appendix A. IV

TABLE II-5

Equations for SR-E: Kepler Orbit Time of Flight

Given data:

K
c, e, l, m
x_1, z_1
x_F, z_F

Equations: (Derivation: Appendix A. I)

$$\dot{A} = \frac{1}{2}\left(\frac{K}{C^3}\right)^{\frac{1}{2}}$$

$$B = 1 - e^2$$

In equations which follow subscript i = 1, F

$$\breve{x}_i = \frac{m x_i - l z_i}{c}$$

$$\breve{z}_i = \frac{l x_i + m z_i}{c}$$

$B > 0$:

$$Q_i = \frac{1}{2B}\left[e\breve{x}_i - \frac{1}{|B|^{\frac{1}{2}}}\sin^{-1}\left(B\breve{z}_i - e\right)\right]$$

$B < 0$:

$$Q_i = \frac{1}{2B}\left\{e\breve{x}_i - \frac{1}{|B|^{\frac{1}{2}}}\left[\log 2 + \log\left(|B|^{\frac{1}{2}}\breve{x}_i - B\breve{z}_i + e\right)\right]\right\}$$

$B = 0$:

$$Q_i = \frac{\breve{x}_i \breve{z}_i}{2} - \frac{\breve{x}_i^3}{3}$$

$$t_{1\text{-}F} = \frac{Q_F - Q_1}{\dot{A}}$$

TABLE II-6

Equations for SR-F: Velocity at Specified Point on Given Kepler Orbit

Given data:

K - product of the universal gravitation constant G and the mass m of the central body

a, b, c - the in-plane Kepler orbital elements for the form $ax + bz + c = (x^2 + z^2)^{1/2}$

x, z - point at which velocity is desired in inertial coordinates in orbital plane

Equations:

$$r = (x^2 + z^2)^{1/2}$$

$$a_1 = ar - x$$

$$a_2 = br - z$$

$$a_3 = \frac{(cK)^{1/2}}{a_1 x + a_2 z}$$

$$\dot{x} = a_2 a_3$$

$$\dot{z} = -a_1 a_3$$

Derivation: Appendix A.V

[redacted]

TABLE II-7

Equations for SR-G: Rendezvous Thrust Initiation

Given data:

$I_{sp} g_o$ - Characteristic velocity--product of rocket fuel specific impulse and sea level acceleration of gravity

t^* - time it would take the injection rocket engine to consume an amount of fuel equal to the mass of the entire coasting vehicle $(m_o/\dot{m})$

ϵ_+ - thrust buildup time lag

$R(t)$ - range of rendezvous vehicle relative to target--continuously fed in from measured vehicle data and stored target data

$\dot{R}(t)$ - relative range rate of rendezvous vehicle to target--continuously fed in from measured vehicle data and stored target data

Equations:

Thrust initiation signal:

$$R^*(t) = t^* \left\{ I_{sp} g_o \left[1 - \exp\left(- \frac{\dot{R}(t)}{I_{sp} g_o} \right) \right] - \dot{R}(t) \right\}$$

$$B = \frac{R^*(t) - R(t)}{\dot{R}(t)} - \epsilon_+ \longrightarrow 0$$

Derivation: Section II-B1-- Ascent

[redacted]

TABLE II-8

Equations for SR-H: Rendezvous Thrust Termination

Given data:

$R(t)$ - Same as for Table II-7

$\dot{R}(t)$ - Same as for Table II-7

$t_v - \epsilon_-$ - difference between desired time lapse t_v between primary thrust shutdown and vernier correction and the primary thrust decay time ϵ_-

Equations:

Shutdown signal:

$$S = t_v - \epsilon_- + \frac{R(t)}{\dot{R}(t)} \longrightarrow 0$$

Vernier correction time:

$$t = t_{s \to 0} + t_v - \epsilon_-$$

Vernier correction magnitude:

$$\dot{R} = \dot{R}_{s \to 0}$$

Derivation: Section II-B1-- Ascent Guidance

[redacted]

Now that all of the equations in the basic subroutines have been listed, we describe how these building blocks are used to construct the following programs (P) for the guidance and navigation of the Apollo vehicle.

P-I. Powered-flight steering to hit an aim point ballistically

P-II. Midcourse steering to hit a point fixed in space and time

P-III. Midcourse approach orbit steering

P-IV. Powered-flight tangent orbit steering

P-V. Rendezvous steering and thrust control

P-VI. Midcourse position determination

P-VII. Position and velocity at a specified time from an initial point on a given Kepler orbit.

In the following descriptions of these programs, the applicability of some programs to abort and re-entry guidance will be discussed in the interest of presenting the complete two-body story even though these guidance phases have not been introduced yet.

Figure II-5 shows a diagram of program P-1. As used for ascent guidance, the navigator loads the aim point position and time plus a trajectory shaping function prior to liftoff. Then the present position and velocity data from the inertial platform are processed at high rate through SR-A to generate the pitch steering command during powered flight. (The roll attitude is stabilized to a vertical reference, and yaw is steered to null the component of velocity normal to the guidance plane.) The present position and the desired velocity are fed to SR-C to determine the orbital elements, which in turn feed to SR-E where time of flight is computed. The flight time discrepancy constitutes the thrust termination signal. The data processing through the SR-C SR-E path can be slower than the steering processing through SR-A. This would necessitate an extrapolation of the cutoff signal.

This very same program would be used in identically the same manner for abort guidance in the out-of-atmosphere abort situation during ascent. It would merely be necessary for the navigator to read into the computer the aim point position and time corresponding to an appropriate landing site.

This same program might possibly be used as the atmospheric re-entry guidance scheme as well. To achieve long range and yet to avoid overheating the vehicle, it has been found desirable to skip back out of the atmosphere again after reducing the initial energy somewhat and to coast ballistically to the landing area. If, during the skip portion, the vehicle were steered by program P-I so that if all "thrust" were instantaneously terminated (the atmosphere would disappear in this case), then the vehicle would fall ballistically to the target. Thus, as the vehicle dips down into and then climbs back out of the atmosphere, it would hold itself in a constant state of readiness for the correct

out-of-atmosphere free-fall.

During normally powered flight, of course, the rocket thrust would be terminated when the desired flight time is achieved. During re-entry the atmosphere could not be turned off at will; hence, it would be necessary to accept whatever flight time resulted after the vehicle did in fact climb out of the air. The time error in actuality would be a miss distance as a result of the landing site motion, but could be compensated during the second re-entry. It is possible that the same program could be employed even here. If not, an equilibrium glide or some other technique would have to be used. This use of program P-I would not require the time computation explicitly; however, the navigator could index the aim point location to account for flight time variations. This and several other techniques are discussed more fully under re-entry guidance, Chapter III.

Figure II-6 shows that the same sub-routines as above are used in a somewhat different program logic in P-II. This program would be used for the translunar midcourse steering to hit the aim point just outside the sphere of influence of the moon. The present orbit estimate of position and speed (velocity magnitude) at a desired correction time are fed in, together with the aim point position and time. These data are processed through SR-A to determine the correct flight path angle to give a Kepler orbit through the correction and aim point positions with an unchanged speed at the correction point. The correction time position and new velocity components feed through SR-C where the orbital elements are computed. These, in turn, enable the calculation of time of flight in SR-E. This time is then compared with the desired time. If the times do not match, the correction speed is appropriately adjusted and the process is iterated until a match is obtained. The desired velocity at the correction time is then fed out. Iterating the complicated expression for time of flight means that the computing rate is reduced below that of the steering part of P-I, but this is of no consequence in midcourse.

Program P-III would be used for moon approach and for transearth guidance. The similarity to P-II is apparent in a comparison of Figs. II-6 and II-7. Subroutine SR-B is substituted for SR-A to compute the flight path for tangency. The inputs are changed appropriately: desired pericenter instead of aim point. SR-D is inserted between SR-C and SR-E to compute the coordinates of pericenter for the time computation. This program computes iteratively the velocity at a given correction point and time to yield an orbit tangent to a given circular orbit at a specified time. This is tantamount to controlling the pericenter radius and time to pericenter. Again, computing time is unimportant.

P-IV (Fig. II-8) bears the same similarity to P-I as P-III does to P-II; i.e., SR-B is substituted for SR-A and SR-D is inserted between SR-C and SR-E. This program would process at a high rate the inertially measured present position and velocity data to steer for a condition of circular orbital tangency (maintaining a pericenter altitude). Then, at a somewhat reduced speed, the flight time to pericenter would be monitored against a desired time.

When a match is obtained, a thrust termination signal would be generated. This program would be used in one of two modes for midcourse abort guidance.

In the normal mode it is assumed that there is freedom to choose return time appropriately so that a pre-determined landing site (Edwards Air Force Base) can be reached. In this case the navigator would insert the desired orbital inclination, perigee altitude, and time commensurate with the propulsive capability. The rocket would be ignited and P-IV would steer for the appropriate tangency and terminate thrust when the flight time is correct.

In the emergency mode it is assumed that the quickest return is desired. The existing orbital inclination, the desired perigee altitude, and a ridiculously short time would be inserted into the computer, and the rocket would be ignited. The steering would be the same as before but it would be impossible to reduce the return time to match the desired input. Therefore, the fuel will be exhausted, reducing the return time as much as that amount will allow.

Program P-V processes at high speed the difference between inertially measured position and velocity and stored position and velocity of a phantom through subroutines SR-G and SR-H (Fig. II-9). In the manner described in detail in II-B1, this program controls injection thrust initiation and termination and steers the vehicle to achieve a rendezvous with the phantom. This program would be used for injection guidance into a circumlunar or a near-earth orbit (to rendezvous with a real vehicle). It would also be used for lunar orbit injection and ejection (to get on a desired transearth orbit).

Programs P-I through P-V are concerned with guidance steering in all phases of the mission. Programs P-VI and P-VII are midcourse navigation programs.

P-VII would be used to compute position and velocity at a desired time on the basis of the most recent orbit determination. Figure II-10 shows that the input first feeds into a routine which makes the first estimate of the Z-component of the desired position according to $Z_{Fo} = Z_1 + \dot{Z}_1 (t_f - t_1)$. This Z value is used to compute the corresponding x value from the equation $ax + bz + c = (x^2 + Z^2)^{1/2}$ of the orbit. Then the flight time is determined in SR-E and compared with that desired. If the time is in error, the Z estimate is adjusted appropriately and the process is iterated until a match is achieved. After the time is matched, the corresponding position feeds to SR-F where the velocity is calculated.

In Section IIB-2e two approaches to the midcourse trajectory determination problem were defined. One of these solved the problem in what might be called an indirect manner--smoothing the data, determining the orbit and hence the position all at one time by an iterative procedure. Adapting such a technique to the two-body solution would result in a loss of its essential advantage,

namely its explicit nature. Therefore Program P-VI is the mechanization of the second basic approach described in IIB-2e. Summarizing the description given there, we solve the observation geometry problem directly to smooth the data and determine independently two positions. This is all P-VI does. In a completely separate program--P-II to be precise--we fit the corresponding orbit to these data exactly as though we were computing a translunar midcourse steering correction.

This concludes the description of the two-body study. Its simplicity is apparent, not only in the forms of the equations shown in the sub-routines but also in the programs built out of the sub-routines. Two pairs of these programs are nearly identical in structure. If full advantage is taken of these features in the arrangement of the computer logic, a very small capacity indeed should result. Further investigation of this area is indicated.

h. Four-body studies

Arma and Autonetics, under contract agreement with The Martin Company, conducted studies of the computer requirements for mechanizing the four-body equations on board the Apollo spacecraft. The results are reported as part of their studies of the overall guidance problem in references II-1 and II-2. In this section we will simply analyze those parts of the reports which deal with the four-body mechanization.

The equations of motion of an infinitesimal vehicle subjected only to the gravitational attractions of the earth, the moon, and the unaccelerated sun are:

with respect to earth,

$$\ddot{V}x_iE = -\frac{K_E(Vx_iE)}{[d(V,E)]^3} - K_S\left\{\frac{Vx_iS}{[d(V,S)]^3} - \frac{Ex_iS}{[d(E,S)]^3}\right\} \tag{34}$$

$$- K_M\left\{\frac{Vx_iM}{[d(V,M)]^3} - \frac{Ex_iM}{[d(E,M)]^3} + P\right.$$

with respect to moon,

$$\ddot{V}x_iM = -\frac{K_M(Vx_iM)}{[d(V,M)]^3} - K_S\left\{\frac{Vx_iS}{[d(V,S)]^3} - \frac{Mx_iS}{[d(M,S)]^3}\right\}$$

$$- K_E\left\{\frac{Vx_iE}{[d(V,E)]^3} - \frac{Mx_iE}{[d(M,E)]^3} + P\right.$$

The notation is explained by particular examples:

$V_{xi}M$ is the x_i component (i = 1, 2, 3) of the vector from the vehicle (V) to the moon (M).

$d(V,M)$ is the magnitude of the vector, or simply the distance from the vehicle (V) to the moon (M).

K_E is the product of the Universal Gravitation Constant (K) and the mass of the earth (E).

P is a symbol used to denote higher order perturbation terms engendered by non-sphericity of the earth and the moon.

Equations (34) or (35) can be solved for vehicle motion if the positions of the earth, moon and sun are known. Equation (34) describes vehicular motion relative to Earth and hence treats the sun and moon influences as differences between the vehicle and Earth. Integrating this equation would yield an accurate trajectory relative to Earth, but accuracy of position relative to the moon would be degraded. Equation (35) treats the moon as dominant and considers the earth influence perturbatively. Integration of this equation would give accuracy with respect to the moon at the expense of earth relative position. Arma and Autonetics both considered mechanizations of geocentric equations. Neither company evaluated effects incurred by not switching to a selenocentric equation, such as (35), in the vicinity of the moon.

There are two possibilities for obtaining the positions of the gravitating bodies to enter into equation (34). The ephemerides of these bodies can be stored in the computer memory at appropriate time intervals, or they can be computed from the equations of motion of the bodies, subject to precisely defined initial conditions. The former approach would require interpolating to compute positions at specific times of interest. The latter would require solving the equations:

earth with respect to sun:

(36)

$$\ddot{E}x_iS = -\frac{K_S(Ex_iS)}{[d(E,S)]^3} - \frac{K_M(Ex_iM)}{[d(E,M)]^3}$$

Moon with respect to earth:

(37)

$$\ddot{M}_{xi}E = -\frac{(K_E + K_M)(M_{xi}E)}{[d(M,E)]^3}$$

$$- K_S\left\{\frac{M_{xi}S}{[d(M,S)]^3} - \frac{E_{xi}S}{[d(E,S)]^3}\right\}$$

The simultaneous solution of equations (36) and (37), as written, is complicated by the fact that said equations are coupled. An examination of the two terms on the right side of (36) reveals that the perturbative effect of the moon (the second term) is at most 0.6% of the sun's dominant influence. One might guess that this is negligible and eliminate this term, thereby decoupling the equations. Autonetics did precisely this, but did not evaluate the effect of doing so. There is no argument that the exact solution to (36) will differ very little from the unperturbed Keplerian simplification, but the sun perturbation term in equation (37) is a small difference of two large numbers--one of which is computed with a small error in the simplified version of (36). Thus a large percentage error could possibly occur in this term and, although it is a perturbative term in the motion of the moon, the neglect of this effect is incompatible with the inclusion of terms in (P) due to first and second order oblateness of the earth and of the lunar triaxial elliptic gravitational anomalies.

The Arma vehicle and ephemeris equations were simplified a great deal more, doubtlessly due in large part to the fact that they actually had programmed theirs and had done some digital machine studies. No perturbation terms (P) were included. This is not serious, but the assumptions that the sun and the earth are both fixed in inertial space, and that the moon moves around the earth in a circular orbit (in a plane containing the sun), completely neglect very important physical features. Therefore, the very small storage requirement, 86 words, and the relatively high computation speed quoted by Arma to do the trajectory integration need revision. The requirements specified by Autonetics-684 GP words and 103 DDA integrators-are predicated upon real-time integration of the equations (34) with accelerometers inputs too, (36) simplified and (37). Autonetics' technique of continuously integrating the equations of motion in real-time throughout the flight seems hardly justifiable in view of the protracted free-fall flight time.

[redacted]

Trajectory determination or updating is closely related to the equation of vehicle motion. The Autonetics report gives a brief, vague description of how they propose to update their DDA trajectory integration on the basis of observations. A "rough estimate" of the computer requirements for accomplishing this updating was given as 50 GP words and 18 DDA integrators. Arma, however, gave a clear and complete description of a good technique for least squares fitting a trajectory to observed data. Their storage estimate for their GP computer was 622 words.

Considering the large disparities in the two estimates, it is surprising how closely the final requirements agree. These estimates are both thought to be low since the separate disparities ought to be resolved in favor of the higher of the two estimates. This would seem to effectively double the requirements for mechanizing the four-body equations, taking it from the 700-word class to the 1300-word class. Even at this level careful investigation of the model's accuracy is required. It appears that, rather than integrating (36) and (37) to obtain the ephemerides of the principal bodies, it may prove more desirable to store their locations as functions of time. Further study is certainly indicated.

i. Three-body series approximation study

The feasibility of the three-body series solutions of Grobner, (see Ref. II-4) and Zukerman, (see Ref. II-5) were considered by Martin-Orlando. Since time did not permit evaluation of both series, the work of Zukerman was selected for investigation primarily because numerical results, presented in the above-cited reference, indicate that an accurate solution may be possible.

The equations of motion for the restricted three-body problem, where the earth and moon move in circular orbits, can be non-dimensionalized by introducing the characteristic quantities:

length (d) distance between the centers of earth and moon

velocity (U) the vacuum escape velocity at the surface of the earth

If this is done, the non-dimensional parameter

$$\eta = \left[\frac{K(1-\mu)}{dU}\right]^{\frac{1}{2}}$$

[redacted]

appears. K is the product of the Universal Gravitational constant and the mass of the earth-moon system, and μ is the ratio of the mass of the moon to the total mass of the system. This parameter is small ($\eta \simeq .1$) hence a power series in η is convergent. Zukerman wrote the solution to the non-dimensional equations of motion as a power series in η :

(38)

$$x_i^* = \sum_{j=0}^{\infty} \eta^i x_{ij}^* (t^*)$$

where t* is the non-dimensional time. Knowing the initial position and velocity solution of this series gives position and velocity components as a function of time. Zukerman expanded (38) to the second order and compared numerical results to those of an iterative solution. The numerical results of Ref. II-5 indicated that, to second-order the series solution by direct substitution was not sufficiently accurate; Martin-Orlando therefor expanded it to third order. The details are given in Appendix B.

To evaluate accuracy, the series through the third order terms was programmed in the IBM 7090 digital computer. To improve accuracy, provision was made for a stepwise procedure used in conjunction with the series solution. This procedure consists of evaluating the series at moderate time intervals: the values found at the end of one interval become the initial conditions for the succeeding interval. This stepwise procedure results in a solution whose accuracy is a function of the time interval used.

Direct substitution in the series solution to third order proved only slightly better than second-order direct substitution. For example, at a flight time of 48 hours (based on a 67 hour transearth trajectory), the X position components compared with the numerically integrated value as shown below:

Numerical Integration	Second Order	Third Order
92798.78	46121.04	60894.31

In comparing the stepwise procedure with the numerically integrated values, it was found that the time interval influenced the results in that a large Δt did not give accurate results and that too small a value caused excessive round-off error. The optimum interval was found to be 0.01 hours. It turned out that the third order solution was more susceptible to round-off error: thus, for significant flight times the second order stepwise made actually incurred less error.

The disappointing accuracy results, and the complexity of the equations, dictate the conclusion that this approach is not feasible.

j. Comparison and evaluation

The study of the Approximate Series Solution to the three-body equations of motion indicates that the series investigated is not sufficiently accurate, and does not effect a savings in computer capacity.

Although the studies of the two-and four-body mechanizations, show some promise, a great deal more must be done to evaluate them completely.

Preliminary investigations of the four-body mechanization indicate, though perhaps optimistically, that the problem can be mechanized onboard in a 20 to 30 pound microminiaturized digital computer. Precision ephemerides of the earth, moon, and sun probably should be stored rather than computed. Comparisons of the accuracies of geocentric and selenocentric calculations of the vehicle trajectory should be made for various phases.

The two-body study revealed that adequate accuracy is made possible by the use of a somewhat unusual biasing technique. This technique, itself, suggests further study into the applicability of barycentric rather than geocentric Kepler orbits for more accurate midcourse representations. The two-body guidance equations and programs for various phases are expressible in quite simple forms, and promise little imposition on computer capacity.

Both the two- and the four-body approaches should be examined in a complete closed-loop simulation of the entire guidance problem. This would entail "flying" a mission via digital computer simulation with appropriate navigation and steering laws controlling the vehicle trajectory. Representative instrumentation errors- - statistically distributed- - should be included. In this fashion a complete story about accuracies obtainable, and propulsion requirements, could be attained.

3. Abort

Just as abort techniques change from phase to phase, so do the abort guidance objectives.

During the early portion of the in-atmosphere ascent, the booster-vehicle combination is over the AMR not far from the launch site. In the event of an abort at this time, only the command module and the abort rocket tower are separated; the primary objective is to avoid collision with the booster. This circumstance is quite critical; hence, it is treated in much greater detail in ER12003.

After exit from the atmosphere, the abort rocket tower is jettisoned and thenceforth aborts involve the entire spacecraft, and propulsive control is effected by means of the mission engine. While the vehicle is still being boosted, an abort would be accomplished, by shutting down the booster, igniting the mission engine for use in guiding the spacecraft to the appropriate abort objective. Prior to injection initiation, abort guidance would be precisely the same as the normal ascent guidance: i.e. the vehicle would be controlled, thrust would be terminated, and the spacecraft would fall ballistically to the desired landing area. Possible landing area locations depend upon vehicle location, the present trajectory, and the propulsive capabilities. A study of these flight mechanics aspects also is reported in ER12003.

The same technique as that described above can be carried part way through injection into the cislunar orbit. At some point, however, the orbital energy becomes so high that it is necessary, for the remainder of the mission, to introduce into the guidance scheme a means of controlling atmospheric re-entry in a more explicit fashion. Accordingly, a technique akin to the earth and moon approach scheme is employed, where now the data must be processed rapidly under thrust-accelerated flight. The vehicle would be steered on the basis of present position and speed to achieve the flight path angle required to produce free-fall orbit possessing desired pericenter altitude. The time to pericenter would be monitored against the desired time. Mission-engine thrust would be terminated when a match is attained. Of course the inclination of the return orbit and the desired time to pericenter must be chosen appropriately to lie within the propulsive capability and to achieve re-entry conditions commensurate with landing at a preselected site. Guidance to the landing site during abort re-entry would be exactly the same as that for a normal re-entry.

Ascent- and midcourse- abort, as applied to the two-body mechanization study have been discussed in Section B2g of this Chapter.

4. Rendezvous

The ascent and injection guidance technique described in Section B1 was shown to have many advantages for Apollo's cislunar missions. However, there is also a requirement that the spacecraft be capable of earth orbital missions and therefore should have rendezvous capability.

Rendezvous with a vehicle in a known orbit must be accomplished in two phases. During the first phase, the supply vehicle is guided inertially to near-rendezvous with a moving image stored in the guidance computer; this image represents the best prelaunch estimate of the target-vehicle's orbital motion. With two minor exceptions, this guidance objective is precisely the same as that described in Section B1. First, the injection vernier may be omitted and, second, the moving image is hypothetical in the sense that an intentional offset from the target vehicle would be programmed. This offset accounts for statistical uncertainties in the positions and velocities of both the target and the supply vehicle. (We simply do not yet have perfect tracking capability to

determine the target orbit, nor do we have an inertial guidance system capable of placing us precisely where we want to go.) An analysis of the geometries of the volumes of uncertainty of position dictate the offset. This offset is a function also of the sensing equipment required for phase two of the rendezvous.

This second phase takes over after the supply vehicle has been "ball-parked" by the first inertially guided phase. The supply vehicle now must acquire the target with some kind of an "eye" and somehow process the intelligence seen by this eye in order to ascertain its situation relative to the target. Then, by means of reaction jets, the supply vehicle must control the situation such that a rendezvous is accomplished.

The first studies of such terminally guided rendezvous problems were concerned with completely automatic systems where the most logical choice of the "eye" was a radar and the intelligence processing was accomplished in a computer-autopilot. It became apparent in these studies that the logic used for processing the data could have a pronounced effect upon the fuel required to accomplish the rendezvous from typical initial conditions. Emphasis therefore was laid upon optimal techniques for minimizing fuel consumption.

As a result of this background, the natural tendency when considering a manned system is to seek to make a place for man in a system which conceptually is intended to be automatic. Such approaches usually end up by making the man a "zero meter reader," giving him displays calculated in the digital computer. These displays are intended to cause him to control the vehicle to accomplish an efficient rendezvous. But all the components are there to completely automate the system.

In the Martin study it was decided to investigate the kind of job a man could easily be trained to do with the least possible help. If applicable equipment were already aboard for other purposes, he could use it; additional equipment was to be minimized. As an example, the inertial platform is already onboard; thus there is little reason to ask the man to control vehicle attitude. Accordingly, the attitude was slaved automatically to a local vertical reference. To accomplish rendezvous, the pilot must now use reaction jets to control the vehicle translation along three axes.

An out-the-window analog simulation was set up to represent what the pilot would see looking out a spacecraft window, or via a TV scan of the rendezvous vehicle. Details of the simulation device, and the results obtained by subjects who "flew" it, are presented in Volume II, Chapter XII, Sections A2 and 3 of this Report. It turned out that this simple display (not something which must be calculated in a computer), augmented by radar display of the altimeter measurement of line-of-sight range, enables a high degree of proficiency of manually controlled rendezvous. The fuel required by proficient pilots is comparable to that required by optimal automatic schemes and a well-controlled docking can be achieved easily (even though the altimeter "goes blind" inside of one mile range).

The altimeter is already onboard the vehicle;the only addition required is a transponder in the unmaneuvering target vehicle. It would also be desirable to incorporate a flashing beacon light on the target similar to those employed on modern aircraft . If the initial offset direction is chosen so as to keep the line-of-sight to the target away from the sun, such a flashing beacon should easily be visible for distances up to 50 miles. In close it would be desirable to have a beacon on the supply vehicle to illuminate the target.

5. Lunar Landing

Ultimately, the Apollo spacecraft is intended to land on the moon; and, just as the propulsion tankage is sized for lunar takeoff, the guidance system design should require little or no modification to accomplish this landing. (There is no question concerning takeoff guidance: it would be precisely the same as that for earth ascent and injection.)

The onboard guidance capability described for the translunar phase could put the vehicle on a trajectory which would intercept (at a desirably steep angle) an intended landing point on the surface of the moon with fair accuracy. Two things would have to be done as the vehicle approached the lunar surface along such a trajectory:

(1) The landing stage rocket would have to be ignited at the appropriate time so that altitude and altitude rate would be nulled simultaneously.

(2) The vehicle would have to be maneuvered laterally on the basis of some kind of intelligence measuring lateral error components from the vehicle to the intended landing site.

The first job will require all the elements needed to do the job automatically and hence should be mechanized in this fashion. The objectives are very similar to the rendezvous injection guidance objectives, except that here there is a gravitational attraction between the bodies which must be accounted for in the thrust initiation prediction. This only requires that a (possibly constant) gravity term be added to the injection guidance scheme described earlier. A deliberate attempt would be made to null altitude rate at some positive altitude so that off-nominal rocket performance and/or lunar surface irregularities would not be catastrophic. A second impulse, with duplicate objectives, would be delivered after a brief free-fall following the first deceleration, except that the target altitude would now be very small. The vehicle would then free-fall these last few feet to the surface. The altitude would be chosen so that off-nominal engine performance still would provide tolerable vehicle-fall distances.

During the two deceleration thrusting periods described above, the second task of laterally maneuvering over the intended site must be accomplished. Here the man can play a very essential role because this is a piloting job not particularly easy to automate mechanically. If the pilot could look straight

down the local vertical via stabilized TV camera and were given a display showing roughly how much "on" time remained for the rocket, then he could command the vehicle tilt angle to accelerate laterally in the appropriate direction. Once a desired rate toward the target is established, the vehicle would be righted and allowed to coast. At the appropriate lead time, an opposite tilt would check the motion over the site. By monitoring the remaining "on" time, it would be possible to ensure that all rates are nulled prior to engine shutdown. In the event of a landing in darkness, a light beacon on the moon could be used.

III. RE-ENTRY GUIDANCE STUDY

A. INTRODUCTION

A safe re-entry of the Apollo vehicle into the earth's atmosphere from both the earth orbital and lunar missions must be assured. In addition, flight path control must be provided with sufficient accuracy to land at a pre-selected landing site. These two requirements reflect on every subsystem within the Apollo vehicle. For the purposes of this study, a safe re-entry infers that the crew's deceleration limitations and the heat limits of the structure must be observed during re-entry. One of many possible techniques can meet these two requirements from a flight path control as well as vehicle stability standpoint.

Re-entry from an earth orbital mission has been extensively studied by The Martin Company previously with typical lifting body configurations. Previous studies on re-entry from a lunar orbital mission indicate that range variations are highly sensitive to small changes in initial conditions and to the particular method of lift control used during re-entry. For this reason, a broad and comprehensive investigation of the re-entry control problem was initiated during the present Apollo study.

To implement this program, a number of computer simulation studies have been mechanized. Both a two-dimensional and three-dimensional simulation have been programmed in the Martin analog facility which incorporate heat rate and load factor limits along with a total heat calculation; and which are capable of being coupled with various control laws.

Re-entry guidance techniques which provide control over the re-entry landing point for both skip and non-skip type trajectories have been under study. For the purpose of this report, a skip trajectory is defined as one which exits beyond a point in the re-entry profile where dynamic pressures less than 10 psf are encountered. One of these techniques employs an explicit closed-form guidance law, similar to that proposed for translunar and transearth guidance. followed by an equilibrium glide phase of flight. Arma studies have supported Martin in the evaluation of this technique. A somewhat more complex technique has been investigated which employs the continuous prediction of the lift-drag ratio required to hit the landing site based on the solution of Chapman's Z function. A still more complex but more flexible technique has been studied which utilizes the method of steepest descent to continuously select the optimum trajectory from the standpoint of optimizing flight constraints. In the evaluation of the latter technique, Raytheon furnished The Martin Company with both trajectory studies and computer sizings. In addition to these studies on landing point control, a study has been conducted on a tangent steering law which would skip the Apollo re-entry vehicle (by use of aerodynamic forces) into an earth

orbit between 4×10^5 ft and 2×10^6 ft. A general block diagram of the re-entry control system is shown in Fig. III-1. The five techniques evaluated were:

(1) Explicit intercept steering (EXPLIS).

(2) Explicit tangent steering (EXTANS).

(3) Re-entry range prediction steering (RERPS).

(4) Explicit intercept and equilibrium glide steering (EXPLIS & REGS).

(5) Re-entry optimum trajectory steering (REOTS).

The most promising of these techniques to date is based on solving Chapman's Z function (or the equivalent equations of motion) continuously to predict range, load factor, total heat, etc. Automatic and manual control simulations of this technique have been conducted. Figure III-2 illustrates the manual display used in closed-loop simulation.

B. EXPLICIT HIT POINT STEERING

1. Introduction

This technique uses guidance steering, developed for hitting a fixed point in space, in which the rather simple Keplerian equations apply. The feasibility of such a technique for use during re-entry, in which the flight of a vehicle is primarily a function of aerodynamic forces rather than gravity, is not immediately apparent. In order to better understand its application to re-entry, consider the following example. The Apollo vehicle is re-entering the earth's atmosphere and it has been determined that the range to the target is such that a skip type re-entry must be followed. The explicit hit point steering law is continuously determining the flight path angle required at the present position and velocity to hit the target by following a Keplerian arc. As the vehicle dips into and starts back out of the atmosphere, this technique attempts to drive the actual flight path of the vehicle (γ_a) to the desired flight path (γ_d) by modulating angle of attack (α). In fact, if the atmosphere were "cut off" at some point and γ_a was at that time equal to γ_d, then the vehicle would hit the target down range. It is apparent then that if the vehicle could be held so that $\gamma_a = \gamma_d$ prior to losing effective aerodynamic control, the simple explicit technique would be feasible for control of skip type re-entries. Extending this example, it is also of interest to see just how this law might be used for the non-skip type re-entry and for the second re-entry phase of the skip type re-entry. Analytical and analog computer studies have been conducted on the application of this technique to the Apollo re-entry problem.

2. Development of Guidance Equation

We limit ourselves to the two dimensional consideration of the problem in the guidance plane. In a cartesian frame centered at the center of the earth, the vehicle position and velocity will be denoted X_H, Z_H and $\dot{X}_H$, $\dot{Z}_H$ at any time τ. The target point will be denoted X_T, Z_T and the desired hit time . The equation of a Keplerian ellipse (with focus at the origin) through the vehicle position can be written:

(1)

$$a X_H + b Z_H + c = \left(X_H^2 + Z_H^2 \right)^{1/2} = r_H$$

The derivative of this expression:

(2)

$$a \dot{X}_H + b \dot{Z}_H = \frac{1}{r_H} \left(X_H \dot{X}_H + Z_H \dot{Z}_H \right)$$

provides another relation between the constants a, b, c and this is all the kinematics can say. The third relation depends upon the dynamics and is called Kepler's Second Law:

(3)

$$c = \frac{1}{G} \left(\dot{X}_H Z_H - X_H \dot{Z}_H \right)^2$$

where G is the product of the universal gravitational constant and the mass of the earth. These three equations completely define a, b, and c and, hence the the free-fall trajectory for given X_H, Z_H, $\dot{X}_H$, $\dot{Z}_H$. Our problem, however, is to determine $\dot{X}_H$, $\dot{Z}_H$ so that the resulting path goes through X_T, Z_T at the time T. The requirement that the trajectory pass through the target point gives

[redacted]

(4)

$$a X_T + b Z_T + C = \left(X_T^2 + Z_T^2\right)^{1/2} = r_T$$

Equations (1) through (4) constitute four equations in the five unknowns a, b, c, $\dot{X}_H$, $\dot{Z}_H$. At this point, the usual procedure is to introduce the expression for the free-fall time as the fifth relation. This system cannot be solved in closed form for $\dot{X}_H$ $\dot{Z}_H$; thus an iteration technique is employed. A velocity is guessed which goes through the target point since this can be solved. Then the flight time is checked against T-t. The velocity is modified in successive steps until a match is obtained.

The objections to this procedure are as follows:

(1) The expression for time is complicated, hence iterating it is undesirable.

(2) Even after the perfect or correlated velocity is computed, the vehicle can only steer to null one component or else to establish a preferred ratio of components. Then, as the non-zero components are driven to zero by acceleration, the forcing function (lift-drag) is terminated.

An obvious alternative suggests itself at this point; i.e., redefine the correlated velocity so that we simply steer to hit the target point, regardless of the time of arriving there. In this manner, the troublesome expression for time is eliminated from the steering computation, permitting a solution in closed form. The procedure then would be to monitor the flight time resulting from this steering.

We now consider equations (1) through (4) and

(5)

$$\dot{X}_H = V \cos \gamma$$

$$\dot{Z}_H = V \sin \gamma$$

[redacted]

as six equations in the unknowns a, b, c, $\dot{x}_H$, $\dot{z}_H$ and γ. In addition to the target position x_T, z_T, r_T, the vehicle speed V is assumed known. These equations can be solved to yield a single equation in the desired flight path angle. First of all, a, b, c can be eliminated from equations (1) through (4) leaving a cubic equation in $\dot{x}_H$, $\dot{z}_H$. From physical considerations, it was guessed that this equation must be factorable, eliminating the one root which is always real. When the speed is less than minimum energy, there should be no real root; and when it is greater, there should be only two real roots. The linear factor was found (it corresponded to the degenerate case of two straight lines from the center of the earth to the points x_H, z_H and x_T, z_T) and the resulting quadratic equation was:

(6)

$$G\left(z_H z_T - r_H r_T + x_H x_T\right) + r_H\left[\left(z_H - z_T\right)\dot{x}_H + \left(x_T - x_H\right)\dot{z}_H\right]$$
$$\left(\dot{x}_H z_H - x_H \dot{z}_H\right) = 0$$

Finally, substituting (5) into (6) and dividing through by $-r_H V^2 \cos^2\gamma$ yields:

(7)

$$L \tan^2\gamma + 2M \tan\gamma + N = 0$$

where

(8)

$$L = x_H\left(x_T - x_H\right) - K$$

$$M = \frac{2 x_H z_H - z_H x_T - x_H z_T}{2}$$

$$N = z_H\left(z_T - z_H\right) - K$$

$$K = \frac{G}{r_H V^2}\left(z_H z_T - r_H r_T + x_H x_T\right)$$

The solution for tan $\bar{\gamma}$ is:

(9)

$$\tan\bar{\gamma} = \frac{1}{L}\left[-M \pm \left(M^2 - LN\right)^{1/2}\right]$$

The sign ambiguity is easily settled -- We want the smallest tan $\bar{\gamma}$.

The steering law can be written as

(10) $$\tan\bar{\gamma} - \tan\bar{\gamma}_a = \tan\bar{\gamma}_e$$ (Note:- Indicates inertial axis reference)

(11) $$C_L = K \tan\bar{\gamma}_e$$

3. Basic Guidance Law Studies

It is of interest to examine the variation in the calculated value of tan $\bar{\gamma}$ given by equation (9) during a typical constant skip type re-entry. The value of tan $\bar{\gamma}$ at exit (400,000 feet altitude) following the first dip into the atmosphere is of particular interest since it must match the actual flight path angle at exit ($\bar{\gamma}_{a_e}$) if the same range is to be obtained in the skip portion of flight. A two dimensional constant L/D skip-type trajectory was run on the IBM 709 using the L-2-C configuration aerodynamics. The target coordinates for insertion into equation (9) were chosen from the digital run at 400,000 feet altitude at the start of the second re-entry.

Figure III-3 shows the variation in actual flight angle ($\bar{\gamma}_a$) from the digital run and flight path angle desired ($\bar{\gamma}_d$) from equation (9) as functions of time. Although $\bar{\gamma}_d$ is in considerable error initially, as the vehicle nears the exit condition, $\bar{\gamma}_d$ approaches $\bar{\gamma}_a$ and at exit they are essentially the same. This indicates then that if sufficient control power is available in the latter stages of the first dip, this technique can control the skip-out in such a manner so as to skip the vehicle to the target.

Equations (9), (10) and (11) were mechanized in the Martin analog facility and used to close the guidance loop around the two dimensional equations of

motion program described in Appendix O. Check runs were made in an open loop manner using a constant $\frac{L}{D}$ in the equations of the motion. Recordings were made of γ_a, γ_d, tan γ_e and C_L, as well as the normal recordings of velocity load factor, altitude, total heat, etc. Figure III-4 is a plot of tan γ_e as a function of time for a target range of 4589 nautical miles at 400,000 ft. The initial conditions for this run were:

Velocity = 36,000 fps

Flight path angle (γ) = -7.8°

Altitude = 400,000 ft

C_L = .4185 (held constant)

C_D = .93 (held constant)

The value of tan γ_e goes to zero approximately 15 seconds prior to exit which agrees well with the previous hand calculation.

In the actual closed loop operation, using equation (10) to control the lift coefficient of the vehicle (C_L) with various target ranges, it was found that range was hypersensitive to the gain K in equation (11). For example, using the same run as shown in Fig. III-4 in closed loop fashion, it was found that K must be set at a value of 2.20 to obtain the desired range of 4589 nautical miles. Variation of this gain by 0.05 caused a variation in range of approximate 350 nautical miles. Using the same initial conditions and establishing a target at 9992 nautical miles from entry, a gain of 0.89 was required. A change of 0.01 in this gain resulted in a target miss of approximately 700 nautical miles. These runs were sufficient to indicate the extreme sensitivity of the control law ($C_L = K \tan \gamma_e$) to the gain value. Since this sensitivity is undesirable, several rather simple fixes were attempted such as using $\pm |\tan \gamma_e|^2$ and rate of change of tan γ_e (tan $\dot{\gamma}_e$) as additional terms in equation (10). Both of these approaches reduced the sensitivity, but it was concluded that still other approaches were necessary before this guidance technique could be fully evaluated.

4. Modification to Basic Guidance Law

Two basic approaches available for developing a modification to the guidance law are the empirical and the analytical. First, shaping functions may be developed, utilizing the analog computational program, to drive the error signal to command C_L to the desired value for a nominal trajectory. This approach is somewhat empirical and will be referred to as such. The second technique is analytical and involves linearizing the perturbation equations of the equations

of motion, inserting the guidance law and performing a linear stability analysis of the guidance loop at various points along the re-entry flight path. Both of these techniques have been investigated.

a. Empirical

This approach involves programming for trajectory shaping just as all ballistic missiles are guided. Basically, the procedure consists of adding a programmed, time varying term to the computed or actual guidance law. This programmed term, of course, must fade to zero before the end of the guided phase (skip out of the atmosphere in the present case) in order that the true law can guide without error.

The determination of this shaping program was as follows: A nominal constant L/D run was made from the initial conditions of

Flight Path Angle (γ) = -7.8°

Altitude = 400,000 feet

Velocity = 36,000 feet per second

and recordings of C_L nominal, tan γ_e, and dynamic pressure (q) were made. These recordings appeared as shown in Fig. III-5. Since the value of tan γ_e is driving C_L in the closed loop operation, some shaping to the guidance law is necessary because of the difference between the nominal and guidance law C_L values. The difference itself could be used except that it does not fade to zero prior to exit. We know, however, that although C_L nominal does not fade to zero, the lift (nominal) does just that because of the dynamic pressure (q) as shown in Fig. III-5. Therefore, from the time of $q_{max.}$ on ($t > t_{q_{max}}$), multiplying the ordinates of the difference curve (C_L nominal - $C_{L \tan \gamma_e}$) by the ratio q/q_{max} will develop a function $P(t)$ which has the proper shaping.

Five runs using the L-2-C configuration were made from these initial conditions and plots of the $P(t)$ shaping function for each constructed. Pertinent data on these runs are shown in the table on the next page.

Table III-1

Run No.	C_1	C_D	Range to Target 1
1	0.4185	0.93	4589 n. mi.
2	0.4733	0.93	9992
3	0.35	0.93	1973
4	0.43	0.93	5290
5	0.48	0.93	11250
6	-	-	3250

Figures III-6 through III-10 present a plot of the P(t) functions for runs one through five, respectively. It is observed that this function could be approximated by a straight horizontal line to some time $t = t_f$, followed by an exponential decay to essentially zero at a subsequent time $t = t_z$. Care was exercised in choozing t_z sufficiently far ahead of t_e (exit) so that adequate time for pure guidance is allowed. The modified guidance law is of the form:

(12)

$$C_L = P(t) + \tan \gamma_e$$

where, of course, $P \rightarrow 0$ as $t \rightarrow t_z$ and

(13)

$$P(t) = A e^{-k(t-t_f)}$$

The value of A was determined from Figs. III-6 through III-10 as a function of range and is shown in Fig. III-11. The value of k in equation (13) was developed for each of the five runs and is shown as a function of range in Fig. III-12.

Equation (13) was then mechanized in the analog facility and used to close the loop around the equations of motion. A total of sixty (60) runs was made in which the constants in the function $P(t)$, (A, k, and t_o), were varied for various target ranges. The purposes of these runs were twofold; first, to check the analytical approximation using the exponential decay, and second, to establish the sensitivity of range to the gain term A. Fig. III-11 shows that a good comparison of the analytical value of A and that determined on the analog was achieved. In establishing the sensitivity of range to A, it was first necessary to determine A near the optimum values of t_o and k for all ranges. A study of various combinations of values led to the selection of $t_o = 78$ seconds and $k = 0.24$. Finally, the values of A shown in Fig. III-11 were determined. The sensitivity of range to gain has been decreased by an order of magnitude over that shown for the same initial conditions in Section 3-B-3 of this report. Figures III-13 through III-32 present plots of C_L, velocity, and altitude for runs 2 through 6 utilizing the modified guidance law.

In conclusion, this study has shown that the $\tan\gamma$ steering law can be used to control skips. It also has shown that, using the shaping function approach, different shaping functions will be required for each initial condition. This last factor makes the use of this approach extremely cumbersome.

b. Analytical

Another approach to the modification of the basic guidance law has been pursued along different lines. This approach is based on developing the linearized perturbation equations to both the equations of motion and to the basic guidance law. The perturbation equations for the equations of motion are then Laplace transformed to facilitate a linear stability analysis of the closed loop guidance system. This development is presented in Appendix P of this report. A block diagram of this approach is shown in Fig. III-33. The stabilizing network, of course, must be determined by standard stability analysis techniques for various flight conditions expected to be encountered during re-entry. It is recommended that further work on this approach be completed prior to the final evaluation of the use of the explicit hit point steering for control of skip type re-entries.

5. Summary

This technique is rather simple, and from the development study appears to offer at least a practical skip-control means. However, the application of this technique to non-skip re-entry trajectories appears less promising. Further investigation should be undertaken, particularly since it would offer a simple means of extending the range of a non-skip control technique such as equilibrium glide. This work should be concentrated around the analytical approach discussed previously, followed by either digital or analog closed loop simulations of the modified guidance law.

C. EQUILIBRIUM GLIDE STEERING

1. Introduction

When considering explicit guidance techniques for re-entry, one of the more obvious selections is based on the concept of equilibrium glide. This technique has several features which recommend its investigation:

(1) The simple relationship between range and velocity

(2) Has been studied extensively for sub-orbital velocity re-entries.

(3) The range velocity relationship suggests that it may be applicable to super-circular velocities.

Martin has, after making an analytical investigation of this concept along with a brief analog study, requested Arma's support in this area. The initial work at Martin consisted of developing an altitude damping control technique which would effect a transition from parabolic re-entry velocity to a constant altitude sub-orbital velocity, at which time an equilibrium glide would be made to the target. Arma has greatly expanded on this initial work and has actually demonstrated this technique by closed-loop analog simulation with manual control (Ref. III-1).

The application of the basic equilibrium glide equation to super-orbital speeds has also been studied by Arma. Although it can be shown that the same equation is applicable at this speed, one must use it to steer the vehicle to a target which is associated with a velocity slightly greater than $\bar{u}=1$. Unfortunately a small perturbation away from the equilibrium glide conditions at super-circular velocity is divergent in nature rather than convergent, as in the sub-orbital case. Stability augmentation techniques must be added to prevent this divergence. Some method of transition, such as constant altitude, from super-circular to sub-orbital equilibrium glide must also be provided.

The use of the equilibrium glide technique for the Apollo mission appears feasible, but longitudinal range reduction (in comparison with those techniques which provide a skip capability) and increased total convective heat are characteristics of this approach. For these reasons, it is felt that a combination explicit hit point and equilibrium glide system shows considerable promise as an explicit parabolic re-entry method.

2. Analysis

When considering the application of the equilibrium glide principal to the re-entry guidance of the Apollo vehicle, one must recognize at the on-set that several guidance laws are required, each one being applicable to a segment of the trajectory. That portion of the trajectory to which the most highly developed

guidance technique applies is that portion when the vehicle decelerates from approximately 99.5% of circular orbital velocity to approximately Mach 5. The guidance law for this segment of the trajectory is based upon the concept of the equilibrium glide, which will be summarized in the next paragraph.

a. Sub-orbital equilibrium glide

A quantitative understanding of the equilibrium glide may be gained by considering a vehicle flying in such a way that the lift and centripetal force just balance the gravitational force. This keeps it from falling. Drag is constantly reducing velocity and since both lift and centripetal acceleration are proportional to velocity squared, they tend to decrease. Lift is also proportional to density, so that the balance can still be maintained with constant L/D if the vehicle descends into denser air as it slows down. This type of flight will be called an equilibrium glide. An equilibrium glide trajectory has the following general characteristics:

---- Altitude is always decreasing.

---- Path angle is small.

---- The rate of descent is always increasing at a rate which is small compared to lift/mass.

---- Lift and drag coefficients are constant.

---- Velocity is always decreasing.

The equilibrium glide has a number of properties which make it especially attractive as a tool in re-entry guidance.

---- Altitude is a function only of velocity and lift coefficient.

---- Since heating rate is assumed to depend only upon velocity and density, it too is a function only of velocity and lift coefficient.

---- the distance traveled between any two velocity states depends only upon the velocities and the lift/drag ratio.

---- explicit and simple expressions for the above relationships can be derived.

---- All constant L/D trajectories (sub-orbital velocity) approach equilibrium glide as time progresses because of natural damping of vertical oscillations. This permits the application of the equilibrium glide expression to the latter portion of any constant L/D trajectory.

If equilibrium glide conditions exist, i.e., the lift plus centripetal force balances the gravitational force, density will be a function only of velocity for any given lift coefficient. Knowing the relationship between density and altitude, we can plot a family of altitude versus normalized velocity ($\bar{u}$) curves for various lift coefficients. A family of such curves is presented in Fig. III-34.

Suppose that, at a given velocity and lift coefficient, the vehicle is above the altitude shown in Fig. III-34, then, its lift will be less than if it were on the equilibrium curve because the density will be lower. However, the vehicle cannot remain at this altitude because gravity will now cause it to fall. Moreover, drag will be lower at the higher altitude so that velocity will drop more slowly. Hence, the slope of the altitude versus velocity curve will change in such a way as to bring the vehicle toward the equilibrium curve. This effect may be viewed as a feedback action tending to keep the vehicle on an equilibrium glide. This reasoning leads to the hypothesis that the equilibrium glide is a physically realistic as well as mathematically convenient type of trajectory.

Assuming that the vehicle is on an equilibrium glide, the distance as the normalized velocity drops from $\bar{u}$ to the approach velocity ($\bar{u}_T$) is given by:

(1)

$$\theta_s = \frac{1}{2} \frac{L}{D} \ln \frac{(1-\bar{u}_T^2)}{(1-\bar{u}^2)}$$

The derivation of this formula together with computer runs demonstrating its applicability to sub-orbital guidance appear in Arma document S-10,157.

b. Super-orbital equilibrium glide

The equilibrium glide concept has developed from studying re-entry vehicle behavior at velocities less than circular orbit velocity. The possibility of extending this concept into the super-orbital region now suggests itself. In this region centripetal force exceeds the gravitational force and negative lift is needed to balance the forces. Negative lift can be obtained either by flying upside down or trimming at negative angles of attack.

As the vehicle decelerates from escape velocity to orbital velocity on such an equilibrium glide, the centripetal acceleration drops from 2g to 1g while lift acceleration changes from minus 1g to zero. Thus, to maintain the balance of forces, lift will always be numerically less than centripetal force. Because of this, and because both lift and centripetal acceleration are proportional to velocity squared, altitude must increase as the vehicle decelerates. In this respect, the super-orbital equilibrium glide differs from the sub-orbital

case. As a consequence of this difference, maximum heating rate occurs at maximum velocity in the super-orbital glide. Figure III-35 is a plot generated by Arma which gives altitude as a function of velocity for various lift coefficients for the super-orbital equilibrium glide.

One of the most desirable properties of the sub-orbital equilibrium glide (the tendency of any constant $\frac{L}{D}$ trajectory to approach equilibrium conditions) is absent in the super-orbital region. In fact the tendency is just the opposite. This behavior is illustrated by supposing that, at a given velocity and lift coefficient, the vehicle is above the altitude shown in Fig. III-35. Then its lift will be numerically less than it would be if it were on the equilibrium curve because density will be lower. The lift, which is negative, is then insufficient to balance the centripetal acceleration and the vehicle rises even farther from the equilibrium curve. Thus, although the forces are in equilibrium when the vehicle is on the curve, any disturbance in the equilibrium causes the vehicle to rise or fall at an ever increasing rate. In this sense, flight at constant negative lift coefficient is inherently unstable in altitude. Morth and Spever in Ref. III-2 have developed an approximate formulation for the rate of divergence away from the equilibrium glide path (which is dependent only on velocity, scale height, local value of gravity and velocity) measured as time to double amplitude. The rate of divergence varies from 20 seconds at 35,000 fps to 70 seconds at 26,500 fps. The significance of these rates are twofold: first, the rate of divergence is rather slow; and, second, control system response must be faster than these rates if damping of the divergence is to be obtained. In other words, the guidance system must incorporate stability augmentation at super-orbital velocities.

An analytical approach to determining just what this stability augmentation must consist of can be obtained by developing the perturbation equations to the equations of motion for equilibrium conditions similar to that shown in Section B of this Chapter. By performing a Laplace transformation of the perturbation equations and studying the characteristic equation of the system from a stability standpoint, evaluation of the coefficients can be made at various points along a typical parabolic re-entry and the control terms needed to stabilize the system can be developed.

Assuming that the vehicle is constrained to fly a super-orbital equilibrium glide, equation (1) is applicable, provided that $\bar{u}_T$ is greater than unity. In the super-orbital region the guidance system functions in such a way as to bring the vehicle over a specified point on earth at a specified $\bar{u}_T$ (which would be approximately 1.0005). The guidance systems calculates the $\frac{L}{D}$ command needed to do this. The $\frac{L}{D}$ command, together with actual rate of climb and actual lift and drag accelerations, is incorporated into an error function which changes angle of attack in such a way as to bring the vehicle onto an equilibrium glide at the command L/D. This guidance technique overcomes the unstable altitude characteristic of the super-orbital equilibrium glide.

The equilibrium glide concept is not applicable at orbital speed. Between $\bar{u} = 1.05$ and $\bar{u} = 0.995$ a different type of trajectory, possibly constant altitude, is desirable.

3. Skip Range Control

The range covered after re-entry can be substantially increased by skipping out of the atmosphere and re-entering a second time. The behavior of the vehicle outside the atmosphere can be described by the relatively simple equations of a Keplerian arc. Thus, if the desired point of re-entry is specified, the desired path angle at exit can be calculated from the vehicle's velocity and position at exit. The atmosphere does not end abruptly, so the exact instant of exit is undefined. This difficulty is overcome by continuously maintaining the flight path angle at a value such that, if the atmosphere should disappear at that instant, the vehicle would follow the Keplerian arc to the re-entry point. The required path angle changes with time, and aerodynamic forces are required to bring about the change. As the vehicle gains altitude, the available aerodynamic force diminishes. This type of control and the guidance law which commands the vehicle are discussed in Section B of this Chapter. It should be clear that the accuracy of such a system need only be within the maneuvering capability of the vehicle from the initial conditions of the second re-entry. This is so since it is proposed that equilibrium glide control be used to control range during the second entry.

In the actual use of such a system, the range to the target, based on expected re-entry conditions, would be used to select the skip mode or super-orbital equilibrium glide mode of control prior to re-entry. If the skip mode is selected, a subsequent switch to equilibrium glide must be made prior to the second re-entry.

4. Analog Simulation

An analog simulation of the Apollo re-entry has been constructed in the Arma Computational Laboratory. (See Fig. III-36.) A man can be placed in the control loop, and he can vary angle of attack by moving a control stick. Both positive and negative angle of attacks are possible. The aerodynamic characteristics of Fig. III-37 have been inserted into the computer. A control system based on damping the super-orbital re-entry to achieve constant altitude flight was used for these simulated flights.

Figure III-38 is a sample of a controlled trajectory. Angle of attack and altitude are recorded as functions of down range distance. The vehicle enters at escape velocity and -7.4 degrees path angle (lower end of design corridor). The pilot holds maximum positive angle of attack until the rate of descent ceases. This procedure minimizes the depth to which the vehicle descends into the atmosphere, and thereby minimizes the heating rate at the first altitude minimum.

When the vehicle starts its first climb, the pilot attempts to level the vehicle at 265,000 feet. He is aided in this procedure by an error function calculated by the computer and displayed on a meter. The error function is the difference between a "desired" rate of climb and the actual rate of climb. The pilot moves the stick to bring the error function to a null. "Desired" rate of climb is proportional to the difference between 265,000 feet and the actual altitude.

This control method takes no account of distance from the target in the damping phase. However, it does prevent the violent skipping which would occur with an open loop flight. Altitude control is applied in the trajectory of Fig. III-38 until the velocity falls below orbital velocity. From then on, the pilot controls angle of attack in such a way as to bring the vehicle to the preselected target on an equilibrium glide. He is aided in this process by the chart in Fig. III-39. The chart is a plot of $(1-\bar{u}^2)$ versus distance from the target for four equilibrium glides at various angles of attack.

A pen traces the actual $(1-\bar{u}^2)$ versus distance from the target on the chart. The pilot observes the angle of attack corresponding to the pen position. This is the command angle of attack. He then moves the stick until the actual angle of attack agrees with command angle of attack. The trajectory ends at $(1-\bar{u}^2)$ of 0.96 (approximately Mach 5). At this velocity, as Fig. III-39 shows, the distance to go is practically zero. Thus the vehicle has flown through the specified approach point at the specified velocity.

Figure III-40 illustrates the performance of the above control system in the presence of off-nominal re-entry conditions. Two trajectories are shown, both of which have re-entry at the same velocity and path angle, but at different distances from the target. Figure III-41 is the equilibrium glide chart with recordings of the same two flights superimposed. Both flights reach $(1-\bar{u}^2)$ of 0.96 with practically zero distance to go. The longer flight follows the lower angle of attack curve, which corresponds to the higher $\frac{L}{D}$.

5. Summary

The application of equilibrium glide concepts to the Apollo re-entry problem has been demonstrated employing man to perform the transition from supercircular speeds to the sub-orbital region of flight. Using this technique, total range capability is limited to below that required in the present Martin operational concept of 10,000 nautical miles. The application of super-orbital equilibrium glide control shows promise as a means of controlling range while at super-orbital velocities which will undoubtedly provide better range control. This technique should be pursued further to establish its exact limitations and capabilities, however, it still appears impractical to expect 10,000 nautical mile range utilizing this technique in conjunction with the comparatively low L/D vehicles considered for the Apollo mission. Range extension can be

obtained by using this technique in conjunction with a skip-control guidance law, such as Explicit Hit Point Steering as described in Section B. This combination could prove to be an extremely simple and sufficient re-entry guidance system for the Apollo vehicle.

D. RE-ENTRY RANGE PREDICTION STEERING (RERPS)

1. Introduction

A variety of systems and combination of systems have been studied for directing a maneuverable vehicle through the earth's atmosphere to a predetermined let-down point without exceeding defined temperature and deceleration limits. Studies of systems, for example, which employ fixed trajectories about which perturbations are made, have indicated that a favorable termination of let-down from circular velocity can be accomplished if the deviations of the actual initial conditions of entry are close enough to the values stored in a computer memory, and if a sufficient number of perturbation variables are employed in the computation. This approach is inherently limited, however, to the variety of initial conditions and degree of trajectory diversification capable of being stored in the computer memory.

Inasmuch as the re-entry guidance system will be required to handle wide variations in abort and entry conditions and also considerable deviation from established atmospheric standards, interest has been stimulated in the search for a system which embodies a more universal application and does not depend on computer stored information, but which continuously calculates and predicts the remainder of the flight trajectory based upon present in-flight conditions. In addition to increased flexibility, a continuous prediction system affords an advantage in its direct application to a display of predicted flight range conditions and hazardous situations to the pilot in a manner in which maximum control is afforded.

The main problem with any continuous-prediction technique is the complexity of the equations employed to mechanize the prediction. To maintain accuracy and speed in spite of limited input information and restrictive amounts of computing equipment, a satisfactory compromise must be realized. It will be the purpose of this section under re-entry to elaborate on the studies that have been made to determine the overall form of the prediction system in light of Apollo requirements.

2. Technique

The re-entry range prediction steering technique involves, essentially, a fast solution of the collapsed equations of motion of the vehicle as it traverses the flight trajectory. By inserting a desired lift-drag ratio and solving the equations for range, a comparison may be made between the predicted range

and the actual range as determined in the guidance computer and appropriate changes made in vehicle angle of attack in order to bring the predicted range in line with that desired. If this operation can be accomplished with sufficient speed, genuine closed-loop range control is possible. Studies conducted thus far indicate that such a system is indeed feasible.

The complete equations of motion for a vehicle entering the earth's atmosphere are by nature complex and difficult to solve even with large high-speed digital computers. The feasibility of in-flight solution of these complete equations for the purpose of controlling range, deceleration and heat absorption becomes questionable because of the restrictions placed upon the size and complexity of airborne type computers. It is, therefore, both mandatory and desirable to reduce the mathematical and computational complexity of the reentry guidance and control scheme to a minimum.

Among the different approaches investigated, the method developed by Chapman (Ref. III-3) to approximate the solutions obtained with the complete equations of motion offers a substantial saving in computational complexity. In essence, he has reduced the motion equations to a single, ordinary, nonlinear differential equation of second order by rejecting terms which contribute only negligibly to the solution and by the introduction of a particular mathematical transformation.

Assumptions. The physical and mathematical assumptions made in the development of the "Chapman" equation restrict its application to a particular range of altitudes and initial conditions which are, however, within the range of extremes predicted for the Apollo mission. The basic assumptions used in the development of the collapsed equation are:

(1) Atmosphere and planet are spherically symmetric.

(2) Variations in atmospheric temperature and molecular weight with altitude are negligible compared to any variation in density.

(3) Peripheral velocity of the earth is negligible compared to the velocity of the Apollo vehicle.

(4) The small change in distance from the planet center is negligible compared to the fractional change in velocity in a given increment of time.

(5) The flight path angle γ is sufficiently small that the component of drag is large compared to the component of lift in the horizontal direction.

Equations of motion. The two component equations of motion which Chapman has collapsed are the classical:

$$(1) \quad -\frac{d^2h}{dt^2} = -\frac{dv}{dt} = g - \frac{u^2}{r} - \frac{L}{M}\cos\gamma + \frac{D}{M}\sin\gamma$$

and

$$(2) \quad \frac{du}{dt} + \frac{uv}{r} = -\frac{D}{M}\left(\cos\gamma + \frac{L}{D}\sin\gamma\right)$$

where:

h = altitude

v = vertical velocity component (along direction of radius vector)

u = circumferential velocity component normal to radius vector

r = distance from earth center

L = lift force

D = drag force

m = mass of vehicle

γ = flight path angle relative to local horizontal

Initially, the term $\frac{uv}{r}$ in equation (2) is dropped. This is equivalent to the restriction of assumption (4). Next, an independent variable $\bar{u}$ (ratio of horizontal to circular satellite velocity u/u_c) is introduced and employed as the independent variable along with a new dimensionless dependent variable Z formed through a transformation of the two original motion equations. Z is defined as:

$$(3) \quad Z = \frac{\rho \bar{u}}{\left(\frac{M}{C_D A}\right)}\sqrt{\frac{r}{\beta}}$$

where:

ρ = density of the atmosphere

C_D = drag coefficient

β = atmospheric density decay parameter

Through the process of mathematical manipulation, Chapman's final Z function results:

$$(4)\quad \bar{u}z - \left(z' - \frac{z}{\bar{u}}\right) = \frac{1-\bar{u}^2}{\bar{u}z}\cos^4\gamma - \sqrt{\beta r}\,\frac{L}{D}\cos^3\gamma$$

The physical meaning of each of the terms is perhaps helpful:

$\bar{u}z''$ = vertical acceleration

$-\left(z' - \frac{z}{\bar{u}}\right)$ = vertical component of drag force

$\frac{1-\bar{u}^2}{\bar{u}z}\cos^4\gamma$ = gravity-centrifugal force

$-\sqrt{\beta r}\,\frac{L}{D}\cos^3\gamma$ = lift force

A brief investigation of the analytic strength of the Z function and its ability to predict almost all of the important trajectory parameters associated with an Apollo-type entry, has led to a detailed study of the possibility of using it as the primary entry range control law for the Apollo mission. With this one differential equation it is possible to closely predict, for example, the following important motion parameters if the initial flight path angle (γ), flight path circumferential velocity ($\bar{u}$), and lift-drag ratio (L/D are known:

Circumferential distance (longitudinal range)

$$(5)\quad \frac{\Delta S}{r} = \frac{1}{\sqrt{\beta r}}\int_{\bar{u}_2}^{\bar{u}_1}\frac{\cos\gamma\, d\bar{u}}{z}$$

Corresponding elapsed time

$$(6) \qquad t = \frac{1}{\sqrt{\beta g}} \int_{\bar{u}_2}^{\bar{u}_1} \frac{\cos\gamma \, d\bar{u}}{\bar{u} z}$$

A dimensionless function proportional to total heat absorbed

$$(7) \qquad \bar{Q} = \int_{\bar{u}_2}^{\bar{u}_1} \frac{\bar{u}^{3/2} d\bar{u}}{z^{1/2} \cos^2\gamma}$$

Horizontal component of deceleration

$$(8) \qquad a_h = g \frac{\sqrt{\beta r}\, \bar{u} z}{\cos\gamma}$$

Flight path angle γ as a function of velocity

$$(9) \qquad \sin\gamma = z' - \frac{z}{\sqrt{\beta r}\, \bar{u}}$$

A dimensionless function proportional to heating rate

$$(10) \qquad \bar{q} = \bar{u}^{5/2} \sqrt{z}$$

Approach. Inasmuch as the Z function affords an approximation of the solution of the complete equations of motion, the philosophy has been to check in detail the Z function solutions with results obtained on the IBM 7090 digital program in which the complete equations are included. Comparison has shown excellent correspondence even for relatively long (> 15,000 nautical miles) ranges and multiple skips where ballistic ranges must be computed as a function of predicted exit conditions.

Equation mechanization. The Z function has been mechanized in the analog facility so that γ, Z, and range ($\frac{\Delta S}{r}$) are readily available as functions of velocity ($\bar{u}$) for any combination of initial conditions. X - Y plotters are employed to produce graphs of these variables versus $\bar{u}$, which are extremely useful in the preparation of ground traces or "footprints" showing longitudinal and lateral range as functions of L/D ratio and γ_i.

Inasmuch as the Z function's prediction ability has been shown to be invalid in small neighborhoods of Z=0, it has been necessary to begin prediction only after the value of Z approaches the numerical value of 0.01. This restriction, which incidentally evolves from assumption four, requires that ballistic equations be used for altitudes above 260,000 feet. This means that insofar as the Z function predictions are concerned, atmospheric entry and exit begins at 260,000 feet. The limitation of a Z minimum of 0.01 results primarily from a scaling restriction in the analog simulation. The magnitude of the variation of Z, especially when negative $\frac{L}{D}$ ratios are studied, limits Z to a value consistent with analog accuracy. Any flight computer hardware would be designed so that the minimum Z value would be 0.001. This change in $Z_{minimum}$ would move the exit and entrance prediction boundaries to approximately 300,000 feet. This limit reduces any velocity error at exit (due to that portion of the atmosphere above 300,000 feet) to a few fps.

The basic analog mechanization employed to study the range prediction system is shown in Fig. III-42. When this system is operated in closed-loop fashion, the aerodynamics and the inertial dynamics are closed through a complete three-dimensional analog program that contains the 1959 ARDC model atmosphere. By means of this combination, a continuous input of velocity, range to go, deceleration and flight path angle allows a fast solution of the Chapman Z equation and the associated parameter predictions.

Specifically, the re-entry range prediction system operates in the following manner:

(1) Prior to entry, the mid-course guidance system computes the expected entry conditions and supplies the range computer with the following inputs (see Fig. III-43):

(a) Z_i = (initially defined as 0.001)

(b) Z'_i = $d\bar{z}/d\bar{u}$

(c) $\bar{u}_i$ = $V \cos \gamma / V$ circular

(d) γ_i = flight path angle

(e) R_{tg} = range to go

(f) I_i = initial flight path inclination

(2) The range prediction computer solves the motion equation for a series of L/D ratios and selects a ratio corresponding to the range to go.

(3) At physical entry into the earth's atmosphere (300,000-ft altitude) the vehicle begins to decelerate. This deceleration is measured by the inertial platform and is a direct function of velocity, altitude and vehicle configuration. The deceleration input, in conjunction with the change in velocity and flight path angle, is sufficient information to up-date the initial conditions so that a new range prediction, based upon flying the same constant L/D ratio, may be made.

(4) The newly predicted range is compared with the desired range to go and an additional range prediction made, based upon whether or not the difference between the predicted range and the desired range is high or low.

(5) The span of the two predicted ranges should include the desired range and a simple empirical relationship is solved for the L/D ratio and corresponding angle of attack needed to hit the target. This angle of attack is flown until the output of the next examination is completed. This whole process of examination and testing can be completed by the prediction computer on the order of once every second early in flight when the total trajectory is comparatively long, and two or three times per second as the terminal portion of flight is approached.

3. Performance Boundary Investigations

The range prediction technique has been extremely helpful in defining the performance boundaries for the re-entry vehicle as a function of initial conditions. Inasmuch as atmospheric entry has been assumed to take place at 260,000-ft altitude (Z=0.01) for the purpose of this study, Figs. III-44 and III-45 present the change in the initial flight path angle limits for a 30-mile guidance corridor as a function of altitude. Reference to any value of γ at 260,000 feet may therefore be referred to the corresponding γ at 400,000 feet.

Figures III-46 through III-49 are ground range traces for initial γ^s from -3° to -6°. These diagrams were prepared by solving for lateral range as a function of constant roll angle in conjunction with longitudinal range versus L/D ratio solutions as illustrated in Fig. III-50. The lateral range (R_y) equation used in this study consists of the following:

(11) $$Ry = Y_1 + Y_2$$

where:

(12)
$$Y_1 = L/D\ (3438)\ \ln \bar{a}\ \sin \phi_B \sin \phi_C$$
$$Y_2 = 620\ (L/D)^{1.78} \sin 2\phi_B$$

and where:

(13) ϕ_B = Vehicle bank angle about velocity vector

ϕ_C = Earth central angle which is equivalent to $\frac{\Delta s}{r}$ in radians

The derivation of the lateral range equation is based upon curve matching techniques as employed by Frank and Perrine. Actual range calculations employing this expression have shown good correspondence with results obtained with the IBM 7090 complete three-dimensional equations of motion. Inspection of the ground traces or "footprints" indicates the maximum lateral and longitudinal range attainable with any L/D ratio between 0.8 and 0 and any roll angle between 0 and 90°. Actually, the performance boundary includes negative L/D ratios to the value of -0.8 and roll angles up to and including 180°. Because both of these extremes result in a very fast build-up in deceleration and, conversely, short ranges, the resulting boundaries are, in general, off of these footprints. The points of constant bank angle are denoted by dashed lines which intersect the lateral range lines for constant L/D ratios at 10 degree intervals.

The longitudinal range limit is denoted by the ballistic skip apogee line at the center of the diagram. This line represents exit conditions which put the apogee during ballistic flight above 400 nautical miles and into the Van Allen Radiation Belt. This limit is controlled in the range prediction system by actually computing the apogee each time a ballistic exit is made. The apogee radius (r_a) prediction equation to be mechanized in the computer is:

(14)

$$r_a = r \left[\frac{\bar{u}_e^2}{1 - \left[1 - \bar{u}_e^2 \left(2 \frac{\bar{u}_e^2}{\cos^2 \gamma_e} \right) \right]^{1/2}} \right]$$

The apogee limit may be set at any desired altitude in order to account for possible computational inaccuracies or an alternate method used to determine the skip peak. A method used on the analog computer to avoid the complexity in equation (14) involved explicitly solving the flight path angle (γ_e) velocity ($\bar{u}_e$) relationship for a 400 nautical mile apogee on the IBM 7090 and constructing a graph of the allowable and unallowable exit conditions (see Figs. III-51 and III-52). This $\bar{u}_e$ versus γ_e relationship can be programmed on a function generator and the predicted exit conditions examined to see if the apogee restriction is met. When the examination is made, if an unallowable exit relationship is predicted, the computer does not continue to compute the remainder of the trajectory but immediately recycles and picks an L/D ratio somewhat lower than the previous value for trial prediction. The decreasing incremental change in L/D for such a computation has been initially set at 0.05 L/D for simplicity, however, this value could easily be made some empirical function of the apogee prediction. It should be noted that any computation and recycle time involving the trajectory up to initial exit would be only a fraction of the total solution time so that a number of predictions like this could be made in less time than would be normally required to solve the total trajectory.

4. Closed-Loop Range Control Operation

Because no closed-form solution for range is presently available for low L/D vehicles entering the atmosphere at shallow angles, a fast iteration of the equations of motion is necessary to give a closed-loop type of control. Furthermore, to make fast computation as simple as possible, it is important that the number of variables required for each range prediction be held to an absolute minimum. The Chapman Z function, being of second-order, requires two initial conditions (Z_i and Z') for solution each time a prediction is to be made. Compared to standard trajectory computations, which require either altitude or pressure inputs in addition to information on the aerodynamic parameter $M/C_D A$, the prediction equation requires only the effect of these variables in the form of horizontal deceleration (Au). Since this parameter is already available from the inertial platform, no additional instrumentation is required for the re-entry guidance system. It should be emphasized that the relation between density and geometric altitude will be essentially unknown during entry since variations in atmospheric density may fluctuate as much as 20% from a so-called standard day, especially at high altitudes.

The fact that predictions made during the flight in the atmosphere assume an exponential density decay ($\sqrt{\beta r}$ = constant) results in a major portion of any range prediction error for any single computation. However, any system which does not actually sense pressure (a formidable task considering the environmental extremes present during re-entry) will be confronted with this problem. The prediction technique's basic attribute, its ability to work in closed-loop fashion and always strive to null any error in the system, well equips it to handle this problem.

Analog simulation. The motion equation programmed in the analog simulation is:

$$(15)\quad \frac{\bar{u}\, d^2 z}{d\bar{u}^2} - \frac{dz}{d\bar{u}} + \frac{z}{\bar{u}} - \frac{1-\bar{u}^2}{\bar{u}\, z} + \sqrt{\beta r}\left(\frac{L}{D}\right) = 0$$

The deletion of the cosine γ terms does not appreciably affect the prediction accuracy as long as γ is small.

Two initial conditions are required for solution of equation (15) in addition to the independent variable $\bar{u}$; they are Z_i and Z_i'. Z_i is computed continuously in the complete equations of motion section of the computer, being a function of deceleration (Au) and velocity ($\bar{u}$), the equation for Z_i is:

$$(16)\quad Z_i = \frac{K\, Au}{\sqrt{\beta r}\, \bar{u}}$$

where:

K = A correction factor used to adjust the deceleration input for a trial prediction using a drag coefficient other than that used originally. It will be a function of the slope of the C_D curve.

The value of Z' is also determined each time in the computer equations of motion and consists of:

$$(17)\quad Z_i' = \left(\frac{dz}{d\bar{u}}\right)_i = \sqrt{\beta r}\, \sin\gamma + \frac{z_i}{\bar{u}_i}$$

Both Z and Z′ are fed into the prediction portion of the computer and are available as initial conditions whenever a range prediction for a new L/D ratio or a change in velocity are made.

During closed-loop operation, whenever the predicted range using a particular L/D ratio fell below or above the desired target range, an additional prediction was made using a higher or lower L/D ratio in addition to an interpolation which was used to solve for the new L/D ratio required to hit the target. The incremental change in L/D for the trial prediction is actually important only to the extent that it should be large or small enough, depending upon whether or not the initial prediction overshot or undershot the target, to bracket the desired range when combined with the original prediction in one single iteration. The closer the trial L/D ratio is to that ratio which will just hit the target, the closer the actual interpolation will be when the nonlinear aspects of the L/D versus longitudinal range relationship are considered. Fig. III-50 illustrates this highly nonlinear trend especially in the vicinity where the initial flight path angles approach the overshoot boundary. The choice of the trial L/D ratio was, therefore, determined using the following relationship:

$$(18) \qquad (L/D)_T = \frac{R_P (L/D)_P}{R_D}$$

where: $(L/D)_T$ = The trial L/D value

R_P = Predicted range with $(L/D)_P$

R_D = Range desired

$(L/D)_P$ = The L/D ratio used in the initial range prediction.

This solution for $(L/D)_T$ is carried out within the range prediction computer and inserted in the Z function for solution along with the corrected initial conditions of Z and Z′ . The correction of the initial condition for the trial prediction is accomplished through knowledge of the C_{D_P} (prediction drag coefficient) value used in the initial range prediction and its relation to the position of C_{D_T} (trial drag coefficient) on the drag polar. For example, if we examine the 410 drag curve in Figs. III-51 and III-52, we can see that if we

desired to pick our $(L/D)_T$ value at 0.58 with initial condition data from $(L/D)_P$ = 0.66, we would have to multiply Z_i for the $(L/D)_T$ prediction by the ratio of $(C_D)_T/(C_D)_P$ or 0.288/0.31. This would give a K factor for equation (16) of 0.929.

The solution for the actual L/D ratio to be commanded of the vehicle L/D_C is accomplished by the following interpolation:

$$(19) \qquad (L/D)_C = (L/D)_P \pm (\Delta L/D)_C$$

where:

$$(\Delta L/D)_C = \frac{R_P - R_D (\Delta L/D)_A}{\Delta R}$$

$$(\Delta L/D)_A = (L/D)_P - (L/D)\ T$$

$$\Delta R = R_p - R_t$$

R_T = Range predicted using $(L/D)_T$

The interpolated value of $(L/D)_C$ is commanded as an angle of attack and is actually flown in the equations of motion for a short period of time before a new prediction is again made, using the value of $(L/D)_C$ as the value of $(L/D)_P$ in the next interpolation.

The actual time between successive solutions in the analog simulation was varied from an upper limit of 10 to a lower limit of one second. As expected, the time between solutions was found to be proportional to the exit condition errors and consequently to the range discrepancies at second entry for comparatively long runs. Short range targets, especially those which did not require a ballistic skip, did not demonstrate as critical a dependency on this variable. In any case, to maintain reasonable prediction accuracy, solution times of less than five seconds are found to be necessary.

Deceleration limiting. An examination of Fig. III-53 shows the maximum load factor that would be experienced during initial entry for various entrance angles and for various L/D ratios. It is obvious from this figure as well as from Figs. III-44 and III-45 that lift-modulation is required for entrance angles close to five degrees (260,000 feet) and larger. In order to provide a means whereby the range prediction system can restrict the maximum deceleration (A_M) to six g's, a simultaneous prediction of G_{MAX} as a function of velocity ($\bar{u}$) is predicted along the flight path with the following calculation:

$$(20)\quad A_M = \sqrt{\beta r}\ \left(\bar{u}^2\right)_{MAX}\ \sqrt{1+(L/D)^2}$$

A constant value of 26.5 is used for $\sqrt{\beta r}$ in this expression inasmuch as this value is most representative of the actual atmospheric decay constant extent in the vicinity of the initial critical dip into the atmosphere.

The modulation process consists of solving for the time at which six g's or any other deceleration limit will occur with the use of the following integration (equation (6)):

$$\text{Time (t)} = 27 \int_{\bar{u}_t}^{\bar{u}_i} \frac{d\bar{u}}{\bar{u}^2}$$

A limit switch in the prediction computer throws the time integrator into hold when the predicted value of A_M reaches the designated limit. In this manner, a lead time is provided which allows for modulation before the deceleration limit is actually exceeded. The required increase in $(L/D)_p$ to limit deceleration $(\Delta L/D)_L$ is computed with the following relationship:

$$(21) \qquad \left(\Delta\ L/D\right)_L = K\left(\frac{\Delta G}{\Delta t}\right)$$

where: ΔG = the predicted change in G from now until it reaches some specified value

Δt = the predicted change in time from now until G reaches some specified value

K = a gain factor

It can be seen that the $\left(\frac{\Delta G}{\Delta t}\right)$ term is actually the rate of change of acceleration and as such is well suited for deceleration limit adaptation.

Heating considerations. In order to avoid disastrous heating conditions during re-entry, some method of controlling both the total heat absorbed by the vehicle during flight and the ablator loss rate of the ablative shield at any time must be devised. The RERPS system does not only predict these important heating parameters as a function of known present flight conditions but also controls them by proper flight trajectory modification.

The rate of ablation from the protective nose-cone is both a function of the vehicle configuration and the particular flight trajectory. The prediction computer solves the following relationship for the ablation rate ($\dot{m}$):

$$(22) \qquad \dot{m} = a + b\,\bar{u}^2\,\dot{q}_c$$

where:

$a+b$ = constants which depend upon ablator material

$$(23) \qquad \dot{q}_c = \left(K V^3 \rho^{1/2}\right) = \text{constant } (\bar{q})$$

$$\bar{q} = \bar{u}^{5/2} z^{1/2}$$

Whenever the predicted rate of ablator loss exceeds a predetermined value (depending upon the amount already lost compared to the amount left) corrective flight path action is demanded by either the pilot or the prediction computer. In a critical ablator loss rate prediction, the computer will immediately call for an increase in C_L by means of an angle of attack command rather than a demand for a higher L/D ratio. This is necessary because of the shape of the drag curve (Fig. III-52) and the possibility of actually decreasing C_L by a demand for an increased L/D ratio on the right-hand side of the curve.

The total convective heat absorbed prediction (Q_s) is determined with the following calculation in the prediction computer:

(24)

$$Q_S = \text{CONSTANT} \sqrt{\frac{m}{C_D A R}} \; \bar{Q}$$

where:

$$\bar{Q} = \int_{\bar{u}_f}^{\bar{u}_i} \frac{\bar{u}^{3/2} \, d\bar{u}}{Z^{1/2} \cos^2 \gamma}$$

The most obvious correction for a critical total heat prediction is to shorten flight time by lowering the L/D ratio which, in turn, enables the vehicle to descend quickly and, therefore, limit the total heat input. It has been found necessary, however, to override the commanded decrease in L/D during the period of initial entry because the high drag portion of the drag curve is being modulated at that time and total heat predictions (based upon the heat absorbed during the entire trajectory assuming present conditions) are likely to appear critical. Because of this problem, it has been decided to observe but not to control the total heat parameter until γ initially reaches 0° (minimum altitude of initial penetration). For an indication of the control logic associated with heat determination, see Fig. III-43.

5. Terminal Flight Considerations

The terminal portion of re-entry is climaxed by the initial deployment of a small drogue chute at some altitude between 100,000 and 60,000 feet and the subsequent deployment of a large main chute at approximately 15,000 feet. The drogue chute is triggered as a function of velocity and the main chute as a function of barometric pressure. The re-entry range prediction steering system is particularly adaptable to this type of terminal recovery, as trajectories resulting from the employment of parachutes or drag devices can be found by modifying the K parameter in the initial condition equation for Z_i (equation 16). The range of velocities over which initial chute deployment can vary are from a $\bar{u}$ of 0.045 to a $\bar{u}$ of 0.083. Velocities above or below these values result in vehicle instability or squidding problems with the drag chute. When an optimum deployment velocity is chosen this value of $\bar{u}$ will be the minimum velocity for which the range integration in equation (5) is made. Insofar as the range control system is concerned, therefore, it will be controlled to arrive at the target when the final velocity $\bar{u}$ is attained. At this time, the guidance computer will call for deployment of the drogue chute and the vehicle will descend to the target. The actual ground range covered from drogue chute deployment to touchdown is less than 15 nautical miles even if the vehicle angle of attack is positioned to give maximum C_L. The portion of this range contributed during the descent of the main chute is 1.6 nautical miles maximum. In order to account for the range attained during the drogue chute deployment portion of flight, the final values of γ , Z, and Z' at $\bar{u}_f$ would either be placed in the primary range prediction computer, with the appropriate modification to the K term in the Z_i equation to account for the increased drag of the chute, and the terminal range solved for in a serial fashion, or the back-up computer could be used for a simultaneous solution and the ranges added. Whatever the procedure, the re-entry range prediction steering system can be adapted to account for this terminal portion of flight.

6. Abort During Boost

The re-entry range prediction system could also be used in an emergency abort during the boost phase of flight. The guidance system would furnish the information necessary for the choice of an adequate landing point in addition to controlling deceleration and target range. Recoveries from a number of abort conditions have been demonstrated in a manned closed-loop analog simulation by Wingrove, et al (Ref. III-5) employing the Chapman range prediction guidance scheme. In all cases, normal recoveries were made and the pilot succeeded in reaching an in-flight selected landing site. It should be pointed out, however, that the lift-drag ratio limit of the re-entry vehicle configuration will also limit the maneuvering capability in an emergency return and will result in a series of possible re-entry trajectories in which the maximum deceleration limit of six G's will be exceeded. However, because of its ability to predict g history as well as range, the RERP system offers considerable control in limiting the extreme decelerations likely to be encountered in an abort situation.

7. Rotating Earth Considerations

The re-entry study phase has primarily been concerned with demonstrating feasibility. Thus, some of the side effects that would normally constitute part of a complete study have been disregarded since they would necessarily make the job of mechanization and evaluation even more complex. The effect of earth rotation, for example, on the re-entry range prediction system was neglected because a large part of the IBM 7090 digital trajectory data employed to check the analog simulation did not include this effect. To account for this effect, which will indeed have to be done for any re-entry range control scheme, does not actually entail much more complexity in this range prediction technique since most of the necessary input parameters are already available in the re-entry computer program.

The earth's rotation with respect to the great circle route of the vehicle in space will have essentially two effects on the range control system. First, the aerodynamic forces acting on the vehicle will be a function of the relative velocity with respect to the fluid medium. Since the air mass has a velocity with respect to inertial space the relative velocity will therefore be a combination of the inertial velocity of the entering vehicle and the velocity of the air mass as a result of earth's rotation. Secondly, and this is the major of the two effects, the location of the destination will be changing with respect to the vehicle's great circle route.

The relative velocity between the air mass and the vehicle can be adequately approximated by allowing the independent variable $\bar{u}$ in the differential equation (1) to be the sum, or difference, of the inertial velocity of the vehicle and the component of the earth's rotation, in the plane of the great circle at the target. The $(1-\bar{u}^2)$ term in equation (1) should, however, contain the inertial velocity rather than the relative velocity since it represents the inertial centrifugal force in the trajectory equation. This is also true for the ballistic range equation. The range prediction integration (5) should include the relative velocity as an integration limit as the range to go should be zero when $\Delta\bar{u} = 0$.

To determine the distance the target will move during re-entry, relative to the great circle route in space, it is necessary to predict the time remaining during the trajectory. Equation (6) calculates time for that portion of a flight which is in the atmosphere (below 300,000 feet altitude or $Z \geq 0.001$), and the time expended during ballistic flight is determined by the following relationship:

$$(25) \qquad t_B = \frac{\Delta S_B}{K_e \bar{u}_e \cos \gamma_e}$$

where: ΔS_B = Ballistic range

$\bar{u}_e$ = Exit velocity

γ_e = Exit flight path angle

K_e = Eccentricity correction factor (constant for apogees less than 400 nautical miles)

Total time along the flight trajectory would then be a combination of the initial atmospheric-entry time up to skip-out, ballistic-range time and the final second-entry-to-target time. The total predicted time of flight can be used to determine the longitudinal range contribution as a function of earth rotation (ΔS_{LO}) with the following relationship:

(26)

$$\Delta S_{LO} = K_{LO} \left[t_B + \frac{1}{\sqrt{\rho g}} \int_{\bar{u}_f}^{\bar{u}_i} \frac{d\bar{u}}{\bar{u} z} \right] \text{ in nautical miles}$$

where: K_{LO} = 0.2498 cos I (Spheroidal earth)

and I = Flight path inclination with respect to equator.

The corresponding change in lateral target position as a function of time can also be determined by substitution of the K_{LO} constant with a similar one representative of lateral range (K_{LA}). The K_{LA} constant is merely the component of K_{LO} , therefore, the change in lateral target position as a function of the L/D ratio chosen to reach the target and the corresponding flight time is:

(27)

$$\Delta S_{LA} = K_{LA} \left[t_B + \frac{1}{\sqrt{\rho g}} \int_{\bar{u}_f}^{\bar{u}_i} \frac{d\bar{u}}{\bar{u} z} \right]$$

where:

$K_{LA} = 0.2498 \sin I$ (Spheroidal earth)

E. RE-ENTRY OPTIMUM TRAJECTORY STEERING

1. Introduction

During re-entry of the Apollo vehicle, certain requirements must be fulfilled by the guidance system. These requirements include maximum heating restrictions, satisfactory acceleration levels for the vehicle occupants and equipment and specified landing position. An ideal guidance scheme should determine the trajectory which minimizes the heat input to the body surface, constrain the flight path to one having acceptable acceleration limits and specified landing position and finally, provide signals to the control system to accomplish such a re-entry trajectory.

A promising technique for achieving such an optimum guidance system employs the Calculus of Variations. In past years, resort to variational techniques for providing guidance equations has been practically impossible due to the complicated nature of the indirect methods and their associated split boundary conditions. Tedious iteration schemes are an unfortunate necessity for obtaining extremal paths by the indirect methods of variational calculus.

Recently, several breakthroughs have occurred which show promise of applying direct methods of variational calculus to future guidance systems. Nearly simultaneously, Kelly (Ref. III-7) and Bryson, et al. (Ref. III-8) published methods incorporating direct variational techniques for obtaining extremal solutions with an associated reduction in computing time. Both methods make use of the system of equations adjoint to the small perturbation equations about a nominal trajectory. This adjoint system yields influence coefficients which, in turn, correct the nominal trajectory in an optimum fashion. Convergence of the method to the true optimum is accomplished by "steepest descent" methods.

These direct variational methods are actually linearized solutions to the Mayer Problem of the indirect method of the Calculus of Variations. The approximation involves replacing the non-linear trajectory equations of motion by a nominal trajectory and a linear, small perturbation system of equations. The adjoint of equations of the direct method corresponds to the Euler-Lagrange equations of the indirect method and the influence coefficients in the direct method correspond to the Lagrange multipliers in the indirect method. The significant advantage of the direct method is its ability to determine near optimum solutions in relatively few computer cycles.

To apply a direct variational technique to the Apollo vehicle, an on-board computer would be programmed to determine the lift commands which, in turn, would be inputs to the control system. Boundary conditions consisting of

position, rate and attitude data would be provided to the computer by either on-board sensing devices or ground control linkages. To account for errors in the system (primarily input position and rate data), the trajectory could be continually optimized from the vehicle's present position to the desired touch-down point. The system would become increasingly accurate as the impact point is neared. The significant advantage lies in the ability to guide the vehicle in a manner which would optimize some pertinent parameter such as minimizing the heat input to the body, minimizing the flight time, etc.

Since the methods of Refs. III-7 and III-8 are the first direct trajectory optimization methods to show promise for future guidance on schemes, work is continuing to evolve a simple, direct optimum (or at least near optimum) guidance technique to be applicable for the Apollo vehicle.

A direct variational method capable of optimizing load factor, heat input and range is presently being developed and prepared for programming on the IBM 7090 computer (see Appendix Q). The program will provide a means of determining the optimum re-entry trajectory from a performance standpoint as well as serving as a tool for studying optimum re-entry guidance techniques.

2. Mathematical Development

The optimum re-entry procedures in Appendix Q provide sufficient information not only to determine the optimum re-entry trajectory, but also to control the vehicle to follow an optimum re-entry path. To explain how the optimization procedure will accomplish this task, we will consider the various phases involved in the optimum re-entry; namely, re-entry point determination, optimization, initiation and control.

Re-entry point determination--Prior to re-entry, during the midcourse return voyage from the space destination, measurements are taken of the vehicle's position and the time rates of change of position. These data are, in turn, used to determine the position, velocity and time when the vehicle is expected to initiate its re-entry into the earth's atmosphere. These position, velocity and time estimates are continually updated as the vehicle approaches the re-entry initiation point.

Optimization--Using the estimated position, velocity and time data, at re-entry initiation, the optimum re-entry trajectory is computed on-board the vehicle prior to re-entry. As the computer iterates on the optimum solution the updated estimates on the initial conditions are continually accounted for. Finally, when the vehicle arrives at the re-entry initiation point an optimum re-entry trajectory has been computed and is stored in the computer memory for subsequent use.

Initiation--At the re-entry initiation point, the optimum trajectory stored in the computer memory should be very nearly consistent with the actual position

and velocity. Very small deviations may exist because the computation time required to generate the optimum solution will necessarily cause some lag in updating the initial conditions. However, the influence coefficients which correspond to the optimum solution can be used to correct for these small differences, as will be shown subsequently.

Control--During re-entry of the vehicle, unpredictable disturbances may cause the vehicle to deviate from the precalculated optimum trajectory. Such disturbances could arise from deviations in the atmosphere properties used in the calculations, winds, gusts, etc. By utilizing the information calculated along the optimum trajectory, these disturbances will be corrected by a "Lambda Matrix Control" technique in order to allow the vehicle to satisfy its landing location requirements, acceleration, altitude and dynamic pressure requirements and still minimize the heat transferred to the vehicle.

This "Lambda Matrix Control" scheme uses a precalculated matrix of time-variable "gains" to multiply an error matrix (i.e., deviations in position and velocity from precalculated values) to yield deviations from the nominal control variable programs. These time-variable "gains" are precalculated very simply from the impulse response functions and influence functions obtained in the determination of the optimum trajectory. They are determined in such a manner as to ensure that the vehicle satisfies the terminal constraints with the least deviation from the pre-calculated control variable program. This criterion ensures that the least penalty in "pay-off" function is paid while still satisying terminal constraints. Since little equipment will be required to provide these corrections, the computer could continue to iterate on the optimum trajectory to further account for these disturbances.

The method for providing these control corrections will now be discussed. The nomenclature as well as explanation of quantities involved is presented in Appendix Q. The analysis will account for events which occur at and subsequent to re-entry initiation. Since the method for determining the optimum trajectory is presented in Appendix Q it will be assumed that it has been precalculated and stored in the computer memory. For simplicity in presentation, the analysis will be restricted to two-dimensional trajectories. The results can easily be extended to three-dimensions.

At initiation of re-entry ($t=t_o$) let the deviations of measured initial conditions, $x(t_o)$, $h(t_o)$, $V(t_o)$ and $\gamma(t_o)$ from those estimates initially used, in the optimum re-entry calculations $\bar{x}(t_o)$, $\bar{h}(t_o)$, $\bar{V}(t_o)$ and $\bar{\gamma}(t_o)$ be denoted by:

(1)
$$\delta V(to) = (V-\bar{V})_{to} \qquad \delta Q(to) = 0$$
$$\delta \gamma(to) = (\gamma-\bar{\gamma})_{to} \qquad \delta \psi(to) = 0$$

$$\delta x(to) = (x-\bar{x})to \qquad \delta\phi(to) = 0$$

$$\delta h(to) = (h-\bar{h})to \qquad \delta\theta(to) = 0$$

The influence functions $\lambda_i^{(jh)}$ evaluated at $t=t_o$ can be utilized to determine the effect which the deviations have on ζ_f, χ_f, ψ_f, ϕ_f and θ_f ; heat transfer, range, acceleration altitude and dynamic pressure parameters. These influence functions have been predetermined for the optimum trajectory and are available in the computer memory.

Thus

$$(2)\quad \begin{bmatrix} d\zeta_f \\ d\chi_f \\ d\psi_f \\ d\phi_f \\ d\theta_f \end{bmatrix} = \begin{bmatrix} \lambda_V^{(\zeta h)}(t_o) & \lambda_\gamma^{(\zeta h)}(t_o) & \lambda_\chi^{(\zeta h)}(t_o) & \lambda_h^{(\zeta h)}(t_o) & \lambda_q^{(\zeta h)}(t_o) & \lambda_\psi^{(\zeta h)}(t_o) & \lambda_\phi^{(\zeta h)}(t_o) & \lambda_\theta^{(\zeta h)}(t_o) \\ \lambda_V^{(\chi h)}(t_o) & \lambda_\gamma^{(\chi h)}(t_o) & \cdots & & & & & \lambda_\theta^{(\chi h)}(t_o) \\ \lambda_V^{(\psi h)}(t_o) & \lambda_\gamma^{(\psi h)}(t_o) & \cdots & & & & & \lambda_\theta^{(\psi h)}(t_o) \\ \lambda_V^{(\phi h)}(t_o) & \lambda_\gamma^{(\phi h)}(t_o) & \cdots & & & & & \lambda_\theta^{(\phi h)}(t_o) \\ \lambda_V^{(\theta h)}(t_o) & \lambda_\gamma^{(\theta h)}(t_o) & \cdots & & & & & \lambda_\theta^{(\theta h)}(t_o) \end{bmatrix} \begin{bmatrix} \delta V(t_o) \\ \delta\gamma(t_o) \\ \delta\chi(t_o) \\ \delta h(t_o) \\ \delta\zeta(t_o) \\ \delta\psi(t_o) \\ \delta\phi(t_o) \\ \delta\theta(t_o) \end{bmatrix}$$

or abbreviated

$$(3)\qquad [dX_f] = [\lambda(t_o)][\delta_y(t_o)]$$

The values of $d\chi_f$ are the deviations from the optimum or desired values caused by the initial condition errors $[\delta y(t_o)]$. Since we desire to have the $d\chi_f$ equal zero (i.e., no deviations from the optimum final values), we will determine the correction to apply to the precalculated optimum driving function $\bar{\alpha}(t)$ to account for the deviations $[\delta y(t_o)$ and cause $(d\chi_f)$ to vanish. By means of Equation (68) of Appendix Q we have

$$(4)\quad \begin{bmatrix} K_Q \\ K_\chi \\ K_\psi \\ K_\phi \\ K_\theta \end{bmatrix} = [A]^{-1} \begin{bmatrix} dQ \\ d\chi \\ d\psi \\ d\phi \\ d\theta \end{bmatrix} \qquad [A] = \begin{bmatrix} I_{QQ} & I_{Q\chi} & I_{Q\psi} & I_{Q\phi} & I_{Q\theta} \\ I_{\chi Q} & I_{\chi\chi} & I_{\chi\psi} & I_{\chi\phi} & I_{\chi\theta} \\ I_{\psi Q} & I_{\psi\chi} & I_{\psi\psi} & I_{\psi\phi} & I_{\psi\theta} \\ I_{\phi Q} & I_{\phi\chi} & I_{\phi\psi} & I_{\phi\phi} & I_{\phi\theta} \\ I_{\theta Q} & I_{\theta\chi} & I_{\theta\psi} & I_{\theta\phi} & I_{\theta\theta} \end{bmatrix}$$

or abbreviating (4) we get

$$(5)\quad [K] = [A]^{-1} [d\chi_f]$$

Since $(d\chi_f)$ in Equations (2) and (4) will be small quantities we can apply a weighting factor (W) to each term, thus

$$(6)\quad [K] = [A]^{-1} [W][d\chi_f]$$

Substituting Equations (3) into (6) gives

$$[K] = [A]^{-1}[W][\lambda(t_o)][\delta_y(t_o)] \tag{7}$$

The influence coefficients corresponding to α can be written in matrix notation as

$$\begin{bmatrix} \lambda_\alpha^{(\varphi h)}(t) \\ \lambda_\alpha^{(\chi h)}(t) \\ \lambda_\alpha^{(\psi h)}(t) \\ \lambda_\alpha^{(\phi h)}(t) \\ \lambda_\alpha^{(\theta h)}(t) \end{bmatrix} = \begin{bmatrix} \lambda_v^{(\varphi h)}(t) & \lambda_\gamma^{(\varphi h)}(t) & \lambda_\chi^{(\varphi h)}(t) & \lambda_h^{(\varphi h)}(t) & \lambda_\varphi^{(\varphi n)}(t) & \lambda_\psi^{(\varphi n)}(t) & \lambda_\phi^{(\varphi h)}(t) & \lambda_\epsilon^{(\varphi h)}(t) \\ \lambda_v^{(\chi h)}(t) & \cdots & & & & & & \lambda_e^{(\chi h)}(t) \\ \lambda_v^{(\psi h)}(t) & \cdots & & & & & & \lambda_e^{(\psi h)}(t) \\ \lambda_v^{(\phi h)}(t) & \cdots & & & & & & \lambda_e^{(\phi n)}(t) \\ \lambda_v^{(\theta h)}(t) & \lambda_\gamma^{(\theta n)}(t) & \lambda_\lambda^{(\theta h)}(t) & \cdots & & & & \lambda_e^{(\theta n)}(t) \end{bmatrix} \begin{bmatrix} g_{\alpha v}(t) \\ g_{\alpha \gamma}(t) \\ g_{\alpha x}(t) \\ g_{\alpha h}(t) \\ g_{\alpha \varphi}(t) \\ g_{\alpha \psi}(t) \\ g_{\alpha \phi}(t) \\ g_{\alpha \theta}(t) \end{bmatrix} \tag{8}$$

where $g_{\alpha\lambda}$, $g_{\alpha h}$, $g_{\alpha\phi}$ and $g_{\alpha\theta}$ are zero in the formulation of (See Appendix Q).

(9) Abbreviating Equation (8) we get $[\lambda_\alpha(t)] = [\lambda(t)][g(t)]$ transposing

$$[\lambda_\alpha(t)]^* = [g(t)]^*[\lambda(t)]^* \tag{10}$$

The correction to $\bar{\alpha}(t)$ can be obtained from Equation (56) of Appendix Q and can be written in matrix form as

$$\delta\alpha(t) = \begin{bmatrix} \lambda_\alpha^{(\varphi h)} & \lambda_\alpha^{(\chi h)} & \lambda_\alpha^{(\psi h)} & \lambda_\alpha^{(\phi h)} & \lambda_\alpha^{(\theta h)} \end{bmatrix} \begin{bmatrix} K_\varphi \\ K_\chi \\ K_\psi \\ K_\phi \\ K_\theta \end{bmatrix} \tag{11}$$

or abbreviating

$$\delta\alpha(t) = \left[\lambda_\alpha(t)\right]^* \left[K\right] \tag{12}$$

Substituting Equation (7) and (10) into (12) yields

$$\delta\alpha(t) = \underbrace{\left[g(t)\right]^* \left[\lambda(t)\right]}_{\Lambda_1(t)}{}^* \underbrace{\left[A\right]^{-1}\left[W\right]\left[\lambda(t_o)\right]}_{\Lambda_2(t_o)} \left[\delta y(t_o)\right] \tag{13}$$

$$\therefore \quad \delta\alpha(t) = \left[\Lambda_1(t)\right]\left[\Lambda_2(t_o)\right]\left[\delta y(t_o)\right] \tag{14}$$

Thus $\delta\alpha(t)$ is the correction to be added to the precalculated optimum trajectory to account for disturbances which cause deviations from this optimum. If in computing the optimum, the integrals I_{xy} (Equation (68) Appendix Q) are evaluated continuously along the trajectory then t_o in Equation (14) can be replaced by any arbitrary time τ, where a disturbance occurs and the re-entry trajectory could be continually corrected. The method, however, is only good for small disturbances about the precalculated optimum. If the disturbances accumulate to a point where they are no longer in the linear range of the influence functions, then deviations in the boundary conditions occur. To compensate for this possibility, updated optimum trajectories can be calculated during re-entry to supplement the above guidance technique.

By the second method discussed in Appendix Q for determining an optimum solution, the re-entry guidance correction technique is as follows:

[redacted]

$$(15)\quad [dF]_T = \begin{bmatrix} \lambda_V^{(Fh)}(t_o) & \lambda_\gamma^{(Fh)}(t_o) & \lambda_\chi^{(Fh)}(t_o) & \lambda_h^{(Fh)}(t_o) & \lambda_Q^{(Fh)}(t_o) & \lambda_\psi^{(Fh)}(t_o) & \lambda_\phi^{(Fh)}(t_o) & \lambda_\theta^{(Fh)}(t_o) \end{bmatrix} \begin{bmatrix} \delta V(t_o) \\ \delta\gamma(t_o) \\ \delta\chi(t_o) \\ \delta h(t_o) \\ \delta Q(t_o) \\ \delta\psi(t_o) \\ \delta\phi(t_o) \\ \delta\theta(t_o) \end{bmatrix}$$

or abbreviated

$$(16)\quad [dF]_T = [\lambda(t_o)][\delta y(t_o)]$$

Once again the value of $(dF)_T$ is the deviation from the minimum value of F at t = T obtained for the precalculated optimum trajectory. To correct the $\alpha(t)$ function to account for the errors in initial conditions, $\delta y(t_o)$, we compute a new value of K by Equation (79) of Appendix Q.

$$(17)\quad K = \frac{1}{I}[dF]_T$$

where $I = \int_{t_o}^{T} \left[\lambda_\alpha^{(Fh)}(t)\right]^2 dt$ obtained during prior optimization.

The correction can then be determined by

$$(18)\quad \delta\alpha = K\,\lambda_\alpha^{(Fh)}$$

[redacted]

[redacted]

where

$$(19)\quad \lambda_{\alpha}^{(Fh)}(t) = \left[\lambda_v(t)\ \lambda_y(t)\ \lambda_x(t)\ \lambda_h(t)\ \lambda_Q(t)\ \lambda_\psi(t)\ \lambda_\phi(t)\ \lambda_\theta(t)\right]\begin{bmatrix} g_{xv}(t) \\ g_{xy}(t) \\ g_{xx}(t) \\ g_{xh}(t) \\ g_{x\psi}(t) \\ g_{x\phi}(t) \\ g_{x\theta}(t) \end{bmatrix}$$

which can be abbreviated

$$(20)\quad \left[\lambda_{\alpha}(t)\right] = \left[\lambda(t)\right]\left[g(t)\right]$$

Combining (17) (18) and (20) gives

$$(21)\quad \delta x = \left[\lambda(t)\right]\left[g(t)\right] I^{-1}\left[dF\right]_T$$

Substituting (16) into (21)

$$(22)\quad \delta x = \underbrace{\left[\lambda(t)\right]\left[g(t)\right]}\ \underbrace{I^{-1}\left[\lambda(t_o)\right]}\left[\delta_y(t_o)\right]$$

$$\delta x = \Lambda_1(t)\quad \Lambda_2(t_o)\left[\delta_y(t_o)\right]$$

[redacted]

Evaluating I at various values of t, then t_c in Equation (22) can be replaced by any arbitrary time, τ , where the disturbance occurs. This latter method requires less calculation than the previous method, which indicates that there is much room for improvement and simplicity in the further development of an optimum re-entry guidance system.

3. Results of Study

To evaluate this technique for the Apollo re-entry during the study phase, a working agreement was arranged with the Raytheon Company, who has a direct variational method (Ref. III-9) presently programmed on an IBM 704, to supply typical re-entry trajectories tailored to the Martin operational concept.

Due to the time schedule on this proposal, Raytheon was unable to prepare new computer programs to handle all the trajectory constraints of interest to The Martin Company, or to handle any three dimensional trajectories. The techniques are fully developed and have been tested on other problems, however. The Apollo trajectories which have been calculated made use of an existing program, substituting the vehicle characteristics provided by The Martin Company. The program used was the one similar to that described in Appendix Q for re-entry from escape speed. The control variable in the planar problem is angle of attack, α . With this problem, we were able to maximize or minimize total heat absorbed or final range subject to the constraint that the "pilot" remain conscious.

The lift and drag coefficients, furnished by Martin (with a change of zero lift axis) are shown in Fig. III-54. Six optimum control variable programs were obtained. The results are summarized in Table III-2. Perhaps of most interest are the trajectories for minimum total heat. The two cases calculated were for initial flight path angles γ_0 of -5.3° and -8°. The results are shown in Table III-2 and Figs. III-55 through III-58. In the $\gamma_0 = 5.3°$ case, negative lift is required to keep the vehicle in the atmosphere while the speed is reduced to circular satellite velocity. After this, small positive lift is required to avoid excessive accelerations due to large dynamic pressures. In the $\gamma_0 = -8°$ case positive lift is required to keep the entry sufficiently shallow to satisfy the acceleration tolerance constraint. To minimize total heat, the trajectory should be fairly steep; a fact noted already by several authors. Hence, roughly speaking, positive lift should be kept to the minimum value consistent with the acceleration constraint.

The minimum range cases (Table III-2 and Figs. III-56 through III-60) are seen to be very similar to the minimum heat cases. This is simply verification that minimizing heat leads to very rapid entry. The maximum range cases involve insignificant accelerations and heating rates. Very delicate angle of attack control at the initial re-entry would be necessary to provide the long skip, which is nearly a complete orbit. Even at the second re-entry, several hundreds of miles variation in landing position is possible. This reduces the initial guidance accuracy requirement substantially on these long glide cases.

The maximum range cases (Figs. III-56 through III-61 and Table III-2) are indicative of the higher total heats that might be absorbed. Heat absorption perhaps 25% greater than the maximum range cases might be obtained with just the proper α program.

In the minimum heat and minimum range cases, the high accelerations occur in a single "pulse". A peak acceleration of eight g's is seen to be typical. The heating rate curves have a similar shape. The peak rate rises with increasing steepness of initial entry angle.

F. EXPLICIT TANGENT STEERING (SKIP INTO NEAR ORBIT)

1. Introduction

During the early portion of the Apollo program, an operational concept was evolved which required a skip into orbit upon returning to the earth from a lunar mission. This concept has many attractive features from a guidance and control standpoint such as good control over landing site selection, updated re-entry conditions during orbit by means of ground tracking or airborne measurements, and the fact that the vehicle could use developed techniques during the re-entry from an earth orbit. The obvious disadvantage of such a concept would be the weight of propellant required to achieve and de-orbit from the desired near-earth orbit and the added complexity required of such a system. In order to evaluate this concept, a program was initiated on the Martin analog facility which incorporated a control steering law to modulate lift during the initial re-entry from the parabolic approach speeds in such a manner that a minimum impulse would be required to achieve an orbit whose perigee was greater than 400,000 feet and whose apogee was less than 400 miles. The configuration used for this study was the L-2-C with the aerodynamic characteristics shown in Fig. III-62. Lift to drag ratio was obtained by rolling the vehicle about the velocity axis with the vehicle at maximum C_L angle of attack, thus changing C_L while maintaining a fixed C_D .

2. Description of Study

The explicit tangent steering law attempts to modulate lift so as to produce a trajectory that is tangent to a target orbit of a desired perigee altitude. The steering law commands a change in lift proportional to the error between the γ_d (γ desired) and (γ actual) through the relationship:

(1) $\tan \gamma d - \tan \gamma a = \tan \gamma e$

(2) $C_c = K \tan \gamma_e$

(3) Where $\tan \gamma d = \pm \sqrt{C/A}$

(4) and

$$C/A = 1 + \frac{r^2 V^2}{r_c \mu \left(2 \frac{r_c}{r} - \frac{r_c V^2}{\mu} - 2 \right)}$$

C_L = vehicle lift coefficient

r = earth's radius in feet

V = vehicle velocity, fps

r_c = desired tangent target radius, feet

μ = universal gravitational constant, ft^3/sec^2

In order to simplify the mechanization of this law on the analog computer, an approximation was developed which is of the form

(5) $$C/A = \frac{-\Delta h}{r_c^2 V^2} \qquad \Delta h = h_a - h_c$$

h_a = vehicle altitude at time (t) feet

h_c = desired tangent target altitude feet

This approximation is developed in Appendix R.

Employing the three dimensional analog program described in Appendix O, the tan γ control law was used to close the guidance loop. Seventy-three runs were made on the Martin analog facility in which the initial conditions within a forty mile design corridor were varied (γ_i at 400,000 feet from -5.3° to -8°). The target orbit radius (r_c) was varied as was the gain (K) in the steering law (equation (2) to study the effects of these parameters on the additional velocity requirements to achieve the desired orbit. Velocity, altitude and C_L as a function of time were recorded during the run.

3. Results of Analog Study

Figures III-63, III-64 and III-65 show the incremental velocity (ΔV) requirements (at the apogee of the skip to achieve a circular orbit of that radius) as a function of the steering law gain and initial conditions for various target orbit altitudes (P_d). It can be seen that the ΔV requirements are hypersensitive to control law gain at the upper end of the design corridor. Skip-out

beyond 400 nautical miles would be very difficult to control. As the entry angle steepens, the sensitivity decreases but the velocity requirements increase, as one would expect. Sensitivity to gain increases as the target orbit altitude is increased.

Figure III-66 is a cross plot of the above data showing the ΔV requirement as a function of the target orbit radius ($P_{\perp}$) for the minimum ΔV cases evaluated. This plot indicates that in order to minimize ΔV, target orbits would have to be chosen based on initial entry conditions. This would not be difficult to do on-board the Apollo vehicle but it is also clear that the function of target orbit altitude and initial flight path angle is non-linear. Figure III-67 presents fuel required as a function of ΔV assuming an ISP of 300 seconds. This figure is useful in converting the previous results into vehicle weight penalties. Fig. III-68 again points out that a single desired target altitude will not minimize the ΔV requirements for all permissible entry angles, and that ΔV requirements rapidly increase as the re-entry angle steepens.

Figures III-69 through III-81 present typical traces of C_L, velocity and altitude as a function of time for the minimum ΔV required for a series of entry angles at 400,000 feet.

4. Summary

The purpose of this study was to evaluate the feasibility of a typical lifting body vehicle using aerodynamic lift to control a skip re-entry in such a manner so as to minimize the velocity required to achieve a circular orbit between 400,000 feet and 400 nautical miles. This study has shown that such a technique is theoretically feasible and that velocity requirements will vary from 145 fps to 1300 fps depending on the initial entry angle. The actual operational feasibility for application to an Apollo re-entry depends on the advantages gained by such a technique and the weight penalty to the vehicle. Assuming a requirement of approximately 500 fps to de-orbit and no penalty to the vehicle to carry the propulsion system through the first heat pulse, a weight penalty as high as 1500 lbs could be manifested.

G. TWO ROLL PROCEDURE FOR RE-ENTRY RANGE CONTROL

1. Introduction

The purpose of this study is to develop an emergency re-entry range control technique which would have the following characteristics:

(1) Be as simple as possible.

(2) Not require precise measurement of altitude and flight path angle at re-entry.

(3) Avoid load factor and heating limits.

During the initial re-entry into the atmosphere, some form of aerodynamic control is required to prevent random skip-out. The system developed in this analysis controls the skip, and therefore the range and apogee altitude, through a two-roll procedure in which negative lift is applied between rolls. The system is based on the measurement of load factor (N) and the rate-of-change of load factor with time (dN/dt). The time at which a load factor of one is reached is taken as a reference point for measuring time (t*) to roll initiation (see Fig. III-82); the range to target is also in reference to this point. The $(dN/dt)_{max}$ is used together with the range from target to determine the required time of roll initiation (t*) and the time between rolls (Δt) to achieve the desired range (see Fig. III-83).

The system described in Fig. III-83 will provide the desired range to target if nominal conditions exist. Studies to determine the effects of off-nominal conditions are included in this report.

At the beginning of this analysis, the roll technique for range control was investigated because of its potential as a primary control system. While the results indicate that the accuracy is probably not good enough for a primary system, the two-roll procedure could be used for emergency back-up. It is felt that the accuracy of the two-roll system shown in this analysis could be improved by further study.

2. Method Of Calculation, And Assumptions

All computations were made on the IBM 709 digital computer using a point mass two-degree of freedom program. The top of the atmosphere was assumed to be at 400,000 feet. Flight within the atmosphere was computed by integrating the appropriate equations of motion. Flight at altitudes above 400,000 feet was computed from the Keplerian free-flight equations. A spherical non-rotating earth is used throughout. Also the ARDC 1959 Standard Atmosphere is used in all cases except for sensitivity studies where the effects of changing atmospheric density is considered. The flight plan developed is as follows: (see Fig. III-84):

(1) Re-enter atmosphere at 400,000 feet at 36,000 fps. Initial re-entry is at C_L max to minimize heating.

(2) Measure load factor N and count time from the point where N = 1 g.

(3) Measure range to target from the point where N = 1 g.

(4) Measure the maximum rate of change of load factor with time.

(5) Using the information in (3) and (4) above and nominal performance of the vehicle, a time of roll initiation (t*) and a time between rolls (Δt) are determined from stored data. Rolls are assumed to occur instantaneously.

(6) Free-flight from exit to second re-entry.

(7) Re-enter and fly to target at the appropriate L/D. For this analysis, (L/D) max is used from the second re-entry point to target. However, the L/D could be varied during this portion of flight to provide control over the touch-down point.

For this study, machine calculations were made for flight from the initial re-entry to the second re-entry point. Range from the second re-entry to the touch-down point was obtained from the cross plot of re-entry range data shown in Fig. III-85.

Although this entire analysis is based on digital computations, it was anticipated that analog facilities would be used to augment the digital data. Accordingly, curves were developed which (1) define exit conditions for an apogee altitude limit of 400 nautical miles and (2) defines apogee altitude and free-flight range for exit conditions which avoid exceeding the 400 nautical mile altitude boundary. These curves are presented in Figs. III-86, III-87, III-88.

Figure III-85 shows the re-entry range capability of a vehicle having an L/D of 0.73 and a W/C_DA of 50 for a satellite type re-entry. The Model 410 vehicle has an (L/D) max of 0.73 and a W/C_DA of 166. The difference in re-entry range due to changing W/C_DA from 50 to 166 is small at an L/D of 0.73. Therefore, the data of Fig. III-85 were used in this analysis for determing re-entry range from the second-re-entry to impact.

Figure III-86 shows the free-flight range and exit conditions for a constant apogee altitude of 400 nautical miles. Since 400 nautical miles was used as an upper altitude limit in this analysis, Fig. III-86 provides boundary conditions on velocity and flight path angle at exit. Figures III-87 and III-88, respectively, provide free-flight range and apogee altitudes for various exit conditions which have the conditions of Fig. III-85 as an upper limit.

A weight of 6400 lb is used in all calculations. Assumptions pertaining to altitude, time and load factor limits are given in the section on "Two Roll Procedure with C_L max constant."

[redacted]

LIST OF SYMBOLS

A	Aerodynamic reference area	ft^2
C_D	Drag coefficient	
C_L	Lift coefficient	
q	Dynamic pressure	lb/ft^2
N	Load factor = $\sqrt{L^2 + D^2}\ \frac{1}{W}$	g's
t	Time referenced to initial 400,000 ft re-entry point	sec
t^*	Time of roll initiation measured from N-1 g	sec
Δt	Time at negative lift	sec
ρ	Atmospheric density	$slugs/ft^3$

[redacted]

3. Aerodynamic Data

Aerodynamic data for the Model 410 vehicle is shown in Figs. III-89, III-90 and III-91. Figure III-89 shows aerodynamic coefficient data estimated from Newtonian impact theory. Figure III-90 shows nominal lift and drag coefficient data and also shows curves with the nominal lift and drag coefficients increased by 10 per cent. The off-nominal curves were used for sensitivity studies. Figure III-91 shows lift coefficient data as a function of dynamic pressure for both 6 g and 10 g modulation. The data shown in Fig. III-91 were obtained from Fig. III-90 and the following equation:

$$N = \frac{1}{W/C_D A} \sqrt{1+(L/D)^2}\ q$$

The curve of θ_G shown in Fig. III-89 provides the direction of the resultant load factor with respect to the vehicle centerline. This information is useful from the standpoint of human factors in determining allowable g limits on the pilot.

A reference area of A = 78.54 ft^2, corresponding to a circular base area, is used for all aerodynamic coefficient data.

4. Results

a. Early studies

In the process of generating the data necessary for defining a range control system, early studies were concerned with determining applicable re-entry angles, load factor time histories, the effects of time of roll initiation on range and whether C_L max or (L/D) max should be used after roll initiation. From corridor width studies, it was determined that applicable re-entry angles varied from approximately -5.5 to -10 degrees. Load factor time histories for $C_{L\,max}$ are shown in Fig. III-92 for various re-entry angles. The significance of the Fig. III-92 data is that it provides: (1) the time reference at which N=1 g and t* = 0, (2) the maximum slope (dN/dt max of the load factor time history and (3) the magnitude of N max for a given re-entry angle. The maximum load factor and the time for N=1 g are shown in Fig. III-93. The maximum rate of change of load factor with time is plotted in Fig. III-120. It should be noted that while the time for N=1 g is used as a reference point for measuring time to roll initiation, it has been convenient in this analysis to plot all data as a function of time from 400,000 feet. Figure III-93 provides the relationship between roll time as referenced from N=1 g and as plotted with reference to 400,000 feet. Figure III-93 shows that for a maximum allowable load factor of six g's,

lift modulation would be required for all re-entry angles larger than approximately -6.65 degrees. Likewise, for a maximum of 10 g's, lift modulation would be required at angles larger than approximately -7.7 degrees.

Initial investigations of range control by application of negative lift were based on a one-roll procedure. This procedure is the same as that described in the section on "Method of Calculation and Assumptions" except that the second roll is omitted. The first range control computations were made for the purpose of obtaining a comparison between using C_L max and (L/D) max after roll initiation, i.e., during the negative lift portion of the trajectory. Figures III-94 and III-95, respectively, show this comparison for a re-entry angle of -7.5 degrees. As can be seen from the curves, the (L/D) max case was much more sensitive to roll time than the C_L max case. Similar results were obtained for a re-entry angle of -5.5 degrees (not shown). On the basis of these data, it was decided to use C_L max rather than (L/D) max after roll initiation.

Figures III-96 and III-97, respectively, show range and apogee altitudes flown at a constant C_L max for re-entry angles of -6.5, -7.0 and -7.5 degrees. Also shown is a re-entry at -9.8 degrees with lift modulated to avoid exceeding 10 g's. Similar data are shown in Figs. III-98 and III-99 for re-entry angles of -7 and -8 degrees with modulation as required to avoid exceeding six g's. These curves show that with a one-roll procedure, satisfactory sensitivities with respect to time of roll initiation are attained only at large re-entry angles where the g's are high and the range capability small. On the basis of these curves, it was concluded that a one-roll procedure could not be used to obtain a satisfactory range control system and an investigation was begun on a two-roll procedure.

b. Two-roll procedure with C_L max constant

Preliminary calculations revealed that range sensitivity to time of roll initiation could be appreciably reduced by employing a two-roll procedure. This method is the same as that for the one-roll procedure except that a second roll from negative to positive lift is performed after a specified time interval (Δt). With the addition of the new control parameter (Δt), curves of range, apogee altitude and maximum load factor were obtained as a function of time of roll with (Δt) held constant. These families of curves are shown in Figs. III-100 through III-108 respectively, for re-entry angles of -5.5, -6.5 and -7.5 degrees. Boundaries are imposed on these curves corresponding to the following limits:

(1) The time of roll initiation could not be earlier than that for $(dN/dt)_{max}$ since $(dN/dt)_{max}$ is one of range control parameters.

(2) The maximum allowable time to the initiation of the first roll is that corresponding to the point of range discontinuity found for the one-roll procedure.

(3) The minimum time between rolls was arbitrarily chosen as five seconds.

(4) The maximum allowable load factor was arbitrarily set at 10 g's.

(5) The maximum apogee altitude limit was taken as 400 nautical miles.

(6) The minimum apogee altitude limit was arbitrarily set at 400,000 feet.

Figures III-100, III-103, and III-105 show that within the above limits, the range control available varies from approximately 3000 to 15,000 nautical miles. However, for ranges greater than approximately 10,000 nautical miles, the sensitivities of range with respect to both the time of roll initiation and the time between rolls are quite large, especially for the re-entry angles of -5.5 and -6.5 degrees. Also, in the regions where these sensitivities are reduced, the range capability is reduced and the load factors are fairly high. No attempt has been made to determine optimum combinations of t and Δ t for controlling range from these curves.

c. Two-roll procedure with load factors modulated to 6 g's max

Curves showing range and apogee altitude for the case where load factor is limited to 6 g maximum by lift modulation are presented in Figs. III-109 through III-116 for re-entry angles of -5.5, -6.5, -7.5 and -8 degrees. A comparison of these curves with the unmodulated data of Figs. III-100 through III-108 shows that at the same re-entry angle, the range sensitivities with respect to time of roll initiation have been reduced. At the same time, there is no apparent increase in range sensitivities with respect to time between rolls; the load factors have been reduced and the overall range control capability has remained essentially unchanged. Again, no effort has been made to pick optimum operating conditions from the curves. However, conditions have been selected on the basis of minimizing the error sensitivities due to time of roll initiation and a summary plot relating (dN/dt) max, Δt , t^* and range is shown in Figs. III-117.

5. Sensitivity Studies

Range sensitivities were determined for re-entries with six g modulation for the following off-nominal conditions:

(1) Ten per cent increase in lift coefficient

(2) Ten per cent increase in drag coefficient

(3) Change in atmospheric density ρ of $\pm$ 50 per cent

(4) Change in initial velocity of $\pm$ 100 feet per second

In determining the range sensitivities of the above items, it was assumed that nominal conditions would be used in the guidance system and that off-nominal conditions would not be detected. In computing the sensitivities, account was taken of the fact that off-nominal conditions could cause small variations in the re-entry angle for the same (dN/dt) max. Load factor time histories for both nominal and off-nominal conditions are shown in Figs. III-100 through III-102 and Figs. III-118 through III-121 respectively. These curves show that at a given re-entry angle very little change in (dN/dt) max occurs due to increasing C_L and C_D by 10 per cent. The same results were obtained by changing the re-entry velocity by $\pm$ 100 feet per second (curves not shown). However, changing the atmospheric density by a factor of two caused off-nominal (dN/dt) max vs γ_e relationships. This is shown in Figs. III-122 and III-123. In making the sensitivity calculations (dN/dt) max was held constant and the appropriate re-entry angles were obtained as indicated in Fig. III-123.

A summary of the sensitivity data is shown in Table III-3. It should be noted that the points used for sensitivity calculations were selected at random and no attempt has been made to optimize the selection of t* and Δt for minimum range sensitivity. Also, while only C_L max and six g modulation have been investigated in this analysis, it is possible that the optimum amount of modulation for minimum range sensitivity would be some other value, say five or seven g's. Additional study would be required to determine optimum conditions for minimum range sensitivity.

To obtain some indication of the range error which might result due to a combination of off-nominal conditions, root-sum-square (RSS)* calculations were made for the first two cases given in Table III-3. These calculations are shown in Tables III-4 and III-5. The results show that for a target range of approximately 10,000 nautical miles, the RSS error is approximately 4000 nautical miles. For a target range of approximately 6000 nautical miles, the RSS error is approximately 1800 nautical miles. These results are shown only to indicate the magnitude of errors which might be obtained with the two-roll range control procedure. It should be emphasized again that the points used in the error calculations were arbitrarily selected. Also, the off-nominal values of the variables considered are arbitrary. Because of these arbitrary conditions, it is difficult to draw conclusion as to the significance of these errors other than to consider the order of magnitudes obtained. A more rigorous error analysis should be based on:

(1) Definition of 3σ variations in the variables considered.

---

* The root-sum-square error is obtained by squaring the individual errors, summing the squared values, and then taking the square root of the summation.

TABLE III-3

Summary Of Sensitivity Data

Nominal Conditions								Range Increment For Off-Nominal Conditions					
Ref. Fig. No.	γ_e	t_1	Δt	t^*	Range	$\frac{\partial R}{\partial t^*}$	$\frac{\partial R}{\partial \Delta t}$	+1.1 C_L	+1.1 C_D	1.5ρ_{Std}	.5ρ_{Std}	+100 FPS	-100 FPS
		From 400,000 ft.	Between rolls	From N=1g	Re-entry to target	$\Delta t = c$	$t^* = c$						
-	Deg	Sec	Sec	Sec	N mi	N mi/ sec	N mi/ sec	N mi	N mi	N mi	N mi	N mi	N mi
11A	-5.5	73	35	11	10,100	0	-1200	+3550	-3000	+2000	-550	+1600	-900
11A	-5.5	75	40	13	6250	+100	-550	+1350	-1650	+800	-300	+600	-500
11A	-5.5	82	50	20	4350	+250	-200	+800	-1150	+550	-550	-	-
12A	-6.5	72	10	26	14,300	0	-3000	+4700	-4500	(1)	-3000	-	-
12A	-6.5	78	20	32	4450	+150	-350	+1650	-1000	+625	-600	-	-
13A	-7.5	72	10	34.5	6850	0	-750	+3500	-1500	+1200	-1350	-	-

(1) Exceeds 400 nautical mile altitude limit

TABLE III-4

Root Sum Square Calculation

Reference Conditions:
Fig. III-109 $\gamma_e = -5.5°$
$\Delta t = 35$ sec $t_1 = 73$ sec
Re-entry Range To Target = 10,100 Nautical Miles

Variable (x)	$\partial R/\partial(x)$ (Average Values)	$\Delta(x)$	ΔR N Miles	$(\Delta R)^2$ (N Miles)^2
t*	0 N mi/sec	1 sec	0	0
Δt	1200 N mi/sec	1 sec	1200	1.44×10^6
L/D	3300 N mi/10%	10%	3300	10.89×10^6
ρ	1300 N mi/50%	50%	1300	1.69×10^6
ΔV	1250 N mi/100 FPS	100 FPS	1250	1.56×10^6

$$\sum |\Delta R|^2 = 15.58 \times 10^6$$

$$\sqrt{\sum (\Delta R)^2} = 3950 \text{ N mi}$$

TABLE III-5

Root Sum Square Calculation

Reference Conditions:
Fig. III-109 $\gamma_e = -5.5°$
$\Delta t = 40$ sec $t_1 = 73$ sec

Re-entry Range To Target = 6250 Nautical Miles

Variable (x)	$\partial R/\partial(x)$ (Average Values)	$\Delta(x)$	ΔR N Miles	$(\Delta R)^2$ $(\text{N Miles})^2$
t*	100 N mi/sec	1 sec	100	$.010 \times 10^6$
Δt	550 N mi/sec	1 sec	550	$.303 \times 10^6$
L/D	1500 N mi/10%	10%	1500	2.250×10^6
C_D	550 N mi/50%	50%	550	$.303 \times 10^6$
ΔV	550 N mi/100 FPS	100 FPS	550	$.303 \times 10^6$

$$\sum(\Delta R)^2 = 3.169 \times 10^6$$

$$\sqrt{\sum(\Delta R)^2} = 1780 \text{ N mi}$$

(2) Nominal control parameters t* and Δ t which have been selected on the basis of minimizing range sensitivities.

(3) Considerations of the ability of the vehicle to correct errors in range after the second re-entry.

In the event that it would be necessary to use an emergency-back-up guidance scheme, the primary consideration could be survival and possibly also recovery of the vehicle. In this case, it would seem possible to designate a number of alternate landing areas such that the range from re-entry to target would not be excessive. Under these conditions, the two-roll procedure could be further developed to provide a simple, reliable range control system with sufficient accuracy for emergency use.

6. Conclusions

(1) A variation in range from approximately 3000 to 14,000 nautical miles can be obtained with the two-roll range control procedure.

(2) Range errors of the order of 1800 nautical miles could result for a target range of 6000 nautical miles.

(3) The range sensitivities become extremely large for target ranges of 10,000 nautical miles or greater.

(4) The possibility of designating alternate landing areas for emergency use could reduce the required target ranges to the extent that acceptable range sensitivities could be obtained.

(5) Additional work would be required to define acceptable target ranges for the various re-entry conditions possible.

(6) The two-roll range control procedure is sufficiently simple so that the required maneuvers could be performed by the pilot, if necessary.

(7) Only a small amount of additional equipment would be required for the emergency range control system.

7. Supplementary Data

Fig. III-85 shows the re-entry range capability of a vehicle having an L/D of 0.73 and a W/C_DA of 50 for a satellite type re-entry. The Model 410 vehicle has an (L/D) maximum of 0.73 and a W/C_DA of 166. The difference in re-entry range due to changing W/C_DA from 50 to 166 is small at an L/D of 0.73. Therefore, the data of Fig. III-85 was used in this analysis for determining re-entry range from the second re-entry to impact.

Figure III-86 shows the free-flight range and exit conditions for a constant apogee altitude of 400 nautical miles. Since the 400 nautical mile altitude was used as an upper altitude limit in this analysis. Figures III-86 provides boundary conditions on velocity and flight path angle at exit. Figures III-87 and III-88, respectively, provide free-flight range and apogee altitudes for various exit conditions which have the conditions of Fig. III-86 as an upper limit.

H. SELECTION OF TECHNIQUES

The previous sections have discussed several possible re-entry techniques which were investigated for application to the Apollo re-entry. The constraints placed upon and requirements of the re-entry guidance technique are:

(Req)	Range Capability	--	-2000 - 12,000 n. miles
	G limit	--	Maximum of six g's
Constraints	Heat Shield	--	Must provide indication as to whether heat shield will be overtaxed
	Skip-out limit	--	Must provide measure of skip-out altitude and limit this to 400 nautical miles
(Req)	Accept initial conditions of	--	Angle of attack $-5.3^\circ \leq \gamma \geq -8^\circ$
			Inertial velocity up to and including 36,500 fps
	Altitude	--	300,000 to 400,000 feet

To evaluate these techniques, the analysis in the previous section along with computer estimates and the capability of the technique to meet these constraints and requirements must be considered. In addition, the applicability of the technique to rotating earth considerations, three dimensions, manual control and the required inputs from the guidance system must be compared. Table III-6 presents this comparison. The purpose of this table is two-fold. First, it presents a rather complete resume' of the techniques studied and those criteria considered in arriving at the recommended system selection. Second, it points out those criteria which have not been considered in the present studies of some of the techniques.

Careful review of this comparison indicates that at the present point in the study of the various techniques the re-entry range prediction steering, the optimum trajectory and the complete equations of motion approaches appear to be

TABLE III-6

Re-Entry Techniques

	1	2	3	4	5	6
	Explicit Hit Point Steering	Equilibrium Guide	1 + 2	Range Prediction Steering	Optimum Trajectory	Eq. of Motion
Allowable range (Naut. Mi.)	15,000	Limited to 7000 nautical miles	15,000	15,000	15,000	15,000
Controlled skip	Yes	No	Yes	Yes	Yes	Yes
Stored trajectories necessary	No	Yes (manual)	Yes (manual)	No	Yes	No
Control load factor	Override only	Override only	Override only	Predicts + Controls	Controls to stored trajectory	Predicts + Controls
Terminal range control	(1)	None	None	Predicts end point cond-- Deploys chute and predicts chute trajectory	Yes	Yes
Altitude or pressure input required	Yes	For transition Yes	Yes	No	Yes	Yes
Computer requirements	Guidance computer can be used	Guidance computer can be used	Guidance computer can be used	Guidance computer can be used--2 sec solution	Additional 100# wt in guidance computer	Considerable increase in computer complexity or twice solution time
Closed loop operation	Yes	Controls to Nominal	Semi	Yes	Controls to a fixed trajectory	Yes
Heat limiting	(1) Not considered in present study	High heat-- Controls only to a fixed trajectory	Controls only to a fixed trajectory	Predicts total heat and can limit to some desired minimum	Yes	Can be incorporated
Manual control tie-in	Yes	Yes	Yes	Yes	Yes	Yes
Lateral range control	(1)	Can be controlled for $\bar{u}$ below value of one	Can be controlled below $\bar{u}$ of one	Yes	Yes	Yes
Rotating earth considered	(1)	Can be incorporated	(1)	Can be incorporated without very much complication	Yes	Yes--at increased complexity
Range control solution	Explicit	Explicit	Explicit	Iterative	Iterative	Iterative
Apogee limiting	(1)	----	(1)	Yes	Control to a stored ref.	Yes

Note:

(1) Not considered in present study

equal in their capability to satisfy the Apollo re-entry guidance requirements. The one exception to this conclusion is the onboard computer requirements. A more careful analysis of this item is necessary to evaluate the computer requirements in these three approaches. The use of the following types of computers were considered and estimates of both weight of computer and required solution time determined.

General purpose - digital

DDA - general purpose digital

Analog

Analog - digital

Table III-7 lists the computer weights and solution time for each of the techniques.

TABLE III-7

Technique	Computer Type	Time per solution	Weight (lb)
Re-entry range prediction steering	GP	1.99 sec W/O heat pred	21
		3.66 " W heat pred	
	Analog	0.1 sec	30
	DDA-GP	1.0 sec W/O heat pred	30
Optimum trajectory	GP	two to three minutes	100
Equations of motion	GP	5 sec W/O heat pred	21
		7.3 sec W heat pred	
		(Based on same number of time solution as (1))	

These estimates were based on detailed listing of the applicable equations for each technique, the computing logic necessary and any conversion either digital to analog or analog to digital required.

The above table indicates that at the present time (status of investigation of applicable equations) the optimum trajectory technique imposes a severe

penalty on the vehicle in order to incorporate it as a re-entry guidance technique. It is felt that considerable simplification of the application equations along with anticipated advances in computer development would again make the optimum trajectory technique attractive. The computer differences in the equations of motion approach and the re-entry range prediction steering approach (approximation to the equation of motion) is somewhat more subtle. One must compare the time of solution required using the same size computer. The computer requirements for the Apollo midcourse guidance have been established as a general purpose digital computer weighing twenty-one pounds. Table III-7 compares the time of solution, utilizing this computer, for both the approximate and exact equations of motion approach. This time of solution is based on the same number of time points in each technique, utilizing a rotating coordinate system in the exact equations.

Simulator studies have indicated that a minimum time of approximately four seconds will be tolerable between control changes during critical portions of the re-entry profile. The re-entry range prediction steering (approximate equations of motion) technique requires four seconds of time for the required two solutions whereas the equations of motion would require approximately 10 seconds. Since simulation studies have shown that the accuracy of the approximate technique is sufficient for control during re-entry and the required computer time is less than minimum time allowable, the re-entry range prediction steering technique is recommended for the Apollo re-entry guidance approach.

I. SUMMARY

The re-entry guidance technique studies for Apollo included the evaluation of both explicit and iterative techniques. Closed-loop analog or digital simulations where conducted on each of these techniques. In general, the simulations were simplified by using a two-dimensional, non-rotating earth program including only the vehicle force equations. Each of the techniques evaluated has shown promise for specific application during re-entry, but further study is required to fully establish their limitations.

The explicit hit point steering system offers a rather simple technique to control exit conditions which, in turn, control the skip range for skip-type re-entries. The equilibrium glide technique controls re-entry range but is limited in the guaranteed longitudinal range from entry and must be modified to incorporate acceleration and heat limiting. The optimum re-entry trajectory approach seems to work well because of its inherent ability to minimize or maximize constraints, but requires approximately five times the computer weight required by the other techniques.

The results of the studies have indicated that the re-entry range prediction steering technique will meet the re-entry guidance requirements of the Martin operational concept. This technique has been studied extensively by analog simulation and its feasibility demonstrated for both skip and non-skip type re-entries. Further work on this technique should include a detailed sensitivity investigation which must be conducted on a digital simulation program in order to establish accurate error partial evaluations.

IV. MECHANIZATION

A. PROBLEM AREAS AND ESSENTIAL CONSIDERATIONS

Analysis of the previously described guidance concept studies indicate that a number of problem areas and essential design factors must be considered in the mechanization of Apollo's guidance system. Although the number of these areas is quite large, it is believed worthwhile to explore them to a limited extent in this report. The problem areas briefly discussed immediately below are not necessarily presented in their order of importance.

1. Installation and Configuration

The guidance system chosen must not penalize, compromise or have any significantly adverse effect upon the overall configuration.

2. The Crew

The astronauts' operational capability must be fully integrated into the system design. This concept leads to design simplicity in certain portions of the system. This in turn leads to increased reliability. The astronauts must be given pertinent information on the status of the mission in the form of displays. Further, provision must be made for periods when the astronauts are not fully capable of performing normal navigational tasks.

3. Reliability

Since the system is manned and operates over a relatively long period, reliability becomes a serious consideration. To ensure reliability, redundancy of techniques and equipment is required. System simplicity must also be a design goal. By assigning a number of tasks to the astronaut, simplification results in certain portions of the system. High reliability also dictates the use of long life components such as gas bearing gyros, and minimizes moving parts, e.g., static storage in the computer.

4. Windows

Since cutting openings in the heat shield presents problems, the number and size of windows should be kept to a minimum. The guidance system designer is faced with choosing the type of windows, namely flat or domed. The flat window is easier to fabricate and interferes least with the aerodynamic shape of the vehicle; its field of view, however, is restricted. While the dome window offers a large field of view, it is difficult to build to the accuracy required and involves a "bump" on the vehicle's aerodynamic profile.

5. Tie-ins

Space navigation instruments primarily measure angles such as angle of star, included angle of a body, and sextant reading. When more than one component is involved--e.g., platform and tracker--a common reference, from an angular standpoint, must be provided. This can be accomplished by several means such as mounting the tracker directly on the platform, providing a rigid structural tie between tracker and platform, or providing optical or electrical links between components.

6. Window versus Periscope

The guidance system designer also may choose between two methods of looking out of the vehicle: via a direct viewing window or by means of a periscope. The window gives the astronaut a direct view of the heavens and minimizes sealing problems. The periscope allows the astronaut a potentially larger field of view, but his instantaneous field of view is relatively limited, and he has the problem of adjusting to an unnatural viewing area. The periscope also presents the problems of a sliding seal and a loss in optical accuracy.

7. Look Angles

Ideally, the astronaut and his equipment can see any portion of the sky at a given time. In particular, a view of the earth and moon with background stars is essential. Therefore, the guidance system design must incorporate the maximum possible viewing capability.

8. Rotation of the Vehicle

Any guidance system chosen should minimize rotation of the vehicle in space. This conserves fuel and weight.

9. Radiators

The vehicle must have radiators for transmitting heat generated within the vehicle to outer space. The guidance system chosen must not compromise radiator effectiveness by causing these radiators to receive part or all of the sun's radiation for a prolonged period of time.

10. Antennas

Antennas are mounted on the vehicle to communicate with the earth. Ideally such communication is uninterrupted: the selected guidance system chosen should minimize such interruption.

11. Accuracy

Accuracy allowing arrival at the prescribed periselenium, proper lunar orbit altitude, and required re-entry corridor must be built into the system. Finally, accuracy in the system conserves fuel for midcourse corrections.

12. Instrumentation

Navigational measurements are quite varied, e.g., star tracking, body center, body diameter, and occultation. The question arises: Should one instrument make the varied readings, or should a separate instrument be used for each type of reading?

13. Weight

Weight obviously should be kept to a minimum to avoid penalizing the configuration and overall mission.

14. Size

Because of the limited space in the re-entry module, size of the guidance equipment should be minimized.

15. Power

Guidance component power requirements should be kept as low as possible to minimize power source weight. Shutting down or reducing power on certain components during particular phases of the mission should be considered.

16. Availability

Because of the relatively short time between go-ahead and first system delivery, serious consideration should be given to the state of development of selected guidance components and techniques.

17. Degree of Automaticity

By integrating the crew into the guidance operation, simplification in certain portions of the system can be realized resulting in an increased system reliability. This concept also allows the crew to control the guidance function. In some cases, however, the crew may be incapacitated for such reasons as sickness, fatigue, restrictions in space suits and emergency operation. To cope with such situations, a certain amount of automaticity should be considered. The navigator is thus enabled to do his job with a minimum of manual motion, for example, to initiate automatic operation by merely pushing a button. Accuracy of manual versus automatic operation should also be considered.

18. Fuel Requirements

Guidance system design efforts must consider fuel requirements. In this case fuel is taken generally to mean propulsive fuel for course corrections and attitude changes. Fuel for supplying electrical power has already been mentioned. System accuracy, particularly during ascent, has a decided effect on fuel requirements. Fuel expenditure is also a consideration in the selection

among restricted two-body and three- or four-body computation. Finally, in defining the attitude changes required by the guidance system, the amount of fuel to be expended should be taken into consideration.

19. Environment

Normally, the guidance equipment within the cabin will operate essentially in a room environment. This presents no abnormal problems. However, situations such as loss of cabin pressure must be guarded against, and the method of cooling and sealing becomes important. Any equipment operating in a vacuum presents several problems involving de-gassing of lubricants and other materials, extreme temperatures and arcing problems. Micrometeorites, reentry heat, and space radiation must also be considered. Within the cabin, manual system operation should be compatible with the space available and with the capabilities of the crew.

Obviously no system will completely satisfy all of the above criteria and problem areas. The system selected, however, should entail minimum overall penalty and one involving relatively few difficult design and operational problems.

B. APPROACHES STUDIED

As has been seen, the selection of guidance criteria hinges upon such factors as reliability, the number of windows required and the degree of automaticity. Several guidance system approaches have been studied, with these and other points in mind. These approaches include:

1. Multiple Windows

This concept assures that in any vehicle orientation, the body of interest--earth, moon or star--can be seen from at least one window. This results in minimum vehicular rotation and attendant fuel savings. The structural problems, however, are compounded in cutting the necessary three or more windows through the heat shield. Problems of tying equipment together by structural or optical means, the internal space situation, and the establishment of crew duties in the face of multiple windows around the periphery of the vehicle also assume major importance.

2. One Window

The use of a single window would minimize the structural problem of cutting holes in the heat shield. However, this approach raises two questions: would the system have only one optical instrument? or would plug-in capabilities for other instruments be available? With the one instrument approach, no redundancy is contained in that portion of the system; with the plug-in approach, only one optical instrument can be used at a time. Rotation of the vehicle is also inherent in this scheme.

3. Two Windows

This scheme doubles the structural problem of cutting windows in the vehicle, and retains the problem of limited viewing. However, the attendant provision for two instruments enjoys advantages of redundancy for reliability, since two instruments can be used simultaneously. Furthermore, if the two windows are located adjacent to each other the tie-in problem can be minimized by the use of direct structural connection and by the use of synchro loops.

4. No Windows

With this approach, an optical instrument (or instruments) looks through a hole in the vehicle skin. Problems encompassed in optically flat windows, differential pressure and sunlight glare on the windows are eliminated. However, the problems of operating the equipment in a vacuum and the sliding seal now must be faced. Lubricants would boil off, extreme sun-and-shade temperature fluctuations would be experienced and micrometeorites would bombard the optical equipment. This approach also precludes the navigator's direct participation in the guidance operation.

5. Manual System

This approach minimizes automaticity. Stars would be manually acquired and tracked to align inertial reference monitoring corrective maneuvers and re-entry. Measurements for trajectory determination would be very basic, in that they would be based upon sextant readings and occultations times. While maximum system simplification and additional reliance on astronaut activities would result, this approach does not allow for periods of astronaut incapacity, and would limit the amount of basic data that could be fed into the system.

6. Automatic System

This approach entails complete automation of guidance operations. The astronaut would merely push buttons to initiate guidance operations; thereafter, his function would be limited to monitoring operations. This concept takes the burden of precise measurement off the astronaut, but does not fully utilize his capabilities, and thereby limits data handling capacity and capabilities. This approach by its very nature is also the most complex and complicated.

7. One System

The one-system approach assumes that each subsystem in the overall system would possess extremely high reliability and therefore would not fail during the mission. Such a philosophy is overly optimistic. Although system weight, size and complexity would be minimized, this approach would impose limits on both automatic and manual functions, and on the amount of basic data fed into the system.

8. Two Systems

In this approach, two complete systems would be available for guidance. Redundancy for reliability is therefore automatically provided. Also, the intermixing of automatic and manual functions, with resultant increases in basic data acquired, becomes feasible. The increase in complexity over that of the one-system approach is obvious.

9. Three Systems

This entails a two-system operation backed up by a third system. This cautious approach gives the greatest insurance of bringing the vehicle and crew back safely despite malfunction of the primary equipment. This is the cautious approach but attendant increases in complexity, system weight and the scope of crew functions are self-evident disadvantages.

10. Radio System

A pure radio guidance system has also been considered. This approach will not be discussed in detail here because of the basic Martin concept of providing self-sufficent, independent onboard guidance capabilities. This concept does not preclude ground-tracking data being made available to the astronaut for use at his discretion.

C. SELECTED APPROACH

The above discussion makes it obvious that a number of conflicting problems are involved in selecting an optimum guidance system. It is also apparent that a number of approaches could arbitrarily be considered the best method to handle the guidance function. Table IV-1 compares the various approaches previously discussed, in relation to the most pressing problems involved. It is recognized that other approaches and combinations of approaches are possible: In fact, literally dozens of different guidance configurations are possible. To present all of them, however, would make evaluation awkward; only the more representative are therefor presented. Without elaborating upon each system shown in Table IV-1, it is apparent that the two-window, two-system and three-system approaches offer the most in desirable features and least of undesirable ones. The three-system approach involves two primary systems, with a tertiary system ensuring a safe but not necessarily accurate re-entry. The only real disadvantage of these approaches is the requirement for reorientation of the vehicle when taking measurements. This reorientation is due to the limited viewing capability. Such a disadvantage is not considered serious, however, since attitude control of a space vehicle is an established technique having been perfected on Viking, Vanguard and other rocket projects. Adequate time and fuel is available for these maneuvers.

Approaches	Affect on Installation and Configuration	Utilization of Astronauts Capability	Reliability	Number of Windows	Tie-in Problems	Vehicle Maneuver Requirements	Effect of Enviroment	Comments
Multiple windows	X	O	O	X	X	O	O	
One window	▽	▽	▽	▽	O	X	O	
Two windows	▽	O	O	▽	O	X	O	Adjacent windows
No windows	▽	X	▽	O	▽	▽	X	Push-through instruments exposed to space
All manual input	▽	O	O	▽	▽	▽	▽	
Pure automatic	▽	X	▽	▽	▽	▽	▽	
One system	▽	▽	X	▽	O	X	▽	One opening
Two systems	▽	O	O	▽	O	X	▽	Two adjacent openings
Three systems	▽	O	O	▽	O	X	▽	Tertiary system for re-entry, two adjacent openings

LEGEND:
O - Good
▽ - Average or Inconsequential
X - Bad

Table VI-1 Comparison of Various Guidance System Approaches

The Martin approach is one utilizing the two-window, two-system criteria. This concept involves complete redundancy in techniques and equipment. One window is used for an automatic instrument while the other is utilized for manual operation. While two systems exist, subsystems of one system may operate in conjunction with the other. In essence, then although ostensibly a two-system approach, only a single integrated system is actually involved.

The two systems are arbitrarily called the automatic and manual input systems. The automatic system consists of an astro-inertial platform and a digital computer. The astro-inertial platform uses gyros to establish an inertial reference, and accelerometers to measure accelerations. This unit also can automatically acquire and track stars for updating the inertial reference coordinate system. This unit has the further capability to track a celestial body other than a star--in this case a partially illuminated earth or moon--and to determine the body's center with respect to the stellar background and its apparent angular diameter.

During ascent the digital computer uses acceleration data to calculate position, velocity and steering signals. The computer also accepts line-of-position and ranging data derived from celestial-body tracking, to determine the vehicle's orbit and to correct it where necessary. These inputs are also used in injection into and ejection from a lunar orbit. The computer has the further capability of guiding the vehicle to the proper re-entry corridor and, using Chapman's technique, of directing the vehicle to the prescribed landing area.

The manual input system derives its inputs primarily from a manually operated optical instrument called a telesextant. This unit is capable of:

(1) Determining the angular coordinates of a given star.

(2) Determining the angular coordinates of the center of a celestial body, such as the earth or moon, even though said body is only partially illuminated.

(3) Determining the apparent angular diameter of the partially illuminated celestial body.

(4) Sextant measurements of the angle between a given star and a given landmark on the earth or moon.

(5) Light-gathering sufficient for observing an occultation of a 9th magnitude star by the moon.

(6) Measuring the lunar latitude of a star occultation.

(7) Angular coupling with other units in the primary and alternate systems.

(8) Automatic and manual read-out of angles.

(9) Remote controling instrument positioning.

Outputs from this unit are fed to both the automatic and the manual input computers. The computers solve for position, velocity, orbit and steering information.

A miniature platform is included in the manual input system. This unit is slaved to the astro-inertial platform. It can measure acceleration data and accept angular information from the telesextant for alignment purposes. In addition to serving as a replacement for the primary platform in the event of an emergency in midcourse, this unit is used during thrusting phases as an operating redundant subsystem.

In emergency situations such as a failure of the astro-inertial platform, the telesextant would align the miniature platform. A failure of one of the computers would be detected by abnormal readings; self-checking capabilities would command switchout of the malfunctioning unit.

Obvious advantages of the two-window, two-system approach include:

(1) Redundancy of techniques and equipment; this provides the highest possible reliability.

(2) The advantage gained by integrating the systems so that the largest possible amount of basic data is fed into the system.

(3) The advantage gained via the use of lower-powered units in midcourse.

(4) Automatic capabilities sufficient to takeover in the event of crew incapacity, and the provision of the greatest possible amount of data acquired and used.

(5) A direct-viewing window available to the astronaut enables him to make telesextant measurements, and allows general observation of the heavens. It also fulfills other purposes, such as photography, when the portable telesextant is removed. Other methods of making observations necessary for navigation, such as by periscope and by equipment pushed up through the skin, entail the sliding-seal and unnatural-view problems. The pushed-up instrument not only presents the sliding-seal problem; it also incurs problems in presenting data to the astronaut. While this could be done by a video link to the display panel, the problems are alleviated by the window.

(6) By locating equipment close together, accurate tie-in can be accomplished. In the proposed system, the astro-inertial platform and the

telesextant are adjacent and mounted on the same structure. The miniature platform is also mounted on this structure.

(7) By providing manual input capability, full utilization of the astronauts' faculties is made possible. The astronauts' function, in relation to the automatic system, is that of knob turning, throwing switches and general control of the system. With manual function, more data can be taken, and the capability of "resting" part of the system is made possible. This results in decreased power requirements and increased reliability.

(8) In the selected approach the equipment operates normally in a room environment; problems engendered by exposing precision equipment to space environment are therefor nonexistent.

(9) Finally, the selected system calls for only proved techniques and equipment modifications--primarily miniaturization. Astro-inertial platforms and star-trackers have been flying for many years in connection with such programs as SNARK, B-52, B-58 and Hound Dog. Astro-inertial platforms also are involved in the Skybolt and B-70 projects. Miniature inertial platforms are integral to such programs as F-104G, A2F, WF2, W2F and P3V programs. Digital computers have flown in the Atlas and Minuteman missile, and are also involved in the A3J, Hound Dog and Skybolt weapon systems. The telesextant is a combination of two well-known instruments--a theodolite and a sextant. Since the system concept involves such proven equipment, development time would minimize and planned schedules would be met.

Some disadvantages of the selected approach have already been touched on. These include:

(1) Such a closely integrated approach requires that the vehicle be rotated when taking observations. It has already been mentioned that this is not a serious objection, since attitude control is a tried, proved, perfected technique. In Chapter V, "Operation," it will be shown that reorientation requirements have been held to minimum. There is, however, the fuel weight penalty involving some 100 pounds, but this is small compared to the approximately 6000-pound weight of the overall command module fuel required for the lunar orbit mission.

(2) Any guidance scheme providing visual observation requires that holes be cut in the vehicle. Windows in the selected scheme require larger holes, for a reasonable field of view, than would be required for periscopes or pushed-up instruments. These windows also must be of optical quality and would operate in a rather unfavorable environment. This is discussed in Section E4 of this Chapter.

(3) Obviously, the two-system approach is more complex than a one-system approach, with attendant weight and size penalties. Advantages, however, far outweigh the drawbacks--said advantages include a 200-fold increase in reliability, reduced power requirements during most of the mission, full integration

of the astronaut into the guidance function; and the provision of automatic guidance operations during incapacitation of the crew. Finally, the increase in the amount of data inputs also greatly enhances system accuracy.

The next section of this report presents detailed descriptions of the various subsystems selected. How these subsystems are tied together, the data flow and how the equipment is operated will be found later in this chapter and in Chapter V, "Operation."

D. CONSIDERATIONS AFFECTING CHOICE OF SUBSYSTEMS

1. Astro-Inertial Platform

As discussed in the preceding section, the recommended guidance approach utilizes an astro-inertial platform as the basic sensing unit of the primary system.

From the viewpoint of functional requirements, this unit must be capable of establishing an inertial reference by gyros, and of measuring vehicle accelerations by accelerometers. It must also be able to automatically acquire and track stars for updating the inertial reference coodinate system. The unit must be further capable of tracking a celestial body other than a star--in this case a partially illuminated earth or moon--and of determining this body's center with respect to the stellar background, and its apparent angular diameter.

The choice of a specific type astro-inertial platform to meet the above general requirements, and to best satisfy the specific performance criteria for each of the various flight phases, involved the following prime considerations.

(1) Performance--accuracy, flexibility and mission compatibility.

(2) Automaticity.

(3) Installation--astro-tracker field of view, window and environmental requirements.

(4) Simplicity and reliability.

(5) Physical characteristics and development status.

(6) Growth potential.

Careful study of the above considerations, and of possible compromise solutions, resulted in the recommendation for an astro-inertial platform housed in a pressurized container, and using a single flat window for sighting stars and other objects. Two-degree-of-freedom gyros and three linear

accelerometers are mounted on the platform inner gimbal, which is suspended by four gimbals (azimuth, inner-roll, pitch, outer roll). This configuration provides complete vehicle freedom about all axes and preserves orthogonality of the three inner gimbals during the critical re-entry phase. The astro-tracker unit is also mounted on the platform to provide optimum accuracy; this unit can be rotated with respect to the platform about two axes to allow automatic stellar search and acquisition within a reasonably short time interval. Also, the platform instruments and gimbal angle pickoffs should be in digital form for direct use in the computer as needed, whereas gimbal angle signals, properly resolved, should be available in analog form as needed for vehicle attitude control. The platform should also be capable of reduction in power requirements to lower power supply fuel weight. It should also provide for automatic alignment by a programmed star-pair search and acquisition, as well as by manual sightings.

Significance of the above prime considerations, insofar as they affect the recommended type of astro-inertial platform, is discussed below.

a. Performance

Using digital pickoffs such as code wheels to provide telescope gimbal angle signals, angular accuracies of three seconds of arc can be expected for star sighting. Instrument misalignments will slightly degrade this performance. To minimize gyro torquer errors, the platform coordinate frame of reference will remain fixed in inertial space during inertial computations. However, the gyro torquing rate must be sufficiently high to allow slewing to a new star pair, or to the earth or moon for necessary sightings. The desirability of torquing the gyros, and platform, to a local vertical reference frame during re-entry will be further evaluated in terms of torquing linearity and computational simplification.

Another significant performance consideration is the number of astro trackers to be located on the platform. One possibility is to use three star trackers, two of them being continuously fixed on a star pair while the third changes stars; a continuous progression of stars could thus be tracked, confining the tracking function to a very small area of sky. Although this would aid the computational problem, it is not considered necessary in view of the digital computer capabilities and low gyro drift while switching from one stellar source to another. Since more than one tracker is not required, reliability considerations dictate against such a scheme.

b. Automaticity

Some simplification could be achieved by aligning the astro-inertial platform, during flight, with the aid of a manually operated optical unit (see Appendix G). This could eliminate the need for one of the two gimbal axes associated with the platform telescope mount, as well as the need for storing

star tables in the computer. However, complete automaticity is deemed necessary to allow for possible crew incapacitation.

c. Installation

It is considered necessary to operate the astro-inertial platform in a pressurized container, using a window for sighting stars and other objects. With the altitude-azimuth type of telescope gimbaling planned, the telescope gimbal angles enable hemispherical coverage. However, hemispherical coverage implies a hemispherical window, or a complicated pyramidial window. Hemispherical windows of the required size and quality have not as yet been manufactured. The refraction correction at each one of the junctions of the pyramidial window are in opposite directions, thus causing loss of image quality and necessitating complicating corrections for difference in refraction between the vacuum outside the vehicle and the pressurized gas within the telescope enclosure. For this reason it is suggested that a flat window providing a 90- to 120-degree cone be used. Note that the innermost window forms an integral part of the platform housing rather than an integral part of the vehicle. This is done to allow environmental control within the platform enclosure, from completion of factory assembly through the various installation operations and usage. In other words, this excludes such foreign materials as screwdrivers, curious fingers, and dirt. To preserve equipment cleanliness, cooling will be provided by a liquid-to-air heat exchanger. The installation should also be such that stars can be tracked after atmospheric exit, but before injection into the translunar trajectory. This would eliminate gyro drift during this period and allow considerable relaxation of guidance restrictions on parking orbits. Likewise, staging or vehicle configurations should provide some degree of protection against the worst of aerodynamic heating encountered during atmospheric exit and re-entry.

d. Simplicity and Reliability

This consideration is very closely related to the degree of automaticity provided, and to the platform power requirements. Complete automaticity, defined as the ability to safely return to earth in the event of complete and sudden incapacitance of all crew members, is best provided by continuous operation of the astro-inertial platform in accordance with programmed stellar data. It can be argued that continuous operation may prove more reliable than intermittent operation because of power transients, thermal cycling, etc. This of course depends upon the design criteria (e.g., continuous or intermittent operation) specified for the various components and the extent of test programs covering component reliability development. Closely associated is the type of optical detector employed (e.g., phototube or solid state) and the development status of this unit.

e. Physical Characteristics and Development

The obvious desirability of minimizing size, weight, and required power of the astro-inertial platform must, of course, be evaluated against possible conflicting advantages associated with using existing equipment (i.e., component development and qualification cast savings, use of existing hardware, etc). For example, though the stellar platforms being developed and tested for the B-70 programs could be utilized, they would impose significant penalties: platform weight and required power would be four to six times that anticipated with the next-generation subminiaturized astro-inertial platforms. Also, the reliability of existing optical detectors suggests the need for additional developmental advances. It was therefore necessary to develop a new astro-inertial platform, using subminiature components currently in various stages of developmental testing and therefore compatible with the time phasing of the Apollo program.

f. Growth Potential

Applicability to other missions is considered an important goal because: (1) the larger production potential on which to base reliability history; (2) in a more sophisticated mission, it will avoid another development cycle. For instance, the optical-inertial guidance system, when assisted by radar altimeter, fulfills all of the functional requirements for guidance and control on a journey to the surface of Mars and return. It should also be generally adaptable to a larger family of terrestial applications, thereby providing a larger bulk of reliability experience and cost writeoff.

2. Digital Computer

The Apollo guidance computer, must adhere to the restricted volume, and the weight and power limitations inherent in the Apollo mission. It must, however, handle computation and provide data storage of a magnitude usually associated with large-scale computers. These conflicting requirements (large capacity, small size and weight, and low power consumption, versus high reliability with a minimum of environmental control) can be reconciled only by judicious selection of computer components, and intelligent organization.

The general features of a desirable component for this application are sharp switching threshold at rapid repetition rates, moderate- or low-power consumption, ability to maintain a state without external regeneration, and operation unaffected by temperature variation. Desirable organizational features include rapid access to storage, programming flexibility, and rapid arithmetic operations. These can be achieved either by parallel computation or by high-pulse repetition frequencies and time overlaps in the phasing of a computing cycle. The ability to perform certain real-time computation on measured variables independent of the main stream of programming, at rates determined by the variation of the input variables, is a great aid to computer speed. This is

usually achieved by utilizing a certain number of storage registers, addressable by the main program in a digital differential analyser configuration that operates independent of and simultaneously with the main program.

In addition, the computer organization must be sufficiently flexible to be readily adaptable to programming a variety of missions, and to accommodate the changes that will undoubtedly occur in the navigation and guidance techniques during the development program.

The computer organization should be able to accommodate temporary power transients and failures. This could be achieved by periodically storing the entire state of the computer control circuitry. In the event of a power failure, the last-stored state would be used to re-initiate computation. Such a design assumes a storage access that is non-volatile and semi-independent of the main program.

The most important subsystem in the guidance computer is the storage facility. The computations required for navigation and guidance consist of a sequence of calculations that depend upon rapidly-changing inputs. These sequences must be appropriately repeated to update results for effective vehicular control. The computation requires a considerable amount of access to stored data during each sequence.

Two essentially different storage facilities or modes are required: one for temporary storage of computed data for subsequent readout; another to handle data stored prior to the mission for use throughout the entire mission--interrogated but never disturbed.

Obviously, the storage facility must be designed on the basis of currently estimated requirements. At the same time, it would be desirable if the internal organization (for example the address structure) were such that additional storage could be provided with a minimum of redesign.

Because of rapid changes current in computer technology, the time specified for developmental completion of a particular computer has a profound effect on the organization and components selected for that computer. Components and techniques, particularly those applicable to storage, are being developed so rapidly--and along so many diverse directions--that the operating principles of the computer components, and the logical organization and the methods of fabrication thereof depends largely upon how far into the future development completion is projected. There are many developmental computer components, potentially superior to currently available components, that have not yet reached the state where they could be considered for use in a computer to be developed in 1961.

Thin films of magnetic material having different reluctance characteristics along different directions have been arrayed in storage cells having low dissipated power per switching cycle, extreme compactness and cycle times, and an

order of magnitude faster than those attainable with magnetic core stores. In addition, this type of device lends itself to techniques of fabricating whole arrays of storage cells, rather than individual cells. However, difficulty has been experienced in obtaining sufficiently uniform films for large arrays.

Cryotron storage and logic elements have been developed that also lend themselves to fabricating techniques whereby large arrays may be formed as a unit. Principle problems of these techniques are those associated with the operation and integration of the required cooling unit. Despite the many superior characteristics of this techniques, these problems have not been reduced to the level where a cryotron computer development in 1961 is feasible.

There exist many other developmental techniques and components superior to present techniques, such as techniques of semiconductor insulator and conductor deposition on a substrate; in deposited arrays of diodes, transistors, resistors and their interconnections. Such techniques hold the promise of reduced size, integrated fabrication of large systems or major circuits, and the increased reliability that seems to be inherent in combined fabrication and interconnection.

The above remarks are intended to emphasize the significance of the 1962 final development date on the computer configuration.

3. Miniature Platform

It has been shown in the preceding sections that a requirement exists for an alternate or miniature inertial platform. In the guidance operational concept (see Chapter V) this platform would be used as a redundant unit during ascent, lunar orbit injection, lunar orbit ejection, and re-entry as a redundant unit. In midcourse it is a redundant attitude reference, to be used only in emergency situations, therefore all power is turned off except for temperature control. This platform is initially aligned by slaving to the astro-inertial platform; however, in midcourse its inertial coordinate reference is obtained from the telesextant in the event of failure of the astro-inertial platform.

The requirements, based on the above, become quite obvious. They are:

a. Long life

Since this unit must operate for a relatively long time, it must possess a high reliability: something in the order of 5000 to 10,000 hours MTBF. This indicates the use of long-life components such as gas spin bearing gyros (the gyro spin bearings are usually the limiting factor in the life of a platform). Direct-drive torquers should also be seriously considered since they involve fewer moving parts. Finally, the electronics associated with the platform must possess the highest possible reliability.

b. Drift

The random drift in the gyros should be of the order of 0.01°/hr so that, if this unit becomes the primary attitude reference, frequent realignments by telesextant readings are unnecessary.

c. Size, weight and power

Platform size and weight should, of course, be minimized so that the overall configuration is not penalized. Since the mission is relatively prolonged, the platform's power requirements must be low to minimize power supply fuel weight in the event this unit is used in midcourse. Further, provision should be made to reduce power during the periods when the platform is not actively used. This is accomplished by cutting back power on the gyro wheels, gimbal torquers, synchros and electronics. This results in a further reduction in power supply weight.

d. Pickoffs

Ideally, both analog and digital pickoffs should be mounted on the platform gimbals. The analog would be used in a direct slaving mode from the astro-inertial platform during critical mission phases. Since all guidance computations are performed in a digital computer, digital readout is also desired. In this case, however, digital only is recommended, with astro-inertial readings compared to the miniature reading in the digital computer with the difference being fed to the gyro torquers of the miniature unit. Accuracy of the pickoffs need not be as precise as in the astro-inertial platform and telesextant. Approximately one minute of arc is sufficient for the redundant role.

e. Accelerometer accuracy

The accelerometers are primarily used to measure vehicle acceleration during thrusting. An accuracy of 10^{-4} g in linearity and bias is adequate for this application. However, to cover emergency operation during critical phases of flight (ascent, lunar orbit injection, lunar orbit ejection, and re-entry) an accuracy of 5×10^{-5} g should be specified.

f. Number of gimbals

Commands may be issued to orient the vehicle in any direction, ascent, observing, correcting, lunar orbit, and re-entry--in brief, during any phase of a lunar mission. All-attitude platform freedom platform then is indicated. This, of course, requires four gimbals.

g. Environment

For most of the mission time, the platform will operate in a benign environment of room conditions and zero gravity. Design must be incorporated,

however, to cope with the ascent and re-entry accelerations. Provision also must be made for loss of internal cabin pressure. Cold plate temperature control and hermetic sealing are indicated. Insulation of the unit to reduce heater power requirements are also recommended.

h. Development status

A number of small platforms are in production or at least in development. To meet Apollo's planned schedule, a platform should be selected that is well along the developmental road.

4. Telesextant

The requirement for a manually operated optical unit to make midcourse celestial measurements has been established. This unit would be used to track stars to update the miniature platform orientation when this unit is in use, to monitor the astro-inertial platform and to make navigational measurements using stars, earth and moon. The telesextant is the only really new component in the system: astro- and inertial-platforms, digitals computers, and radio altimeters have already been developed and put in operation in existing and proven guidance systems. Fortunately, the telesextant combines two old and well known techniques, namely, telescopic (or theodolite) and sextant measurements. Telesextant requirements are detailed in the succeeding paragraphs.

a. Star tracking

The unit should be capable of manually tracking bright navigational stars to 5 to 10 seconds of arc, or better. This precision is required for properly aligning the miniature platform and for use as an inertial attitude reference in the event of an astro-inertial platform malfunction.

b. Sextant capability

This instrument must have the ability to measure "angles in the sky," such as the angle between a given star and a given crater on the moon. One such measurement gives a cone of uncertainty, two measurements provide a line of position. Therefore, six sextant readings are required to determine the vehicle's orbit. The accuracy of this measurement should be of the order of 5 seconds of arc.

c. Body diameter measurement

This reading, which measures the included angle of a nearby partially-illuminated body, infers the range to that body. Again, the accuracy objective should be 5 seconds of arc, or better. The sextant may be used for this measurement.

d. Body center measurement

Determining the direction to the center of a celestial body, in this case a partially illuminated earth or moon, with respect to a known inertial coordinate system provides a line of position. Three such lines of position, separated by discrete times, is sufficient to determine an orbit. These measurements which should also be accurate to 5 seconds of arc, may or may not be made using the sextant portion of the instrument.

e. Angle readout

Angle measurements--azimuth, elevation, polar--should be read-out both visually and automatically. The visual readout should be accurate to one second of arc to prevent the degrading of overall accuracy. Use of this type of readout implies a manual method, such as a keyboard, for inserting data into the computer. The automatic readout should be as accurate, but the requirement of such an accurate pickoff being of reasonable size dictates some relaxation in accuracy specifications. Automatic readout provides redundancy, and navigator relief and it permits more readings to be taken in a given time.

f. Light-gathering power

The telesextant's main telescope will be used for observing occultations of stars behind the edge of the moon. To provide a reasonable density of stars for occultation purposes, stars up to the ninth magnitude may be used. The telesextant's light-gathering power should be sufficient to observe not only stars of the ninth magnitude, but those that are somewhat dimmer (10th to 11th magnitude) so that the navigator will not be required to observe occultations of stars at the outer limit of his visibility. The problem of diffraction patterns of the moon and stars also may come into play. This is discussed further in Chapter V, Section C.

g. Lunar latitude measurement

When an occultation of a star against the edge of the moon is observed, it is helpful to know the lunar latitude at which occultation occurred so that a true line of position can be established. Otherwise only a cylinder, or a segment of of cylinder, of position is determined. The Martin technique of making this measurement is as follows: (1) the telesextant horizontal crosshair is lined up with two known lunar landmarks; (2) a rotation is then made about one of the craters to the point of the occultation; and (3) the lunar latitude is inferred from this angle. The accuracy of this measurement is not critical and $\pm$ 0.1° is adequate for this navigational technique.

h. Inter-unit couplings

The requirement of transmitting angles from the telesextant to the miniature platform has been discussed. The requirement for coupling to the astro-inertial

platform to monitor this platform is also inherent in the guidance concept. The requirement to stabilize the telesextant from either platform should also be included. The vehicle is in a control-system limit cycle and may be rotating as much as 40 arc sec/sec. This poses a problem to the navigator who is attempting to make measurements with an accuracy of the order of a few seconds of arc. It is desirable therefore to stabilize the telesextant to conform with vehicle motion. The problem of the pickoff errors then becomes important. This dictates the manual slewing of telesextant to impart angular rates to the unit; in other words, aided tracking must be provided.

Other desirable but not necessary features of the telesextant include automatic star tracking. This feature may add unnecessary complication without materially increasing accuracy or utility. Also, it would be more convenient if all the above mentioned functions were performed by one instrument. If this proved impractical, two or more instruments would be used: Martin therefore gave consideration to making this a plug-in type instrument. With this concept, the instrument may be removed when not in use, thereby giving the astronaut an unobstructed view of the heavens and the capability to perform other functions such as photography and the performance of other scientific measurements. Other advantages are pointed out in the detailed discussion of the telesextant in Section E4 of this Chapter.

It would be desirable for the basic optics in the instrument to have a precision of one to two seconds of arc so as not to add materially to the error of a given reading. Other features include the capability of taking readings rapidly, more readings in a given time resulting in more accurate navigation. Manual operations and navigator fatigue should be considered with regard to this aspect. A further aid to the navigator would be a provision to vary the instrument's light-gathering power. This feature would be used in occultation observation to bring in the star or stars of interest without presenting too many stars to make identification a problem.

The accuracy requirements on the overall guidance system are primarily dictated by a safe and accurate re-entry so that an accurate landing may be made. Not only must the vehicle arrive at the proper re-entry point, but the initial conditions at that point should be well defined. The accuracy goal of the re-entry corridor is 1.7 nautical miles one sigma. Five-second accuracy measurements in midcourse (lines of position) give rise to a positional error approximating 5 miles. Stadiametric readings on the earth from 40,000 miles out result in a range error of 1.2 nautical miles when the angle is read to an accuracy of 5 seconds. This accuracy is degraded somewhat by earth irregularities.

Further discussion on the accuracy aspects will be found in Chapter VII, "Error Analysis." It appears then that 5 sec of arc, with an improvement factor of 3 or more in smoothing, is a good figure and that number will be the accuracy objective.

Secondly, it must be determined what can be achieved in a reasonable size and complexity. Theodolites accurate to one second of arc have been built for many years. The best presentday sextants have an accuracy of about 10 seconds of arc. The best flying star-tracker in the 10-second class is the Autonetics N3 Astro-Inertial System. Nortronics' Snark and Skybolt systems have accuracies of the order of 20 seconds of arc. Future Nortronics systems (e.g. the A-11 Astro-Inertial System) will have errors of 10 seconds, or less. A considerable portion of the error in the automatic systems is in readout. Five seconds of arc then is not an unreasonable goal in terms of equipment in the time period of Apollo. Another consideration is how accurately the navigator can take readings--in other words, what variances will be incurred by the operator in taking successive readings? In an attempt to answer this question, The Martin Company procured a mariner's sextant and made a number of tests. These tests included the use of three different operators performing the two basic sextant jobs, that is, stadimetric and star-on-landmark. Results of these tests are shown in Table IV. These tests were performed using an earth globe and a star simulated by the shiny end of a wire about 3/32" diameter against both a black and white background. These objects were positioned with a black background simulating space conditions. It will be seen that the minimum spread approximates $\pm$ 10 seconds of arc if certain "bad" readings of a given set are disregarded. The instrument used had a half clear glass and a half fully-silvered glass for combining the two images; this made superposition somewhat difficult. Therefore, with a better instrument, use of a partially silvered mirror for combining light and a trained operator, the spread in readings was estimated at 5 seconds of arc.

How accurately the information can be read out of the instrument also must be considered. The accuracy of the visual readout is not a problem. What may be a problem is navigator fatigue in taking a time-consuming, large number of readings.

From the above tests, it was found that the minimum time to take a single reading was about 30 seconds. A trained operator using a more efficient instrument, could doubtlessly be faster but with the time required to punch the readings into the computer, 30 seconds appears to be a reasonable number. An automatic readout will permit readings to be taken several times faster. However, an automatic readout to one second of arc for such a compact instrument does not appear to be compatible. It is felt that a relaxation to 10 seconds of arc for the automatic readout will provide a useful addition to the instrument, and is in keeping with the state-of-the-art in pickoffs. This accuracy is also compatible with the human error in taking the measurements.

TABLE IV-2

Test Results Of Sextant Readings

Stadimetric Operator A	Stadimetric Operator B	Stadimetric Operator C
	Black Background	
6° 11' 40"	6° 11' 50"	5° 56' 10"
6° 11' 20"	6° 11' 15"	5° 57' 00"
6° 11' 50"	6° 12' 00"	5° 56' 40"
	*White Background	
6° 11' 40"	6° 11' 40"	5° 56' 20"
6° 12' 00"	6° 12' 00"	5° 56' 40"
6° 11' 15"	6° 11' 55"	5° 56' 10"
6° 11' 20"	6° 11' 25"	5° 56' 10"

Stadimetric	Star on Point on Labrador Coast	Star on West Tip of Africa
Operator A	Operator A	Operator A
	Black Background	
21° 27' 50"	17° 50' 10"	21° 53' 30"
	17° 51' 10"	
21° 28' 30"	17° 49' 00"	21° 53' 25"
	17° 50' 30"	
21° 27' 50"	17° 47' 30"	21° 53' 15"
	17° 48' 50"	
	17° 51' 45"	21° 53' 45"
21° 27' 40"		

*Best results were consistently made while using a white background.

5. Radio Altimeter

One of the most fundamental measurements to be made by the guidance system is that of ranging to the nearest body, either the earth or moon. The resultant altitude information is vitally necessary as an input to the guidance system particularly during (1) earth orbiting before going into the translunar phase, (2) during the moon approach and moon orbit phase, and (3) during the earth approach and re-entry phase. During all these phases, accurate altitude measurement is extremely important.

A radio altimeter is the only state-of-the-art approach to this measurement problem. The altimeter should have a range well in excess of 1000 miles, and be accurate to within less than one-half mile. It should include a display capability so that the navigator will have data on altitude immediately available to him, on a realtime basis.

E. SUBSYSTEMS

1. Astro-Inertial Platform

Various astro-inertial platform proposals were evaluated, using as criteria the prime considerations discussed in the preceding section (D. Considerations Affecting Choice of Astro-Inertial Platform).

A platform tentatively chosen as being most compatible with the guidance system design criteria is that proposed by Autonetics. In addition to providing a fully automatic capability, its design is evolved from the background and experience gained in developing astro-inertial platforms for the alternate Snark guidance system (N2C) and for the B-70, and in developing the highly reliable components needed in the Minuteman NIO inertial guidance system.

The optical-inertial system is illustrated in general by the mock-up in Fig. IV-1. The weight of the package illustrated (including platform electronics, star tracker and housing) would be approximately 50 lbs. Power consumption would normally be in the vicinity of 100 w, with perhaps 150 w during rocket motor burning periods (which require larger gimbal driving torque). In general, the circuits will be designed power lean.

The platform uses two miniature, case-rotated free-rotor gyros (Fig. IV-2) to provide attitude stabilization; because they are two-axes gyros, two gyros suffice for complete stabilization. The acceleration sensors are quartz accelerometers encoded to give velocity information (as shown in Fig. IV-3). The dynamic range of these instruments is such that the same instruments are used for main boost, injection, and orbit correction velocity measurements. A single telescope, requiring approximately a six-inch window, is mounted on the platform for star and horizon tracking. The telescope slewing time between stars is at a rate commensurate with that necessary for correcting gyro drift.

The platform has complete gimbal freedom and digital gimbal angle pickoffs of sufficient resolution (either 14 bit, 80 arc sec/count or 15 bit, 40 arc sec/count) for boost autopilot rate-sensing purposes. All electronics, except the power stages, are microminiaturized. Required alternating voltages are generated by switching the supplied d-c voltage.

The platform gimbal system, shown schematically in Fig. IV-4, uses a combination of external and internal gimbals. The platform gimbal configuration has been used at Autonetics since 1954 and is currently being used on the Autonetics stellar-inertial system and on the Hound Dog program. As in Minuteman, the gimbal torquers are direct drive. Slip rings are provided on two axes (outer roll and azimuth) which, with flexible wiring across the axes, allow complete freedom.

The telescope optical system is a folded reflector system similar to that used in the Autonetics N3B. It will utilize a solid state detector for size and weight minimization and reliability augmentation. This detection technique is currently being developed by Autonetics on company funding, and preliminary daylight test data have substantiated its feasibility.

a. Case-rotated miniature free-rotor gyro

The miniature free-rotor (MFR) gyro is essentially a smaller scale version of the G6 gyro currently in use on the Minuteman program. (Free-rotor gyro-research at Autonetics was started in October, 1954.)

The MFR gyro has been under development at Autonetics for the past three years. During the first year a model was built of a one-half size G6 gyro. This unit demonstrated feasibility of the small diameter spherical gas bearing and the motor and torquer elements. During the past two years the MFR gyro has been developed as a research program sponsored by contract AF 33(616)-6368 with WADC. Under this program two case-rotated gyros (Fig. IV-2) have been built and tested. The present development program is nearing completion, with several months of evaluation testing being the only remaining task.

The observed performance data on the MFR Model 2 research gyros are consistent with Apollo design goals. Test results and physical characteristics are classified, but are presented in Reference 2.

b. Quartz accelerometer

The quartz accelerometer is shown schematically in Fig. IV-3, whereas Fig. IV-5 shows a physical instrument and an exploded view of the interior parts.

In the quartz accelerometer (actually fuzed silica is used) the proof mass is an electrostatically restrained fuzed silica reed. The reed is clamped between

two fuzed silica blocks which also support electrode blocks over the free area of the reed. Appropriate evaporated coatings are applied for electrodes and circuitry. The acceleration-caused deflection of the reed is sensed by a capacitance bridge and used to apply control voltages that null the deflection via the electrostatic forces. Construction is extremely simple due to techniques developed for making the reed.

Advantage is taken of the dimensional stability of fuzed silica to reduce the dimensions, and thereby the required restoring voltages (under 100 v) to an extent that semiconductor electronics can supply the necessary active circuit elements. A simple linearizing circuit is used to make the control voltage proportional to the acceleration rather than the square root of the acceleration. The linearizing circuit works on the principle that with a bias voltage V_b plus a control voltage V_c across the gap requiring the greatest electrostatic force, and $V_b - V_c$ across the other gap, the total restoring force F is:

$$F = K(V_b + V_c)^2 - K(V_b - V_c)^2 = 4KV_bV_c$$

The control voltage is also encoded to form a pulse train, each pulse of constant charge. Thus the pulse rate is proportional to control voltage and acceleration and each pulse represents a velocity increment. The program has been funded on internal research funds. Studies started in the summer of 1959, and testing of the first model started in October, 1960. Two units are currently being tested at $\pm$ 1 g and with vibration. Performance has been consistent with the first model goal (adequate for Apollo) listed in Fig. IV-3, without any proven incapabilities of reaching the ultimate goal. The preliminary encoding circuitry tests to date have been intermediate in accuracy between the two goals and circuitry more adapted to final requirements including microminiaturization, is currently being prepared for test.

2. Digital Computer

a. General features

The computer selected as being typical for Apollo operation will be fully developed at the end of 1961; it draws upon components and techniques that have reached a high degree of development at the present time. (See Ref. II-1.) The organization and structure of the computer represents the highest degree of simplicity, compactness, low power consumption and integrated fabrication methods that are attainable using magnetic core storage and silicon semiconductor logic; it is the result of a program begun in 1958 for the development of an advanced ballistic missile computer. In spite of its small size (0.40 ft^3)

weight (21 lb) and power consumption (55 W), its capacity is fully adequate for the Apollo mission. It will have a random access storage of 4096 words, accessible within 27 sec and it will perform a multiplication within 135 sec.

Although rotating magnetic drum or disc memories enjoy a high state of development, the high computing capacity required for the Apollo mission and the nature of the computations to be performed make any but a random access type memory impractical. Although the long access time of serial memories can be partly offset by judicious programming, the present uncertainty as to the exact program requirements and the requirements for programming flexibility to accommodate possible changes in guidance and navigation concepts and various missions, seemed to rule out dependence on programming sophistication for rapid access.

The requirement for non-volatile random access storage using presently developed components and techniques indicates a core storage technique. The greater part (90%) of the storage is to be used for constants and program instructions; there will be no need to write into this portion of the storage during the computation. The remainder of the memory is for temporary storage of intermediate results and provisions must be made for writing in as well as reading out. It would be desirable to include both types of storage into the same organization for simplicity and flexibility for future re-apportionment or expansion.

The storage requirements are satisfied by an array of two aperture cores consisting of 4096 22-bit words, selection being word-organized. The component and wiring economy that can be realized by bit-oriented storage is more than offset by the instrumentation problems that arise when the storage cell is used to participate in the selection process. It is felt that the additional circuitry involved in a word selection system is easier to accommodate than the problems associated with discrimination against half-selected cells and control of drive currents, especially when precise temperature control is not contemplated. A common addressing system is possible using non-destructive flux-switching interrogation.

The most important property of these components is that there is the possibility of ascertaining the state of an element without altering that state; this makes possible a non-destructive readout, so that data do not have to be regenerated in interrogated storage elements. This is an advantage in that the integrity of stored data is never jeopardized when it is read from storage as it is in destructive readout systems that require a read-write cycle for storage interrogation. This system also decreases vulnerability of stored data to temporary power failures. A common addressing system is possible for word-organized two-aperture core memories driven by fast pulses.

The division between the two portions of the memory can be made by merely disabling the write circuitry in the part that is to be used for read only, after the appropriate data have been read in. This is a more flexible arrangement

than certain types of non-destructive read systems that contain fixed information by virtue of the physical orientations of the storage cells, or the wiring interconnections between cells. In such systems, all the data pertaining to a particular mission must be wired into the computer when it is constructed; any changes must be made by interchanging physical components. A memory of 4096 words is presently considered adequate for the computation associated with all variations of the Apollo mission. Further study will probably indicate additional capacity. If this need should arise, it could be provided without disrupting the present internal organization of the computer.

The arithmetic and control portions of the computer are composed of semiconductor "or" and "and" circuits cascaded between inverting amplifiers and clock pulse strokes. Standardized individual circuits are fabricated on flat cards and are interconnected by printed wiring on large circuit cards which are interconnected through leads brought out to one edge. This type of circuitry is conventional except for the well developed fabrication techniques and the high degree of compactness that have been realized. Serial magnetostrictive delay lines are used for some arithmetic registers.

The arithmetic is performed in a serial mode at a 1 mc/sec pulse rate requiring 27 sec to complete a basic add order on two numbers stored in the appropriate arithmetic registers. Data are retrieved from storage in a parallel mode and require 27 sec for retrieval. The arithmetic and control organization is conventional except for some provisions for shortening the time required for some arithmetic instructions.

b. Organization and logical design

General. The computer operates in the serial linary synchronous mode with a clock frequency of 1 Mc/sec. It operates in conjunction with a random access magnetic core storage array of 4096 words. The storage is word selected by means of a decoding matrix driven by the address selector register; the data from a selected location being read out in parallel.

Word structure. Data are stored in units (words) of 22 bits length. A 22-bit word may represent numerical data or instructions. Numerical data are stored in binary fixed point, fractional notation. Negative numbers are represented in 2's complement form because of the serial arithmetic processing. (See Fig. IV-6.)

Instruction Code. Instruction words are 22 bits in length and are used in a single-address instruction code. Thirteen bits are reserved for the operand address; twelve are actually used to select among the 4096 storage positions. The additional bit can be used to expand the storage to twice its size if this is necessary. The operand address bits may also indicate the amount of shift in some special shift operation instructions. Five bits are used for the operation codes. There are in all 21 operations that can be programmed on the computer; these instructions span all the conventional instructions that are required to

generate sophisticated general purpose programs and include add, subtract, multiply, divide, square root, shift, read, write, transfer, conditional transfer, compare, complement, and a special write instruction to address the portion of the memory reserved for permanent data and instructions. The write addressing circuitry of a portion of the memory (3712 words) which is reserved for permanent data will be disabled during the ground checkout procedure after data has been stored and checked. With the exception of the write instruction, all instructions may address any storage location. During the mission, the write instruction will be able to address only the 384 storage locations reserved for temporary storage. There are additional temporary storage registers associated with the arithmetic unit which take care of temporary storage required during the execution of an arithmetic instruction.

Operation time. The time required for execution of a representative list of instructions is shown below:

Add, subtract	27	sec
Multiply	135	sec
Divide	324	sec
Square root	324-594	sec
Conditional transfer Write Transfer	27	sec

Arithmetic unit. The arithmetic unit consists of a conventional accumulator register for execution of fast instructions (add, subtract, etc.); a special unit for executing slow instructions ... multiply, divide, and square root ... operates independently, simultaneously and under the control of the main arithmetic unit. By means of judicious programming, this feature can be used to save computation time by eliminating or reducing the necessary interruption of the main program to execute slow instructions. Provisions are made for double or single precision.

The arithmetic and control unit circuitry consists of cascaded standard gate, inverter-amplifier, and multivibrator circuits, except for four magnetostrictive delay line units which are used for temporary storage associated with the arithmetic operations.

Storage unit. The storage unit consists of two aperture "transfluxor" ferrite magnetic cores, arranged in 128 word planes, each plane containing 32 words. The address selection system is word-oriented (see Fig. IV-7). On a read instruction, the address selector register energizes the plane and word line of

a selected word through a selection matrix, while the data in that location are read out in parallel through sense lines which thread corresponding bit locations of every word location in the storage. To detect a stored '1', the sense line detects the switching of elastic flux direction in the two legs of the small aperture (see Fig. IV-8), caused by a current pulse in the write line of all bits in a selected word. The original direction of flux is then restored by a current pulse through this sense line. Data is contained in the core by virtue of the algebraic sum of the flux in the two legs of the core surrounding the small aperture, and no amount of interrogation, as described above, will alter this. Altering this state, i.e., writing, is accomplished by driving all cores to saturation in the one state by a pulse of current through an "erase" line through the large aperture, then switching those cores that are to contain a zero into saturation in the opposite direction by the application of simultaneous current pulses through a read-write line through the small aperture and the sense line. When the core is saturated in such a direction that a subsequent pulse through the sense line can drive it out of saturation, the core contains a one; when it is saturated in the direction such that a subsequent pulse through the sense line will not alter its state of saturation, it contains a zero.

The arrangement described above has a number of significant advantages over more conventional random access core memories, which are listed below:

(1) Data are read from storage non-destructively. The state of the core is determined by whether or not it is saturated. This state may be interrogated indefinitely by switching the non-elastic flux back and forth in the two legs of the core surrounding the small aperture, without ever affecting the state of the core, regardless of the regulation of the interrogating circuit drives.

(2) The non-destructive feature has the advantage of flexibility over other non-destructive memories in which the data are wired into the circuit. Data may be read in or out of the permanent storage portion of the memory and subjected to tests at ease any time prior to the decision to disable the write address mechanism.

(3) This method of reading and writing is not dependent upon a high degree of regulation of the address selection and read-write drives, a high degree of uniformity of the BH characteristic of the cores, or any of the problems associated with signal discrimination in noise generated by half-selected cores. As a correllary to this, this system is less susceptible to variation in core characteristics due to temperature variation; cores having been operated in this mode without failure over temperature ranges of 0°C to 100°C.

The memory is divided into a 116-plane unit that is used for permanent storage, to which no write instruction can be addressed, and a 12-plane unit for temporary storage, to which both write and read instructions can be addressed. The only thing that distinguishes these two parts is that the write address mechanism for the permanent part is disabled just prior to launch.

Input-output. The input unit accepts data from the following sources:

(1) Mission program and data inserted prior to launch.

(2) Three accelerometers.

(3) Roll pitch and yaw data from the inertial platform gimbal angles.

(4) Pilot manual input data.

The mechanization of these inputs in the input unit is described below:

Mission program and data inserted prior to launch. The program and associated constants are loaded from an external tape unit. Only by external connection of this equipment to the computer can this operation be initiated. This protects the stored program against accidental modification during the mission.

At the factory, a special routine is stored in the memory which provides for the loading of program information. It contains the memory address in which the first word of the program is to be stored. By continuous address iteration, the entire program is read in sequentially through the input unit via the accumulator to the program memory. As each word is loaded, it is read back and checked against the input. If an error is detected, the memory is erased and the procedure begun anew. The end of the program loading is indicated by a stop program instruction.

Accelerometer inputs. The accelerometer output is in the form of two sinusoids whose difference frequency is proportional to acceleration. This difference frequency is integrated in time to obtain velocity by counting pulses of the difference frequency.

The accelerometer input unit (see Fig. IV-9) consists of three channels, one for each accelerometer. Each pair of accelerometer signals is converted into a sequence of difference frequency pulses that enter a circuit which synchronizes the random-epoch incoming pulses to the timing signals generated within the computer. In each channel, the synchronizer is interrogated periodically, and its output, if any, is read into a three-stage reversible counter. The first two stages have a capacity of plus or minus three counts, and the third stage identifies the sign of the sum. The accumulated count in each channel is read into the input unit accumulator 8000 times/sec, the reversible counters being reset to zero after each readout. The accumulator contains a three word magnetostrictive delay line which stores the velocity in each channel. This information recirculates in the accumulator once every three-word times (81 $\frac{1}{3}$ sec) as inputs from the three channels are sequentially added.

Gimbal angle detection. Gimbal angle information is received from three incremental pickoffs mounted on the platform. Each pickoff produces two pulse

train signals; the sum of pulses is proportional to the magnitude of the change in gimbal angle from some initial position, and the phase relationship between the pulse train determines the sign. These angles are accumulated in the input unit in a manner analogous to the way velocity data is accumulated.

Manual input data. Data read into the computer manually will include such information as star occultation times, lunar parallax angles, earth parallax angles, range data, etc. Provision will also be made for manually initiating and stopping computation, and selecting various computation routines.

Manual data inputs will be introduced into the computer from a shift register actuated by a miniature keyboard. Timing inputs will be introduced by a manually induced transfer of clock register data into an input shift register.

The output unit provides the following types of data:

(1) Analog data to the control system and to display panel.

(2) Digital data to the display panel.

(3) Miscellaneous discrete signals.

Analog data. Digital to analog conversion is performed conventionally by means of a ladder network with switch weighted d-c currents proportioned to 2^0, 2^1---into a summing amplifier. The output of the summing amplifier remains unchanged between inputs to its digital control register, representing a "zero-order-hold" condition.

Digital data. Digital data are transferred directly from the output register to the display control register.

Discrete signals. The computer provides many discrete timing signals under program control, such as engine cutoff, engine start, GSE timing signals, malfunction indication signals, etc. These outputs will be driven by solid state switches under the program control.

c. Physical description

General. Figure IV-10 shows the overall computer package, a typical wafer plane and an individual wafer.

Wafer. Various microminiature components (transistors, capacitors, diodes) will be mounted into wafers to form "and-or" gates, complementary boosters, and flip-flop wafer modules. Wafer modules (0.8" x 0.8" x 0.032") made of alumina are used in the formation of an assembly.

A wafer contains one flip-flop circuit or two 6-input "and-or" circuits or one double inverter circuit. A typical wafer is shown in Fig. IV-10.

[redacted]

Interconnection board. Twenty-four wafers form an interconnection board. The interconnection board is a 1/32 inch thick glass epoxy printed circuit board with an interconnection matrix consisting of vertical lines on one side of the board and horizontal lines on the reverse side. Plated through holes are used to make connections from one side to the other. External connection to the board is accomplished through the use of forty-eight Elco type contacts on the bottom of the board.

Assembly. Thirty interconnection boards form an assembly. Interconnection boards are spaced in a housing on 0.150 inch centers.

Memory. Memory planes are formed by the connection of 64 transfluxor strips on a printed circuit board, each strip containing 22 transfluxors conventionally wired and soldered.

Overall configuration and case design. The case structure shown in Fig. IV-10 houses the electronic assemblies, the air duct for cooling air, and provides space for wiring between assemblies. The air duct contains perforations to allow cooling requirements. The computer contains 30 assemblies protected by an aluminum housing. Three connectors external to the case provide for computer power, input signals and output signals.

Circuit reliability. The microminiature computer circuits are designed to operate correctly under the worst possible combination of component tolerances and power supply voltages. Typical component variations allowed in Arma's silicon semi-conductor circuit design are $\pm$ 10% in supply voltages, ten to one deterioration in back leakage of diodes and transistors beyond their initial high temperature requirement, 45% deterioration in transistor current gain, and $\pm$ 10% variation in resistor tolerances. This concept of design for "worst case" provides a high degree of reliability in the operation of a circuit. In the past two years, Arma has accumulated conclusive data on application of this design approach to operating computer circuitry where 12,000,000 transistor test hours and 72,000,000 diode test hours under operation were accumulated in a typical production computer. This computer was placed on life test and operated continuously without failure for over 6600 hours before the Air Force allocated it for other uses.

Logic circuitry. The basic logic chain consists of cascaded "and-or" inverter groups terminating in a flip flop. The maximum number of inverters between flip-flop retiming circuits is two, permitting up to 12 stages of "and-or" circuits. Under the worst conditions (of voltage, temperature, and circuit parameters), the maximum delay of such a logic chain is 0.3μ sec. A logical "or" is achieved by connecting the output of two or more and-1 circuits, each of which contains an "or" diode at its output.

Transfluxor storage. The microminiature flexible computer employs a transfluxor core plane memory for storage of the program and constants and for temporary storage. The transfluxor is a square-hysteresis-loop ferrite

[redacted]

core with two apertures. Arma has developed techniques to permit the use of these devices over a wide temperature range (0 - 100°C).

Magnetostrictive delay line storage. Dynamic circulating storage loops utilizing a magnetostrictive delay line have been developed by Arma for use in the microminiature flexible computer. The desirable features of this delay line are its reliability, simple construction, small size and light weight.

The magnetostrictive delay line consists of an input transducer, a coil of Ni-Span-C wire and an output transducer. The two transducers are identical in construction. Figure IV-11 indicates the input transducer connected to the line.

A current pulse is applied to the two transmitter coils whereupon a change of length occurs in opposite directions in the magnetostrictive nickel tapes. The push-pull stress pulse, resulting from the rapid change of length, causes a torsional stress pulse on the Ni-Span-C line attached to the ends of the tapes. This stress pulse travels along the line at approximately 0.115 inches per microsecond. The receiving end transmits the stress to two tapes whose mounting is similar to that of the input tapes. The output tapes pass through two coils biased by permanent magnets. These coils sense the presence of the stress pulse by the change of reluctance in the magnetostrictive ribbon. This reluctance change produces a change of flux and hence an induced voltage in the output coils.

3. Miniature Platform

A number of miniature inertial platforms were considered in selecting the alternate platform to be used in the proposed Apollo guidance system. Some of the platforms and systems investigated are presented in Table IV-3 together with the more significant platform characteristics. The Litton P-300G has been selected as typical of a miniature platform fulfilling Apollo requirements. The following discussion of the P-300G platform has been extracted from Litton's publication, number 1453 (see Ref. IV-1).

TABLE IV-3 Platform and Systems

Co.	Designation	Application	Size (ft^3)	Wt. (#)	Accuracy	Status	Remarks
Kearfott		407 missile (French)		Platform 18	600-1500 ft in 300 NM CEP	Design	Librascope builds digital computers. Also in early production on AJN-8 attitude and heading reference for B-52G. Doppler damped.
Litton	P-200	WADD Dev. WF2, W2F, A2F, F104G, CF-104, P_3V	Platform 9-1/2" dia., 14-1/2" long cyl. Plat + elec 1.1	Platform 30 Elec 22 Dig Comp 40	1 NM per hr of flt CEP	Quantity Prod	Delivered 65,600 on order, present rate 12/mo max 40/mo. Two axes gyros, jewel pivots, floated. Four gimbal geared torquers.
	P-300	WADD Dev. for Dyna-Soar type vehicles	Platform 0.225 Elec 0.2 Dig Comp 1.0	Platform 15 Elec 18.5 Dig Comp 35	1 NM per hr of flt CEP	Development	First unit delivered mid '61 Beryllium construction in components and gimbals.
	P-300G		Platform 0.225 Elec 0.2 Dig Comp 1.0	Platform 15 Elec 18.5 Dig Comp 35		Development	Same as P-300 except the two axes gyro uses gas lubricated spin motor bearings.
Minneapolis Honeywell	MIG	Centaur, Osprey	Platform 0.5 Elec 0.5	Platform 28 Elec 18	1 NM per hr of flt	Production	Four Gimbals - uses three MIG gyros and three pendulous type accelerometers.
	Sub-Miniature Platform		Plat + Elec 8" dia - 12" long cyl	Platform 16 Elec 5	1 NM per hr of flt	Development	Four gimbals - uses three MIG gyros and three miniature hinged pendulum accelerometers. Electronics mounted on end bells of basic platform package. Four gimbals. Direct drive torquers.
Nortronics	LINS			Platform 25 Elec 25 Dig Comp 60	1 NM/hr CEP	Development	Company - sponsored effort

a. General description

The inertial subsystem consists of the following major units:

(1) Inertial reference unit.

(2) Inertial reference electronics unit.

Figure IV-12 is a block diagram showing the relationships between these units.

A summary of subsystem physical characteristics is presented in Table IV-4. The environmental capabilities of the subsystem are summarized in Table IV-6.

TABLE IV-4

Inertial Subsystem Physical Characteristics

Unit	Weight Lb	Volume Cu Ft	Power Watts
Inertial Subsystem			
Reference unit	15.0	0.245	51.0*
Reference electronics unit	18.5	0.410	180.0
Total	33.5	0.655	231.0

*Note: Additional heater power of approximately 100 watts is required for normal applications.

TABLE IV-5

Inertial Subsystem Environmental Capability

(a)	Vibration and acceleration	Designed for ± 20 g linear acceleration
		± 10 g vibration
(b)	Thermal characteristics	
	Inertial reference unit	

TABLE IV-5 (cont)

Inertial Subsystem Environmental Capability

Internal operating temperature	+ 57.2 C
External cooling air temperature	+ 30 C (max)
Storage temperature limit	- 55 C to + 85 C
Electronic Units	
Operating temperature limits	- 55 C to + 71 C*
Storage temperature limits	- 62 C to + 85 C

*Cooling gas required.

b. Inertial reference unit

The inertial reference unit (P-300G), pictured in Fig. IV-13, consists of a stable element employing two floated, two-degree-of-freedom gas bearing gyros and three floated, torque-balance accelerometers supported by a set of gimbals permitting vehicle angular freedom in azimuth, pitch, and roll. The stable element can be maintained in a prescribed orientation by torquing the gimbals with angular error signals derived from the gyro pickoffs. A redundant inner roll gimbal is provided to prevent gimbal lock; this allows the vehicle complete maneuverability without affecting the stable element. A summary of P-300G characteristics is found in Table IV-6.

TABLE IV-6

Summary, P-300G Inertial Reference Unit

Basic design	Three-axis, four gimbal
Weight (pounds)	15.0
Size (inches)	6 x 6.5 x 10
Volume (cubic feet)	0.245
Power (watts)	51 (plus 100 watts for heater power)

TABLE IV-6 (cont)

Summary, P-300G Inertial Reference Unit

Gyros (G-300G)	
Number	Two
Type	Two-degree-of-freedom floated (gas spin bearings)
Size (inches)	2.1 x 2.9
Weight (pounds)	Two
Accelerometers (A-300)	
Number	Three
Type	Floated, torque-balance, non-integrating
Size (inches)	0.80 x 0.80 x 1.50
Weight (ounces)	2.6
Orientation error	Three seconds of arc
Synchro output error (per axis)	Two min of arc over $\pm$ 10°; Five min of arc full range
Servo bandwidth	40-50 cps
Acceleration	Greater than $\pm$ 20 g

c. Gyros

In a stabilized platform employing two-degree-of-freedom gyros, the gyro instrument errors are the limiting factors in stabilization accuracy (since there are no cross-coupling errors due to rotor precession). It is therefore of extreme importance that the design configuration achieve high accuracy.

The development of self-acting, gas-lubricated bearings makes it possible to improve the performance of the precision gyro by approximately one order of magnitude. Basically, the gas-lubricated bearing assembly consists of simple

sleeve bearings and thrust pads similar to the oil-lubricated bearings used on large machinery. The difference between gas and oil-lubricated bearings is that a gaseous lubricant requires a much smaller clearance between the bearing surfaces. About one-twentieth the clearance commonly used in oil-lubricated bearings is used in the gas bearing.

The significant features of a gas bearing are as follows:

(1) There are no highly stressed areas in the gas-lubricated bearing. In a ball bearing, near-point contact exists between the ball and the race; in a gas-lubricated bearing, the load is distributed over the entire bearing surface. Since the area supporting the load in the gas bearing is approximately 2000 times greater than that of the ball bearing, the surface stress in the gas bearing is reduced by a comparable amount. The reduced stress level means a significant reduction in structural creep and thereby improved day-to-day repeatability.

(2) No metal-to-metal contact occurs between the bearing surfaces once the rotor is started; therefore no bearing wear occurs during the operation of the gyro. Because excessive liquid lubricant causes mass shift, ball bearings used in a precision gyro must be run with practically no lubricant; gas-lubricated bearings, on the other hand, run in a continuous bath of lubricant - the ambient gas. So the life expectancy of the gas-lubricated bearing is virtually unlimited. For this reason, a substantial saving in overhaul time and money can be expected with the use of a gas bearing.

(3) Reduction of mechanical noise is the third significant feature of the gas-lubricated bearing. In a ball bearing, small irregularities in the balls and races cause appreciable mechanical vibration; in a gas bearing, the bearing load is distributed over a large area, and small irregularities in the bearing surface do not cause relative movement of the bearing and journal centers. Reduction in vibration means a reduction in drift due to torque-rectification.

(4) The thermal conductivity through a gas-lubricated bearing is much greater than that through an equivalent ball bearing because of the much greater surface area of the gas bearing. Consequently, the temperature distribution over the float will be much more uniform with a gas bearing. Thermal gradients are therefore minimized.

A summary of design parameters for the G-300G gyro is given in Table IV-7. (See Fig. IV-14.)

TABLE IV-7

Model G-300G Gyro Specifications

Performance	
Random drift rate	0.005 to 0.001 deg/hr
Mass unbalance	0.01 deg/hr/g
Anisoelasticity	0.003 deg/hr/g^2
Maximum torquing rate	3000 deg/hr
Operating life	20,000 hr
Mechanical	
Fully floated instrument	
Degrees of freedom	Two
Angular momentum	0.7 x 10^6 gm-cm^2/sec
Size	2.1 in. by 2.9 in.
Weight	2.0 lb
Electrical motor	
Voltage (line-to-line running)	52 v
Frequency	400 cps $\pm$ 0.01%
Synchronous speed	24,000 rpm
Power/phase (running)	1.0 w
Runup time (65 volts line-to-line)	1.0 min (maximum)

TABLE IV-7 (cont)

Model G-300G Gyro Specifications

Pickoff (each axis)	
Excitation voltage	15 v
Excitation frequency	5000 cps
Excitation power	0.070 w
Output scale factor	100 v/rad
Torquer (each axis)	
Scale factor	30 deg/hr/ma
Nonlinearity	0.005%

d. Accelerometers

The accelerometer for the P-300G Inertial Reference Unit is denoted A-300. A-300 is a miniature, single axis, torque balance, pendulous type accelerometer.

The sensitive element is a floated pendulum mounted on a pair of jewel-and-pivot bearings and equipped with an electromagnetic pickoff and torquer. The sensitive axis of the instrument is perpendicular to both the pivot axis and to the line joining the center of mass and the center of buoyancy; hence, an acceleration along the sensitive axis results in a torque acting upon the floated pendulum which tends to rotate the pendulum about the pivot axis. This rotation, however, is immediately sensed by the pickoff which generates a signal to control the accelerometer torquer current by means of an external amplifier in such a way that the pickoff signal is continuously maintained at a null. As a result, the current through the torquer coils becomes a precise measure of the applied acceleration. The high pickoff sensitivity and restoring amplifier gain keep the relative rotation of the pendulum with respect to the case limited to a small fraction of a milliradian even in the presence of maximum acceleration. As a result, the directional accuracy of the sensitive axis is maintained, and cross-coupling effects are negligible. A calibrated precision resistor, mounted externally to the instrument, converts the torquer current to a voltage that is a precise measure of acceleration. This voltage is applied to the input of the digital conversion circuit. (See Fig. IV-15.)

Design characteristics of the A-300 miniature accelerature accelerometer are summarized in Table IV-8.

TABLE IV-8

Characteristics of Accelerometer Model A-300

Size	0.80 x 0.80 x 1.50 inches
Volume	0.825 cu in.
Weight	2.6 oz
Orientation Error	3 seconds of arc
Pickoff excitation	15 v rms at 5000 cps
Pickoff power	50 mw
Torquer scale factor	2.0 ma per g
Maximum acceleration	Greater than $\pm$ 20 g
Threshold acceleration	Less than 2×10^{-5} g
Bias uncertainty	2×10^{-5} g
Nonlinearity and scale factor	2×10^{-5} of applied acceleration

e. Gimbal system

The gimbal system for the inertial reference unit employs a four-gimbal, three-axes configuration, including one redundant gimbal to eliminate the possibility of gimbal lock during vehicle maneuvers. The azimuth, pitch, and outer roll gimbals have unlimited freedom about their respective axes, but the inner roll gimbal is limited to $\pm$ 20 degrees of freedom. The resultant system, when servo-stabilized, allows unlimited maneuverability of the carrier vehicle. In the P-300G inertial reference gimbal system, the signal generators and torquer motors are direct drive, gearless units. This arrangement permits higher angular output accuracy within minimum size and without the need for special, low-backlash gearing in the case of the signal generators. The torquer motors approach the high efficiency of geared units by proper design and application of the direct drive components.

f. Thermal control

Although the gyros and accelerometers are designed to function over a wide temperature range, the operating temperature of these instruments must be

held nearly constant in order to achieve highest accuracy. A nearly constant instrument operating temperature is achieved by maintaining the platform housing interior to within 1.6° C of an average temperature of 57.2°C, and by using film heaters to maintain the instruments within 0.5°C of an average temperature of 71° C. Since total dissipation of the instruments and gimbal components is small, accurate temperature control is possible with a minimum of heating and cooling equipment.

g. Electronics

The inertial data subsystem electronics unit contains all the circuitry necessary for operation of the inertial reference unit and for communication with a digital computer. It consists essentially of electronic circuitry mounted on etched circuit boards which, in turn, are mounted on heat sinks that provide good heat paths to the case walls.

The inertial reference electronics unit contains the gimbal servo amplifiers, accelerometer restoring amplifiers, redundant azimuth gyro axis caging amplifier, the various power supplies for the subsystem, platform temperature control circuits, the digital converter and various switching functions.

The digital converter contains the analog-to-digital conversion circuits for converting accelerometer analog outputs to binary incremental velocity data for a digital computer, the precision gyro pulse torquing circuits that are controlled by torquing commands from a digital computer, and the emergency pendulous leveling circuits for the platform.

The circuitry in the reference electronics unit is based on extensive use of d-c amplification. This approach greatly reduces the number of bulky elements such as transformers and coupling-capacitors and, therefore, permits a higher density of packaging. The direct drive gimbal torquer is an ideal component for use with d-c amplifiers, permitting a reduction on the order of one-third of the number of components required in platform servo amplifiers driving conventional, geared a-c torquers. Use of d-c amplifiers must be carefully controlled, however, to minimize system errors caused by amplifier drift. This requirement has been satisfied for the electronics units used with the P-300G platform.

h. Development status

The P-300 (a ball bearing gyro version of the above system) is in the advanced stages of development and the first unit is scheduled for delivery in July, 1961. The gas bearing gyros are nearing final development and platforms that will incorporate these gyros could be delivered in 12 to 18 months after July, 1961.

4. Telesextant

The following description of the telesextant is based on the requirements and specifications generated by The Martin Company and outlined in Section IV-D-4. This description is derived from a proposal by Kollsman Instrument Corporation (See Ref. IV-2), modified primarily in nomenclature (e.g., telesextant is a Martin designation) and in the omission of irrelevant material.

a. Introduction

This section describes the Kollsman Instrument Corporation's approach to the design and development of a telesextant. As may be inferred from its designation, this instrument is essentially a precision theodolite, equipped with a sextant attachment and provided with an additional degree of freedom about the theodolite line of sight. In addition, a cursor is provided for the measurement of lunar occultations.

The telesextant enables the astronaut to employ semiautomatic and manual operational procedures in the following navigational modes:

(1) Sextant - through the measurement of sextant angles between selected stars and specific lunar features (e.g., craters).

(2) Stadiometry - through the measurement of apparent earth and lunar diameters (during the various applicable phases of flight).

(3) Occultation correlation - through the measurement of time and the location of lunar occultations.

A detailed description of the equipment operation during the navigation modes is presented later in this section.

The design of this instrument is planned to permit the efficient participation of an astronaut in the navigation of a spacecraft. Such participation is deemed essential for the following basic reasons:

(1) Human capabilities in the performance of particular functions are superior to those of automatic equipment (e.g., occultation detection).

(2) Psychological considerations suggest the involvement of the astronaut within the overall navigational scheme.

A block diagram representative of the complete navigational system (with emergency equipment omitted) is presented in Fig. IV-16. Functionally, the telesextant is integrated within this scheme to fulfill the following requirements:

(1) The unit can serve as a primary source of celestial coordinate inputs to the navigation system for establishing lines, or surfaces, of position along the trajectory.

(2) In the event of malfunctions within the automatic astro-inertial measuring unit, the astronaut is able to provide the required celestial navigation data to the central digital computer.

(3) In the event of complete or partial power failure, the derived celestial navigation data can be read by the astronaut and employed (in conjunction with precomputed data) to calculate the necessary navigational information.

(4) The astronaut is provided with monitoring capabilities over the automatic astrotracker in that he can observe the inputs to the automatic astro-inertial navigational system.

An additional feature of the described equipment, not explicitly specified as a requirement, permits it to function as a theodolite. The resulting ability of the equipment to relate celestially referenced data with the spacecraft's axes (through elevation and bearing angles) makes it possible to align initially both the primary and secondary inertial platforms.

The design of the instrument is influenced by the limitations of human capabilities as well as the size and weight restrictions imposed on the spacecraft equipment. As discussed in greater detail later, the effects of weightlessness, body motion, fatigue and visual acuity must be all considered in the choice of parameters for the final equipment configuration. However, much remains to be learned regarding the optimum integration of human and automatic equipment functions. (Significant human-factor investigations are contemplated within the basic design and development phase of the program.) Some of the conclusions and recommendations presented in this document are based upon a limited, but significant, number of human-factor experiments conducted at the facilities of the Kollsman Instrument Corporation. It is expected that these efforts will be expanded and coordinated with data derived from the cognizant industrial and governmental organizations.

The telesextant, described in the major portion of this document, does not represent a finalized configuration. Instead, it is a representative approach of the design of semiautomatic and manual equipment. It embodies extensive experience in three principal regimes--the development of sophisticated optical equipment, the development of advanced electromechanical equipment, and the development of equipment engineered for human operation.

b. Equipment description

(1) Prime equipment

The complete navigational instrument is comprised of three separate units. They are the telesextant, the electronics unit, and the remote control equipment. The telesextant, depicted in Fig. IV-17, has, as its design objective, a weight of approximately 20 pounds and a volume of about one cubic foot. The electronics unit is estimated to weigh approximately 3-1/2 pounds and occupy a volume of about 0.1 cubic feet. The remote control equipment is given only functional coverage in this document because it is believed that the controls will be integrated within other equipment receiving adjustments by the astronaut.

For descriptive purposes the instrument has been broken down into the following categories: electromechanical, optical and electronic equipment.

(a) Electromechanical description

The telesextant comprises all of the optical and electromechanical components that are required for the automatic and manual drive, as well as the readout of the five significant angles whose geometric relationships are depicted in Fig. IV-17. As will be described later, all required outputs for the various navigational modes are obtained from the precision measurement of specific combinations of these angles. Stabilization of the instrument against motion relative to the required sighting points is accomplished in a number of automatic and aided modes, as described fully later.

The telesextant's sub-base will be the male part of a Tribrach-type kinematic mount, consisting of three hemispherical surfaces 120° apart at a radius of approximately 4 inches. When the instrument is in its working position at the overhead vehicle window, the three spherical surfaces of the Tribrach will mate with three female fittings (at about 8 inches diameter) in a right-angle bracket fixed to the vehicle wall alongside the window. The three fittings and their adjustments will permit aligning the telesextant to the reference axis of the capsule; the kinematic nature of the mounting will permit repetitive positioning of the instrument within seconds of arc.

While in use, the instrument is retained against its mount by a nondeforming spring clamp. When not in use the instrument may be unclamped from its mount (single lever) and slid along a guiding track to a compartment alongside the window - leaving the window clear for observation. In its closed storage compartment, the instrument is protected from the acceleration force of launching and from accidental contact with crew members.

The electromechanical equipment associated with the telesextant is shown in Fig. IV-18. The five angular settings are equipped with manual drives and optical readouts. In addition, all drives except that associated with the cursor are also provided with the electromechanical rotary components required for the various stabilization modes.

A precision resolver is mounted upon each shaft. For automatic readout purposes, one winding of the resolver is excited by a reference voltage. The resulting output is representative of the angular position of the shaft. When it is desired to slave the shaft to a remote source, the resolver serves as a position receiver and error readout.

Each shaft also provides the mounting for a drive motor, rate generator, clutch and gearing. The motor provides the driving function for remote control signals. The rate generator is employed for stability purposes, and the clutch is used to disable the manual drive during the various powered stabilization modes.

(b) Optical description

The optical system shown in Fig. IV-19 combines conventional theodolite techniques with the following:

(1) A dual-objective system.

(2) A unique sextant feature.

(3) A long focal-length, precision, pointing telescope.

(4) An erect-viewing, multiple-function eyepiece.

(5) A wide-field view finder.

(i) Dual objective system

The main, or theodolite, objective is an adaptation of the Maksutov concentric corrector to a Cassegrainian type system. This arrangement compacts a 34-inch focal length into an overall length of 6 inches. The aperture's outside diameter is 2-1/4 inches, with a central obscuration of 1/2 inch; and the field covered is 1° or more.

Parallel to the theodolite telescope is a finder telescope, whose objective consists of a negative front component followed by a positive component. It provides approximately 10° of field coverage, with the principal ray directed over a focal area equal to that of the main objective.

This makes the two objectives compatible to the same erecting and eyepiece system. The two objective lenses are alternately placed in the path of the viewing system by means of a switching prism arrangement in the finder objective path.

(ii) Sextant optics

The sextant system is an array of three mirrors; two are rigidly mounted to the sextant body and one rotates about an axis transverse to the line of sight to

effect the sextant angle. The sextant body can rotate about the theodolite optical axis to effect the polar angle.

Nominally, the planes of the three mirrors cross the optical axes at an angle of 45° and are parallel to each other. Of the two rigidly mounted mirrors, one is in the finder optical path and the other is in the theodolite path. The third sextant mirror is in the path reflected by the other two.

The unique mirror of the group is the one in the theodolite path. It is aluminized in a zone of approximately 1-1/4-inch outside diameter by 1/2-inch inside diameter. These dimensions are chosen to secure the correct balance in brightness between the main theodolite view and the sextant view in both the main objective and the finder objective.

This arrangement utilizes the outer portion of the main objective for the theodolite view and the inner portion of it for the sextant view. During the theodolite situation the inner zone of the finder view is used, but during the sextant situation the central hole of the finder view is used.

The fixed brightness balance, built in by the apportioning of the apertures, is nominally correct, but under certain conditions it must be modified to suit the operator. Therefore, a "dimmer" device is incorporated in the region of the aperture to permit control of the flux entering either the sextant or the theodolite. The assignment of the inner zone of the aperture to the sextant function has the virtue of making the dimmer device as small as possible. A variable diaphragm is a preferred type of dimmer because it does not introduce any refractive effects which could reduce accuracy.

(iii) Reticle system

There are two reticles in the system; one is affixed to the main telescope and the other can be manually rotated.

The fixed reticle is used against a dark field for pointing to stars. To illuminate this reticle, and at the same time avoid obscuring weak stars, it will be projected into the system with a beam splitter. Its pattern will be a solid line perpendicular to the sextant mirror axis and a broken line parallel to this axis. Thus, as the sextant angle is changed the image of a target will be moved along the solid line, and the broken line will mark the reading point of this movement.

The manually rotative reticle, or cursor, will be composed of a radial double line with a scale for reading its rotation about the center of the field. This reticle will contain opaque lines physically located in the focal plane. This type of reticle is always used in an illuminated field.

(iv) Viewing optics

The viewing optics consist of an erecting relay, a fixed 90° deviation prism and an eyepiece. This viewing system is common to the main telescope, the finder telescope and the microscopic readings of the sextant and polar angles. Transferring functions will be accomplished by switching prisms or mirrors. A 60° apparent field, with an approximately 3/4-inch eye relief, can be provided.

(v) Readout optics

The optical systems for reading the sextant and theodolite scales are not shown because of their complexity. As mentioned previously, the sextant and polar angle readout will be switched into the main viewing system. A system which provides simultaneous readout from opposite points on each scale will be provided. This will include a fine reading to one second of arc on both angles.

The theodolite angles of elevation and bearing will be separately and similarly readout through a second eyepiece located alongside the main eyepiece.

The main, or theodolite, telescope is centrally pivoted with respect to the window to command a conical solid angle of view. For an 18-inch window, this cone is a full 70° ($\pm$ 35°).

The sextant angle is also capable of commanding a full cone of 70°. Because the polar angle enjoys 360° of freedom, the sextant mirror can always be placed so that its line of sight is across the theodolite line of sight. This permits any combination of theodolite and sextant angles, up to 60° of incidence to the window, to be achieved without vignetting effects.

(vi) Window consideration

The optical window of a manned space vehicle ordinarily becomes a boundary separating two media of different temperature, pressure and refraction index when the vehicle is in space. Specifically, these media are a vacuum and a life-supporting atmosphere. The effects of these different factors upon the performance of precise optical measurements, such as those of the telesextant, must be very carefully considered. By far the most influential factor is the change of index, which directly contributes to shifting of the line of sight. The effect of a pressure difference upon window bending or distortion is of lesser concern, and the loss of heat through the window will have a more indirect and controllable effect upon the line of sight.

Optical windows may be classified as flat, concentric-spherical or hybrids of these two types.

The flat, parallel window is ideal optically when the optical properties of the medium on both sides are identical. Figure IV-20 shows the errors which

result by using a flat window to separate 20° C air of one sea level atmosphere from a vacuum. The deviation of the line of sight as a function of the angle of incidence goes up to 100 seconds of arc at 60° angle of incidence.

The use of a dome-shaped window bypasses this problem of pointing error if all axes of rotation intersect at the center of the dome. Under these conditions, the dome becomes a weak lens on the optical axis of the system for all pointing directions, and its effect is simply included in the optical design. The requirement that all axes of rotation pass through the center of the dome is extremely critical and not feasible for the preliminary design configuration under discussion.

The telesextant configuration includes one axis which cannot be close to intersection with the other three. This is the axis of the sextant angle. To articulate the sextant mirror to permit the sextant sight line to pass through the center of the dome, the mirror rotation center would have to be located completely outside the structure of the instrument.

Several approaches may be taken to contend with the refraction error across a flat window. One is the computation of a correction for application to the observed sighting angle. The presence of a resolver on each of the theodolite-sextant axes offers the convenience of a "resolver chain" solution in making the corrections to either the theodolite or sextant lines of sight. An extension of this approach would be the automatic application of these corrections by the control of variable wedges in the lines of sight. The instrument sighting angles may then be read out and utilized without further correction.

An alternative method of computing the refraction correction lies in the use of the central digital computer. Automatic compensation of observed sighting angles is again possible.

An entirely different approach, which eliminates the necessity for computation of the angles of incidence to the window (and also overcomes the objections to a dome window), is provided by putting an inverse glass dome between the operator and the eyepiece. This dome, in combination with a plain flat window on the vehicle wall, would then form the ends of an enclosure which could be evacuated by permitting the air to leak out through a valve into space. When this is accomplished, refraction effects at the flat window are entirely eliminated. The dome poses no accuracy problem because it functions as an atmosphere separator in a non-critical viewing space.

The inset in Fig. IV-19 shows the modification of the viewing system required to provide a suitable eye position with respect to the dome. The enforced hands-off operation which results is normally an advantage. For manual emergency operation, the dome can be removed. This would be accomplished by admitting vehicle air into the enclosure by valves in such a manner to prevent direct bleeding of air from the cabin into outer space.

An additional consideration in window design is the prevention of direct sunlight onto or through the window glass, particularly when viewing very dim stars. Such sunlight will tend to be scattered by internal imperfections or scratches upon the glass and, although the scattering points are not imaged on the retina, the extra light will tend to reduce star contrast.

Kollsman has estimated the effect of such stray light upon automatic tracking equipment. Some additional study will be required to determine whether the limitations upon vision are of equivalent significance. It is interesting to note that if a larger meteoritic particle (an infrequent occurrence) produces a major mark on the outer window surface, a readjustment of vehicle attitude can be called for to enable a different portion of the window to be used. In such cases a human operator's powers of inspection and decision are clearly an advantage over automatic equipment.

Thermal shock can sometimes be a problem for glass windows. This is effectively taken care of by use of quartz or 96% silica (Vycor) windows. These materials are practically dictated in spite of their higher cost. Vycor is superior to quartz because it has greater freedom from bubbles and is less expensive.

(c) Electronics

Electronic designs are based on the use of solid state elements and incorporate designs which assure maximum reliability at high efficiency. For instance, the circuitry makes extensive use of transistors as switches in which modulation is accomplished by pulse-width control. Experience has been that transistors used in this manner exhibit high reliability and maximum power efficiency. Wherever feasible, redundant elements are designed into the circuitry to assure highest reliability.

(2) Special test equipment

The telesextant can be tested by well known and conclusive checking procedures involving only simple auxiliary equipment.

With this design, a rotation of 180° can be performed about all four axes of rotation. This enables the user to test for the zero readings of scales and collimation of optics. All scales will be read from two opposite points to eliminate scale eccentricity errors. Scales themselves will be completely certified and can be taken as immutable.

The one unusual feature of the testing will be the necessity of performing all tests with the equipment in each of the two opposite attitudes of mounting. This is necessary because the effects (if any) of gravity must be averaged out to give accurate results in the neutral gravity of space.

The principal item of equipment for performing these tests will be a Tribrach collimator stand, either purchased complete or designed and built at Kollsman. Equipment will also be needed to read out the digital encoders and shaft angle resolvers for comparison to the manual readout scales. This equipment will be designed and built at Kollsman using standard components.

c. Operating characteristics

For reference, the significant operating characteristics are compiled in Table IV-9. The automatic readout tabulation refers to the precision resolver outputs for subsequent conversion to digital form. (The conversion equipment is not considered within the scope of the document.)

d. Design considerations

(1) External factors

(a) General

The telesextant will be used to observe objects (celestial, terrestial and lunar) from a position in cislunar space. Because such observation varies considerably from an observation from within the earth's atmosphere, it is important that this difference be given special consideration.

The earth-based astronomical observation most resembling that of the spaceborne telesextant is the extrameridian observations of the astronomer's altazimuth (with perhaps a 5-inch aperture) and its smaller version, the precision theodolite. The more precise instruments have accuracies approaching 0.1 second of arc. These accuracies are rarely achievable because "good seeing" (clear, calm, uniform-temperature air) is never good enough. Image motion and scintillation, due to atmospheric turbulence and variation in index of refraction, bring about deviations which are a function of the seeing disc, e.g., 10 seconds of arc seeing disc for scale number zero. (See J.O.S.A., v44, No. 4, Comparison of Stellar Scintillation with Image Motion-Roger Hosfeld).

The spaceborne telesextant will be free of these errors because there is no air in space. Furthermore, the accuracy of pointing will be significantly improved because of greater target clarity.

Cislunar observations will result in an absence of atmospheric optical noise. At least 45% of the night-sky brightness (extraneous light) is due to airglow. Cislunar viewing provides increased sky-star contrast. The cislunar sky is blacker than that of earth. Absence of air will also increase star magnitude over terrestial observation by 0.25 magnitude for a zenith star, and by 0.50 magnitude for a star at 30° altitude.

TABLE IV-9

Function	Measured Angles	Automatic Readout Accuracy	Manual Readout Accuracy	Required Stabilization	Field	Operation Angular Limitations
Theodolite Operation	Elevation Bearing	10 arc sec 10 arc sec	1 arc sec 1 arc sec	Elevation Bearing	1° Finder 10°	35° half angle cone
Sextant Operation	Sextant Angle	20 arc sec *	2 arc sec *	Elevation Bearing Polar Angle	1° Finder 10°	± 35°
Stadiametric Measurement	Sextant Angle	20 arc sec *	2 arc sec *	Elevation Bearing Polar Angle (Drive)	1° Finder 10°	70° Diameter
Occultation Measurement	Sextant Angle	20 arc sec *	2 arc sec *	Elevation Bearing	1° Finder 10°	± 35° between star and crater
	Occultation Reticle		1 arc min	Sextant Angle (Drive) Polar Angle (Drive)		Occultation Angle 360°

* Sextant angle is twice the readout angle

Telesextant Operating Characteristics

Space viewing is also free of atmospheric refractions. This will cause an apparent error in a star's observed position that may range as high as 35 minutes at the horizon to 1 minute at 45° altitude. Almost all astronomical observations require that barometric and temperature readings be taken to compute the atmospheric refraction error.

These viewing factors will contribute to increasing accuracy and they need no longer be considered.

Space vehicle viewing, however, introduces another group of conditions that affect accuracy. The apparent position of a star is influenced by the observer's velocity at right angles to the true direction of the star. This phenomenon is known as the aberration of light. On earth, the star's apparent difference in position is due to the velocity of the earth in its orbit (18.5 mps). The maximum for a star at right angles to the earth's motion is the constant of aberration will be 26.6% greater than for the terrestial observer; at 5 earth radii (12%).

(b) Occultation

By the accurate observation of the occultation of a star by the moon, an observer in cislunar space can determine a fine line of position. Combining this information with stadiametric information the observer should be able to fix his point of observation along this line, and thus to know his position in the space between the earth and moon.

The occultation observation should include the actual time within 1/10 second and the point of immersion or emersion relative to the lunar coordinates. The observer must refer this data to the lunar ephemerides, taking into consideration whether the observation is true, apparent or astrographic.

As the moon moves in its earth-perturbed orbit around the sun, it carries a "shadow cylinder" for every star in the universe (in reality cones with negligible apex angles). The diameter of each of these cylinders is the same: 2,160 miles. Any motion of the observer or the moon which changes the direction of the moon-observer axis (with respect to celestial coordinates) will cause the observer to enter new shadow cylinders and to emerge from others.

The most favorable conditions the observer will be able to perceive will be the immersion and emersion of the occulted stars under the following four conditions:

(1) The immersion of a star along a path into the dark limb of the moon.

(2) The emersion of a star along a path from the dark limb.

(3) and (4) The emersion and immersion with respect to the bright limb. However, at the bright limb there is a penalty of three magnitudes, e.g., an emersion at the bright limb would require a seventh

an emersion at the bright limb would require a seventh magnitude star for equivalent accuracy.

The rate of observable star occultations, i.e., the number of stars disappearing and reappearing per unit of time, is a function of:

(1) The subtense solid angle of the moon (or earth)(see Fig. IV-21)

(2) The angular speed of the moon-observer axis with respect to the celestial coordinates.

(3) The density of the observable star population in the direction of the moon (or earth).

For example: consider the frequency of the possible observations of immersions of 10th magnitude stars from the vicinity of the earth. At the earth-moon distance, the moon subtends a solid angle of approximately 0.2 degrees^2. The moon in its eastward motion about the earth moves about 1/2 second of arc per second or 1° per two hours. Therefore, it sweeps a 1° solid angle in four hours. Thus, one star of 10th magnitude (or dimmer) will be occulted every four hours. Of course, the stars are not evenly distributed, and this calculation applies for a region of average density. If, for example, the moon was passing through the Beehive in Cancer, the frequency would be much greater.

This sample calculation of frequency of occultation by the moon observed from the vicinity of the earth is almost the worst case. As the observer moves closer to the moon the angle subtense of the occultating body will increase inversely as the distance. The angular speed will also increase inversely with the distance (for equal motion traverse to the moon-observer) axis. Therefore halfway to the moon the occulation frequency would be on the order of four times the above or once every hour.

(c) Earth and moon surface features

As seen through a spaceborne telesextant, the surtaces of the earth and moon present a set of mapped features which are sufficiently distinct to serve as reference points for star-to-earth or star-to-moon sextant sightings. Because these bodies are spherical, the features most useful as targets are essentially those on the nearest 10% of the surface.

In the case of the earth, the atmosphere significantly degrades the accuracy of any sight to earth landmarks in the same way that celestial references are degraded for astronomers on the earth. Furthermore, earth targets are subject to the obscuration of cloud layers. The availability of reference targets must therefore be investigated.

Lunar observations, however, are favored by the best of "good seeing". The lunar targets for accurate visual reference are also abundant. A rough estimate of the number of craters larger than some diameter d (if d is less than 200 km) on the visible hemisphere of the moon is given by the formula:

$$N = \frac{300,000}{d^2};\ (d \text{ in kilometers})$$

Craters which are convenient as targets, insofar as both recognizability and subtense angle are concerned, can be considered to subtend about one arc-minute as seen by the theodolite-sextant viewer. Taking the magnification of 30 into account to give an actual subtense of 2 arc-seconds and assuming an earth-moon viewing distance, the craters of interest may be estimated to have diameters of 2 to 4 km. By formula, then, some 50,000 craters are available.

It might be well to consider these 2-second subtense craters with the resolving power of terrestrial techniques (for reference, see Gerard P. Kuiper, Symposium on Space Physics, April 1959). In the best existing photographs lunar details down to 0.4 seconds of arc (0.4 mile) are resolvable at the center of the disc. With visual observatory telescopes under ideal conditions of "good seeing", it is possible to resolve 0.1 second of arc.

The preceding consideration of resolving power is based upon ideal terrestrial observation of lunar targets under their best illumination. Lunar references are subject to change of illumination and contrast through change of phase. At 0° phase or full moon, the contrast is least. Although at later phases the craters and mountains along the terminator sometimes offer the best targets, the terminator moves across the moon at about 10 mph or 10 seconds of arc/sec (seen from the earth). Hence, for the sunset terminator, adequate time must be allowed for the observation.

The brightness of details on the dark portion of the moon as seen from earth can be 10 times the brightness of the earth's surface in the light of the full moon. At this level of illumination, details are not revealed with sufficient contrast to permit accurate pointing, but from cislunar space they can serve as coarse references.

(d) Use of earth airglow

The phenomenon of airglow may be utilized as a visual reference for earth diameter measurement. From viewing distances of 100 miles and beyond, the visual constituents of the airglow will be seen as an outer shell of the earth's atmosphere for both the day and night portions of the earth.

The most noticeable and persistent component is the 5577A° (green) line of atomic oxygen, which emanates from a layer of the ionosphere in the region of 56 to 62 miles. When averaged around the whole rim of the earth's disc, the center of this layer should be discernible to about 2 miles.

Although the brightness of the green airglow component is near the limit of vision for an earthbound observer, the viewer from a space vehicle enjoys several advantages. First, he looks edgewise at the shell rather than through it. Second, he is not hampered by the attenuating effect of the earth's atmosphere; and, finally, he sees the glow in contrast to the blackness of outer space.

Kollsman has been conducting an extensive literature search of the line and continuum intensities of the airglow and will continue to evaluate its utility for defining the earth horizon by automatic and visual means. Based upon this work, Kollsman feels that stadiametric measurements by means of airglow are quite feasible for an Apollo vehicle.

(e) Lunar limb

Reference to the limb of the moon for determination of the center of the moon or its diameter by the method used in the telesextant should be a fairly sensitive and accurate process. The lunar topography is such that mountain ranges and crater walls commonly have altitudes as high as 20,000 feet, or roughly four miles. Even at earth-moon distance, these heights subtend 4 seconds of arc. Through the telesextant telescope they subtend more than 2 minutes of arc. The observer using the rotating tangent of the crosshair should be able to average the apparent position of the limb within one-half of this or within 2 seconds of arc or better.

(2) Human factors considerations

The adoption of theodolite-sextant techniques for desired navigational observations of celestial bodies or targets will reduce the equipment complexity and will assure the success of precise angular measurement. The precision and simplicity afforded by the telesextant when it is trained on a complex target (e.g., the crescent of the moon or its features) cannot be duplicated by entirely automatic tracking and logic techniques. Careful attention to human factors will assure that the full advantage of human participation will be realized.

Natural movement patterns, powered assistance and visual aids were essential design features adapted to prevent: tediousness of adjustment and readout; effect of body and instrument motion upon measurements; insufficient brightness and contrast for target comparison; excessive brightness and contrast for dark adaptation; operator overload; and weightlessness.

(a) Natural movement patterns

The most essential step in the provision of natural movement patterns is the placement of the operator, his instrument, the controls and the target in a direct and familiar geometrical relationship. Ideally, the operator should be able to look "through" his instrument toward the target. Up-down or right-left target errors can then be seen in terms of the operator's own reference frame.

In the case of a window location, other than one directly in front of the operator, only a small compromise on the ideal geometry is necessary. Using a right-angle eyepiece, for instance, will enable the operator to sight through an overhead window with comfort.

The up-down, etc., errors of the instrument can be made to appear as up-down, etc., errors of the operator, if an "erect" image of the target appears through the internal optics. The operator normally controls the instrument by knobs, which are affixed to his station panel and which can easily be given the necessary up-down, etc., orientation with respect to the operator.

The resulting up-down control of the image or target is achieved by a drive rotation about the elevation axis. In the overhead configuration shown in Fig. IV-19, this same control will result in a fore-aft swing of the eyepiece with respect to the operator's head. This one point of compromise will mean little during the actual tracking and mensuration of targets because the amount and rate of instrument motion are small. Only during the initial setup, when the operator may prefer to point the instrument by hand through large angles (or when he must resort to hand control during power failure), will the natural movement pattern be violated with an overhead or other nonfrontal window.

(b) Powered assistance

The operating techniques consist of two types of action: aligning the target with respect to a second target or reticle line, and reading of scales. Manipulating the reticle line depends upon the mode in which the telesextant is employed. Several dimensions of adjustment are involved, as discussed under "Equipment Operation" section.

A powered assist in the form of remote rate and displacement controls for each axis is therefore provided to relieve further the operator's loading and thereby to increase the man-instrument accuracy. The remote control feature also protects the instrument from the inadvertent disturbances that are associated with direct hand control.

For theodolite tracking of a star, the two dimensions of up-down and right-left are monitored by control of the elevation and bearing axes, respectively. The need for such tracking is introduced by:

(1) Angular drift of the vehicle in inertial space.

(2) The effects of operator and instrument motions upon the vehicle angular position.

Because of the relatively high vehicle moment of inertia, the effects of (2) will be small. However, as a precaution, the movements of the operator are held to a minimum by virtue of equipment design. All functions, except the readout of theodolite angles, are accomplished using one major eyepiece.

[redacted]

All angular drift to be tracked is essentially constant and is easily accommodated by a rate control (offering a linear relation between axis speed and knob displacement). It is assumed that the attitude drift rate is of the order of one minute of arc per second, or less, and that corrective maneuvers in attitude are withheld during the critical portion of the shot.

Thus, with drift rates effectively cancelled, it is necessary only to adjust the position of the crosshairs by the occasional use of the displacement knob. In the discussion of operation, it will be shown how these displacement adjustments can be sequenced to permit time-sharing with other adjustments.

The elevation and bearing axes drives are employed in all four operating modes (theodolite, sextant, occultation and stadiametric). They assist the instrument's primary optical axis to track the target. In theodolite, sextant and occultation procedures, this target is a star. From a human engineering viewpoint, a starlike target is an ideal reference for two-dimensional tracking by crosshairs.

It will be recognized that the foregoing method of powered assistance is nearly identical to that exploited for tracking by bomb and gunsights from an airborne platform. Although still on a floating platform, the present application benefits over the latter by experiencing nearly constant rates. This fact coupled with the higher optical power of the theodolite-sextant, affords the human operator conditions equivalent to those of an earth-embedded, high quality theodolite.

The polar and sextant axes are similarly equipped with rate-aided drives. Their use in connection with occultation measurements is explained later in the discussion on operation. A special case of fixed rate drive is employed in the stadiametric mode.

(c) Viewing aids

Viewing aids may be considered here to consist of a suitable trade-off of telescope parameters together with various conveniences which further assist the operator's viewing action.

Earlier sections of this report have detailed the preliminary choice of telescope parameters, such as power, field and eye relief. A magnification of 34 assures the discernment of one arc-second in the positioning of targets on the reticle. Because of the small field which necessarily accompanies such high power (1°), a finder telescope is incorporated whose wider field (10°) will greatly facilitate the initial acquisition of targets. Fortunately, the vehicle presents a much more benign vibration environment than an aircraft, and no special provisions for large eye relief and exit pupil are needed. Excessively sized optics are thus obviated.

[redacted]

Other viewing conveniences of importance are:

(1) Dimmer control which gives the operator control over the contrast of targets seen simultaneously, such as star and moon. This feature prevents washout of a weak star by earth or moon light and prevents the high relative brightness of the latter (as seen through the telescope) from momentarily fatiguing the photopic vision (central field of eye where detail is resolved). Special use of the dimmer is made in stadiametric measurements.

(2) Common eyepiece for primary and finder telescopes, together with polar and sextant scale readings.

(3) Nonopaque reticle lines for matching to dim stars.

(4) Use of center of telescope field for all critical settings to minimize the eye movement necessary to keep critical points within the eye's field of acuity. Some deviation from this rule is required for occultation shots, but reticle matching is less critical in such a case. It is particularly interesting to note, however, that the scan of the earth or moon rim during the stadiametric procedure is at the center of the field.

(d) Overload

The concept of requiring an operator to perform several steps in adjusting the controls of the various axes, at first seems to be inconsistent with the accuracy requirement. The situation would become worse if the ultimate visual match were to be achieved through simultaneous adjustments. It has been established that the success with which one operator can adjust two tracking rates to an optimum is limited--hence, the existence of two-man control in gun directors and precision phototheodolites.

The situation is relieved by the fact that rates are set up only as a convenience and not as a solution. Only the final placement of a crosshair on a target (or a target on a target) is to be considered as a determinant of accuracy. All preliminary adjustments can be sequenced at will and each judgement can be made one at a time. Training is necessary to condition the operator to react with little need for concentration and thought.

The readout of the scales, which register the angles of interest, must be carefully engineered to keep mental interpolation to a minimum. Kollsman Instrument Corporation believes that further work on the details of scale presentation will be of value and that a reasonably comfortable resolution of one second of arc is feasible.

Generally, the readout can be conveniently delayed to follow the measurements at the instant of perfect reticle match. Procedures for using a timing

button to delay readings are examined, together with alternative methods, the later discussion of operation.

(3) Accuracy

The significant sources of error that contribute to the overall operational error when the instrument is employed in its normal, or manually aided, stabilization mode are identified below with current estimates of their rms magnitudes:

		Arc-Second	Miles
(1)	Crosshairs on star	2	-
(2)	Crosshairs on crater	3	-
(3)	Star on crater	3	-
(4)	Sextant readout	2	-
(5)	Theodolite readout (elevation or bearing)	1	-
(6)	Correction for internal atmosphere	2	-
(7)	Nonflatness of window	2	-
(8)	Occultation timing (0.1 second)	-	-
(9)	Occultation cursor	60	
(10)	Stadiametric centering of perfect disc	2	-
(11)	Stadiametric centering of crescent	3	-
(12)	Moon diameter irregularities		2*
(13)	Earth diameter irregularities		2*

For any one of the navigational modes, the applicable error sources may be grouped by a root-sum-square method. Since most of the errors are in angle form, the vehicle position error will depend, of course, upon its position along the trajectory. Such computations are beyond the scope of this discussion.

The specific errors associated with each group are indicated below:

Theodolite accuracy. Error items (1), (5), (6) and (7) apply. Their summation is 3.6 arc-seconds.

Sextant accuracy. Error items (3), (4), (6) and (7) apply. Their summation is 4.6 arc-seconds.

*Estimate of average effect in judging target rim in terms of miles at target. The effective rim for the earth is airglow.

Occultation accuracy. Error items (2), (6), (7), (8), (9) and (12) apply. Only (8) and (9) directly affect the significant dimension of interest--namely, the error distance normal to the cylindrical shadow surface of the moon. The factor (8) is trajectory-dependent. The angular accuracy of the occultation base line is affected by (2) to an extent typified by 7 arc-minutes. This error combines with the cursor error (5) to form an occultation error which is along the periphery of the circular cross section of the moon shadow.

Stadiametric accuracy. Error items (4), (6), (7), (10) or (11), and (12) or (13) apply. Thus, using (4), (6), (7) and (11), a "perfect" crescent moon can have its diameter measured to 4.6 arc-seconds.

Verification of sextant angle. Impromptu checks of the sextant angle calibration may be made in flight by utilizing the known angles between star pairs. Thus, a sextant measure of the star-to-star angle will serve to calibrate that particular region of sextant angle for either the sextant or stadiametric modes.

e. Equipment operation

(1) Stabilization modes

The operation of the telesextant requires the positioning of the principal axes of the instrument. Such positioning may be effected (in part) by remote automatic equipment, by remote manual actuation and by direct manual control. The four basic stabilization modes are:

(1) Manual drive.

(2) Manual control (aided).

(3) Automatic stabilization (via inertial-platform-derived outputs).

(4) Automatic following of automatic tracker.

The following functional description of these stabilization modes will make reference to Fig. IV-22. Each mode employs the basic equipment configuration in Panel A of Fig. IV-22. It must be emphasized that the stabilization schemes are only depicted schematically, and in no way do they indicate the finalized selection of components or circuitry.

[redacted]

(a) Manual drive

When no power is available on the spacecraft, the manual drive stabilization mode is employed, and direct positioning of the instrument is required. The prominent control elements in this stabilization mode are shown in Panel B of Fig. IV-22.

With all clutches engaged and power unavailable, manual positioning of the elevation, bearing, polar and sextant axes are possible. The electromechanical components are permitted to rotate passively as shown, and visual readouts of all measurements are provided.

(b) Manual control (aided)

The manual control mode is employed where power is available, but no stabilization signals from remote sources within the spacecraft are employed. The functional diagram of this mode appears in Panel C on Fig. IV-22. Manual control is effected by the use of position and rate-aided tracking circuits, which are remotely actuated.

One feasible aided-tracking circuit is depicted in Panel F of Fig. IV-22. The summation of a position-dependent generator signal and a rate-dependent potentiometer signal is mixed with the (reference axis) shaft-mounted, generator signal. The resultant signal is then amplified to provide a servomotor drive signal, which accomplishes the aided-tracking function.

During this operational mode, the outputs available are both visual (optical) and automatic (resolver signals). The clutches to the manual drive are disengaged, preventing the electromechanical components from rotating.

(c) Automatic stabilization

Where stabilization signals resulting from an inertial platform are available, the telesextant may be stabilized in three axes. This condition is depicted in Panel D of Fig. IV-22. The counterparts of the inertial platform axes are the bearing, elevation and the polar axes of the telesextant. In this mode the resolvers are employed as position repeaters. The bearing, elevation and polar angle commands are transmitted as resolver signals. The outputs of the error windings then function as inputs to the aided-tracking circuits. The resulting signals, combined with the generator outputs, are then amplified and serve as the motor drive signals. During this mode, the clutches to the manual drives are disengaged preventing the electromechanical components from rotating.

With the sextant axis under manual (aided) control, both visual and automatic readouts of the sextant angle are available.

(d) Automatic following of automatic tracker

To allow the astronaut to monitor the operation of the astro-tracker associated with the automatic navigation system, an additional stabilization mode is provided. In this operation the bearing and elevation axes of the telesextant are commanded to follow signals derived from the automatic astro-tracker (or coordinate conversion equipment). Slaving is effected in the same manner described previously in which the resolvers are employed as position repeaters. During this mode of operation, the clutches to the manual drives are disengaged, preventing the electromechanical components from rotating.

The polar and/or sextant angles can be adjusted by the aided-tracking features, described earlier.

(2) Navigational modes

The specific navigational mode employed is dictated both by the particular phase of space flight and by the availability of the required celestial information. As indicated earlier, the equipment is designed to permit sextant operation for triangulation navigation, earth or lunar diameter measurement for stadiametric navigation, and star disappearance and emergence for occultation-referenced navigation. In addition, the instrument also serves as a basic theodolite for precision determination of star bearing and elevation relative to the instrument base. The operation of the telesextant, in effecting these measurements, will be described:

(a) Theodolite mode

(i) Application

In the theodolite mode, a star's direction is displayed in terms of bearing and elevation angles of the instrument's main (or theodolite) optical axis, with respect to the vehicle framework. These angles are available as scale readings, for the operator, or as resolver outputs. With subsequent coordinate rotation, the angular values may be applied as a check on a stable platform.

(ii) Operation

The desired star may be initially located by searching with the finder telescope. Then, by shifting attention to the main telescope, the bearing and elevation axes can be finely adjusted for accurate tracking of the crosshairs on the star. The two tracking axes are adjusted by separate rate and displacement controls. During this operation, the sextant angle is locked at its zero position.

(iii) Readout

Once the crosshairs are properly locked on a star, a reading may be made at any convenient instant. If the scale is read during tracking, a timing button

must be actuated when the scale is at the readout value. In the interest of convenience, the value is preferably a primary mark on the scale rather than a location between marks.

As an alternative to the above method, a "freeze" control can be actuated with the timing button. This step permits reading of the scales, by arresting the elevation and bearing drives, while in a stationary condition.

In the case of power failure the rate drives on the axes become dead. In this case, crosshairs can be manually placed on the star and the timing button pushed, at the same instant. The stationary scales are then read. A variation on this latter situation is to advance the crosshairs slightly ahead of the star and to note its transit of the crosshairs by depressing the times.

The foregoing options for angle readout are generally applicable to the other operating modes, which are discussed subsequently. All readouts are performed through the one eyepiece.

(b) Sextant mode

(i) Application

In the sextant mode, the angle between two celestial targets, as seen from the vehicle, is measured for the purpose of triangulation. Normally, the theodolite field of view is trained on a star and the sextant field of view on the moon or earth (or possibly a second star). The reflectivity of the beam splitter for the reflected (or sextant) optical axis is designed for use on the brighter of the two targets. The angle of interest is registered on the sextant axis. Because the sextant line of sight rotates twice as fast as the deviating sextant mirror, the scale is made to read out double the mirror angle.

(ii) Operation

The desired star is selected and tracked by the same procedure as that used in the theodolite mode. The plane of sextant measurement is then oriented to include the second target by rotating the polar axis. A searching action about the polar and sextant axes will then bring the second target onto the crosshairs and concentric with the original star. This search may be facilitated by first using the larger field of the finder telescope.

The sextant output angle is correct whenever the two targets are superimposed. (The readout would normally, but not necessarily, be made with the superposition of the crosshairs.) This condition may be difficult to perceive because of the contrast between the star and a second target, such as a moon crater or other distributed and shaped light images. The conditions for optimum contrast recognition are set by adjusting the dimmer for the sextant field of view. By this means, the moon or earth target can be dimmed out, in order to check the position of a dim star.

The range of sextant motion is ±35° about the sextant axis and a full 360° about the polar angle. The unusual provision of both directions of sextant declination gives two choices of polar angle for each point in the sextant range. This enables the operator to choose the position which, in conjunction with the theodolite bearing and elevation, gives the least or no vignetting effect from the limitation of the vehicle window.

(c) Occultation mode

(i) Application

In the occultation mode, the theodolite-sextant is employed to observe the time at which a star disappears or emerges from behind the moon's disc and to locate the point of occultation with respect to preselected and identifiable landmarks on the moon's surface. It is assumed that the occultation to be observed is planned both for its approximate time and for the point of occultation.

(ii) Features employed

As with sextant operation, the technique of theodolite star tracking is again employed in combination with an adjustment of the sextant axis to bring a primary target (e.g., crater) of the moon into coincidence with the star. Since the sextant angle may be made as great as 35°, the occultation technique is possible at fairly close range to the moon without concern for the fact that the moon's subtense greatly exceeds the telescope field.

The one additional adjustment required by the operator is the rotation of a cursor line, seen as a radius in the field of view, with respect to the crosshairs. The cursor will be used to line up a secondary target on the moon with respect to the primary target (at its origin of rotation) so that it constitutes a base line. The angle of interest is the angle between cursor and crosshairs at the time of occultation. The angle associated with the primary target will be the angle between the base line and the line to the occultation point, as denoted in Fig. IV-23B.

(iii) Operation

The manner in which these features are used to measure accurately the position of an occultation is illustrated by Fig. IV-23. The field of view is shown as it appears after tracking has been set up on the chosen star (by steps explained in the theodolite mode). The plane of sextant measurement has been preset to pass through the moon. Since the sextant angle is still at zero, the moon (which is beyond the field of view in this example) does not appear.

The sextant and polar angles are then adjusted to bring a primary target of the moon to the intersection of the crosshairs (Fig. IV-23B). This landmark has been preassigned as the pivotal target for the occultation procedure. Therefore, a distinct crater is a likely choice. The cursor is then rotated to pass

through a second target, preselected in combination with the first, for use as a base line. The drive rates of the polar and sextant angles are then adjusted so that the "pivotal" crater remains with the crosshairs.

The operator has now set up simultaneous tracking of the star and "pivotal" crater by one set of crosshairs. Use of the dimmer control on the moon image may be required in order to see the star clearly. It is necessary only to refine both actions by additional observations. Because the star path generally does not go through the pivotal crater but passes above or below it, more frequent adjustment of the crater tracking will be necessary. These latter adjustments are superimposed upon, and will in no way affect, the basic theodolite motion which tracks the star.

Fair warning time of the occultation is provided by monitoring the sextant angle scale. When its reading approaches the value that it will obtain for the moment of star disappearance, the sextant field is shut off by the dimmer. If necessary, the time of occultation is recorded by depressing the timing button.

Immediately after occultation the polar angle must be adjusted in order to sight the pivotal crater on the main crosshair, represented by the solid line in the field of view. Then, at a more leisurely pace, the sextant angle and cursor angles are adjusted. The angle θ may be read off the cursor control. These two latter adjustments may be slightly delayed because the angle θ is relatively unaffected by short range motions of any axis except the polar axis.

The diagrams show occultation at a dark limb of a crescent. This happens when the observer is too near the moon to see a substantial portion of it. This is illustrated in Fig. IV-23. The "pivotal" crater is shown as one chosen near the termination of the crescent. This is done so that the bright portion of the moon will never enter the field of the telescope, through the direct optical path. This assures the ability to see 11th magnitude occultations.

When the occultations are on the bright limb of the moon and faint stars (down to 9th or 10th magnitude) must be used, it is necessary to observe reappearance instead of disappearance. The same procedures would be followed until the entry of the bright limb into the field obscured the star. The tracking is continued with the latest available rates, so that the point of reappearance can be anticipated, by the path of the crosshairs across the moon. At the moment of reappearance the dimmer is opened (exposing the sextant view of the moon) in order to make corrections on the polar angle, the sextant angle and the cursor--thus recording the point of reappearance on the rim. The precision of this measurement depends on the speed of leaving the moon's shadow and the consistency of the tracking rates during occultation. During occultation, the adjustable dimmer may be switched to the theodolite optical path so that the moon information may be kept up to date. The sextant angle must be remonitored so that the dimmer is returned to the star-observing position in time to view the reappearance. Obviously, the most precise occultation measurements can be made when the star is sufficiently bright to be seen against the

view of the moon. In this case, there is no problem of keeping all inputs up to date until the moment of occultation.

When observing occultations of very dim stars, which necessitates alternating the view between the star and the moon, accuracy can be improved by choice of reference craters and proper sequencing of settings.

The very fact that an occultation occurs implies the presence of a continuous angular change between the star and occultating body. If the rates are constant, the rate drives can be used to keep the angular relation up to date. Therefore, the first consideration in improving accuracy is to make the rates as uniform as possible. This is accomplished by choosing the "pivotal" crater so that it lies as near in line as possible with the star's approach to the occultation point.

(d) Stadiametric mode

(i) Application

In the stadiametric mode, the theodolite-sextant is employed to measure the angle subtended by the full earth's or moon's disc. This angle may then be converted to a range measurement. In this application, the radius of curvature of the visible crescent in the case of the moon (or of the visible airglow in the case of the earth) is the quantity directly measured. This measurement is read on the sextant scale.

Inherently, the stadiametric measure is more accurate when the astronaut is closer to the body being sighted. Since this proximity is accompanied by a wide angular subtense of the body, the theodolite field of view will be exceeded. By virtue of its sextant angle feature, the configuration can be easily accommodated to the situation. In addition, the polar angle feature makes possible a visual match of the target rim and crosshair by inspection of phenomena seen only at the center of the field of view.

(ii) Operation

The operation is indicated in Fig. IV-24. The moon is located initially by pointing the theodolite at the estimated center. The theodolite view is dimmed as the sextant view is brought into the field to place the bright edge tangent to the crosshair. The polar axis is then set in rotation. The moon image will describe a circular path. The operator must now adjust the sextant angle until the visible portion of the moon edge appears to slide past and remain tangent to one reference line in the field of view (Fig. IV-24B). To ease determination of this condition, the theodolite axes can be adjusted until the dotted reticle line serves this purpose. The moon edge will now remain tangent to the dotted line at all times (Fig. IV-24C).

If the sextant axis has not been properly adjusted, however, the moon edge will either remain tangent to a circular "hole" in the field or will overlap

completely. After the condition of Fig. 10C has been attained, the angle or the sextant axis may now be read as the stadiametric output.

(iii) Readout

The stadiametric readout is made through the main eyepiece by switching to the sextant scale presentation. The angle read is that which the radius of the body subtends. The body center readout is taken like a normal theodolite reading.

It will also be noted that when the condition in Fig. IV-24C exists, the main telescope is pointing toward the center of the moon. This operation then performs two functions simultaneously--stadiametric and body center determination.

5. Radio Altimeter

a. General

The radio altimeter is shown in block diagram form in Fig. IV-25. It consists of a single speed digital data reduction system, employing an "X" band transmitter and receiver. Most of the circuits are solid state. The altimeter employs an rep-rate of approximately 40 cps and is not required to change ranges for operation between one mile and 10,000 miles. The echo pulses are integrated in an electronic servo which smoothes fading and jitter. The range is measured by counting clock pulses during the propagation time.

The data reduction circuits provide range and range rate information on projection readouts and are presented in decimal form to a 1/8 mile accuracy. These data are stored during the display time and are updated every one and a half seconds. The range is presented in miles, and the range rate in miles per second.

The transmitter power capability is 65 kw peak, employing a four microsecond pulse. By proper data processing, a resolution of 1000 feet can be obtained.

The receiver-transmitter subassembly has a volume of 930 cubic inches and weighs about 30 pounds. Its dimensions are 6.5 by 10.1 by 14 inches.

b. Microwave transmitter and receiver assembly

The block diagram of Fig. IV-25 shows the major portions of the microwave transmitter and receiver assembly. RF energy from the magnetron enters arm 1 of the ferrite duplexed isolator and emerges from arm 2 to the antenna.

Received signals enter arm 2 of the duplexer and are delivered to arm 3. The signals pass through the unfired TR tube and are delivered to the signal

mixers for conversion to IF. The IF-AGC delivers the signal information as video signals of fixed amplitude.

c. Operation of the digital altimeter timing circuits

The digital altimeter uses the transmitted pulse to start a counter. The received echoes stop the counter. The time between the transmitted pulse and reflected echo is a measurement of distance and can be directly displayed, periodically updated, and supplied to the computer.

An analog integrator is employed to smooth data from the echo pulse to provide a noise free pulse to the counter.

d. The range computer and display

A digital display will indicate range data to a precision of 0.5 mile. It will display all ranges from 1 to 2000 miles. This display will be continuously updated at every 64 altimeter pulse intervals, or approximately every one and one-half seconds.

6. Data Link

Tracking data generated by ground based radar stations will be available for use by the Apollo spacecraft guidance system. The Apollo crew will have the option of using either the ground or vehicle derived data for guidance and control purposes.

The tracking data will be sent to the vehicle using the ground-to-vehicle communications link. This link will be one of two possible links, depending on the phase of the mission. During the deep space penetration phase of the mission, the link will be through the deep space S-band communications system. The other phases of the mission will utilize the VHF communications system. These two systems are discussed in detail in the report on Instrumentation and Communications (ER 12011). During the deep space phase of the mission, the basic tracking data are derived from the deep space instrumentation facility. The basic measurements are made by the DSIF stations and transmitted in a format that includes station identification, time, data condition, doppler, two angles and range. Sampling rates may vary from one per second to one per 90 minutes with the present system. This data will be transmitted in digital form, upon request, to the Apollo spacecraft via the S-band communications system. The output of the S-band receiver aboard the vehicle will be a digital signal with a data message format compatible with the on-board computer.

The deep space instrumentation facility will also be called upon to provide the Apollo crew with computed vehicle trajectories and proposed midcourse corrections for purposes of comparison with the on-board systems. These will be generated with the ground tracking data using the computing facilities of the DSIF. This information will be transmitted, upon request, to the Apollo

spacecraft in digital form. The data message format will be compatible with the on-board computer.

During the other phases of the mission (launch and injection and re-entry), the basic tracking data generated by the ground based stations will be used by the vehicle for updating of the inertial guidance system. The basic radars generating the tracking data are the FPS-16 (C-band) and the Verlort (S-band) radars. These radars and the DSIF are discussed in detail in the report on Instrumentation and Communications (ER 12011). The FPS-16 and Verlort radars will generate data consisting of slant range, azimuth, elevation and doppler. This data will be in binary digital form and can be extracted at rates up to 2400 bits per second.

This tracking data will be transmitted (with proper station identification and time information), upon request, to the vehicle using the VHF communication system. The VHF system uses frequency modulation and the binary data will therefore be transmitted using a form of frequency-shift keying. The output of the VHF receiver on-board the vehicle will be a digital signal with the message format compatible with the on-board computer.

The data received on-board the vehicle will be used essentially in two ways: by the computer for computational purposes and directly by the display equipment. The data will be sent, in all cases, directly to the computer where its use will be controlled by the Apollo crew. The use of this data will require the computer to perform coordinated transformations. For this purpose, a program for coordinated transformation and the coordinates of the participating stations will be stored in the computer.

F. OVERALL SYSTEM

1. Physical Characteristics

A summary of the physical characteristics of the subsystems which make up the overall system is presented in Table IV-10.

TABLE IV-10

Component	Wt. #	V. of ____	Power-W max	Power-W norm	Power-W low
Astro-inertial platform	55.0	1.30	150	100	55
Miniature platform	15.0	0.25	150	120	100
Miniature platform electronics	18.5	0.41	180	150	0

TABLE IV-10 (cont)

Component	Wt. (lb)	V. of ____	Power-W max	Power-W norm	Power-W low
Computer No. 1	21.0	0.40	55	55	55
Computer No. 2	21.0	0.40	55	0	0
Telesextant	10.0	0.25	20	20	0
Telesextant electronics	10.0	0.25	20	20	0
Signal conditioner	5.0	0.15	5	5	0
Radio altimeter	30.0	0.5	10	10	10
Total	185.5	3.91	645	490	220

2. Subsystems Integration

Figure IV-26 is a block diagram showing the tie-in between subsystems and with other equipment. The system operation is discussed in Chapter V.

3. Temperature Control

The major portion of the heat generated by the guidance equipment will be transferred through a heat exchange surface to an ethylene glycol solution and finally to the external heat radiators. A small portion of the equipment generated heat will be transferred to the air. The equipment heat exchange surface will incorporate two parallel circuits to permit cooling by two separate glycol systems, either of which can do the entire cooling job. A detailed discussion of the temperature control system may be found in ER 12005.

4. Installation Details

The telesextant and astro-inertial platform windows are located adjacently. The telesextant and astro-inertial platform are mounted on a single structural support fastened to the capsule structure at the astro-inertial platform window area. This single point mounting will prevent any capsule distortion from being transmitted to the support. The miniature platform is also mounted on this support. This installation makes it possible to align all three units electromechanically. Therefore, an optical alignment system is not required.

The window consists of three plates. The innermost is a seal, the next is a redundant seal and the outermost is an insulator. A sun shade hinged near

the nose side of the windows is provided. The change in refraction due to the mediums and to pressure, temperature and humidity is automatically compensated for in the computer.

V. OPERATION

A. GENERAL

1. Information Flow

The flow of information between subsystems is shown in Fig. IV-26. During ascent, the accelerometers on the astro-inertial platform measure vehicle accelerations; accelerometer outputs are fed to the digital computer. The computer calculates vehicular velocity and position and determines appropriate steering signal inputs to the control system. The computer also determines the time to terminate thrust, thereby initiating coast and lunar injection. Discrete signals based on these times are transmitted to the propulsion system.

During the translunar and transearth flight phases, angular data from the astro-inertial platform and the telesextant are fed to the computer for orbit determination. The computer further calculates any necessary corrective velocities. Thus, the vehicle is rotated to the proper direction, thrust is initiated, the accelerometers feed acceleration information to the computer and when the correction velocity has been attained, the computer commands propulsion cutoff.

Injection to and ejection from lunar orbit is similar to ascent. During re-entry, the computer uses accelerometer, platform angular data to calculate the required L/D for the range of the target. The computer then automatically commands the control system to trim the vehicle to the required attitude.

Other information flow includes radio link data which relates vehicle position and velocity to earth coodinates. This information is fed to the computer which transforms the earth coordinates to the navigational reference frame, and sends the data to the displays. Also, at approach to re-entry, the radio altimeter supplies the computer with altitude and attitude rate information. This unit is also used in lunar orbit.

2. Navigator Functions

Figure IV-26 also indicates the commands issued by the navigator and subsequently applied to the control and display panel. The navigator's functions in this mission include:

(1) Monitoring subsystem and system operation during ascent, automatic operation, lunar orbit injection and ejection and re-entry.

(2) Initiating system checkout during coast and other mission phases.

(3) Deciding if and when to abort.

(4) Comparing onboard and ground-based generated navigational data, and deciding which to use.

(5) Initiating automatic star tracking in the astro-inertial platform for alignment updating.

(6) Initiating automatic navigational measurements by the astro-inertial platform.

(7) Making required navigational measurements with the telesextant.

(8) Assessing present trajectory data to determine whether midcourse correction is required.

(9) Deciding upon the time and aim point for such correction, and inserting pertinent data into the control panel.

(10) Controlling vehicle attitude for course correction.

(11) Deciding when navigational measurements should be made.

(12) Switching out malfunctioning subsystems when required; activating and switching to other subsystems to maintain overall system performance.

The integration of the navigator's functions and the basic flow of informance will be further defined in Section D of this chapter.

3. GSE Requirements

The major portions of the guidance system are checked for proper performance and accuracy with the aid of a star reference simulator, and a guidance system test set.

The guidance system test set includes a sidereal gyro test table. Both platforms are removed from the command module and tested to the required system accuracy on this test table. The platforms are then installed in the command module. Rough azimuth alignment is obtained by manually aligning the telesextant with the star reference simulator and properly slaving the platforms to the telesextant. The astro-inertial platform is then switched to automatic track for fine alignment. The miniature platform is automatically aligned with the astro-inertial platform.

All guidance system electronic units (digital computers, power supplies, etc.) will be tested in the command module by applying test signals and sample computation problems through the guidance system test set. The guidance laws and programs, together with required star table data, will be read into the guidance system digital computers and checked by the guidance system test set.

It will be necessary to modify stored guidance data whenever the estimated launch time changes; the guidance system test set will have this capability. Details of the GSE equipment and the testing methods to be used for all phases of the program are discussed in ER 12002.

B. BASIC MEASUREMENTS

Midcourse navigational measurements are varied. Most of these measurements are made with the telesextant; and the details are found in Section E4 of this chapter). These measurements include:

Occultation. The eclisping or reappearance of a star behind a body is observed to give a line of position to the point of occultation (see Section C of this chapter).

Other basic measurements include the tracking of stars and the recording of vehicle accelerations. Navigational stars (50 bright and unambiguous) are tracked for inertial reference updating. This function will take place every 5 to 10 hours automatically, or at the discretion of the navigator, so that the astro-inertial platform is always properly oriented for navigational observations or emergency.

Acceleration measurements described above include vehicle accelerations during ascent, midcourse corrections, lunar orbit injection, ejection and shaping and re-entry. These measurements are made by the accelerometers on the platform and are transmitted to the computer for required guidance computation.

C. INVESTIGATION OF THE OCCULTATION TECHNIQUE

1. Introduction

During the midcourse portion of the flight--both translunar and transearth--an accurate navigation technique can be employed. This technique consists of the observation of the time of occultations. Occultation means the obscuring of a star by the moon or the earth as viewed from the vehicle. Since the moon has no sensible atmosphere, the transition from full starlight to no starlight during the obscuring period will be very brief, and the occultation time more accurately defined. Therefore, although earth occultation data will be very useful, only moon occultations will be given detailed consideration in this report.

At the instant of time when a known star is occulted by the moon, the observer knows his vehicle is somewhere on a cylinder which circumscribes the moon and whose axis is parallel to the line-of-sight to the occulted star. See Fig. V-1. To determine his trajectory, six separate observations are required. Alternatively, if the specific point on the limb of the moon which occults the star is

known, the observer knows his vehicle is somewhere on a line tangent to the moon and pointing to the occulted star. In this case, only three separate observations are required.

During the course of the study of this technique visits were made to the following agencies to ascertain current state-of-the-art limits:

(1) Goddard Space Flight Center, NASA, Greenbelt, Md.

(2) Theoretical Division, NASA, Silver Spring, Md.

(3) Army Map Service, Washington, D.C.

(4) U.S. Naval Observatory, Washington, D.C.

The Army Map Service uses the occultation technique to locate points on the earth surface to an accuracy considerably greater than required for Apollo application. (Ref. V-4, V-8, V-10) However, all their measurements are made at the surface of the earth and can be spaced weeks apart to suit the convenience of the observer. In the lunar vehicle, observations must be made during reasonable portions of the translunar or transearth phases in order to be useful.

The manner in which stars will be occulted by the moon and earth on a nominal Apollo trajectory is depicted in Fig. V-2. This figure shows the stars as viewed from the vehicle. The paths were computed from trajectory and lunar ephemeris data. The typical density of stars up to the 10th magnitude whose positions are accurately known is shown at the lower left portion of this figure. The density is characteristic for any Apollo mission; hence it is clear that more than enough stars are available. See Ref. II-1

Application of occultation technique as briefly described in Section V B.1 to navigation is relatively new; it is therefore believed that a more thorough description of it is warranted.

To evaluate the occultation technique as a navigation aid for a lunar vehicle, there are several problem areas which must be analyzed. These are as follows:

(1) Mathematical justification

(2) Star density

(3) Star identification

(4) Time measurement

(5) Effects of moon irregularities

(6) Instrumentation

These areas are discussed in the following paragraphs:

2. Mathematical Justification

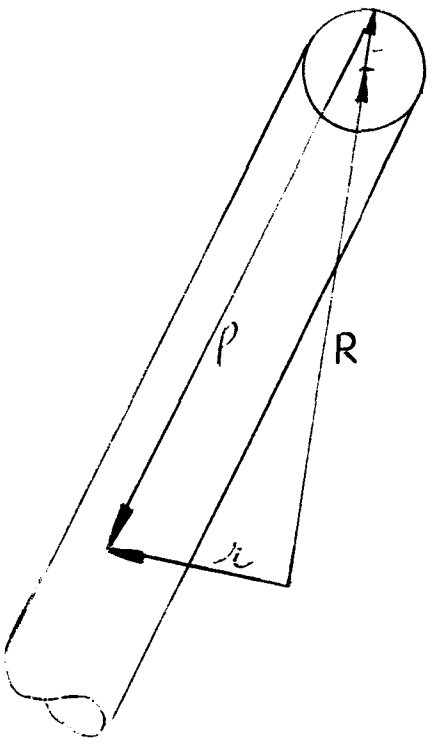

From each occultation can be determined the time of the vehicle's entry into a cylinder oriented in space. The orientation of the cylinder is obtained from the direction cosines of the star which is occulted. To determine a vehicle's position by means of lunar occultations, the following equations are used. From the geometry in the above figure we have:

$$\vec{r}_i = \vec{R}_i + \vec{R}_{mi} + \vec{\rho}_i$$

$$\vec{R}_{mi} \cdot \vec{\rho} = 0 \qquad (1)$$

$$\vec{R}_{mi} \cdot \vec{R}_{mi} = R_m$$

where r_i is the vector from the center of the earth to the vehicle. R_i is the vector from the center of the earth to the moon. R_{mi} is the vector from the moon's center to the point on the rim where occultation occurs. ρ_i is the vector from the point of occultation to the vehicle. Equation (1) gives 5 i equations in the 7 i unknowns (components of r_i, R_{mi} and the magnitude of ρ_i

Since the vehicle trajectory must be on a plane, we have

$$\vec{r}_i \cdot (\vec{r}_1 \wedge \vec{r}_2) = 0 \qquad (2)$$

If a coordinate system is chosen in the plane, the orbit may be written in the form

$$A\alpha_i + B\gamma_i + C = \sqrt{\alpha_i^2 + \gamma_i^2} \qquad (3)$$

where the quantities α_i and γ_i may be defined as follows:

$$\alpha_i = \frac{\vec{\pi}_i \cdot \vec{\pi}_i}{|\vec{\pi}_1|} \qquad \gamma_i = \frac{\vec{\pi}_i \cdot [\vec{\pi}_1 \wedge (\vec{\pi}_i \wedge \vec{\pi}_i)}{|\vec{\pi}_1 \wedge (\vec{\pi}_1 \wedge \vec{\pi}_i)|}$$

The final equation required is the time to traverse the orbit from observations i to $i+1$. This relation is

$$t_{i+1} - t_i = \sqrt{\frac{a^3}{\mu}} \left[b_i - \sin b_i - d_i + \sin d_i \right] \quad \text{where}$$

$$b_i = \cos^{-1} \frac{2a - (|\pi_{i+1}| + |\pi_i| + |\pi_{i+1} - \pi_i|}{2a} \qquad (4)$$

$$d_i = \cos^{-1} \frac{2a - (|\pi_{i+1}| + |\pi_i| - |\pi_{i+1} - \pi_i|}{2a}$$

$$a = \frac{C}{1 - A^2 - B^2}$$

From the above can now be determined the number of observations necessary to specify the orbit:

(1)	5 i equations	7 i unknowns
(2)	i -2 equations	
(3)	i equations	3 unknowns
(4)	i -1 equations	
Total	8 i -3 equations	7 i + 3 unknowns

Thus $i = 6$ or six observations are required.

If it is known where on the rim of the moon occultation takes place then the geometry is simplified.

Equation one becomes

$$\vec{\rho}_i = \vec{R}_i + \vec{\rho}_i$$

This gives three equations in four unknowns (components of $\vec{\rho}_i$ and magnitude of ρ_i).

Thus:

(1)	$3i$ equations	$4i$ unknowns
(2)	$i-2$ equations	
(3)	i equations	3 unknowns
(4)	$i-1$ equations	
Total	$6i-3$ equations	$4i + 3$ unknowns

Thus three observations are required.

3. Star Density

The following tabular data give the number of stars versus visual magnitude in the entire celestial sphere (see Ref. V-1).

Magnitude	Number of Stars
4.0	530
5.0	1,620
6.0	4,850
7.0	14,300
8.0	41,000
9.0	117,000
10.0	324,000
11.0	870,000
12.0	2,270,000
14.0	13,800,000
16.0	71,000,000
18.0	296,000,000
20.0	1,000,000,000

These data are according to Seares and van Rhijn (1925)

Lunar occultations will occur in the general region of the ecleptic; Fig. V-3 shows a plot of average star density in this area of interest. This average density is based on star count data as illustrated on star charts and tables plus

other sources of information (Ref. V-2). However, detailed position information is available only for stars up to the 10th magnitude; hence these are the ones applicable to the navigation problem. The number of stars in this category occulted by the moon obviously depends upon the angular size of the moon as viewed from the vehicle.

Figure V-4 is a plot of the number of stars of different magnitudes up to the 10th occulted by the moon versus distance to the moon. It is very clear from this graph that there are more than enough stars available to employ the occultation phenomenon as a navigation technique.

The next important consideration is the rate at which stars may be occulted. This rate depends on the angular rate of the line of sight from the vehicle to the moon as well as how fast the apparent size of the moon is changing due to motion toward it. To examine this rate an effective diameter of the moon less than the true diameter is chosen since the time of a star occultation in a direction nearly tangent to the edges of the moon would be difficult to define precisely. The sketch below shows this and depicts the chosen effective diameter to be 0.707 times the actual diameter.

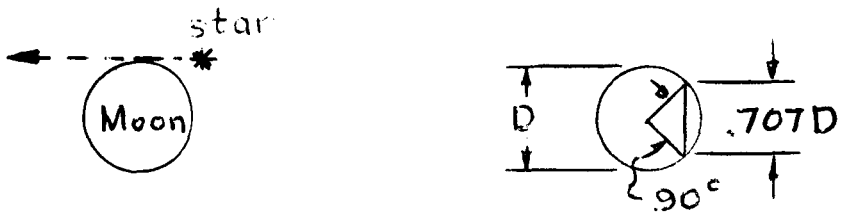

The rate of occultation is then determined by the rate at which the effective diameter occults stars when moving in a direction normal to itself. Figure V-5 is a plot of this rate for different angular velocities of the line of sight with distance to the moon as a parameter.

Thus for angular rates in excess of 0.02 °/hr the occultation rate has an average value of perhaps 3 stars per hour which indicates that the lunar occultation technique is feasible. The effect of the apparent expansion of the moon as it is approached is shown on Fig. V-6.

From this, it can be safely concluded that there are in fact more than a sufficient number of stars available and being occulted for this technique to be applicable.

In addition to available star charts and tables as a source of data, magnetic tapes including the following information for 300,000 stars up to the 10th magnitude are being obtained from the Goddard Space Flight Center, Greenbelt, Maryland.

(1) Identification Number

(2) Right Ascension and Declination (to an accuracy approximating 0.5 sec of arc)

(3) Proper Motion and Precession

(4) Magnitude

(5) Spectral Class

Programming these tapes in an IBM program will make it possible to determine the specific stars occulted by the moon for a given vehicle trajectory.

4. Star Identification

There are three principal ways in which stars about to be occulted can be identified:

Observer experience. Familiarity with the star patterns and constellations will enable the observer to closely match what he sees in the vicinity of the moon with star charts. This would be greatly facilitated by previously plotted nominal trajectories and could further be implemented by a mechanical analogue device to predict occultations (Ref. V-5).

IBM runs employing the magnetic tapes previous described. The observer could then have a listing of times versus stars occulted for a nominal flight.

By using a new star identification technique being studied. This consists of forming triangles of groups of 3 stars. There are a very large number of these triangles since a given star can be a part of many individual and different triangles. Each triangle is normalized by dividing all three sides by the length of the longest side. Data collected indicate that in spite of the many possible combinations, the triangles tend to be dissimilar and when information on star magnitude is factored in, the triangles are unique and can serve to identify specific stars.

5. Time Measurement

There is a cyclic error in the times listed in the ephemeris giving the moon's position and the present universal on Greenwich time. This is due to the fact that since the times of the observations on which the tables are based, the earth's rotational period and other related phenomena have changed. (Ref. V-6) This error was + 0.32 secs in 1955 when the most recent computation was made; there is reason to expect that the errors will decrease, and then increase again due to such phenomena as the periodic nature of the behavior of the earth's axis.

The largest source of error in connection with the occultation problem is in the measurement of time. According to the U.S. Naval Observatory, the above-mentioned correction of 32 sec has a possible error of ± 2 sec. This element of error is due to unpredictable irregularities in earth rotation. Due to its random nature, it cannot be predicted by extrapolation. (Ref. V-7)

6. Effects of Moon's Irregularities

The mass center of the moon is known to within about 0.015 sec of arc in right ascension and 0.01 sec of arc in declination. The geometrical or optical center is 0.6 sec of arc above the mass center in the declination direction. Right ascension is the same for mass and optical center.

The moon's diameter is about 0.5 deg or 1800 arc sec as viewed from the earth. It moves in its orbit at about 1 diameter per hour relative to the star background, or 1800 arc sec in 3600 sec of time.

Mountain Height		Occultation Time
Feet	Arc Sec from Earth	Difference in (sec)
100	0.018	0.036
500	0.09	0.18
1000	0.18	0.36
5000	0.90	1.80
10000	1.80	3.6
15000	2.70	5.4
20000	3.60	7.2
25000	4.50	9.0

The conclusion from the above table is that mountains of the order of 10,000 feet and above will have a significant affect on the occultation time, based on the statements in the preceding section of time measurement.

The details of the irregularities of the moon's edge (or limb) are being carefully plotted. (Ref. V-3, V-9) These details change as viewed from the earth because of libration in longitude and lattitude. Libration in longitude is the apparent rocking motion of the moon due to the fact that, although its period of rotation on its axis is equal to its orbital period, its orbit is not precisely circular. Hence, during one half of its orbit you see a little more around one edge, and during the other half of its orbit you see a little more around the opposite edge. Libration in lattitude is the apparent rocking motion in the lattitude direction due to the fact that the moon's axis of rotation is not normal to its orbital plane.

The total edge zone seen from the earth due to this motion is known as the marginal zone. As has been mentioned, details of this are being studied.

Very little is known about the mountain heights on the side of the moon facing the earth (except for the marginal zone) and of course nothing is known about the back side. Therefore, great precision in measuring the time of occultation (i.e., from 0.01 to 0.1 second) from a lunar vehicle is not possible until this information is obtained. It does not appear that such an order of precision is required at this time.

7. Instrumentation

The unaided eye, which has an integration time constant approximately 0.1 second, can see stars up to the 5th magnitude from the surface of the earth. Assuming the eye aperture is 3mm, the addition of an optical system of a 3" or 75 mm aperture will give an increase of $(75/3)^2 = 625$ in light-gathering power. This amounts to about a 7-magnitude increase ($2.5^7 = 625$). Hence, with a 3" aperture, a 12 magnitude star could just be seen. By going above the atmosphere, an additional 1.5 magnitudes can be gained.

Possible occultation observation modes in increasing order of difficulty are given below.

(1) Disappearance at dark edge (9th magnitude).

(2) Reappearance at dark edge (7th magnitude).

(3) Disappearance at bright edge (possible for 4th magnitude).

(4) Reappearance at bright edge (very difficult--possible for 2nd magnitude).

The reappearance observations are made by tracking the star up to disappearance, then memorizing its motion behind the moon and have the telescope aimed at the exit point.

The moon has a visual magnitude of -12.7. If we are using 8th magnitude stars the difference in brightness is about 10^8. It is therefore necessary to attenuate the light from the moon and star by the use of a neutral density filter or by using a small aperture around the star image in the focal plane to eliminate some of the light from the moon.

The biggest problem is the large amount of scattered light from the optical surfaces within the instrument and the optics must be designed to reduce this stray light to an absolute minimum--even when dark-side occultations are being observed.

One of the advantages of using visual observations rather than automatic (photoelectric) means is due to the noise problem. Light appears in discrete

quanta, and the noise resulting from this discontinuous form of energy is proportional to the square root of the number of quanta per second. Thus, it becomes very easy for the square root of the number of quanta of moonlight passing through the tiny aperture per second to be of the same magnitude as the total quanta from the star per second. Hence, the star would be lost in the noise background and not be observed at all by the photoelectric means. The comparable problem when using visual observation must be examined. It appears that it would not be as severe, since the eye consists of many very small isolated detectors.

The theoretical light level versus time passing thru the optical system is sketched below. This fluctuation is due to diffraction.

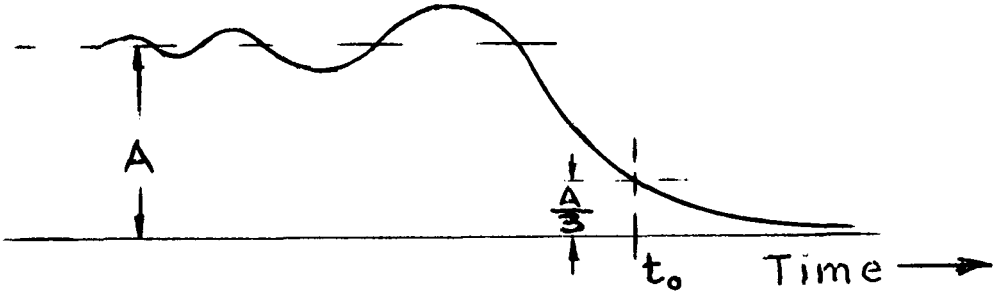

However, it turns out that, due to the noise background, the actual signal received looks as follows:

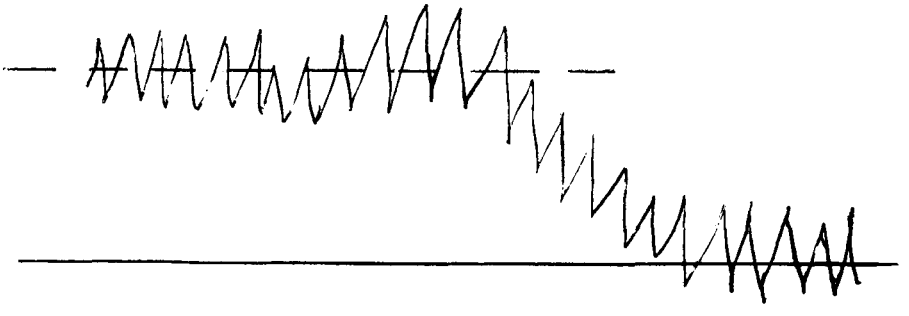

Thus, the diffraction effects are lost in the noise--and the noise must be reduced to a minimum by reduction of stray light and minimizing aperture size.

It would be conceivable to use a vidicon system to measure the occultation. An optical system would be used to produce an image of the moon's edge and nearby identifiable stars on the vidicon tube. The image is scanned and data which define the outline of the edge as well as its location relative to the stars appearing in the vidicon are fed to a computer. The instant of occultation of a

selected star is measured by this vidicon. This system has obvious complexity, even greater than the simple photoelectric system; it is therefore not considered applicable to the Apollo mission.

D. PHASES

Some of the following material relative to the operation of the Apollo guidance system has been taken from "Study Report - Navigation and Guidance System for NASA Apollo Vehicle" Vol. I, (Ref. II-1) prepared for The Martin Company, by Arma, Garden City, N.Y. The operational concepts, however, were originated by The Martin Company; these concepts formed the basis of Arma's study.

The overall operation of the Apollo navigation and guidance system can be summarized simply as follows:

(1) Measured data from the system's sensors are fed to the digital computer. The particular sensors used at a specific point depend on the navigation technique appropriate to that phase of the mission. During ascent, for example, data are derived from the accelerometers on the astro-inertial platform while, during the midcourse portions of the mission, the optical sensors are the primary source of data.

The measured data are processed in the digital computer to yield position and velocity of the vehicle. The detailed nature of these navigational computations varies with the sensors used.

(2) Vehicle position and velocity data are used as inputs to appropriate guidance computations which result in vehicle control commands to achieve the desired guidance objectives. These guidance objectives vary with the phase of the mission. For example, during midcourse translunar flight the guidance objective is to determine proper velocity vector modifications so that the vehicle will arrive at a predetermined periselenium point.

(3) The vehicle control system carries out the commands issued by the guidance system.

The following discussion delineates guidance operation during the various phases of the manned lunar orbital mission--the most complex of Apollo's missions. Times quoted are for the mission requiring roughly 3-1/2 days one way transit time.

1. Prelaunch

During preflight alignment and countdown, the digital computers will be used (in conjunction with the GSE) to control and program all checkout,

calibration, alignment, and program insertion operations. Erection of the primary astro-inertial platform to the vertical is accomplished by nulling the outputs of accelerometers (pendulums) mounted on the platform. Azimuth alignment is accomplished by an optical link to an accurately surveyed external star reference simulator. The secondary platform is also self-erected to the vertical but is slaved to the primary platform in azimuth. Inertial-component calibration data are measured and stored in the digital computers for subsequent use in corrective computations to be performed in flight.

Upon completion of alignment, checking, and calibration operations, reference range parameters and coefficients, and ephemeris data are read into the computer storage. Reading in, and data checking, is performed by the GSE.

At first stage ignition all alignment constraints are removed from the platform so that it is stabilized in inertial space, and accelerometer-data processing is begun. The data are then fed to the digital computer which calculates velocity, position, and steering signals.

2. Ascent

The ascent phase uses the first and second stage boosters and part of the third stage to place the vehicle in a circular parking orbit around the earth at an altitude approximately 650,000 feet. During first stage burning the launch vehicle will follow a pitch program, while during second and third stage burning the explicit guidance scheme described in Chapter II (Guidance Concepts Study) will steer the vehicle to rendezvous with a "phantom" satellite traversing a flight plan compatible with injection onto the required translunar trajectory. Outputs of the accelerometers mounted on the primary astro-inertial platform are fed to the computer which corrects the outputs using the stored calibration data. The corrected data are then combined with computed gravity data and integrated to continuously generate the position and velocity of the vehicle. This information is used to compute guidance signals which steer the vehicle, and which command third stage engine shutdown. The vehicle is then on the desired parking orbit.

3. Parking Orbit and Injection Into Translunar Trajectory

The target point and intercept time toward which the vehicle is coasting while on the parking orbit is a point on the nominal translunar trajectory. Transition from the parking orbit to the translunar trajectory will proceed as follows.

During the parking orbit the digital computer continues to determine vehicle position and velocity, and also generates continuously the position and velocity of a phantom vehicle which is on the nominal translunar trajectory. When the distance between the real and phantom vehicles has been reduced to a predetermined value, the guidance system commands reorientation of the vehicle so that the thrust vector will be parallel to the relative velocity vector and directed in the opposite sense. Third stage engine re-ignition is commanded by the

computer when the position error has reduced to the point where it will become zero the moment that the velocity error between real and phantom vehicles becomes zero (assuming the expected thrust profile). When rendezvous is complete, the computer commands third stage engine shutdown.

The vehicle is in the parking orbit for roughly an hour. During this period, the crew checks the vehicle and its systems, using confirming information from ground communication and tracking facilities. Time is available for realignment of the inertial platforms at the crew's option. If, during the parking orbit period, the vehicle is found unacceptable for the lunar flight, the decision is made to return to Edwards AFB rather than to proceed with injection into the translunar trajectory.

4. Translunar

If injection onto the translunar trajectory has been performed perfectly, the vehicle will coast out to the moon, reaching periselenium at a specific time and point in inertial space. Actually, the vehicle will not be exactly on the nominal trajectory because of such factors as errors in the inertial navigation system, and uncertainty in geophysical constants. Therefore, during the translunar phase, several small corrective maneuvers are executed to insure that the vehicle will pass through the proper lunar orbit injection point at the proper time. The main steps involved in making a corrective maneuver are:

(1) Make manual and automatic navigational observations over a period of time and store in the computer.

(2) Use the data to determine what the vehicle velocity and position will be at the time it is desired to make a corrective maneuver.

(3) Determine what the velocity should be at the predicted vehicle position to achieve the objective of passing through the proper lunar orbit injection point at the proper time.

(4) From the difference between predicted and required velocities at a corrective maneuver time, determine the magnitude and direction of the required velocity increment.

(5) Rotate the vehicle to the required attitude and at the correction time, insert the required velocity increment by applying thrust.

The steps leading up to a corrective maneuver are diagrammed in Table V-1. The operations in this sequence are discussed in the following paragraphs.

As shown in Table V-1, the first step is making navigational observations. The computer has the ability to accept various types of measurements, which can be fed in via key-punch or automatically. The onboard measurements which will be made are:

(1) Star tracking by astro-inertial platform for angular reference updating.

(2) Rim tracking (earth or moon) by astro-inertial platform for range information.

(3) Star-earth landmark angle by telesextant.

(4) Star-moon landmark angle by telesextant.

(5) Subtended angle (earth or moon) by telesextant for range information.

(6) Line-of-position to center of moon by astro-inertial platform and telesextant.

(7) Lines-of-position to edge of moon by occultations using telesextant.

(8) Lines-of-position to earth landmarks using telesextant.

(9) Altitude above earth and moon using radar altimeter.

In addition to data obtained from onboard observations, the computer can accept data transmitted from ground stations via radio link.

When enough observational data have been obtained the next step in the process is determination of the vehicle trajectory. Using processes described in Chapter II "Guidance Concepts Study," a trajectory is found such that if the vehicle were on that trajectory, theoretically perfect observations computed for the same instants as the real observations would give a best fit to the real observations. When the computation of the trajectory shows sufficient accuracy, the determination of the required velocity at the predetermined corrective-maneuver time is commenced.

Taking the predicted position at the desired corrective maneuver time, successive trajectories are computed to find what the velocity must be if the vehicle is to pass through the lunar orbit injection point at the desired time. When the required velocity is determined, its vector difference from the predicted actual velocity at maneuver time gives the direction and magnitude of the required velocity correction.

The final step in the procedure is to decide whether to execute the corrective maneuver or to obtain additional observational data. This is accomplished by comparing the required velocity increment with the velocity uncertainty of the trajectory fitting computation. If the correction is large relative to the uncertainty, the corrective maneuver should be executed. If the correction is not large relative to the uncertainty, the steps of Table V-1 should be retraced.

The entire computing procedure from the time the last observation is made until the required velocity increment is known will take less than one minute.

The steps involved in preparing for and executing a corrective maneuver are as follows:

(1) If the astro-inertial platform requires alignment prior to carrying out the maneuver, the alignment will be accomplished by the star tracker portion of the platform. This is done by tracking 2 or more stars sequentially to obtain an inertial reference and torquing the platform gimbals to alignment with this reference.

(2) When the platform has been aligned, the vehicle control system rotates the vehicle as commanded by the digital computer until its thrust axis is parallel to the direction of the required velocity increment.

(3) When the maneuver time is reached, the engines are ignited and the inserted velocity increment is monitored by integrating the outputs of the accelerometers on the astro-inertial platform. When the required velocity increment has been inserted, the computer commands engine shutdown.

The general sequence of events during the translunar phase of the mission is as follows:

(1) After injection, one hour is utilized in checking out equipment and assessing the overall situation. Ground track information is received via radio link and used in performing the evaluation. The next 1-1/2 hours are spent in making manual and automatic navigation measurements which are fed to the computer. As outlined above, the computer then determines a corrective maneuver which is performed at the three hour point. (Times mentioned are relative to time zero at injection.)

(2) The miniature platform is shut down at this time. During the next 18 hours there is no navigation or guidance effort, but at the 21-hour point a second series of navigation observations is made. Based on these data, any required correction is made at the 25-hour point. Following this correction, further navigation observations are made to refine knowledge of the trajectory. No navigation activity is then performed until the 42-hour point, when a series of observations is begun in preparation for a correction made at the 50-hour point.

(3) The last translunar navigation effort starts at the 74-hour point, and culminates in a correction at the 77-hour point. This correction is based on the tangent steering law and places the vehicle on a trajectory such that it will arrive at the prescribed periselenium within tolerance.

5. Lunar Orbit Injection

After the final translunar corrective maneuver, another set of observations is made to obtain initial position and velocity data for the primary inertial system. When the time for which the initial conditions have been computed is reached, the computer begins calculation of vehicle position and velocity in real time. The computer then commands timely vehicle orientation and engine burning (deceleration) such as to rendezvous with a phantom satellite which is in lunar orbit. This lunar orbit has a periselenium altitude of 50 nautical miles; when the vehicle reaches this point an additional period of deceleration is commanded to place the vehicle in a circular lunar orbit of 50 miles altitude.

6. Lunar Orbit

The operation of the navigation and guidance system during lunar orbit is essentially identical with operation during the translunar phase. Basically, the steps are determination of vehicle position and velocity, followed by execution of small corrective velocity increments to shape the orbit. Optical navigation measurements are made continuously while in lunar orbit; in addition, radar altimeter data are used to augment these observations which emphasize moon landmarks and star setting times. The corrections are made to attain rendezvous with a phantom satellite which defines the reference trajectory, including position along this trajectory as a function of time. Prior to the final lunar orbit the astro-inertial platform and the miniature platform are brought to full power in preparation for ejection.

7. Lunar Orbit Ejection

Ejection from lunar orbit is accomplished by guiding the vehicle to rendezvous with a phantom satellite traversing the desired return trajectory. The maneuver is made directly from the orbiting altitude without going to a lunar parking orbit. Initiation and termination of ejection thrusting is commanded by the guidance computer.

8. Transearth

Transearth guidance operations are almost identical to the corresponding operations during the translunar phase of the mission. Following ejection from lunar orbit, about 2-1/2 hours are spent in making navigation measurements and at the 3-hour point a corrective maneuver is made. Starting at the 27-hour point another series of navigation observations is made, and a correction performed at the 35-hour point. Additional measurements are begun at the 45-hour point, leading to a correction at the 51-hour point. At a range of about 100,000 to 40,000 miles from the earth (5- to 1-hour before re-entry), a series of navigation measurements and a corrective maneuver is effected, at the latter range, in order to trim the trajectory to arrive within the re-entry corridor. Observations are continued until about one-half hour from re-entry to improve re-entry initial-conditions accuracy. At about 8,000 miles out from Earth, re-entry

preparations are begun. Full power is applied to the inertial platforms and the realignment procedure accomplished. When the moment for which the initial position and velocity data have been computed is reached, the digital computer starts computing vehicle velocity and position in real time, and the vehicle is ready for re-entry. The radar altimeter is used for altitude fixes from 2000 miles until jettisoning of the mission module.

9. Re-entry

The real time information pertaining to such factors as vehicle position, velocity, flight path angle, and range-to-go, (as computed by the inertial guidance system) are utilized in conjunction with Chapman's equation to determine the desired L/D ratio. Subject to load factor, heating, and skip considerations the L/D is controlled by modulating angle of attack and roll angle. Lateral maneuvering is achieved by banking the vehicle about the velocity vector. Detailed information relative to re-entry guidance operation appears in Chapter III, "Re-entry Guidance Study." The landing sequence is initiated at about 80,000 ft altitude.

E. OPERATIONAL SEQUENCE

A summary tabulation of guidance operations for the lunar orbital mission is presented in Table V-1. The main events of each mission phase are given, along with the time and other information concerning each item.

TABLE V-1

Lunar Orbital Mission

Phase	Event	Time (approximate)	Initiated or Conducted by	Remarks
Prelaunch	Check-out of all flight systems Erect and align platforms Data stored			
		Time from launch		
Ascent	Launch	0	Guidance computer	Launch time tolerance approximates one hour.
	1st stage burnout	1.6 minutes	Guidance computer	Pitch program
	2nd stage burnout	4.8 minutes	Guidance computer	Guidance based on explicit computation.
	3rd stage shutdown	9.7 minutes	Guidance computer	Crew monitors guidance system.
	Receive ground track confirmation. Check systems. Realign platforms (optional).		Crew plus equipment	In parking orbit
Injection	3rd stage relight	73 minutes	Guidance computer	Crew will monitor
	3rd stage shutdown	76 minutes	Guidance computer	Guidance system
	Vernier phase		Guidance computer	Now in circumlunar flight.
		Time Period (hr)(from injection)		
Translunar	Receive ground track confirmation Check systems Realign platforms	0 to 1	Crew plus equipment	
	Make manual and automatic angle, range, and line-of-position optical measurements	1 to 2 - 1/2	Crew plus equipment	Computer determines course correction required. Miniature platform is shut down after correction is made.
	Correction No. 1	At 3-hour point	Guidance computer	
	Free fall	3 to 21		No navigation effort during this period.
	Make navigation measurements	21 to 24 - 1/2	Crew plus equipment	Computer determines required course correction.

TABLE V-1 (continued)

Phase	Event	Time (approximate)	Initiated or Conducted by	Remarks
	Correction No. 2	At 25-hour point	Guidance computer	
	Make navigation measurements to check trajectory	25 to 28 - 1/2	Crew and equipment	
	Free fall	28 - 1/2 to 42		No navigation effort during this period.
	Make navigation measurements	42 to 49 - 1/2	Crew plus equipment	Computer determines required course correction to get on desired moon approach trajectory.
	Correction No. 3	At 50-hour point	Guidance computer	
	Free fall	50 to 74		No navigation effort during this period.
	Make navigation measurements	74 to 76 - 1/2	Crew plus equipment	Both platforms on full power in preparation for lunar orbit injection.
	Correction No. 4	At 77-hour point	Guidance computer	Correction based on tangent ellipse steering law.
Lunar orbit injection	Decelerate at periselenium	At 84-hour point	Guidance computer	Deceleration results in elliptic orbit around moon.
	Decelerate at new periselenium	At 85-hour point	Guidance computer	Now in circular orbit around moon
Lunar orbit	Data accumulation	As required	Crew plus equipment	Platforms on reduced power after first full orbit. Returned to full power at beginning of final orbit. Radar altimeter used for augmenting optical measurements while in lunar orbit.
	Determination of conditions for ejection	As required	Crew plus equipment	
		Time period (hr) (from ejection)		
Lunar orbit ejection	Accelerate to eject from lunar orbit	0	Guidance computer	Now on return trajectory

TABLE V-1 (continued)

Phase	Event	Time (approximate)	Initiated or Conducted by	Remarks
Transearth	Make navigation measurements	0 to 1/2	Crew plus equipment	Computer determines required course correction.
	Correction No. 5	At 3-hour point	Guidance computer	After correction is made, miniature platform is shut down and primary platform is on reduced power.
	Free fall	3 to 27		No navigation effort during this period.
	Make navigation measurements	27 to 34-1/2	Crew plus equipment	Computer determines course required correction to obtain desired perigee altitude at proper time in a trajectory plane to carry vehicle up the PMR to Edwards AFB.
	Correction No. 6	At 35-hour point	Guidance computer	
	Free fall	35 to 55		No navigation effort during this period.
	Make navigation measurements	55 to 60-1/2	Crew plus equipment	Now approximately 100,000 naut mi from earth.
	Correction No. 7	At 61-hour point	Guidance computer	
	Series of navigation measurements and final correction(No. 8)	61 to 80	Crew plus equipment and computer	This series of measurements over the range occurs from approximately 100,000 to 40,000 miles from the earth (with final correction made at latter range).
	Prepare for re-entry (further navigational measurements)	80 to 85	Crew plus equipment and computer	

TABLE V-1 (continued)

Phase	Event	Time (approximate) Time after reentry	Initiated or Conducted by	Remarks
Re-entry	Re-entry guidance	0 to 30 minutes (for 5000 naut mi re-entry	Manual or automatic control of inertial guidance system	L/D and roll angle are controlled by the re-entry glide steering logic. Crew monitors re-entry guidance.
	Drogue parachute deployment	33 minutes	Sequence initiated by pilot or automatic	At 80,000 feet
	Main parachute deployment	38 minutes	Manual or automatic	At 13,000 feet

F. VEHICLE ATTITUDE REQUIREMENTS

During the midcourse phase, the vehicle will not be allowed to assume any random orientation. The constraints requiring it to be positioned to particular attitudes are:

(1) The radiators must "look" edge-on to the sun so that they can continue to transmit heat out of the vehicle.

(2) The fuel in the rear of the vehicle must be shaded from the sun to prevent boiloff of propellants. This dictates pointing the nose of the vehicle toward the sun as much as possible.

(3) The communication antennas must be able to "see" the earth at all times to ensure continuous contact with ground tracking stations.

(4) The vehicle must be rotated so that the windows can see the body of interest (earth or moon) when navigational observations are being taken.

(5) The vehicle must be reoriented to the required attitude when a midcourse correction is made. This orientation may be in any direction.

These restrictions have led to the concept of "flying" the vehicle with its principal axis parallel to the ecliptic plane (Fig. V-7). The pitch axis of the vehicle is then normal to this plane. Normally, the nose of the vehicle points toward the sun to keep the propellants cool. However, when observations are made, the vehicle will be rotated about its pitch axis so that the field of view of the windows includes the body on which observations are being made. This dictates that the windows be near this plane of action since the earth, moon and sun are approximately in the same plane.

Figure V-7 illustrates a mission taking place during the lunar month when the moon will be in its last quarter phase at periselenium. It may be noted that all vehicle maneuvering is done in pitch in going from earth observation to nose-to-sun attitude and from this latter attitude to moon observation. Future discussion will indicate whether it is more desirable to roll 180° when in the nose-to-sun attitude and then pitch from this point to the moon observation attitude. This maneuver is compatible with the radiators but temporarily blacks out the antennas. It will be shown next that the position of the sun is a factor and this type of maneuver may be dictated.

It is undesirable that sunlight should fall directly on the window at any time. When more is known about operation of equipment in a space environment, this requirement may be found to be mandatory. The problems involved are:

(1) Sunlight obliquely striking the outer surface of the window causes a scattering of the light on this surface. The capability of making observations through the window is reduced.

(2) The heating of the window may cause deformations in the glass, impairing its optical quality.

(3) Sunlight entering the window and striking the optical unit, with the attendant heating, may cause deformation in the instrument, producing a loss of optical accuracy.

(4) Sunlight impinging on the instrument optics causes scattering of light and a loss in viewing capability.

These conditions have resulted in the requirement for a window shade (recommended by Kollsman). The shade is a thin opaque member of approximately the same dimensions as the window. Hinged near the front edge of the window, the shade is positioned at an angle to it which depends on the direction of the sun. Figure V-8 illustrates these angles and the geometry involved for various sun positions. It will be noted that some field of view of the window is lost by the shade -- up to one-half when the sun is 30° to the normal of the window. Ideally, two shades per window, front and back, should be provided. To simplify the shade mechanism, however, only one is recommended. This adds the requirement to rotate the vehicle to the proper attitude to utilize the shade. The front of the window was chosen for the hinge point because the normal attitude of the vehicle is nose-to-sun. In this manner, less maneuvering would be required and the propellants would be kept cooler. This is shown, as well as operation of the shade and the attitude requirements, in Fig. V-9.

Further investigation of the sun and shading problem was made. The angle between the sun and the body of interest was determined from a typical trajectory, assuming different periods of the lunar month. For simplicity, a coplanar case was taken; although it was recognized that the situation would be alleviated to some extent in the three-dimensional case because all bodies do not lie in the same plane. The trajectory chosen was an 80-hour one shown in the Arma study report - Ref II-1 (Fig. V-10). Sun-body angles were tabulated for various periselenium phases. The results are shown in Table V-2.

TABLE V-2

Sun-Body Angles

Time after Injection (hr)	Angle (sun and moon)(deg)	Angle (sun and earth)(deg)
Case 1. New Moon (periselenium)		
10	46	195
20	51	189
30	54	185
40	57	183
50	59	181
60	62	180
70	68	181
Case 2. Crescent Moon After New (periselenium)		
10	1	150
20	6	144
30	9	140
40	12	138
50	14	136
60	17	135
70	23	136
Case 3. First Quarter (periselenium)		
10	44	105
20	39	99
30	36	95
40	33	93

TABLE V-2 (cont)

Sun-Body Angles

Time After Injection (hr)	Angle (sun and moon) (deg)	Angle (sun and earth) (deg)
50	31	91
60	28	90
70	22	91
Case 4. Gibbous Moon before Full (periselenium)		
10	89	60
20	84	54
30	81	50
40	78	48
50	76	46
60	73	45
70	67	46
Case 5. Full Moon (periselenium)		
10	134	15
20	129	9
30	126	5
40	123	3
50	121	1
60	118	0
70	112	1

TABLE V-2 (cont)

Sun-Body Angles

Time After Injection (hr)	Angle (sun and moon) (deg)	Angle (sun and earth) (deg)
Case 6. Gibbous Moon After Full (periselenium)		
10	179	30
20	174	36
30	171	40
40	168	42
50	166	44
60	163	45
70	157	44
Case 7. Last Quarter (periselenium)		
10	136	75
20	141	81
30	144	85
40	147	87
50	149	89
60	152	90
70	158	89
Case 8. Crescent Before New (periselenium)		
10	91	120
20	96	126
30	99	130
40	102	132

TABLE V-2 (cont)

Sun-Body Angles

Time After Injection (hr)	Angle (sun and moon) (deg)	Angle sun and earth (deg)
50	104	134
60	107	135
70	113	134

These data, all for the outgoing leg, show that there are several periods during the lunar month when lighting conditions are not ideal for navigation. In the full moon (periselenium) case, the earth is close to the sun, making observation of that body difficult. In the crescent after new moon phase (periselenium) the moon is difficult to observe because of the proximity of the sun. On the return leg, the mirror image of the problem exists, for the circumlunar case, making the crescent before new moon (periselenium) also an undesirable time for moon observations. These undesirable times are shown graphically in Fig. V-11. The shaded regions represent periods when the sun is a problem. A minimum angle of 30° was chosen because this angle cuts out half of the window field of view. As mentioned earlier about the three dimensional case, the problem is somewhat mitigated, which means, that the shaded areas will shrink.

These investigations indicate that the sun can be a problem in some periods of the lunar month. Theroretically, only one body is required for navigation and this problem can be ignored. However, for the early Apollo missions it is recommended that the poor lighting periods be avoided so that both bodies can be observed without difficulty. For the mission which includes lunar orbiting, ideally a good lighting period would be chosen for the outgoing leg with a wait in orbit until a good lighting situation existed for the return leg.

G. EMERGENCY MODES

The normal operation of the guidance system has been described earlier. It is repeated briefly here to implement a discussion of emergency modes of operation (modes of operation when one or more subsystems malfunction). Normally acceleration and tracker signals from the astro-inertial platform are fed to digital computer No. 1 for navigation and steering signal calculation as well as alignment of the platform (see Fig. V-12). In midcourse and lunar orbit, telesextant angular signals also are applied to the computer for navigational purposes. The miniature platform is operated in parallel with astro-inertial platform during ascent, lunar orbit injection and ejection, re-entry and abort. Digital computer No. 2 receives the same inputs as does No. 1 and its outputs, other than steering and propulsion signals, are fed to the display system.

A malfunction of the miniature platform means that the astro-inertial platform no longer has a standby unit. This applies also to a malfunction of digital computer No. 2. A failure of digital computer No. 1 requires switching over to the No. 2 computer for primary system operation. These emergency modes are relatively trivial and will not be discussed further.

When the astro-tracker portion of the astro-inertial platform malfunctions, the telesextant becomes the primary source of angular information (see Fig. V-13). This unit then supplies the basic navigational information to the computer. For updating of the astro-inertial platform's gimbals, stellar readings are taken by the telesextant and these angles are compared with the platform angles in the computer, the difference being used to tighten the platform to the proper orientation. Otherwise operation is normal.

If there is a malfunction of the entire astro-inertial platform, additional steps must be taken (see Fig. V-14). Not only does the telesextant become the primary angular reference but the miniature platform is the primary inertial guidance unit. Navigational angular data are fed to the computer as in normal operation. Alignment of the miniature platform is maintained by stellar shots by the telesextant, these data being transmitted to the computer, transformed into the proper coordinate system, and fed to the miniature platform as torquing signals.

If the telesextant should malfunction, the primary navigational and alignment data must come from the astro-tracker on the astro-inertial platform (See Fig. V-15). Alignment information for the platform is supplied by the tracker in a normal manner. Navigational data available are in the form of body center and body diameter information from rim tracking. Sextant and occultation measurements are therefore not available. Such an eventuality is considered extremely remote, since redundancy of functions is built into the telesextant. These redundancies are:

(1) Remote or manual positioning.

(2) Automatic or manual readout.

(3) Sextant, body center, occultation, star angle and stadiametric measuring capability.

In the latter item, if the sextant portion of the instrument malfunctions, the occultation and star angle measurements are still available. In the first two items, the emergency capabilities are obvious. Other redundancies built into the unit include manual slewing to remain on an observed object in the event of absence of stabilization signals or aided tracking capability.

In the case of multiple malfunctions such as:

(1) Telesextant and one of the computers

(2) Astro-tracker portion of the astro-inertial platform, the miniature platform and one of the computers

(3) Total loss of the astro-inertial platform and one of the computers

(4) Malfunction of the telesextant, the miniature platform, and one of the computers

Guidance operation will be performed as planned. When two of the same type of subsystem malfunction, such as astro-inertial platform and/or telesextant and miniature platform or both computers malfunction, manual operations, as discussed earlier in Chapter II, must be utilized. Due to the high reliability of each subsystem, such an eventuality is extremely remote.

It will be noted that in the Martin guidance concept a certain amount of automaticity is inherent in the overall system. This portion of the system can take over during periods of incapacitation of the crew, such as sickness, fatigue and space suit operation. This feature can also fill in for the unknowns in the ability of the astronaut to navigate in space.

A further capability must be incorporated into the system; that is, guidance during complete and prolonged incapacitation of the crew. This situation could arise when all of the crew members are stricken with the same dose of radiation from a solar flare. An emergency situation also may exist from a meteorite penetration. Regardless of the cause, provision must be made for any eventuality, at least in the early circumlunar flights.

To cope with such an eventuality, an automatic programmer is provided. A series of lights are presented to the Navigator-Pilot. One that is green denotes that manual control of the vehicle is in effect. To maintain crew control, a button must be pushed every hour. If this button is not pushed, the green light goes off and a flashing yellow light comes on. This display indicates that if the astronaut does not push the crew control button, automatic control of the vehicle will take over. Automatic control is indicated by a red light coming on. This latter event also closes a switch which allows ground control to take over. If the ground decides to allow the on-board programmer to be in control, the guidance system is automatically switched into an abort mode.

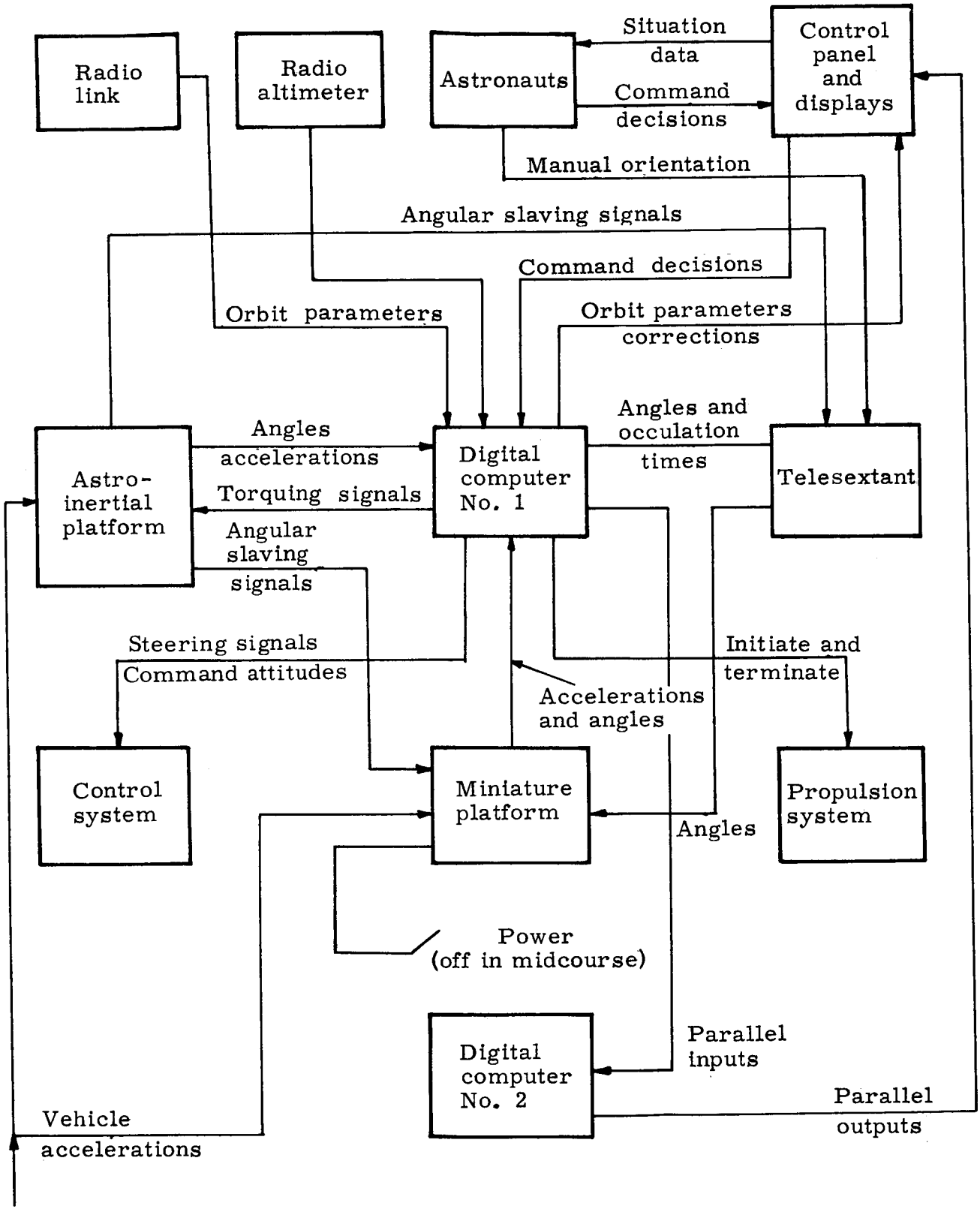

Fig. I-1. Guidance System Block Diagram

MANUAL INPUT

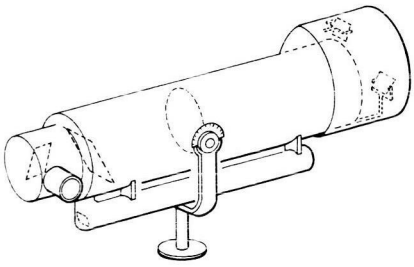

TELESEXTANT

Weight 20 lb
Size 0.64 cu ft
Power 20 watts
Angular accuracy 10 sec arc
Manufacturer--Kollsman

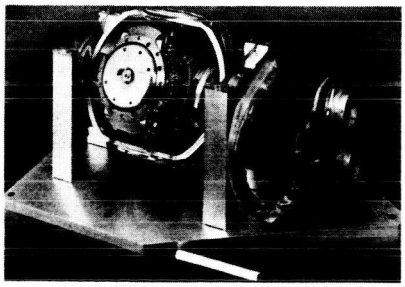

MINIATURE PLATFORM

Weight 33.5 lb
Size 0.65 cu ft
Power 230 watts
Gyros 0.01 deg/hr
Accelerometers 10^{-5}g
Manufacturer--Litton

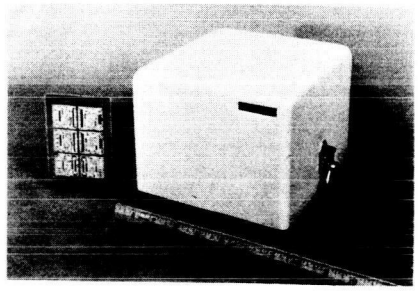

DIGITAL COMPUTER

Weight 21 lb
Size 0.3 cu ft
Power 60 watts
General purpose
Core storage
Microminiature
Manufacturer--Arma

AUTOMATIC INPUT

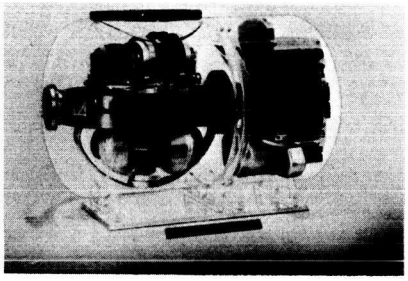

ASTRO-INERTIAL PLATFORM

Weight 55 lb
Size 1.3 cu ft
Power 150 watts
Gyro 0.01 deg/hr
Accelerometers 10^{-5}g
Tracking accuracy 6 sec arc
Manufacturer--Autonetics

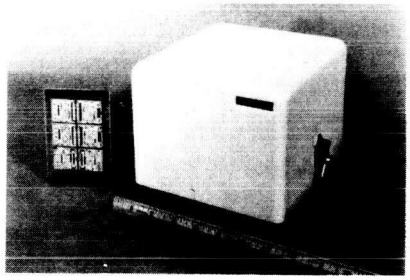

DIGITAL COMPUTER

Weight 21 lb
Size 0.3 cu ft
Power 60 watts
General purpose
Core Storage
Microminiature
Manufacturer--Arma

Fig. I-2. Guidance Components

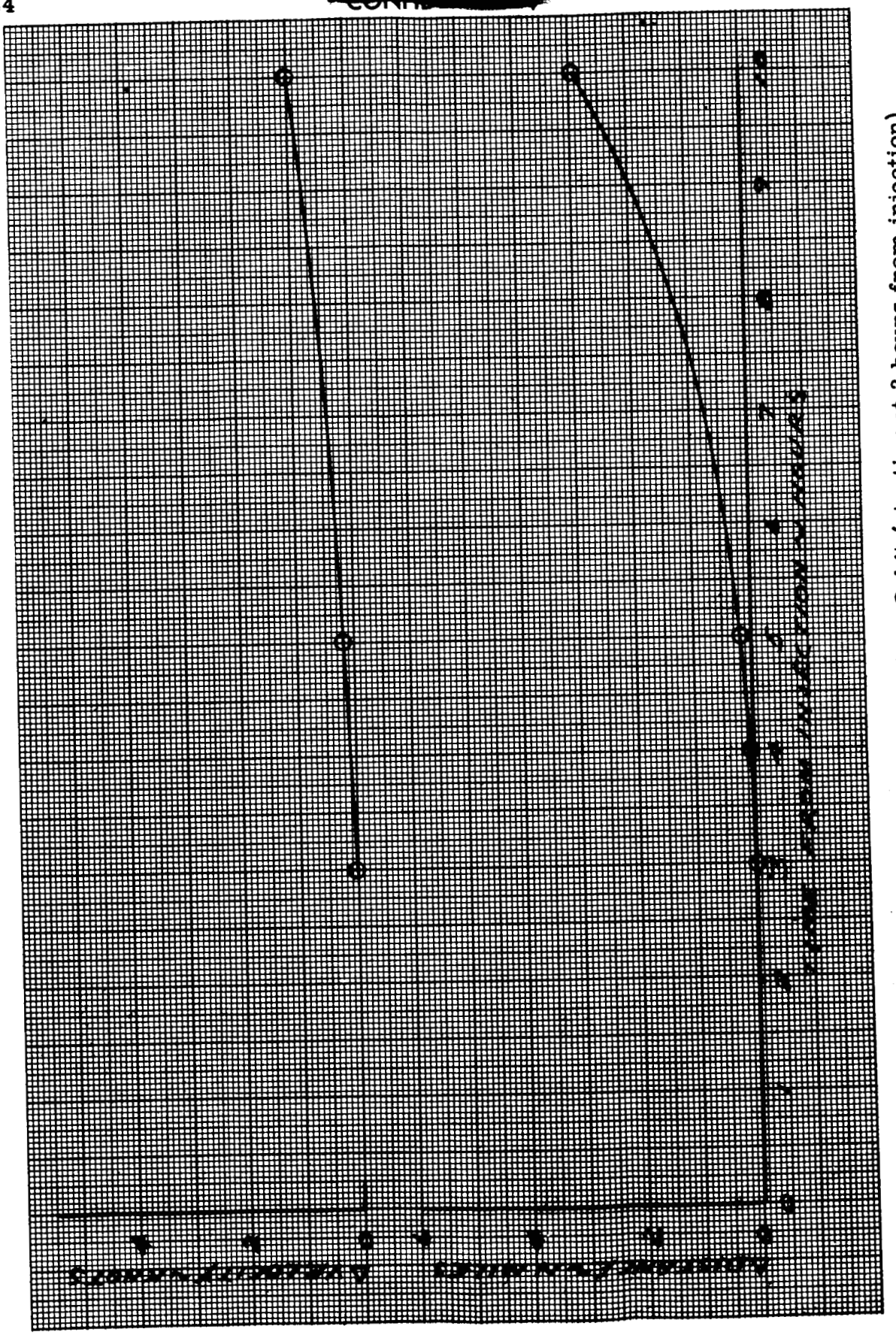

Fig. II-1. Deviation of Kepler Orbit from True Orbit (starting at 3 hours from injection)

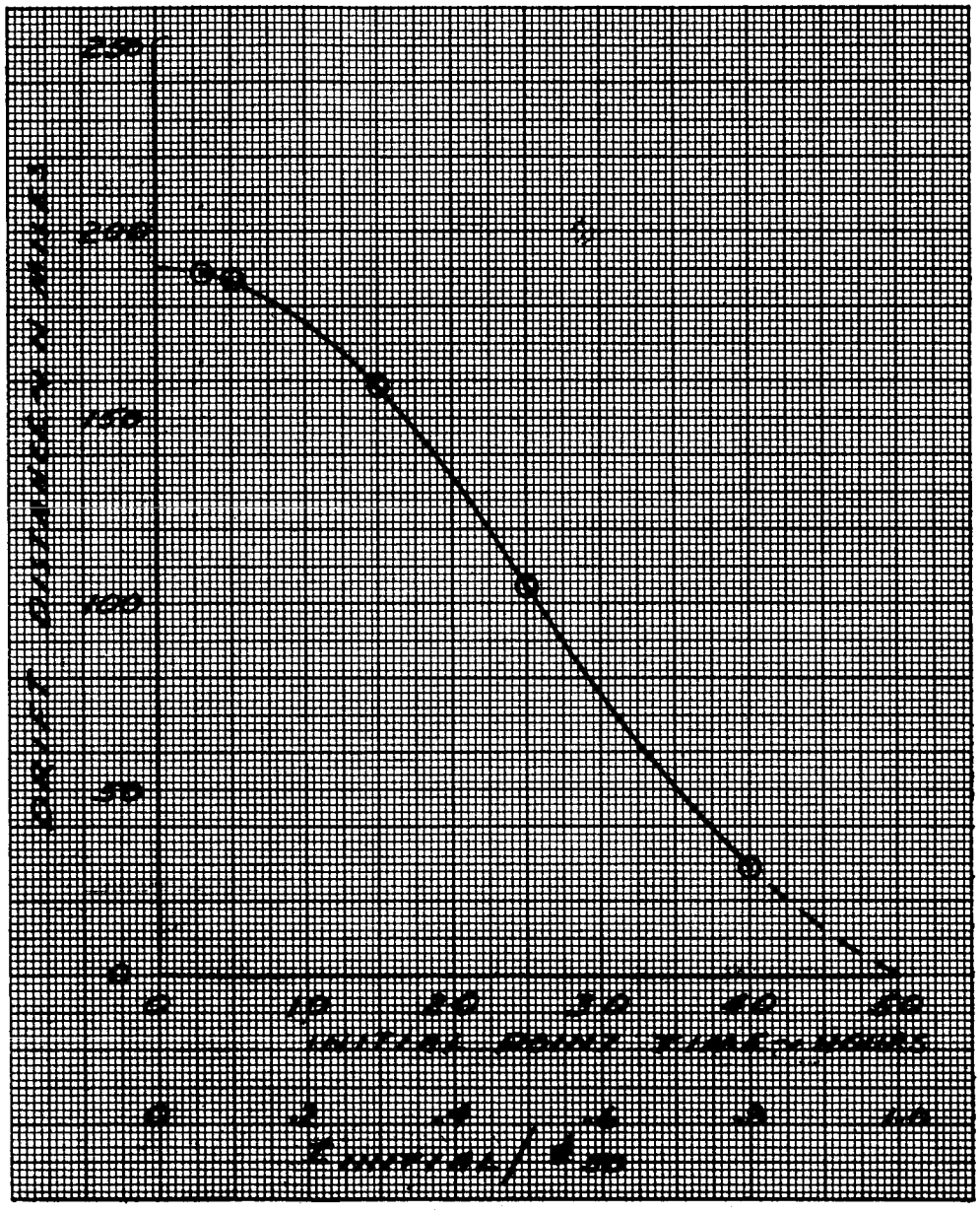

Fig. II-2. Fifty-Hour Drift Distance from Plane Defined at Initial Point

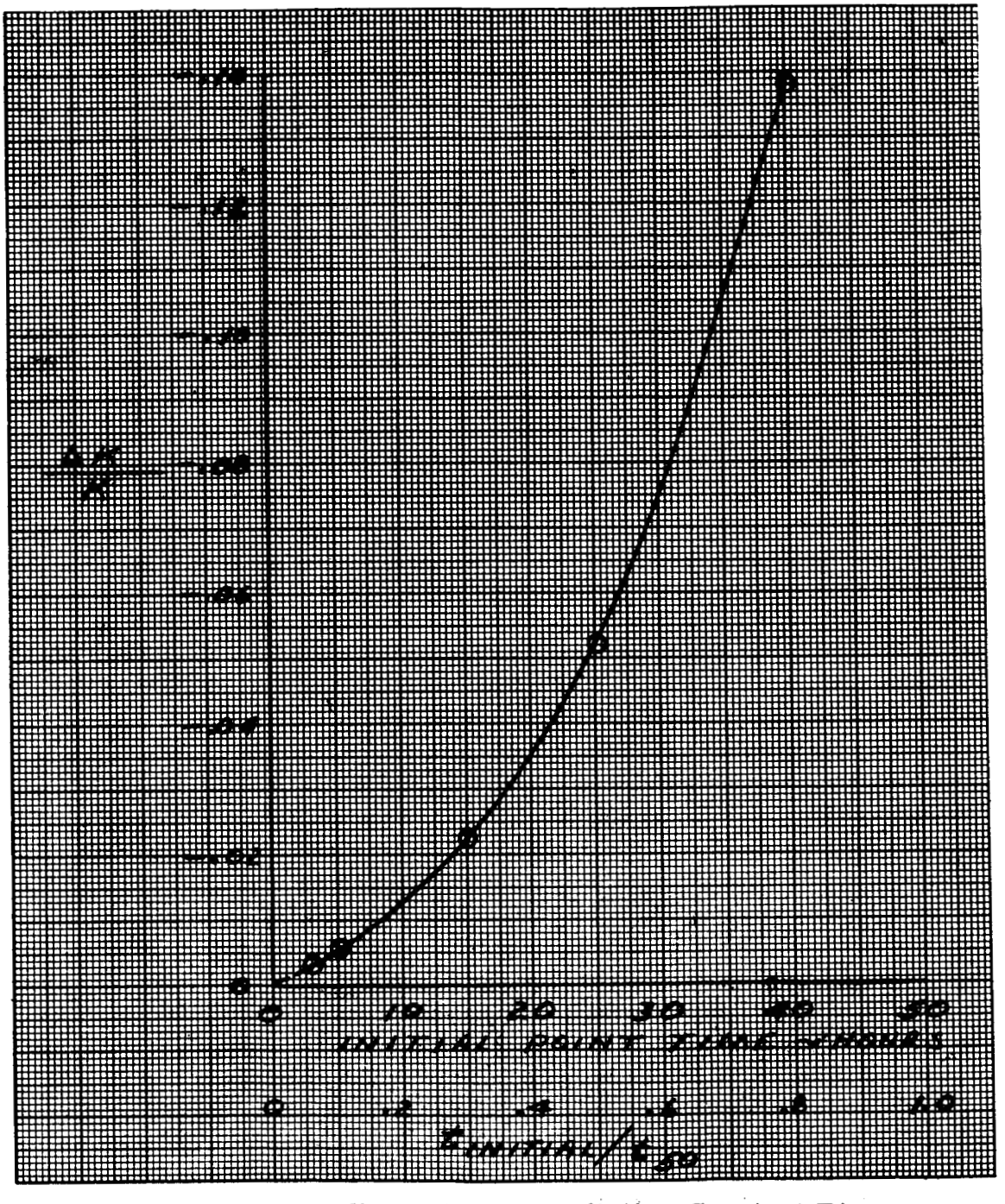

Fig. II-3. Nondimensional Gravitation Constant Bias

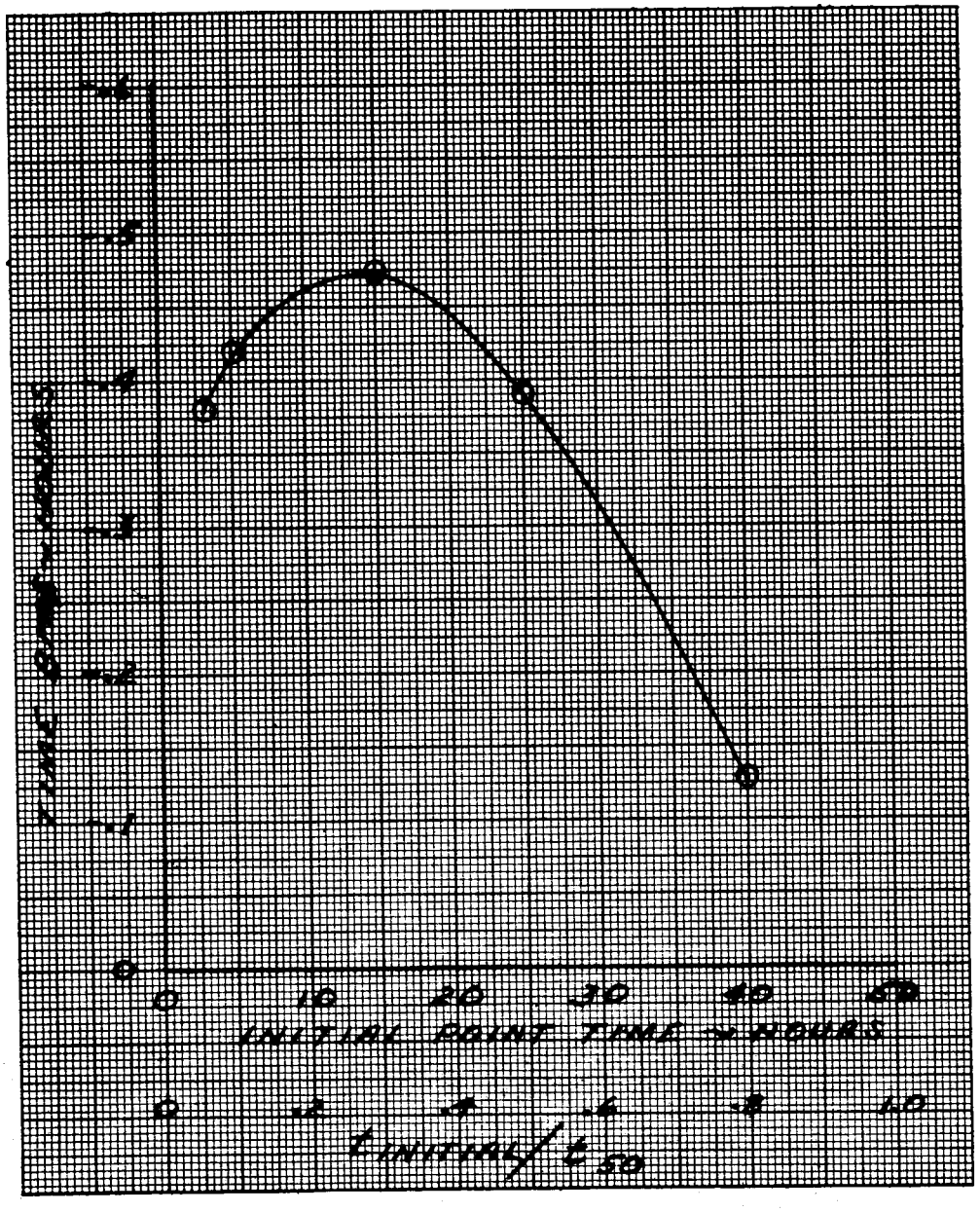

Fig. II-4. Time Bias at 50-hr Point

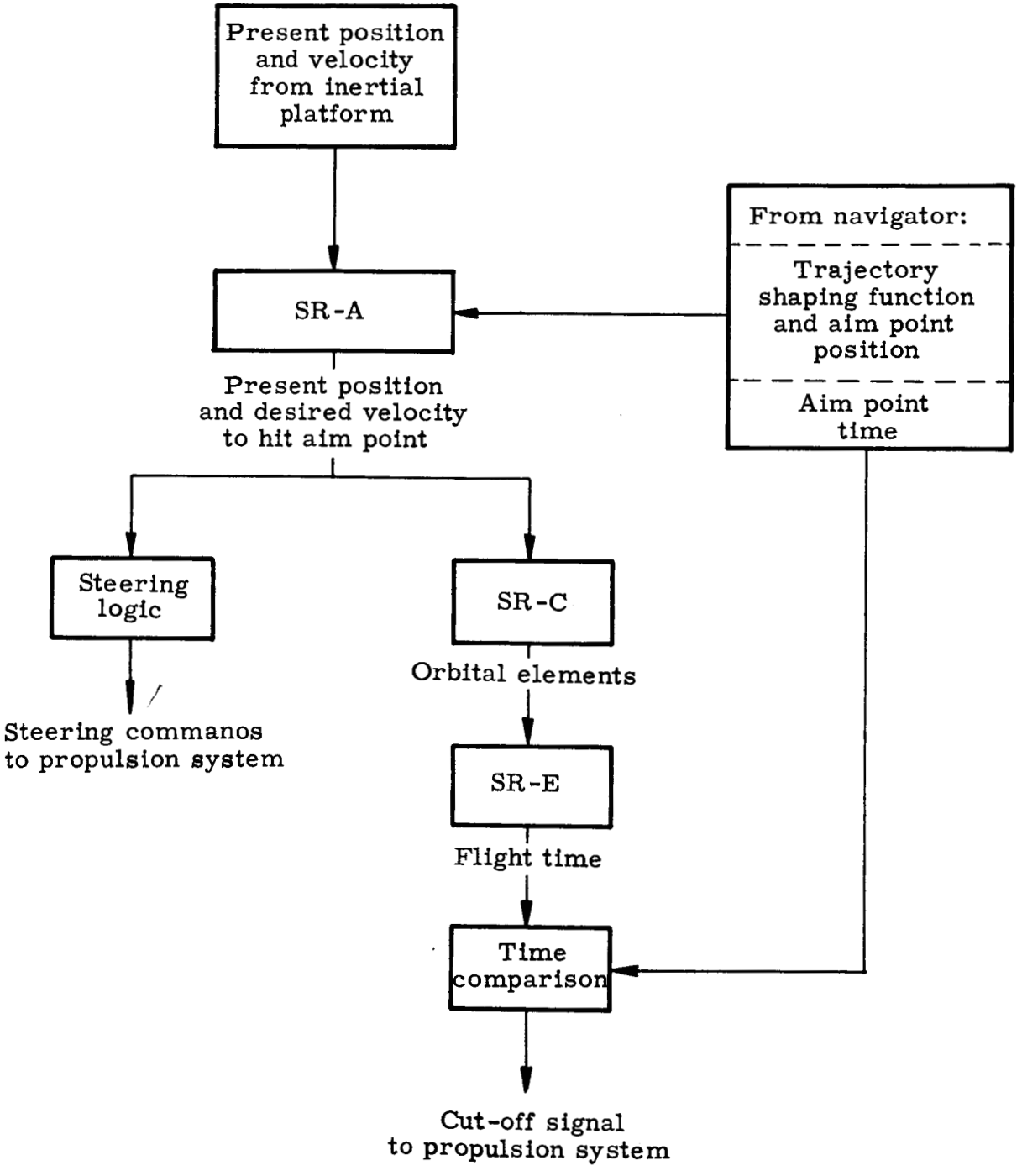

Fig. II-5. Guidance (program P-I)

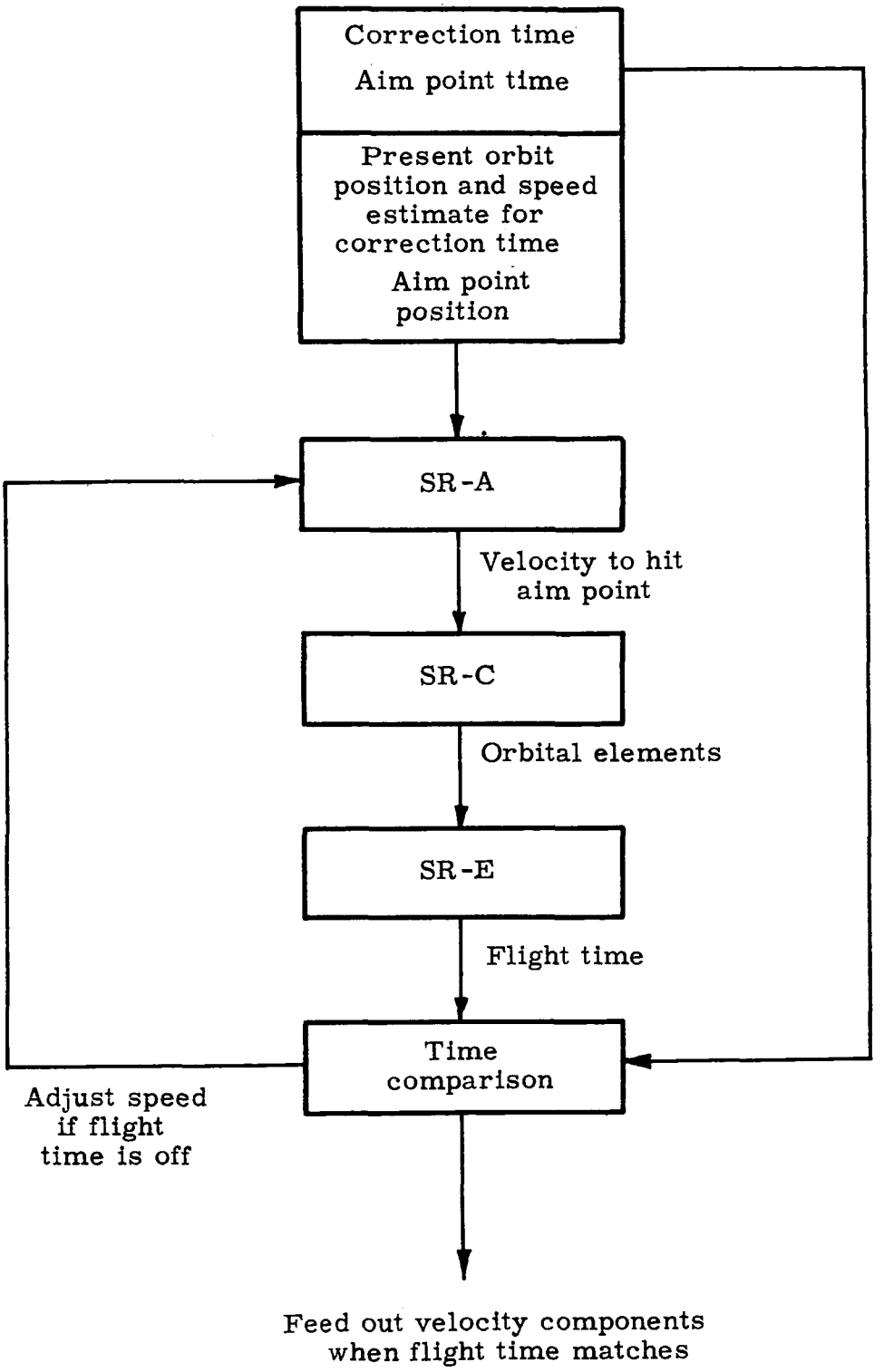

Fig. II-6. Guidance (program P-II)

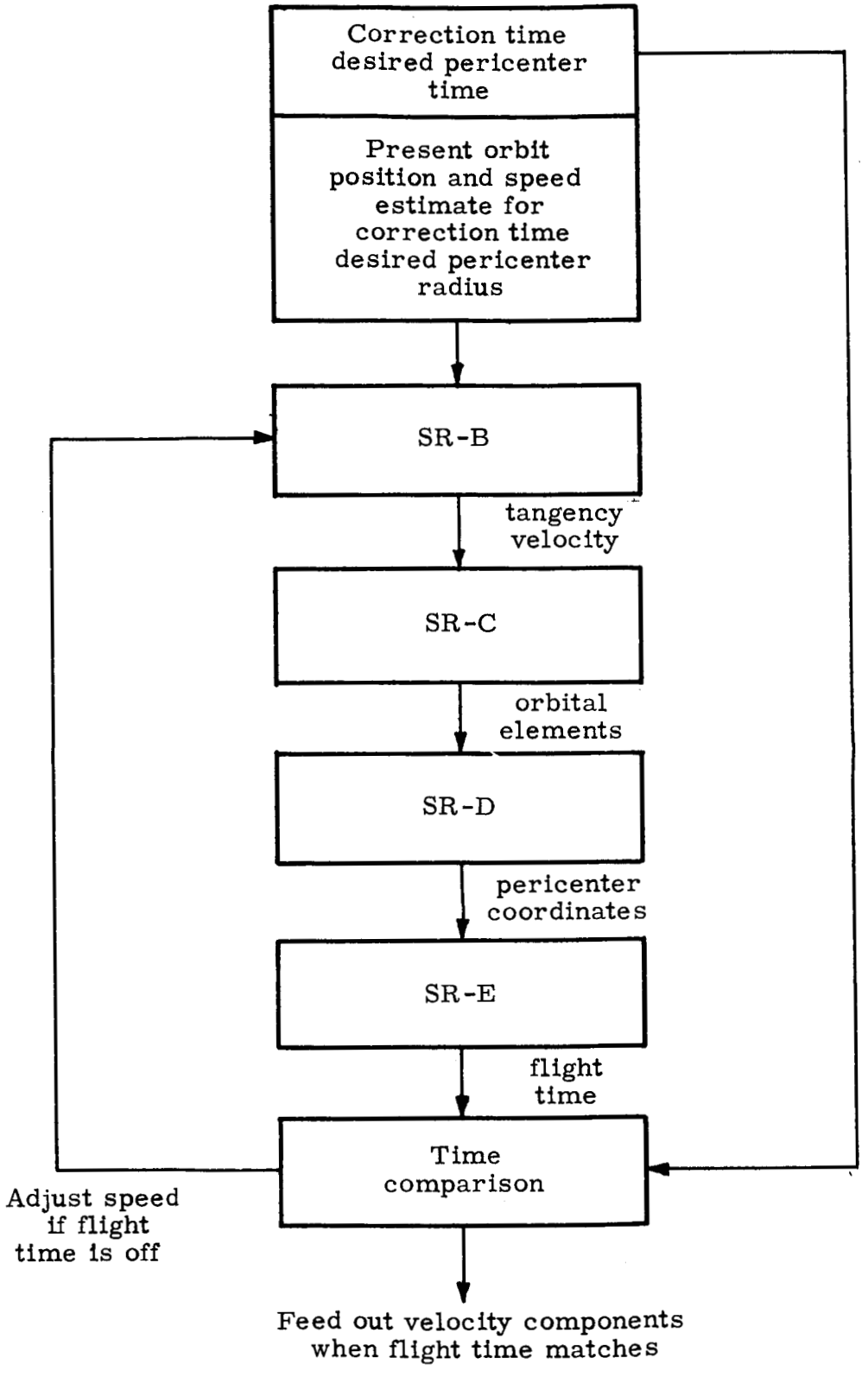

Fig. II-7. Guidance (program P-III)

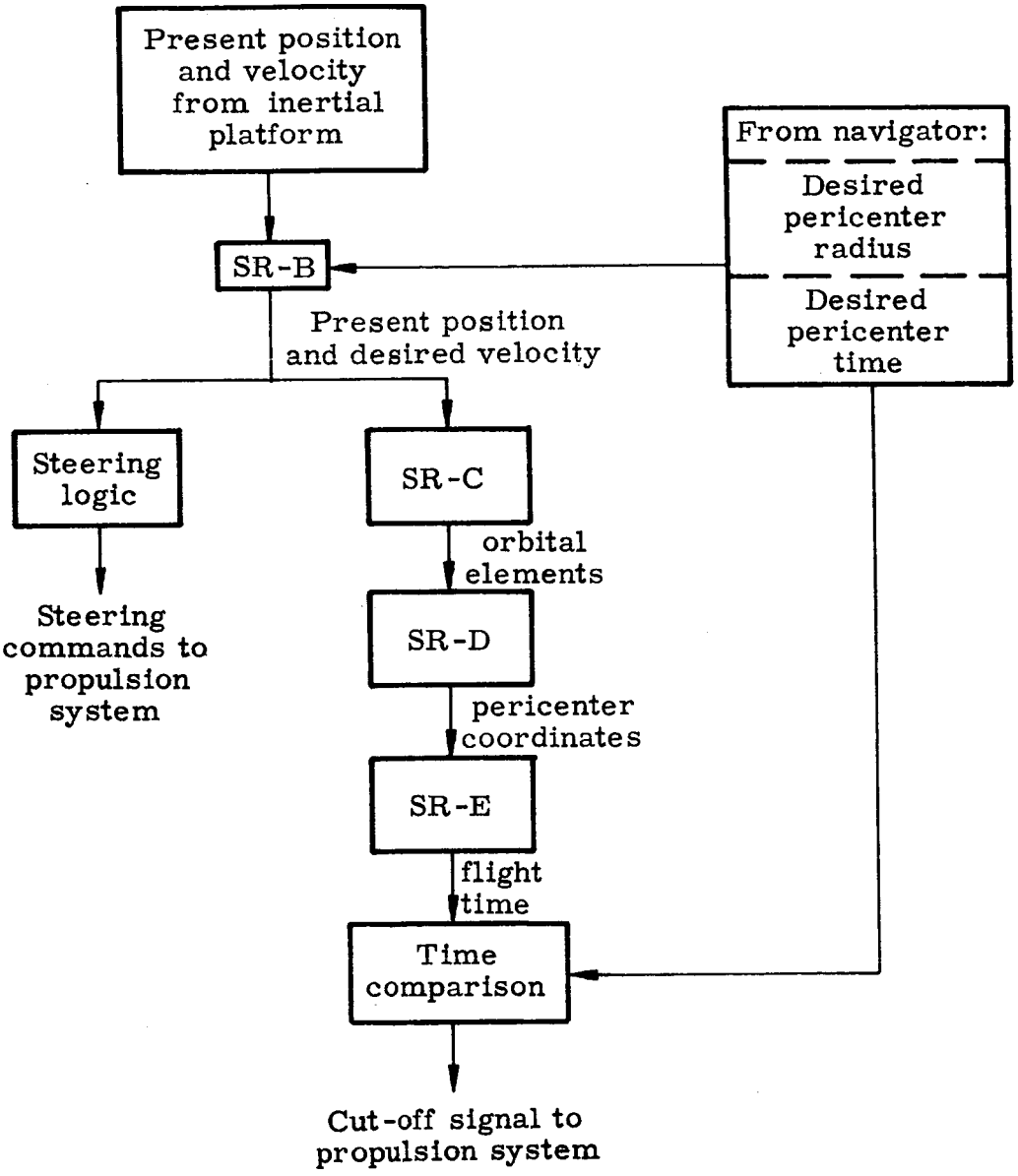

Fig. II-8. Guidance (program P-IV)

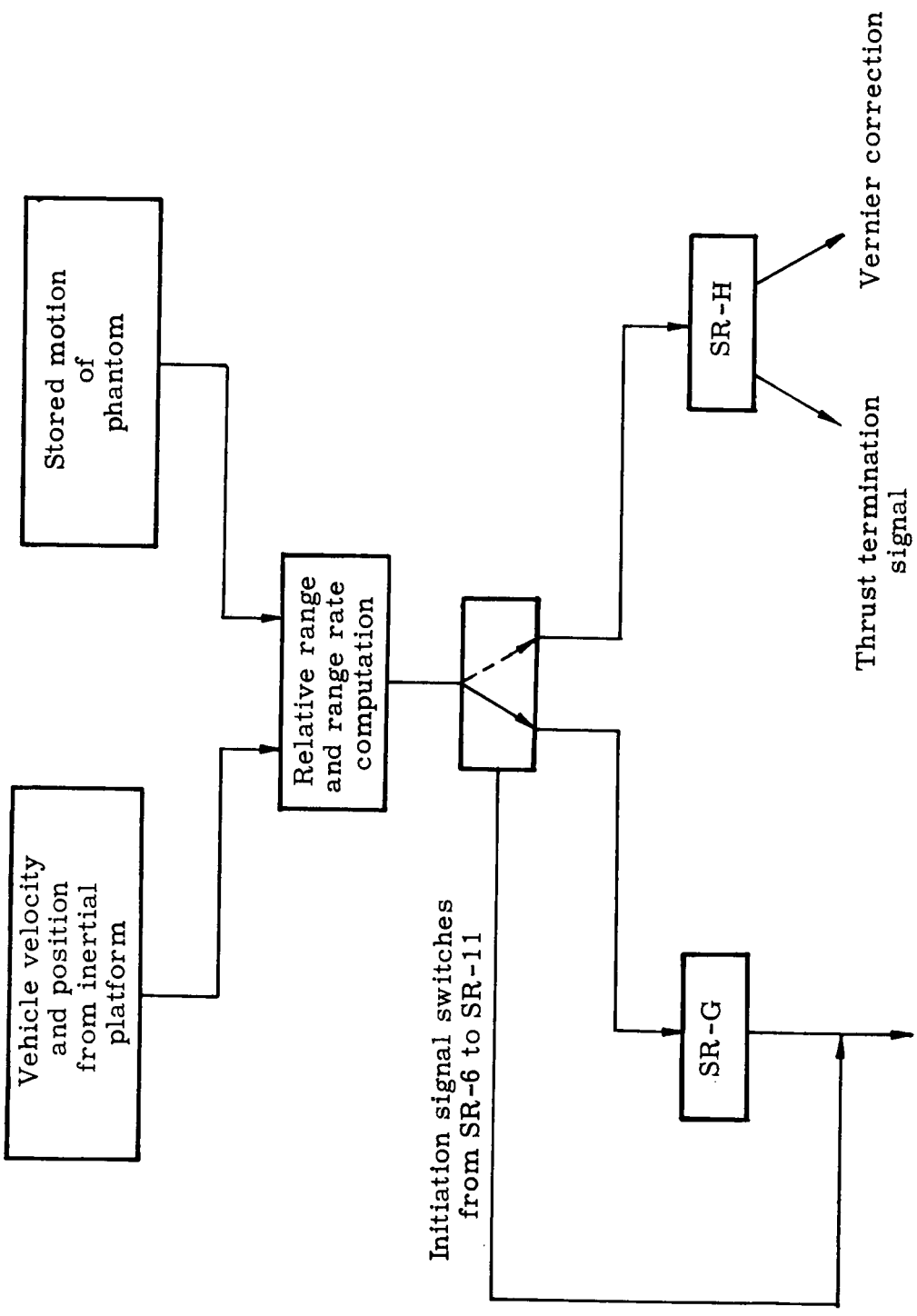

Fig. II-9. Guidance (program P-V)

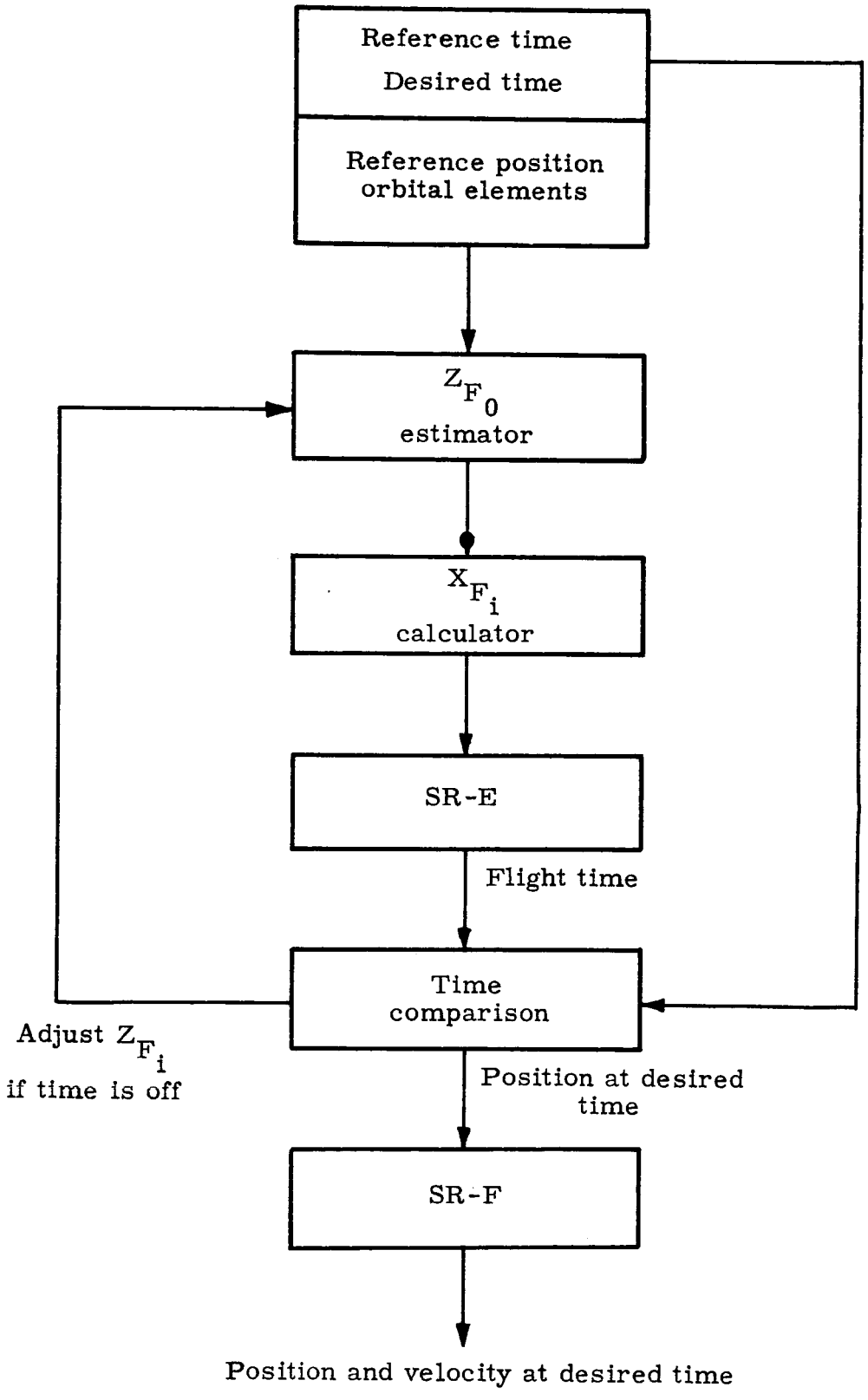

Fig. II-10. Guidance (program P-VII)

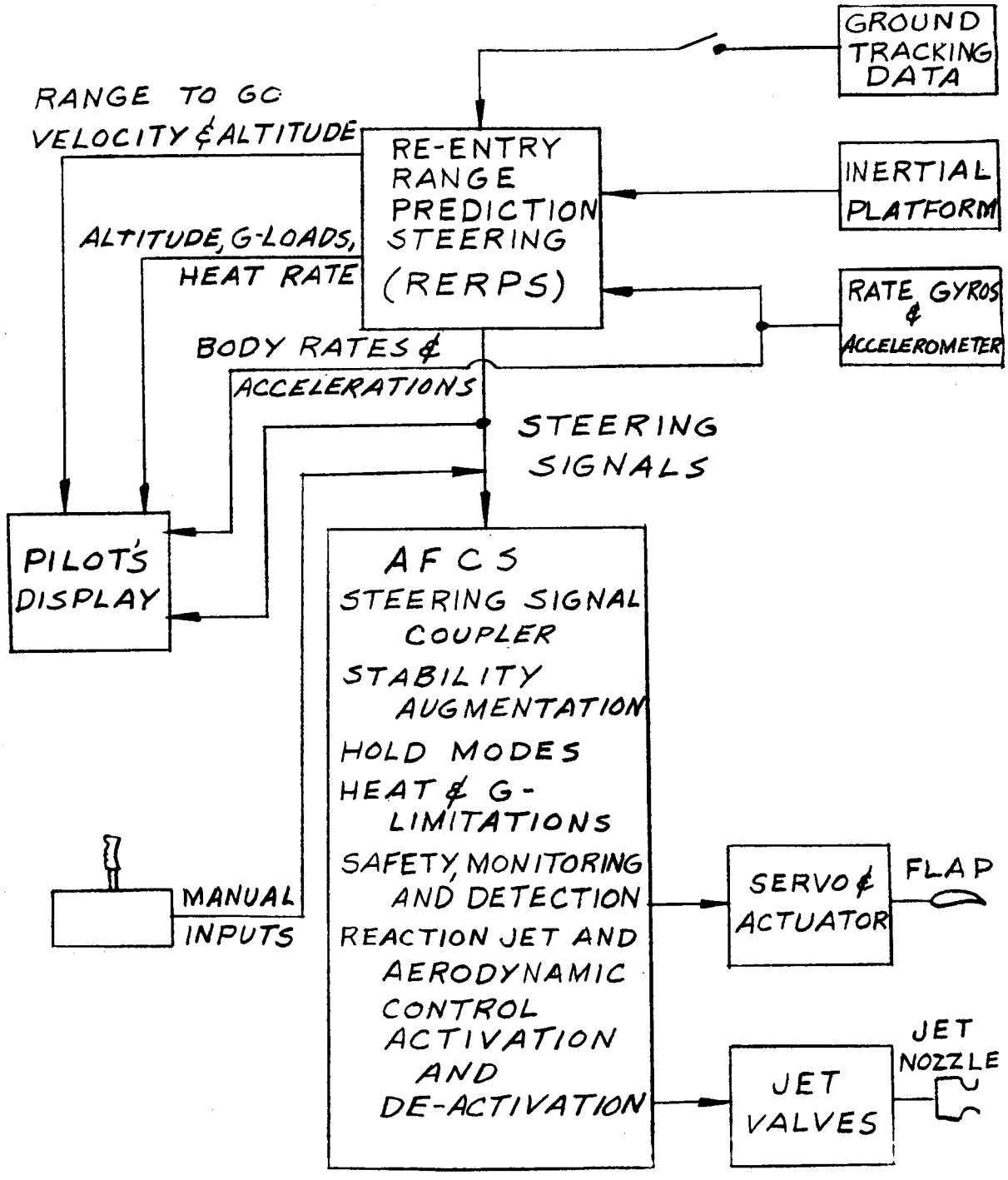

Fig. III-1. Guidance Control Block Diagram

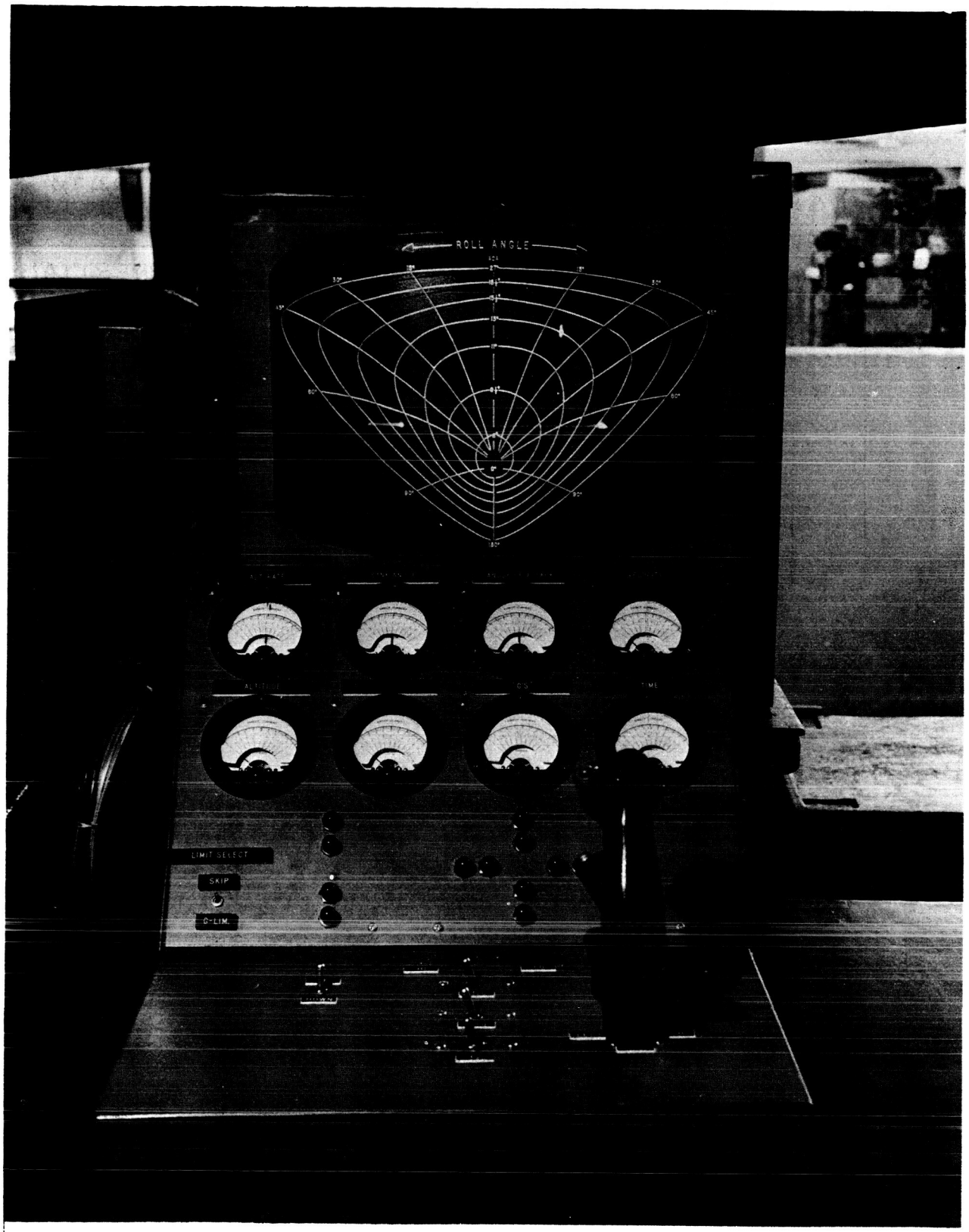

Fig. III-2. Re-Entry Range Prediction System Manual Simulation Display

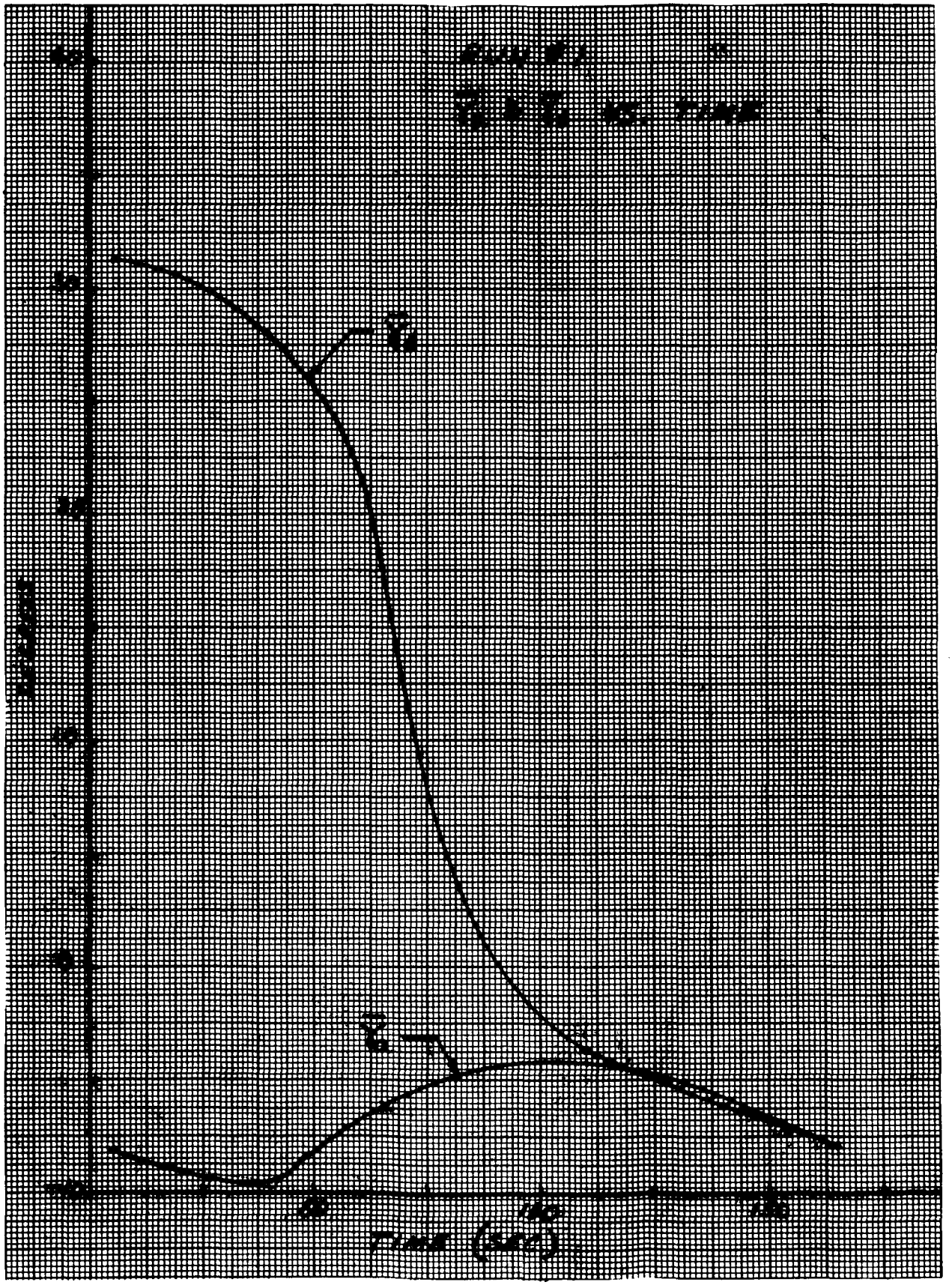

Fig. III-3. Desired Versus Actual Flight Path Angle--Run No. 1

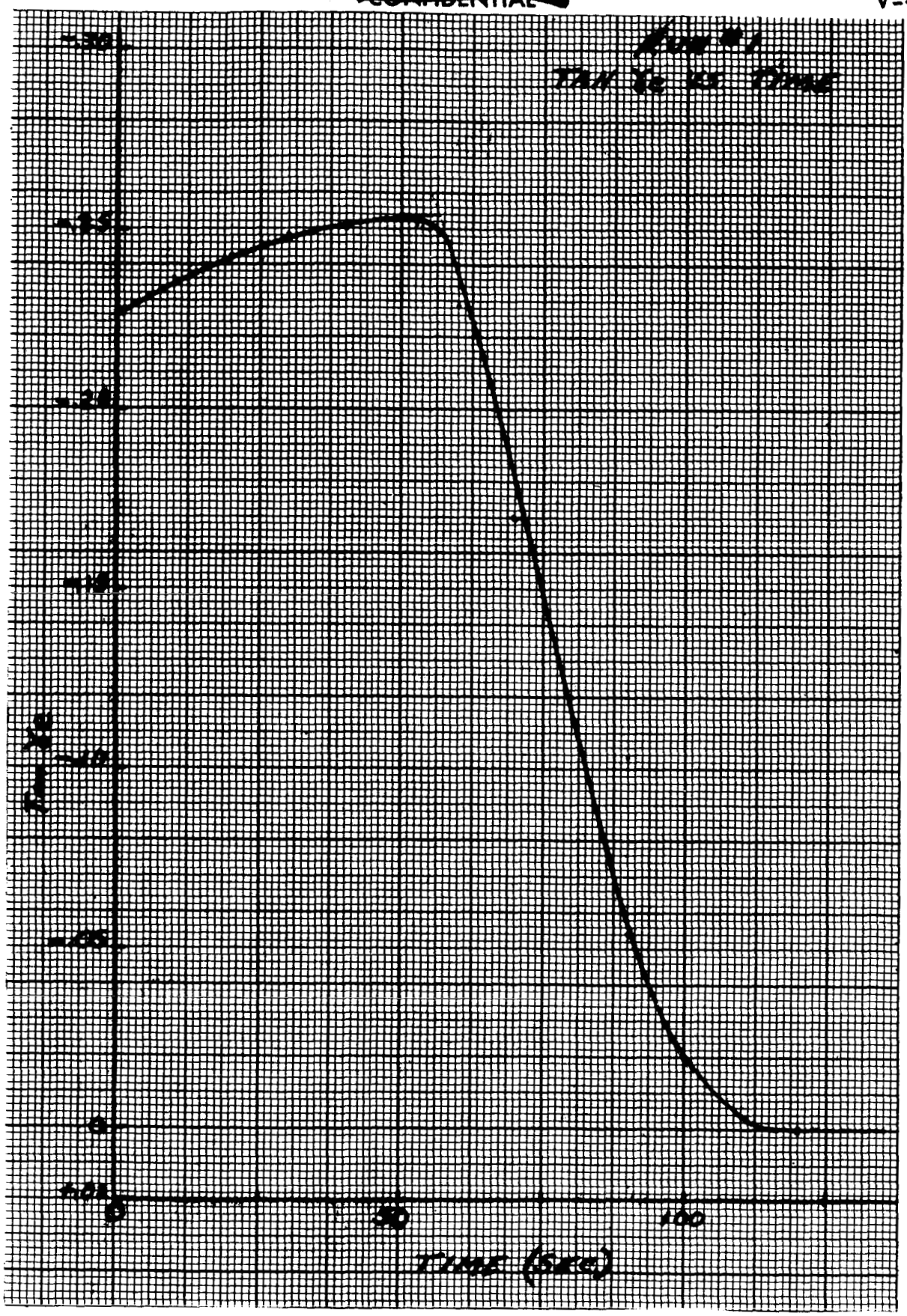

Fig. III-4. Tangent Error (γ_e) Versus Time (Run No. 1)

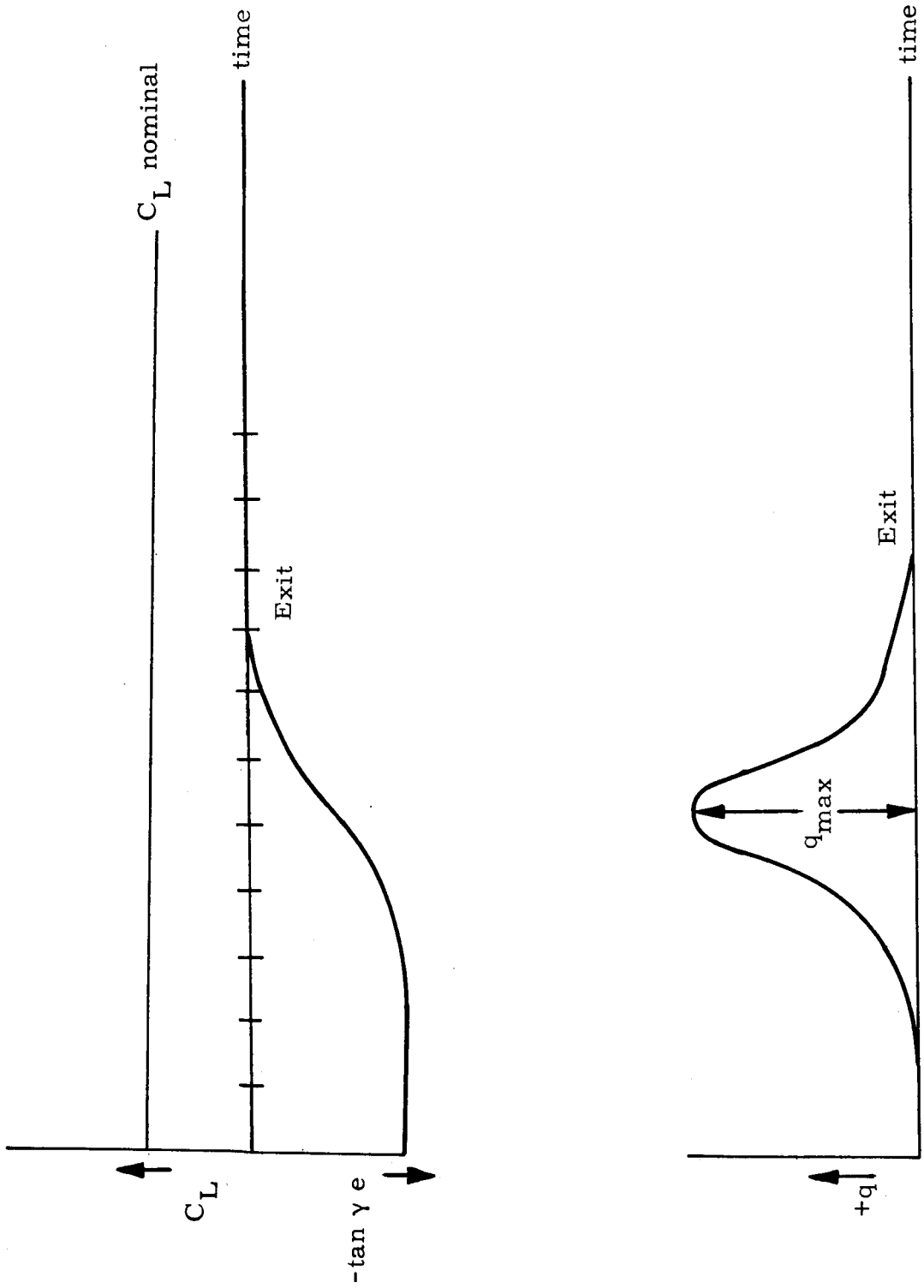

Fig. III-5. Nominal Run for Shaping Program

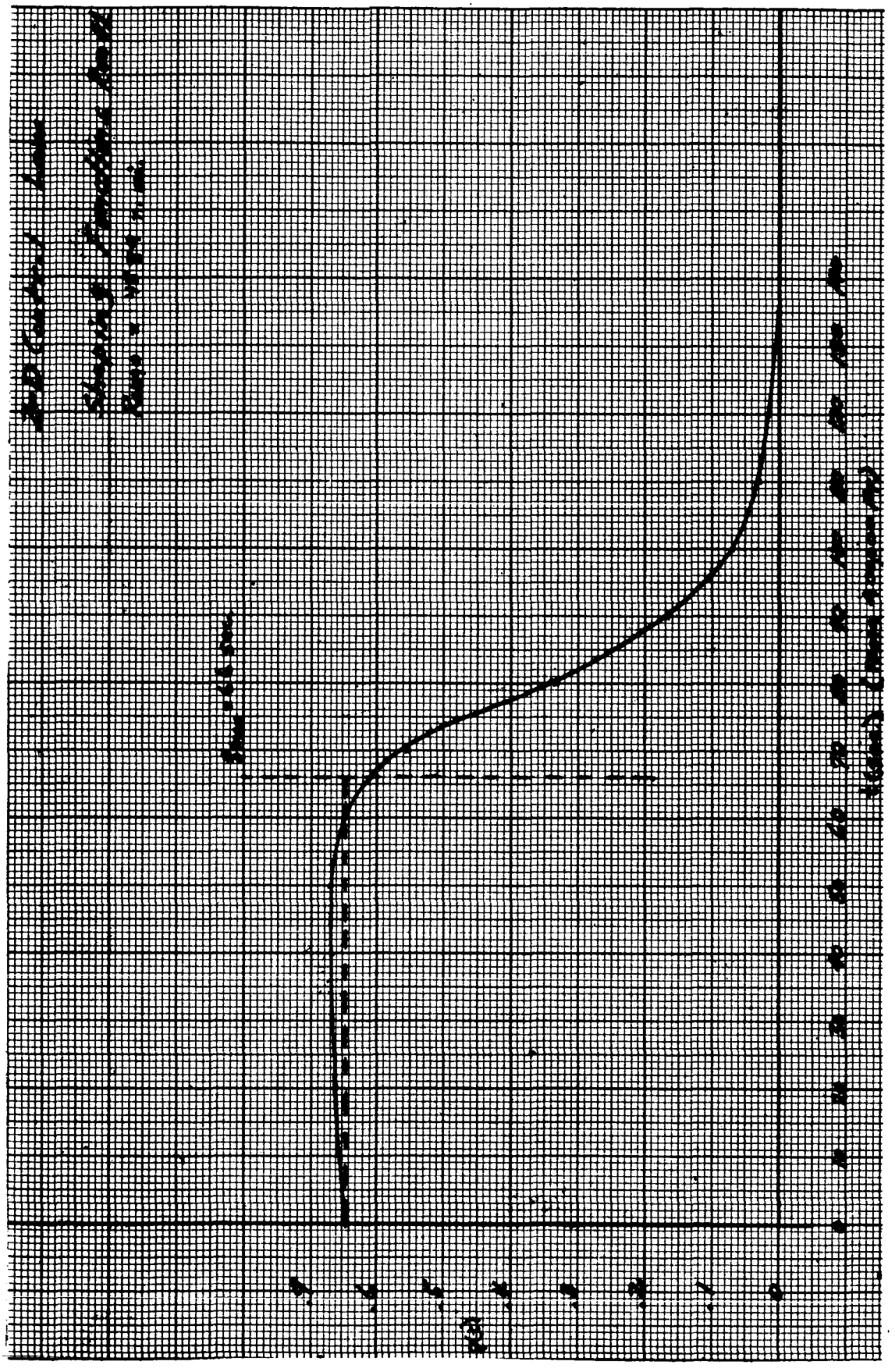

Fig. III-6. Shaping Function--Run No. 1

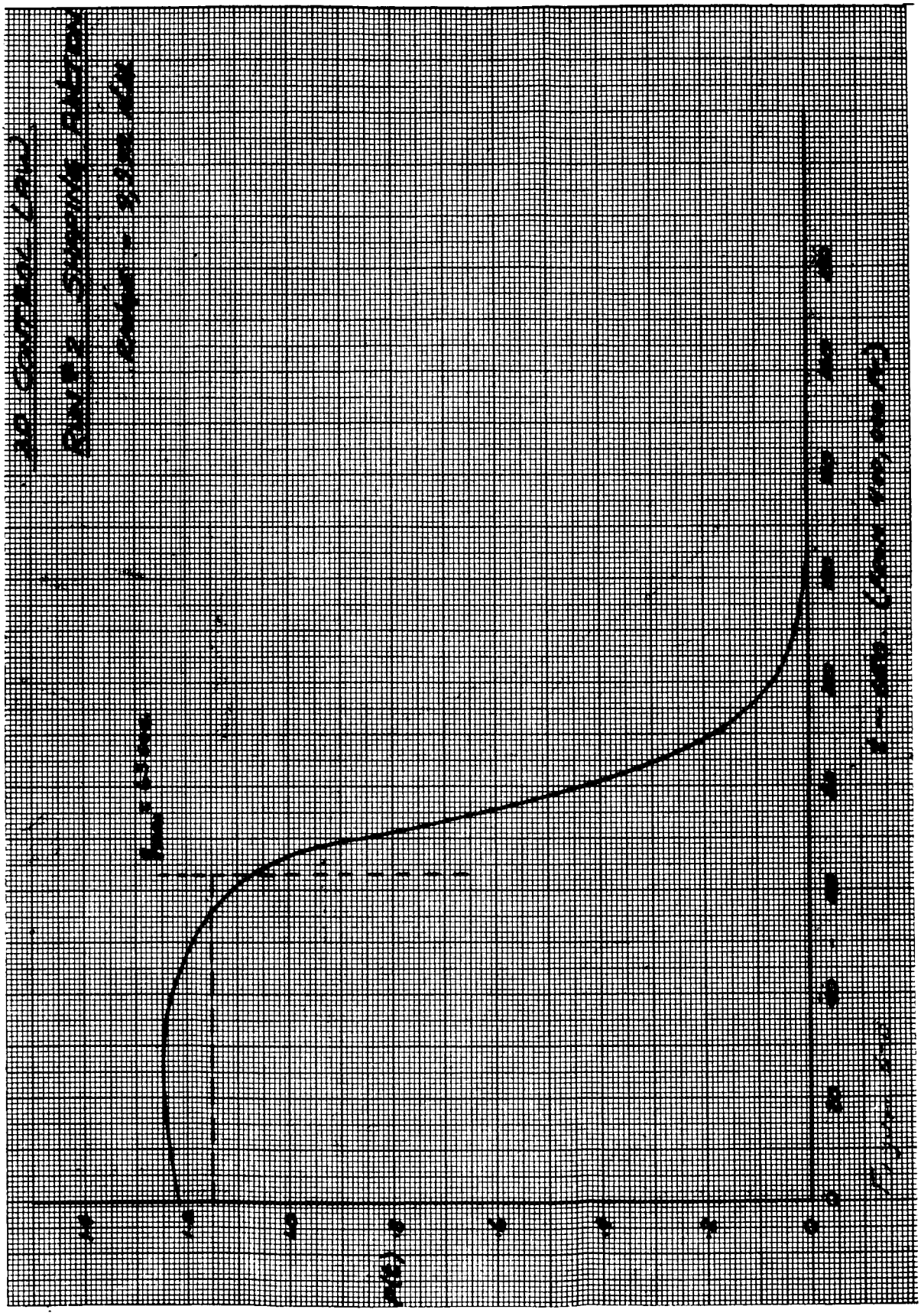

Fig. III-7. Shaping Function (Run No. 2)

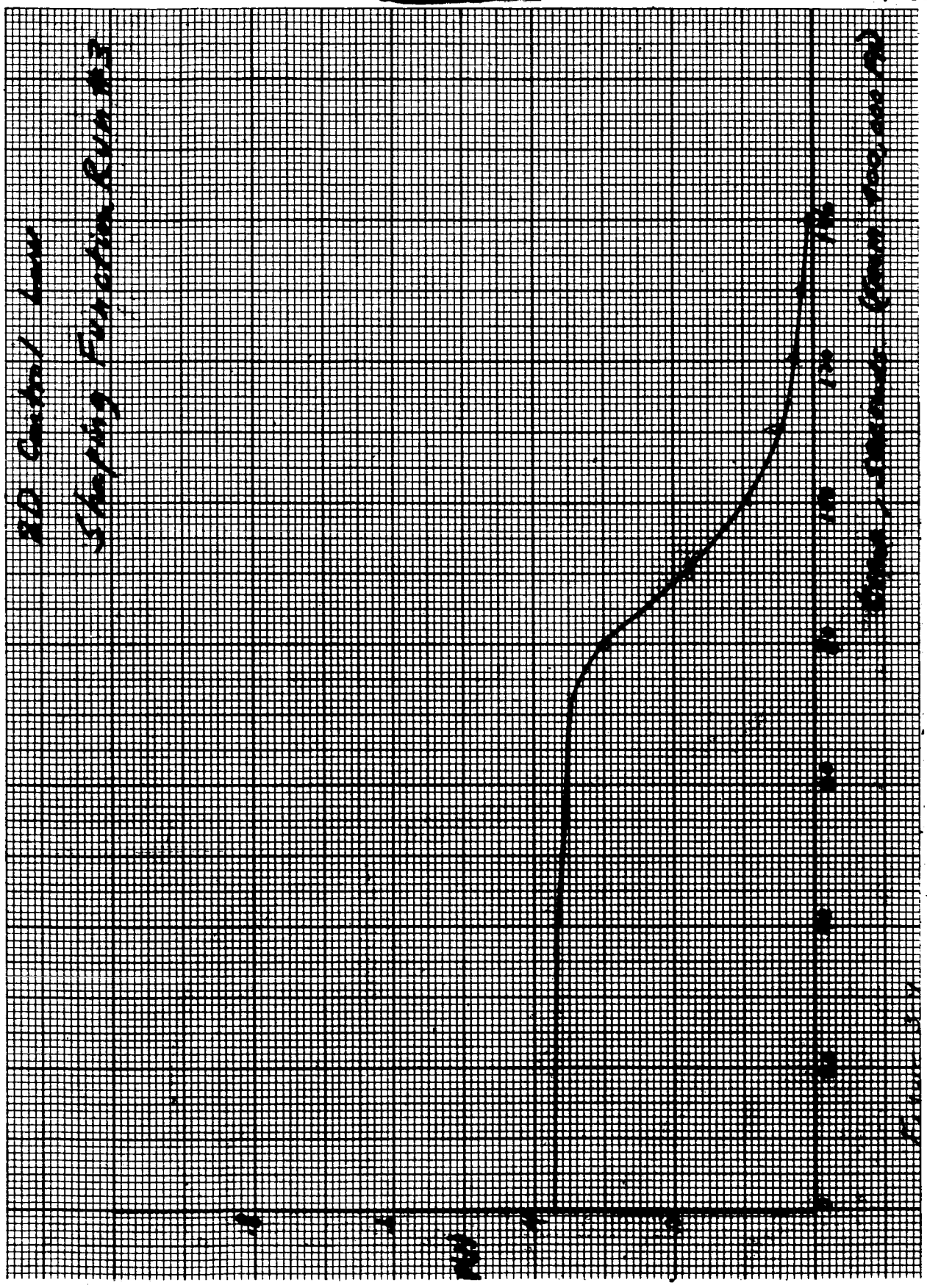

Fig. III-8. Shaping Function--Run No. 3

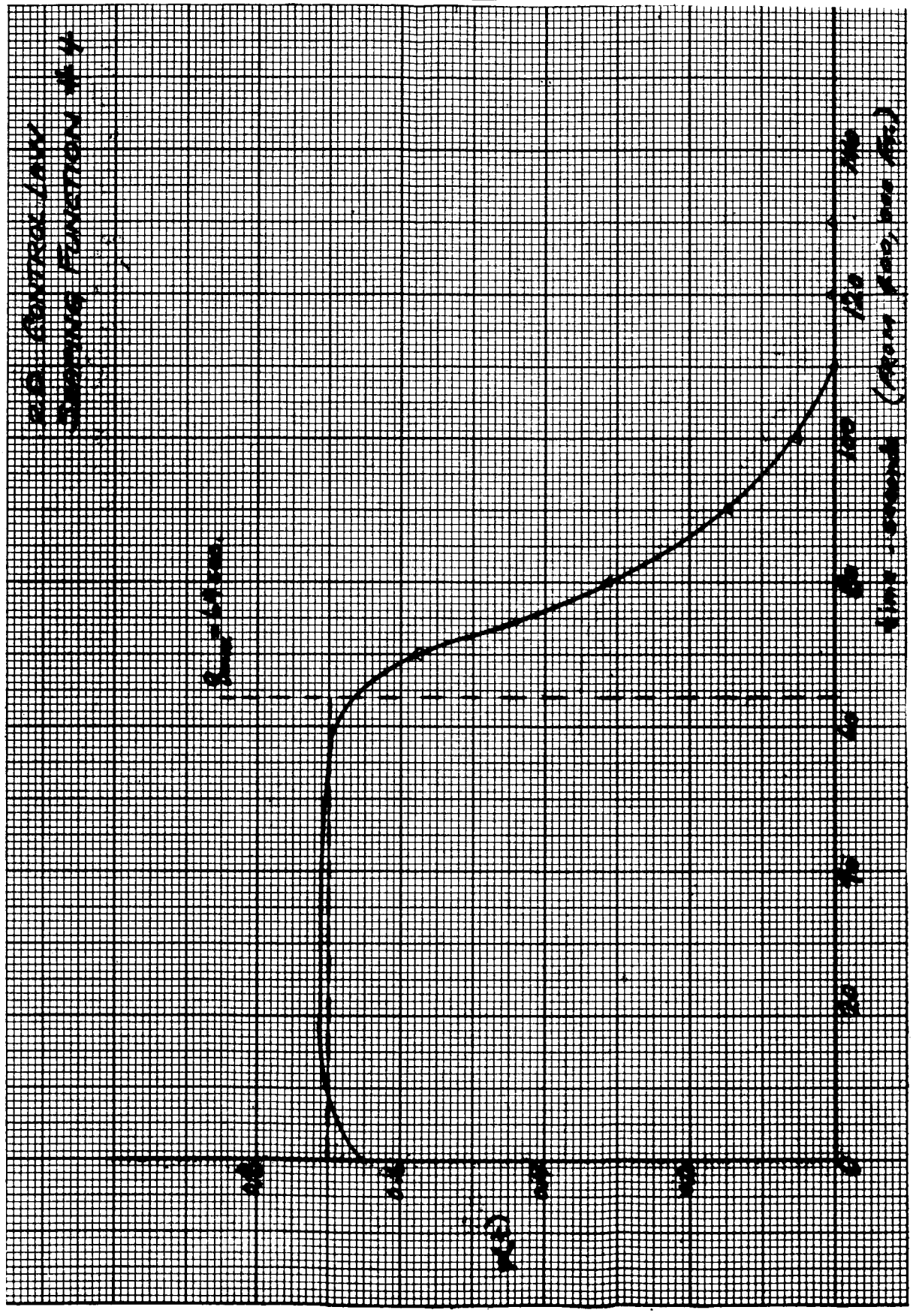

Fig. III-9. Shaping Function--Run No. 4

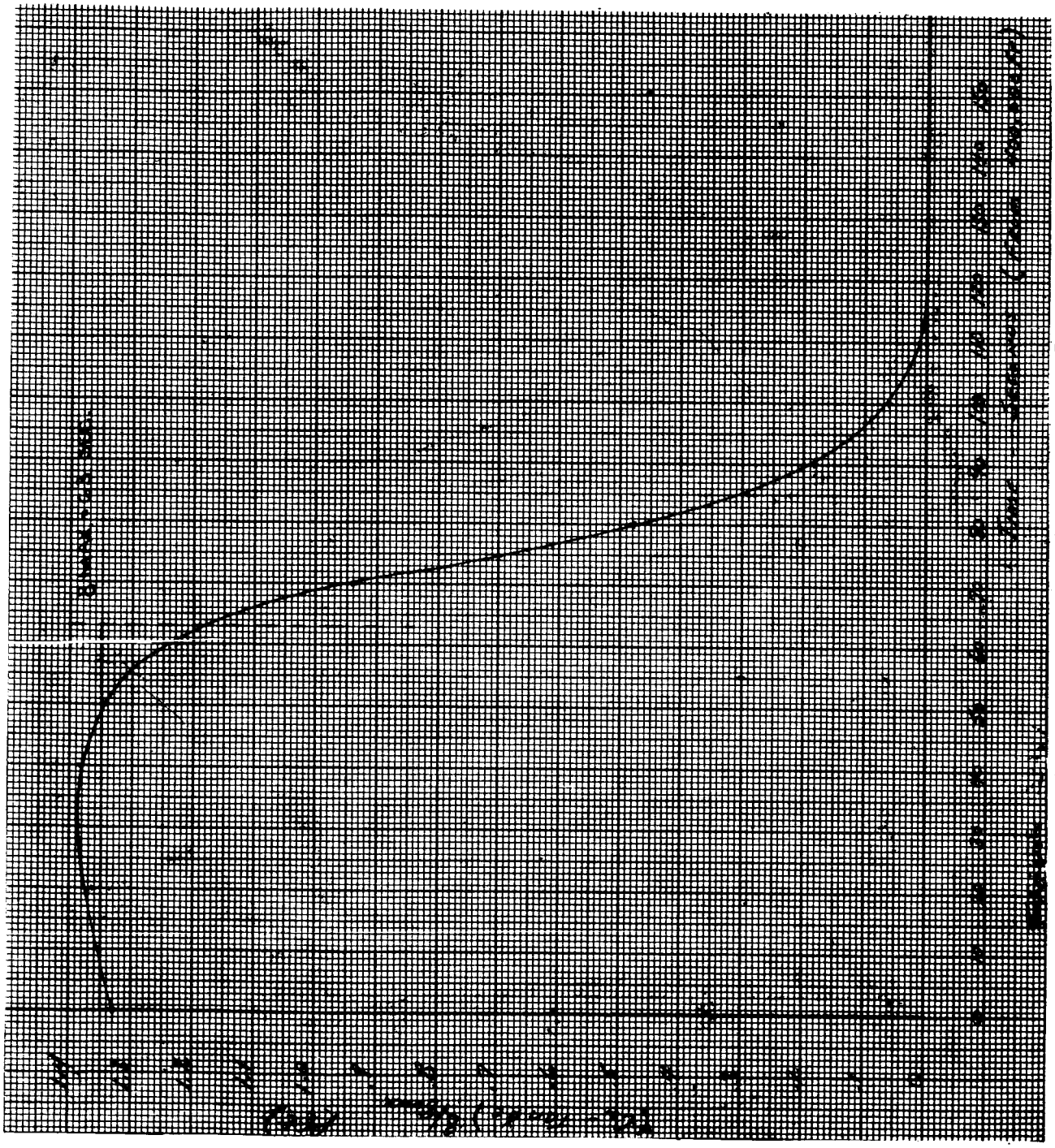

Fig. III-10. Shaping Function--Run No. 5

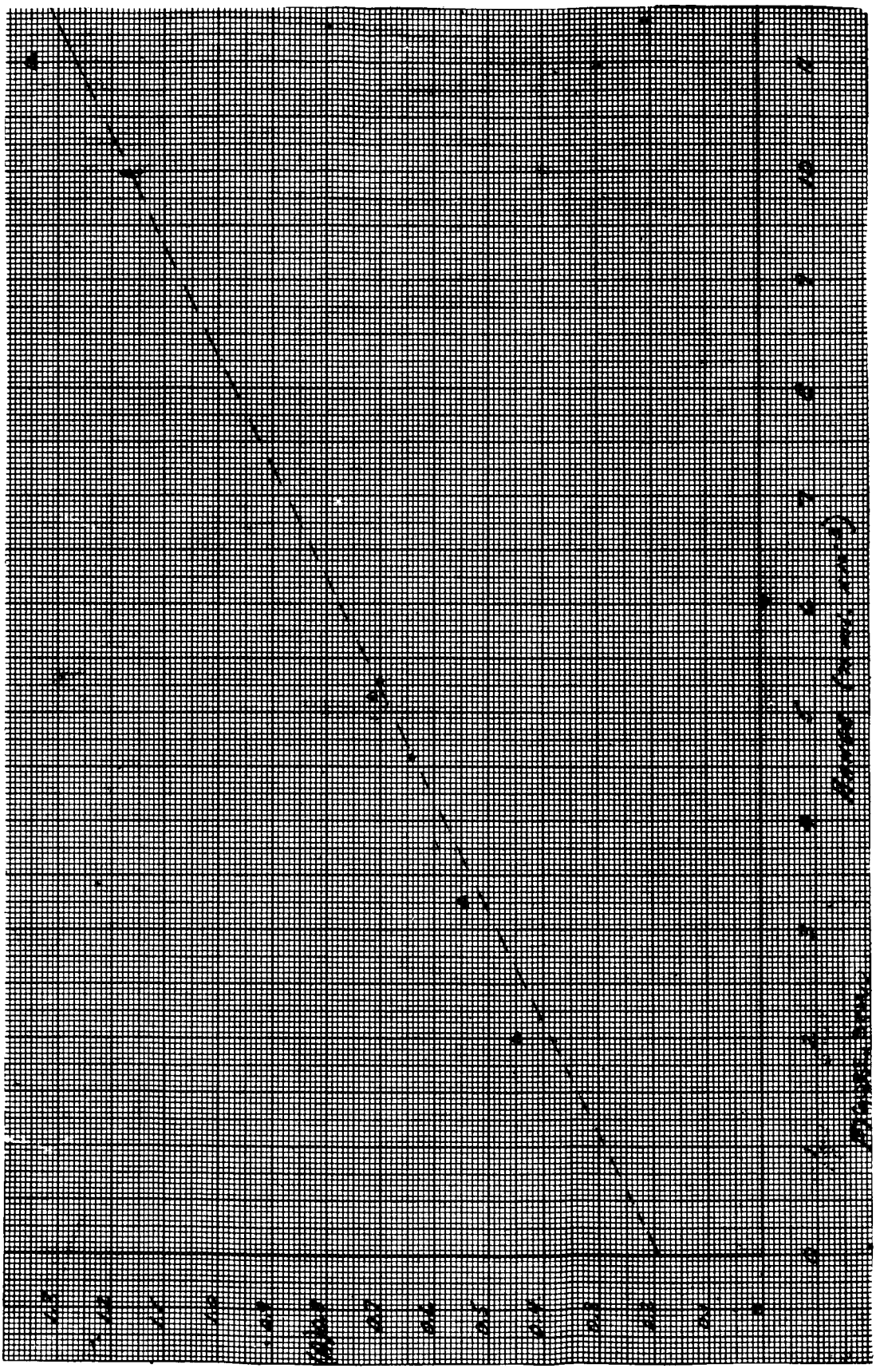

Fig. III-11. Shaping Function Constant (A) Versus Range

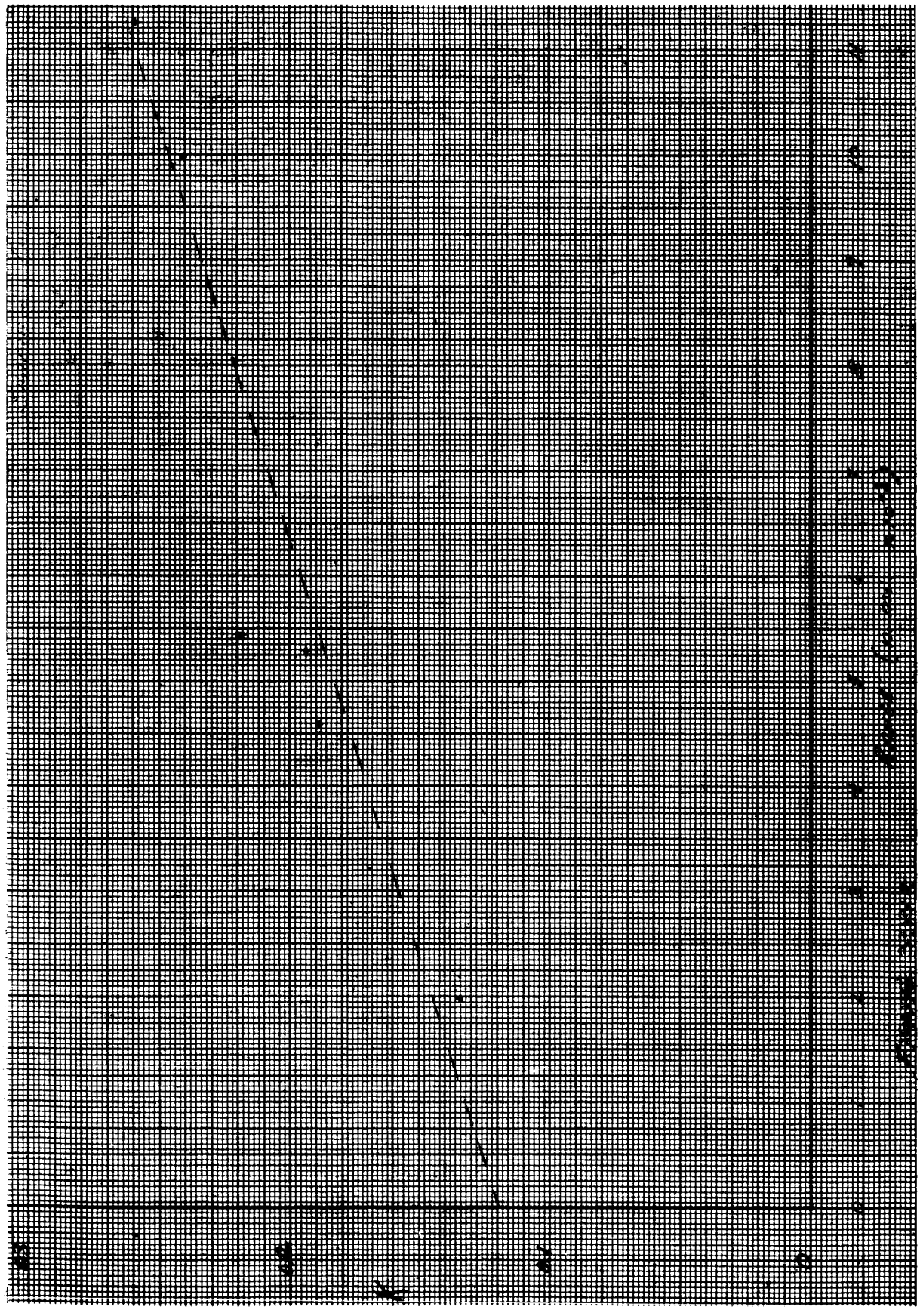

Fig. III-12. Shaping Function Coefficient (K) Versus Range

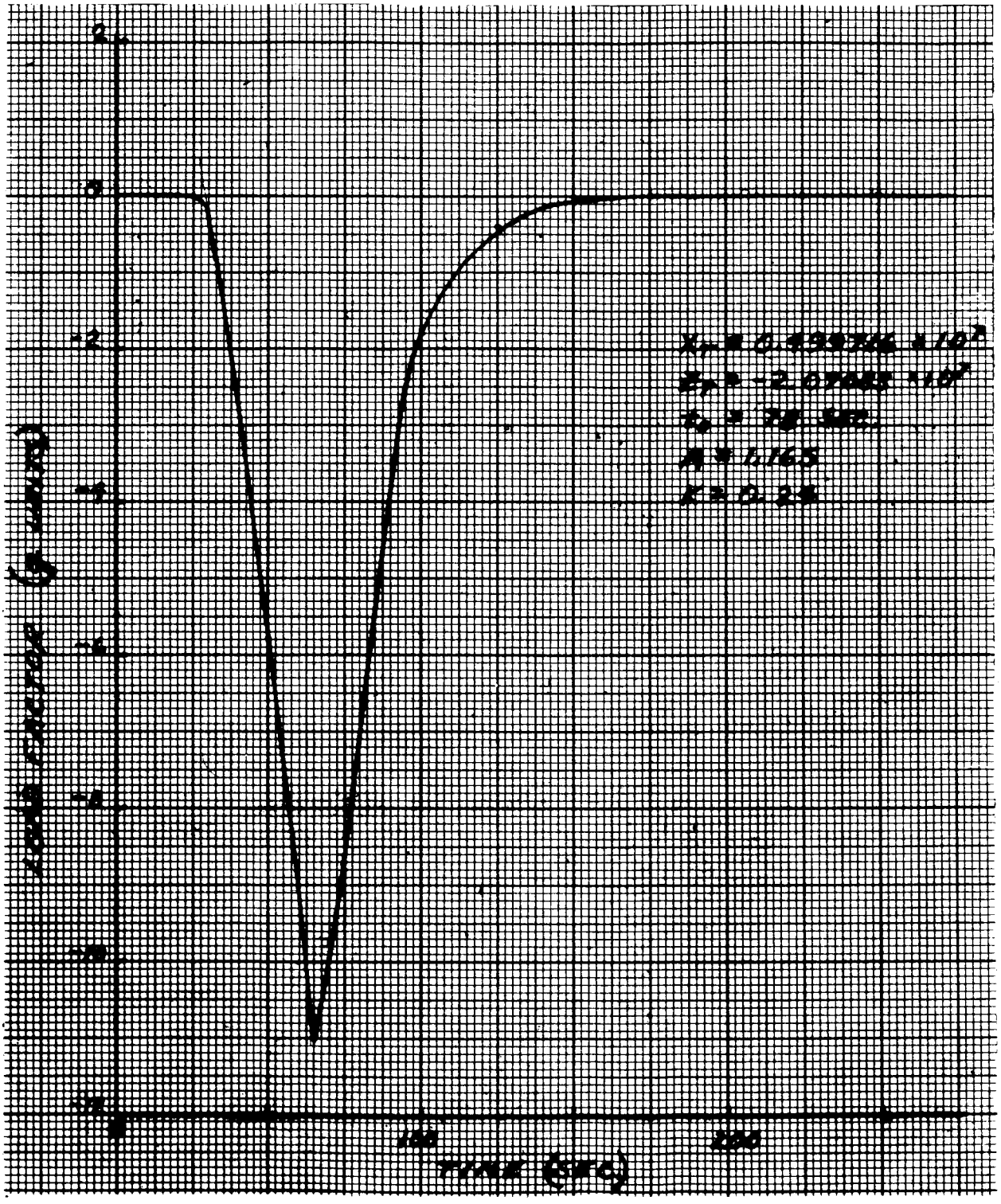

Fig. III-13. Load Factor Versus Time--Run No. 2

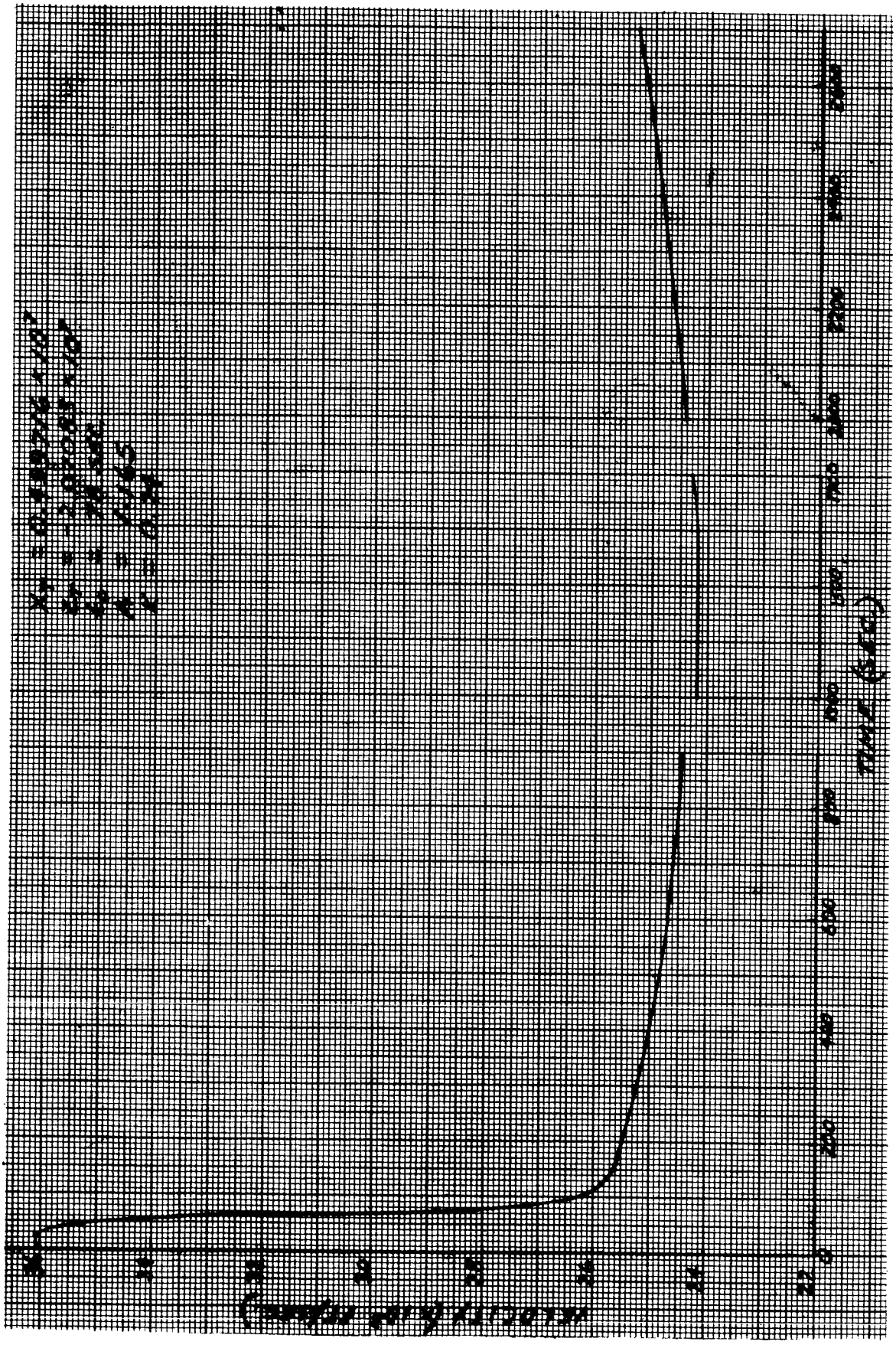

Fig. III-14. Velocity Versus Time--Run No. 2

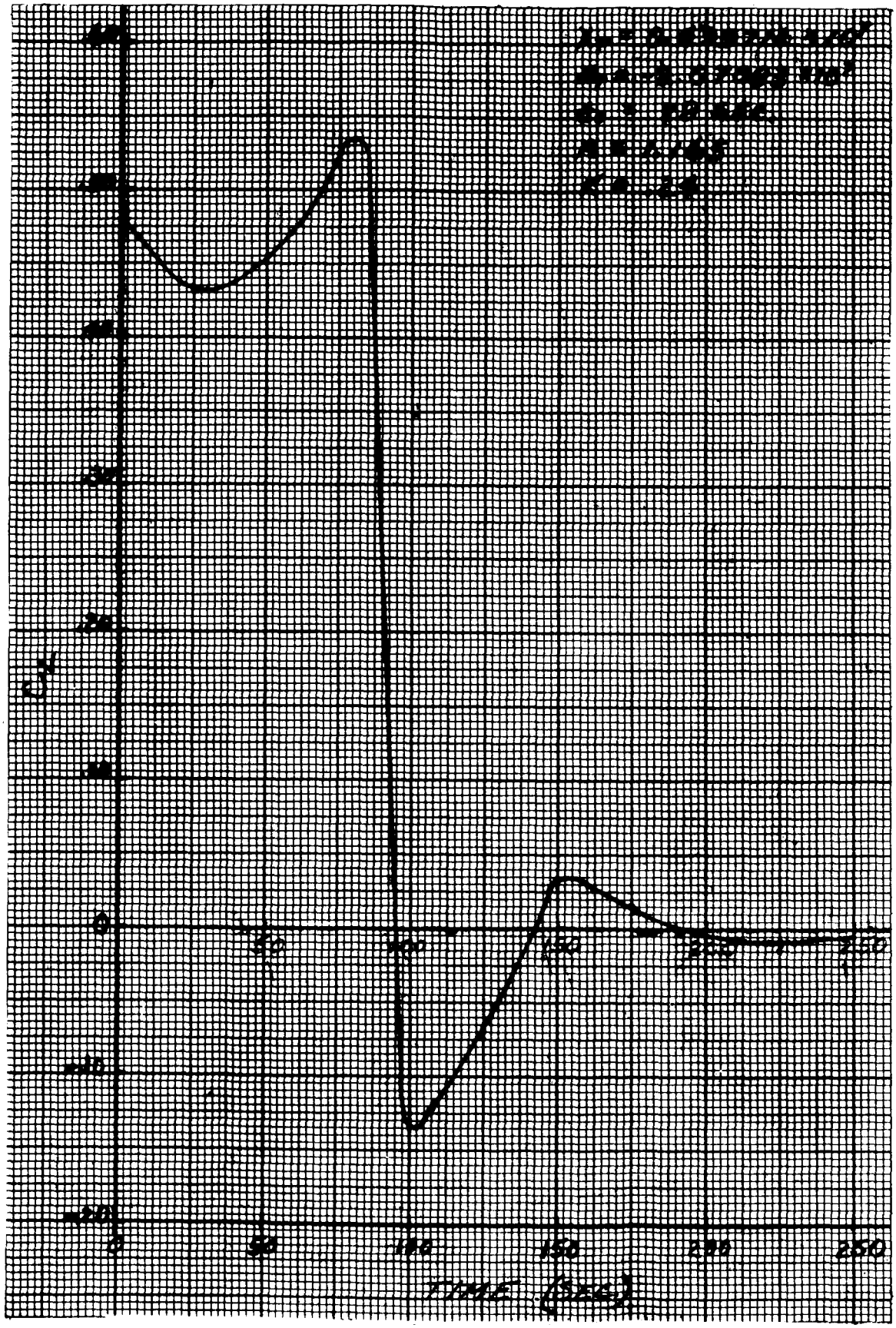

Fig. III-15. C_L Versus Time--Run No. 2

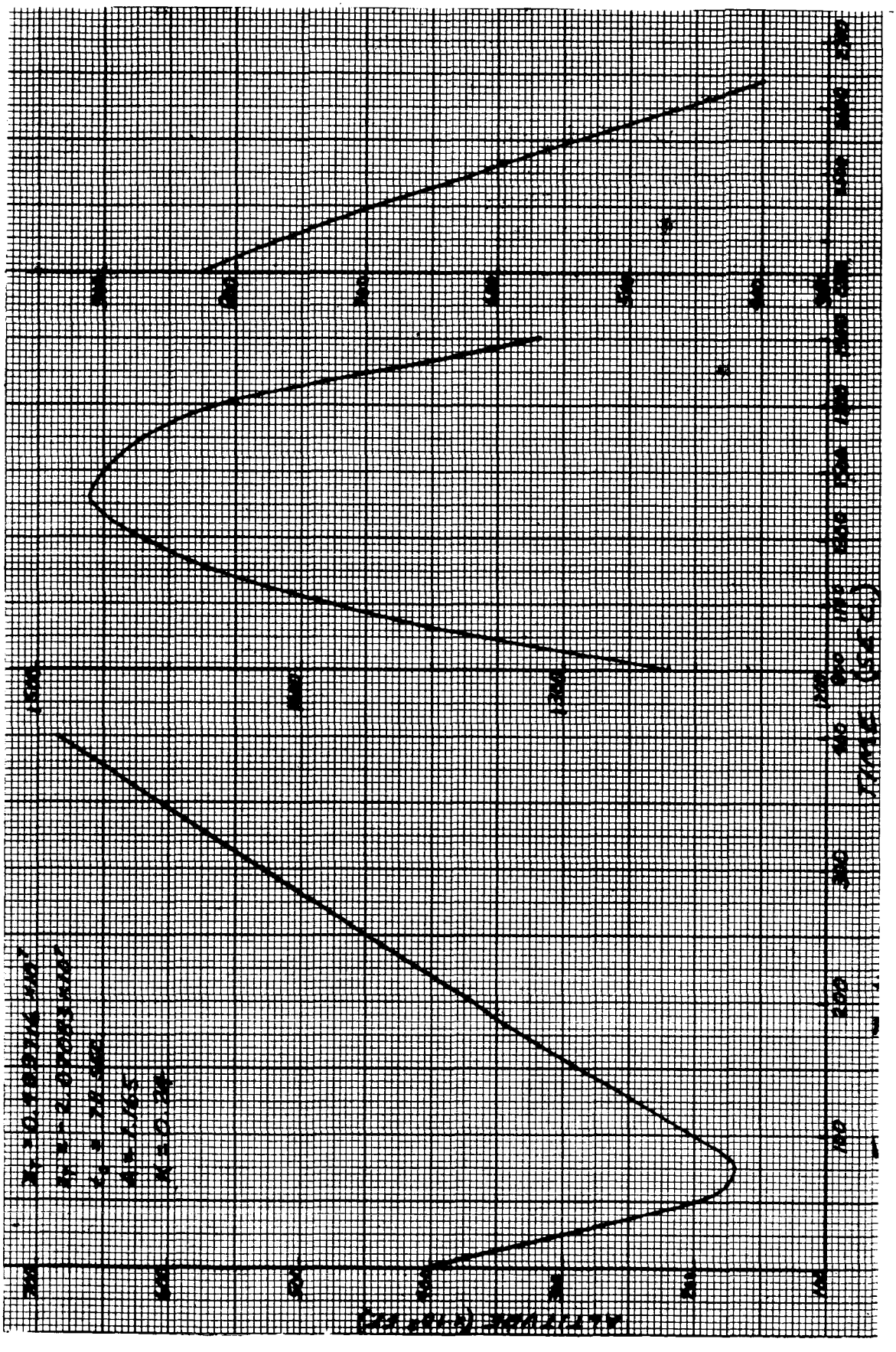

Fig. III-16. Altitude Versus Time--Run No. 2

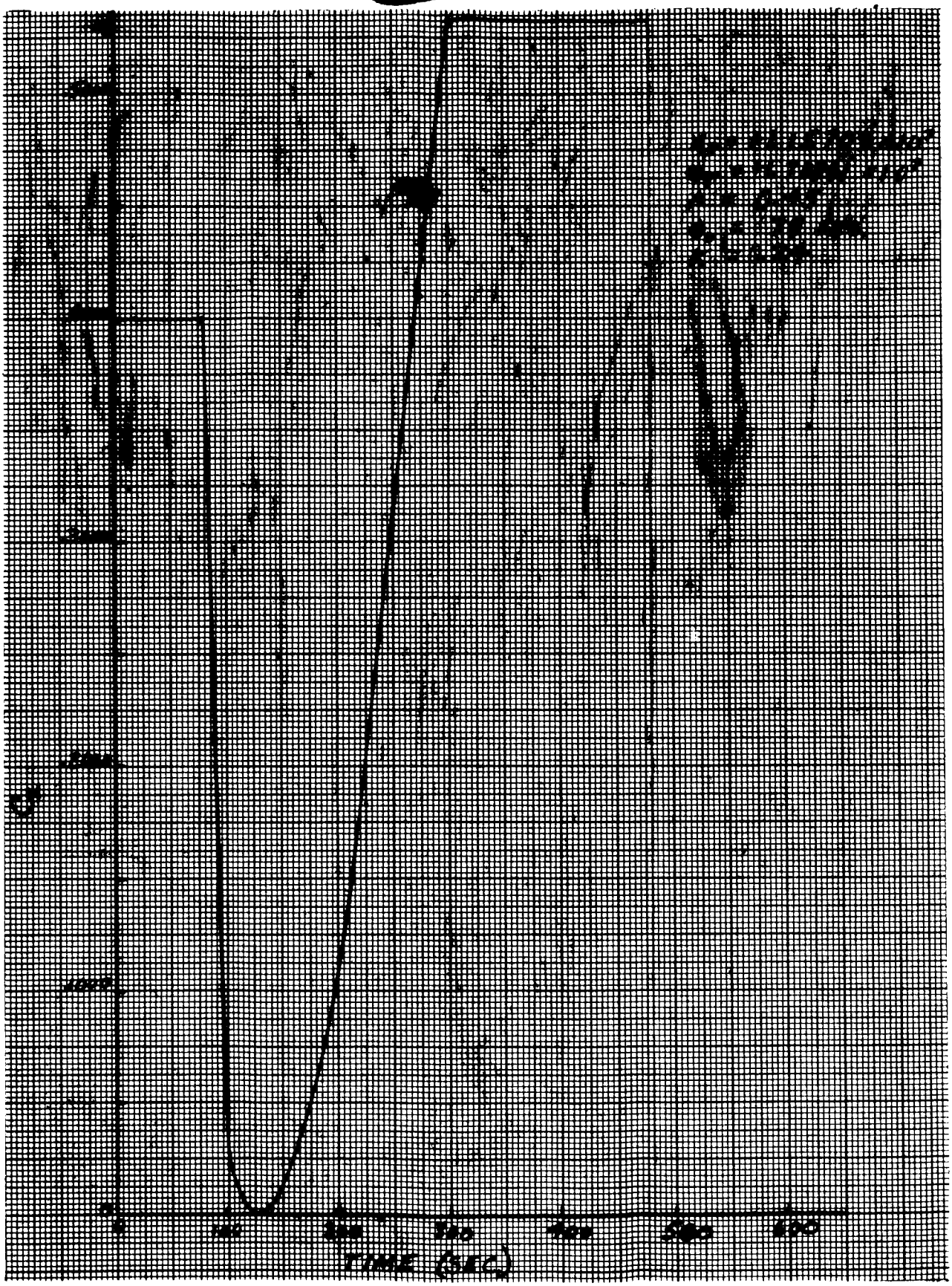

Fig. III-17. C_L Versus Time--Run No. 3

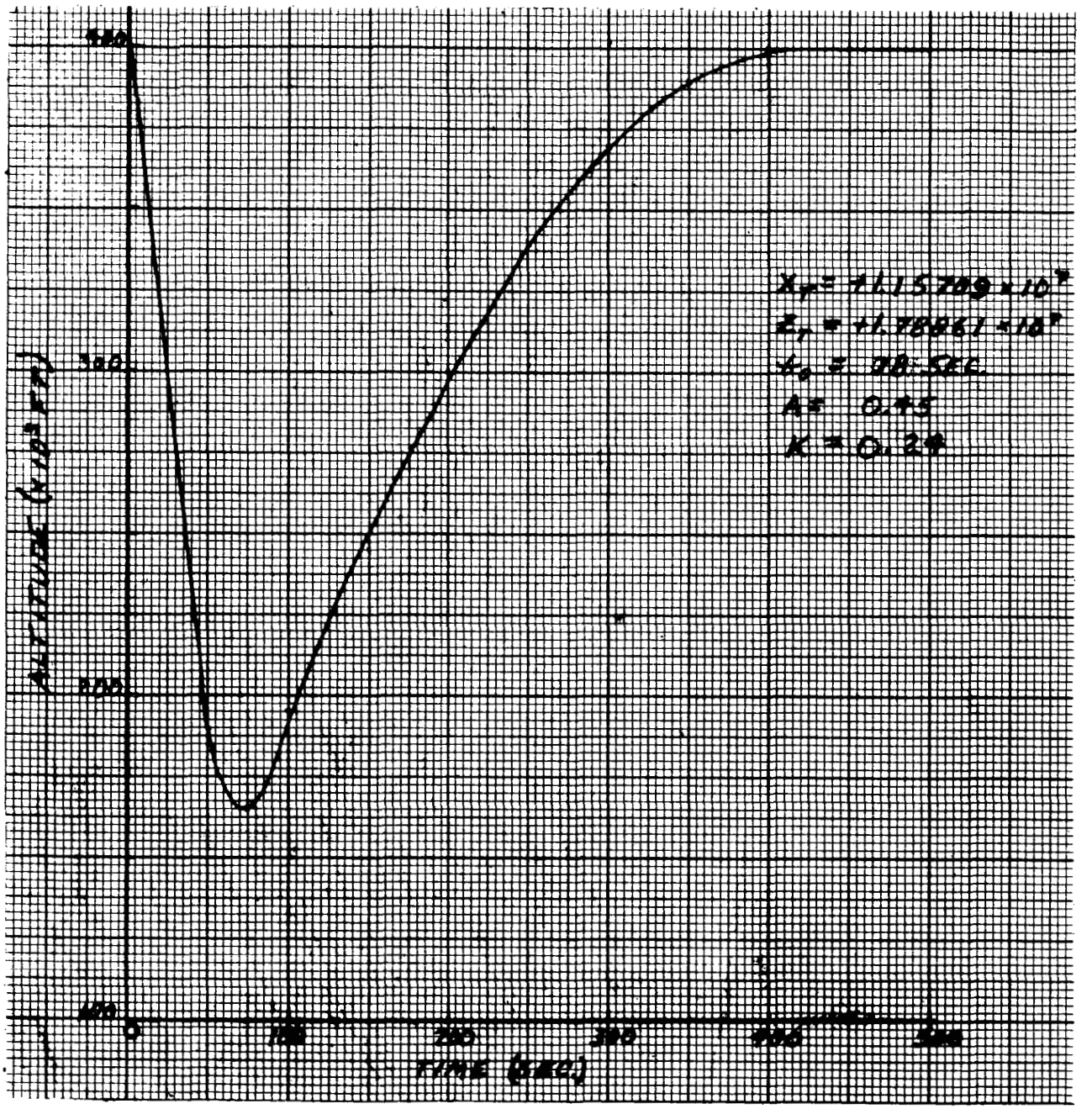

Fig. III-18. Altitude Versus Time--Run No. 3

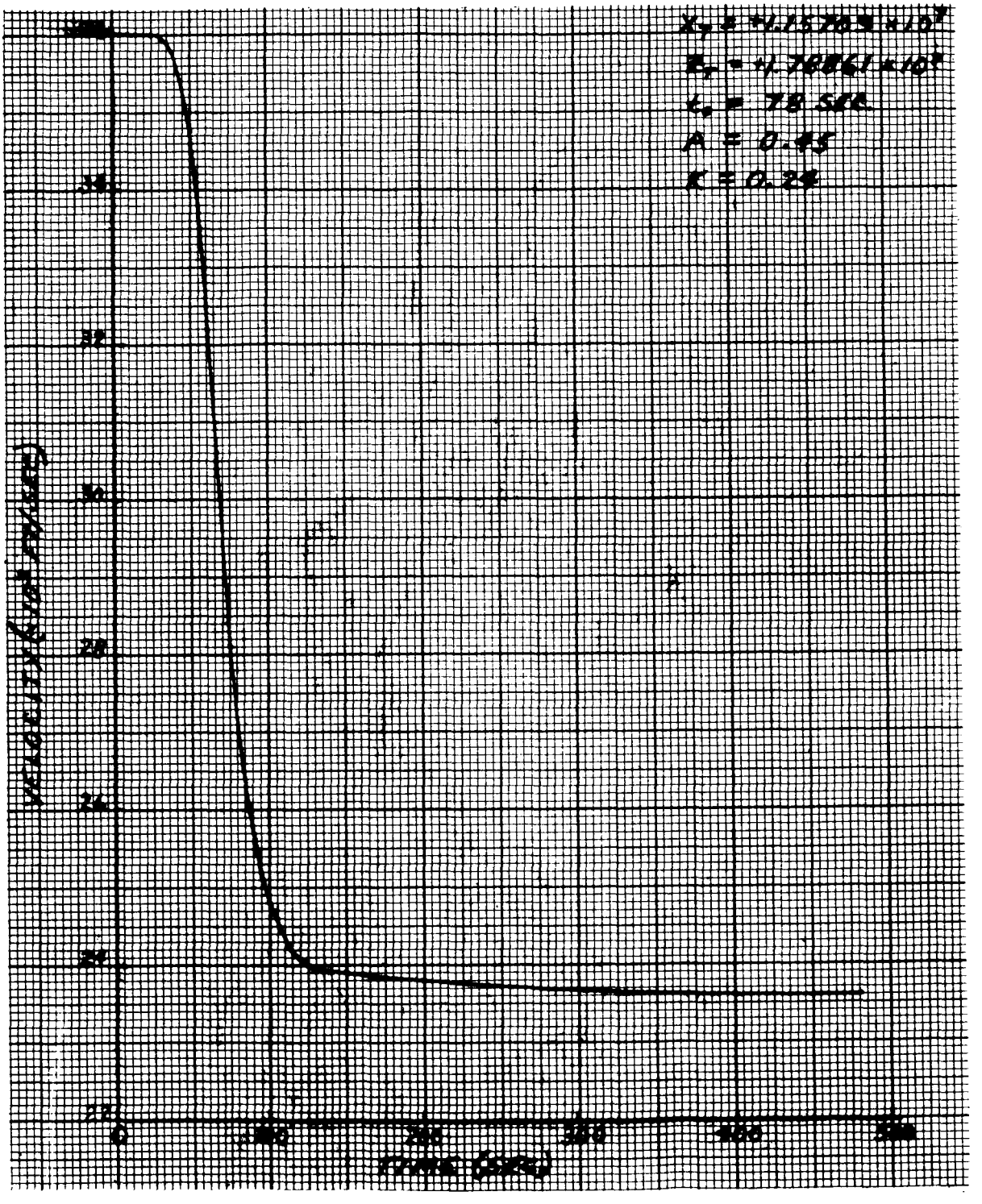

Fig. III-19. Velocity Versus Time--Run No. 3

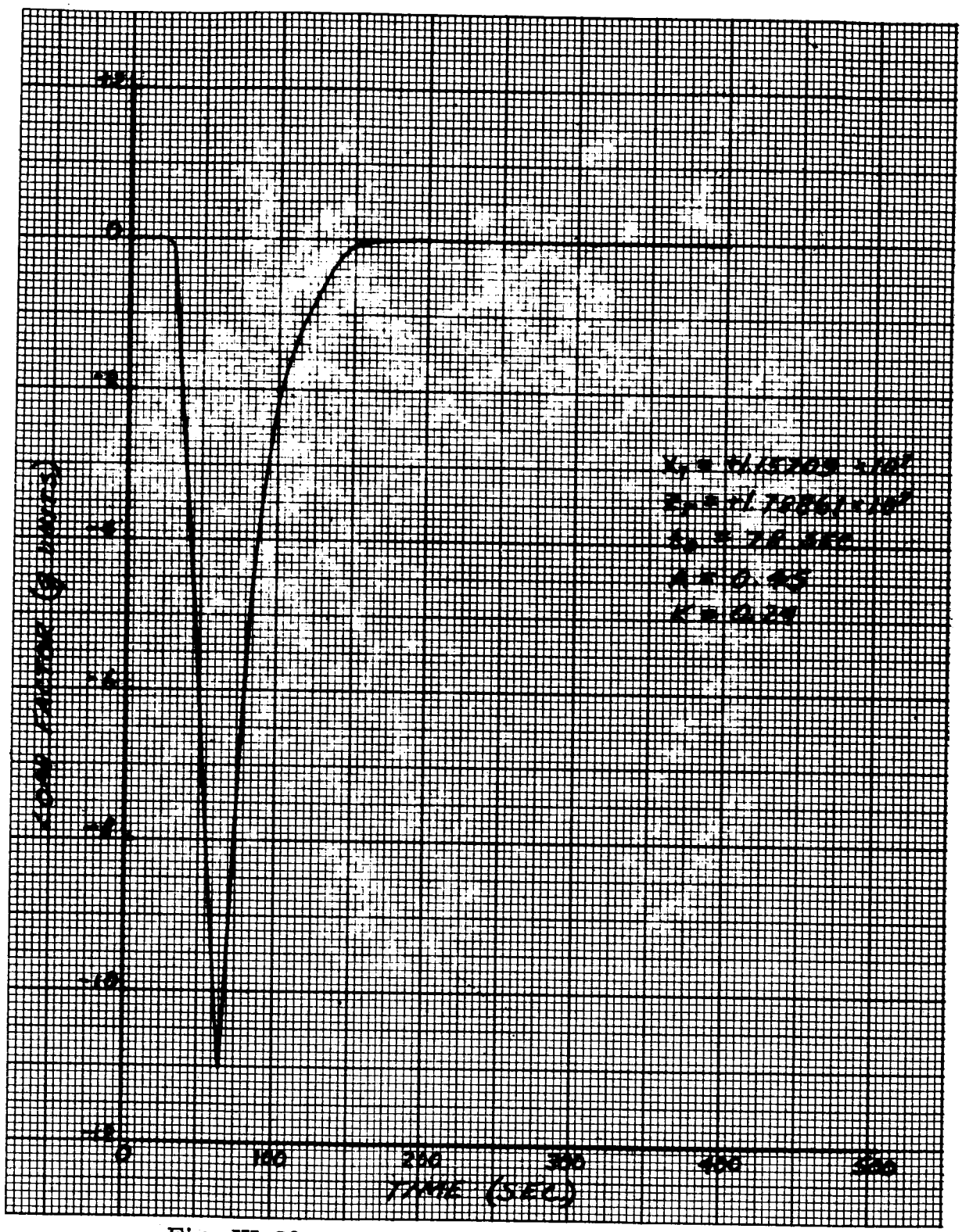

Fig. III-20. Load Factor Versus Time--Run No. 3

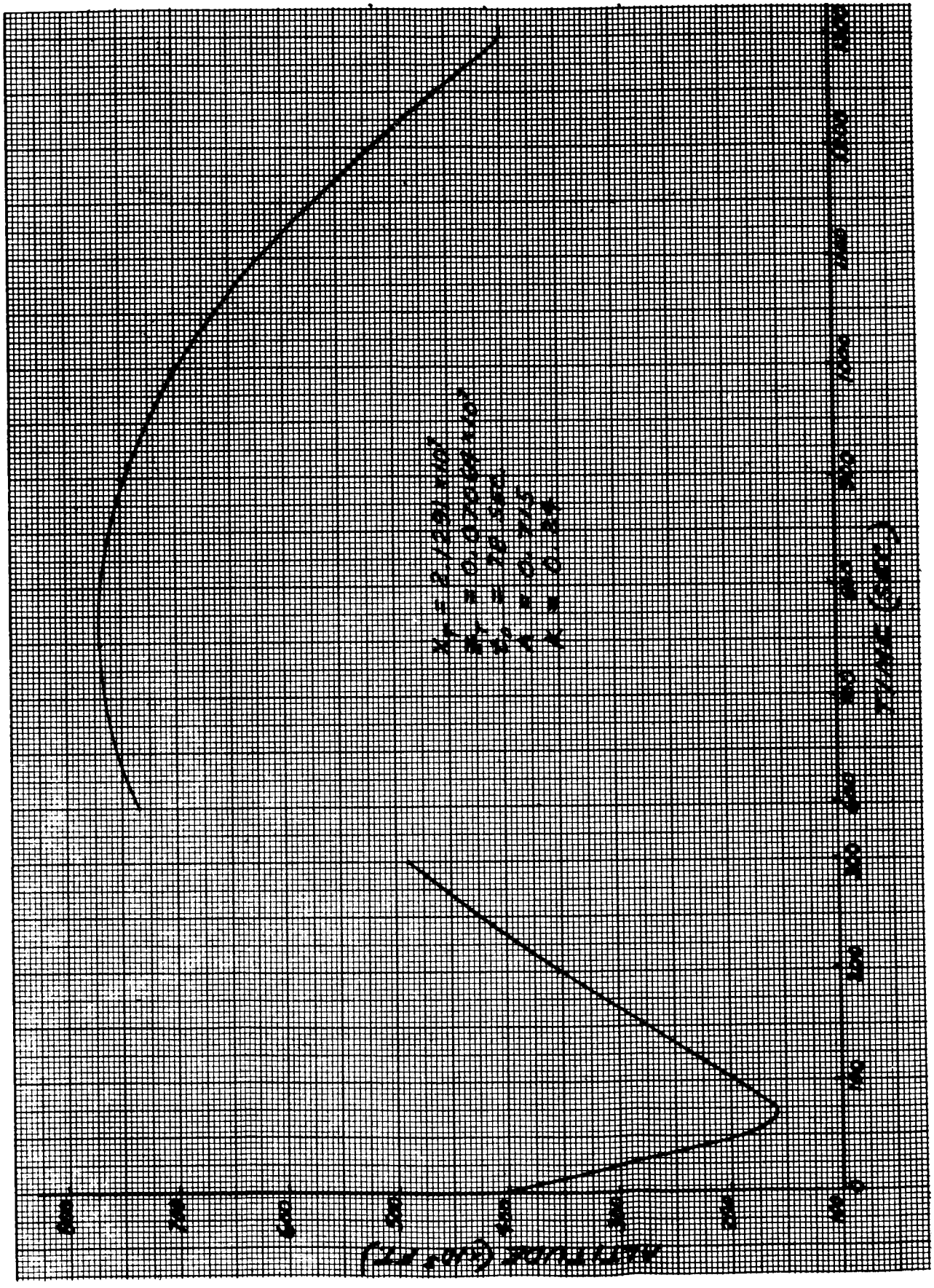

Fig. III-21. Altitude Versus Time--Run No. 4

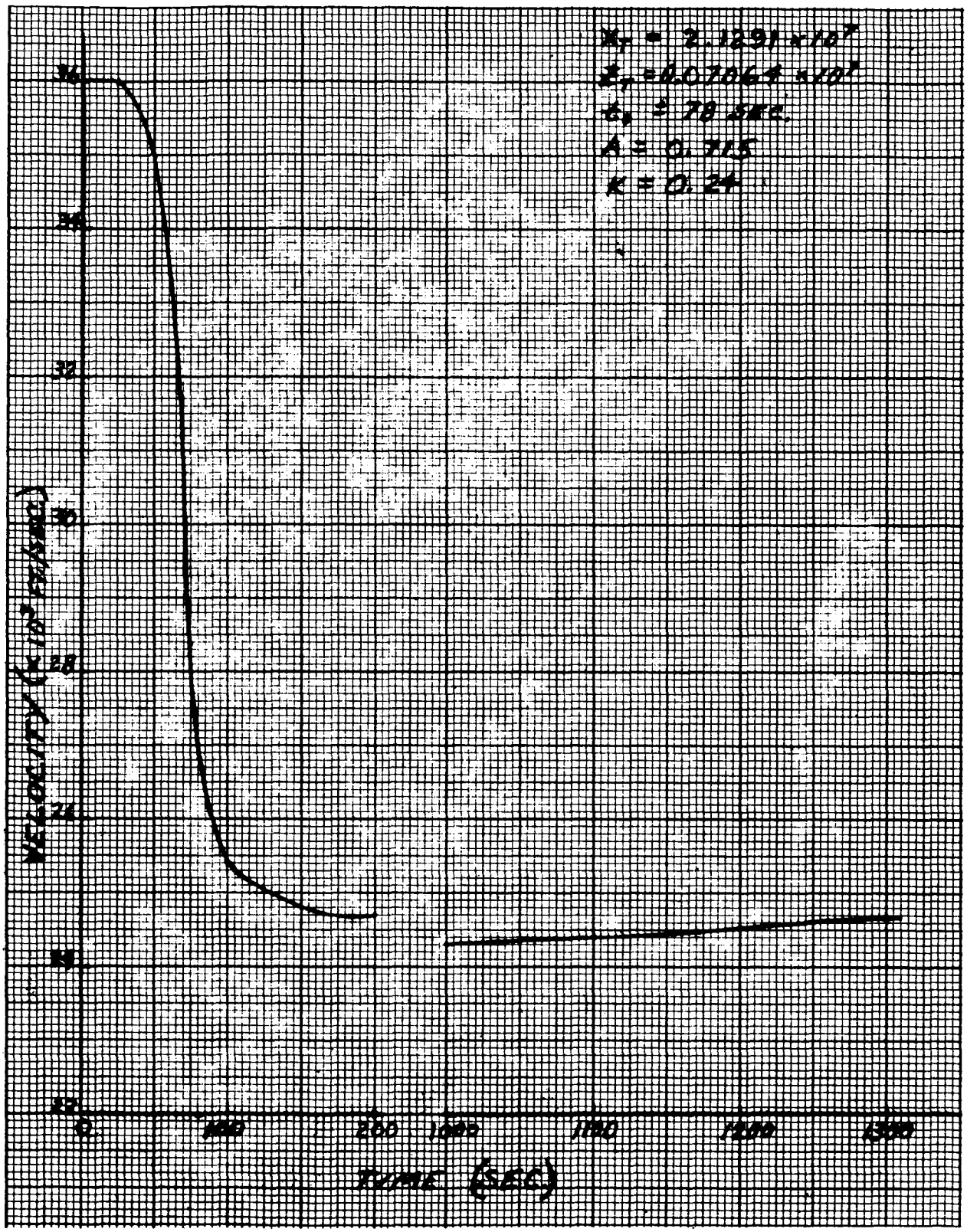

Fig. III-22. Velocity Versus Time--Run No. 4

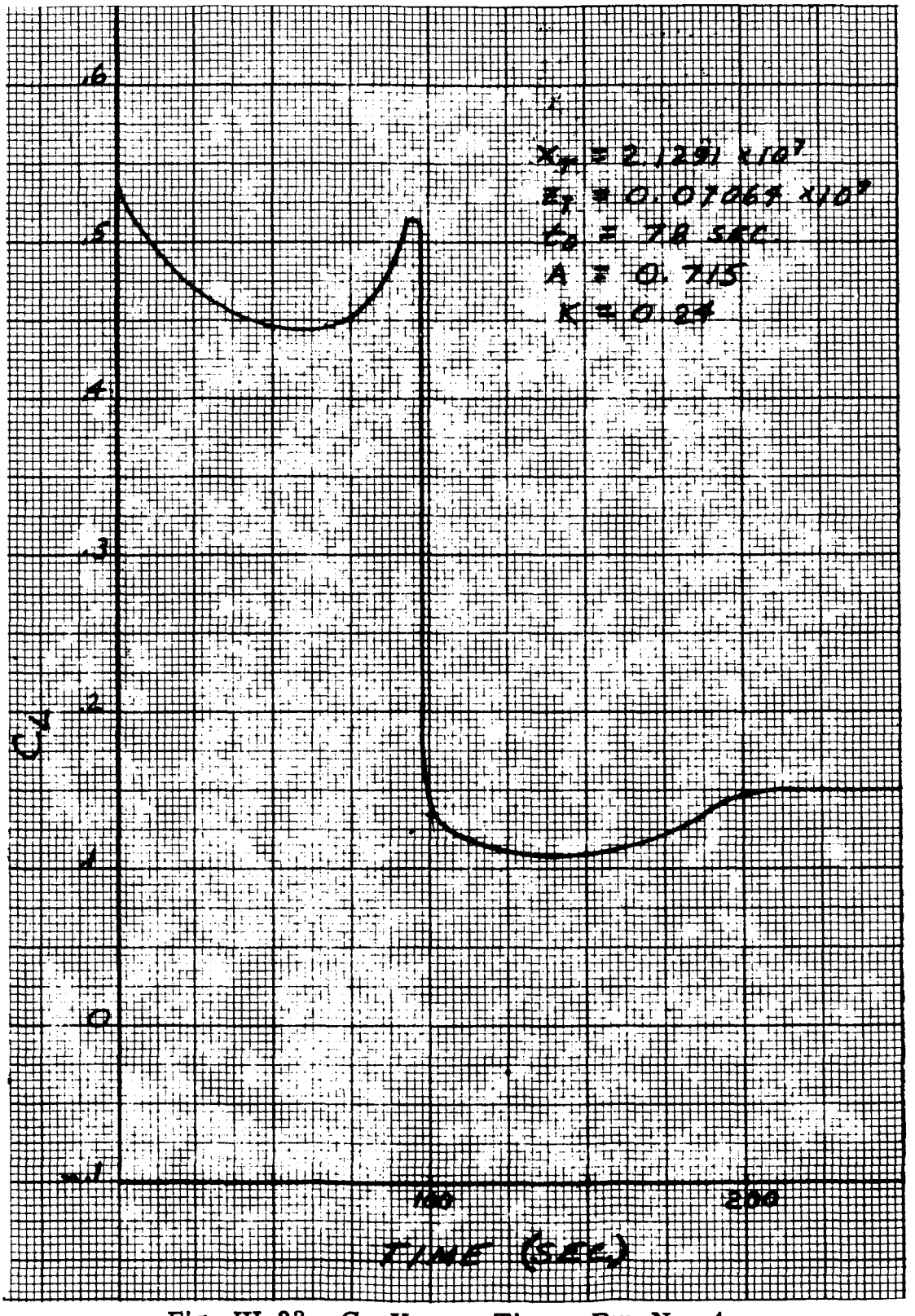

Fig. III-23. C_L Versus Time--Run No. 4

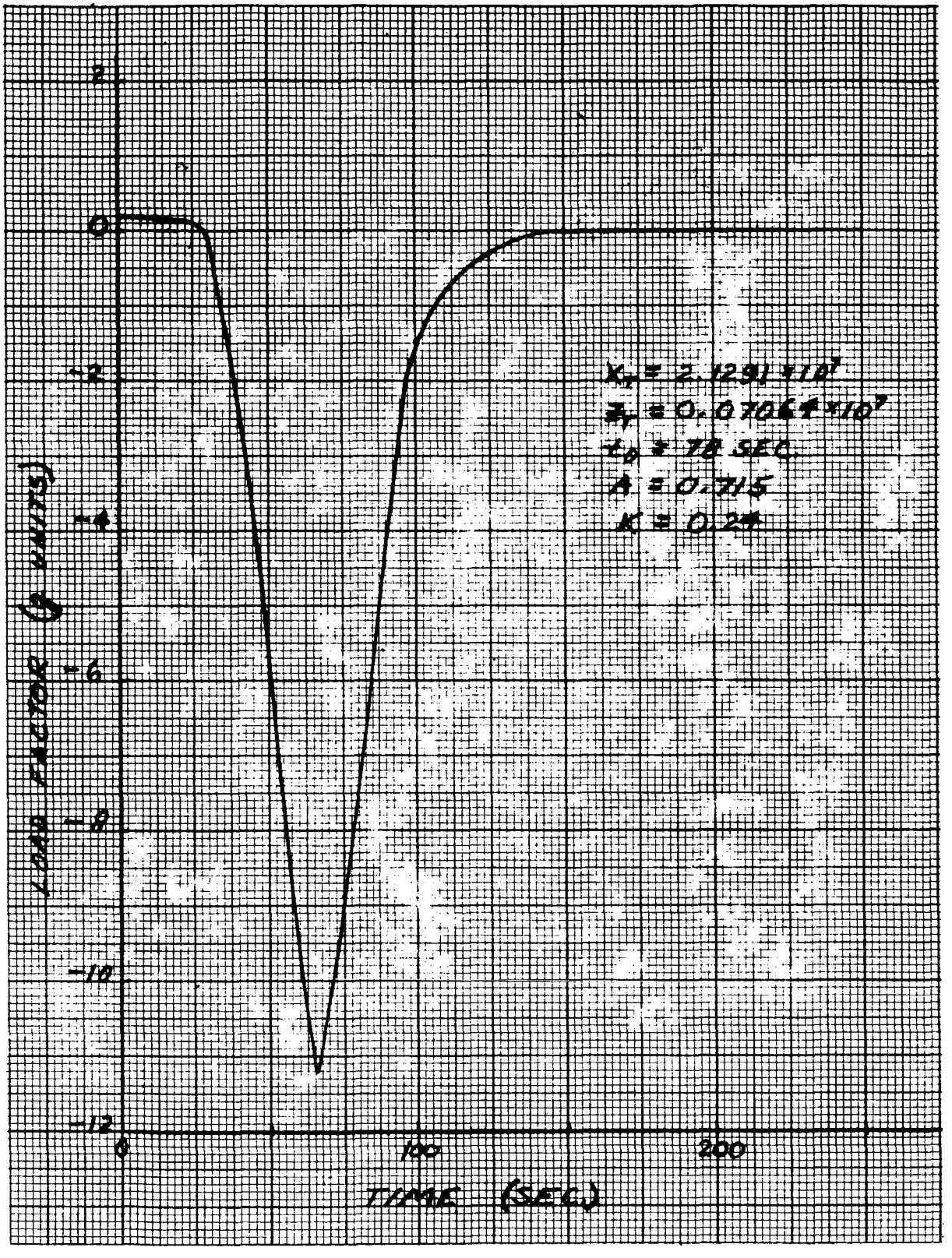

Fig. III-24. Load Factor Versus Time--Run No. 4

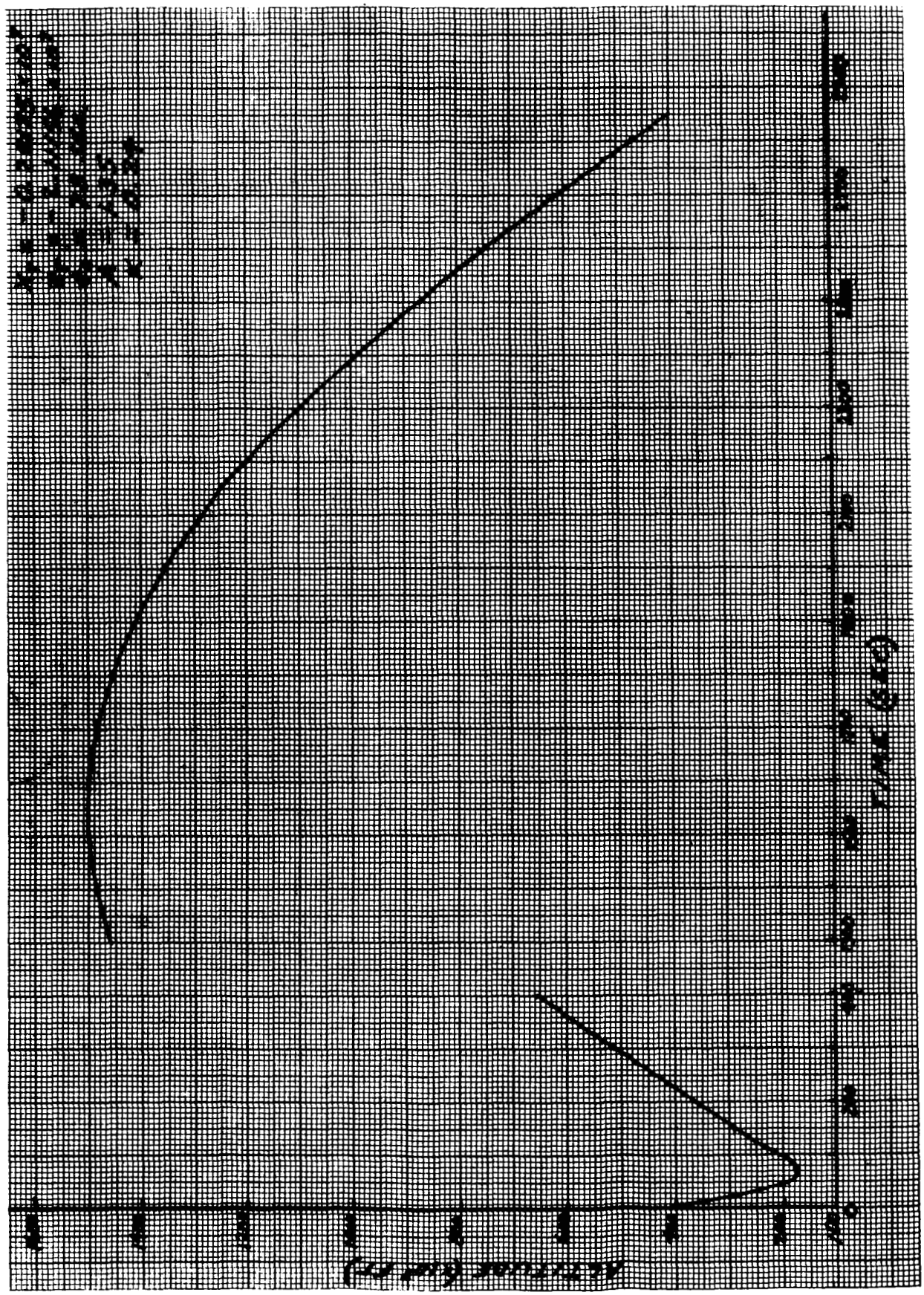

Fig. III-25. Altitude Versus Time--Run No. 5

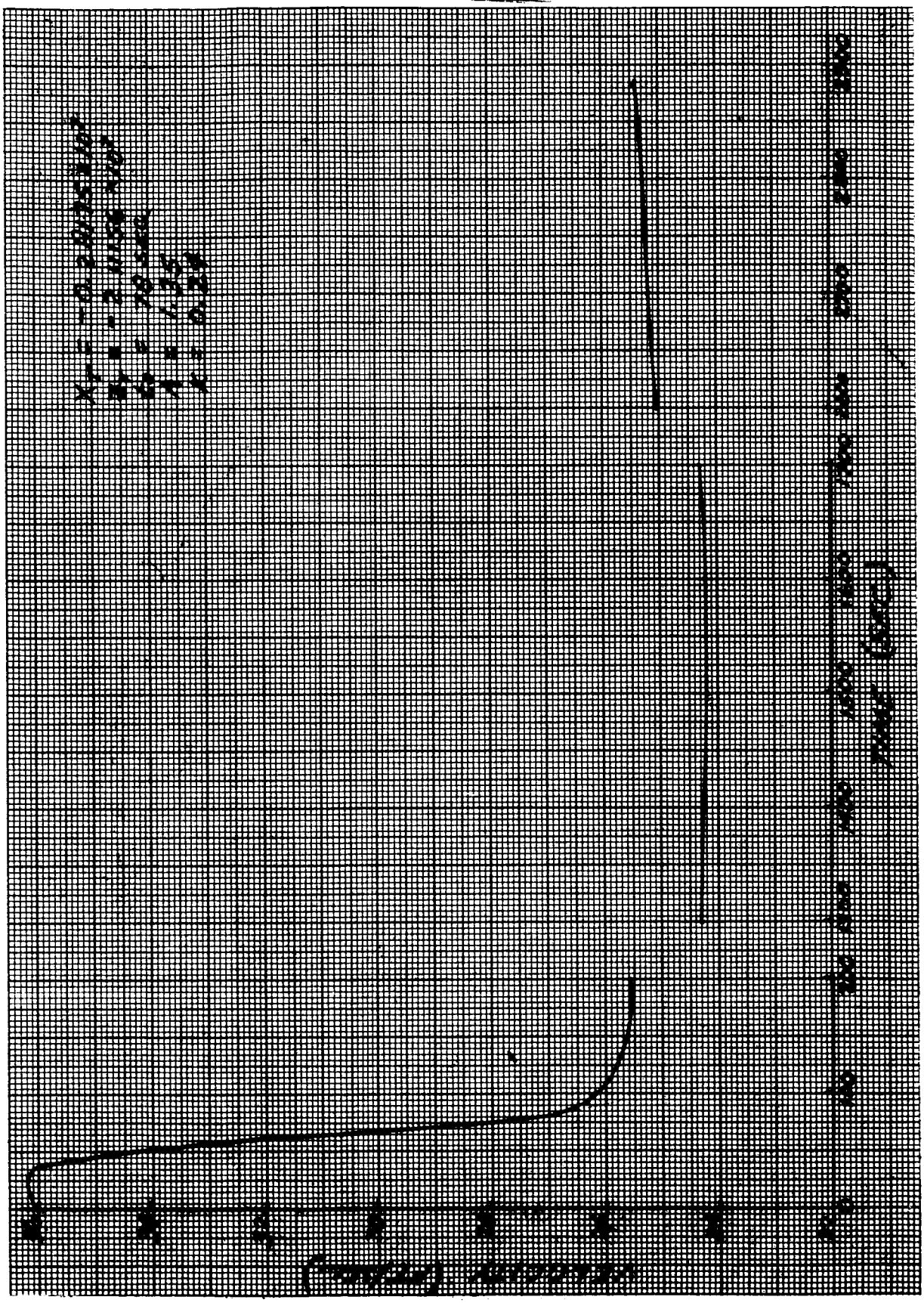

Fig. III-26. Velocity Versus Time--Run No. 5

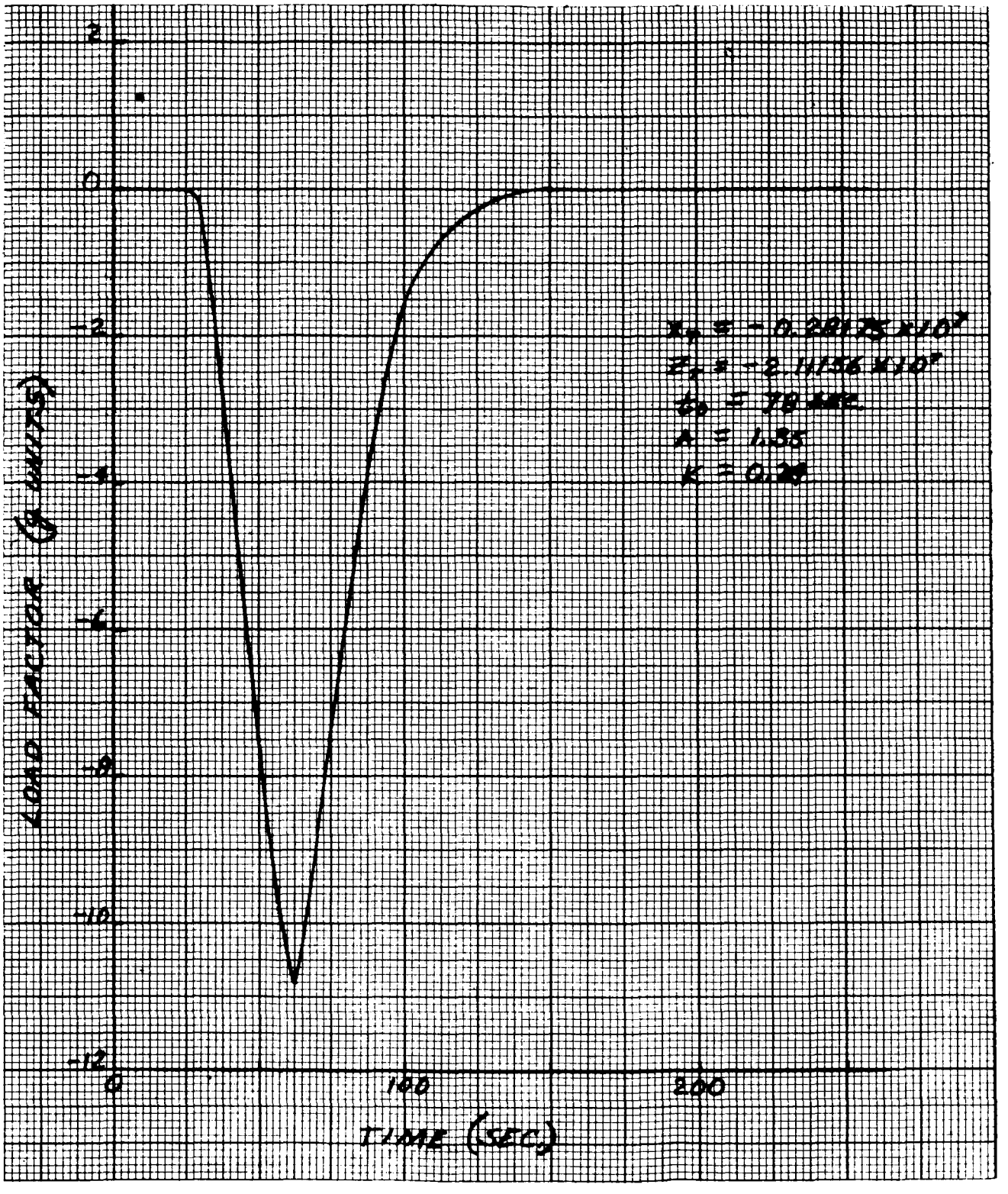

Fig. III-27. Load Factor Versus Time--Run No. 5

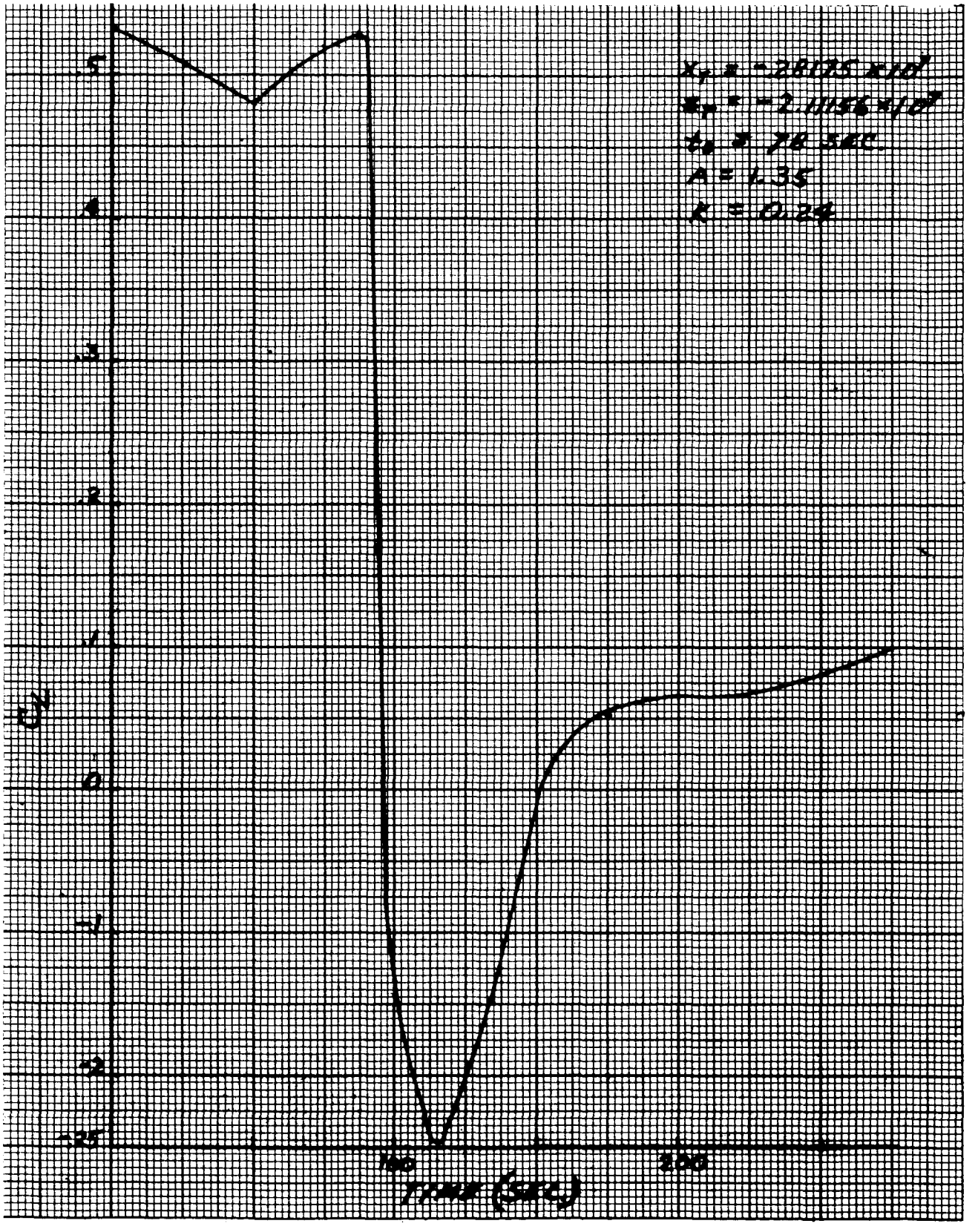

Fig. III-28. C_L Versus Time--Run No. 5

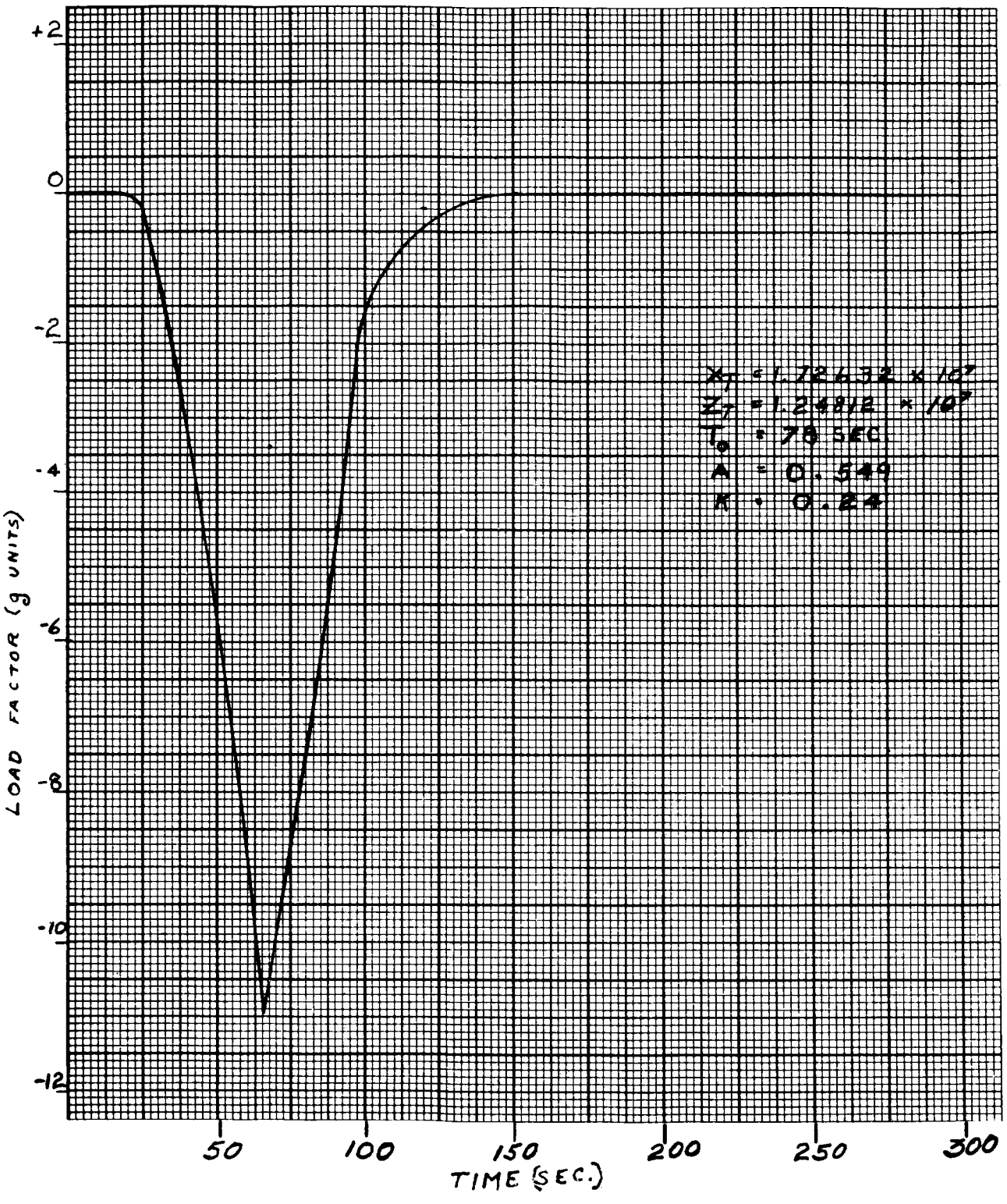

Fig. III-29. Load Factor Versus Time--Run No. 6

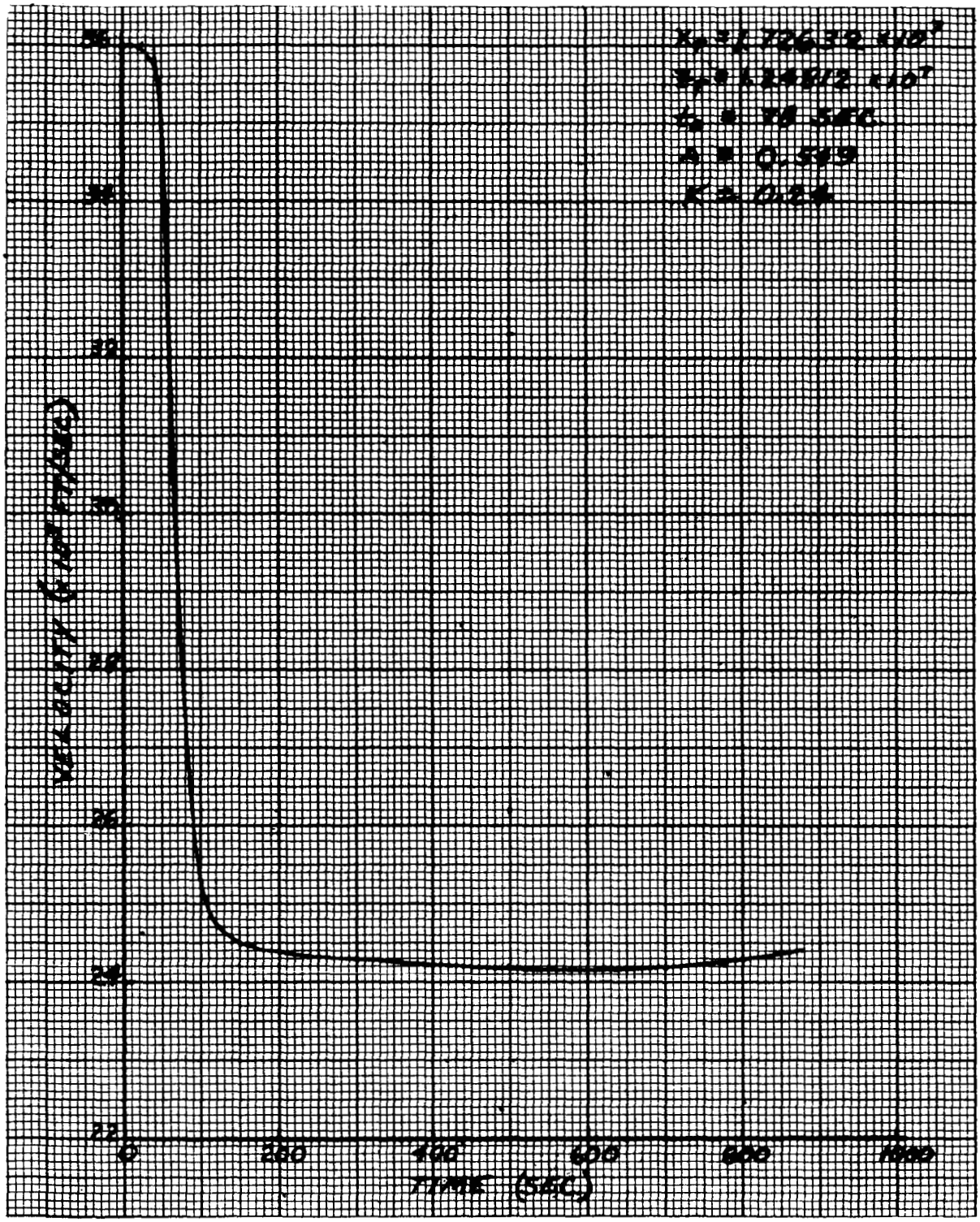

Fig. III-30. Velocity Versus Time--Run No. 6

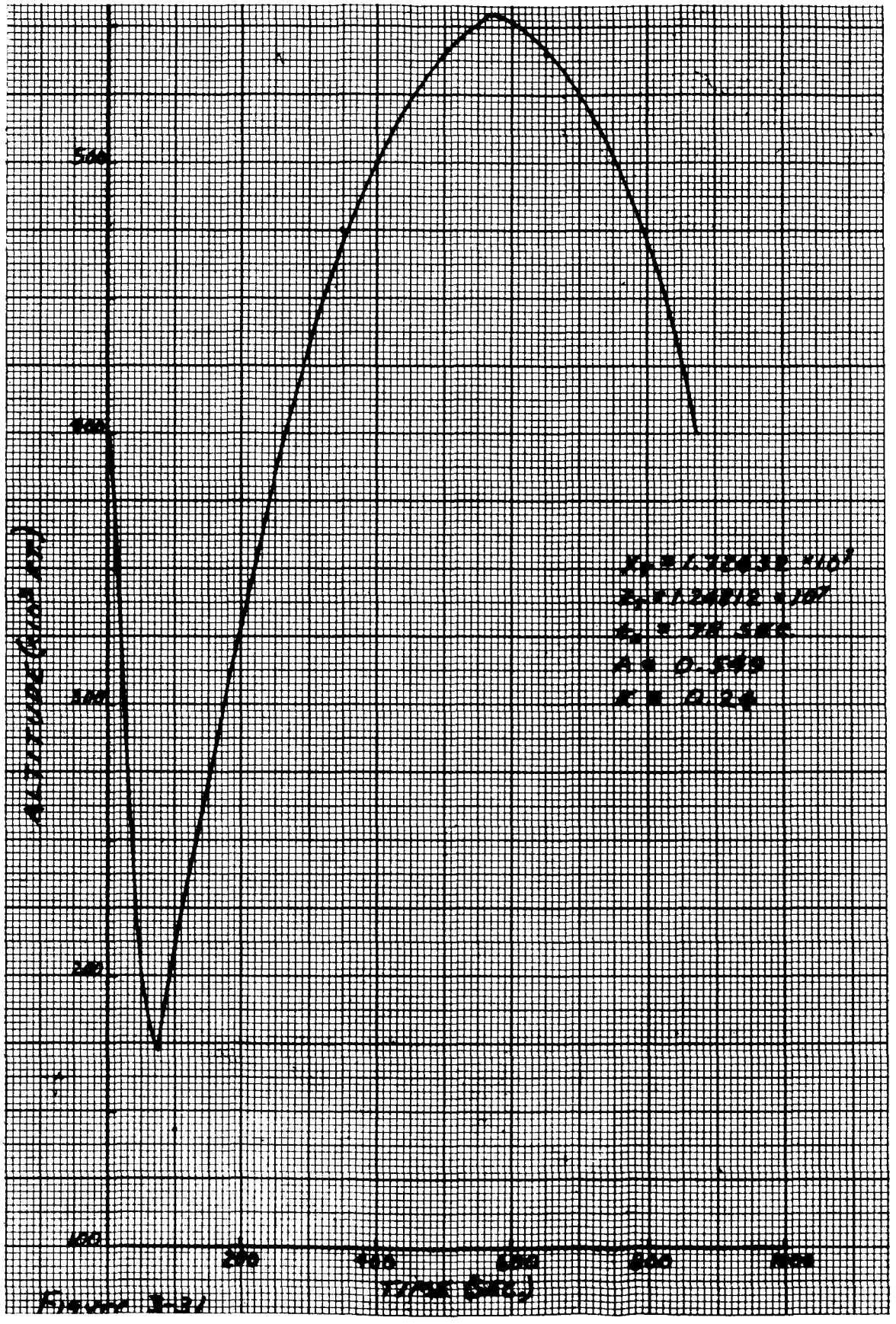

Fig. III-31. Altitude Versus Time--Run No. 6

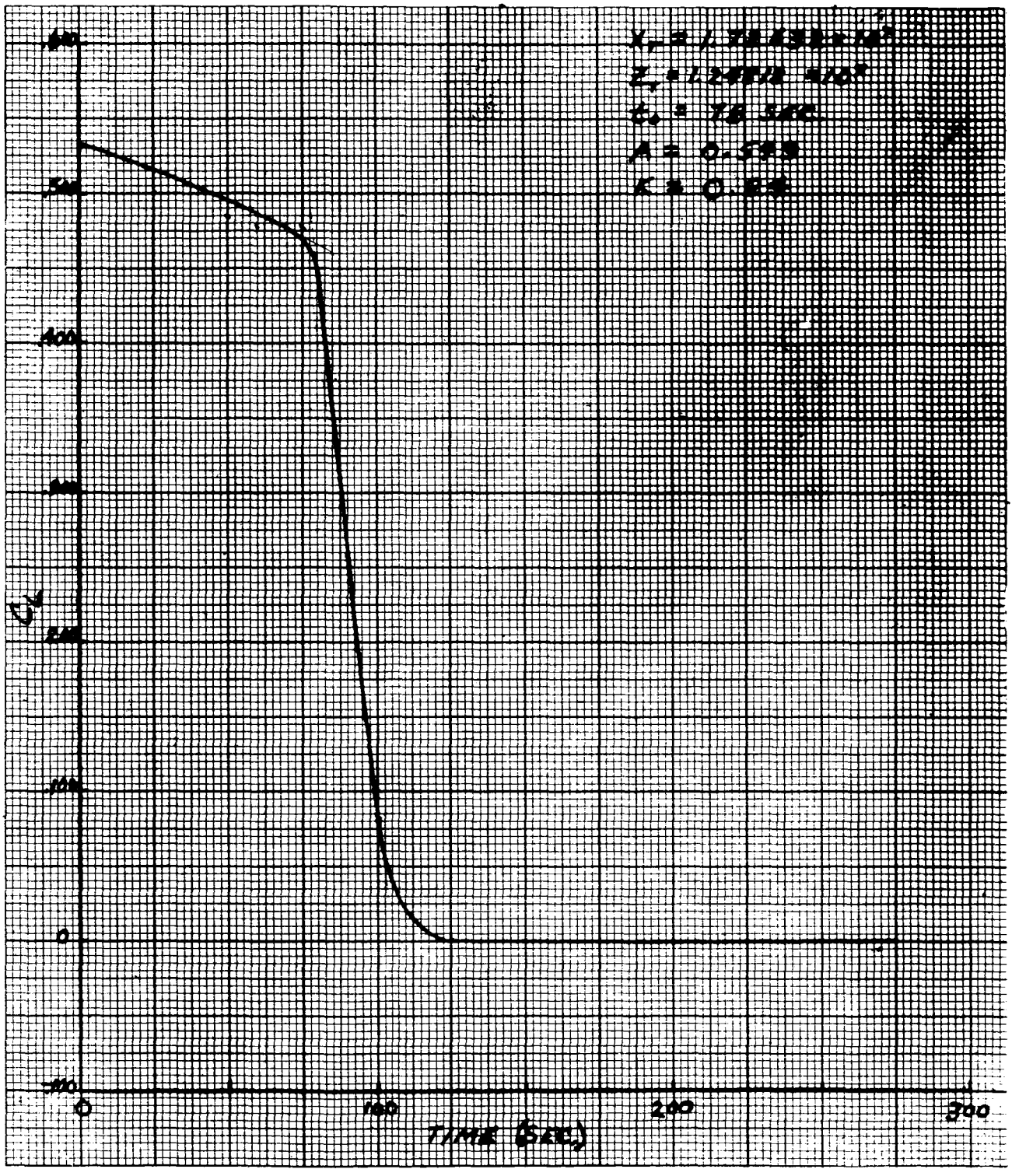

Fig. III-32. C_L Versus Time--Run No. 6

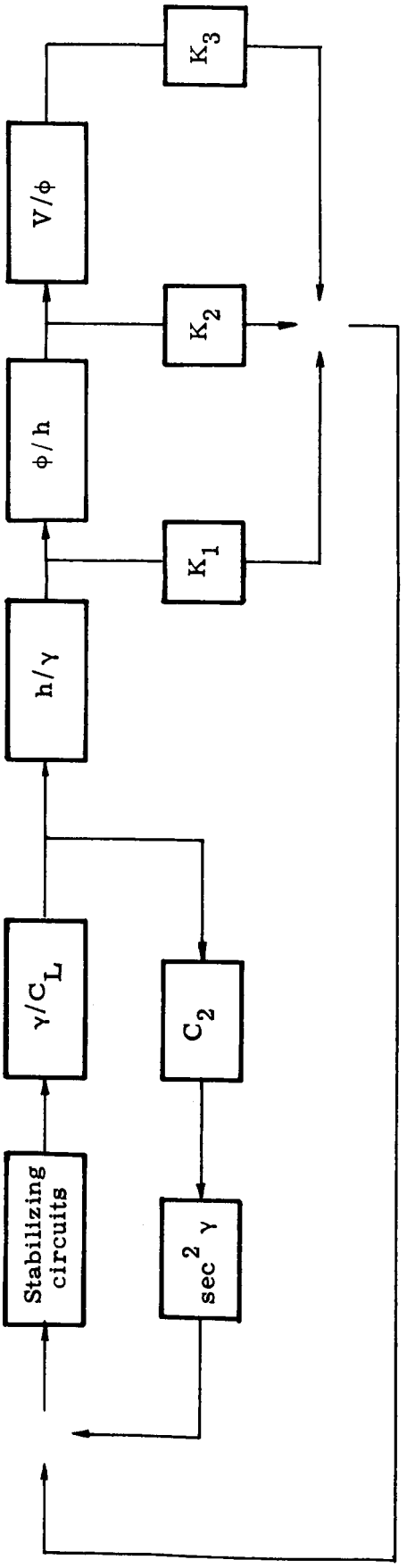

C_L = lift coefficient
γ = flight path angle
h = altitude
V = velocity

θ = earth central angle
K_i = constants
C_2 = constant

Fig. III-33. Block Diagram Linearized Guidance Loop

WING LOADING: $W/S = 30^{\#}/\text{sq. FT.}$

SEA LEVEL DENSITY: $\rho_0 = .0027$ SLUG/CU. FT.

EXPONENTIAL CONSTANT: $\beta = (23,500 \text{ FT.})^{-1}$

$$H_V = \frac{1}{\beta}\left(\ln \frac{-s\rho_0 g r C_L}{2W} - \ln \frac{\bar{u}^2 - 1}{\bar{u}^2}\right)$$

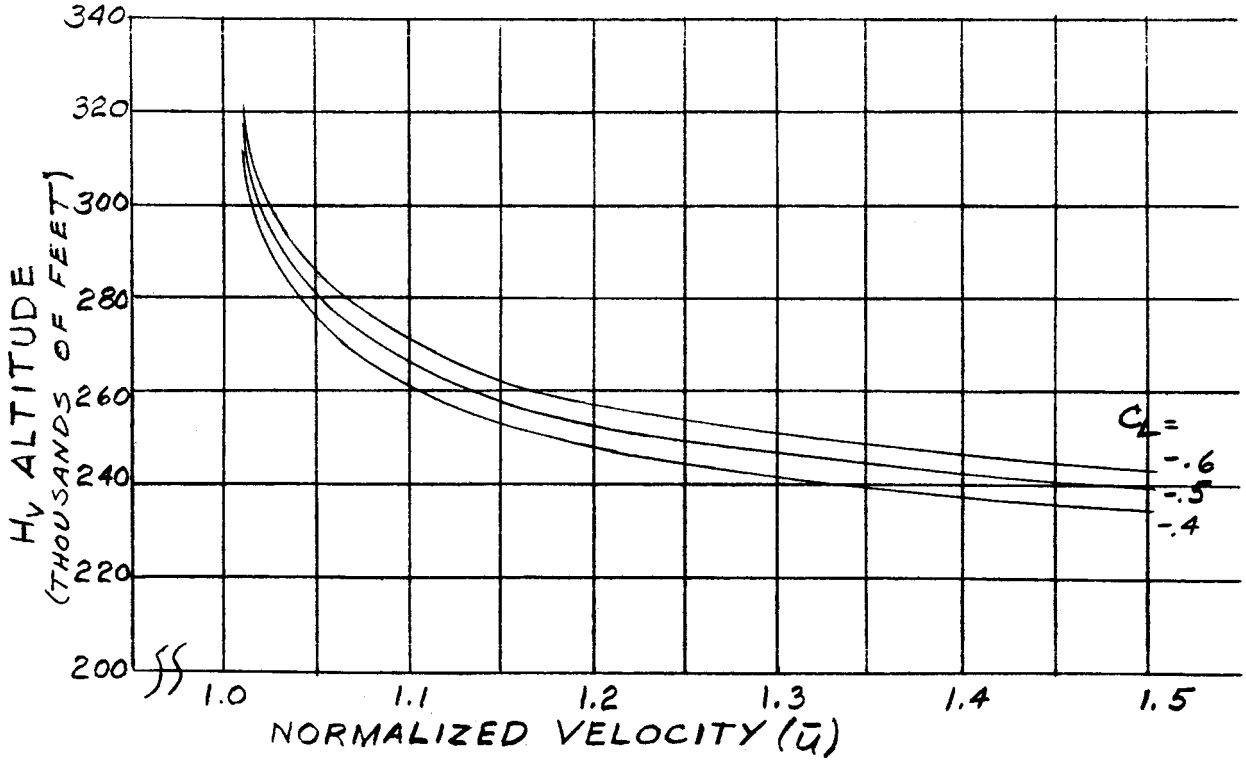

Fig. III-34. Altitude Versus Normalized Velocity for Superorbital Equilibrium Glide

WING LOADING: $\frac{W}{S} = 30^{\#}/\text{sq. FT.}$

SEA LEVEL DENSITY: $\rho_0 = .0027$ SLUG/CU. FT.

EXPONENTIAL CONSTANT: $\beta = (23{,}500 \text{ FT.})$

$$H_V = \frac{1}{\beta}\left(\ln \frac{S\rho_0 g r C_L}{2W} - \ln \frac{(1-\bar{u}^2)}{\bar{u}^2}\right)$$

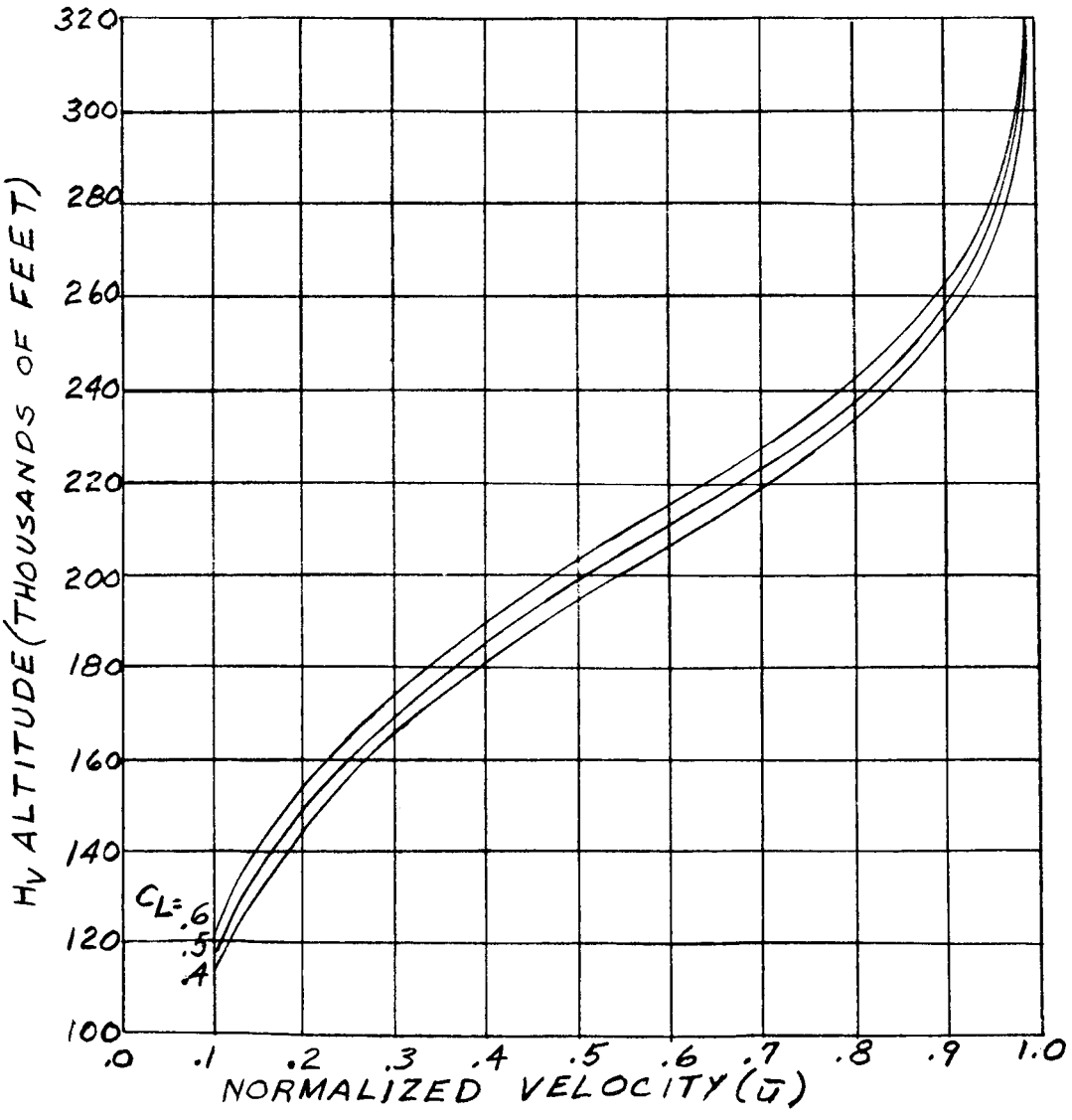

Fig. III-35. Altitude Versus Normalized Velocity for Equilibrium Glide

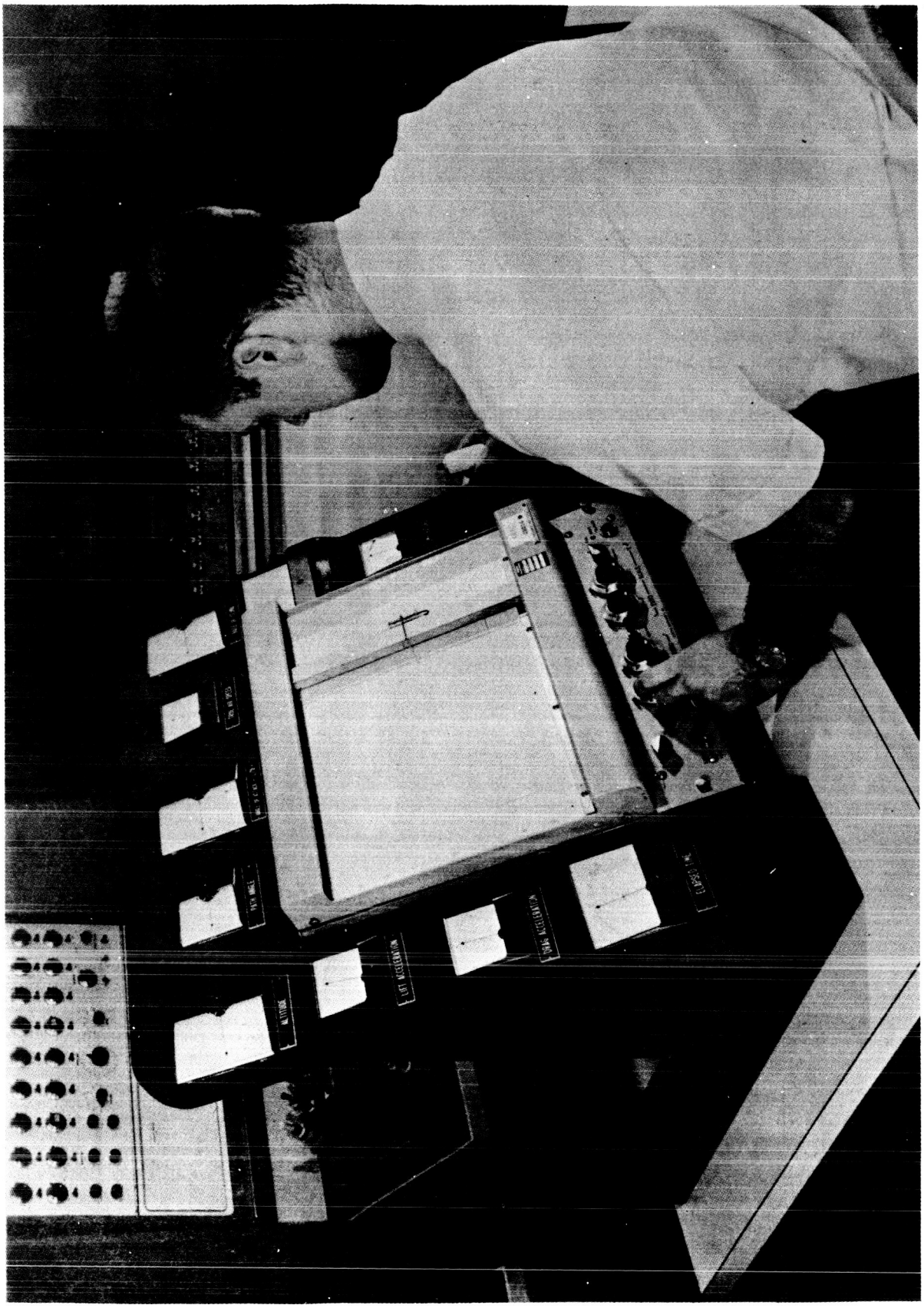

Fig. III-36. Analog Simulator Used for Apollo Re-entry Guidance Problems

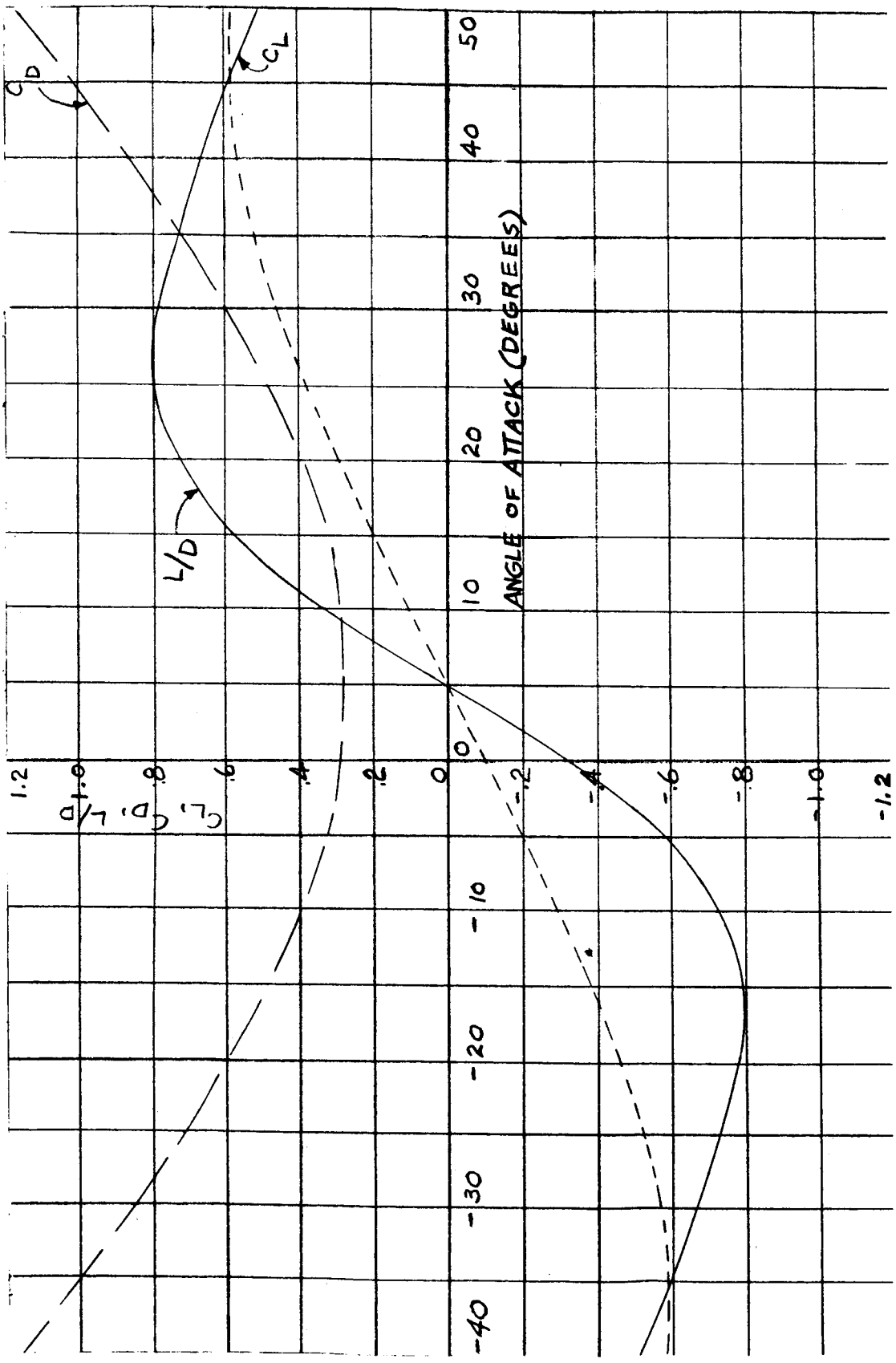

Fig. III-37. Aerodynamic Characteristics of the Typical Apollo Vehicle

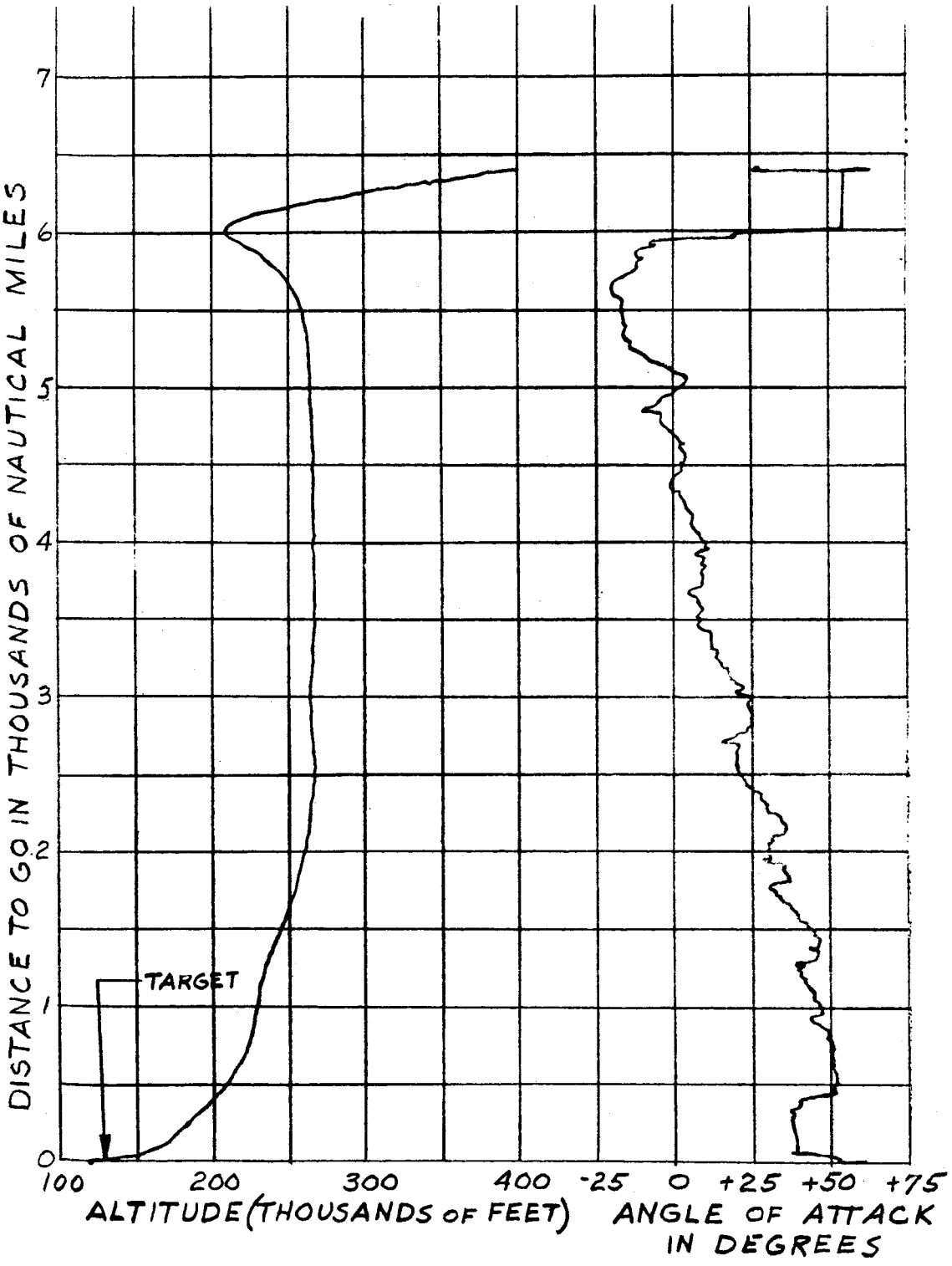

Fig. III-38. Altitude and Angle of Attack Versus Distance to Go for a Closed Loop Trajectory

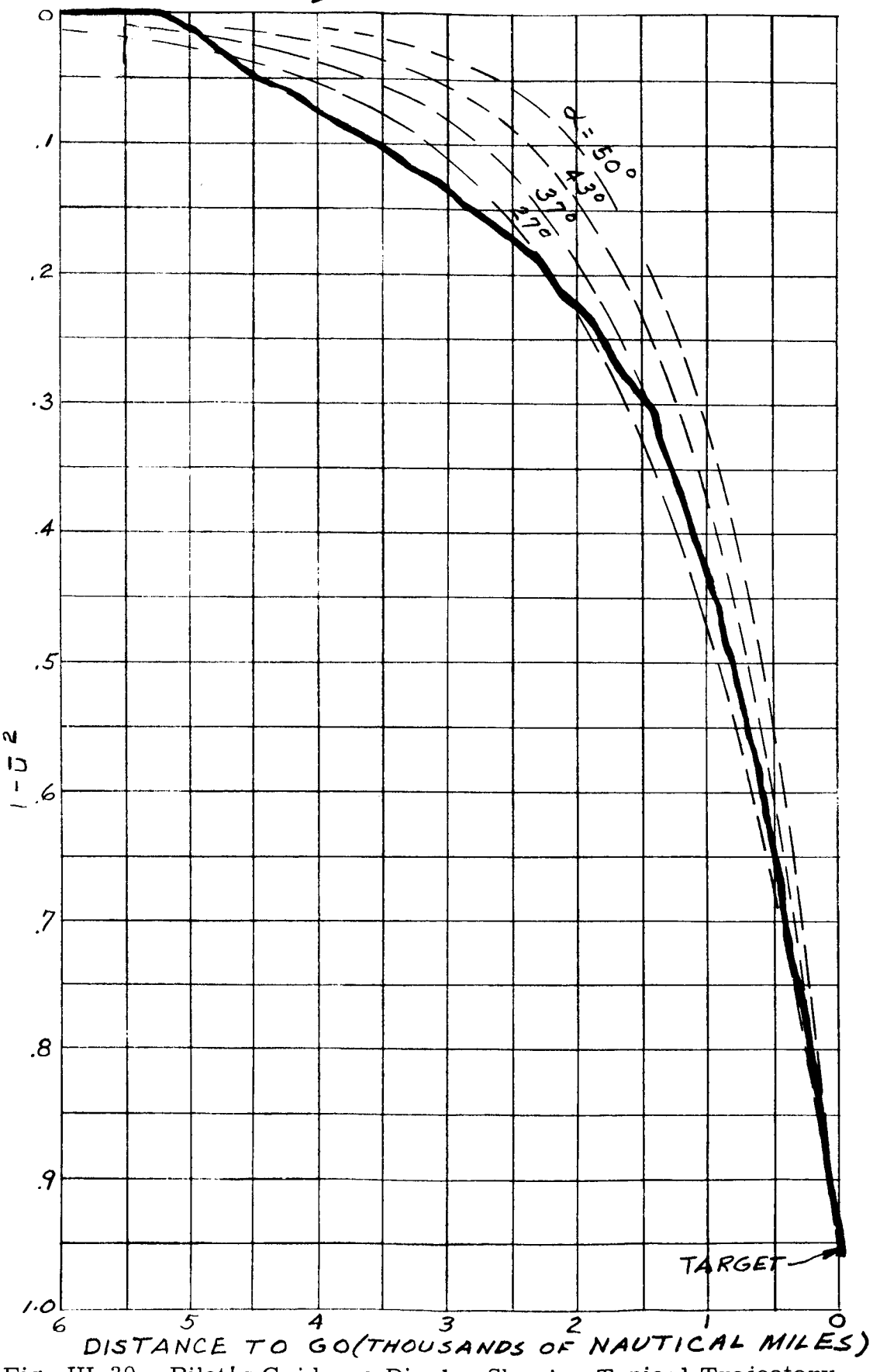

Fig. III-39. Pilot's Guidance Display Showing Typical Trajectory

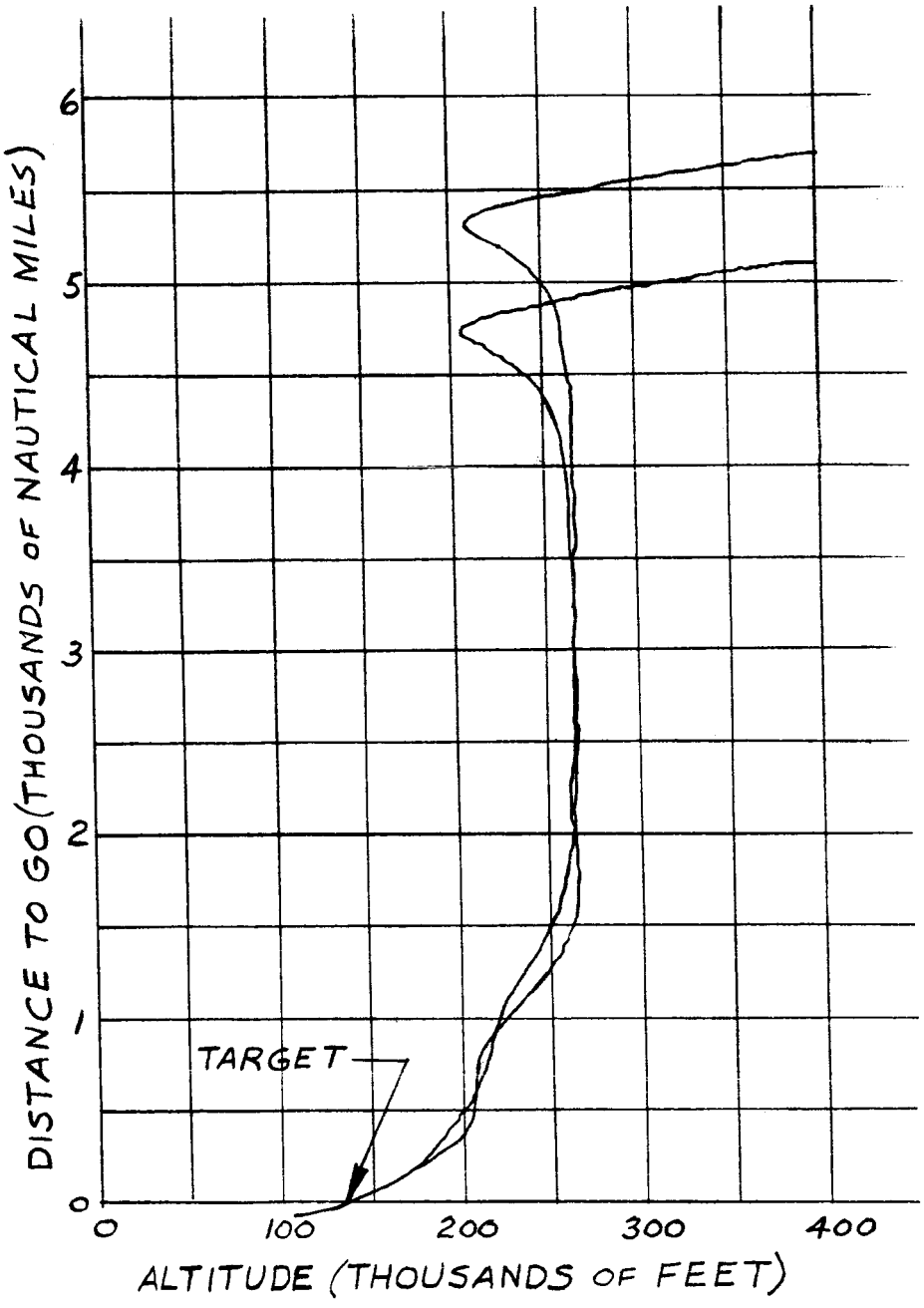

Fig. III-40. Altitude Versus Distance to Go for Two Closed Loop Trajectories to the Same Target

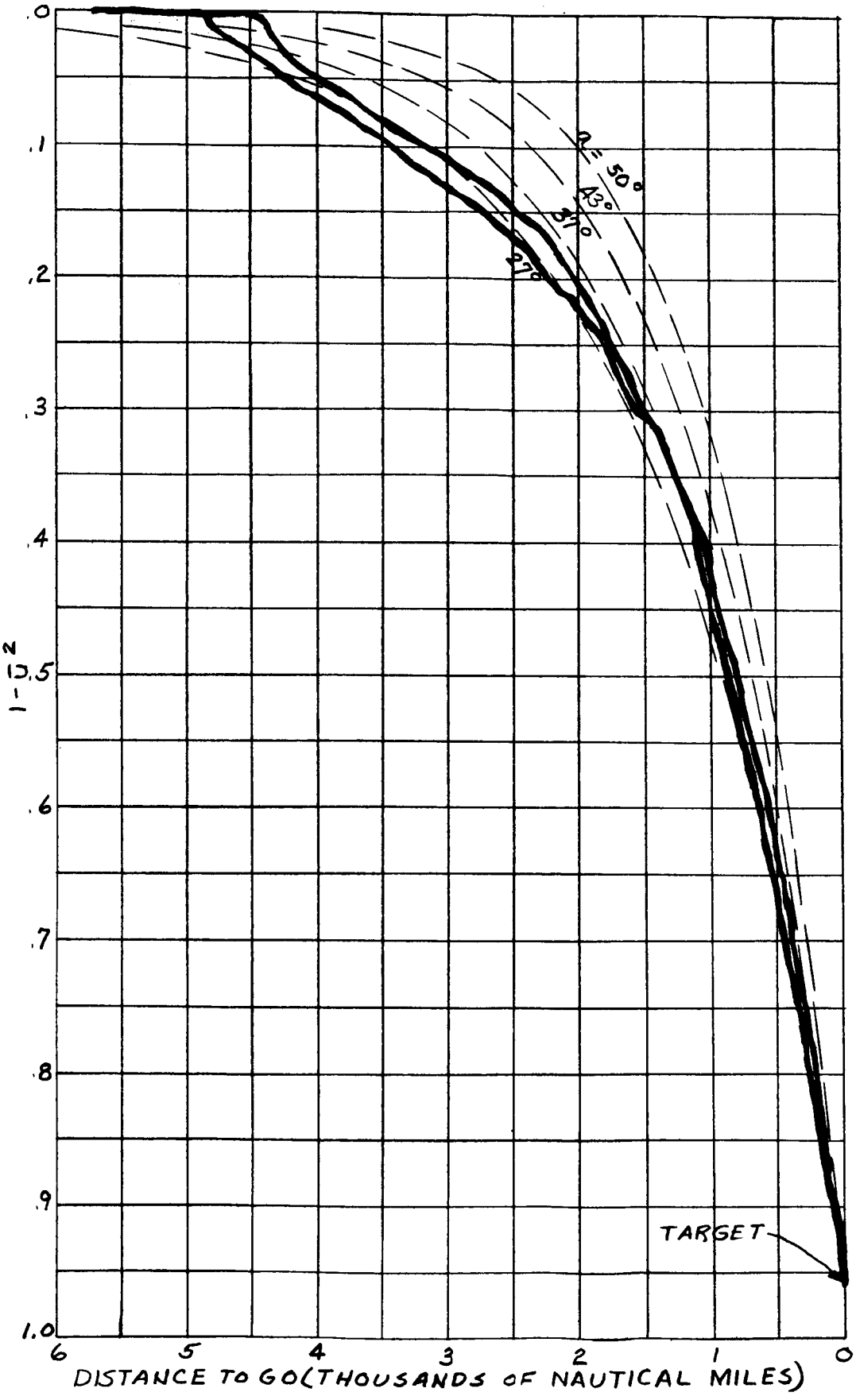

Fig. III-41. Pilot's Guidance Display Showing Two Trajectories

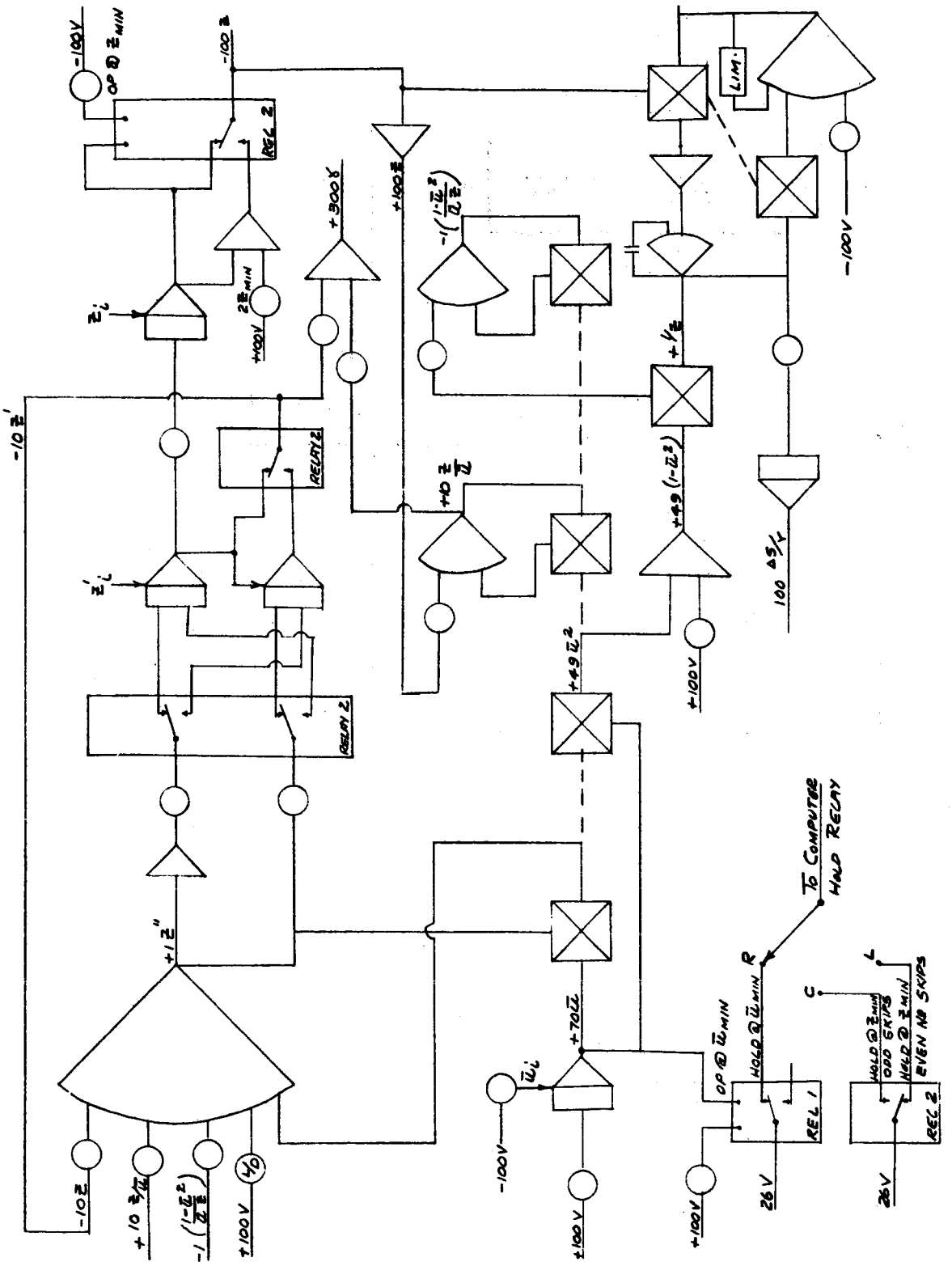

Fig. III-42. Z-Function Analog Mechanization

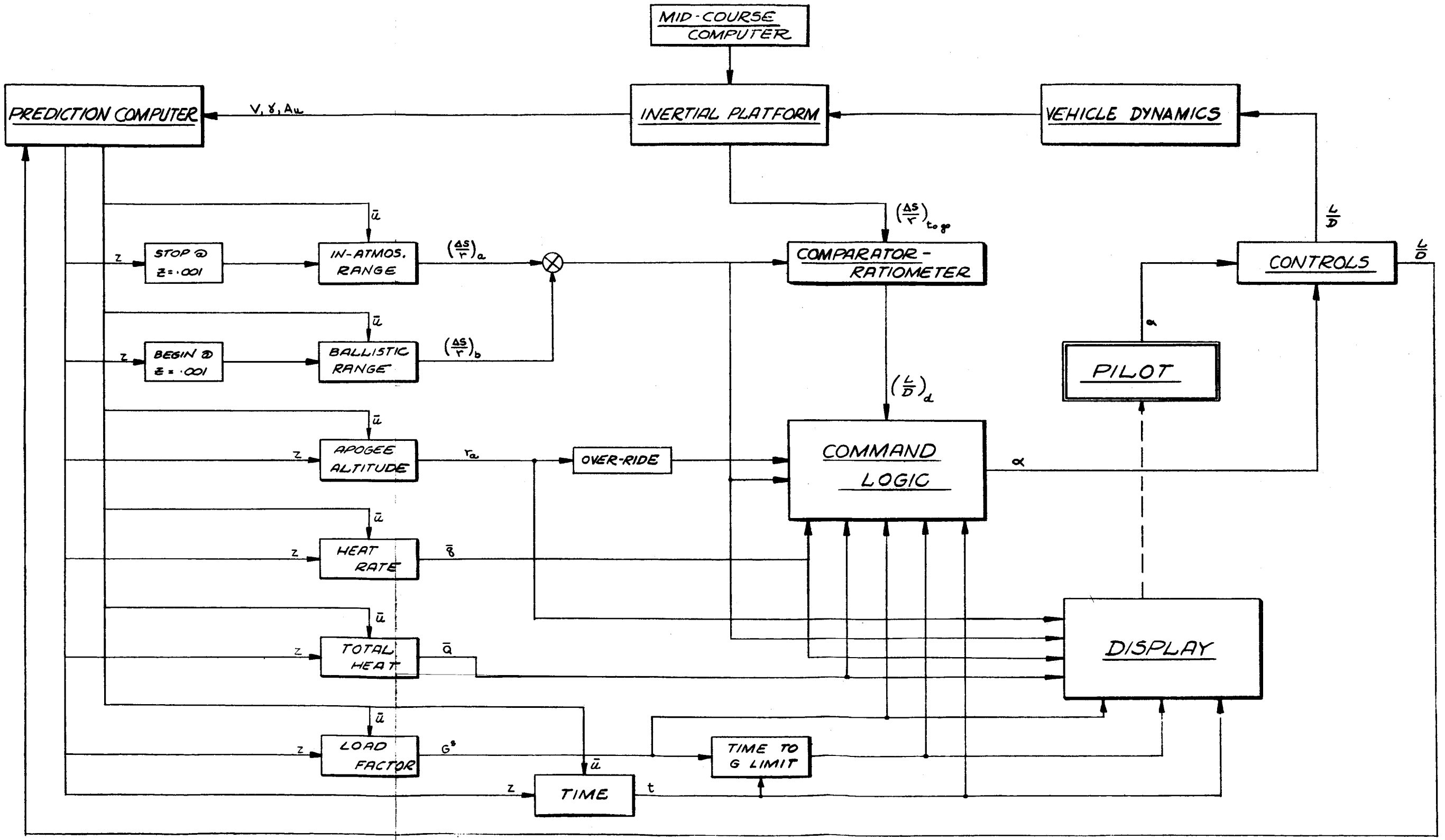

Fig. III-43. Block Diagram, Re-entry Range Prediction System

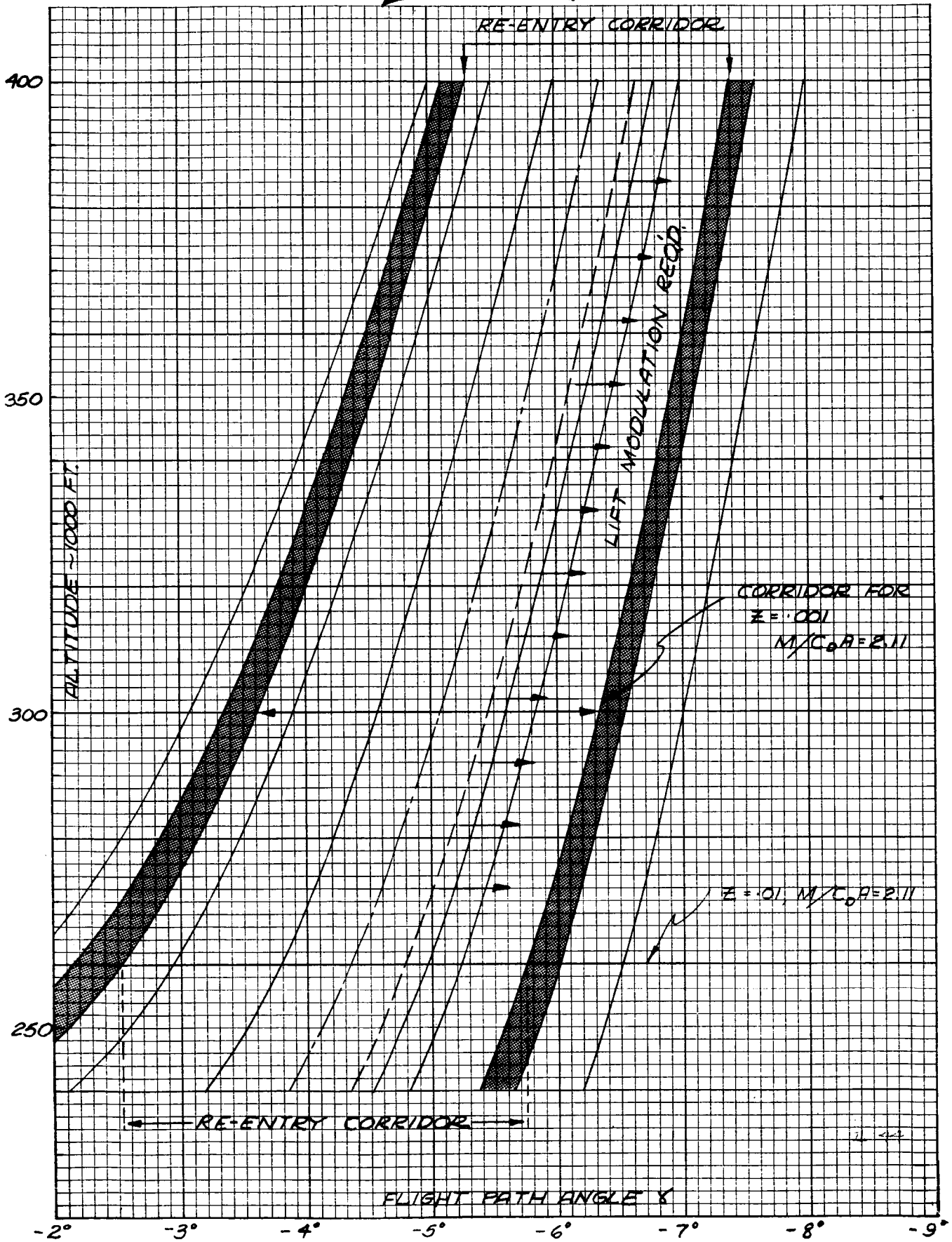

Fig. III-44. Re-entry Corridor Versus Altitude

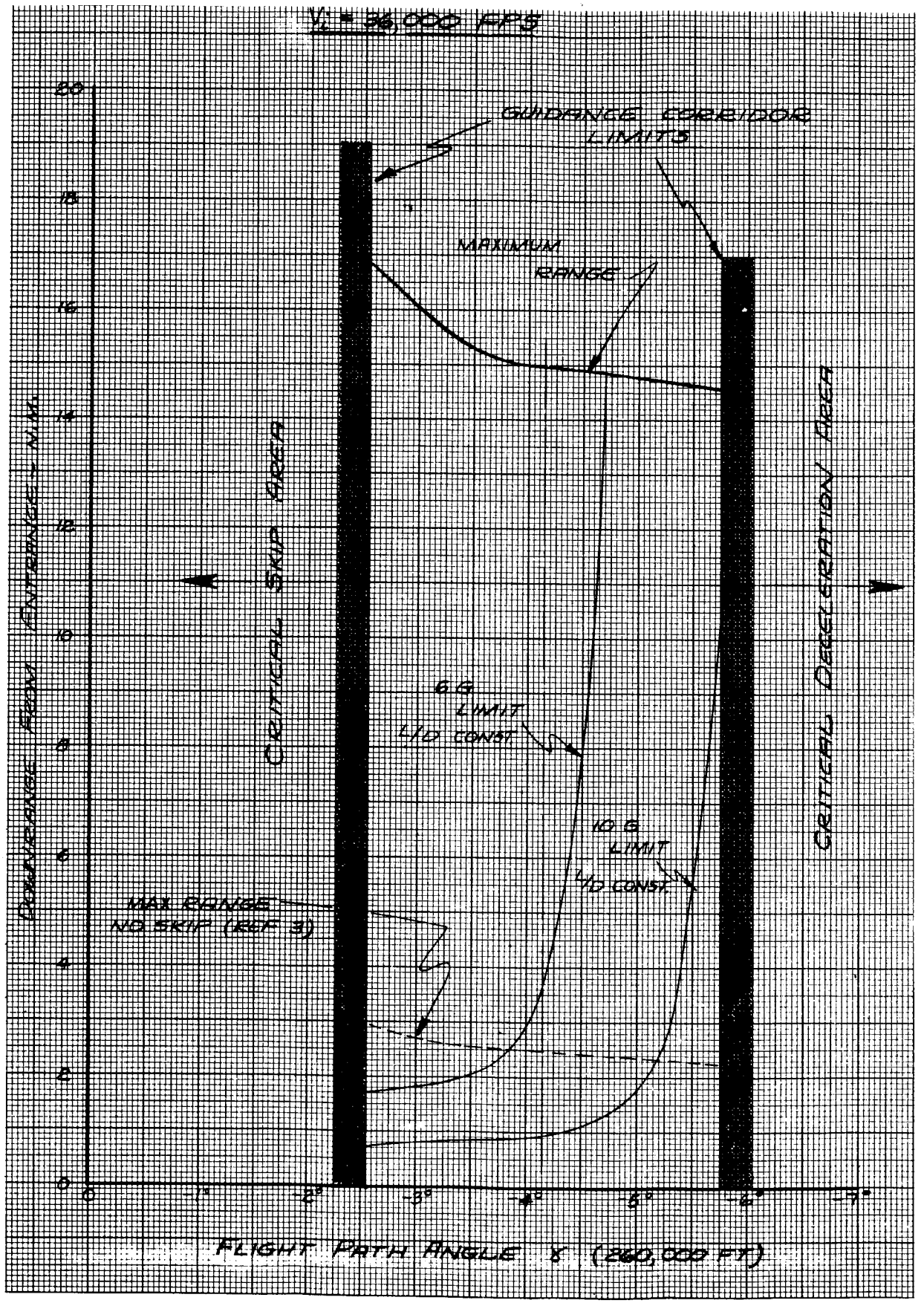

Fig. III-45. Re-entry Boundary Conditions

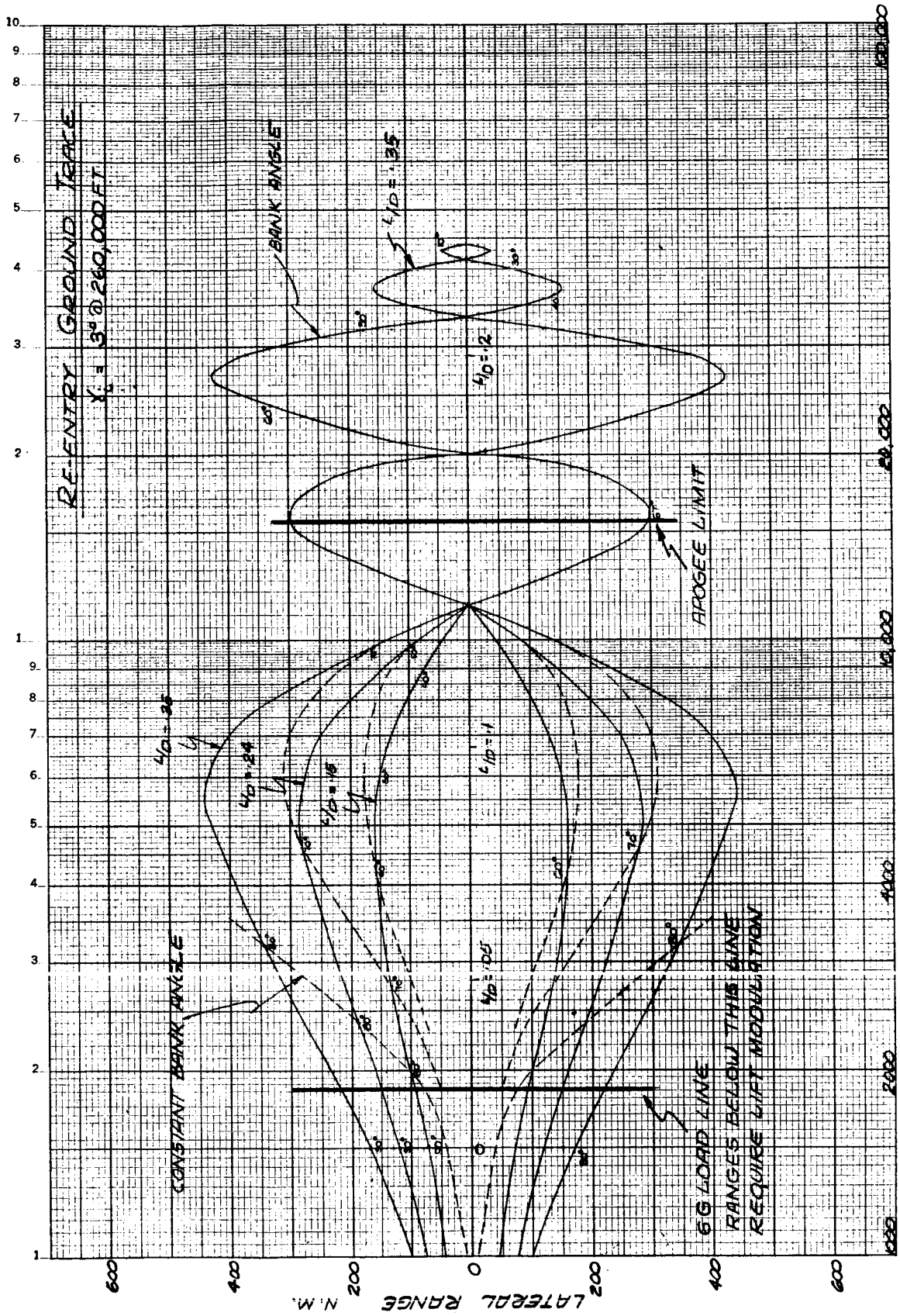

Fig. III-46. Re-entry Ground Trace (γ_i = 3 degrees at 260,000 feet)

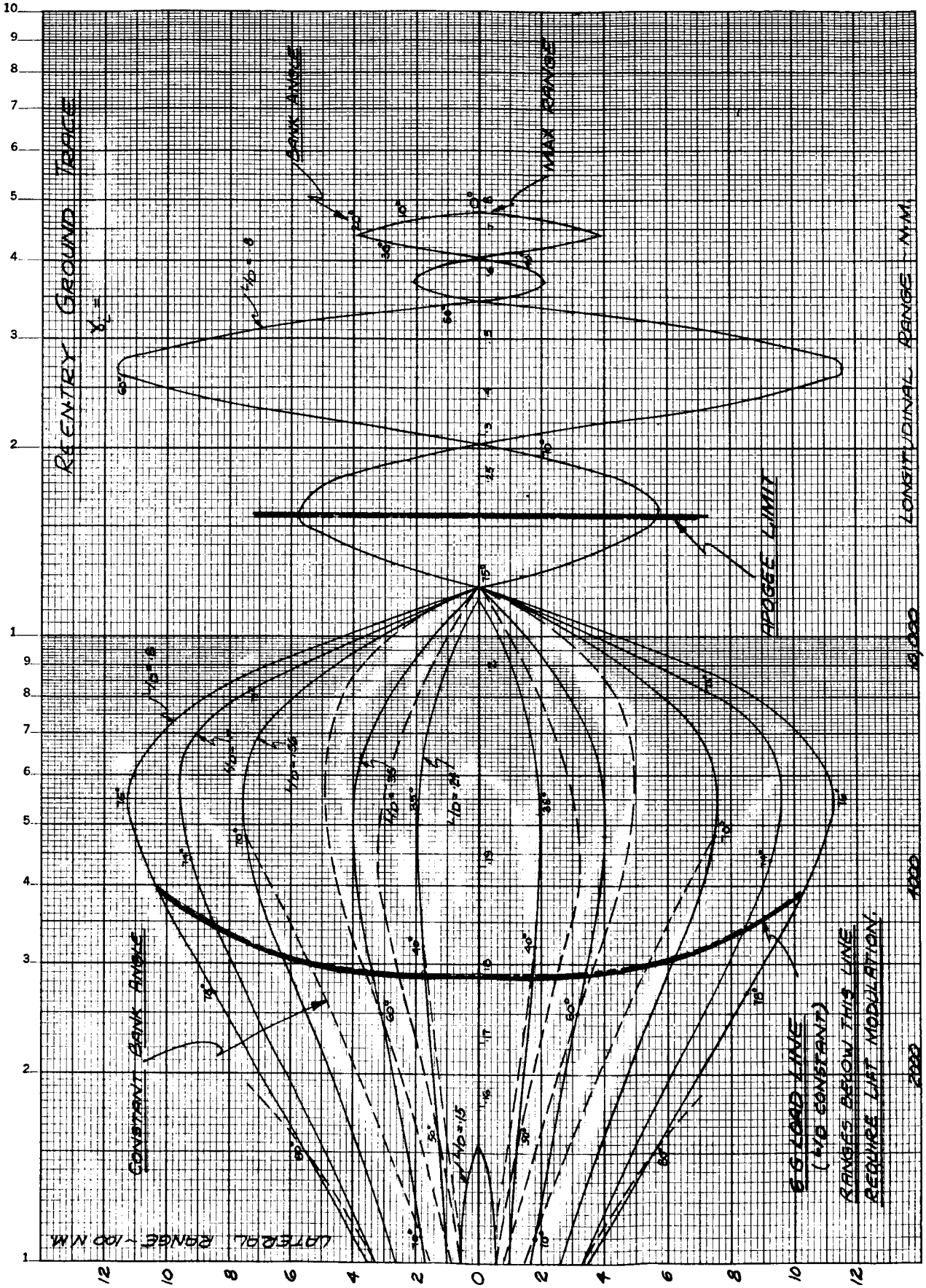

Fig. III-47. Re-entry Ground Trace (γ_i = 4 degrees at 260,000 feet)

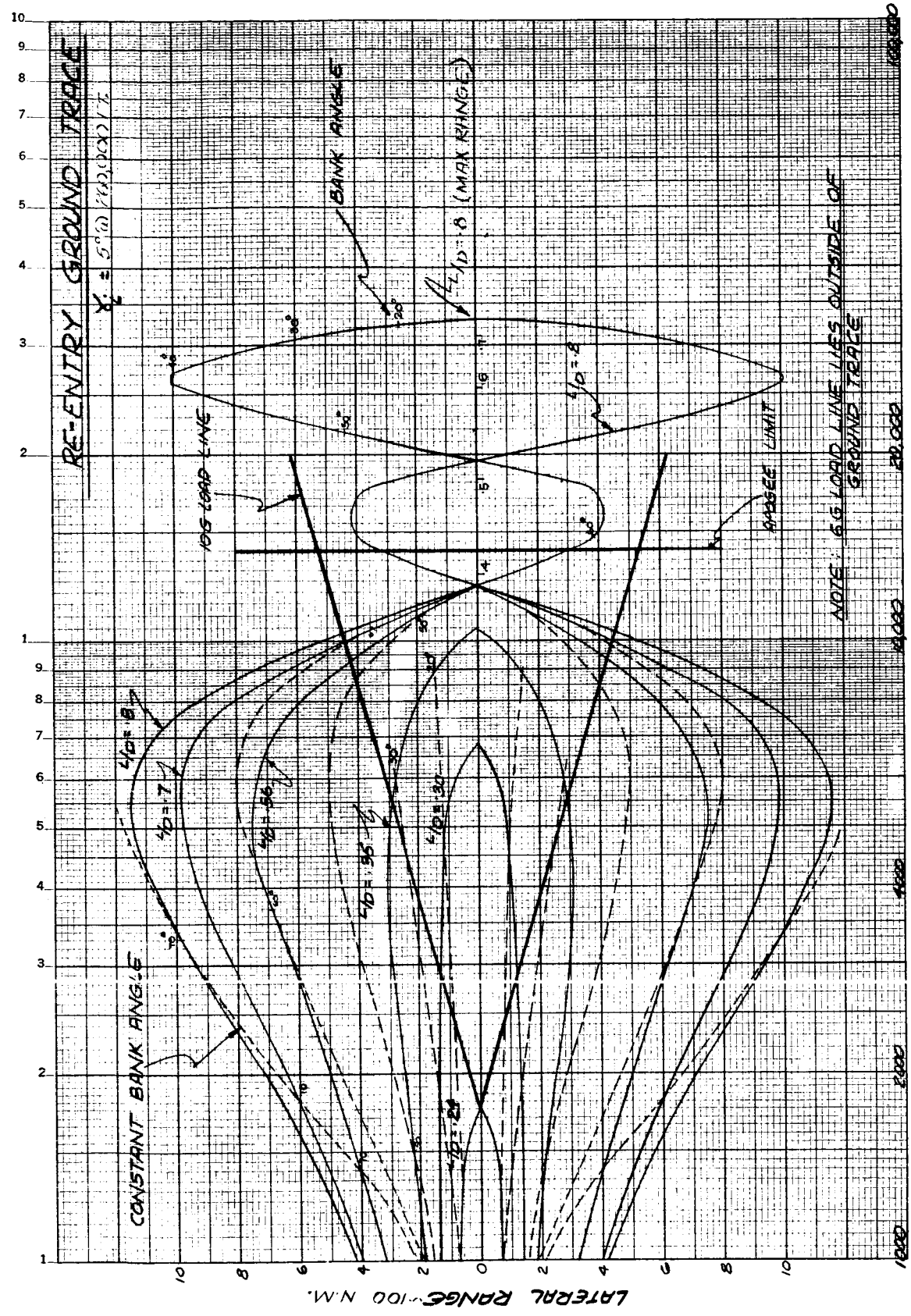

Fig. III-48. Re-entry Ground Trace (γ_i = 5 degrees at 260,000 feet)

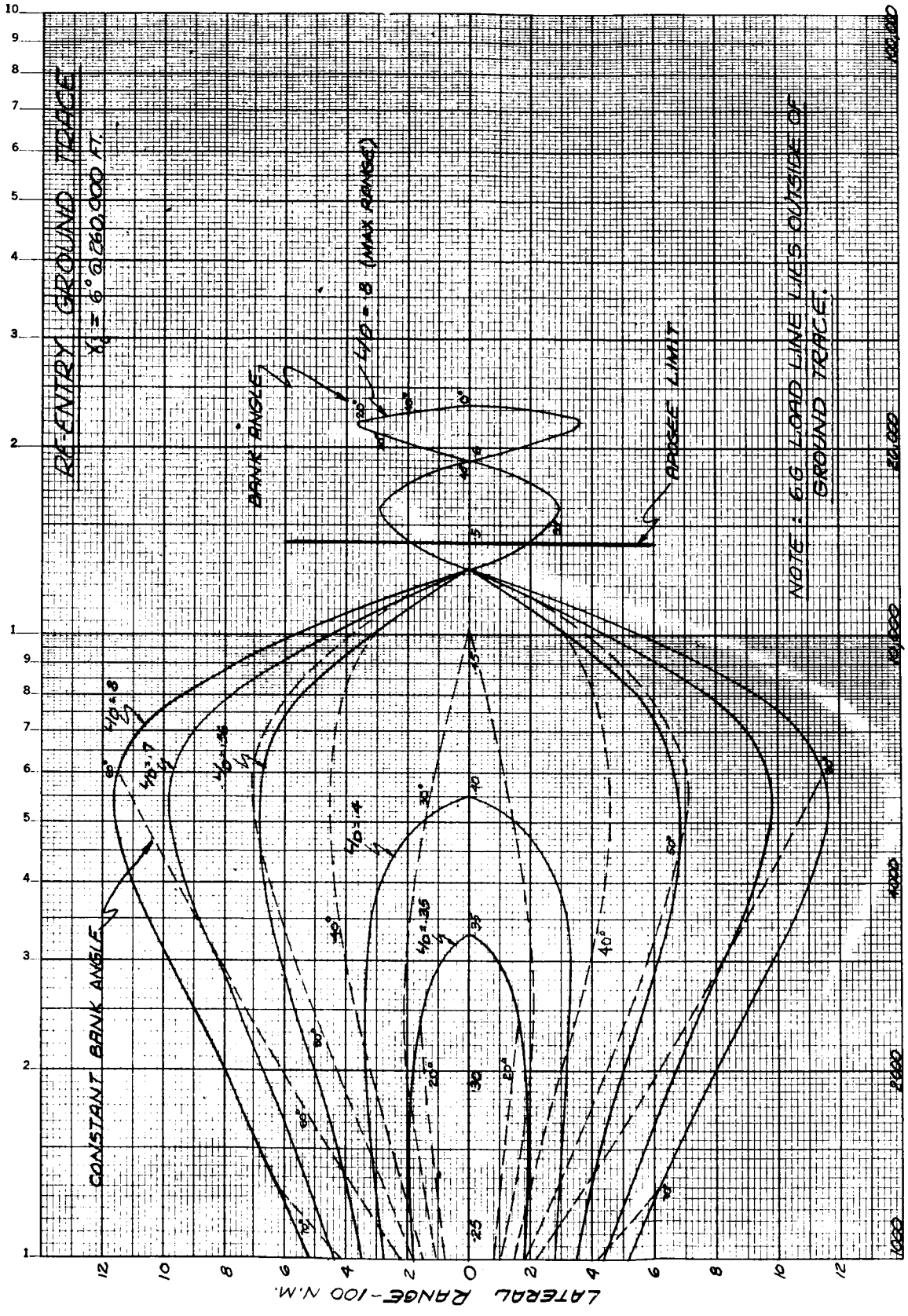

Fig. III-49. Re-entry Ground Trace (γ_i = 6 degrees at 260,000 feet)

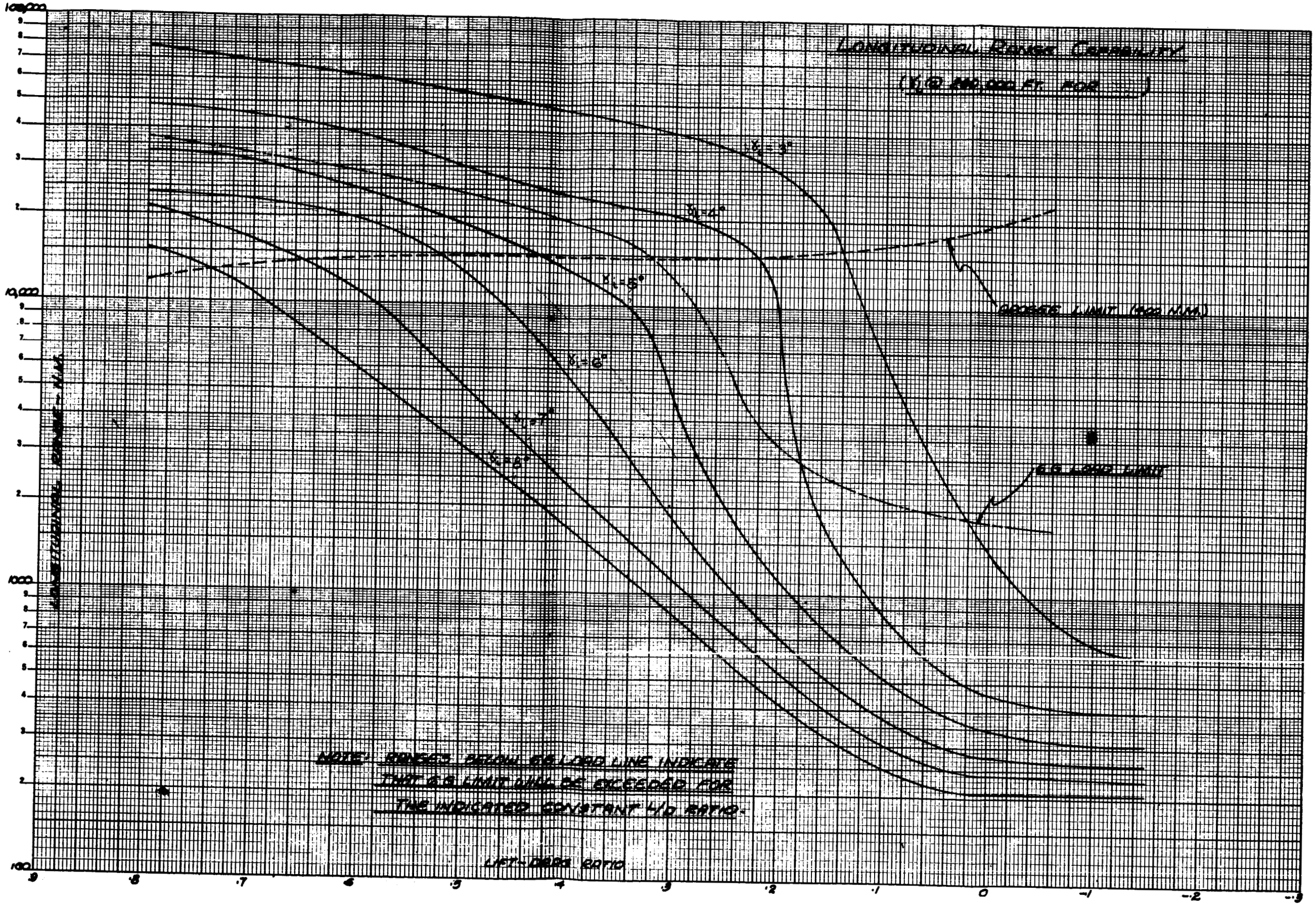

Fig. III-50. L/D Versus Longitudinal Range

CONFIDENTIAL

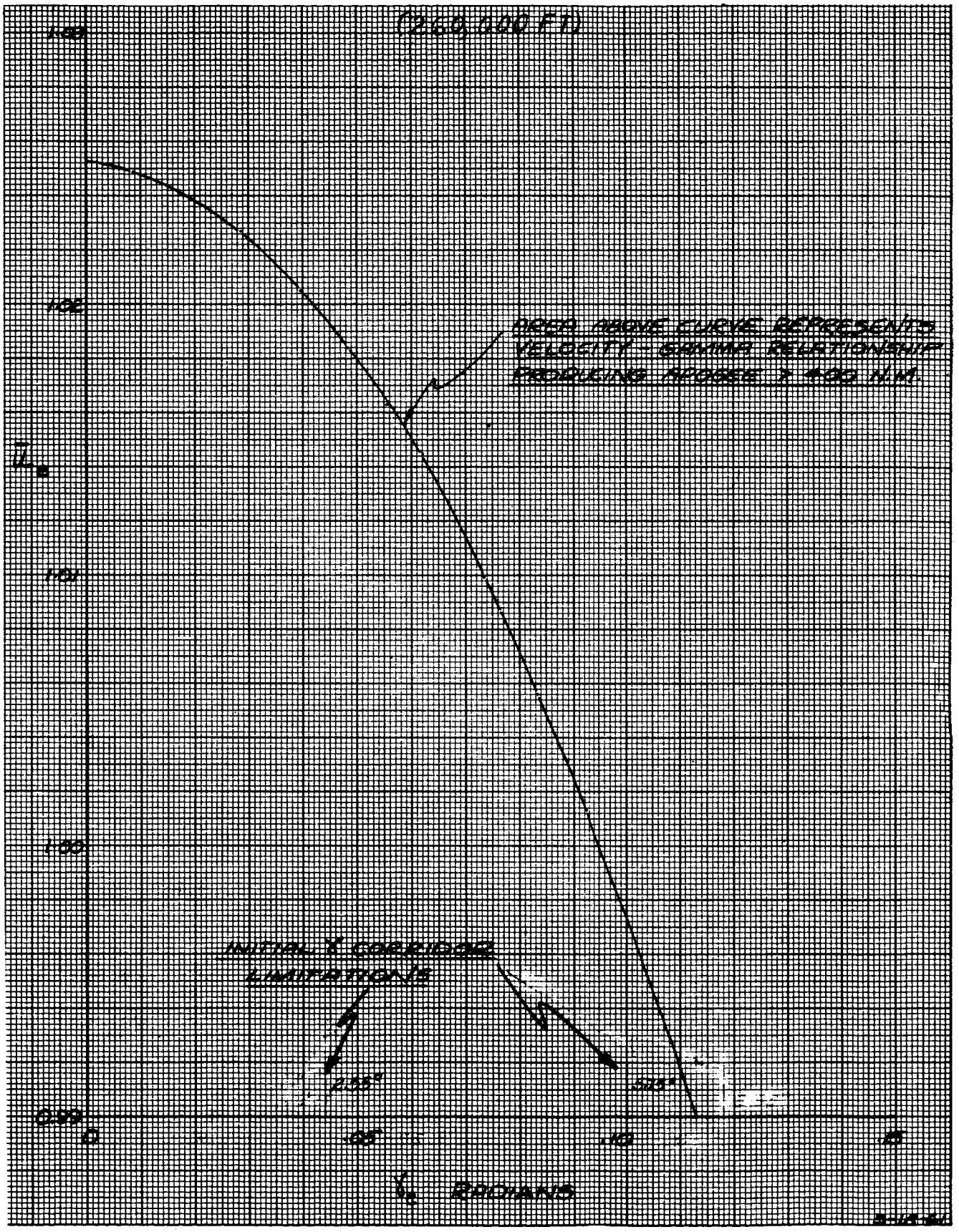

Fig. III-51. Exit Conditions for 400-Nautical Mile Apogee

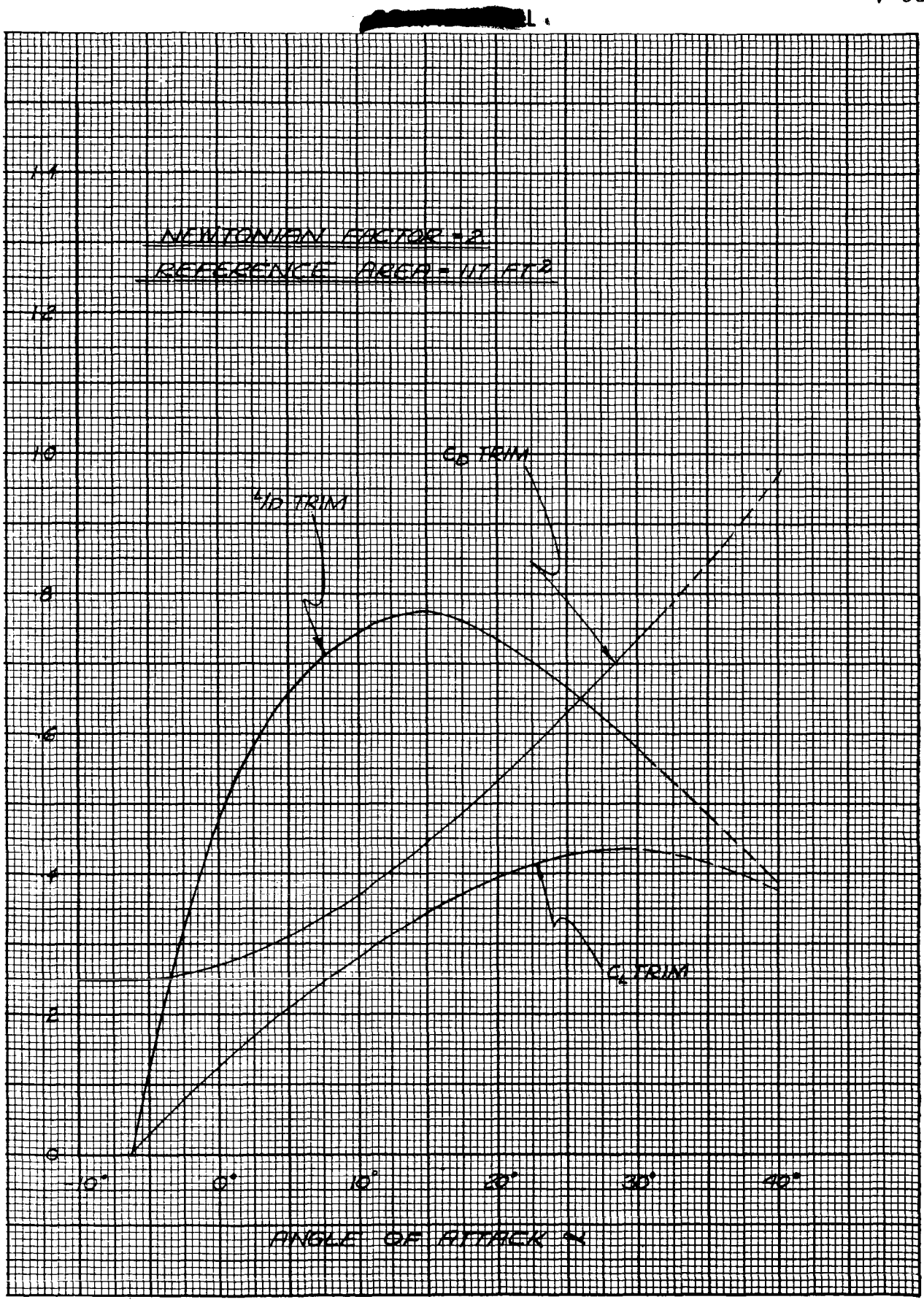

Fig. III-52. Model 410 Aerodynamic Characteristics

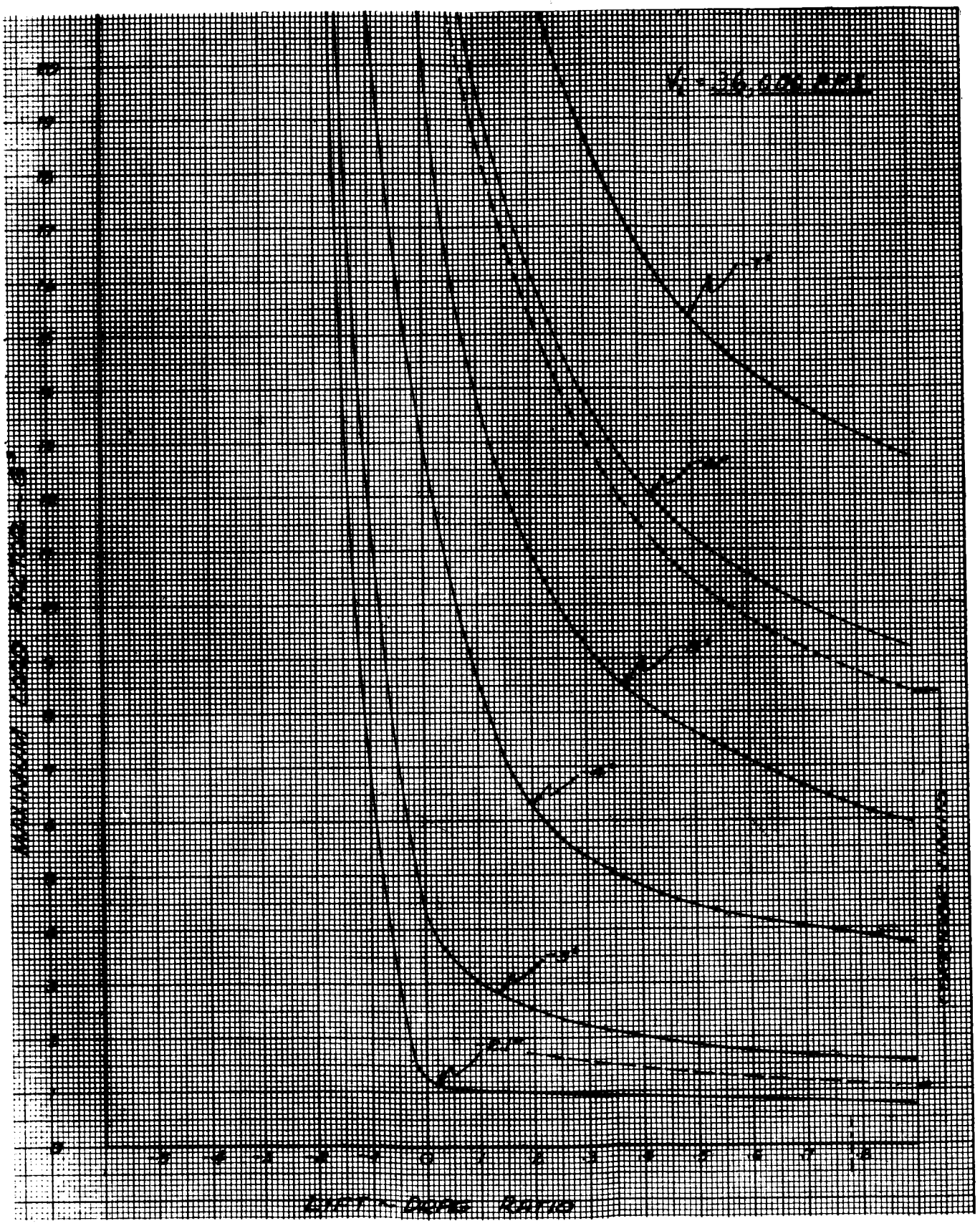

Fig. III-53. Maximum Deceleration Versus L/D and γ_i (γ_i at 260,000 feet)

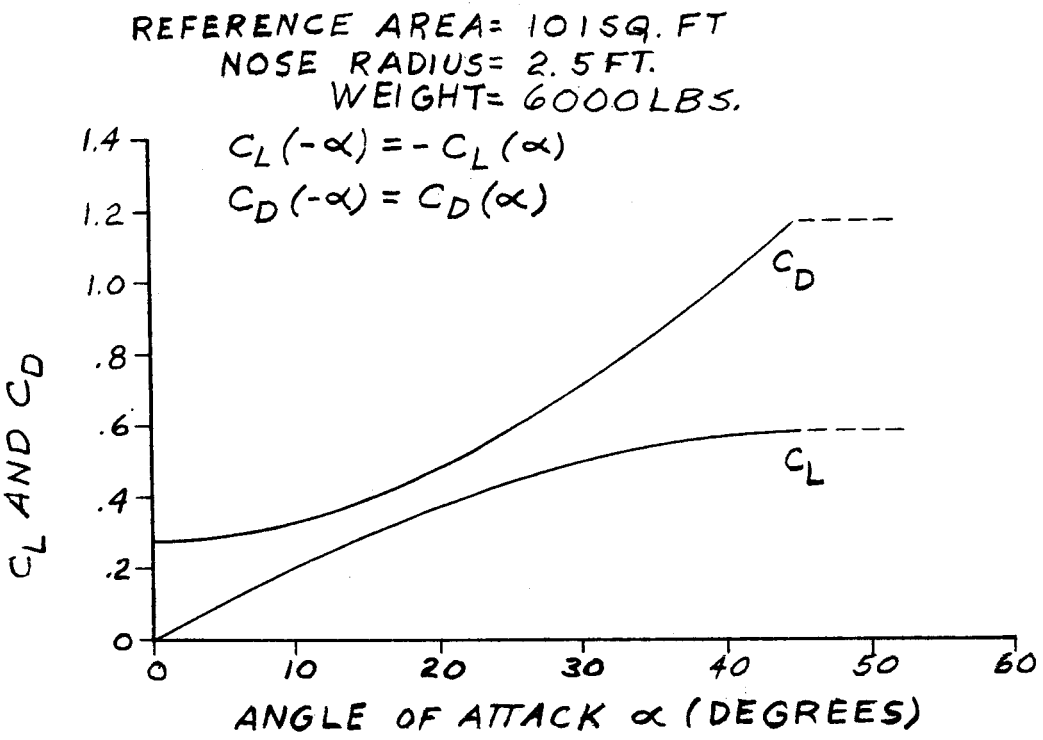

Fig. III-54. Lift and Drag Coefficient Versus Angle of Attack for a Typical Apollo Vehicle

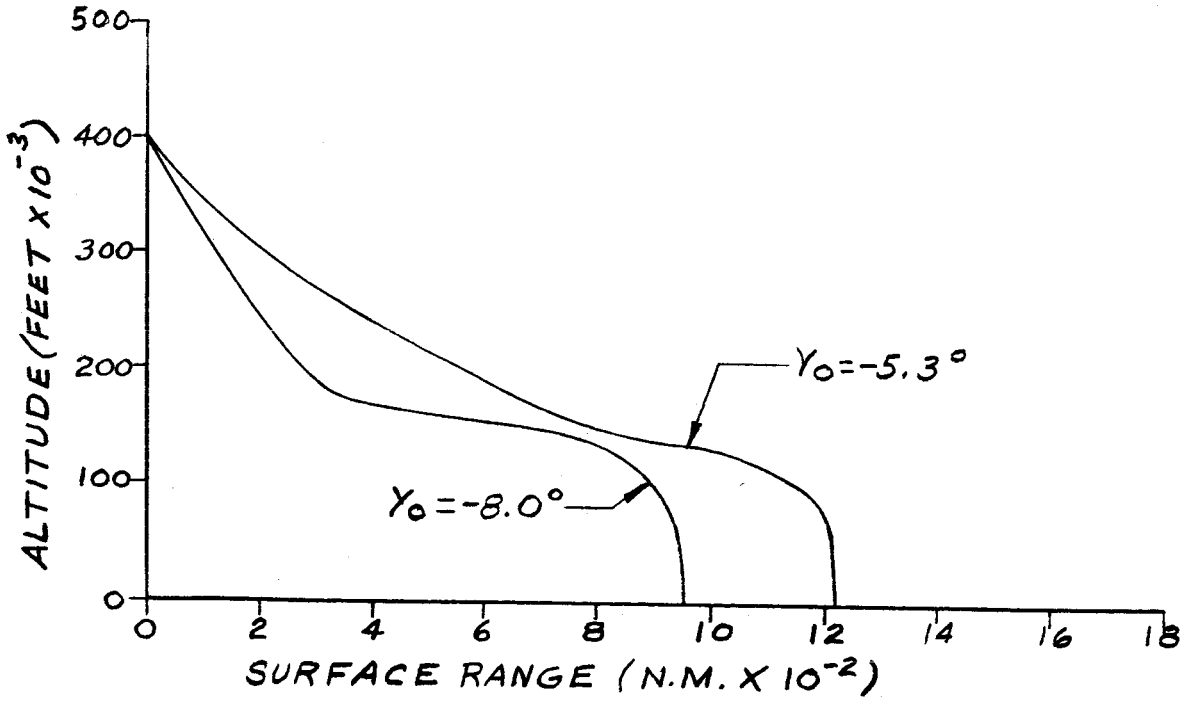

Fig. III-55. Re-entry Trajectories for Minimum Total Heat

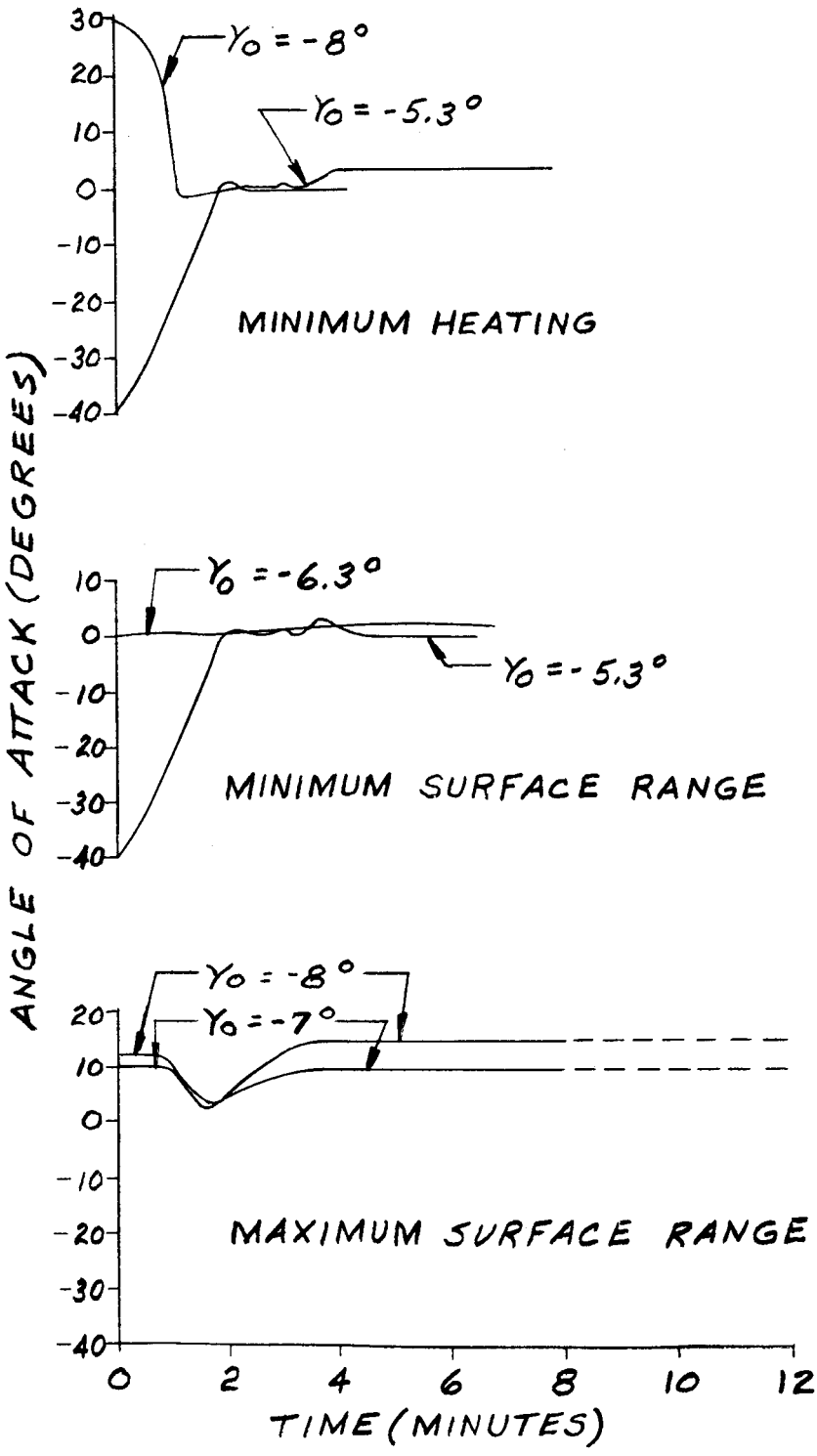

Fig. III-56. Angle of Attack Profiles

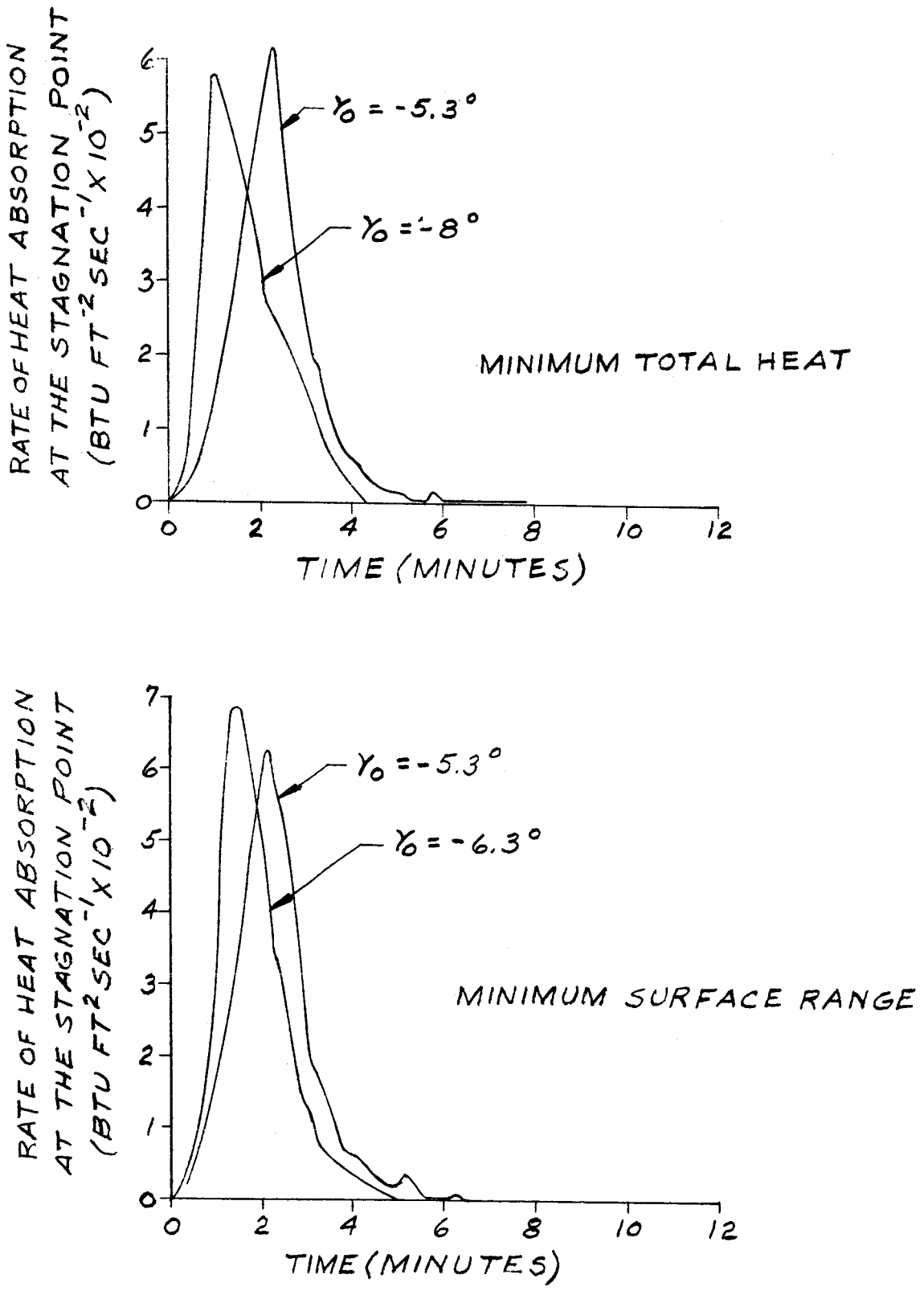

Fig. III-57. Rate of Heat Absorption at the Stagnation Point Versus Time

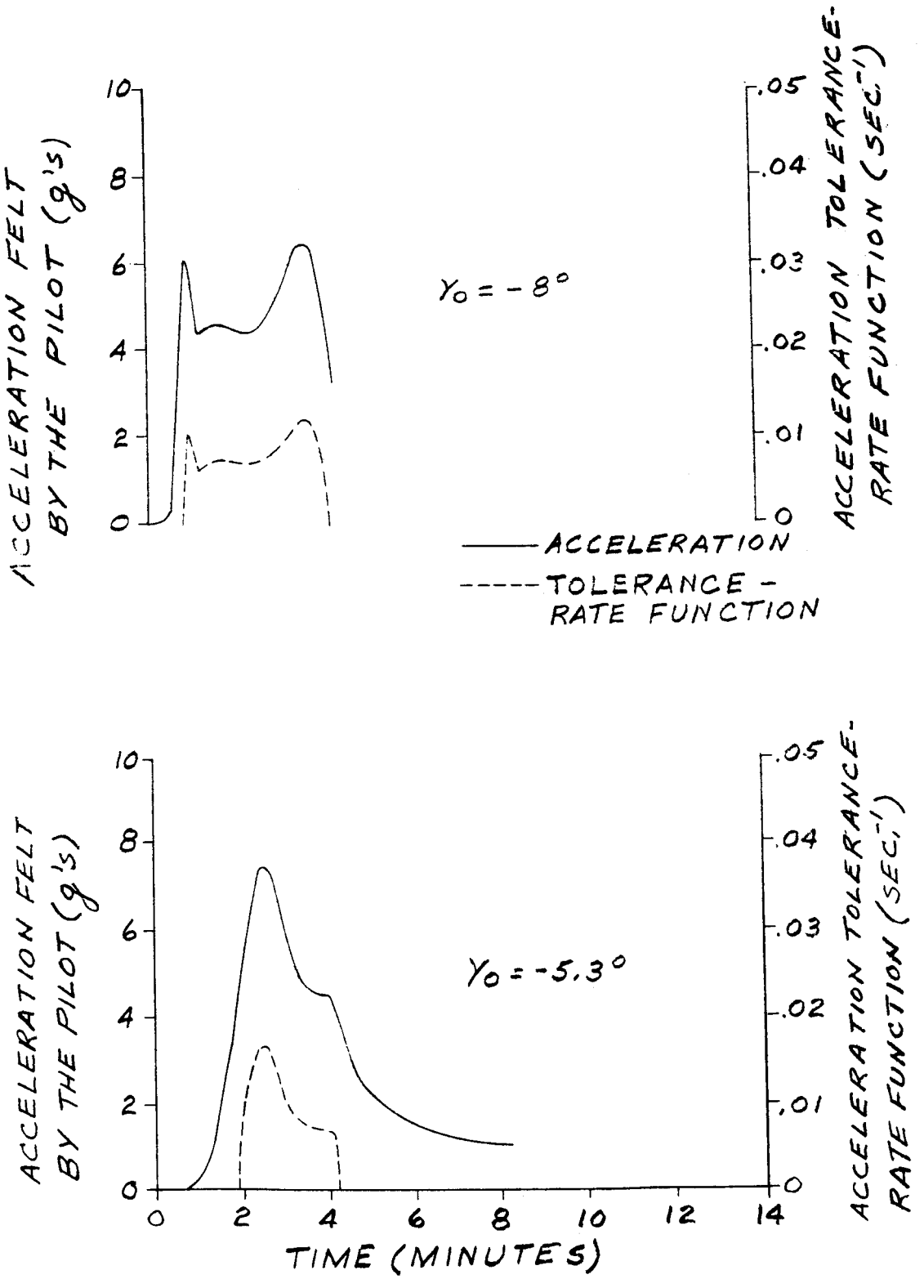

Fig. III-58. Acceleration Felt by Pilot for Minimum Total Heat Trajectories

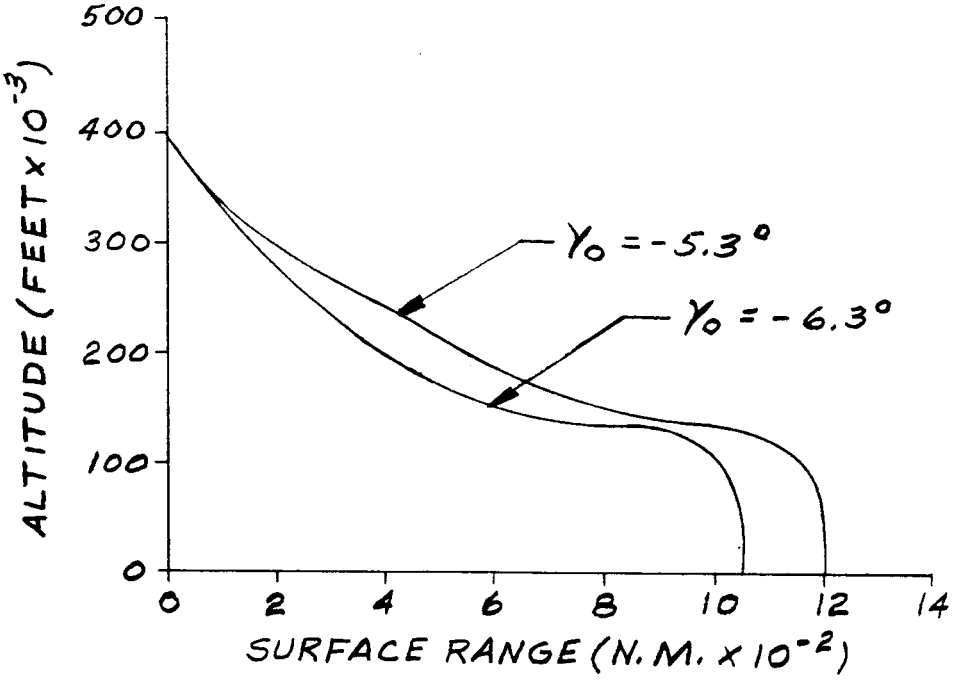

Fig. III-59. Re-entry Trajectories for Minimum Surface Range

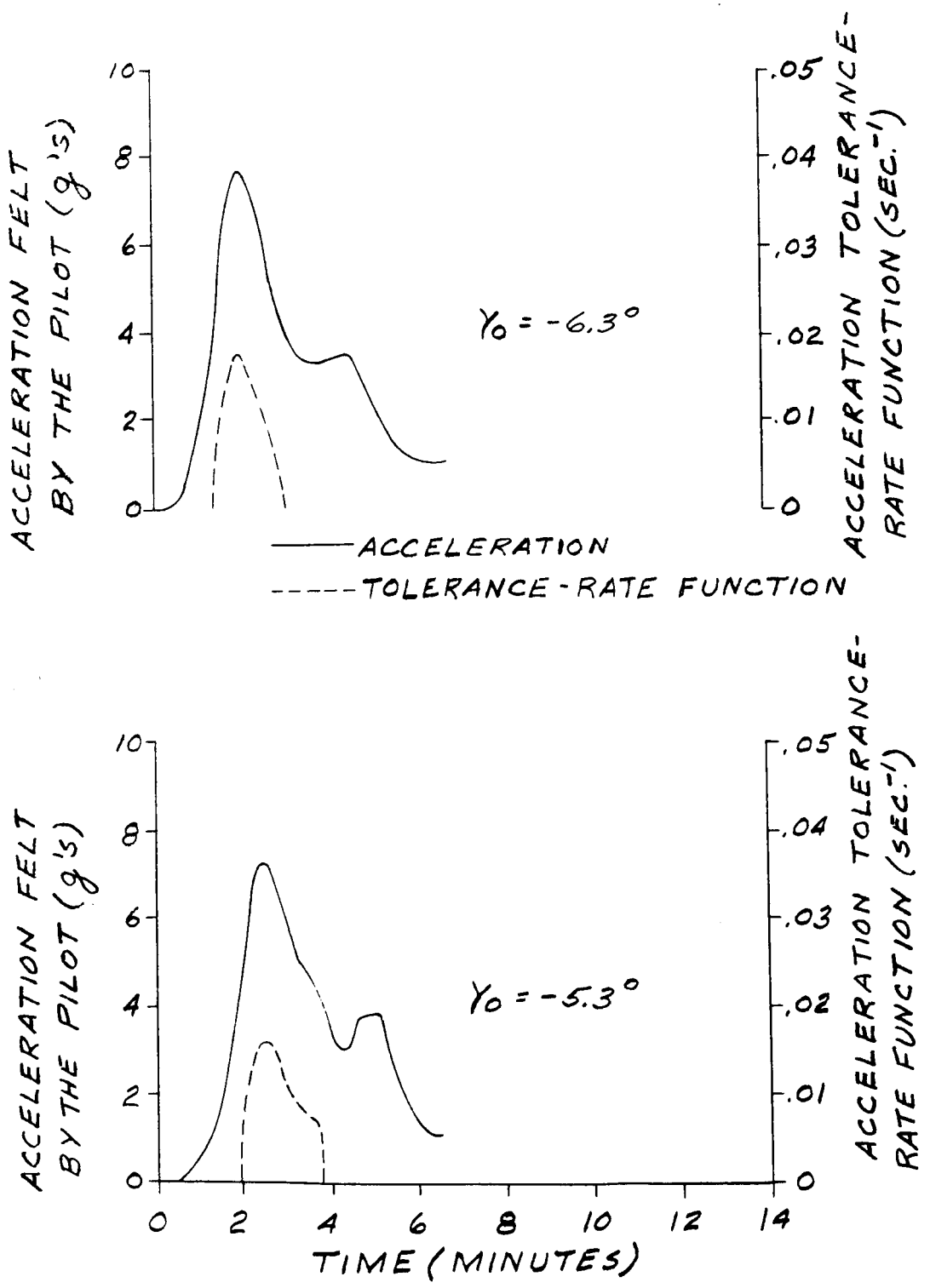

Fig. III-60. Acceleration Felt by Pilot for Minimum Surface Range Trajectories

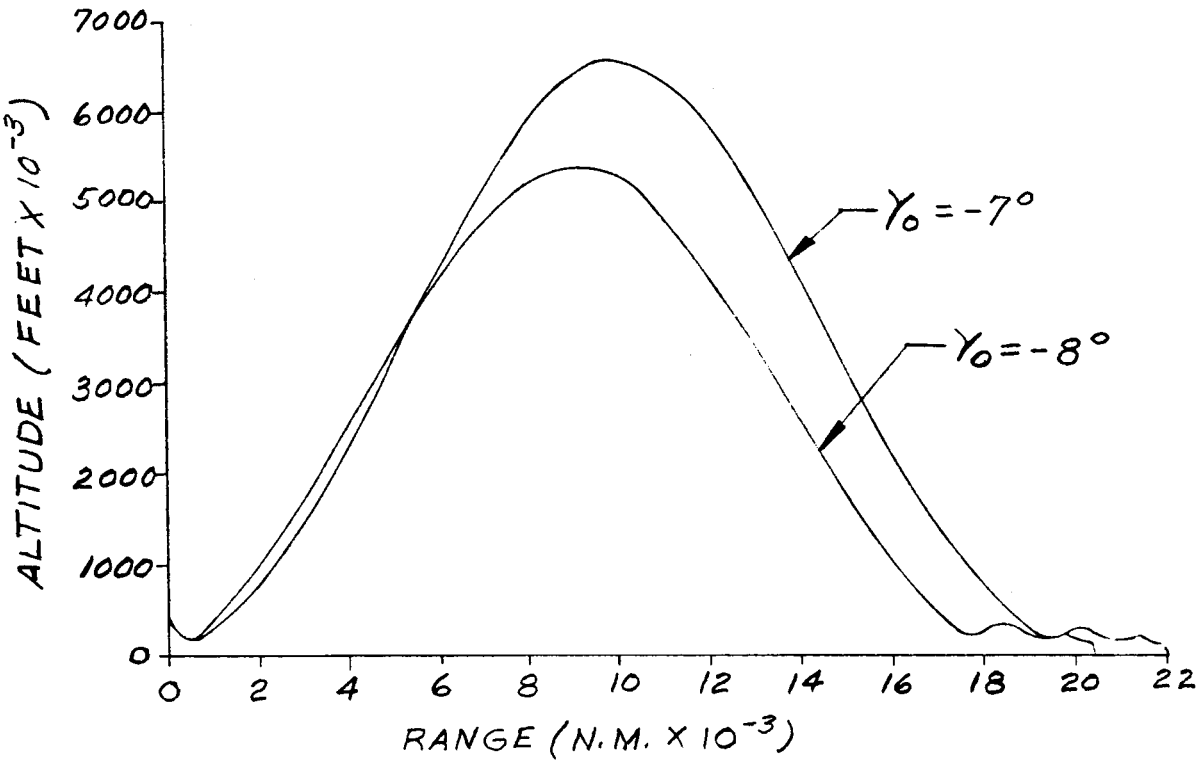

Fig. III-61. Re-entry Trajectories for Maximum Surface Range

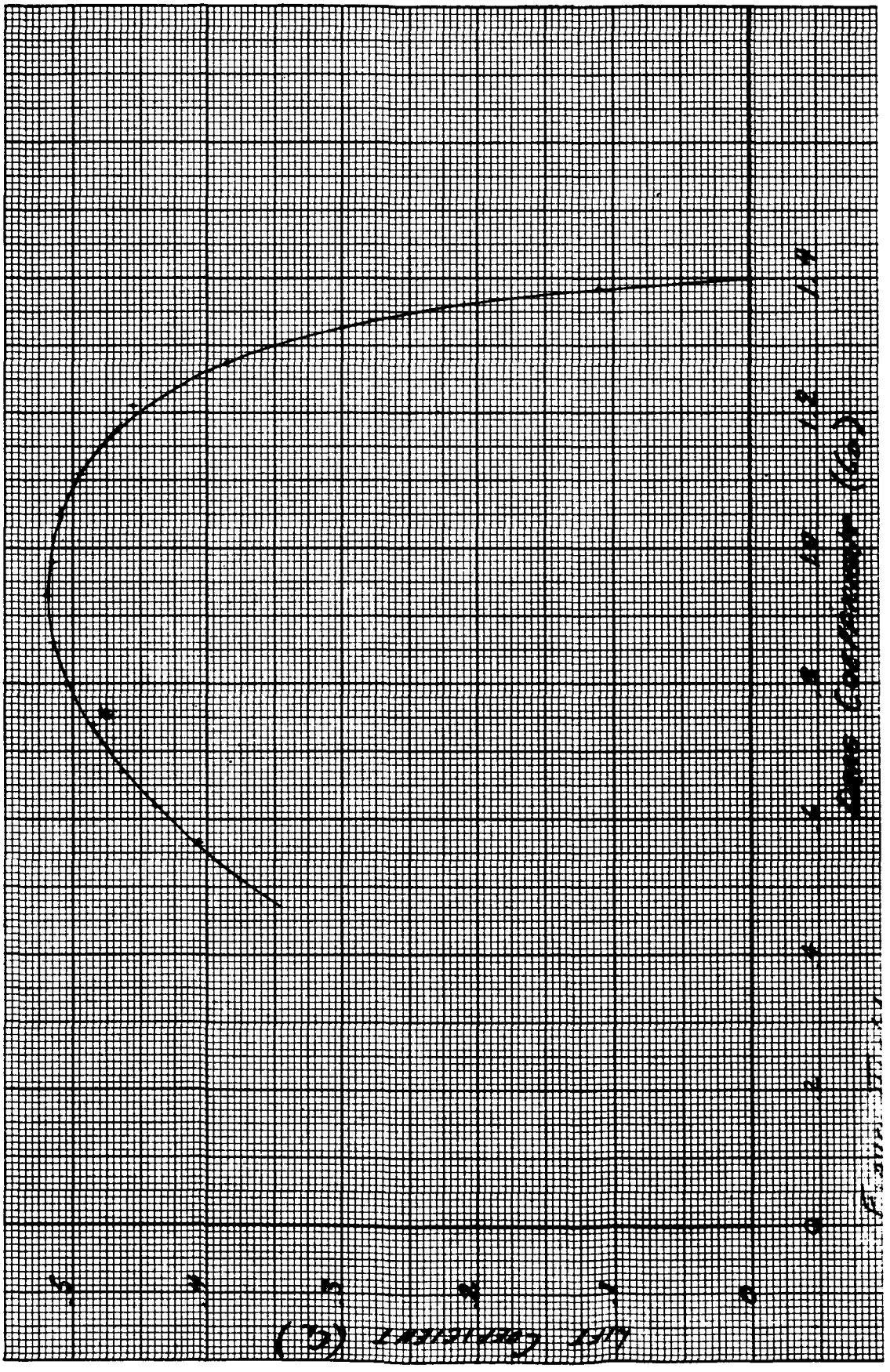

Fig. III-62. L2C Drag Polar

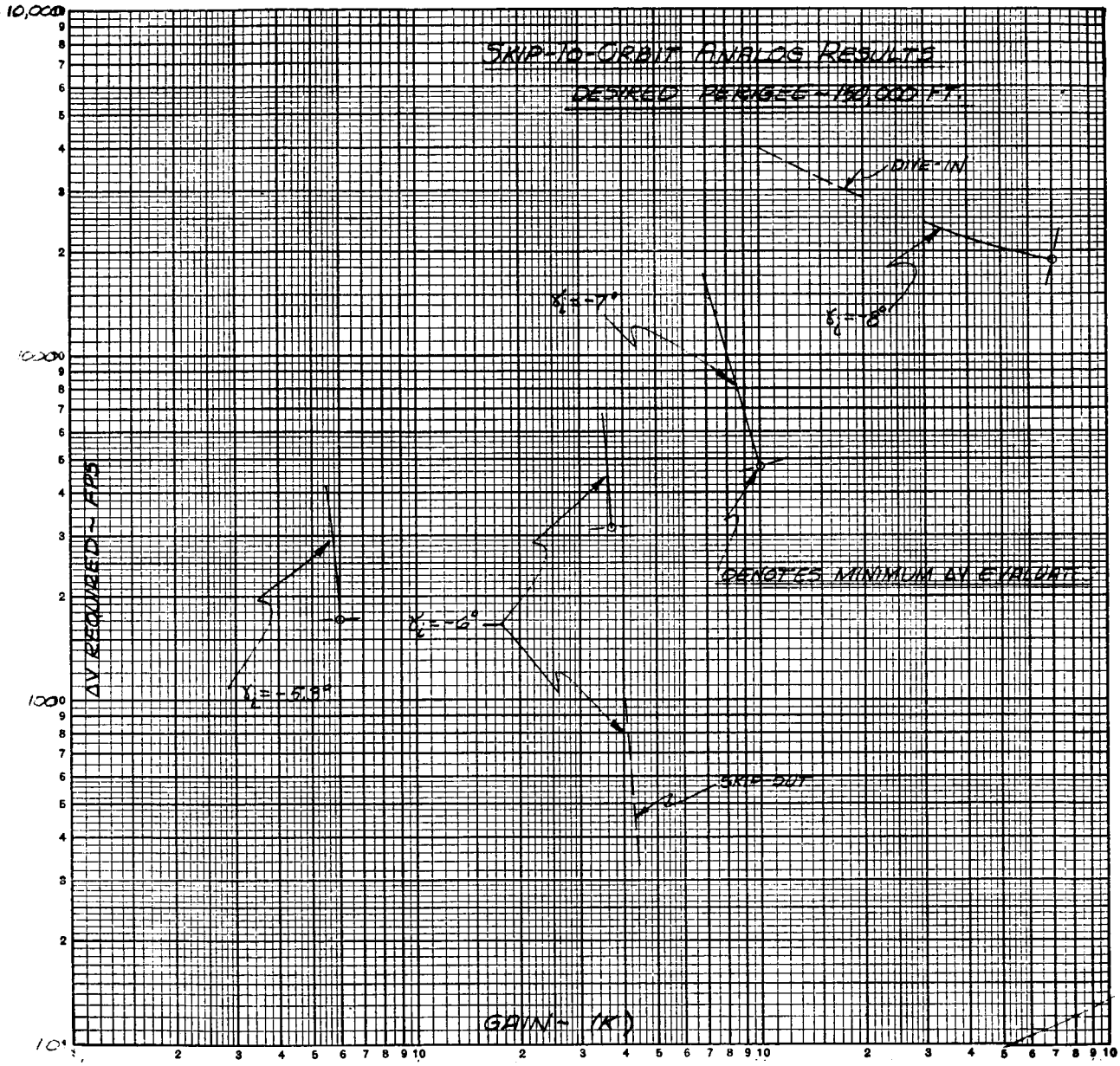

Fig. III-63. ΔV Versus Gain (K) p_d = 150,000 Feet

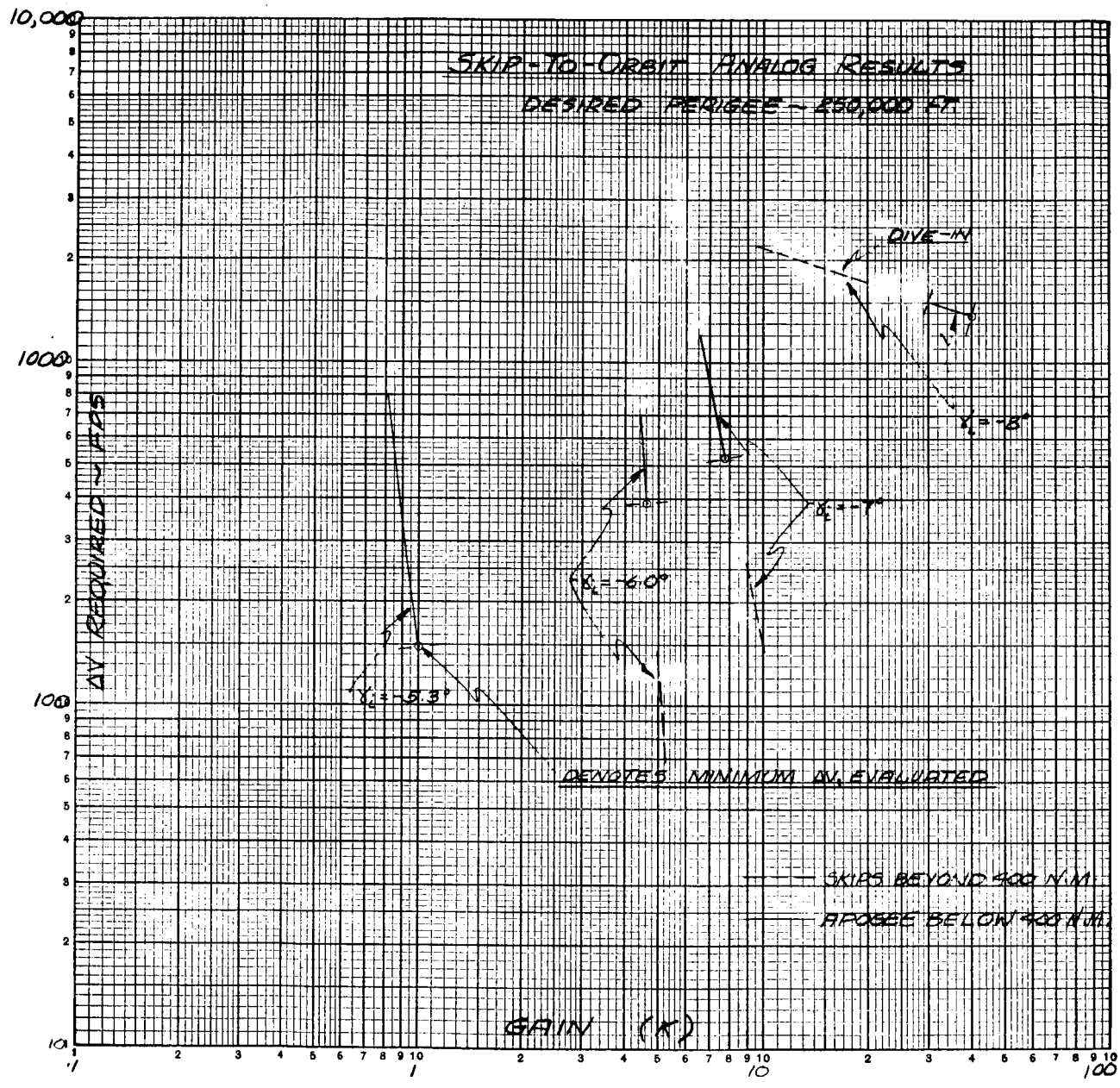

Fig. III-64. ΔV Versus Gain (K) p_d = 250,000 Feet

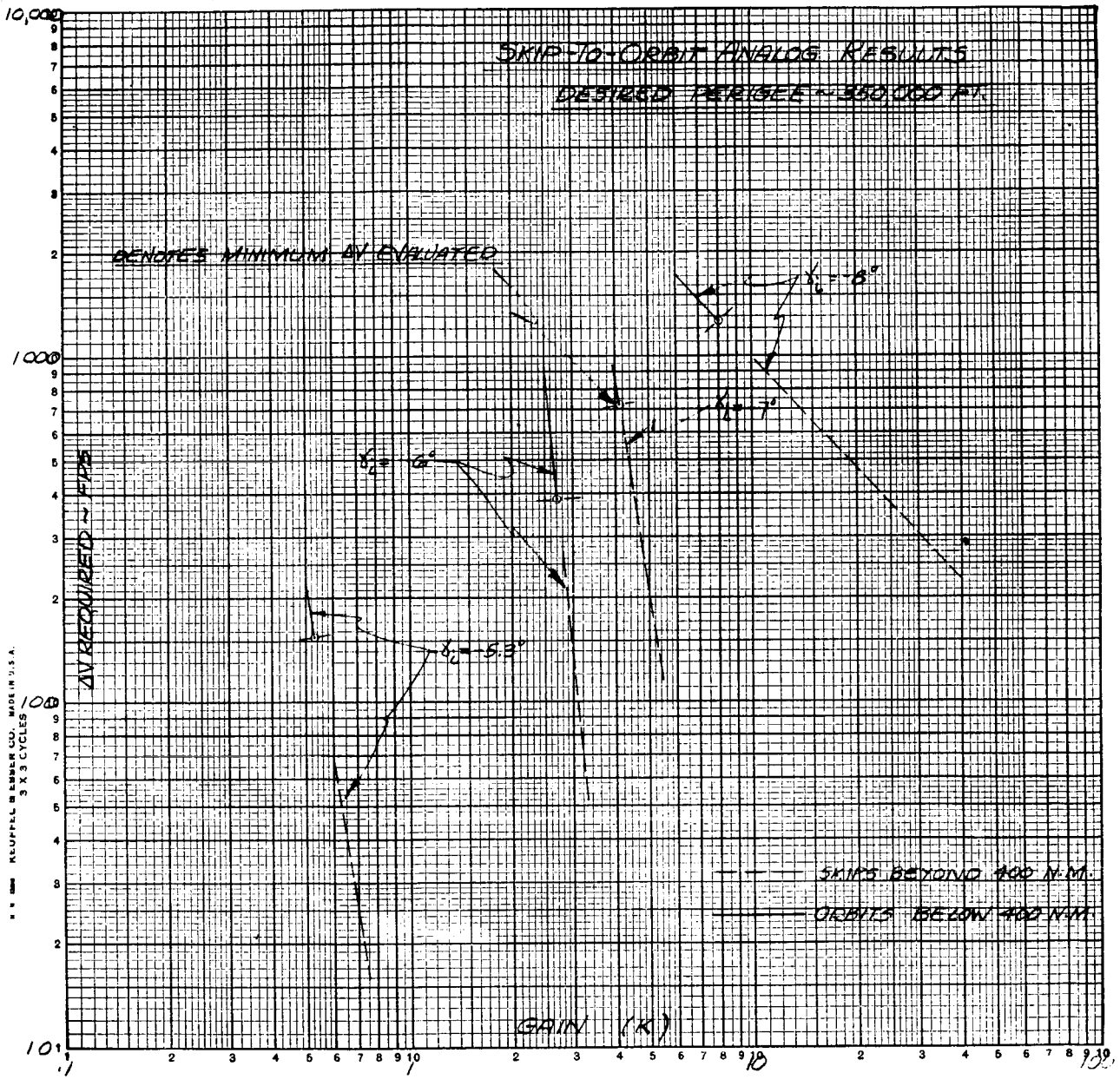

Fig. III-65. ΔV Versus Gain (K) p_d = 350,000 Feet

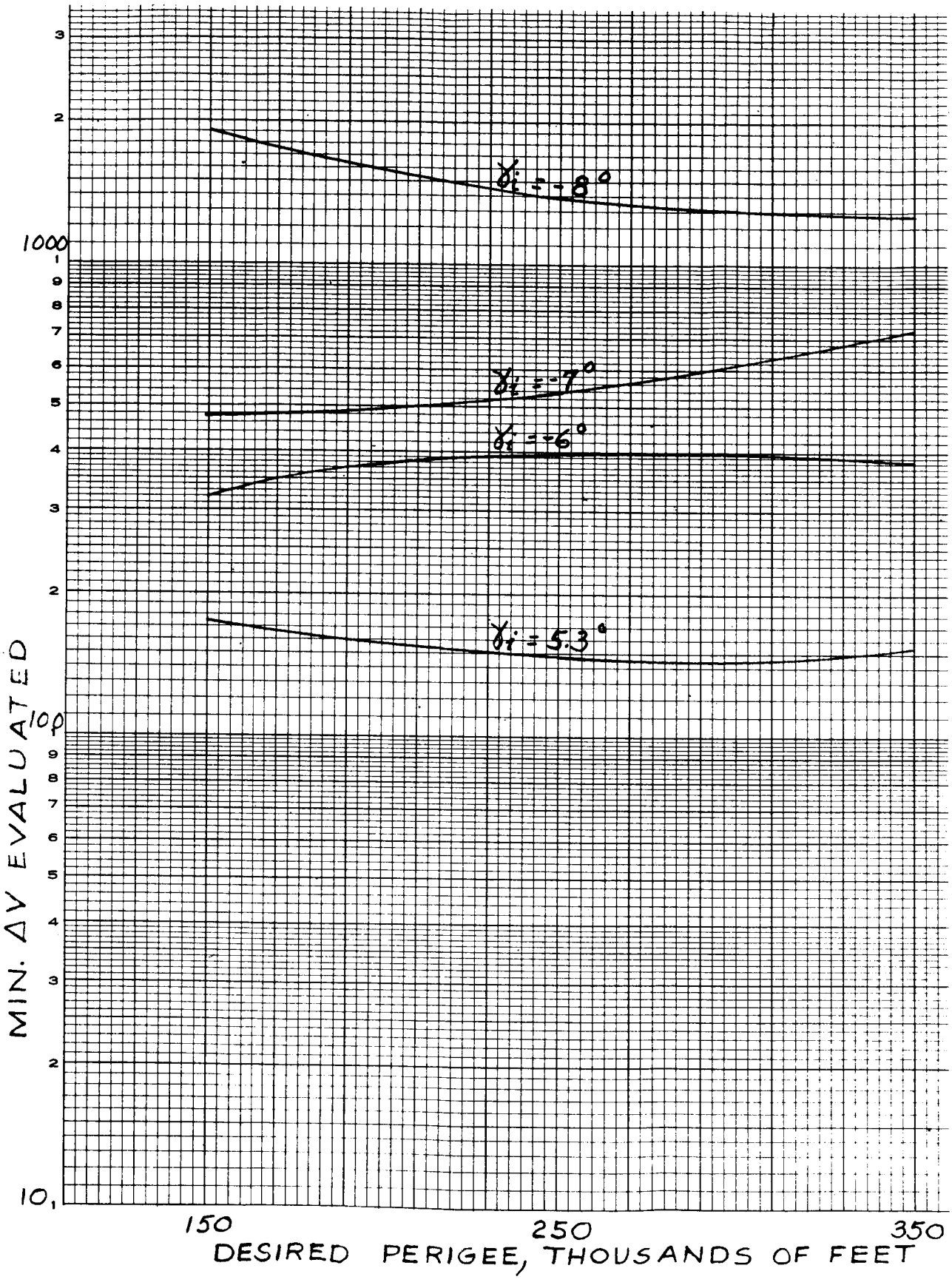

Fig. III-66. Skip to Orbit Analog Results

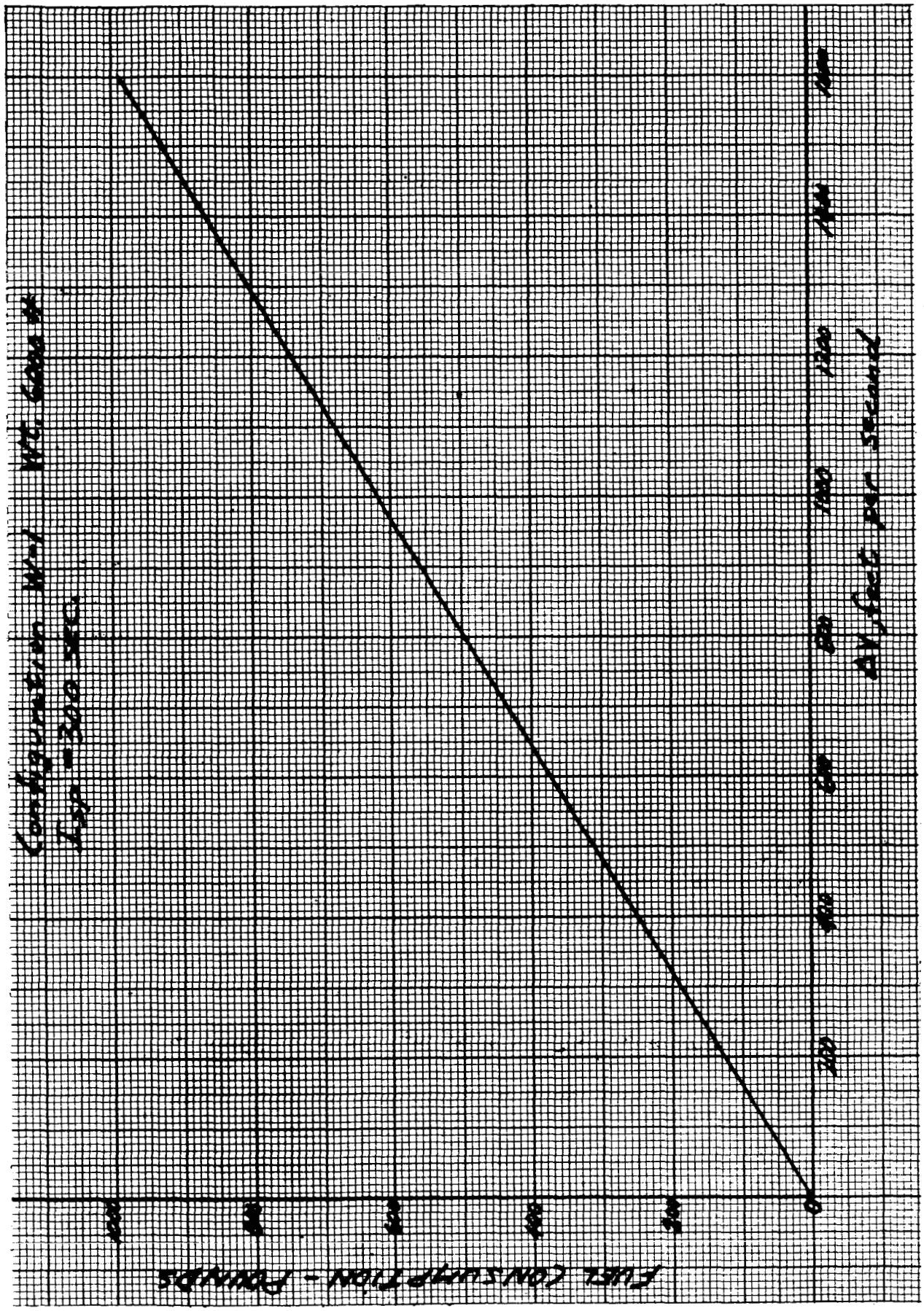

Fig. III-67. ΔV Versus Fuel Consumption (I_{sp} = 300 seconds)

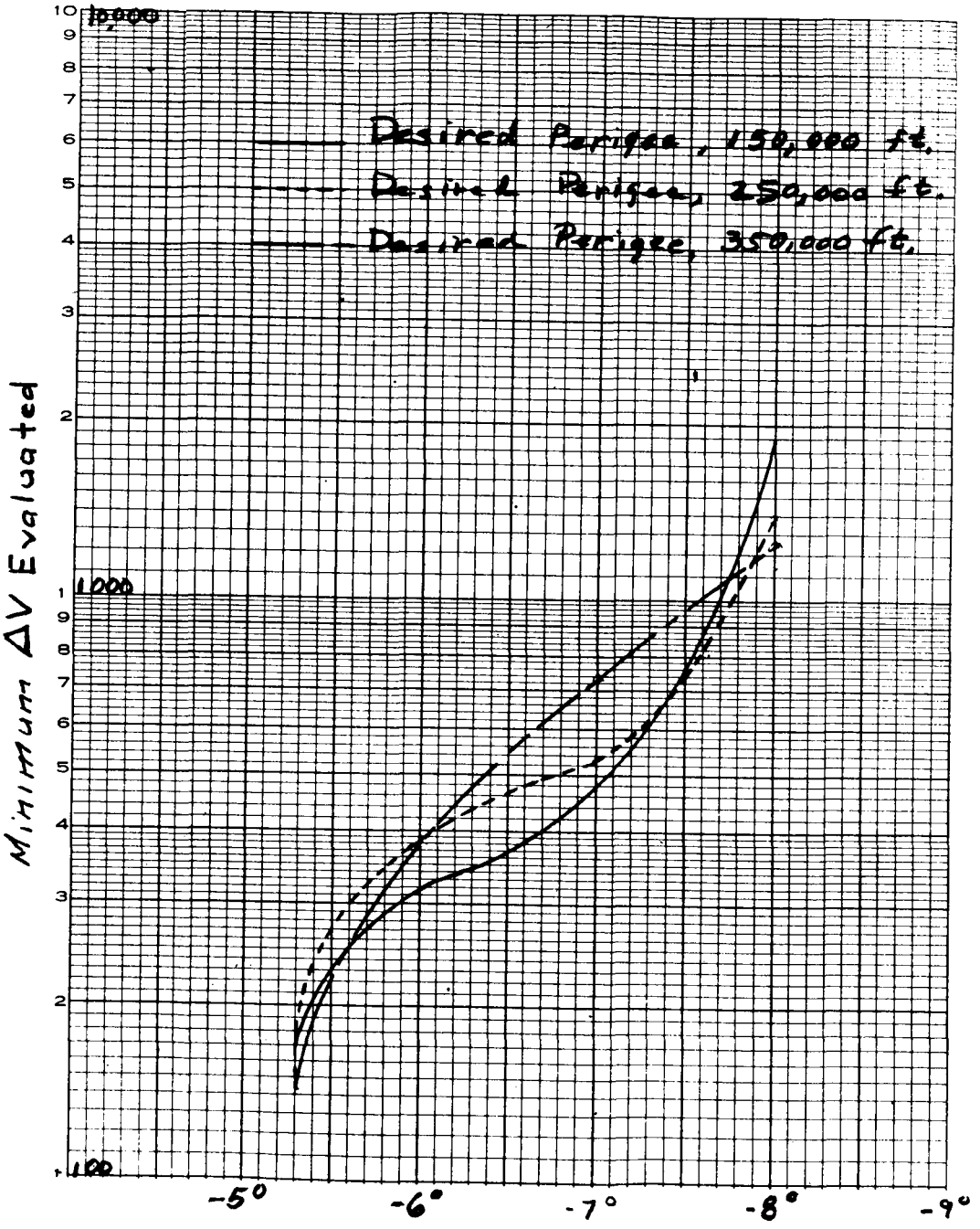

Fig. III-68. ΔV Versus Initial Conditions

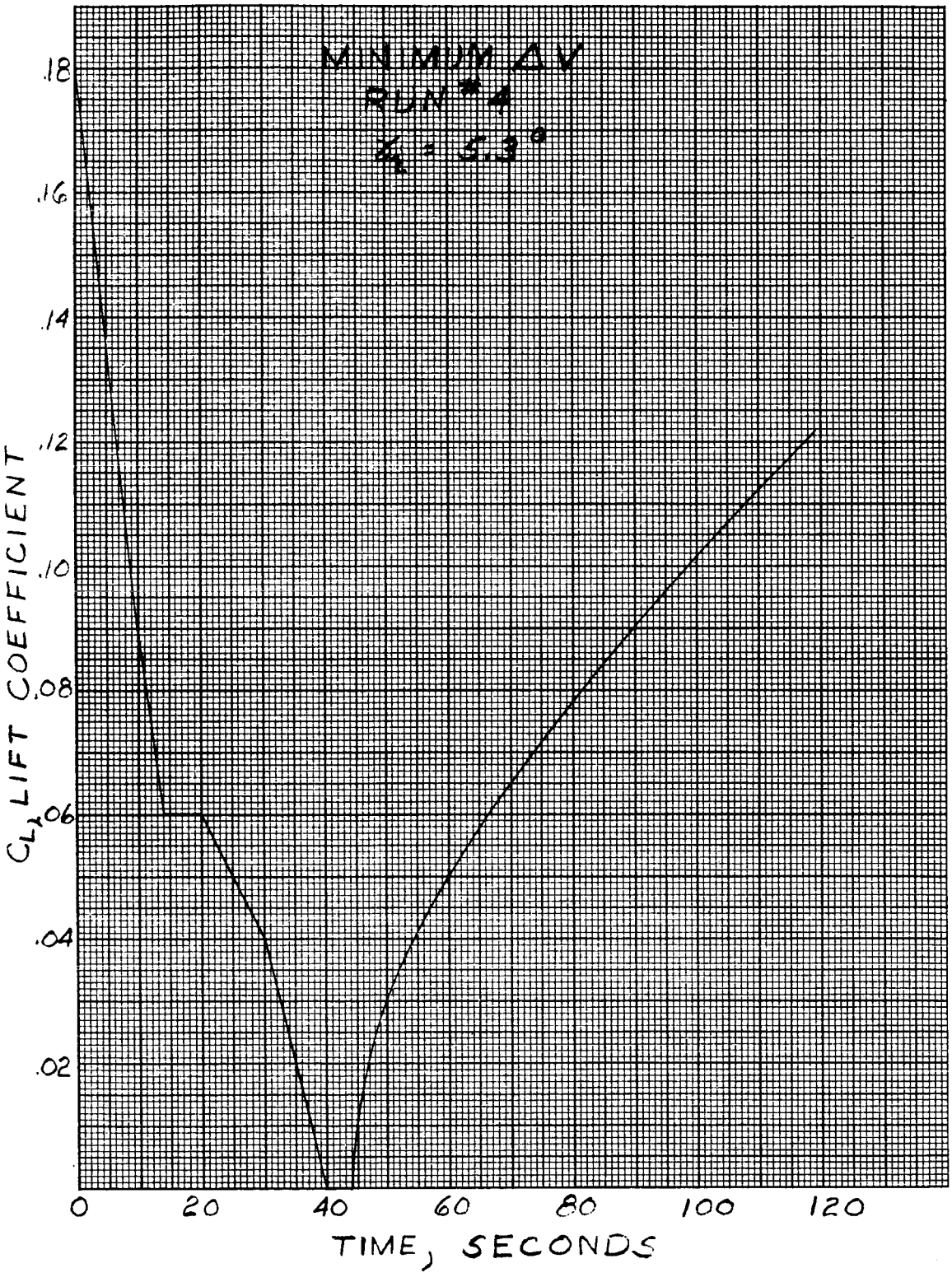

Fig. III-69. C_L Versus Time

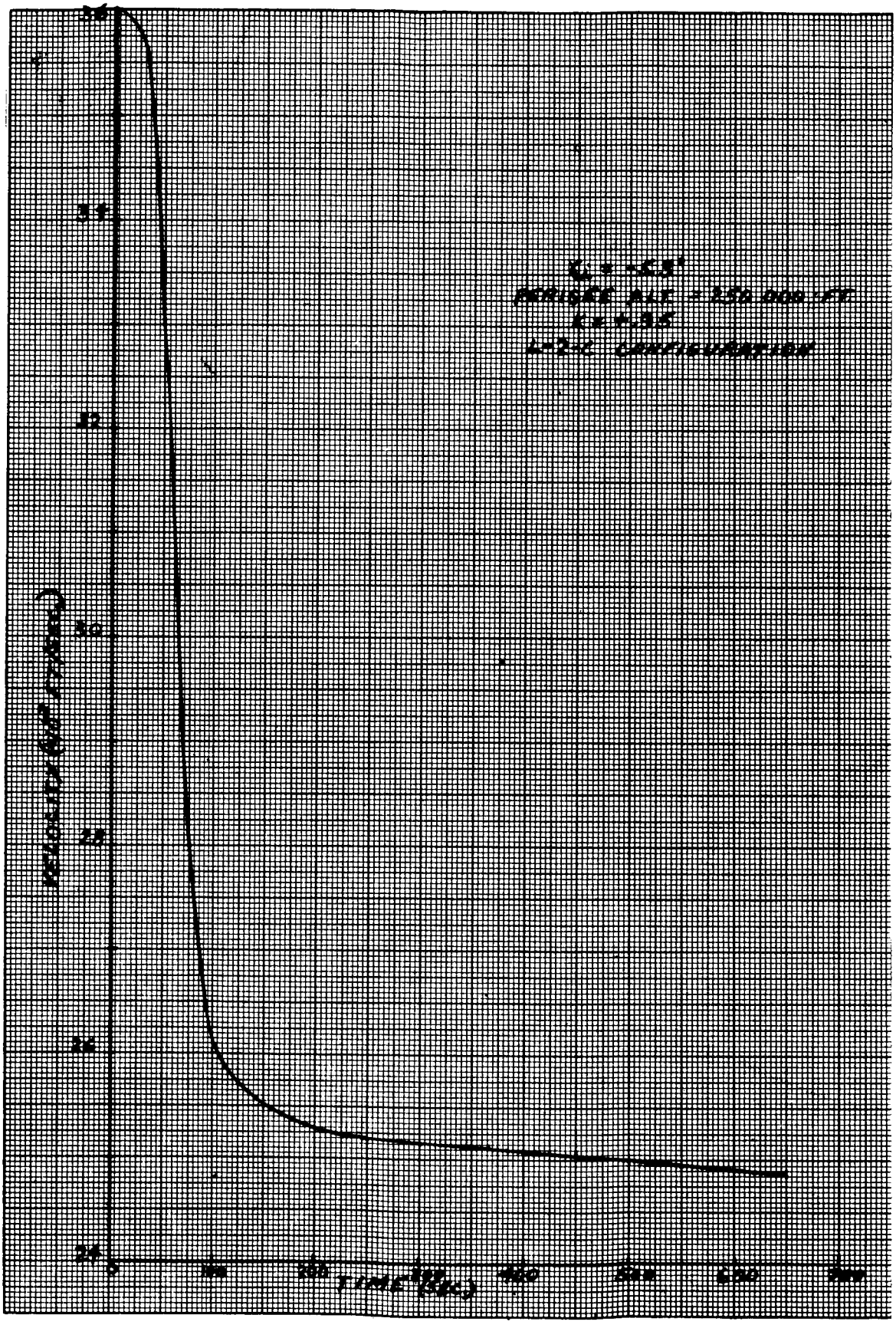

Fig. III-70. Velocity Versus Time (γ_i = -5.3 degrees, p_d = 250,000 feet)

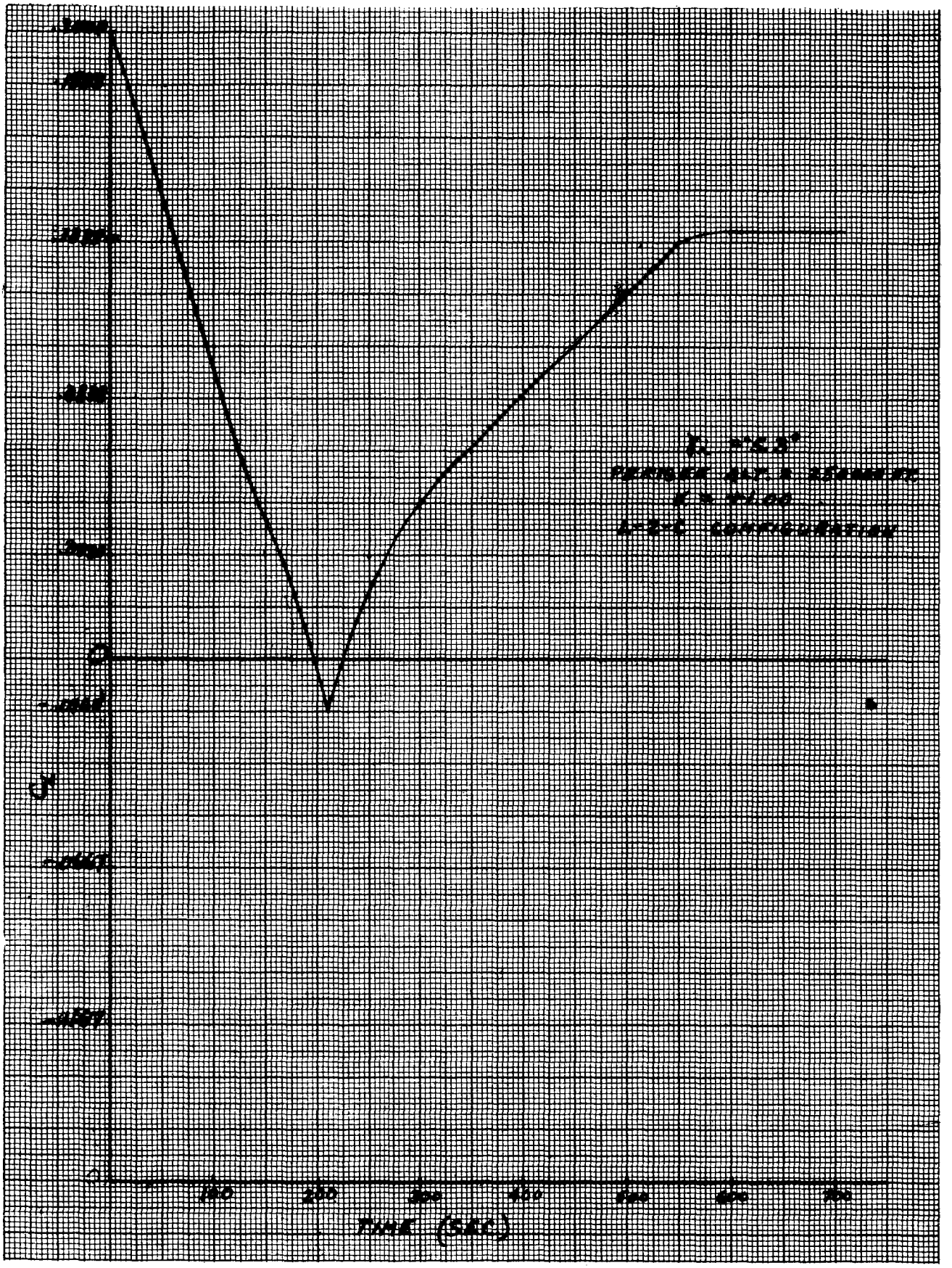

Fig. III-71. C_L Versus Time (γ_i = -5.3 degrees, p_d = 250,000 feet)

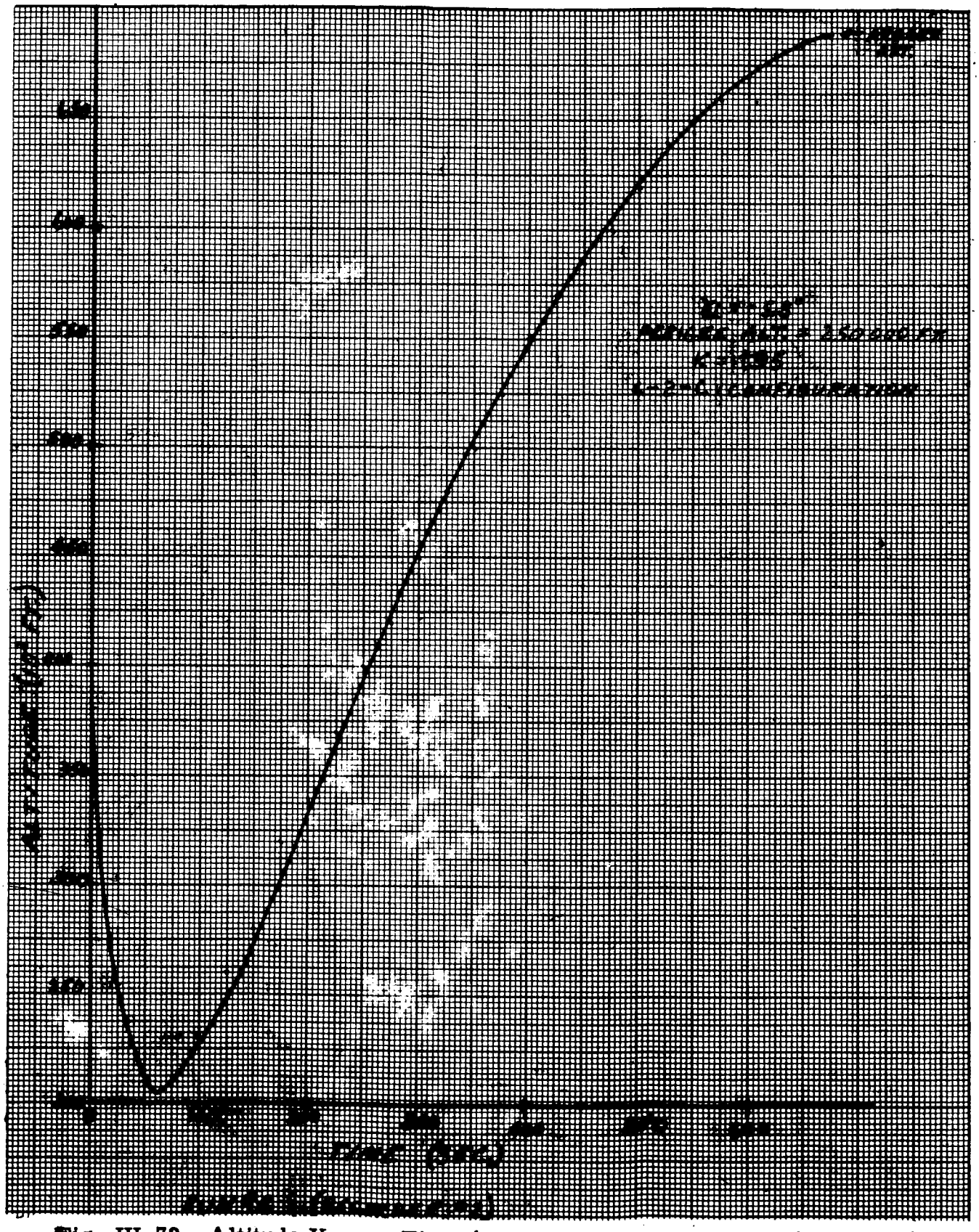

Fig. III-72. Altitude Versus Time (γ_i = -5.3 degrees, p_d = 250,000 feet)

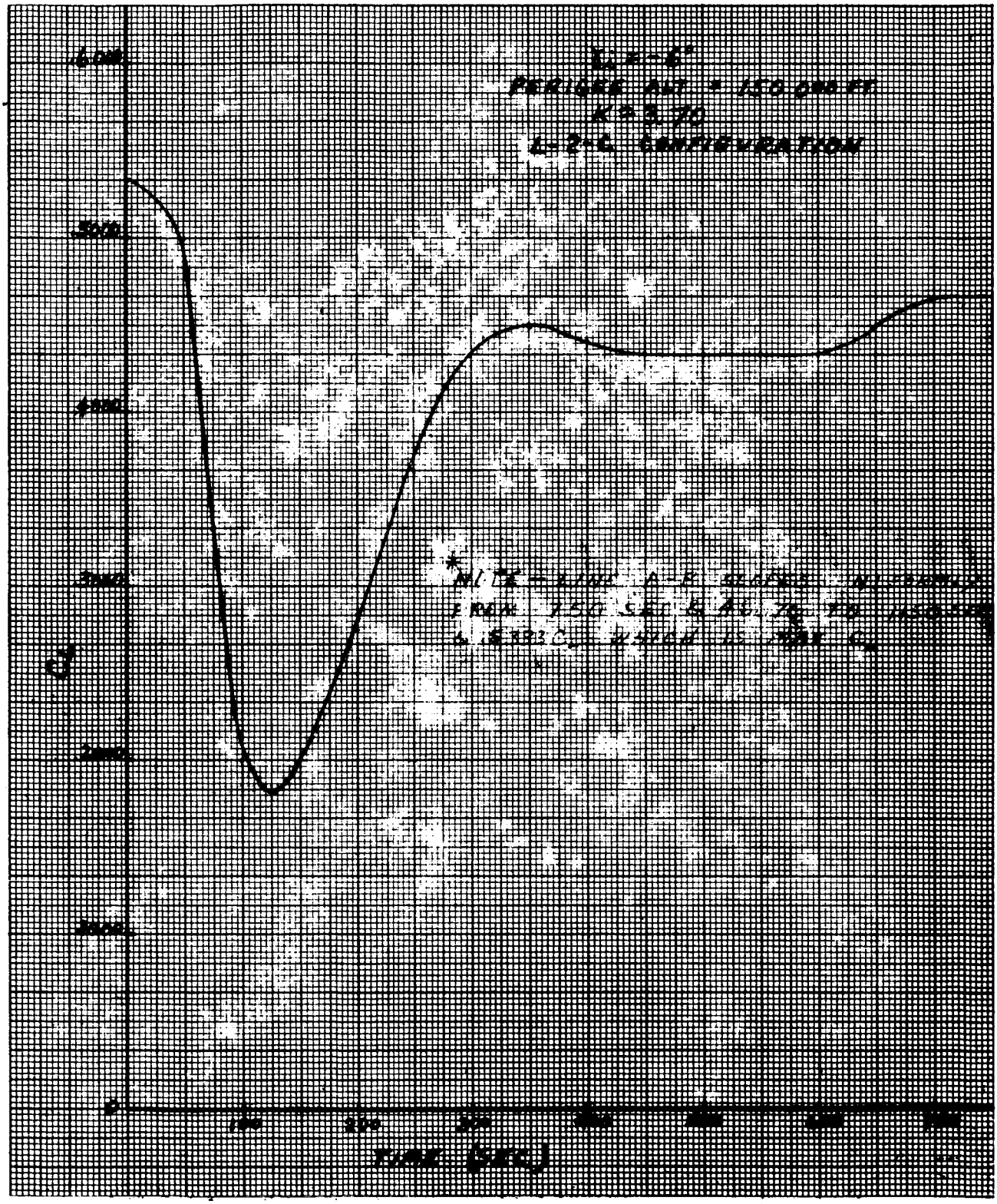

Fig. III-73. C_L Versus Time (γ_i = -6 degrees, p_d = 150,000 feet)

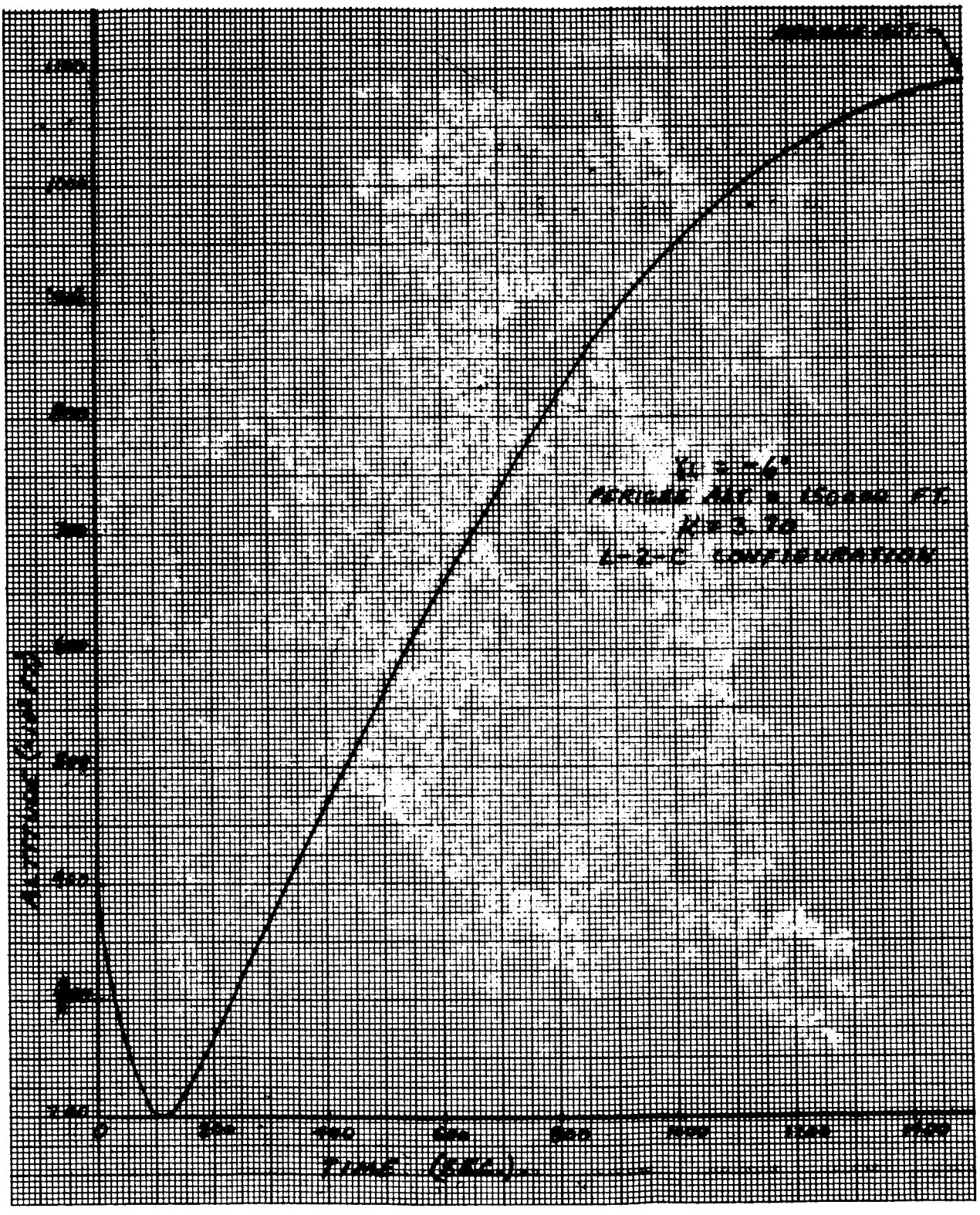

Fig. III-74. Altitude Versus Time (γ_i = -6 degrees, p_d = 150,000 feet)

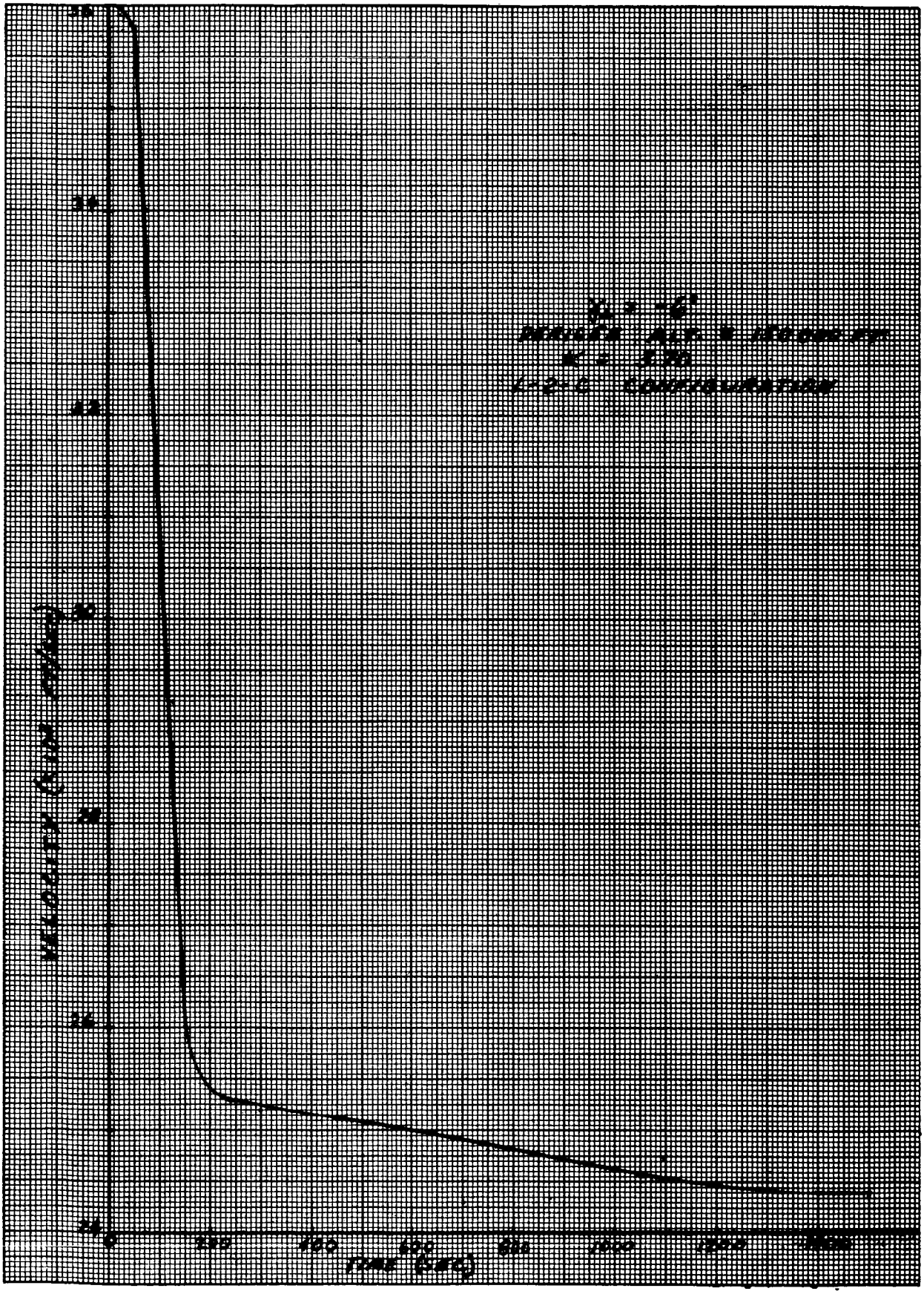

Fig. III-75. Velocity Versus Time (γ_i = -6 degrees, p_d = 150,000 feet)

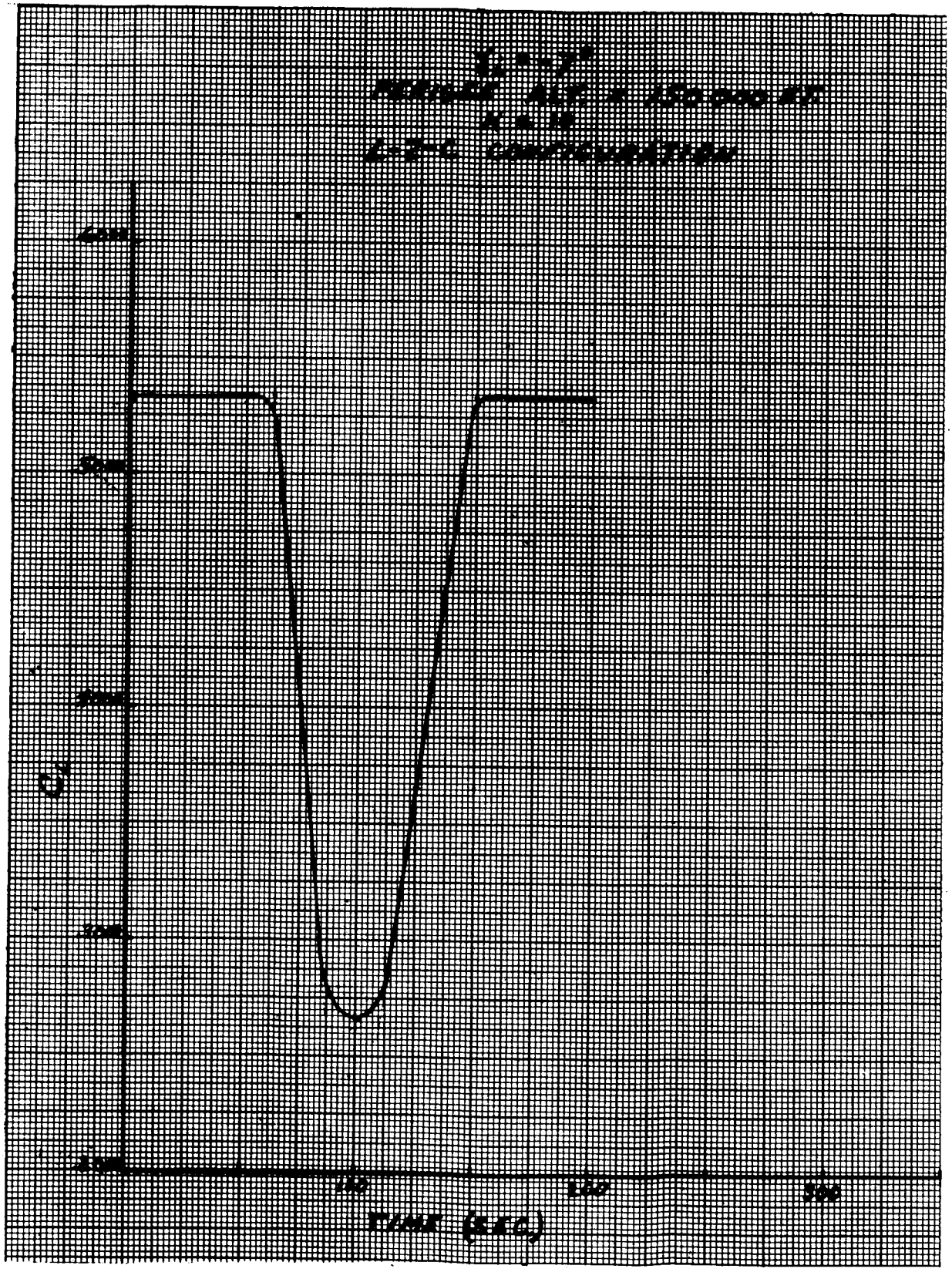

Fig. III-76. C_L Versus Time (γ_i = -7 degrees, p_d = 150,000 feet)

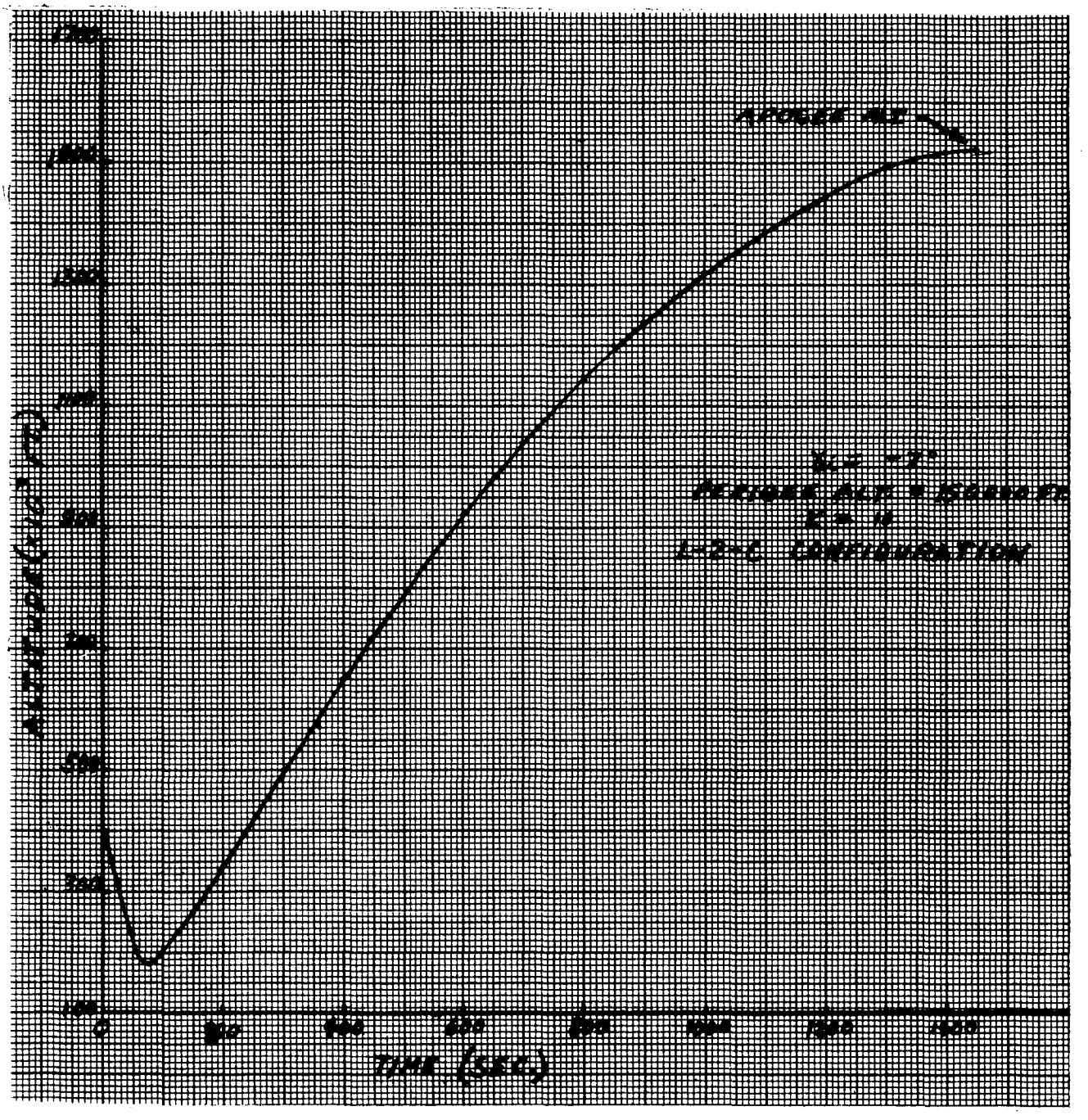

Fig. III-77. Altitude Versus Time (γ_i = -7 degrees, p_d = 150,000 feet)

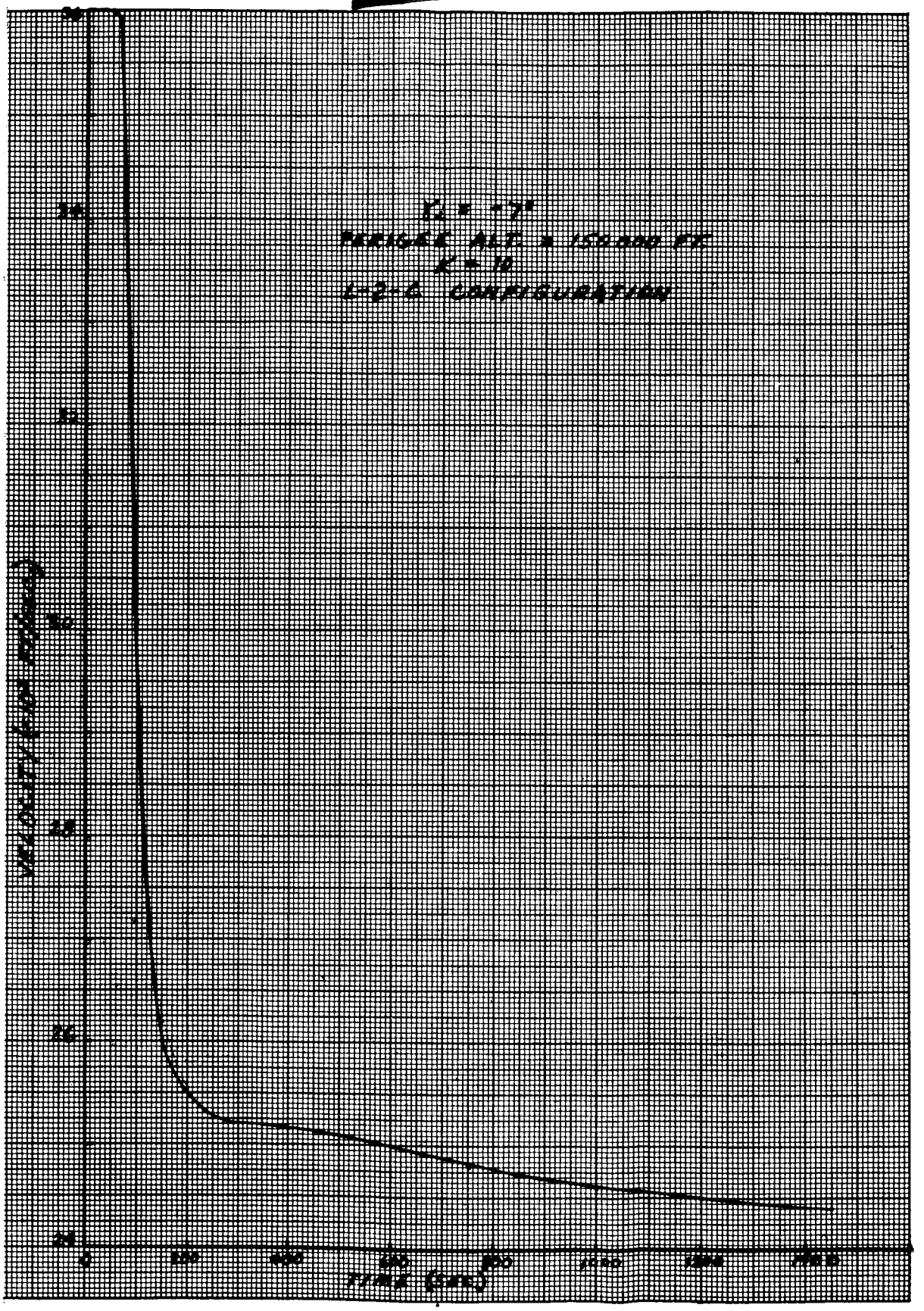

Fig. III-78. Velocity Versus Time (γ_i = -7 degrees, p_d = 150,000 feet)

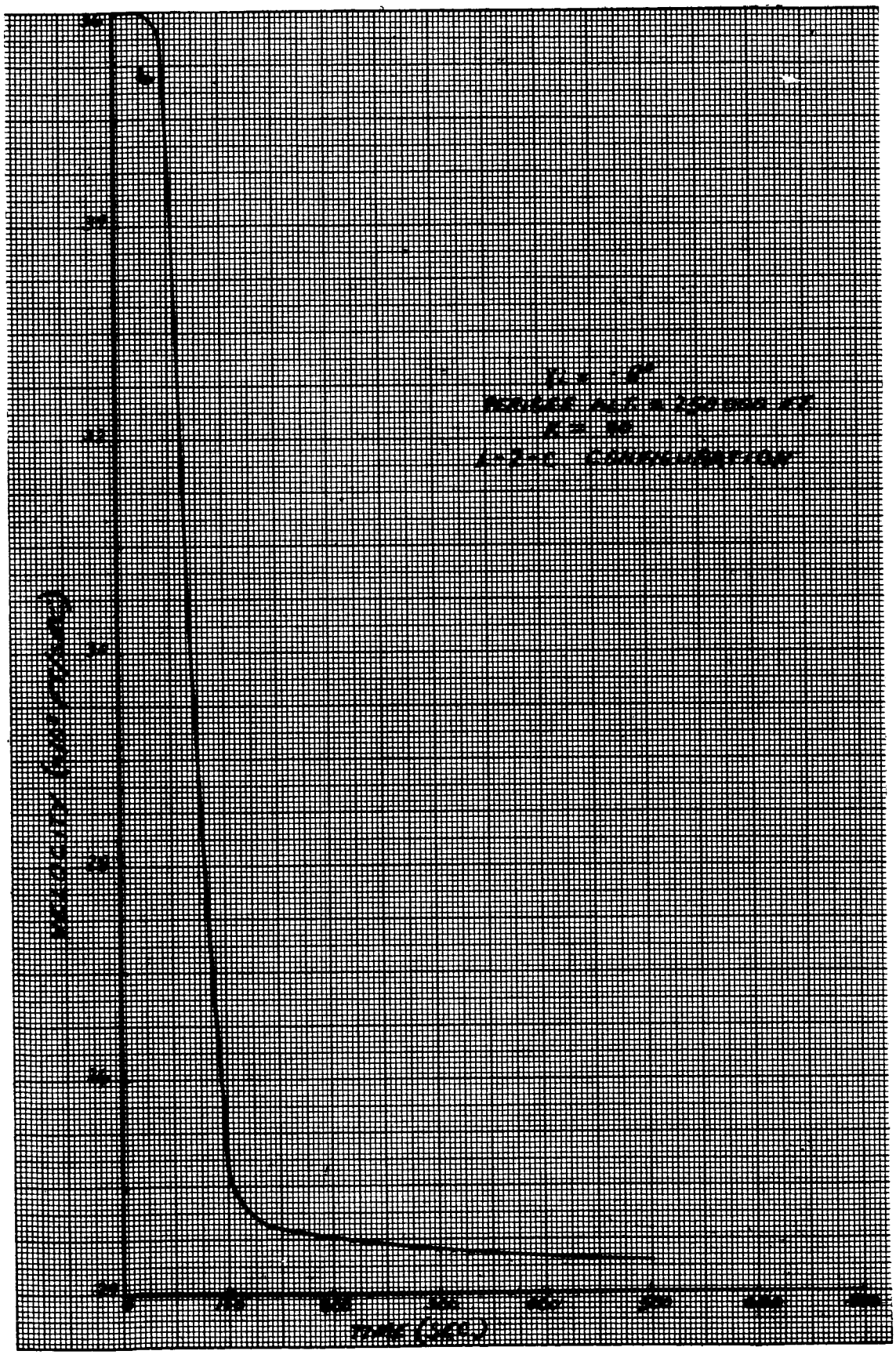

Fig. III-79. Velocity Versus Time (γ_i = -8 degrees, p_d = 250,000 feet)

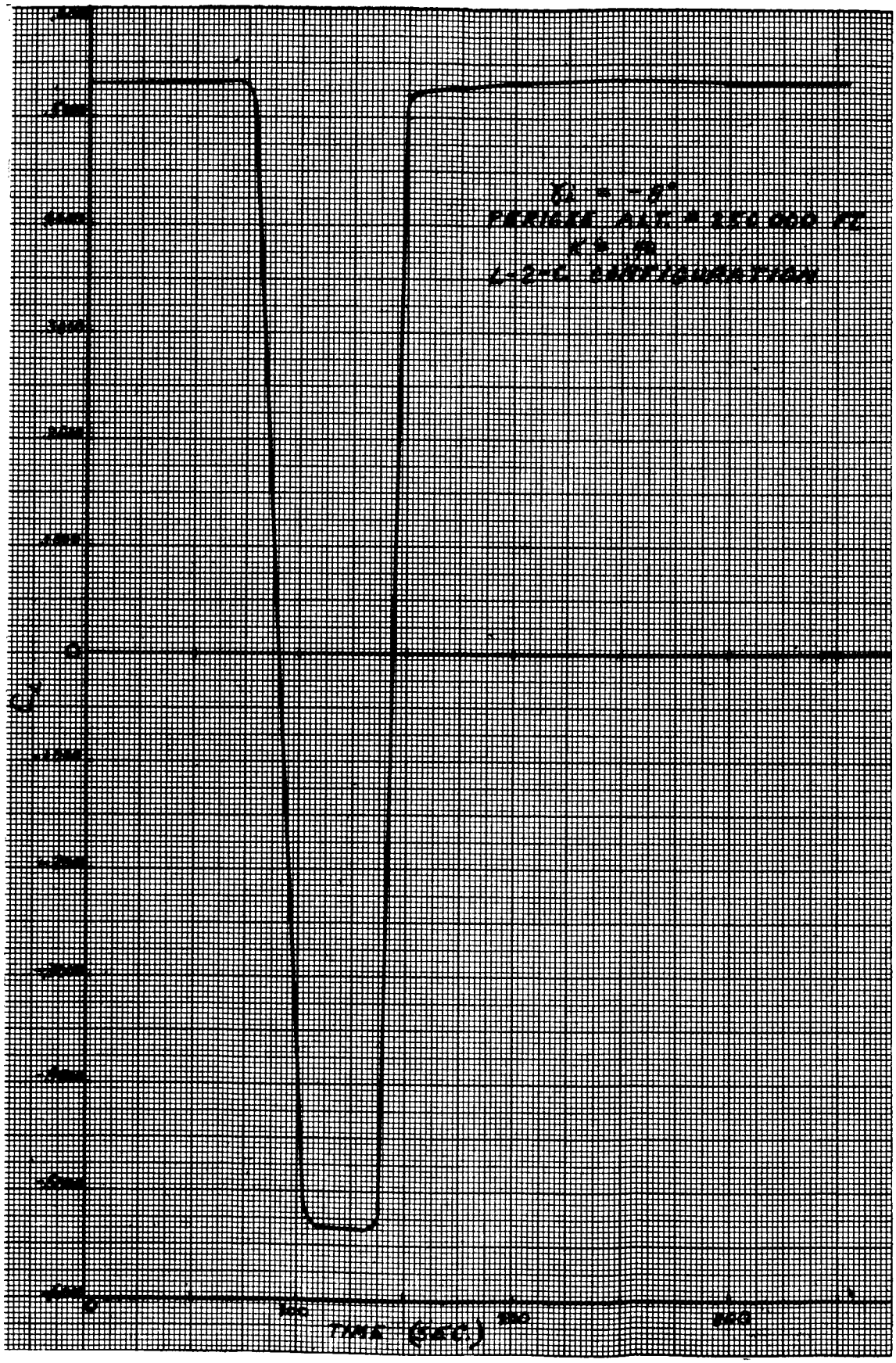

Fig. III-80. C_L Versus Time (γ_i = -8 degrees, p_d = 250,000 feet)

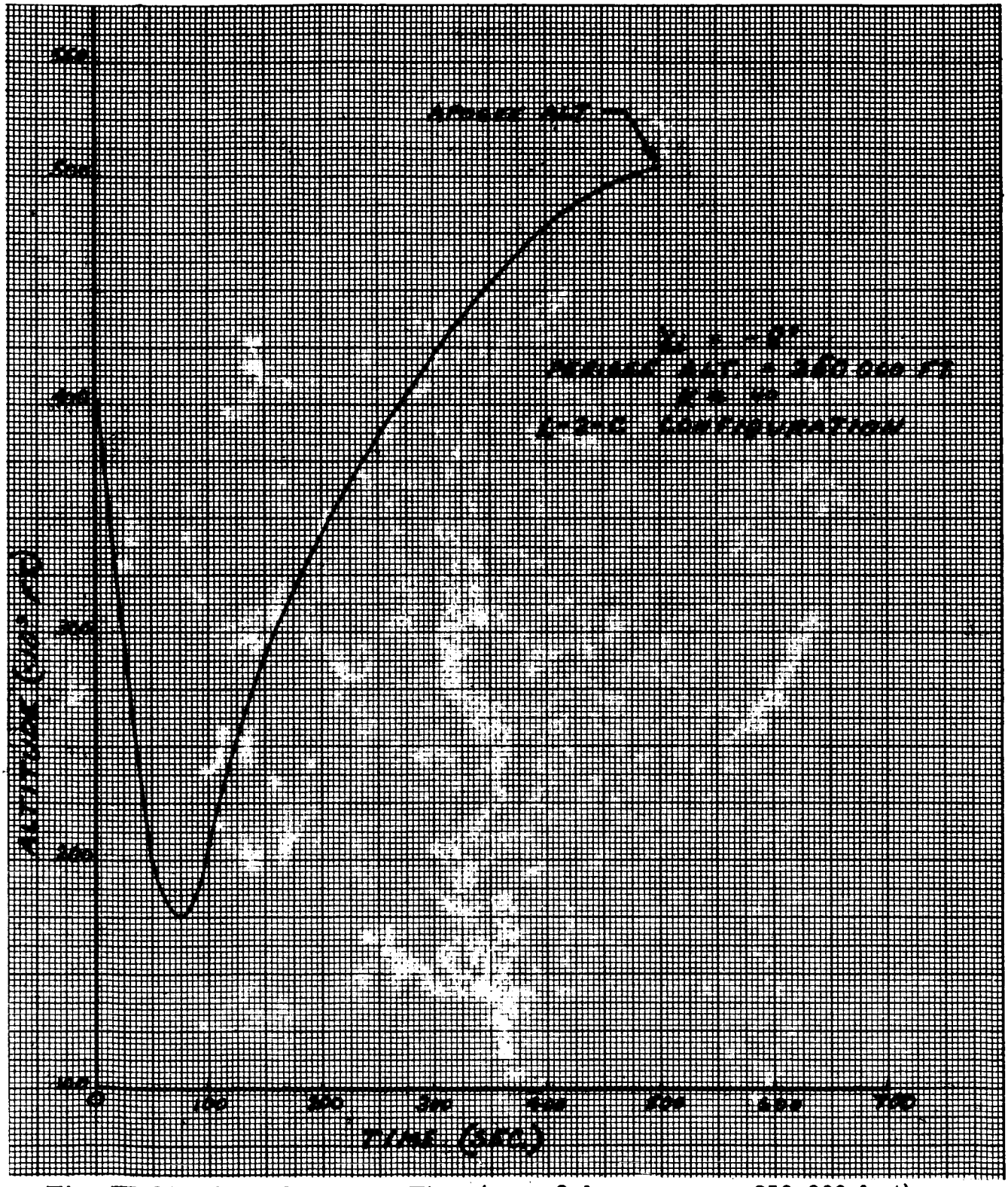

Fig. III-81. Altitude Versus Time (γ_i = -8 degrees, p_d = 250,000 feet)

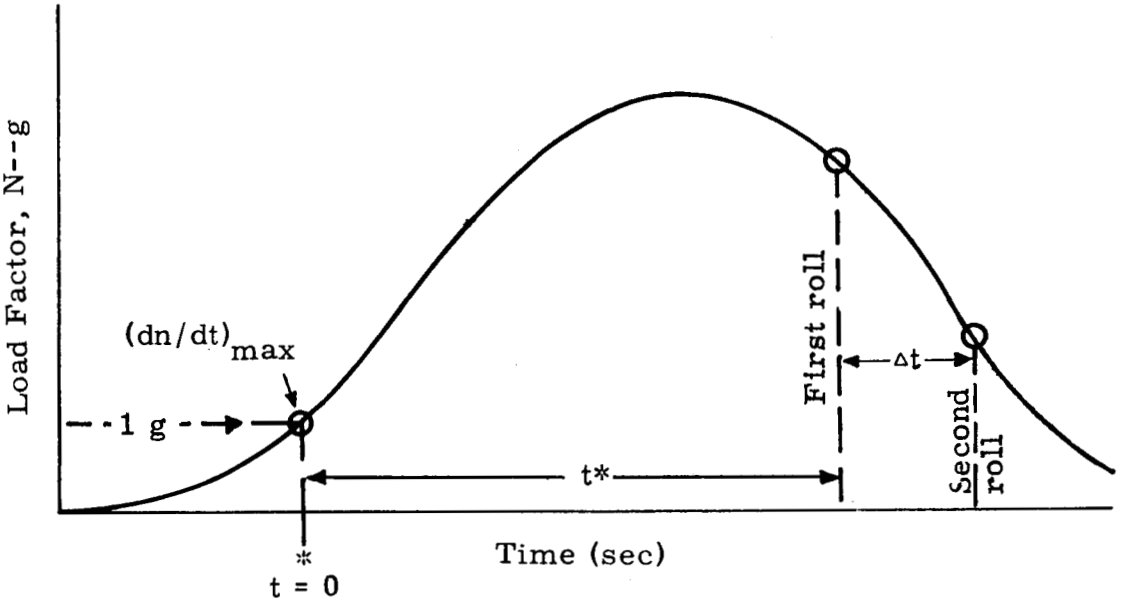

Fig. III-82. Typical Re-entry Load Profile

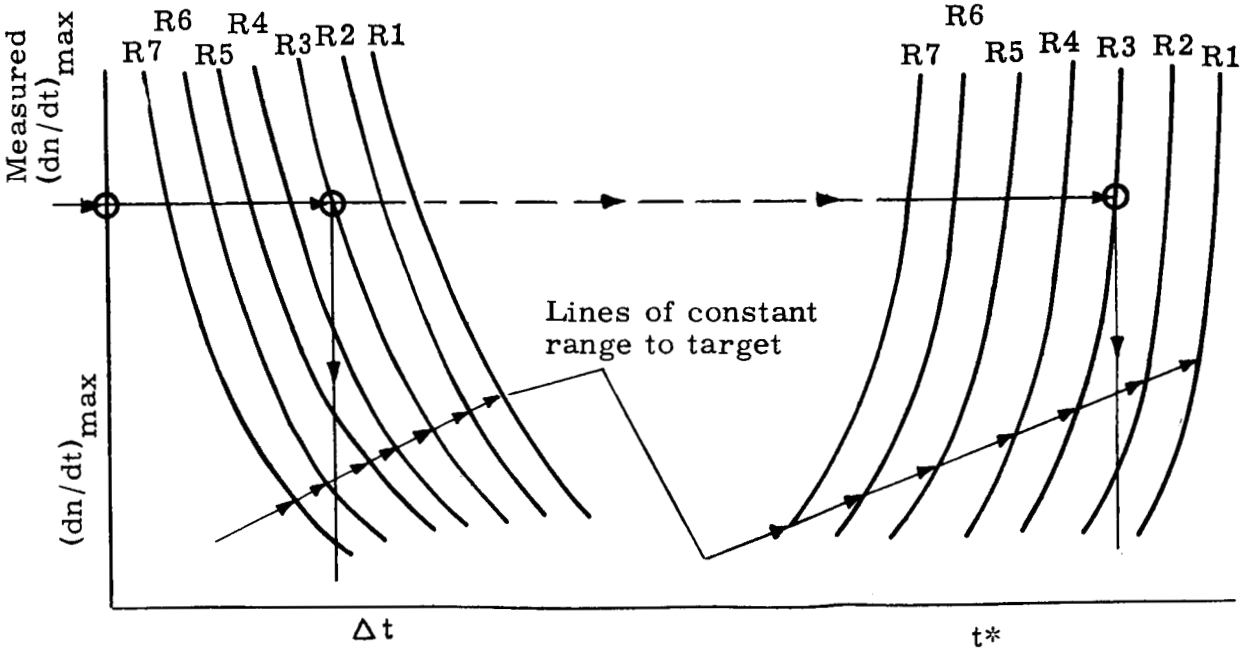

Fig. III-83. t and t* Versus $(dn/dt)_{max}$ for Constant Range

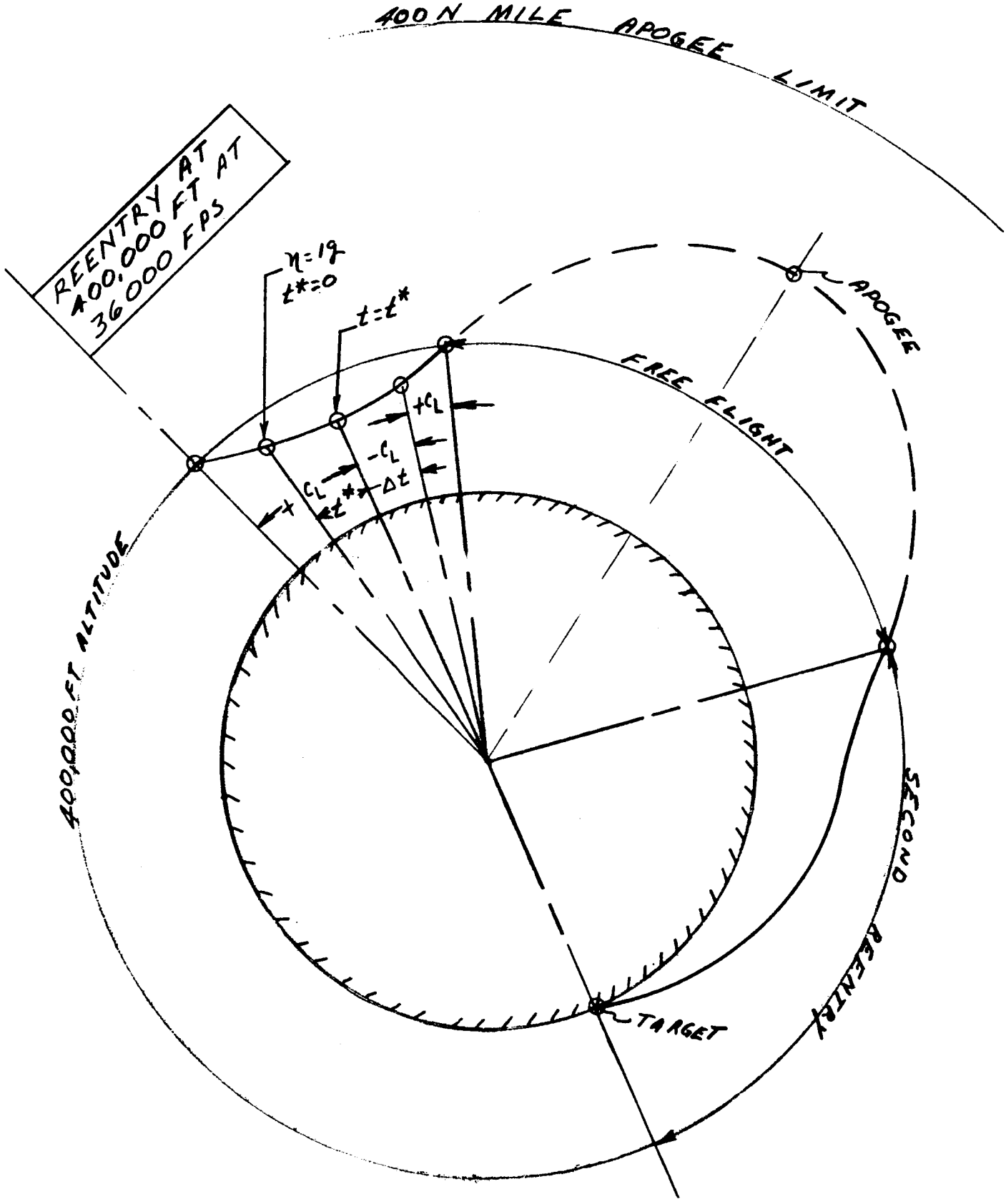

Fig. III-84. Typical Re-entry Flight Trajectory

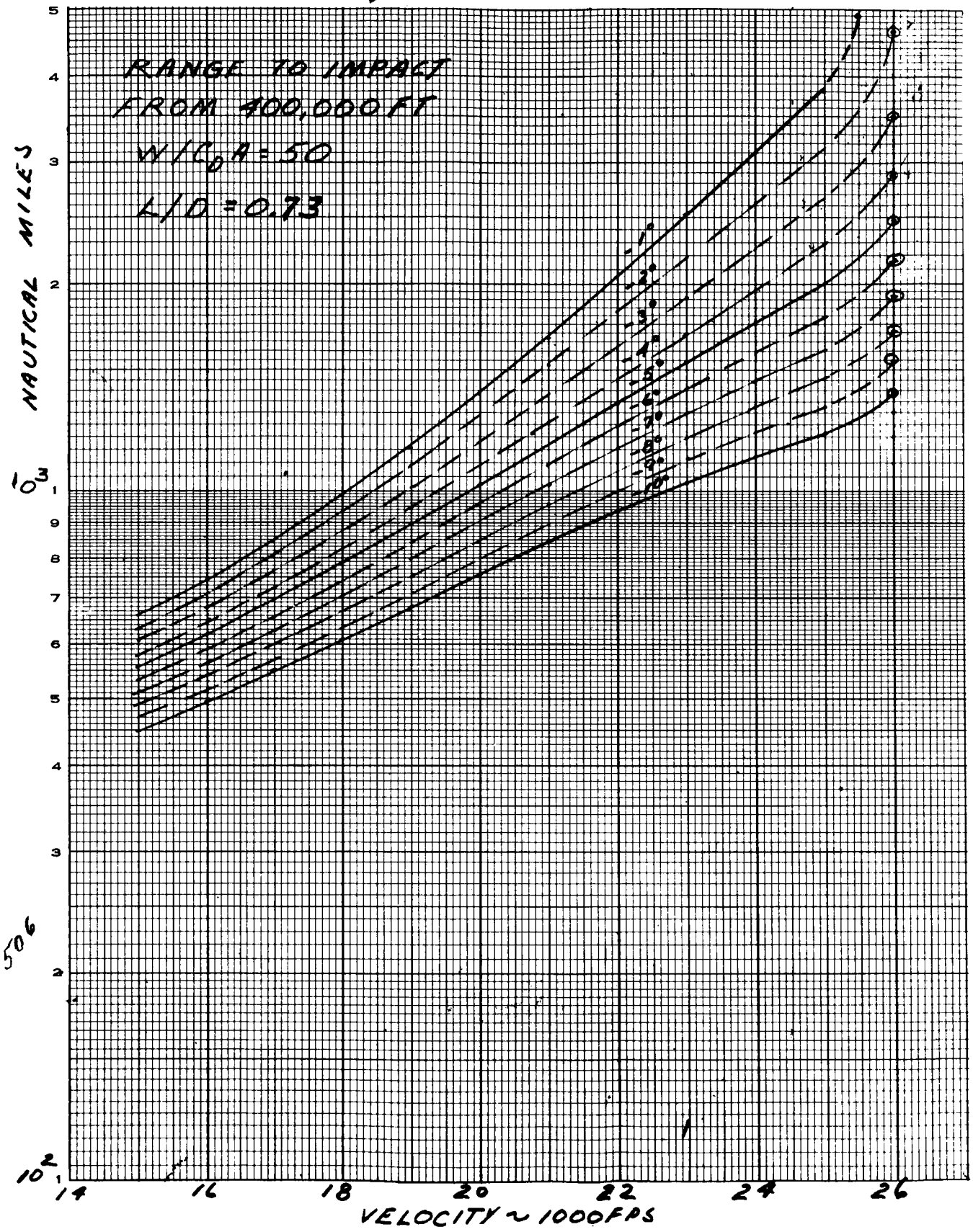

Fig. III-85. Longitudinal Range as a Function of Initial Velocity

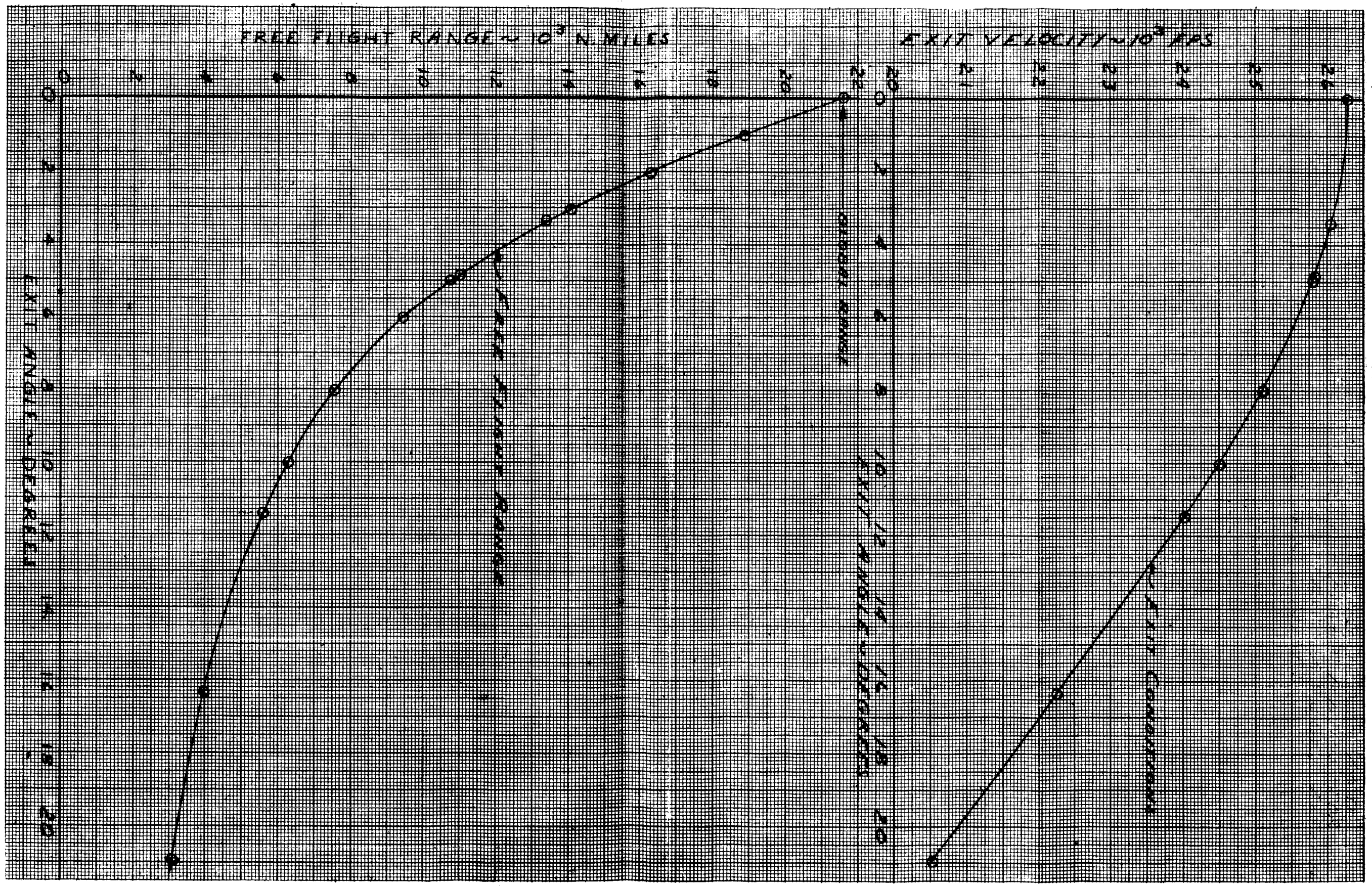

Fig. III-86. Exit Conditions and Free Flight Range for a Constant Apogee Altitude of 400 Nautical Miles

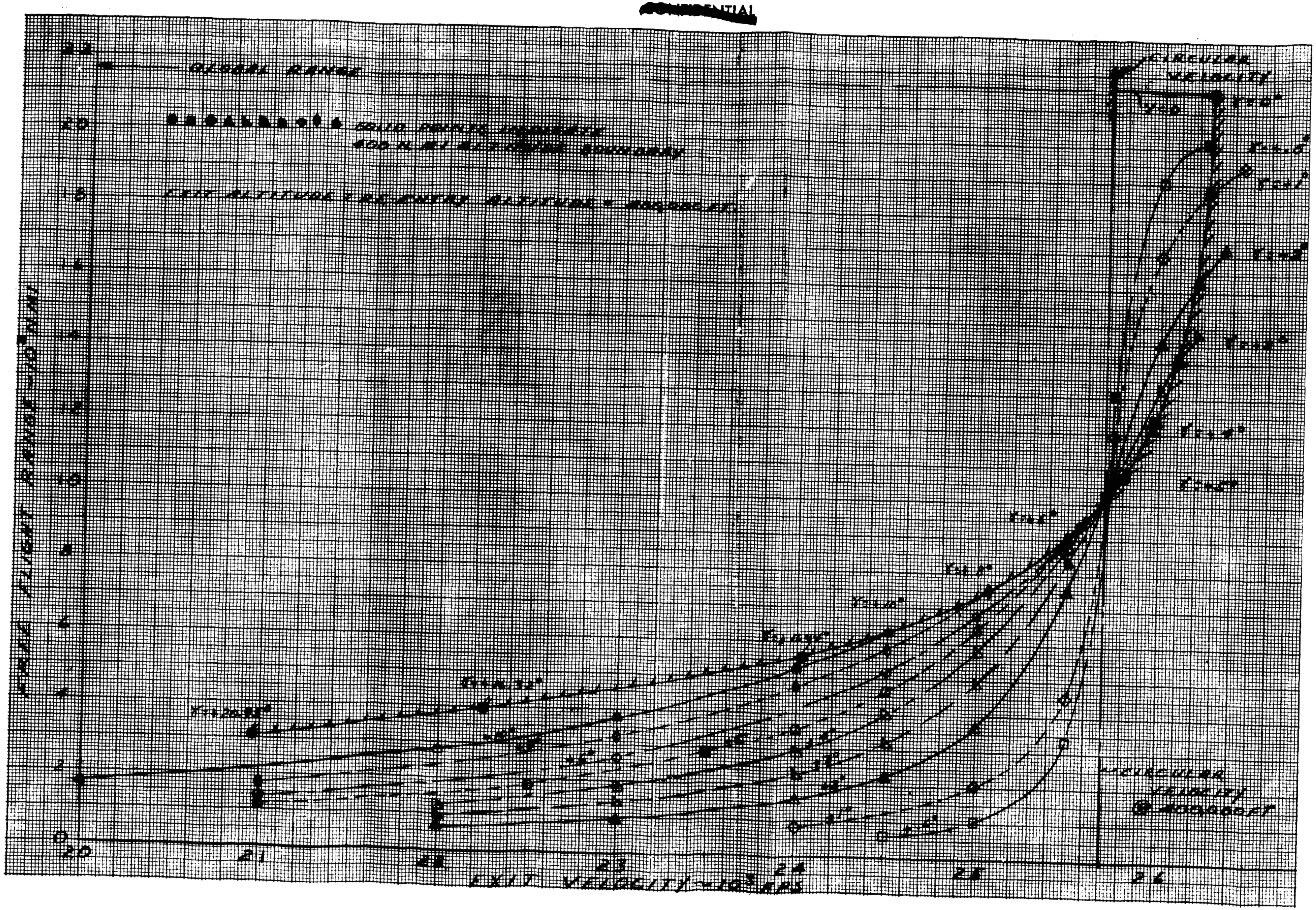

Fig. III-87. Variation of Free Flight Range with Exit Velocity and Gamma

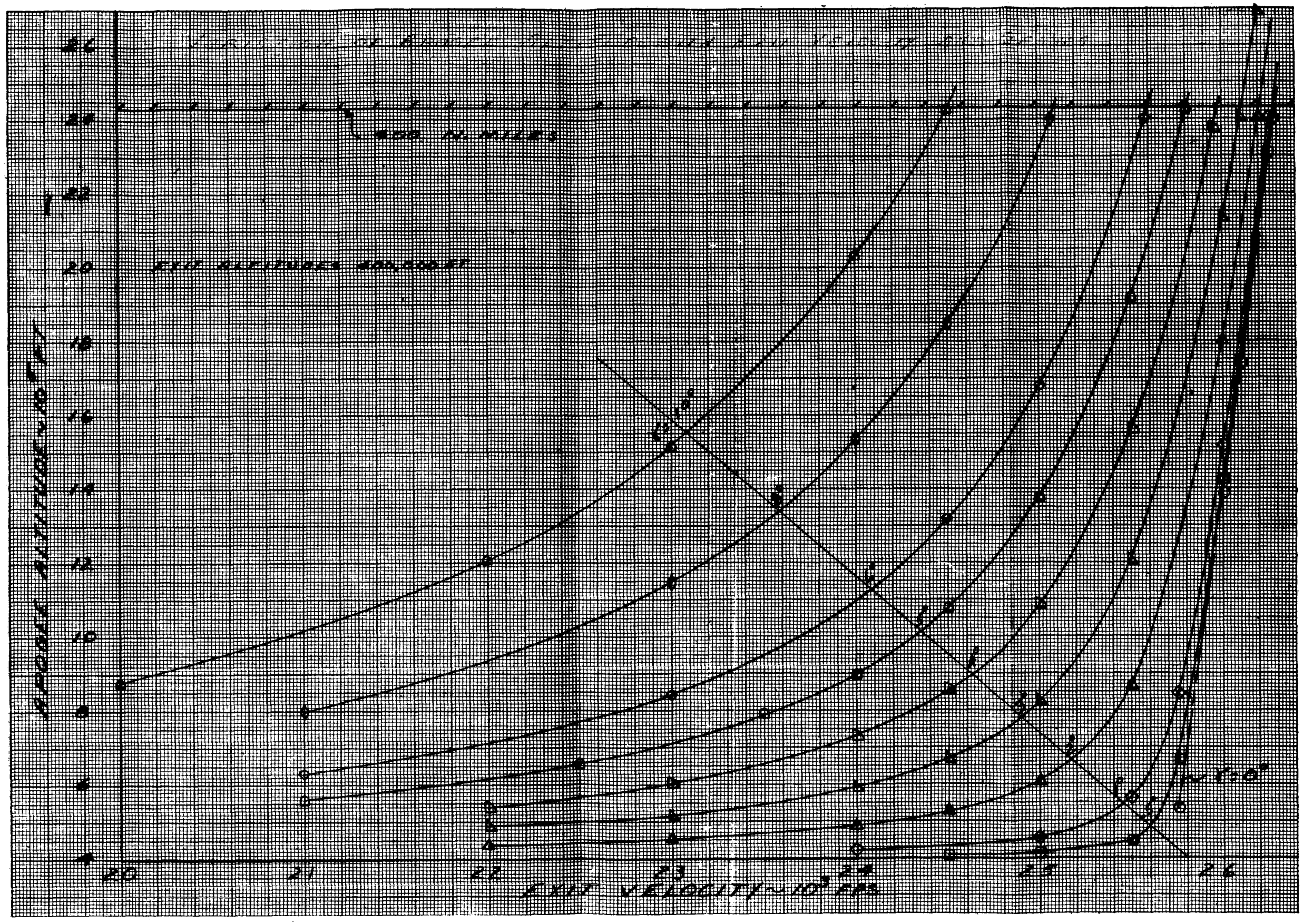

Fig. III-88. Variation of Apogee Altitude with Exit Velocity and Gamma

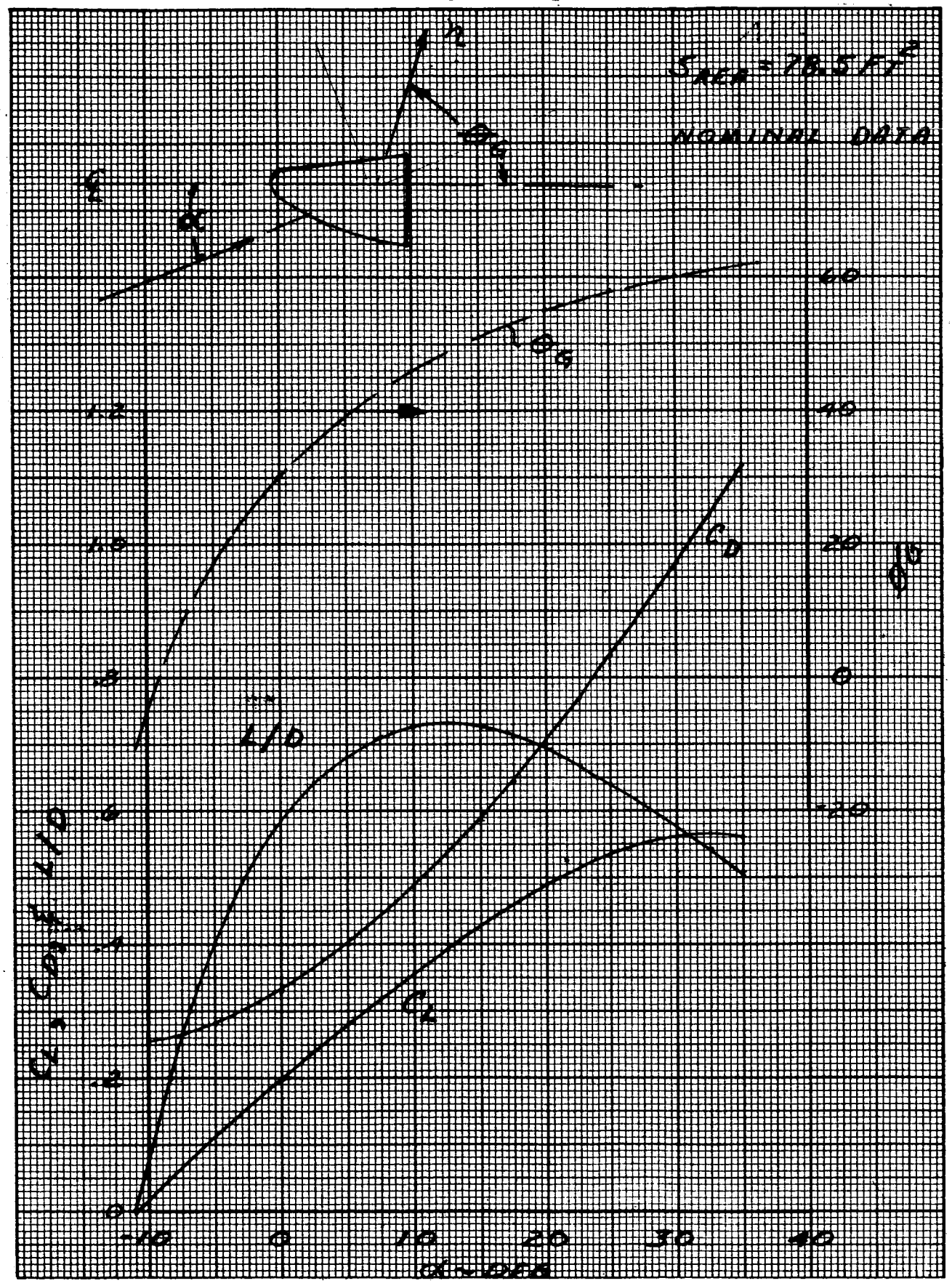

Fig. III-89. Model 410 Aerodynamic Characteristics

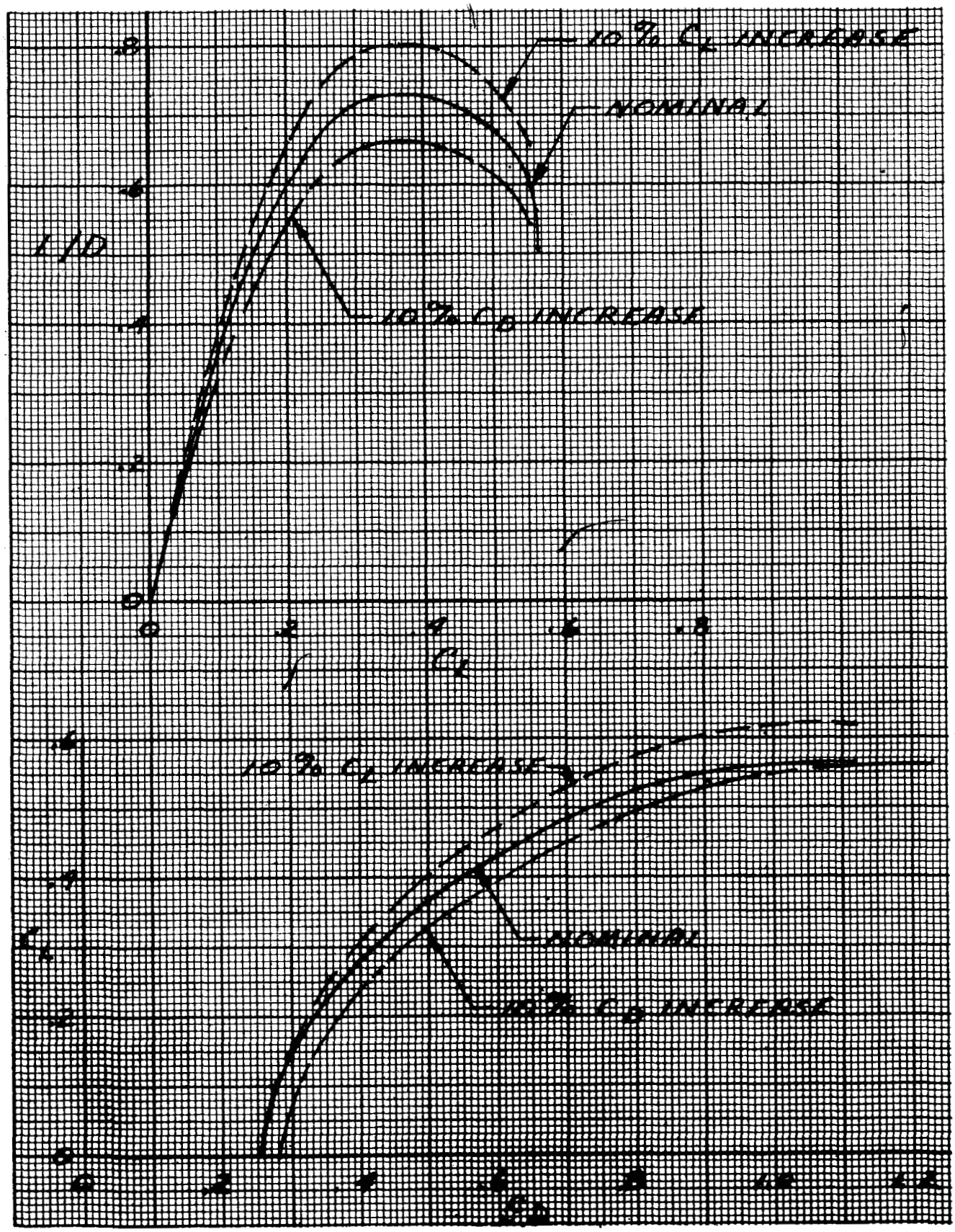

Fig. III-90. Lift and Drag Coefficient Data

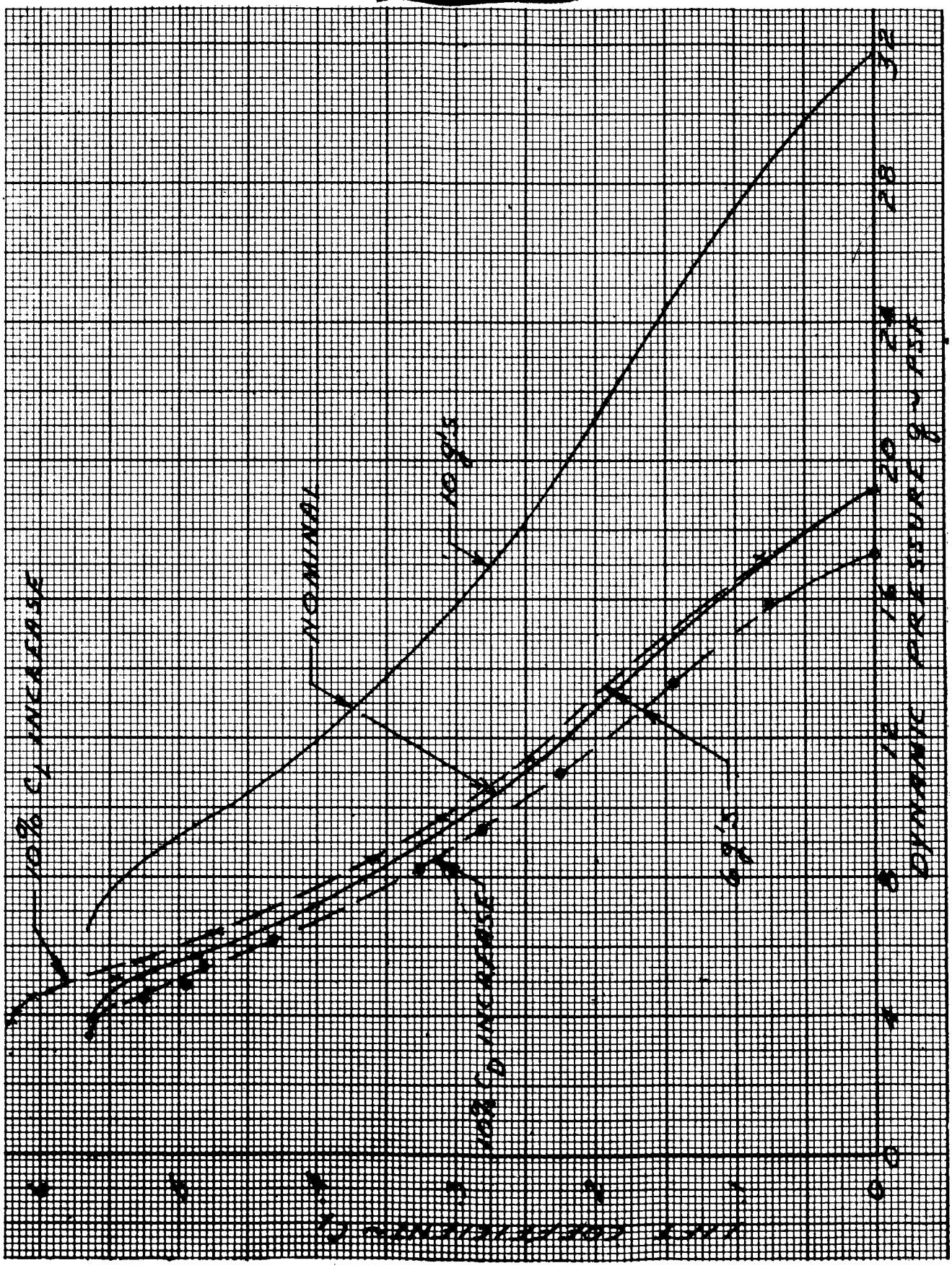

Fig. III-91. Lift Coefficient Versus Dynamic Pressure for 6-g and 10-g Modulation

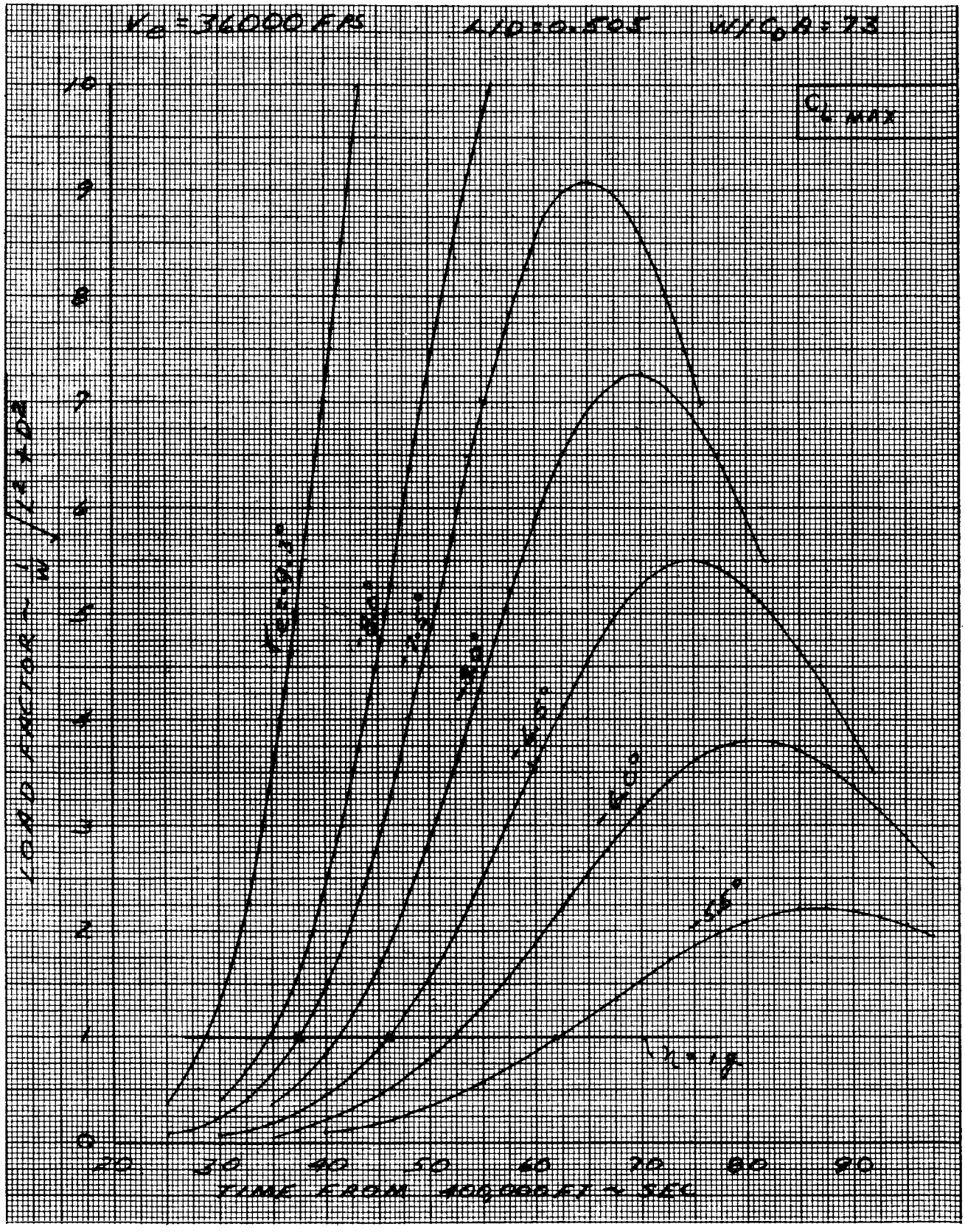

Fig. III-92. Re-entry Load Factor

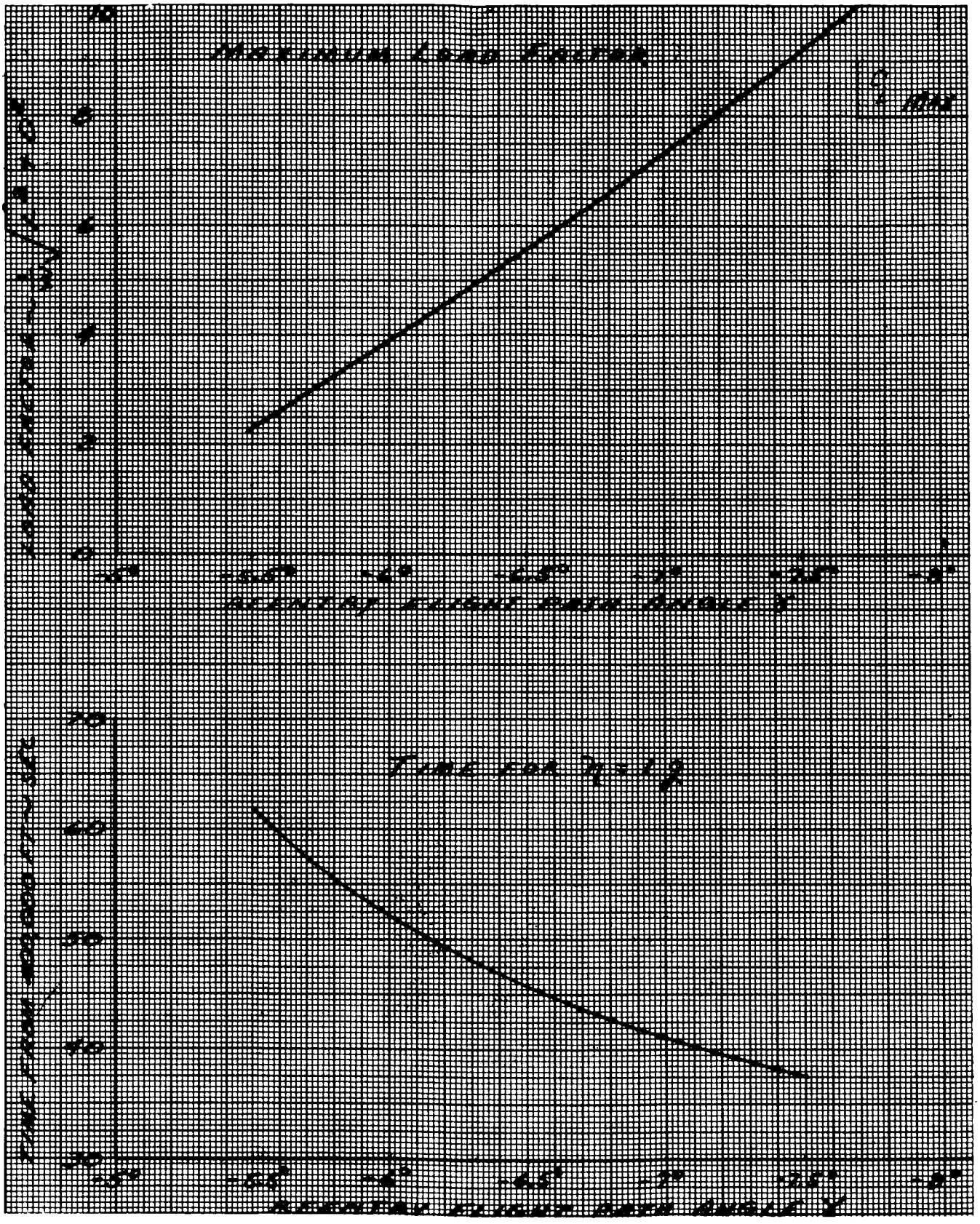

Fig. III-93. Re-entry Load Factor Data

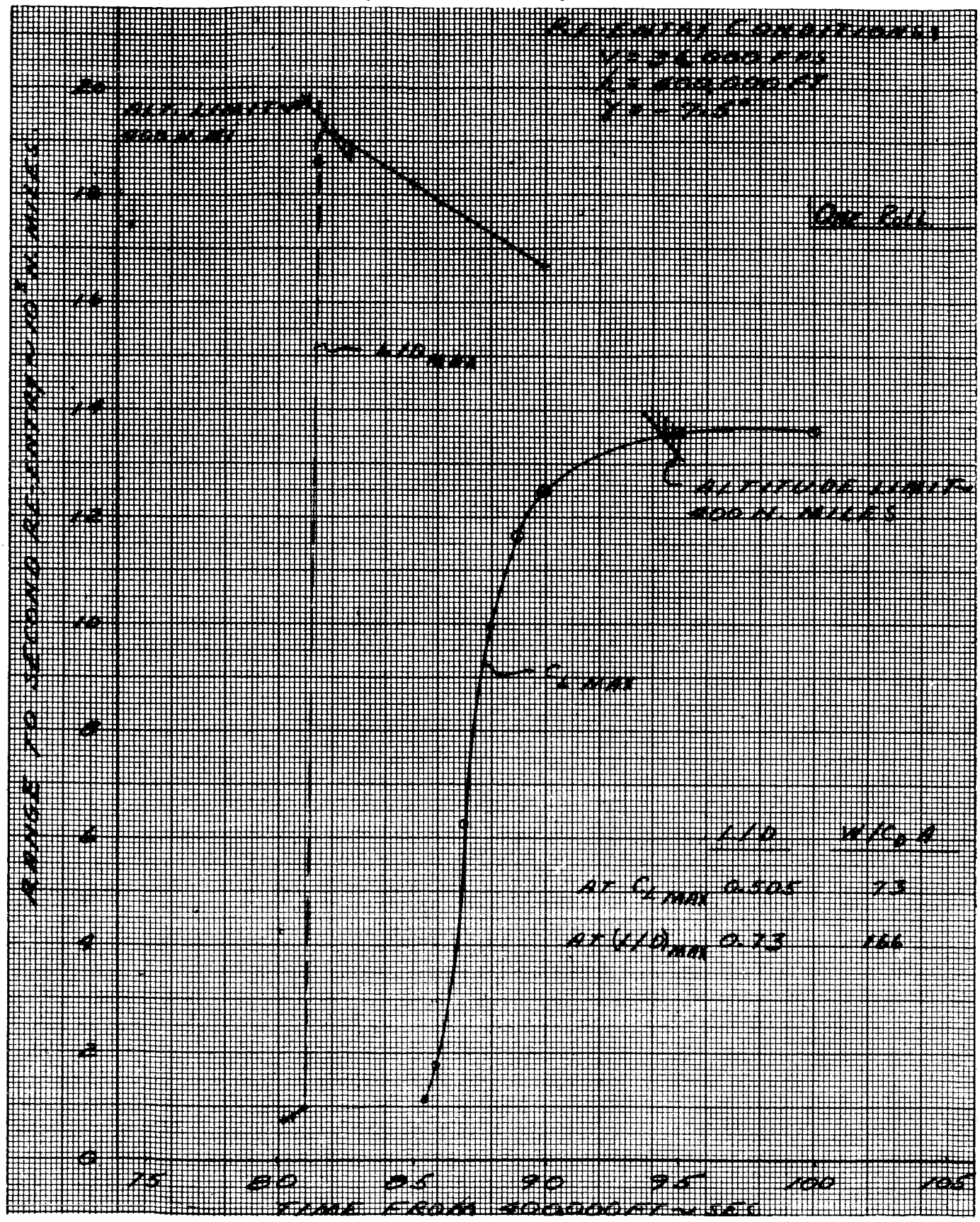

Fig. III-94. Range to Second Re-entry Versus Time at Application of Negative Lift

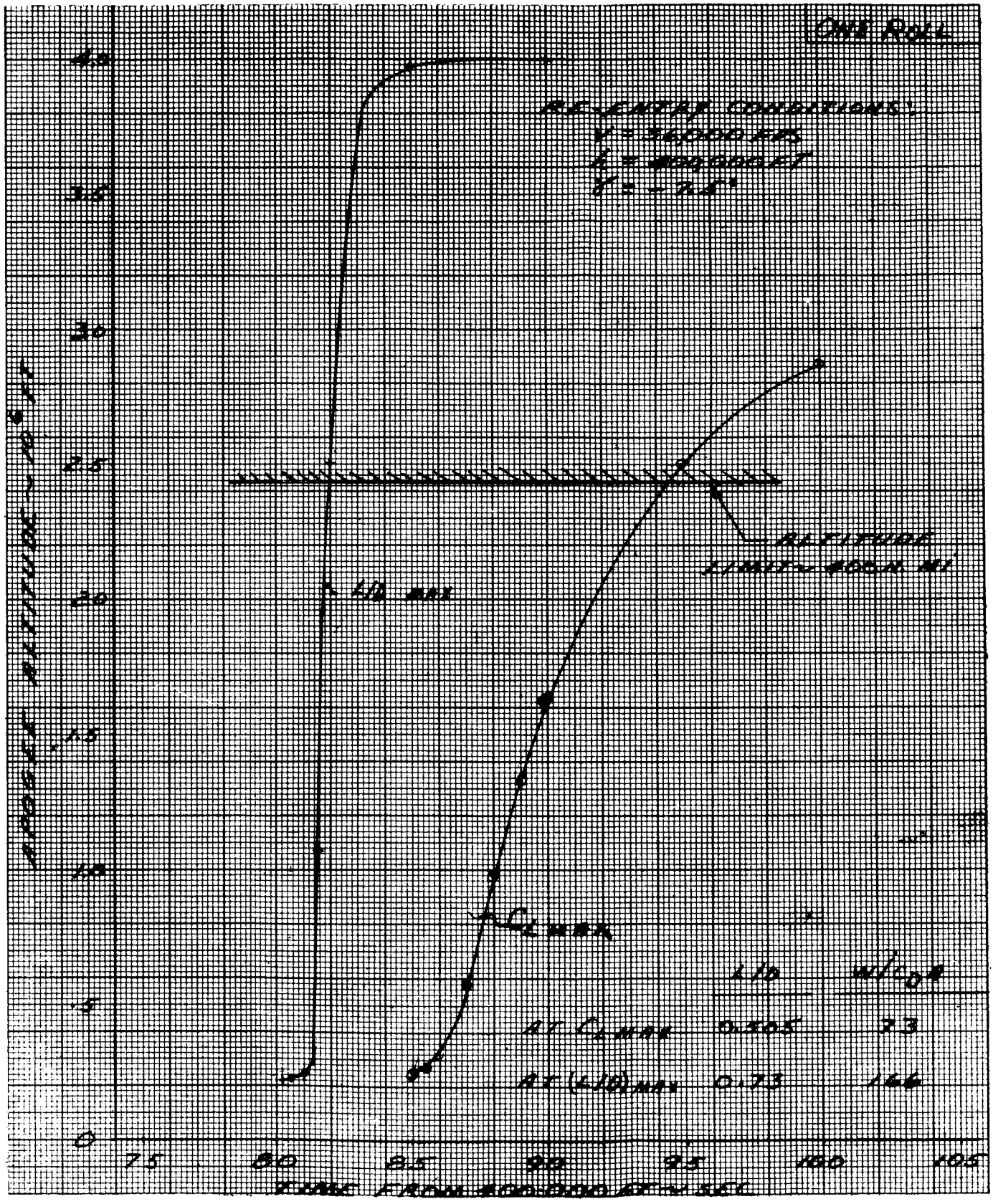

Fig. III-95. Apogee Altitude Versus Time at Application of Negative Lift

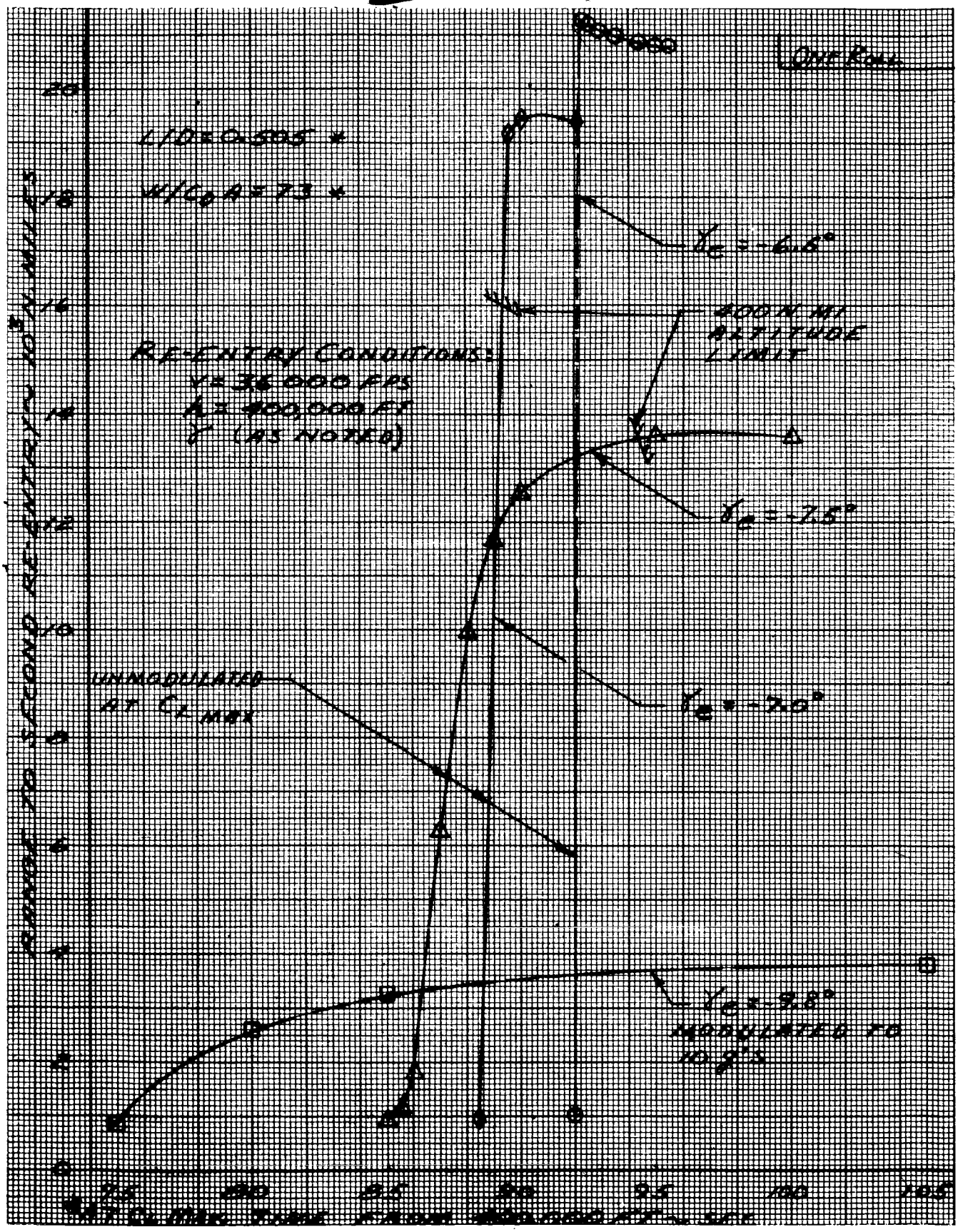

Fig. III-96. Range to Second Re-entry Versus Time at Application of Negative Lift

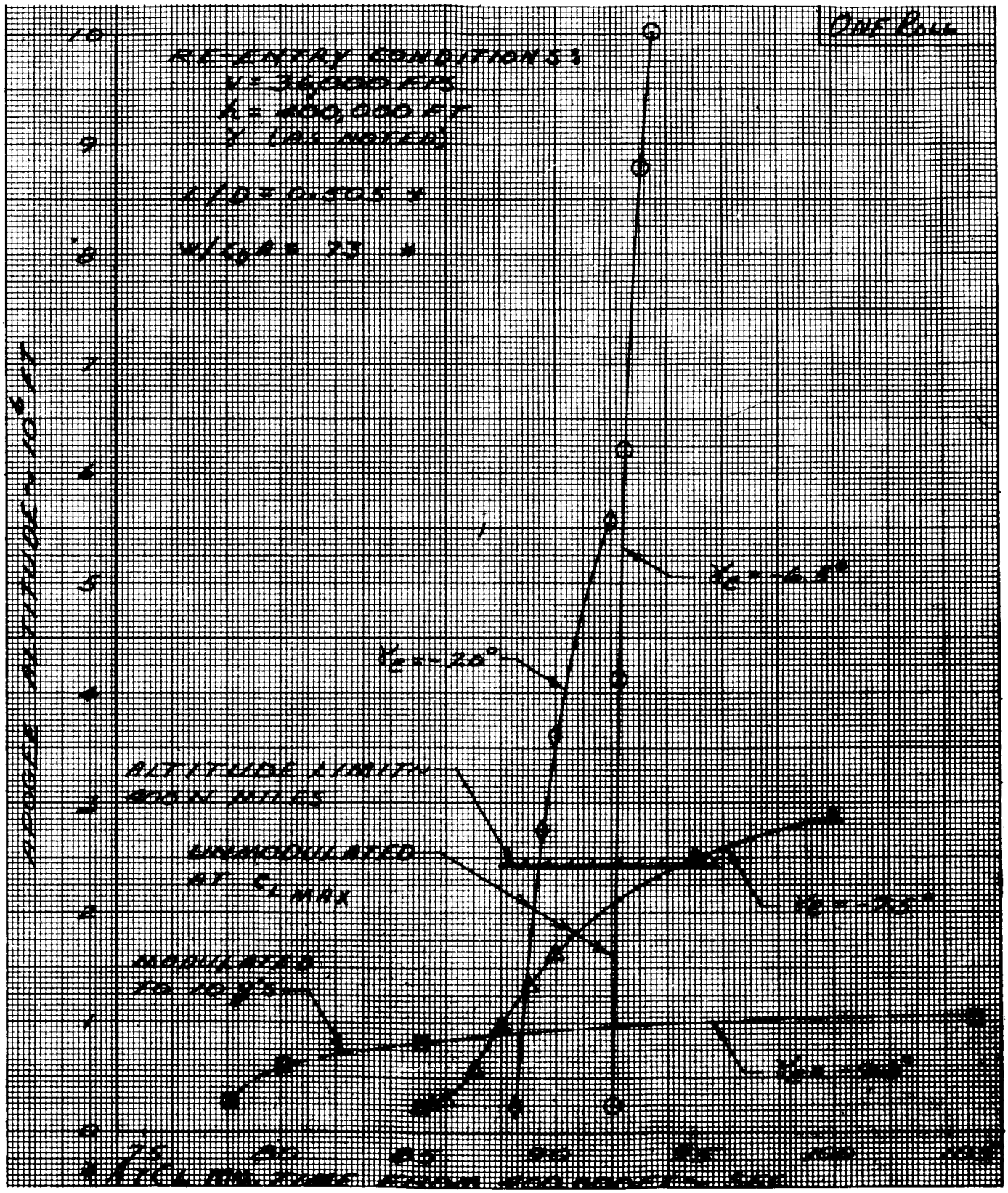

Fig. III-97. Apogee Altitude Versus Time at Application of Negative Lift

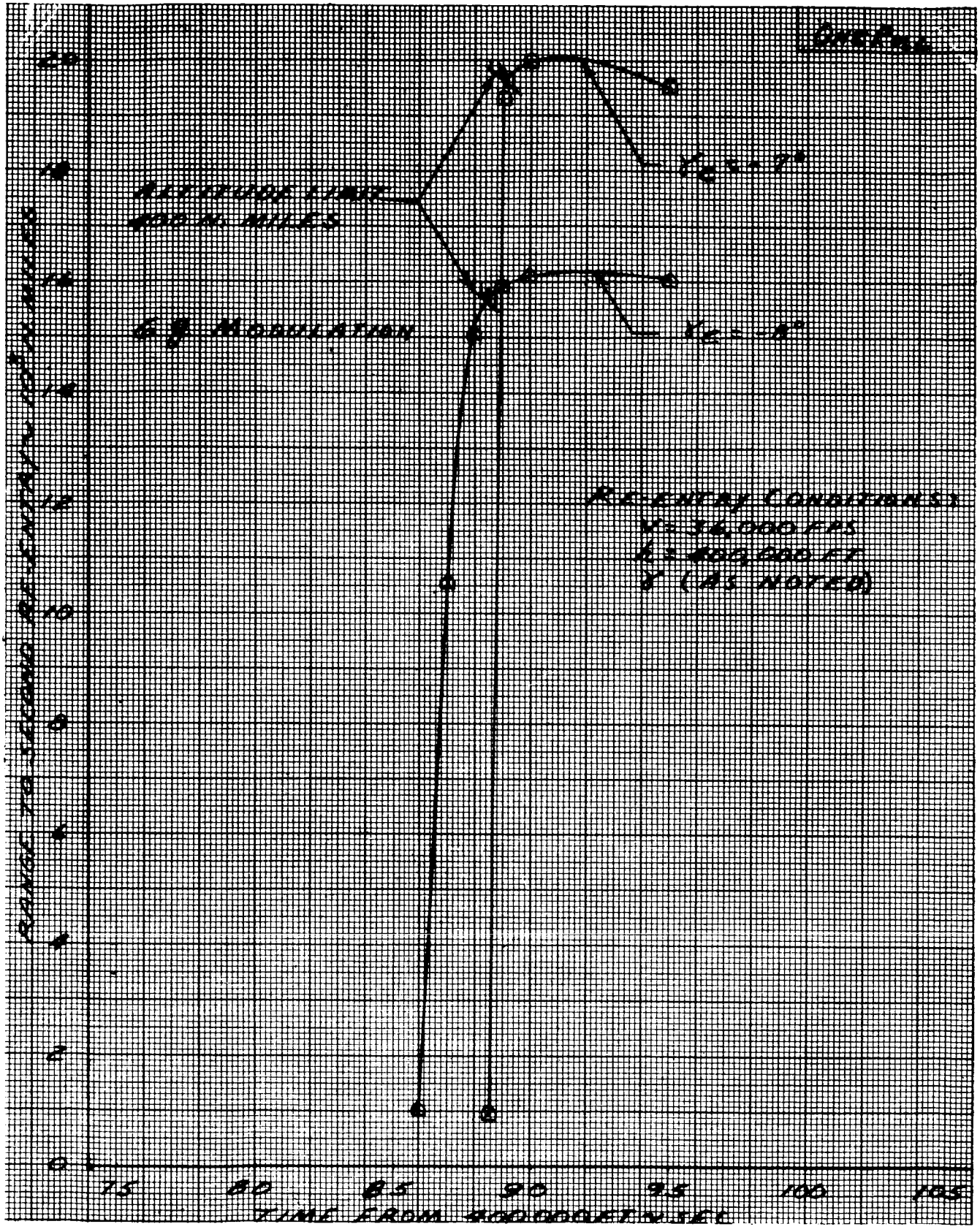

Fig. III-98. Range to Second Re-entry Versus Time at Application of Negative Lift

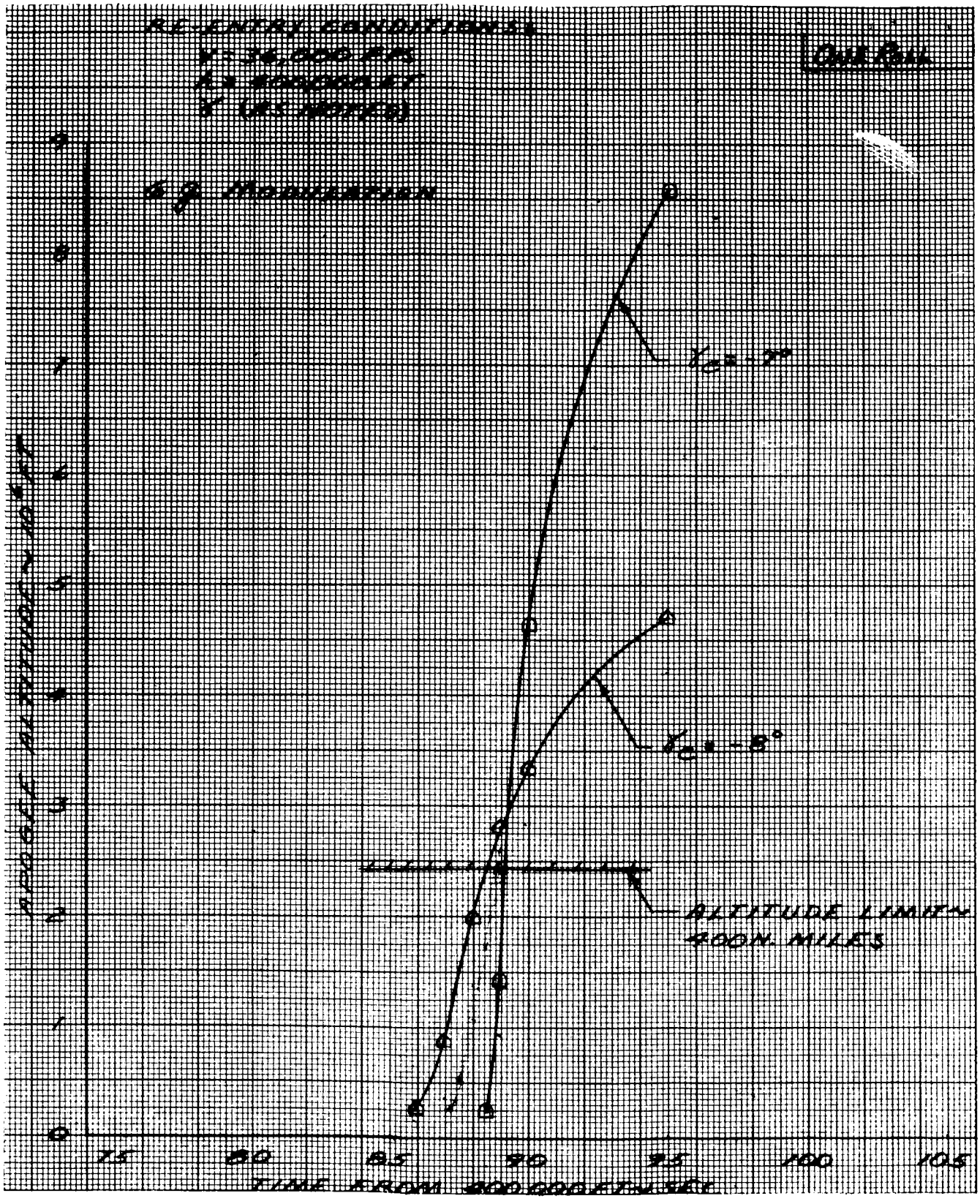

Fig. III-99. Apogee Altitude Versus Time at Application of Negative Lift

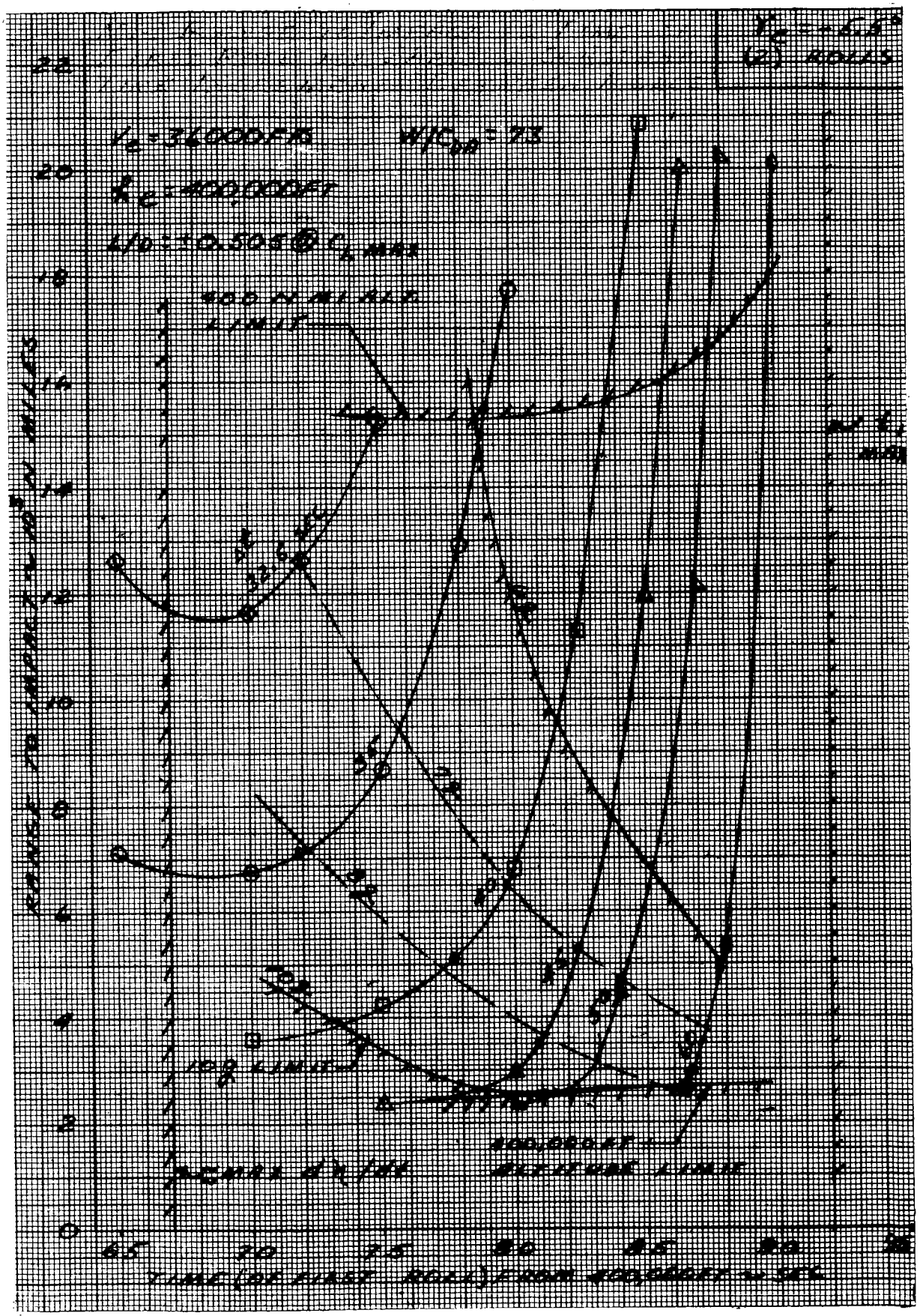

Fig. III-100. Range to Impact Versus Time of First Roll for Various Constant Time Increments Between Rolls

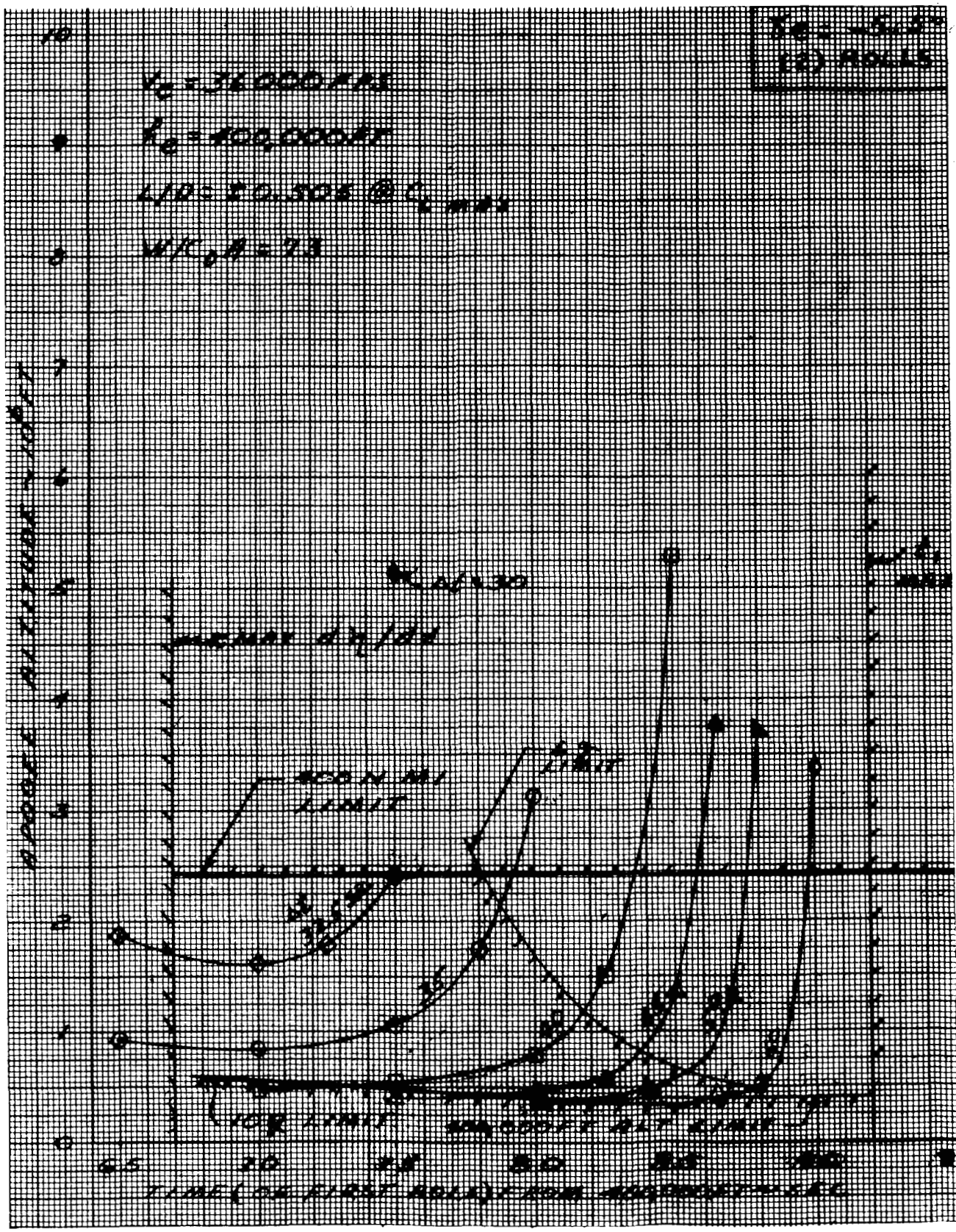

Fig. III-101. Apogee Altitude Versus Time of First Roll for Various Constant Time Increments Between Rolls

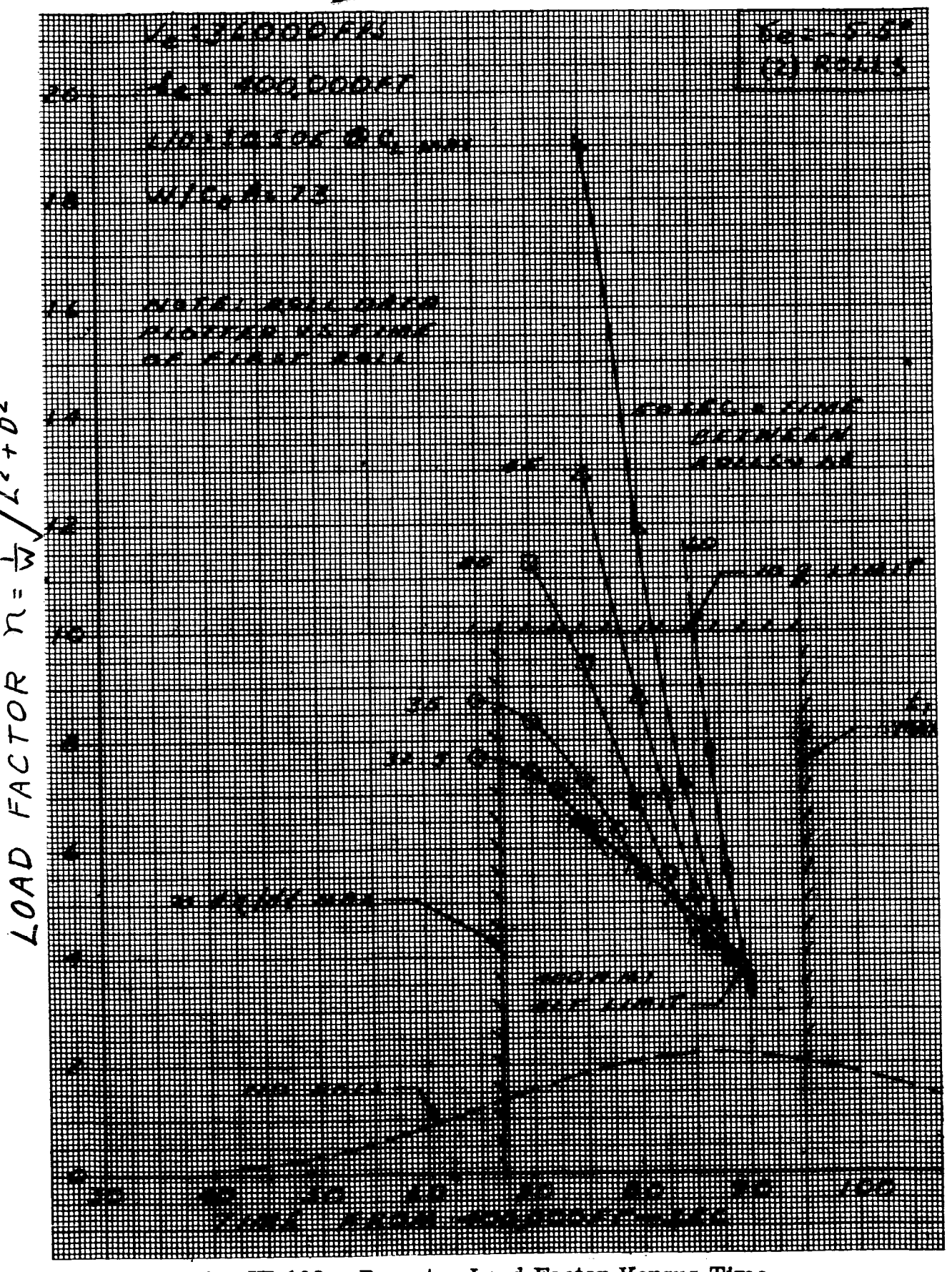

Fig. III-102. Re-entry Load Factor Versus Time

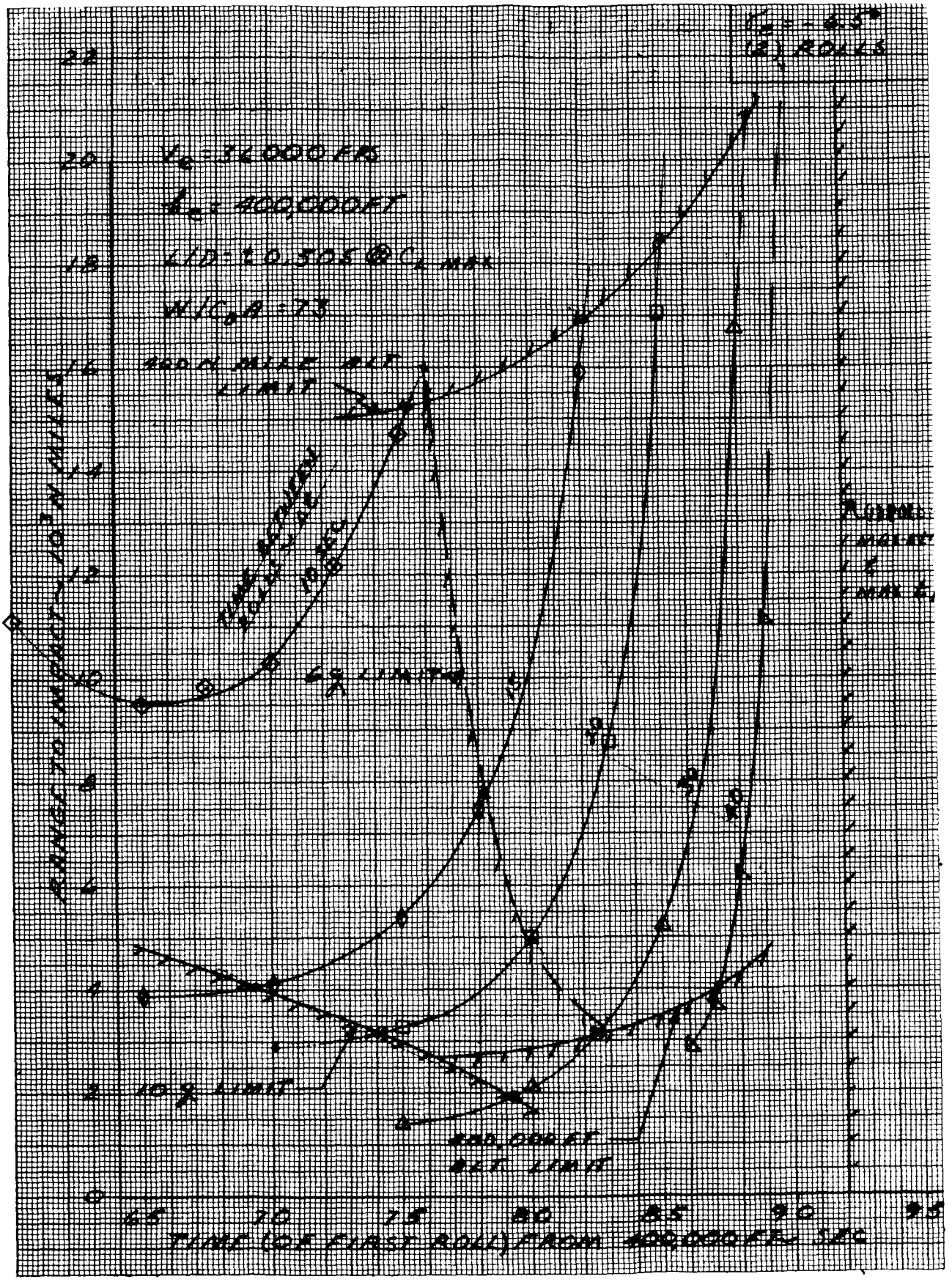

Fig. III-103. Range to Impact Versus Time of First Roll for Various Constant Time Increments Between Rolls

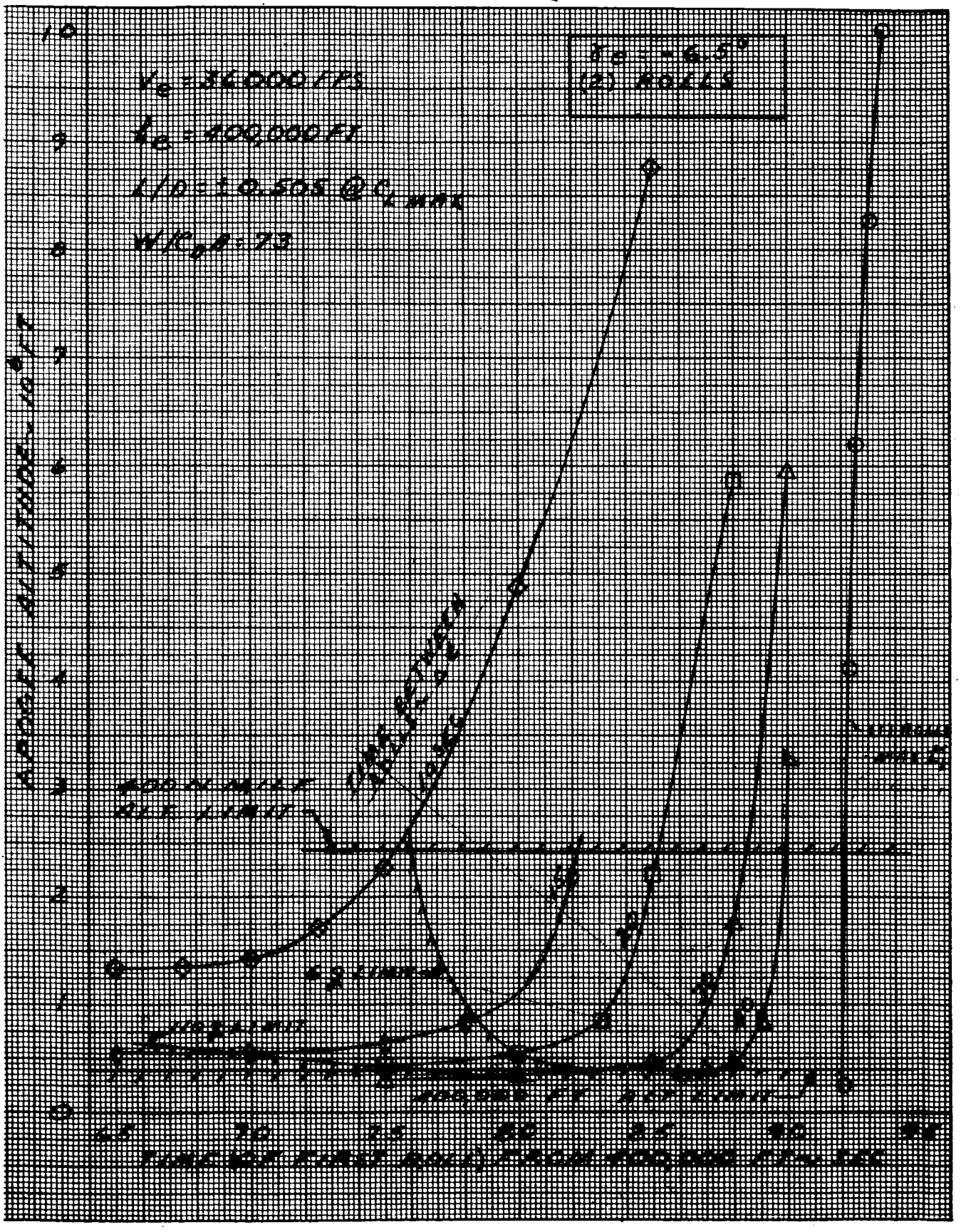

Fig. III-104. Apogee Altitude Versus Time of First Roll for Various Constant Time Increments Between Rolls

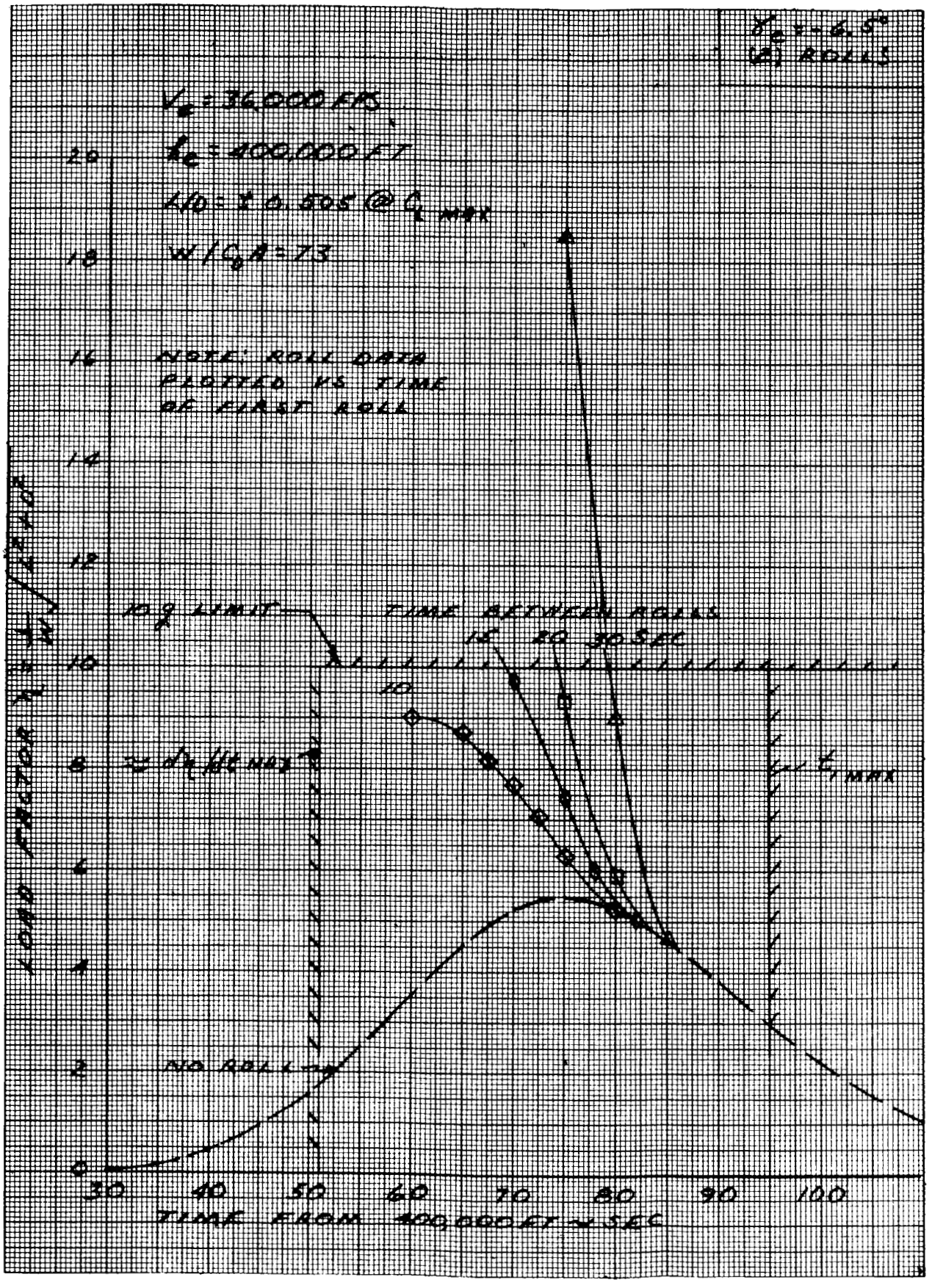

Fig. III-105. Re-entry Load Factor Versus Time

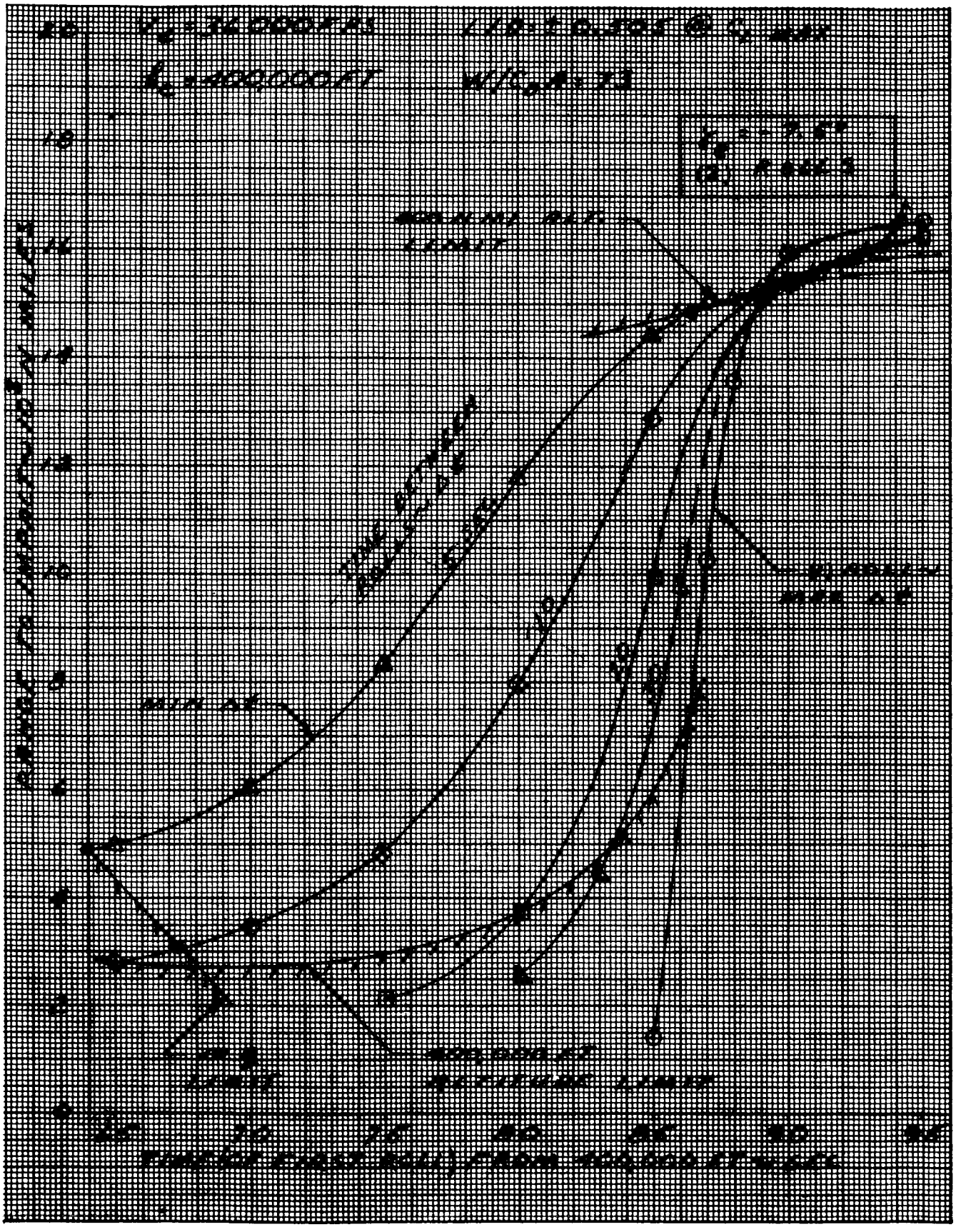

Fig. III-106. Range to Impact Versus Time of First Roll for Various Constant Time Increments Between Rolls

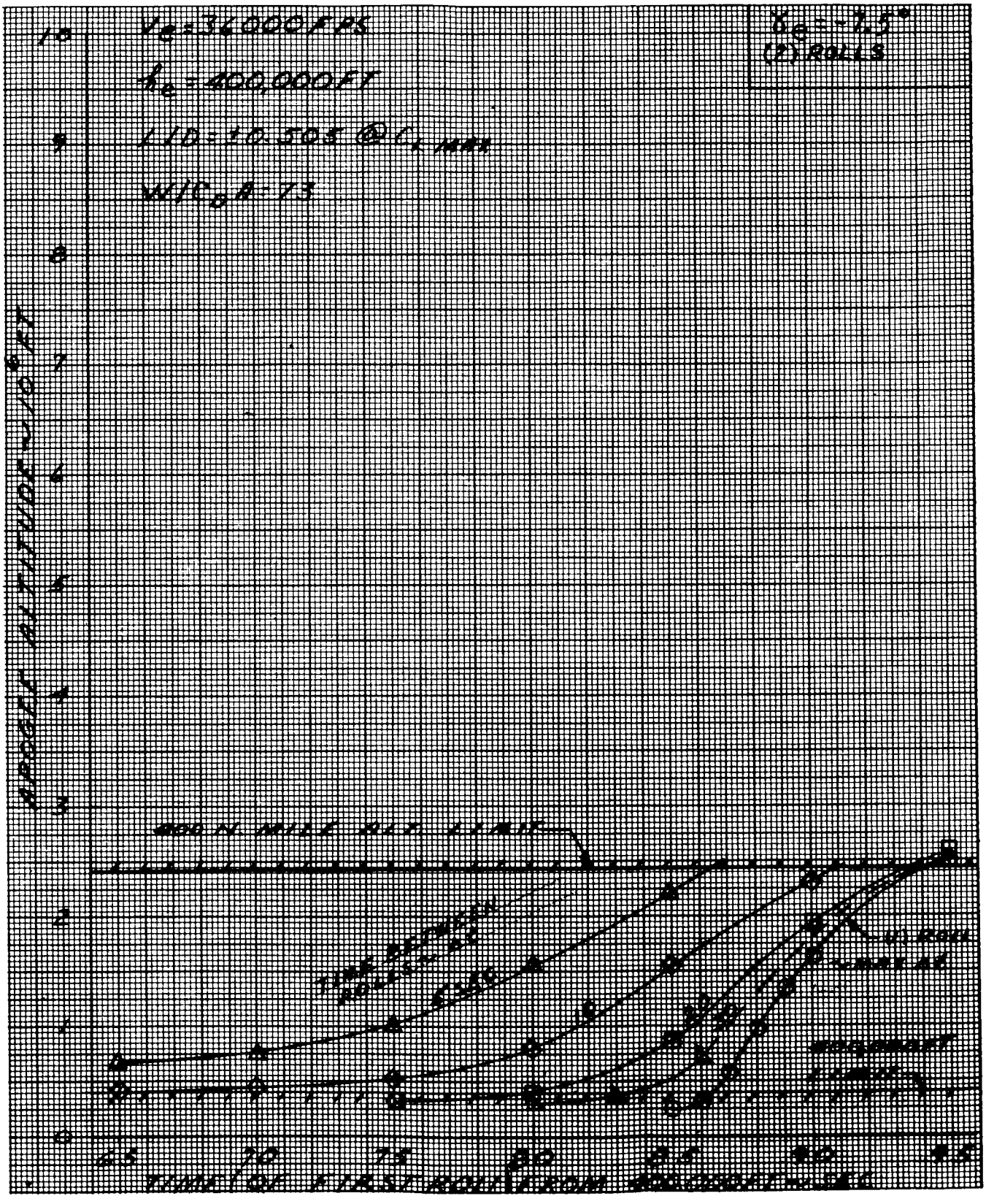

Fig. III-107. Apogee Altitude Versus Time of First Roll for Various Constant Time Increments Between Rolls

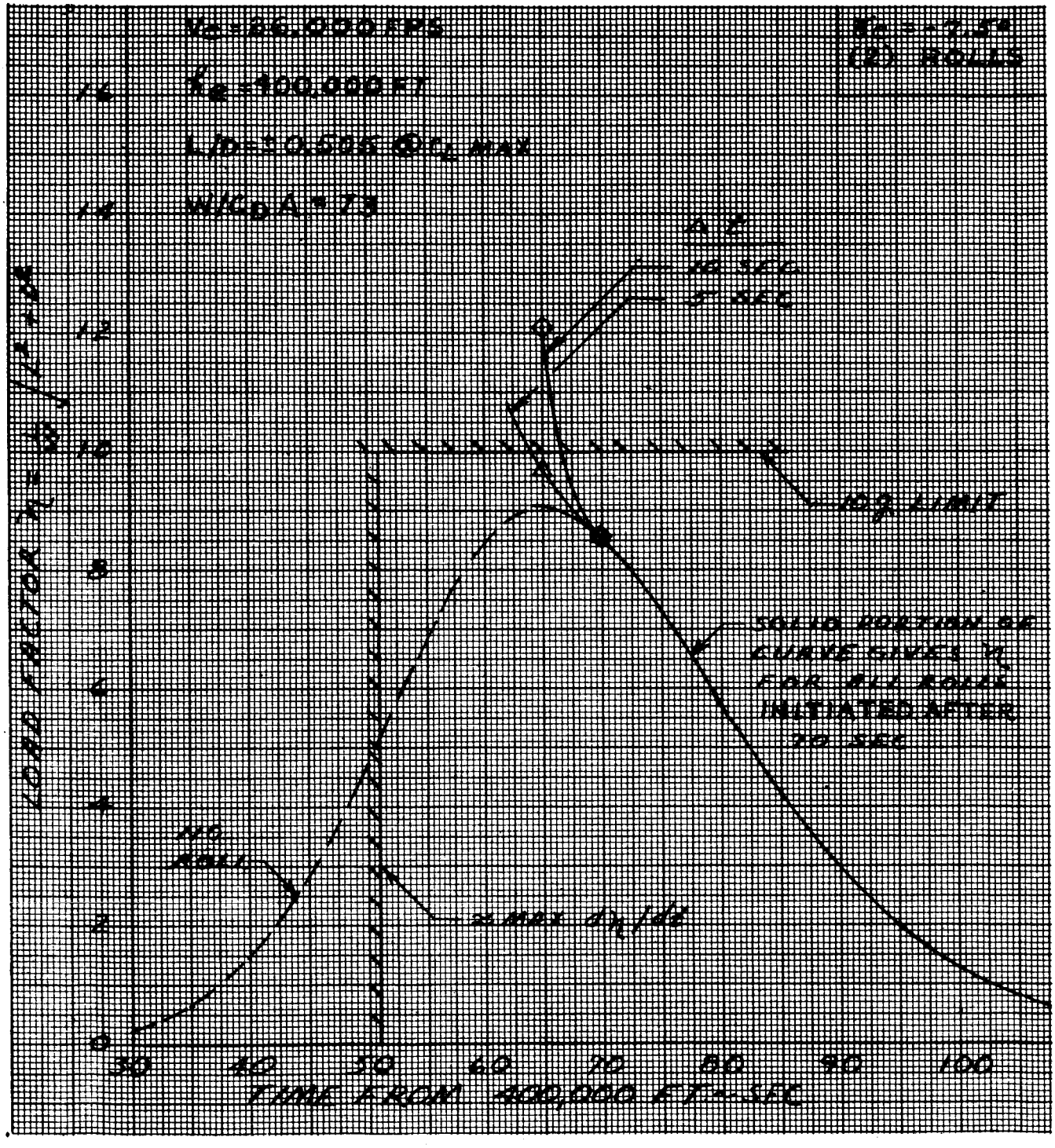

Fig. III-108. Re-entry Load Factor Versus Time

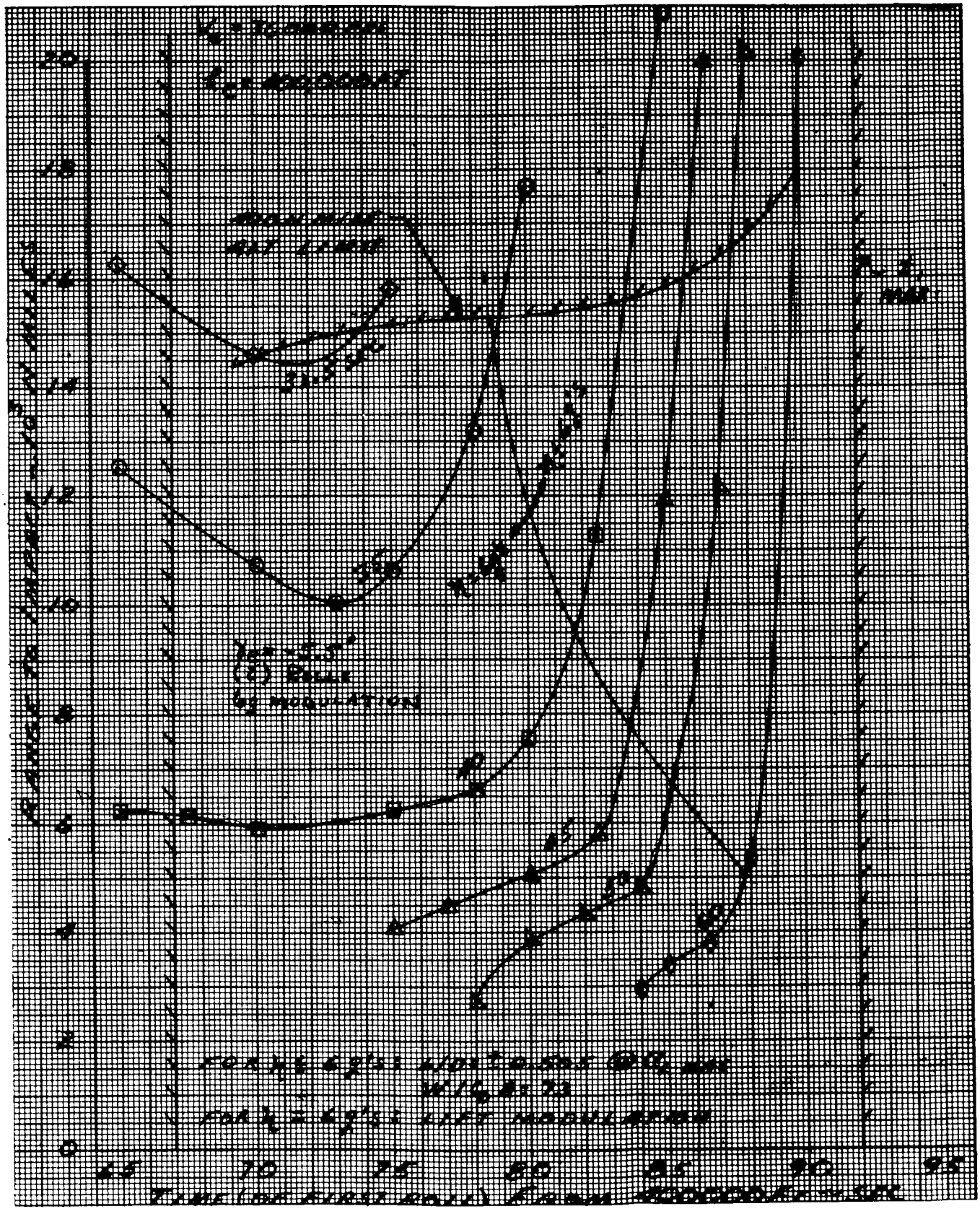

Fig. III-109. Range to Impact Versus Time of First Roll for Various Constant Time Increments Between Rolls

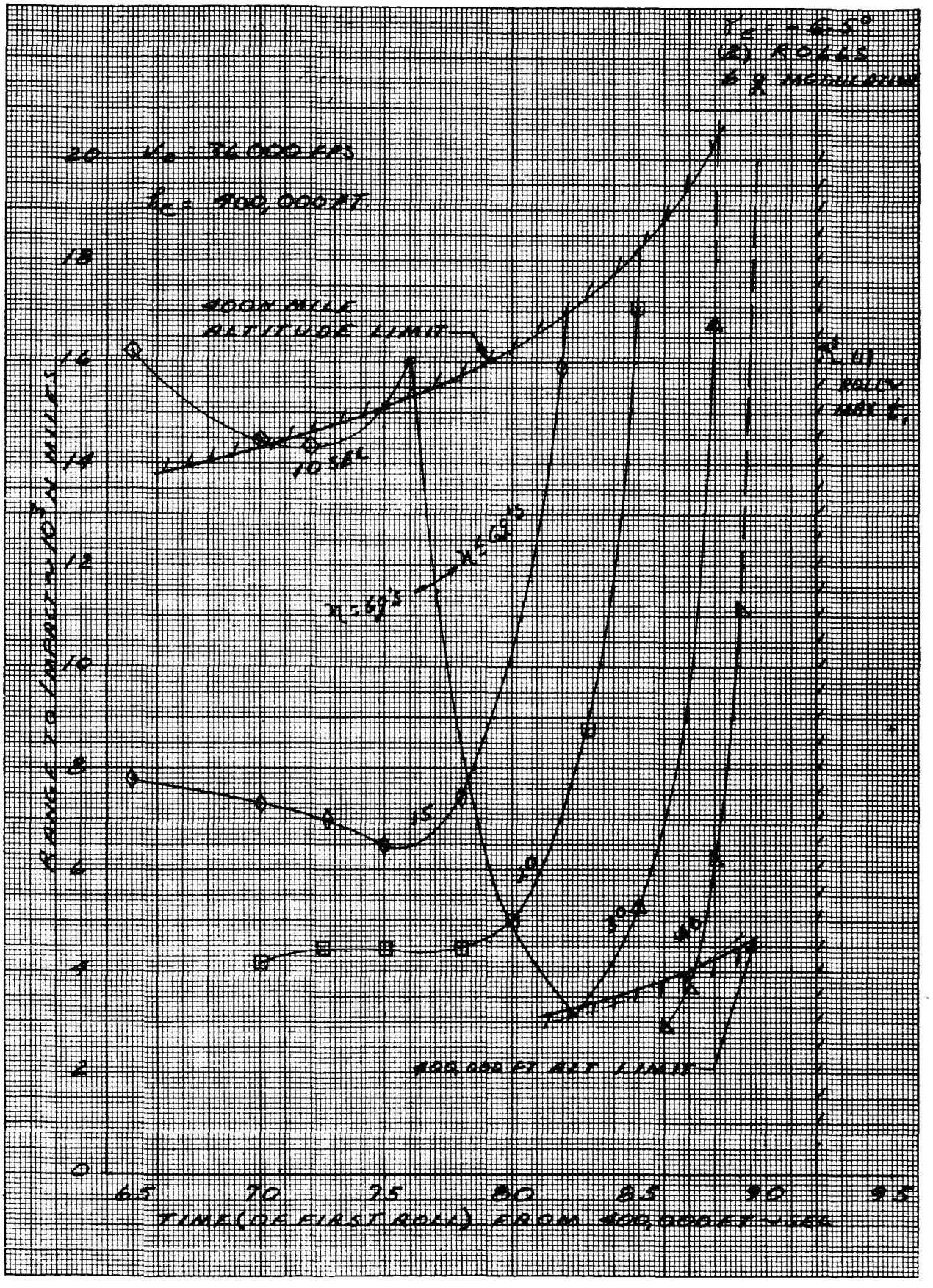

Fig. III-110. Range to Impact Versus Time of First Roll for Various Constant Time Increments Between Rolls

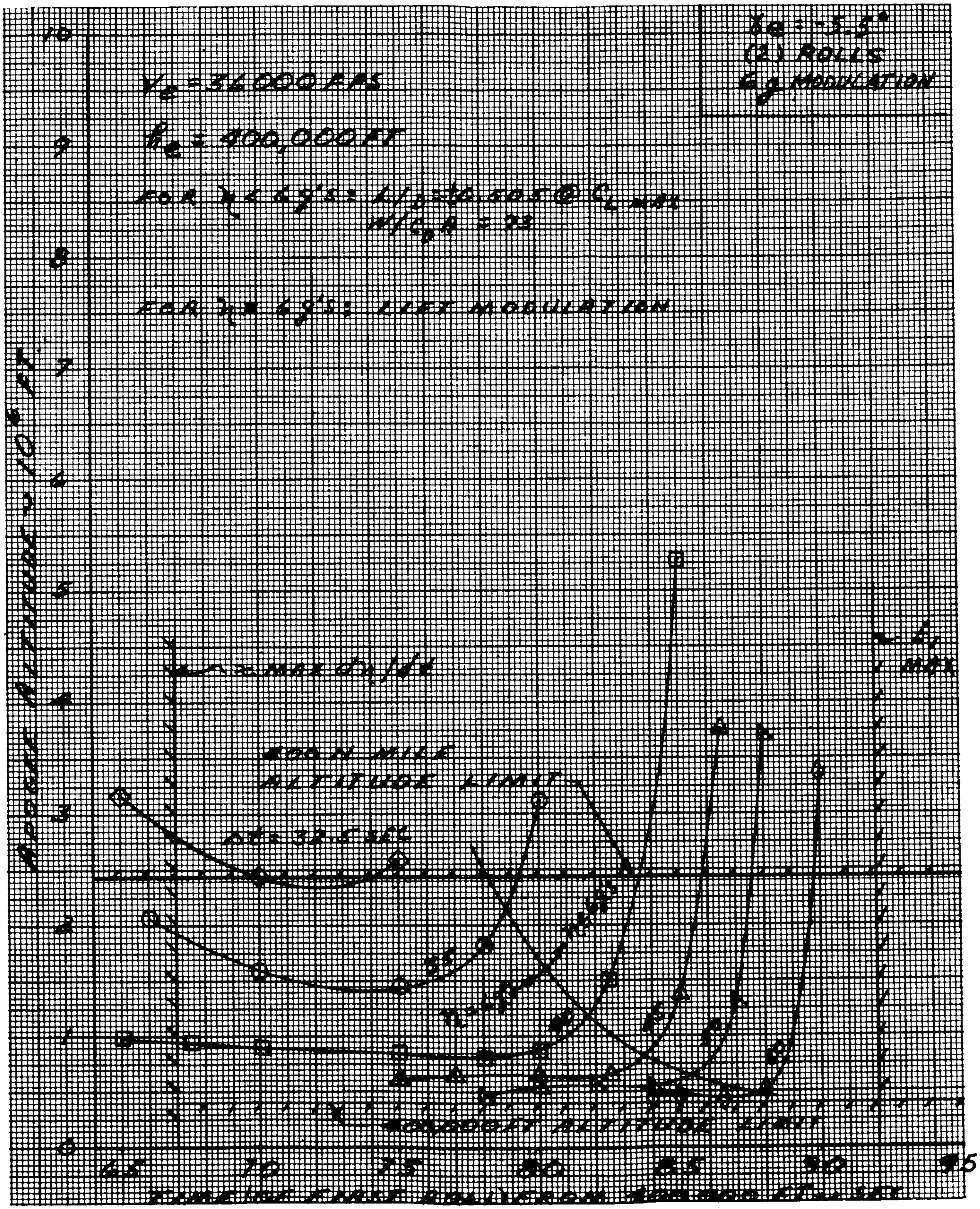

Fig. III-111. Apogee Altitude Versus Time of First Roll for Various Constant Time Increments Between Rolls

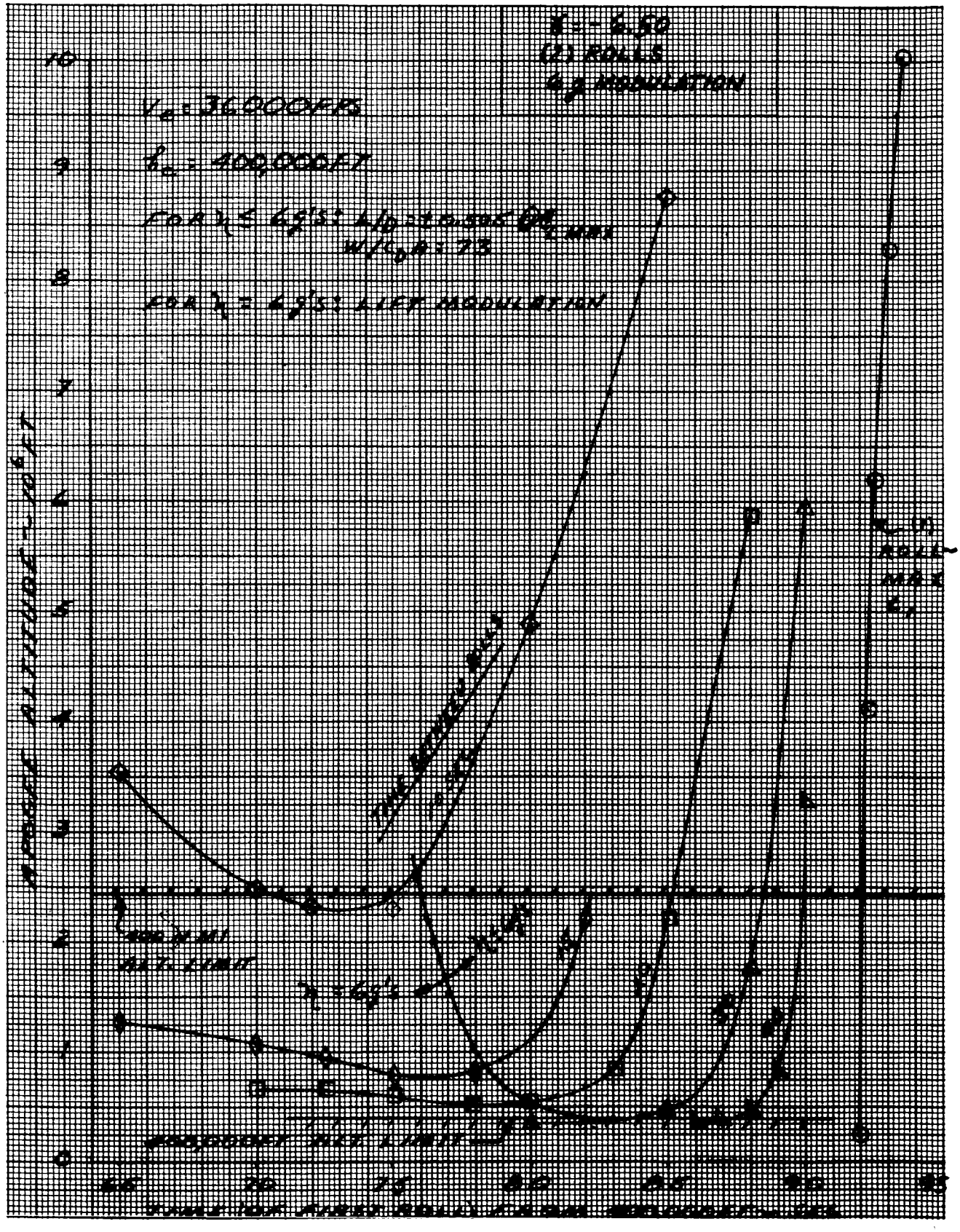

Fig. III-112. Apogee Altitude Versus Time of First Roll for Various Constant Time Increments Between Rolls

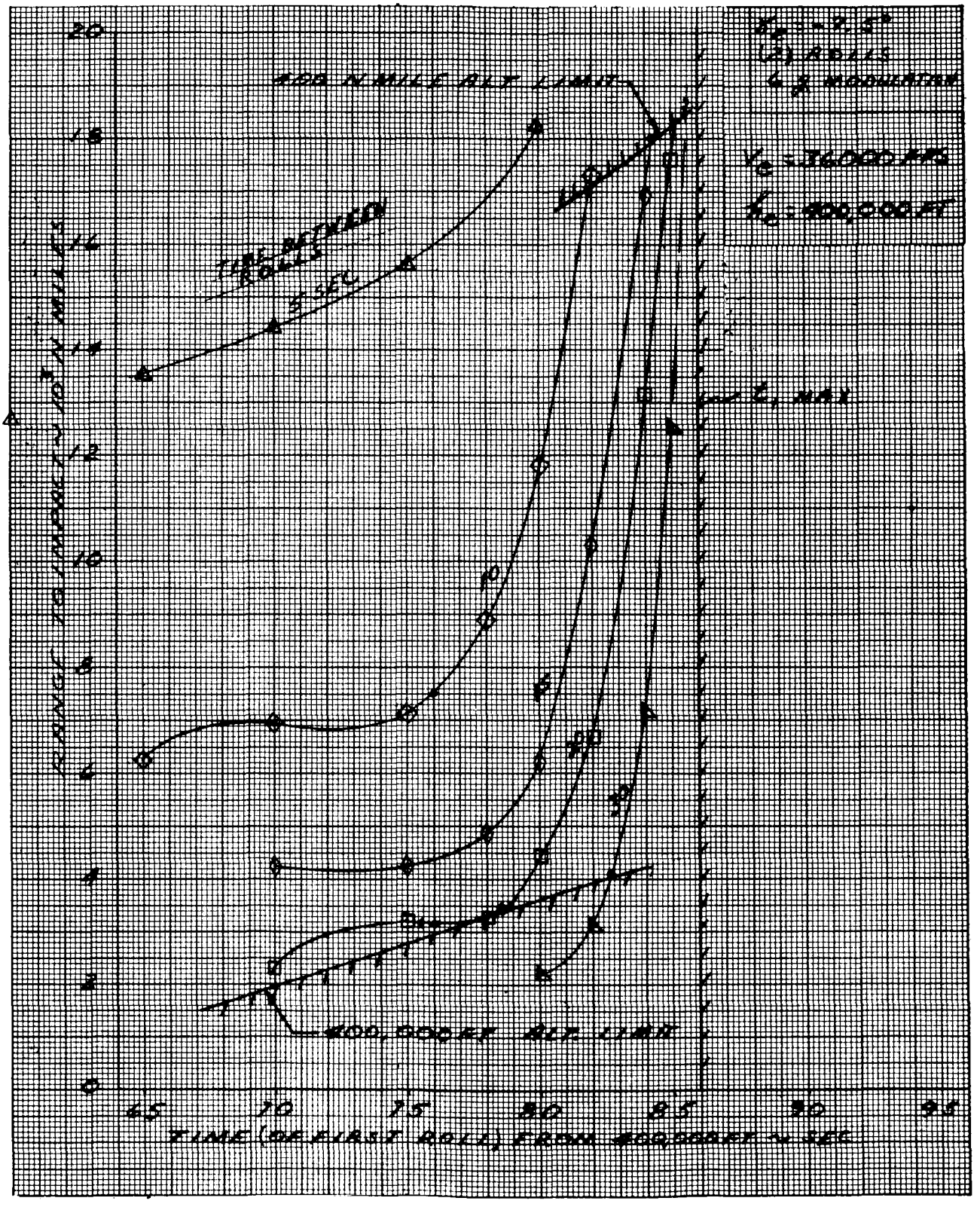

Fig. III-113. Range to Impact Versus Time of First Roll for Various Constant Time Increments Between Rolls

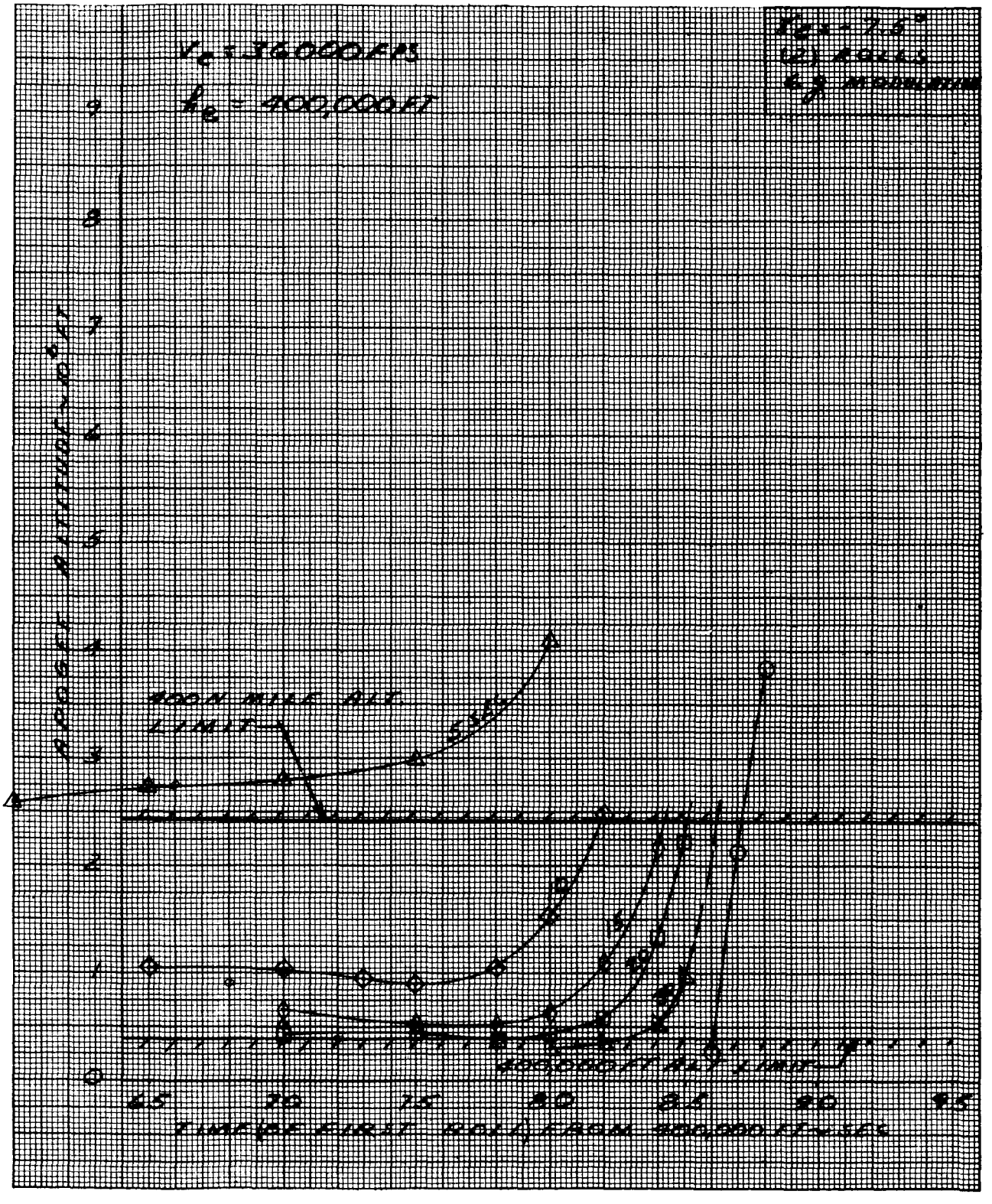

Fig. III-114. Apogee Altitude Versus Time of First Roll for Various Constant Time Increments Between Rolls

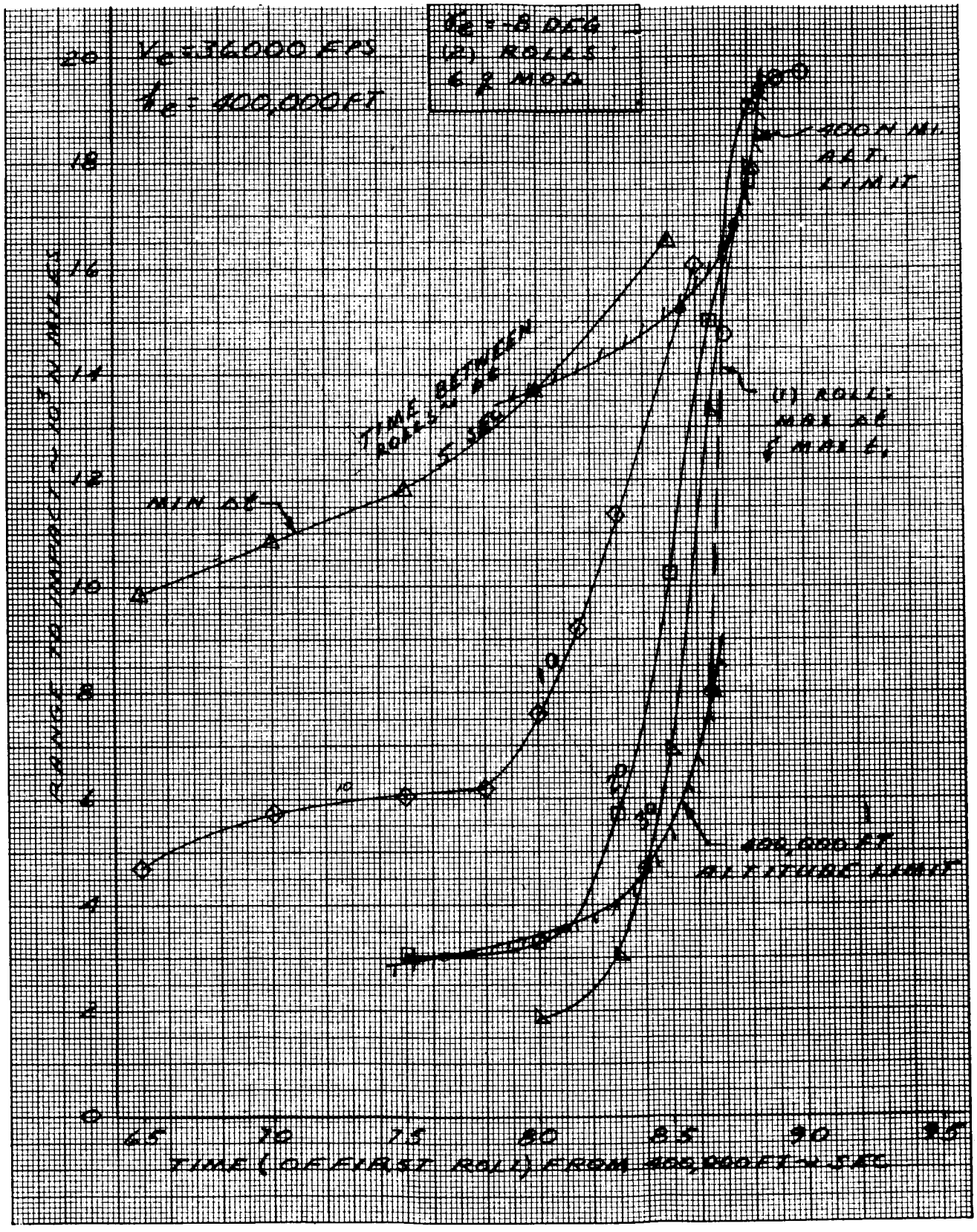

Fig. III-115. Range to Impact Versus Time of First Roll for Various Constant Time Increments Between Rolls

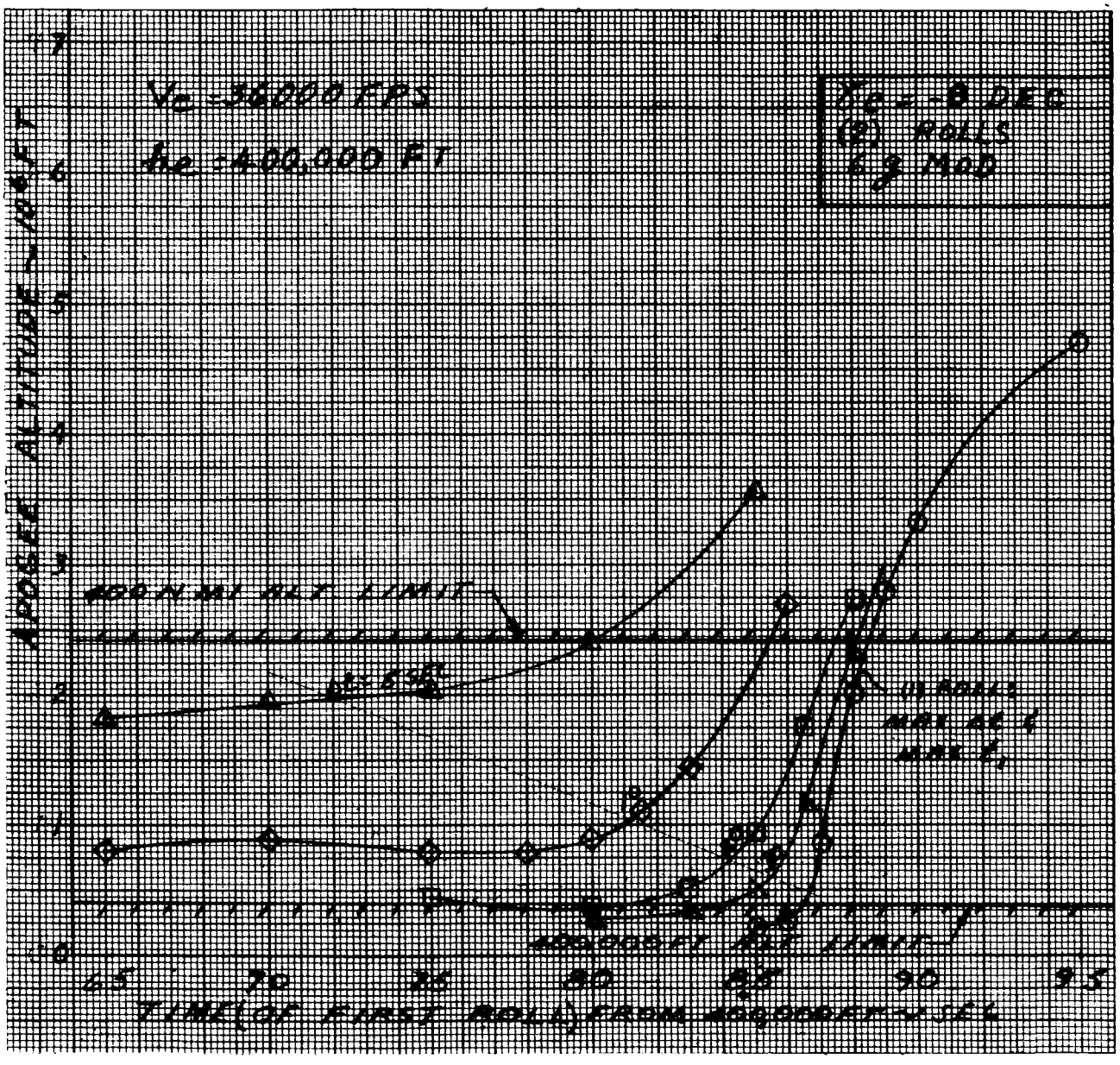

Fig. III-116. Apogee Altitude Versus Time of First Roll for Various Constant Time Increments Between Rolls

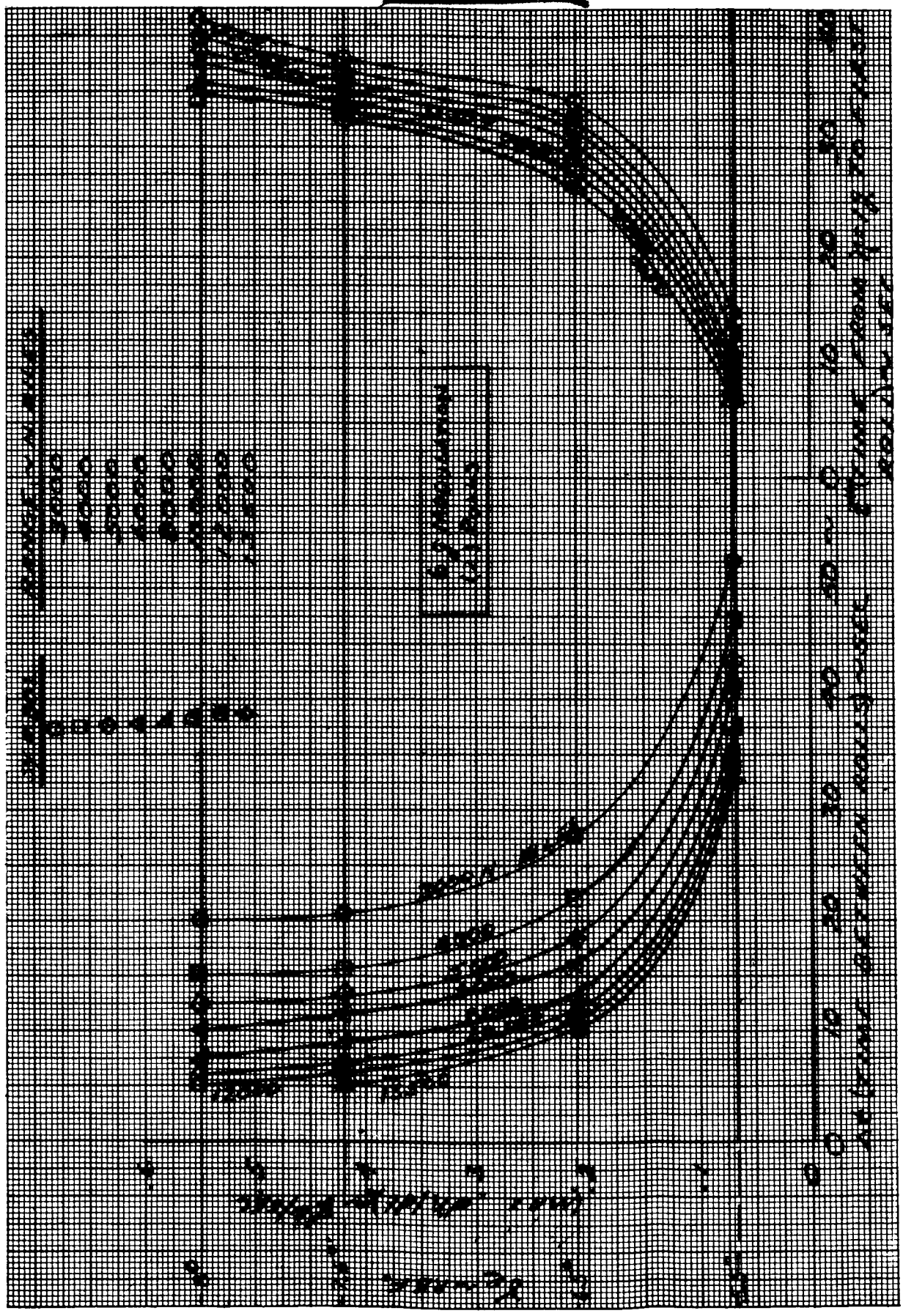

Fig. III-117. Control Parameters (max dn/dt), Control for a Constant Range to Target--Normal Performance

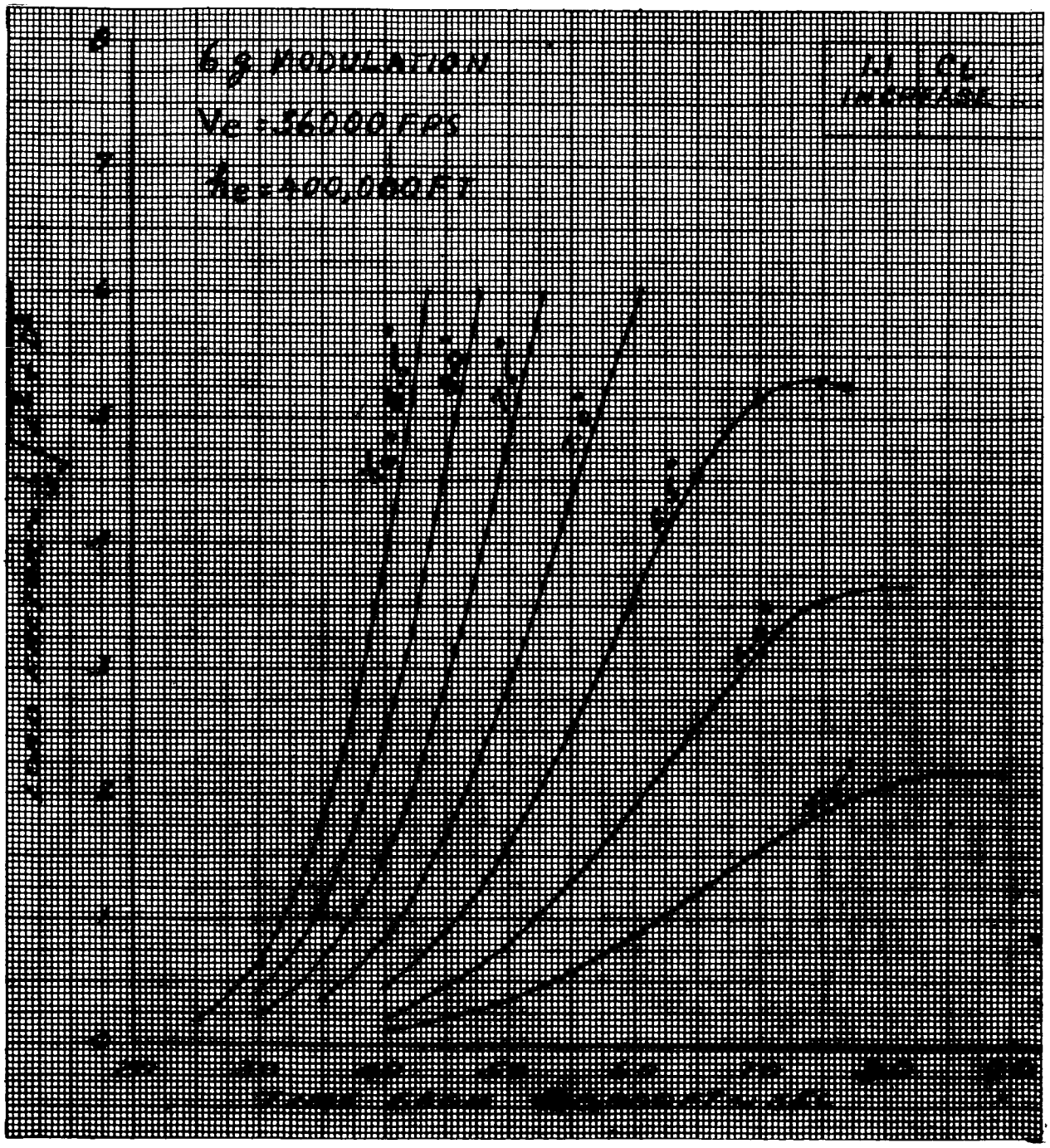

Fig. III-118. Re-entry Load Factor

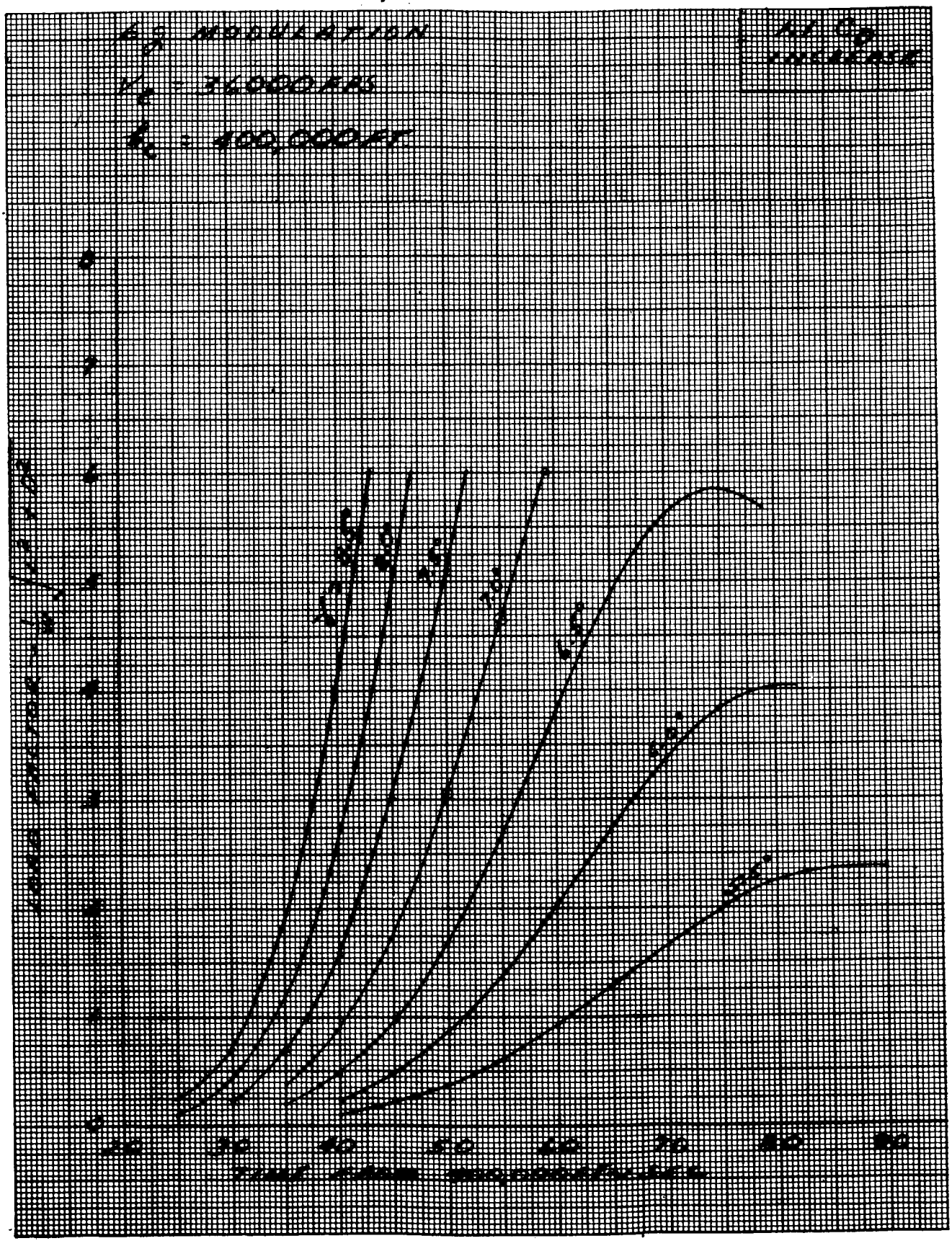

Fig. III-119. Re-entry Load Factor

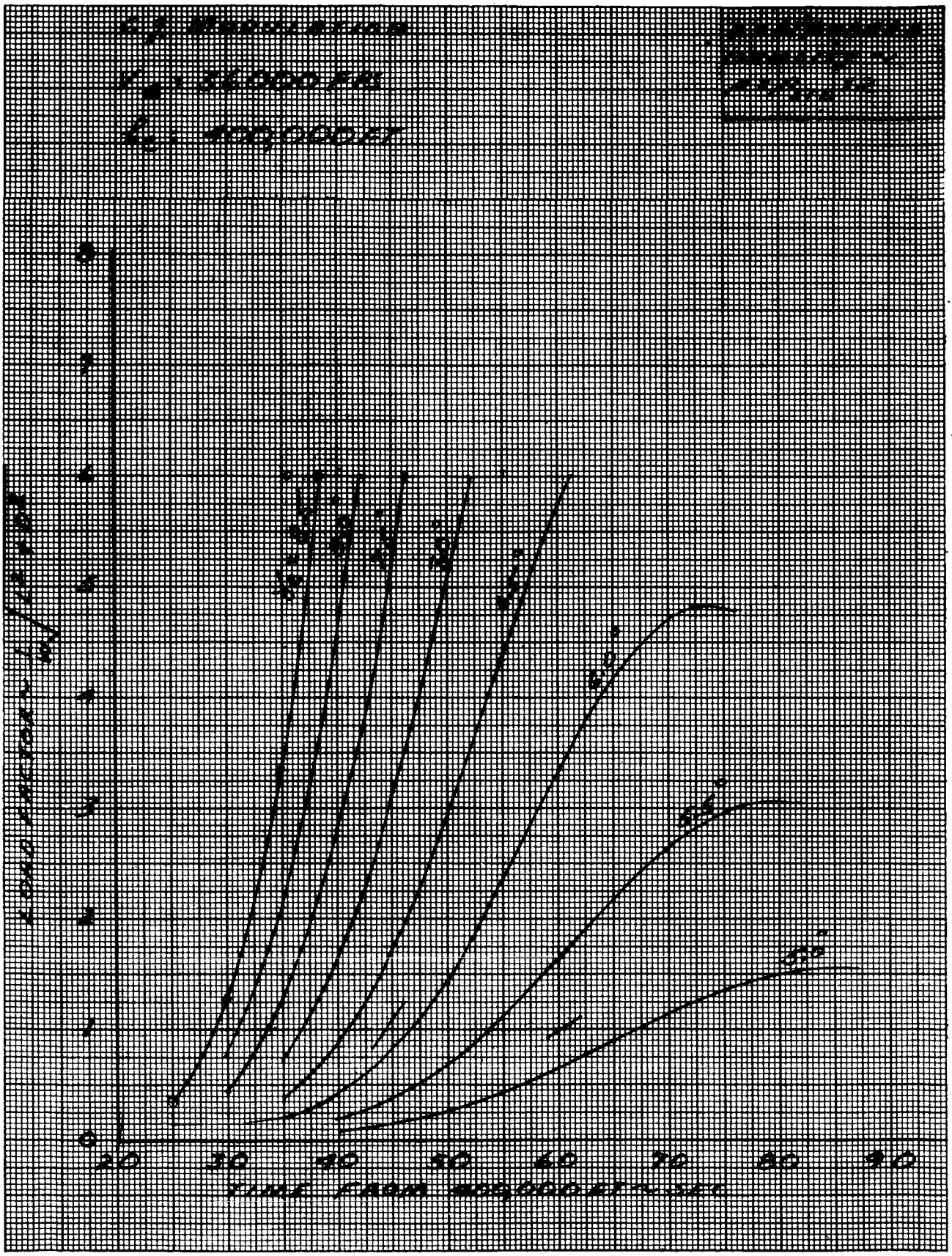

Fig. III-120. Re-entry Load Factor

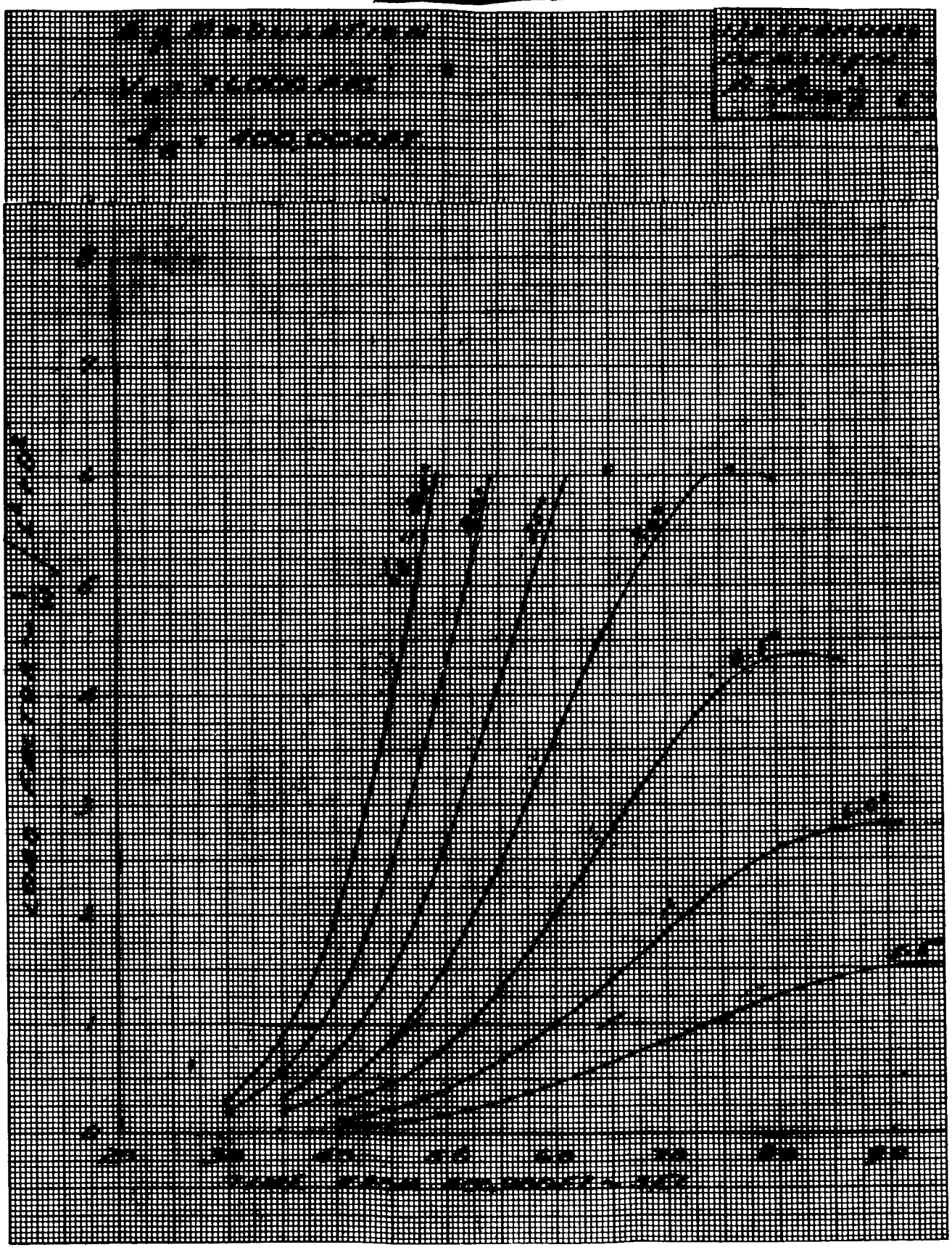

Fig. III-121. Re-entry Load Factor

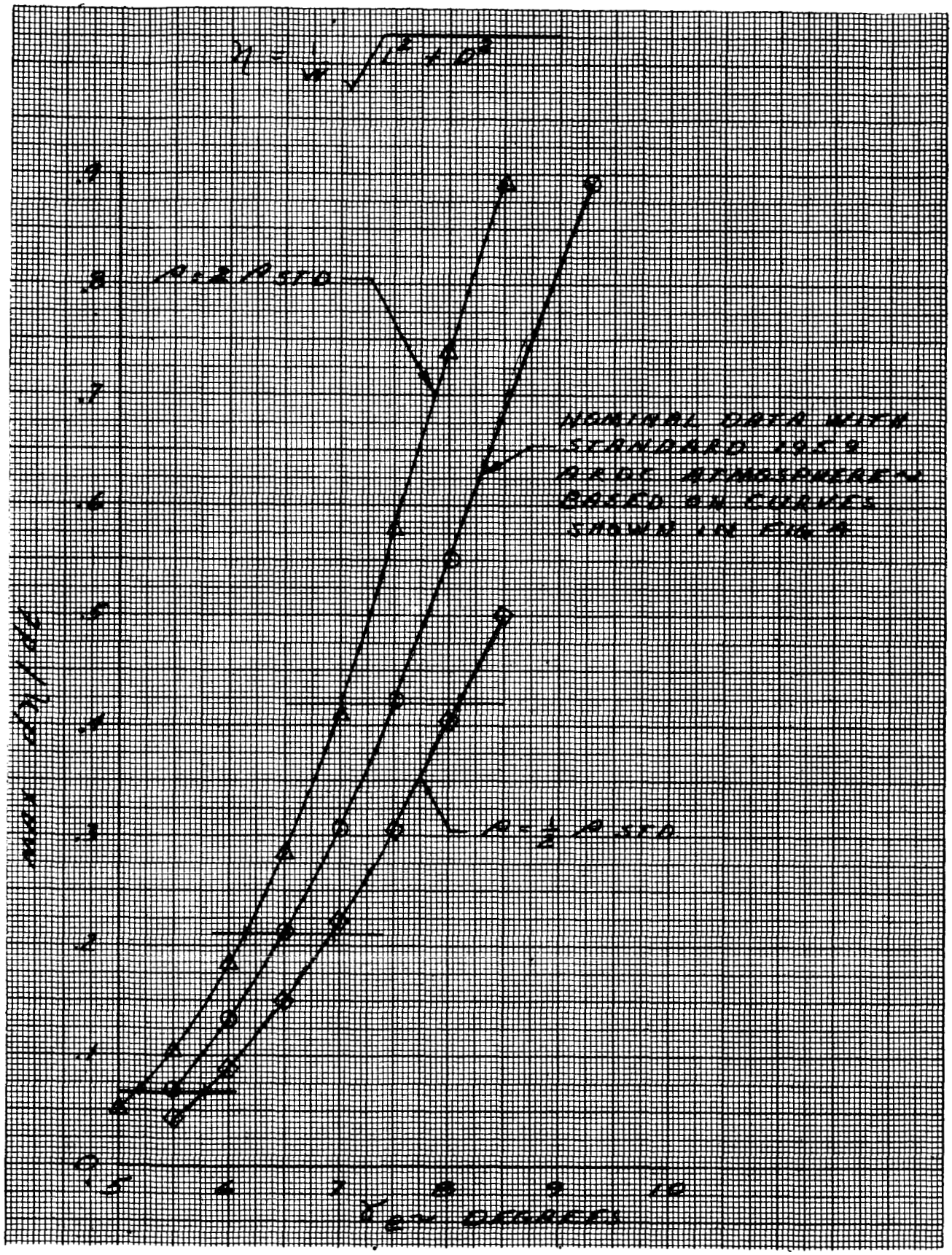

Fig. III-122. Maximum dn/dt Versus Time

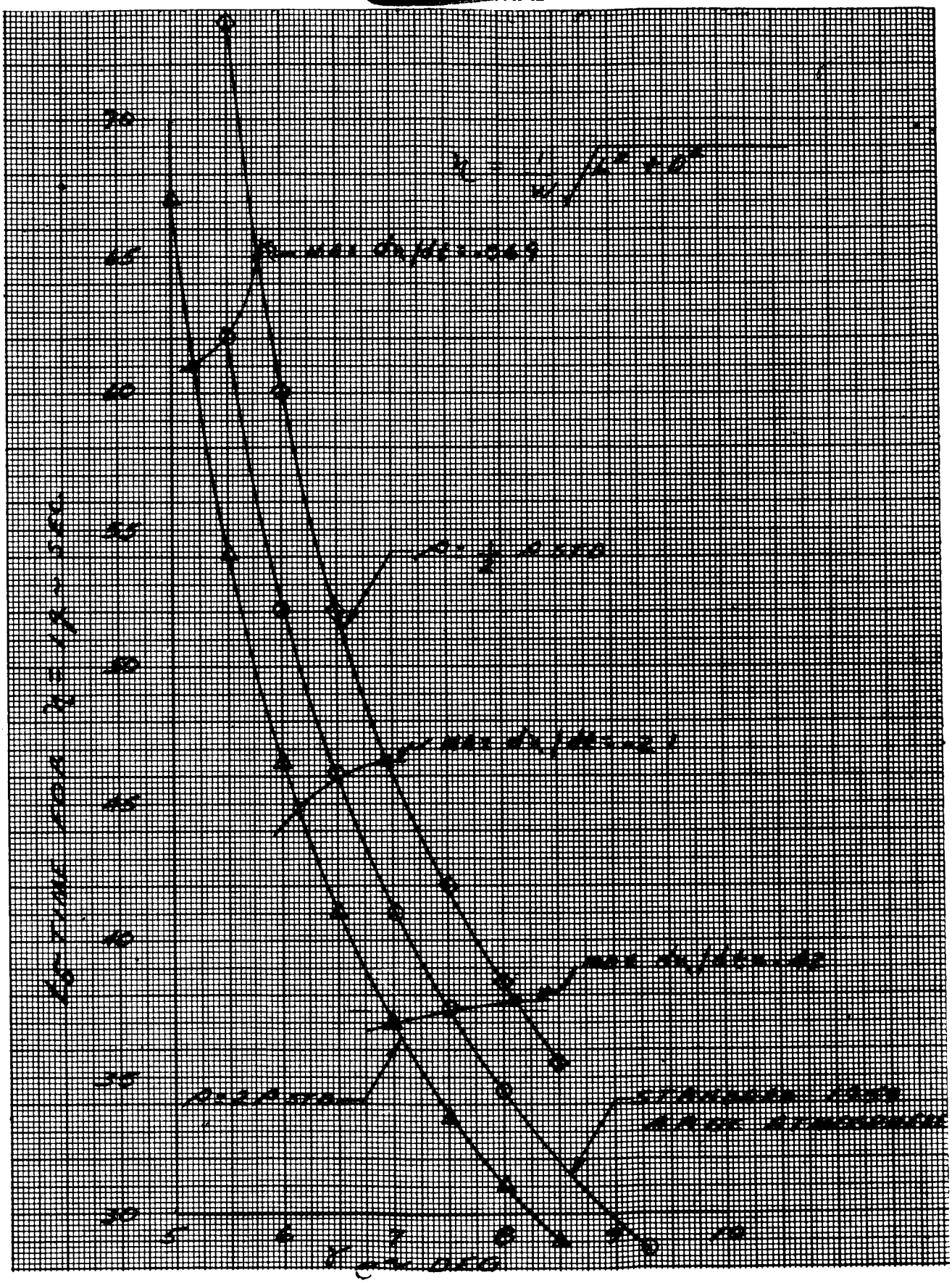

Fig. III-123. Time for n = 1 g Versus γ_e

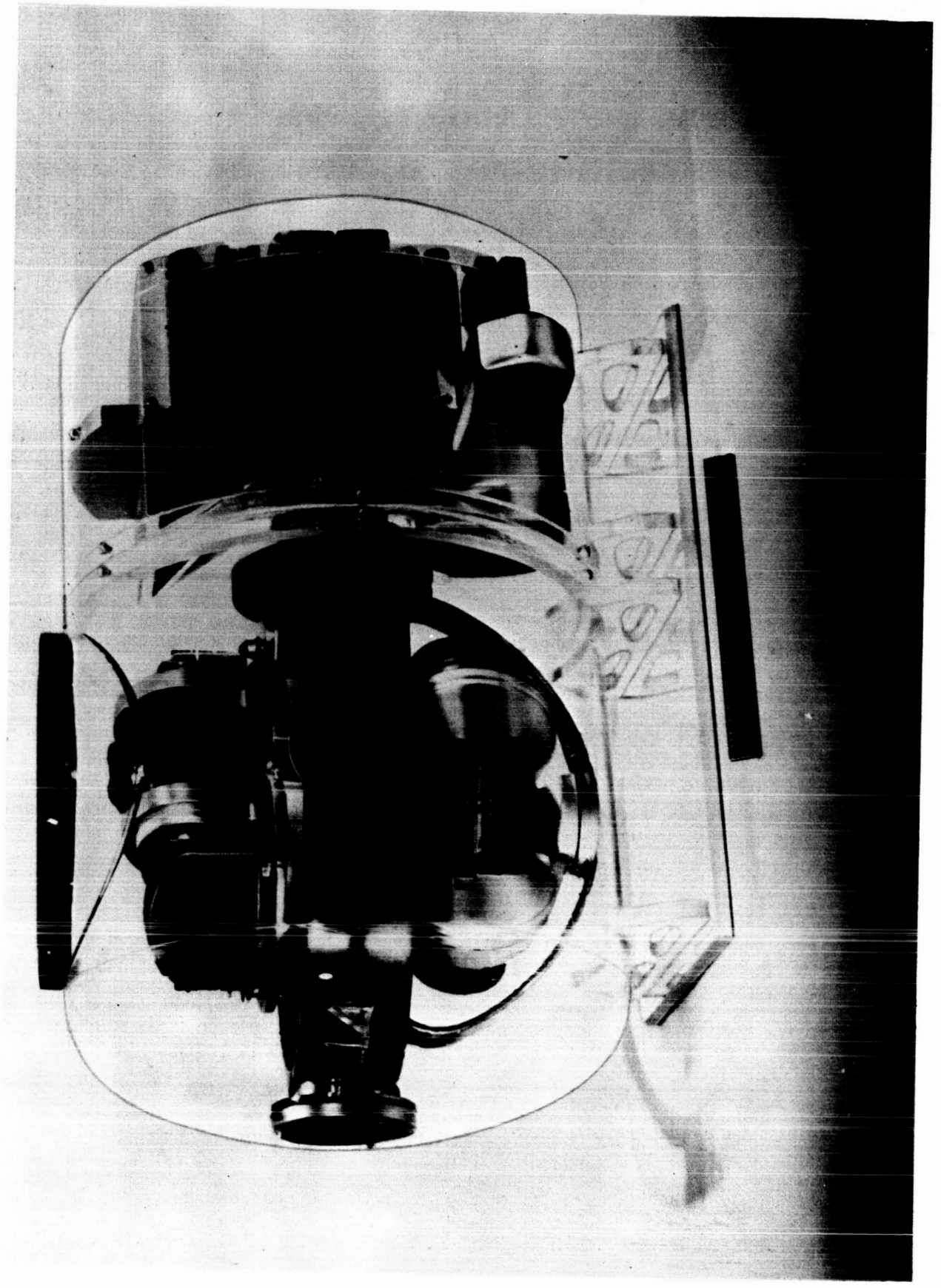

Fig. IV-1. Astro-Inertial Platform

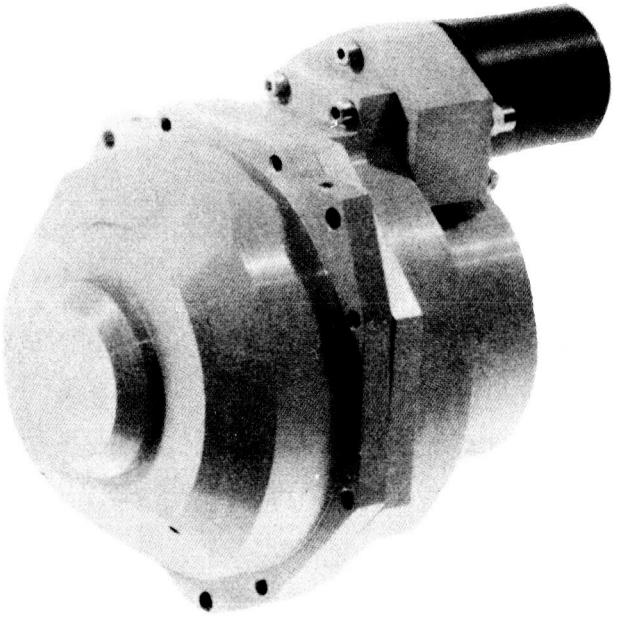

Fig. IV-2. Autonetics Miniature Case Rotated Gyro

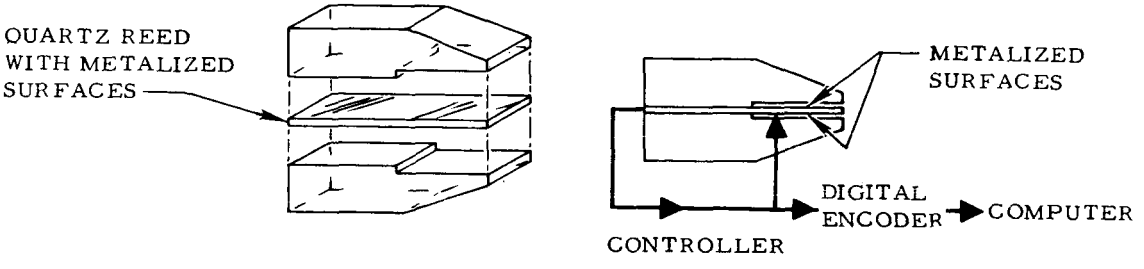

FEATURES

NO WARMUP REQUIRED
HIGH STABILITY
NO BEARINGS
NO LIQUIDS
INTEGRAL PICKOFF BRIDGE

WT 3 OZ

CHARACTERISTICS

SCALE FACTOR 1/100,000 GOAL, 1/20,000 FIRST MODEL
BIAS ACCURACY 1 $\widehat{SEC}$ GOAL, 4 SEC FIRST MODEL
ACCELERATION RANGE ±50g

Fig. IV-3. Autonetics Quartz Accelerometer

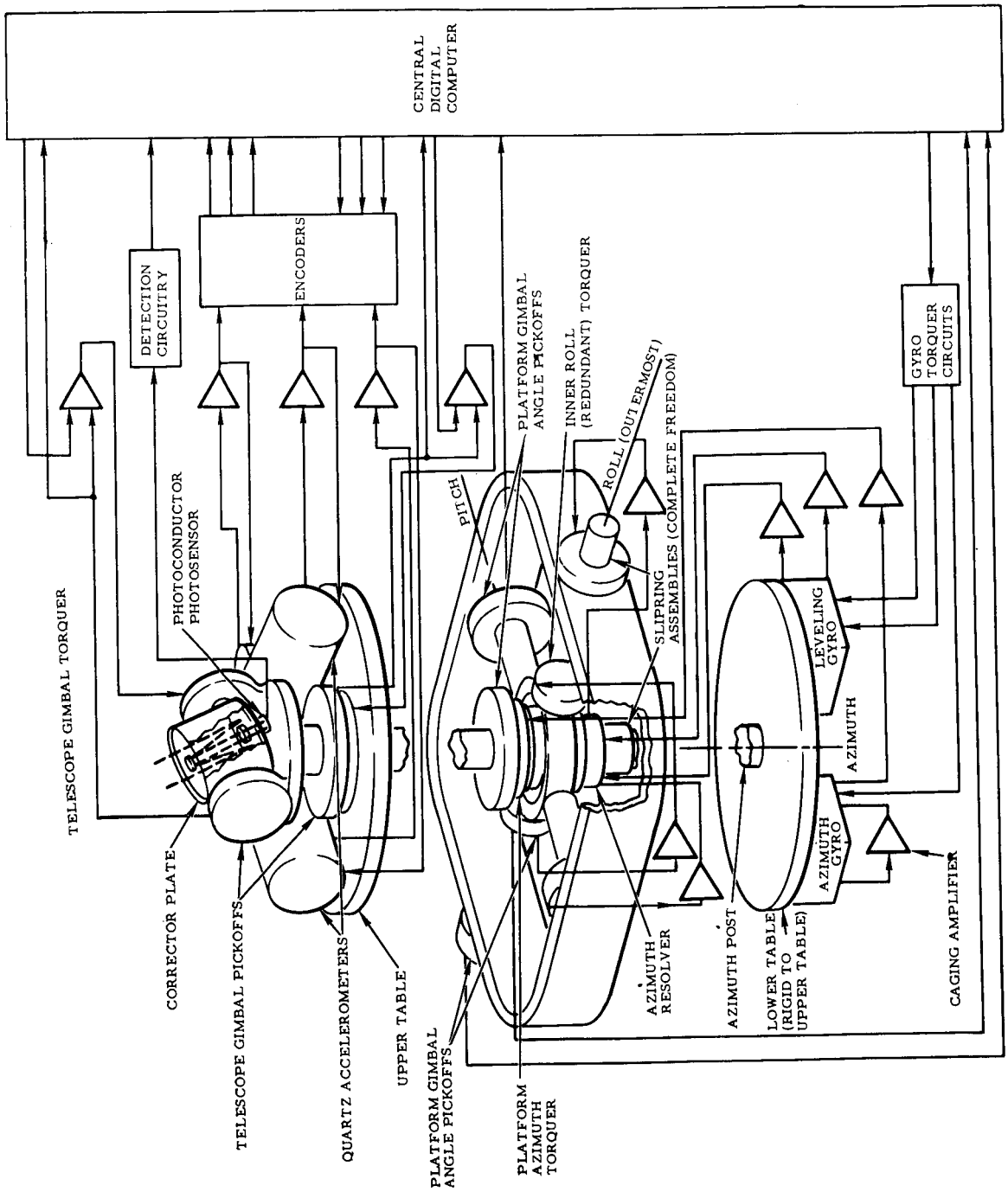

Fig. IV-4. Optical--Inertial System Platform Schematic

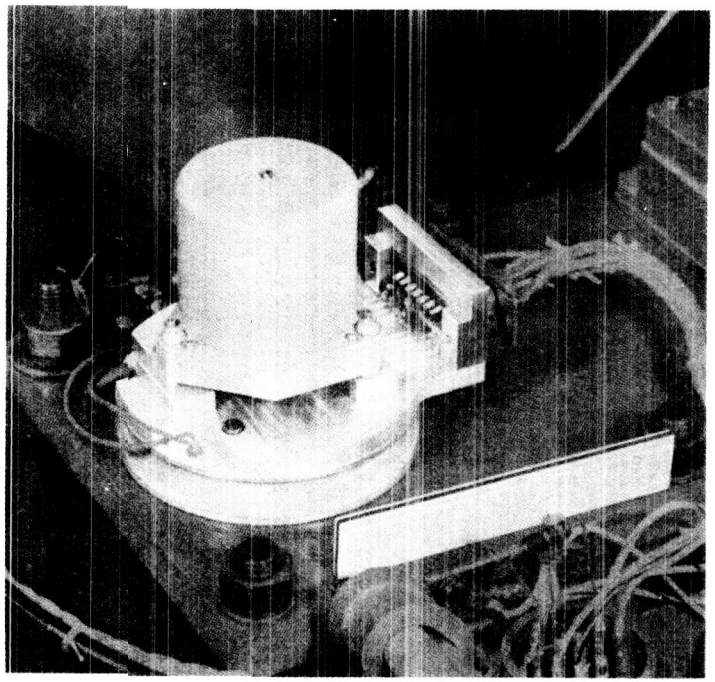

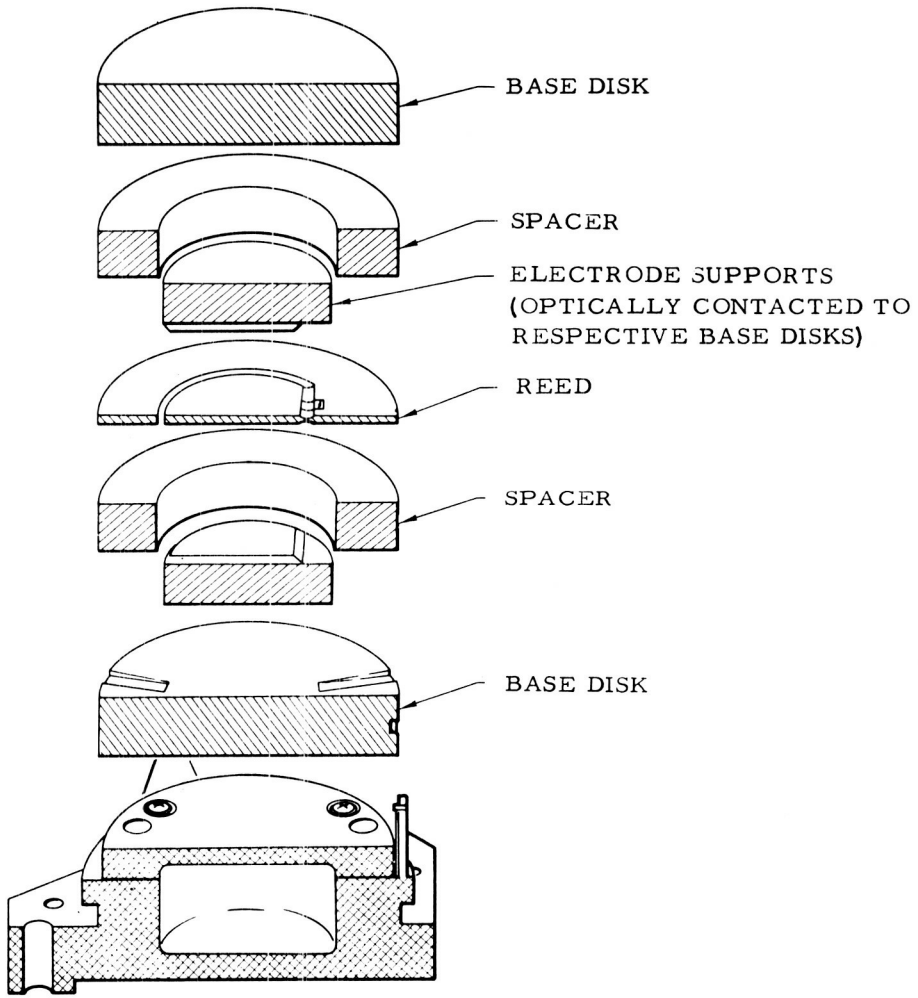

a. prototype instrument

b. exploded cross-section (less cover)

Fig. IV-5. Exterior and Interior of Quartz Accelerometer

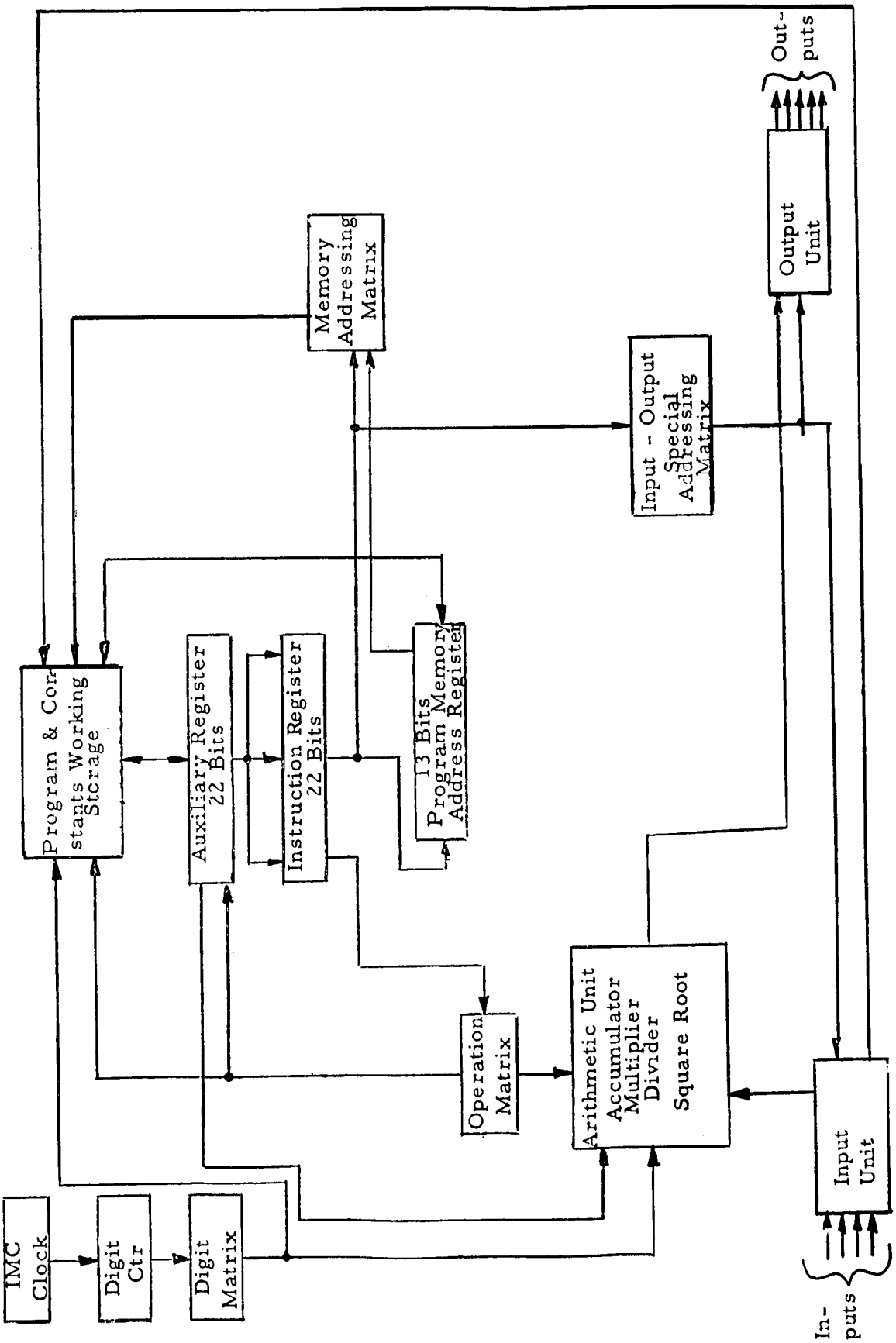

Fig. IV-6. Organization of Apollo Computer

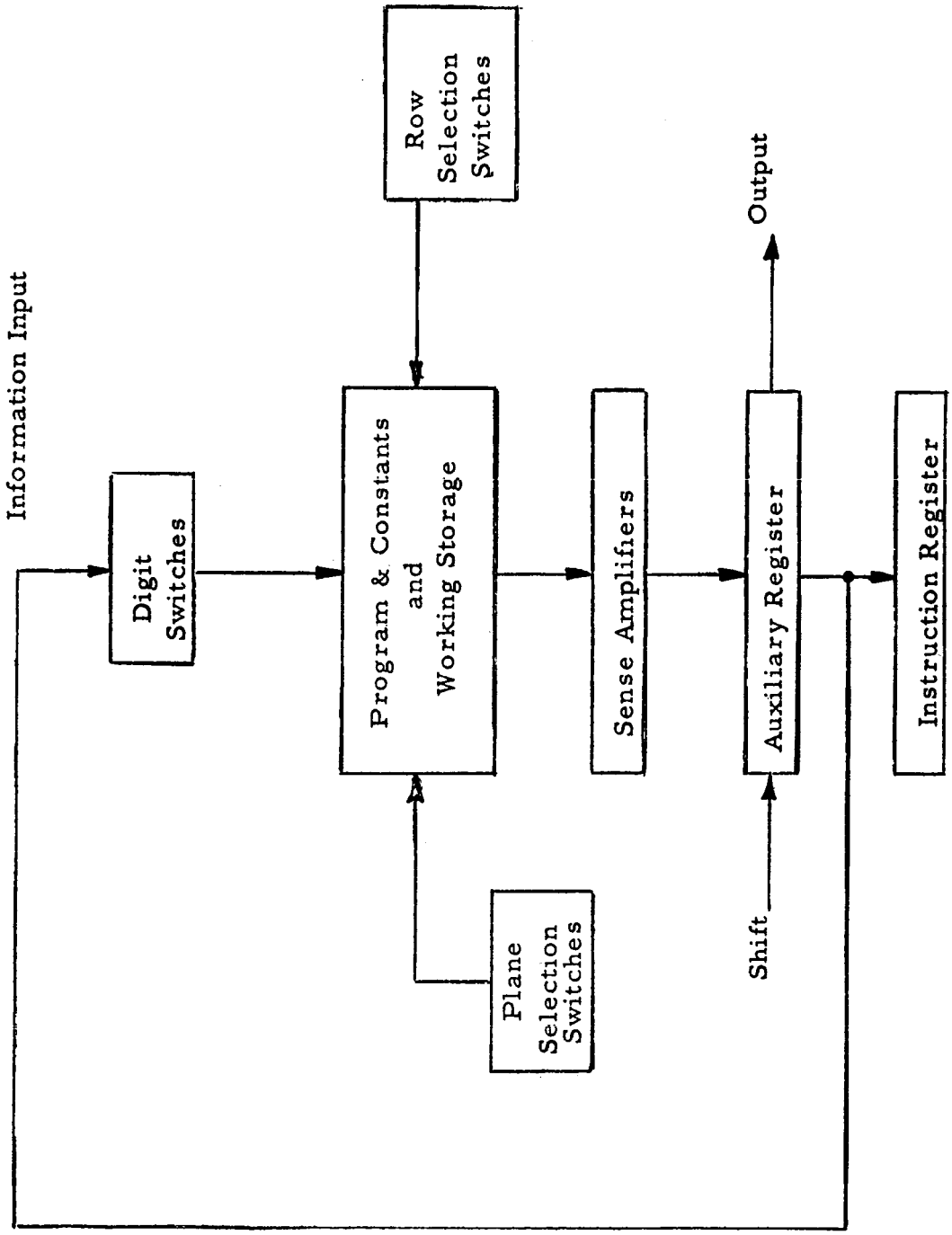

Fig. IV-7. Program Constants and Working Storage

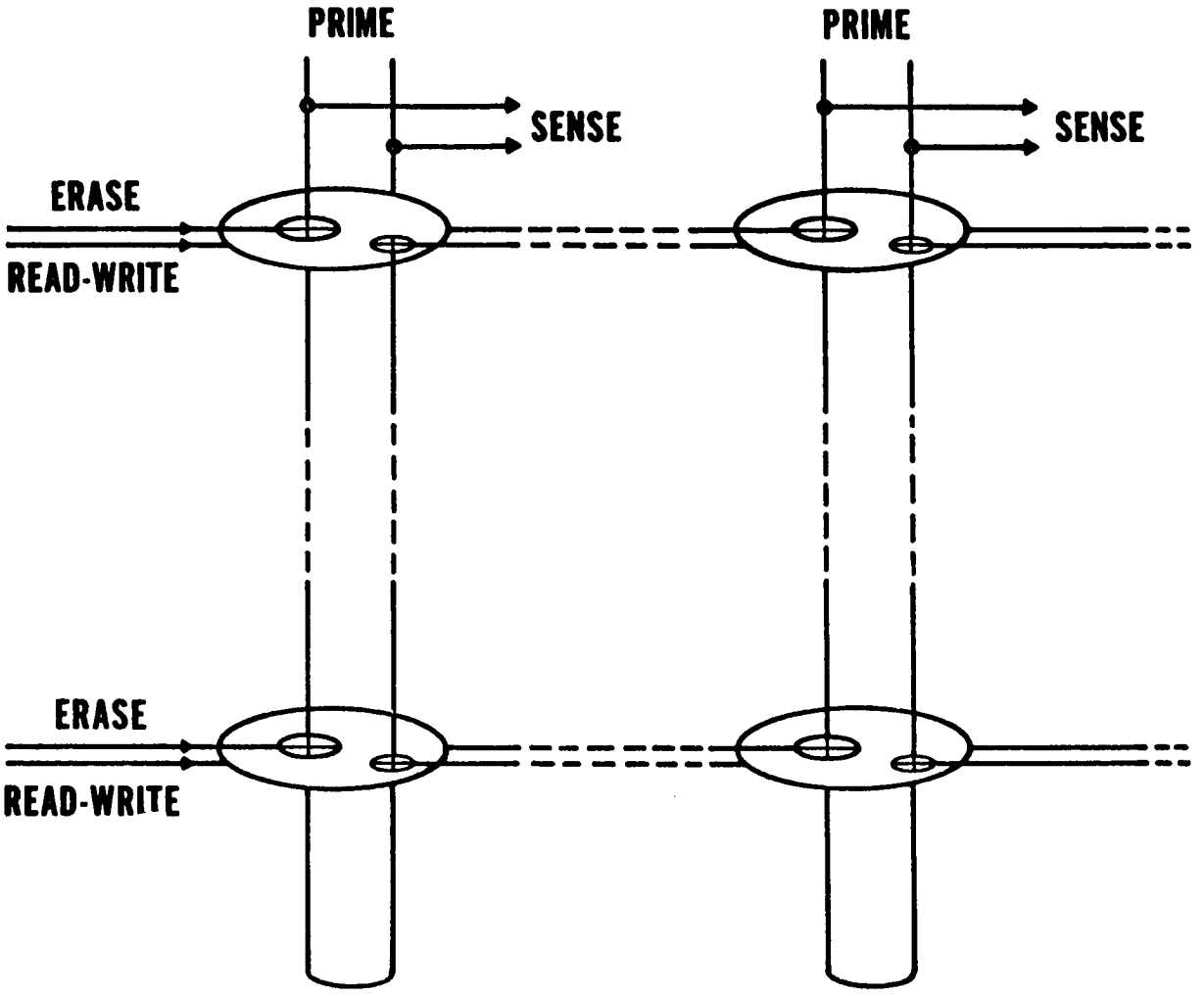

Fig. IV-8. Transfluxor Wiring Configuration

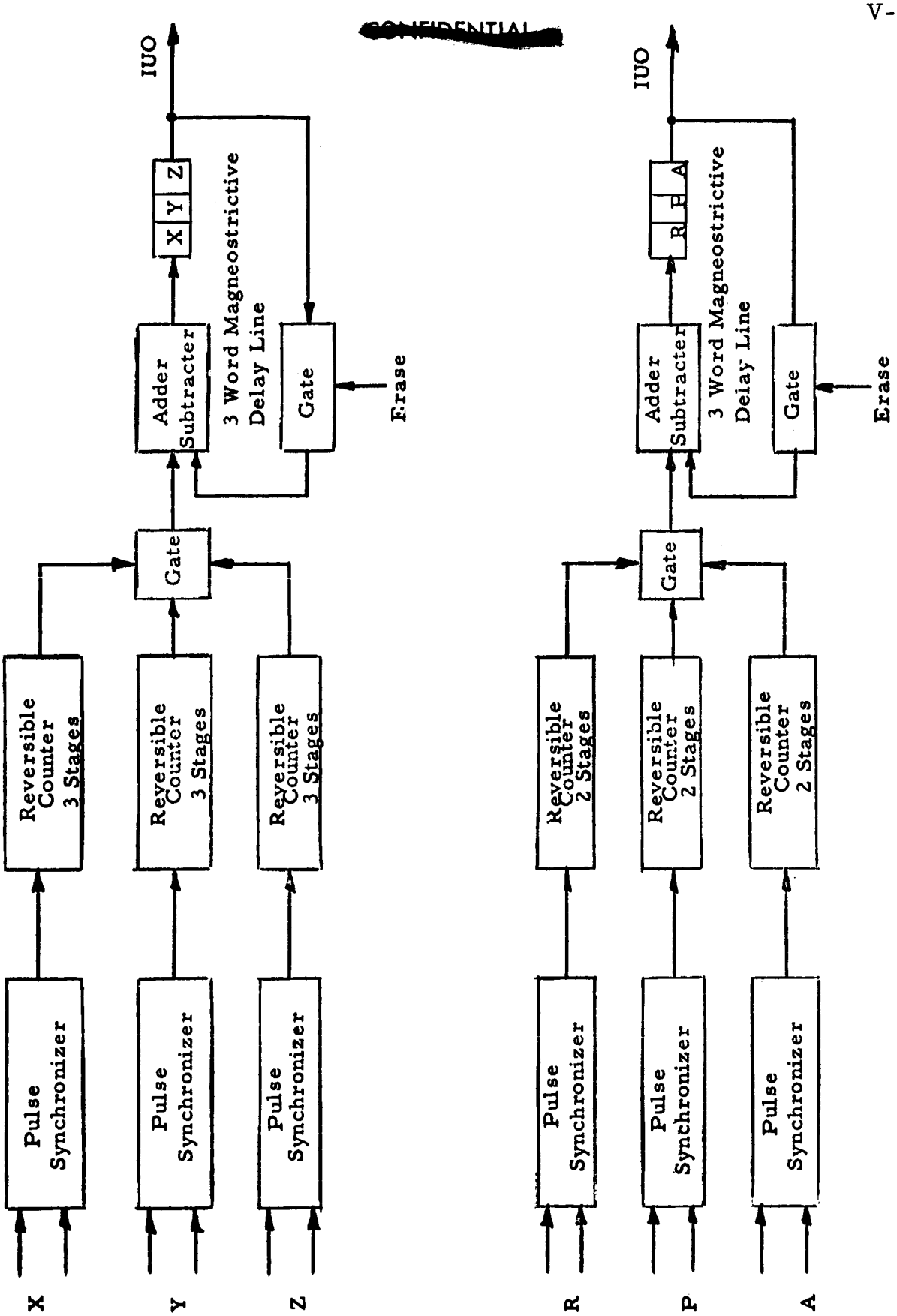

Fig. IV-9. Accelerometer and Gimbal Angle Inputs

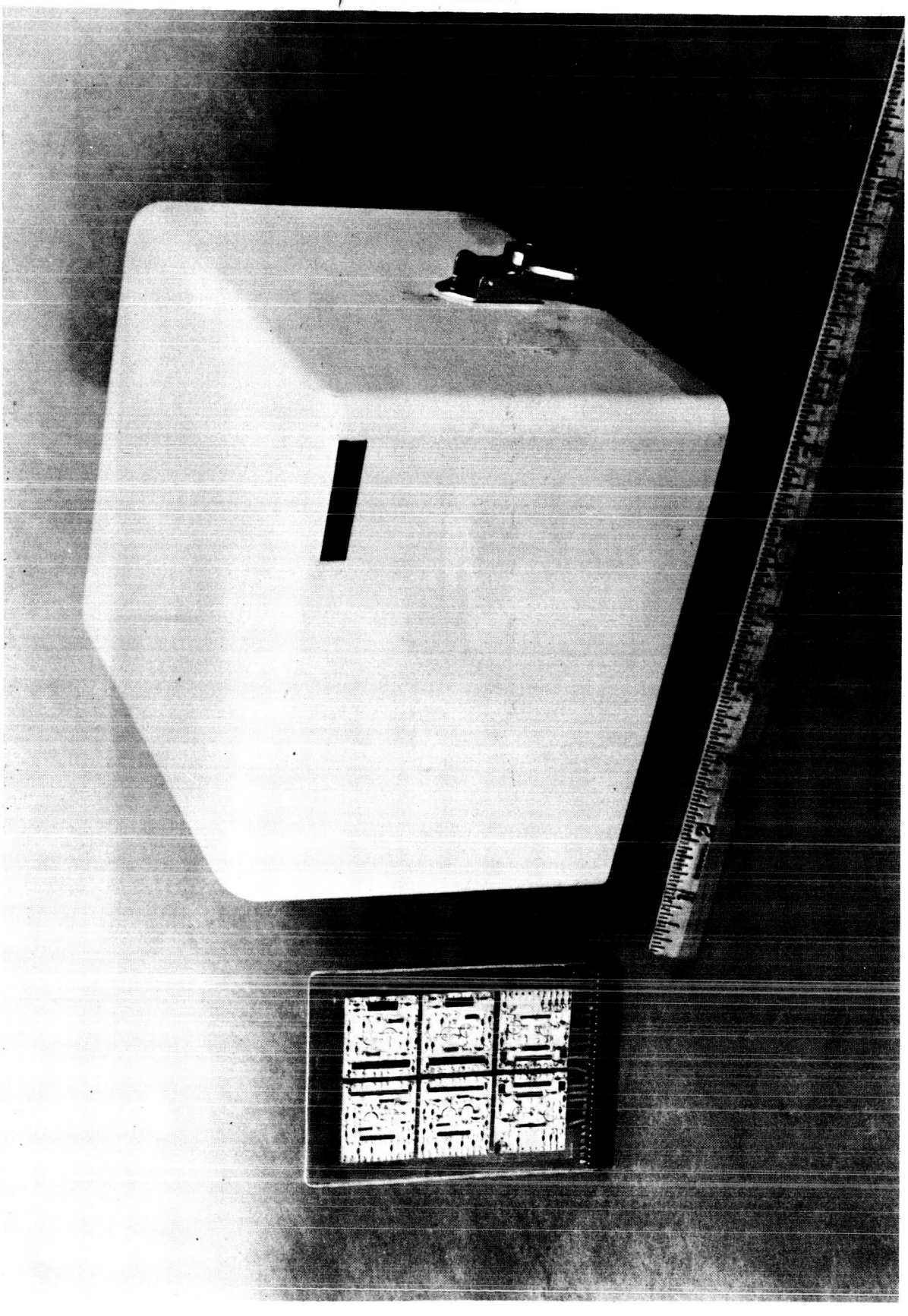

Fig. IV-10. Digital Computer

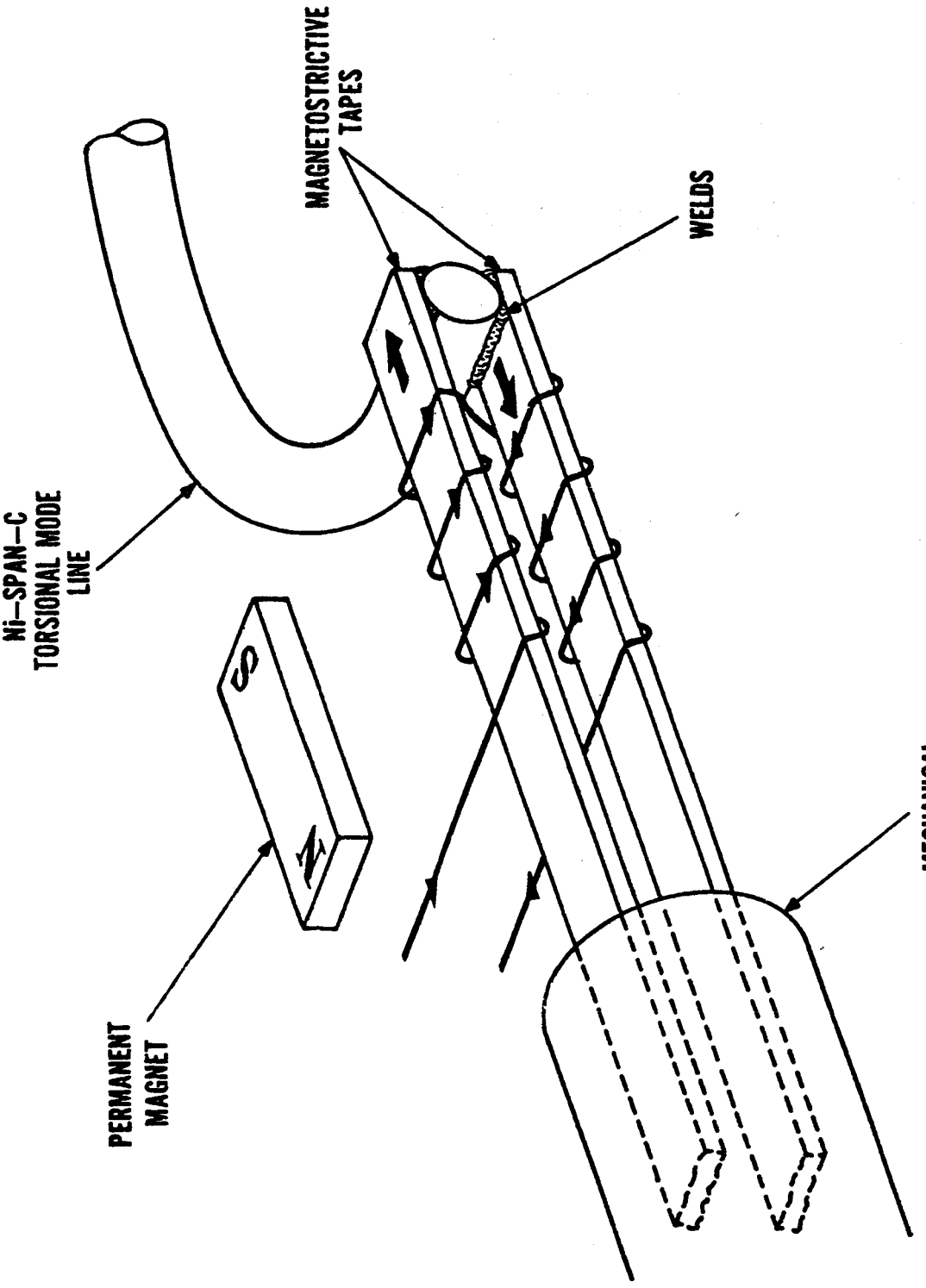

Fig. IV-11. Magnetostrictive Delay Line Input Transducer and Torsional Line

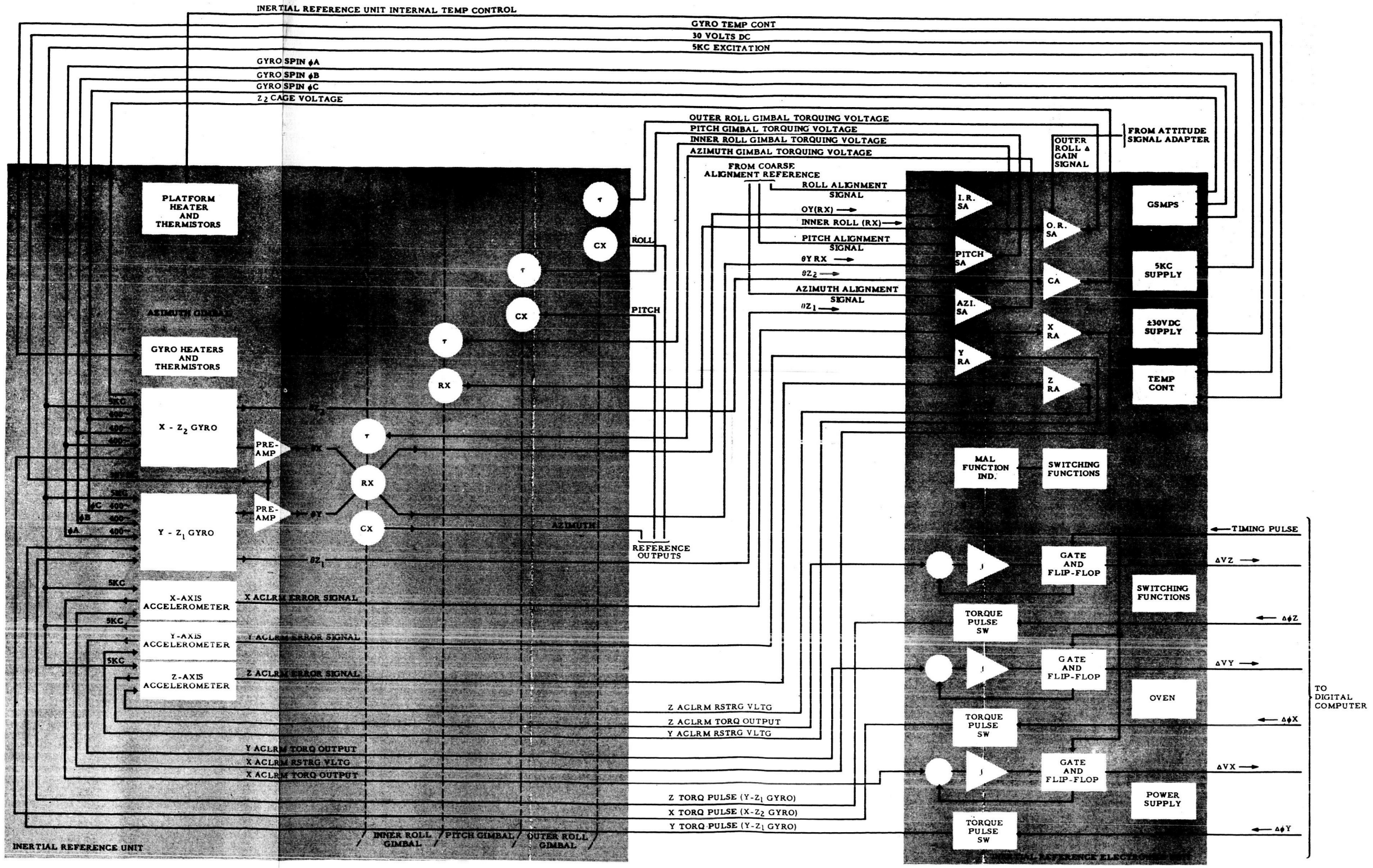

Fig. IV-12. Block Diagram of Inertial Measurement Subsystem

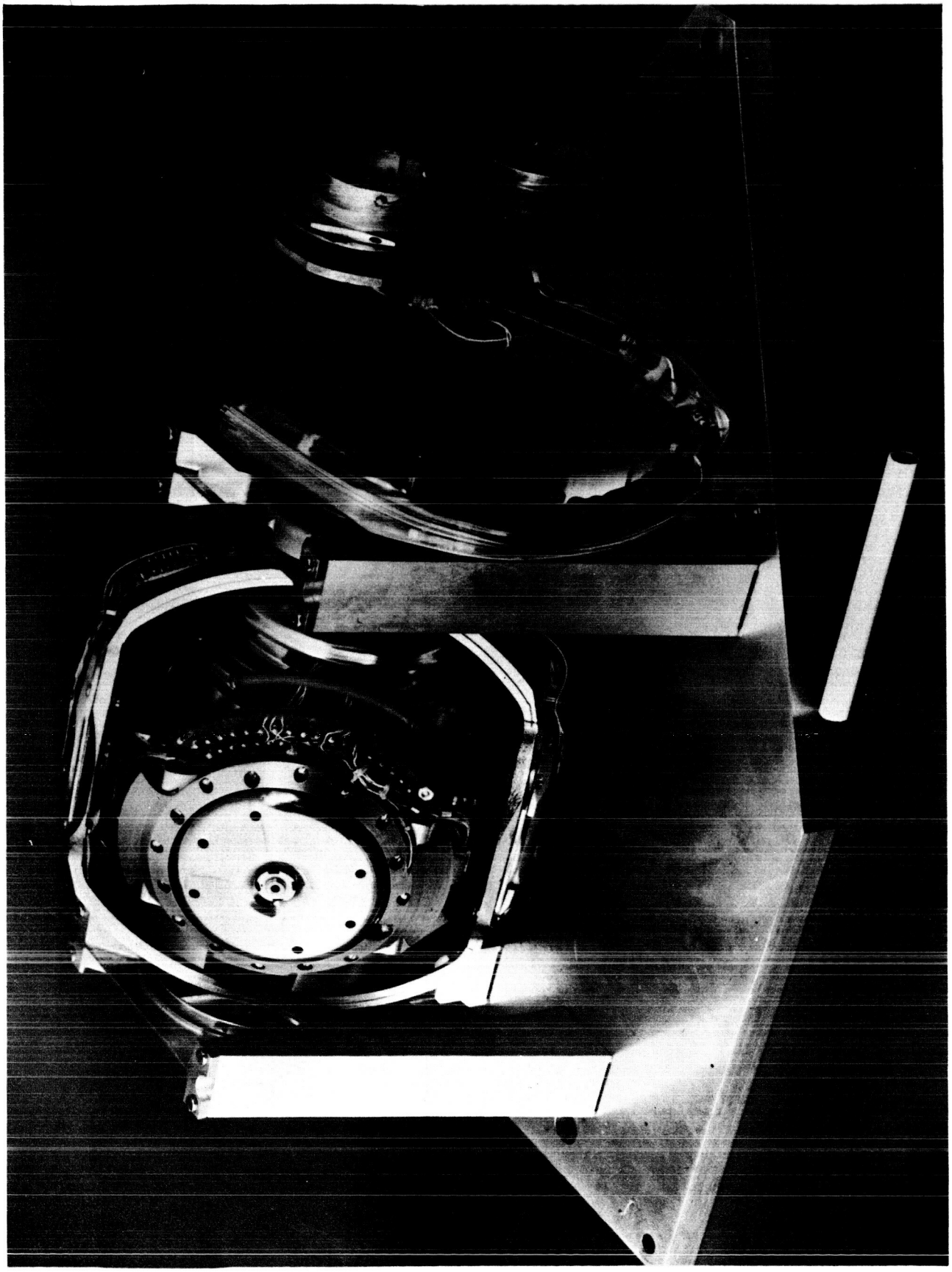

Fig. IV-13. Miniature Platform

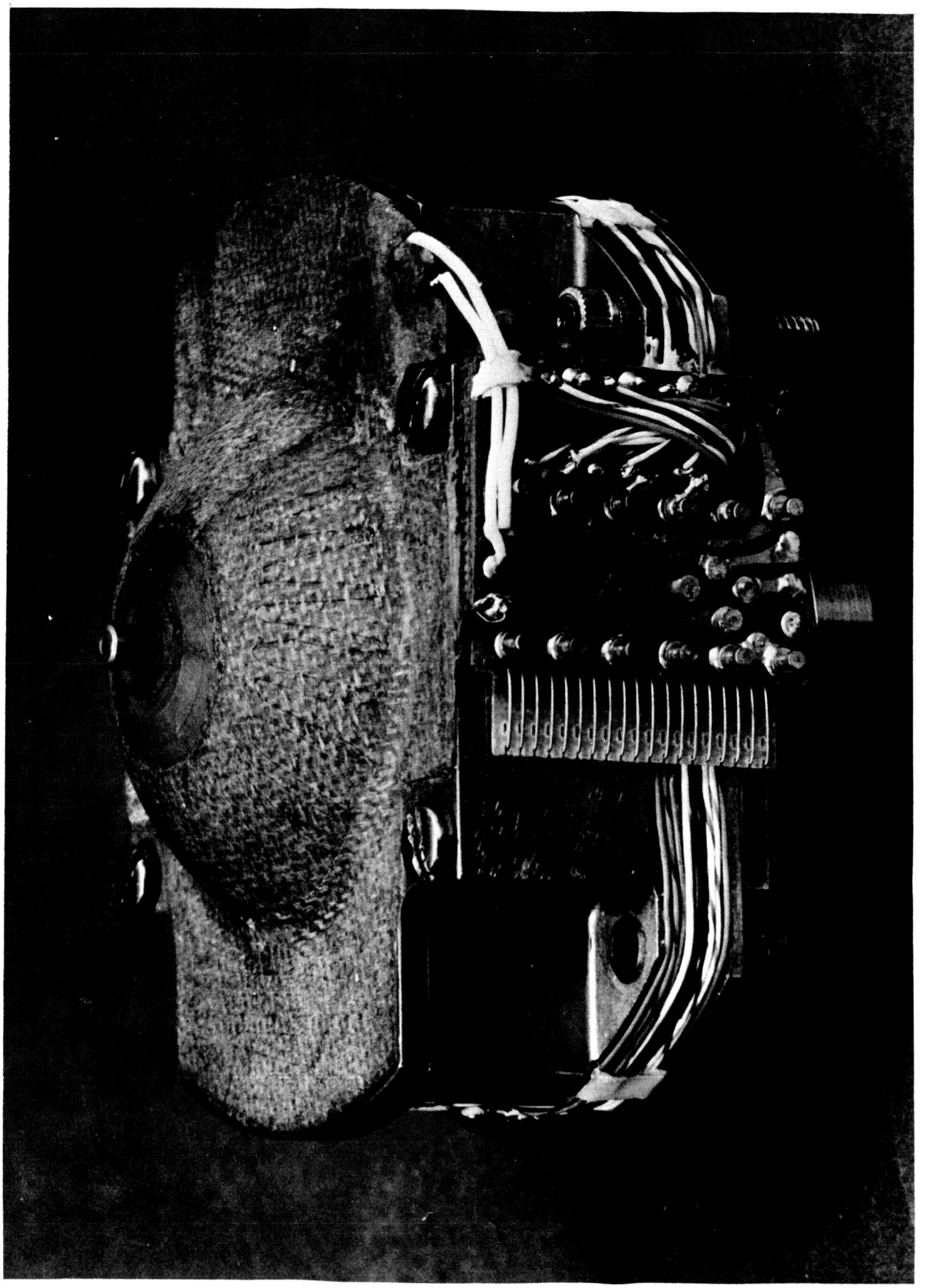

Fig. IV-14. Miniature Platform Gyro

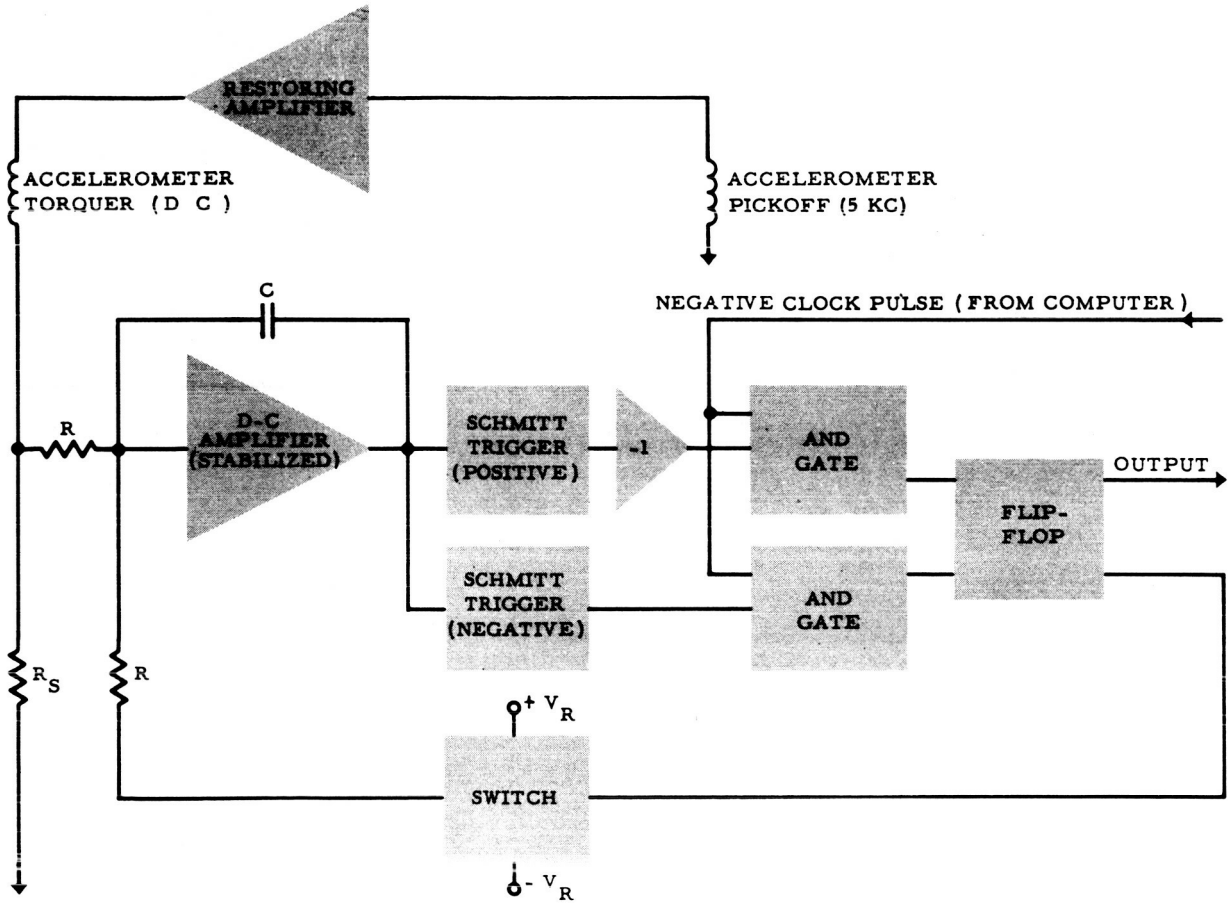

Fig. IV-15. Accelerometer Restoring and Digital Conversion

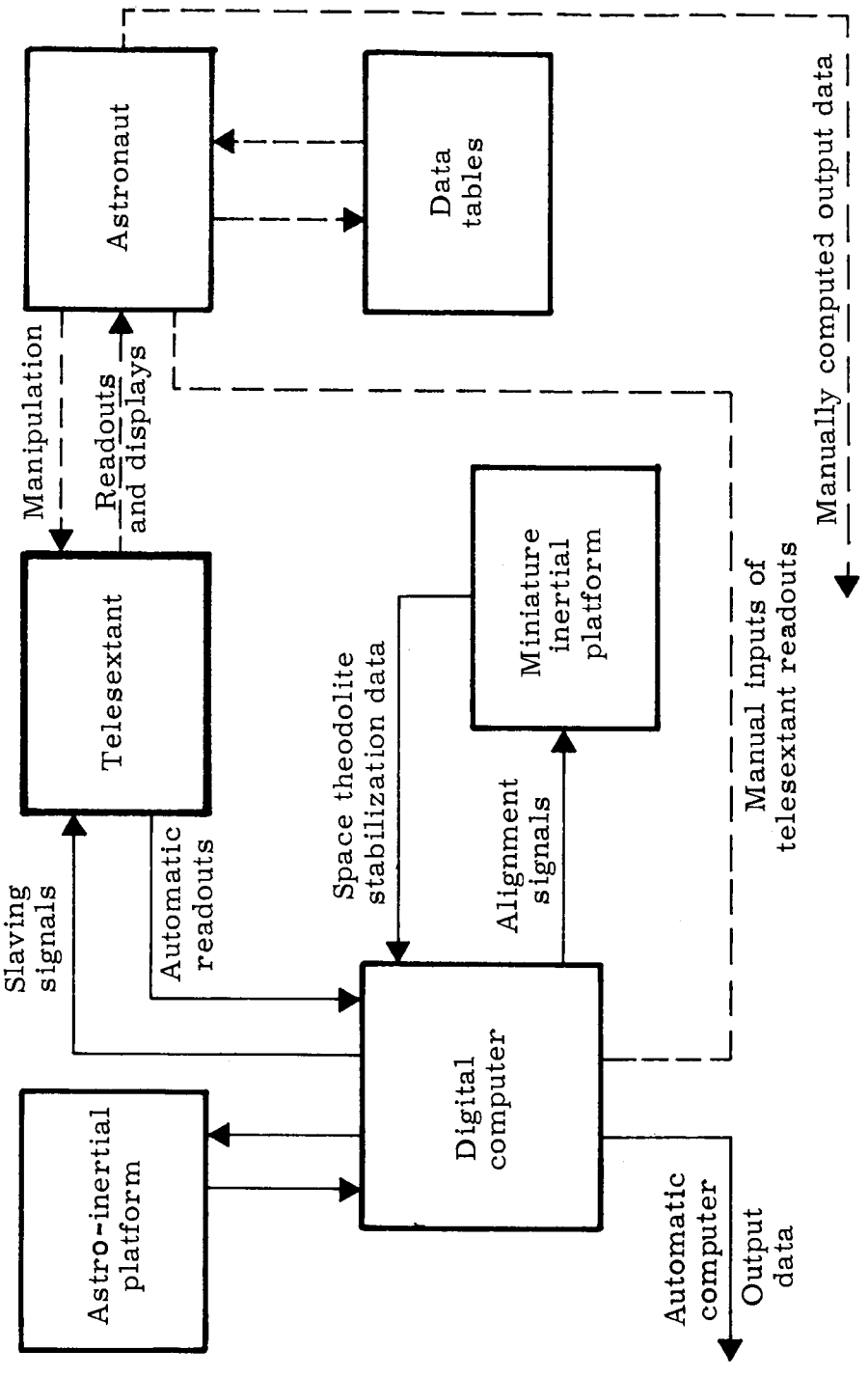

Fig. IV-16. Spacecraft Navigation System

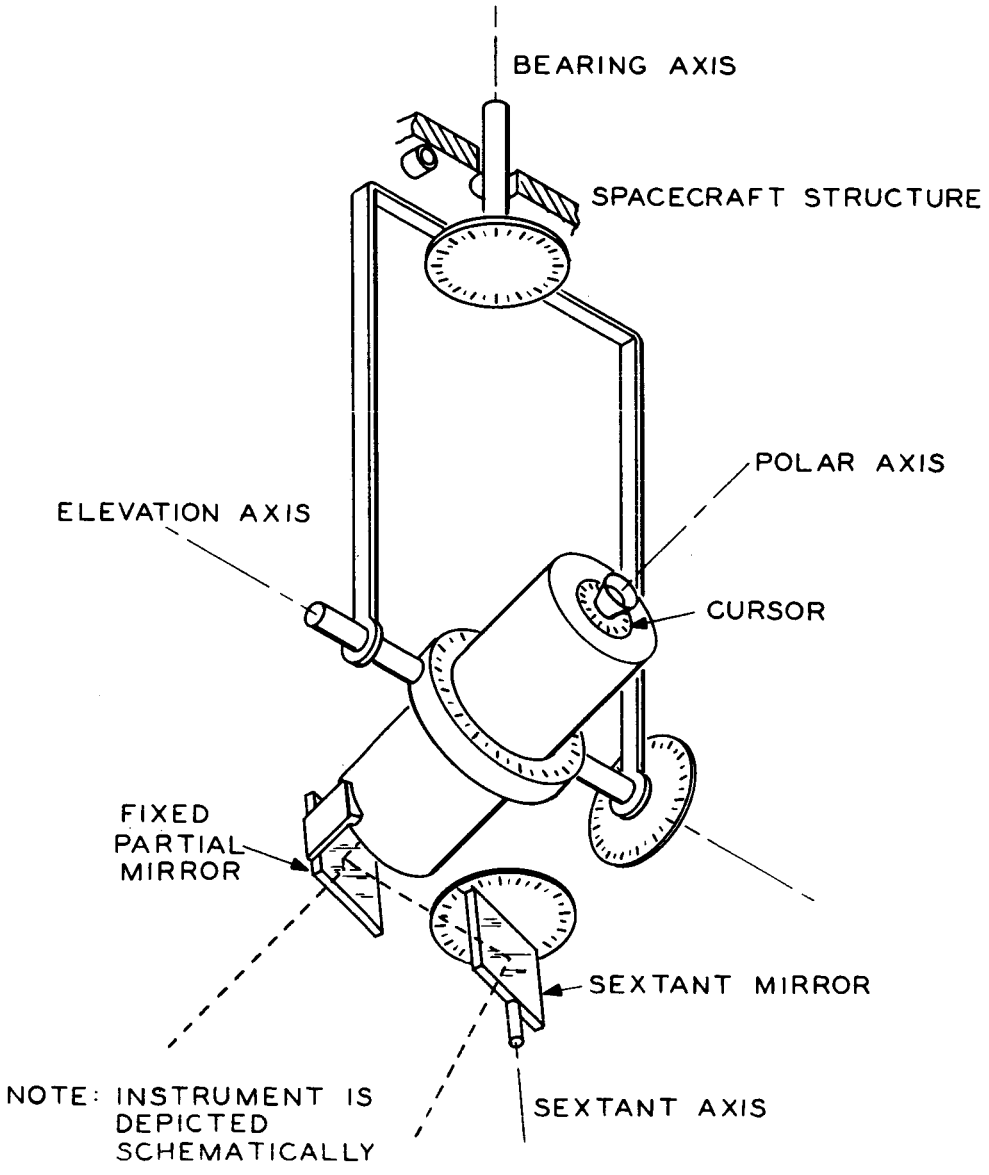

Fig. IV-17. Telesextant

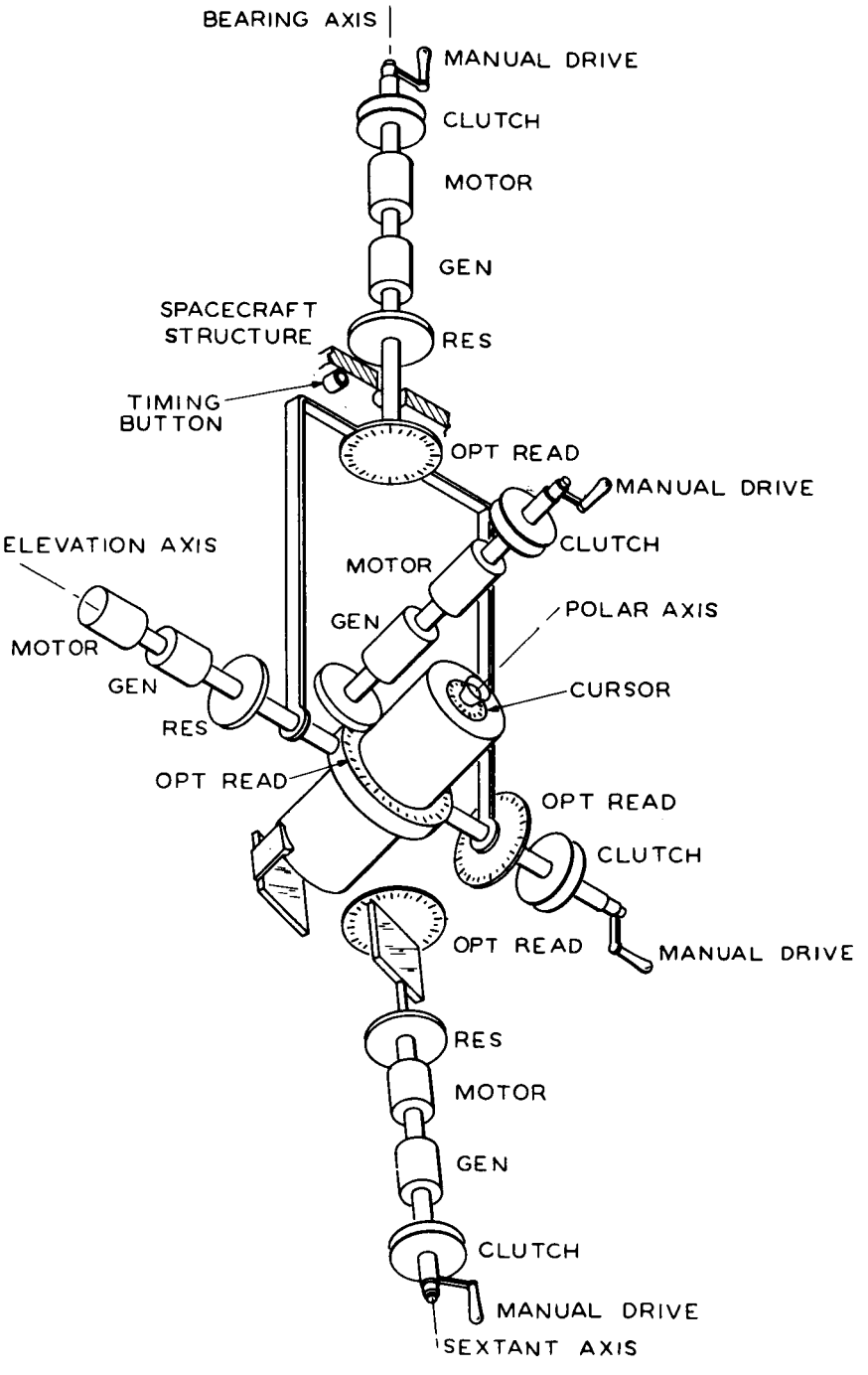

Fig. IV-18. Mechanical Schematic of the Telesextant

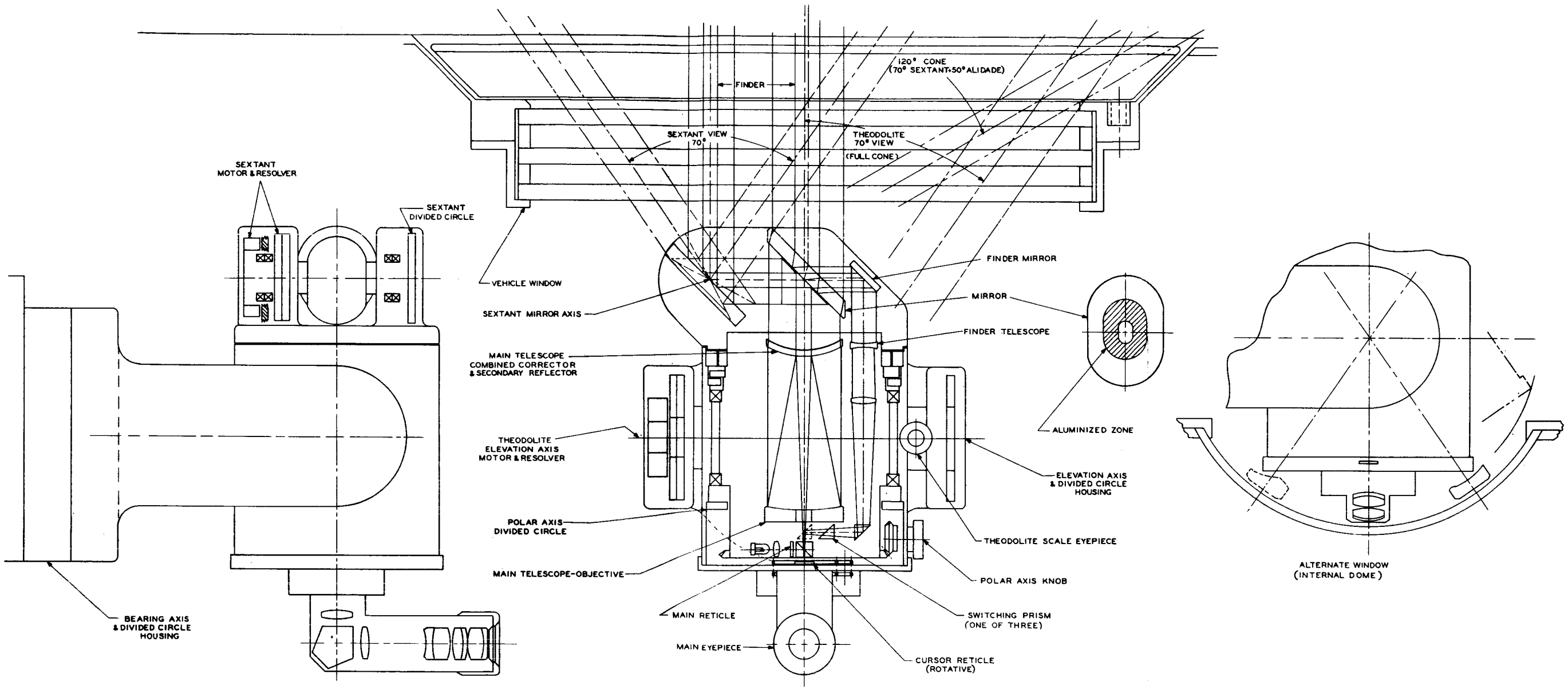

Fig. IV-19. Telesextant

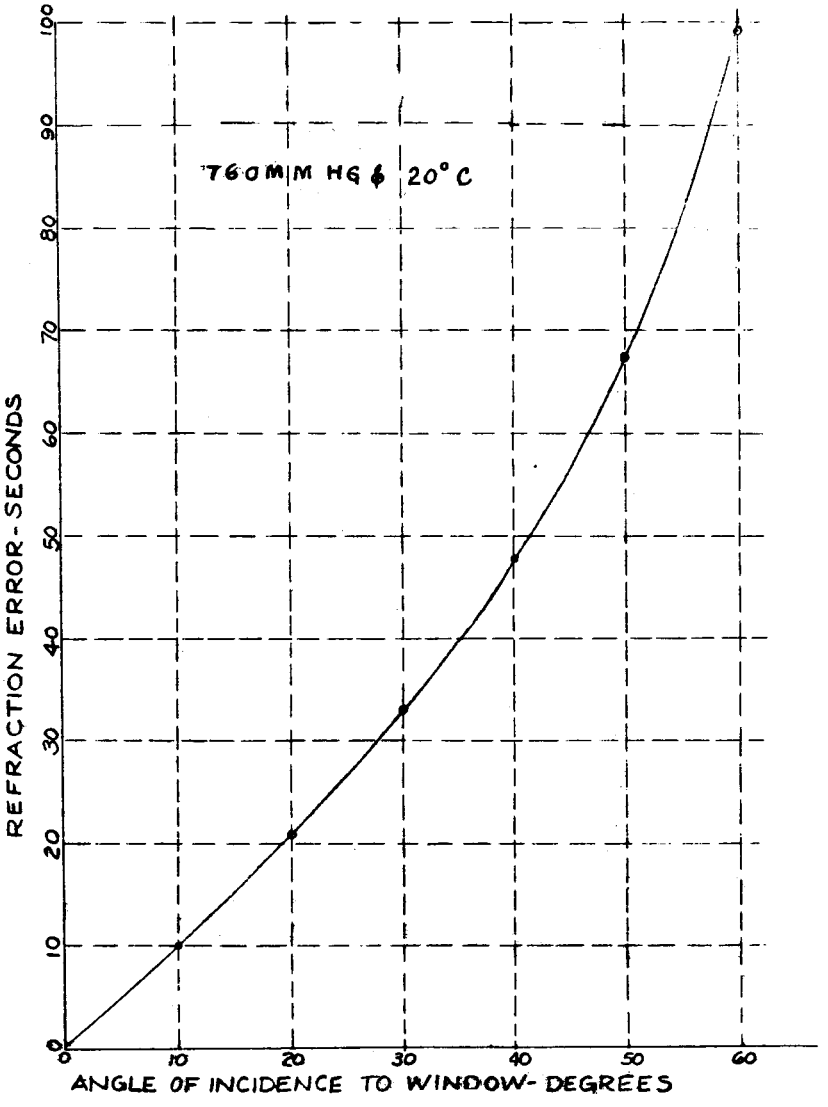

Fig. IV-20. Refraction Through a Plane Parallel Window Between a Vacuum and Air

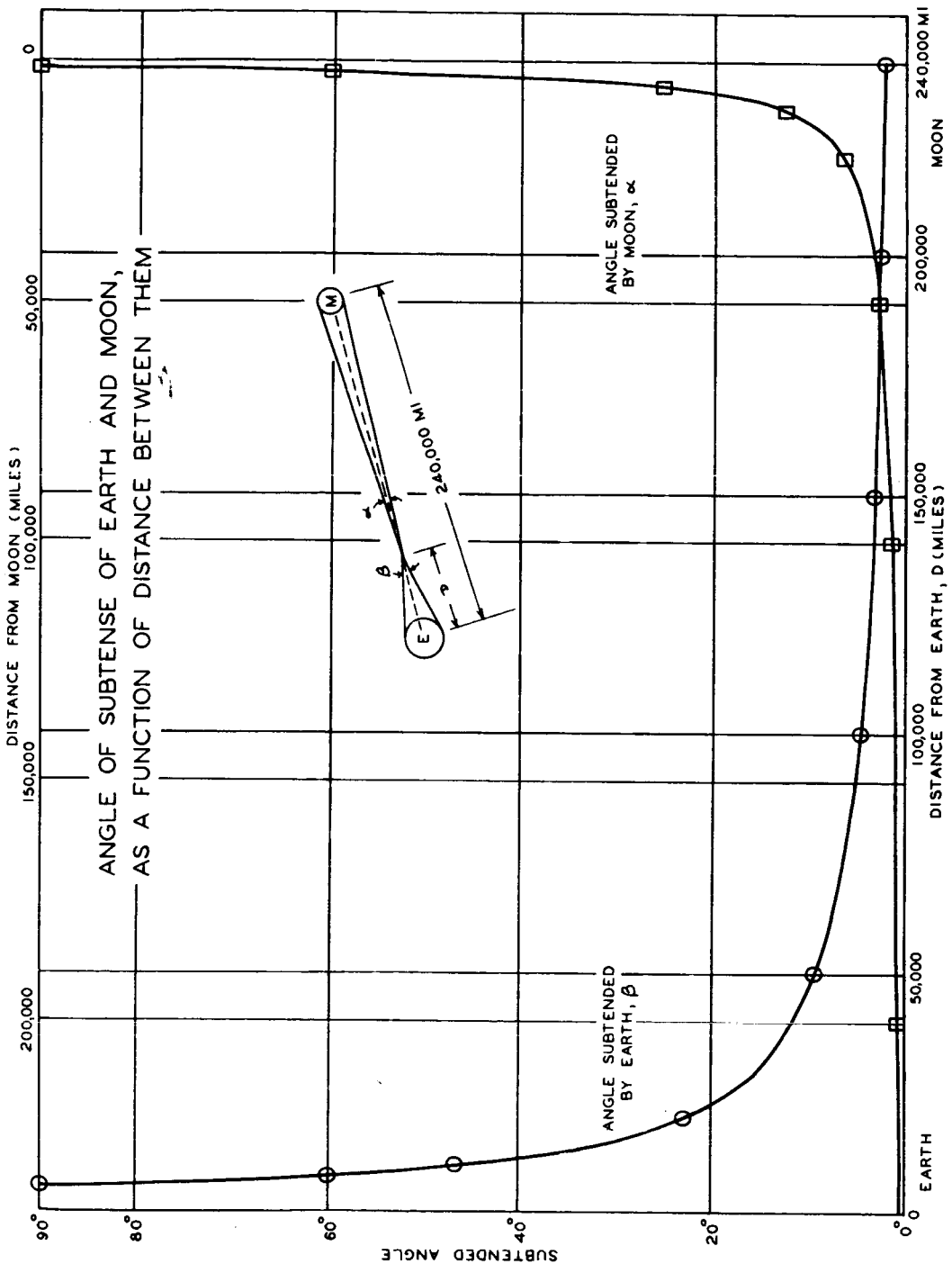

Fig. IV-21. Angle of Subtense of Earth and Moon, as Function of Distance Between Them

(A) EQUIPMENT SCHEMATIC

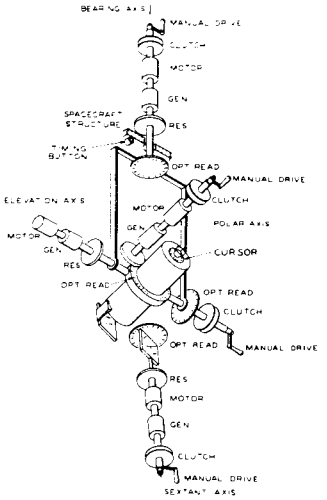

(B) MODE: MANUAL DRIVE

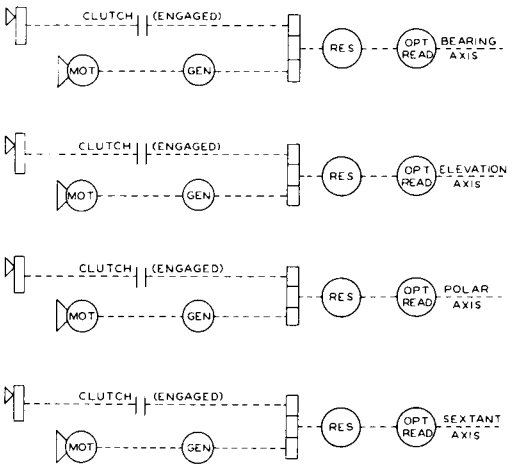

(C) MODE: MANUAL CONTROL (AIDED)

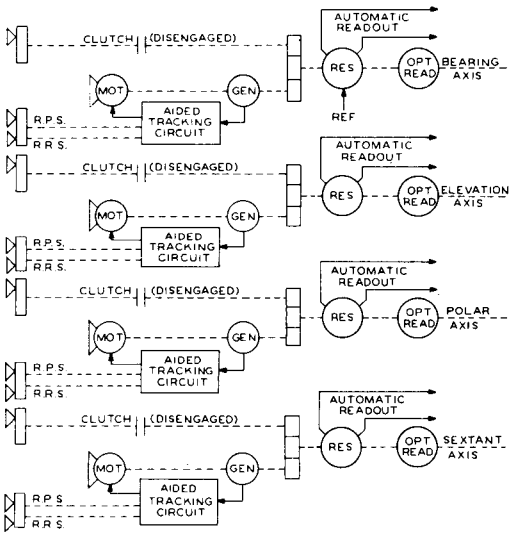

(D) MODE: AUTOMATIC STABILIZATION VIA INERTIAL PLATFORM DERIVED OUTPUTS

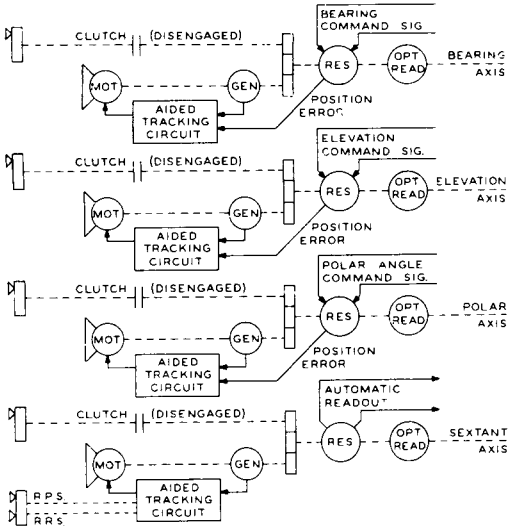

(E) MODE: AUTOMATIC FOLLOWING OF AUTOMATIC TRACKER* (ELEVATION AND BEARING SLAVING)

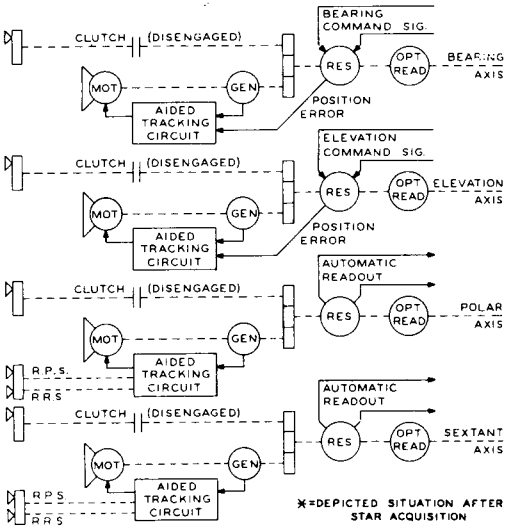

(F) AIDED TRACKING CIRCUIT

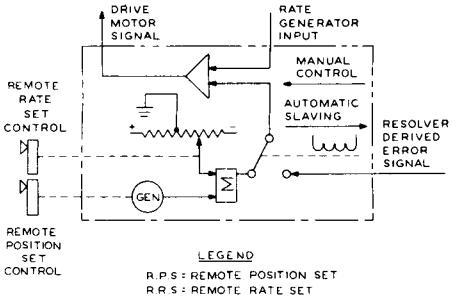

Fig. IV-22. Stabilization Modes and Equipment

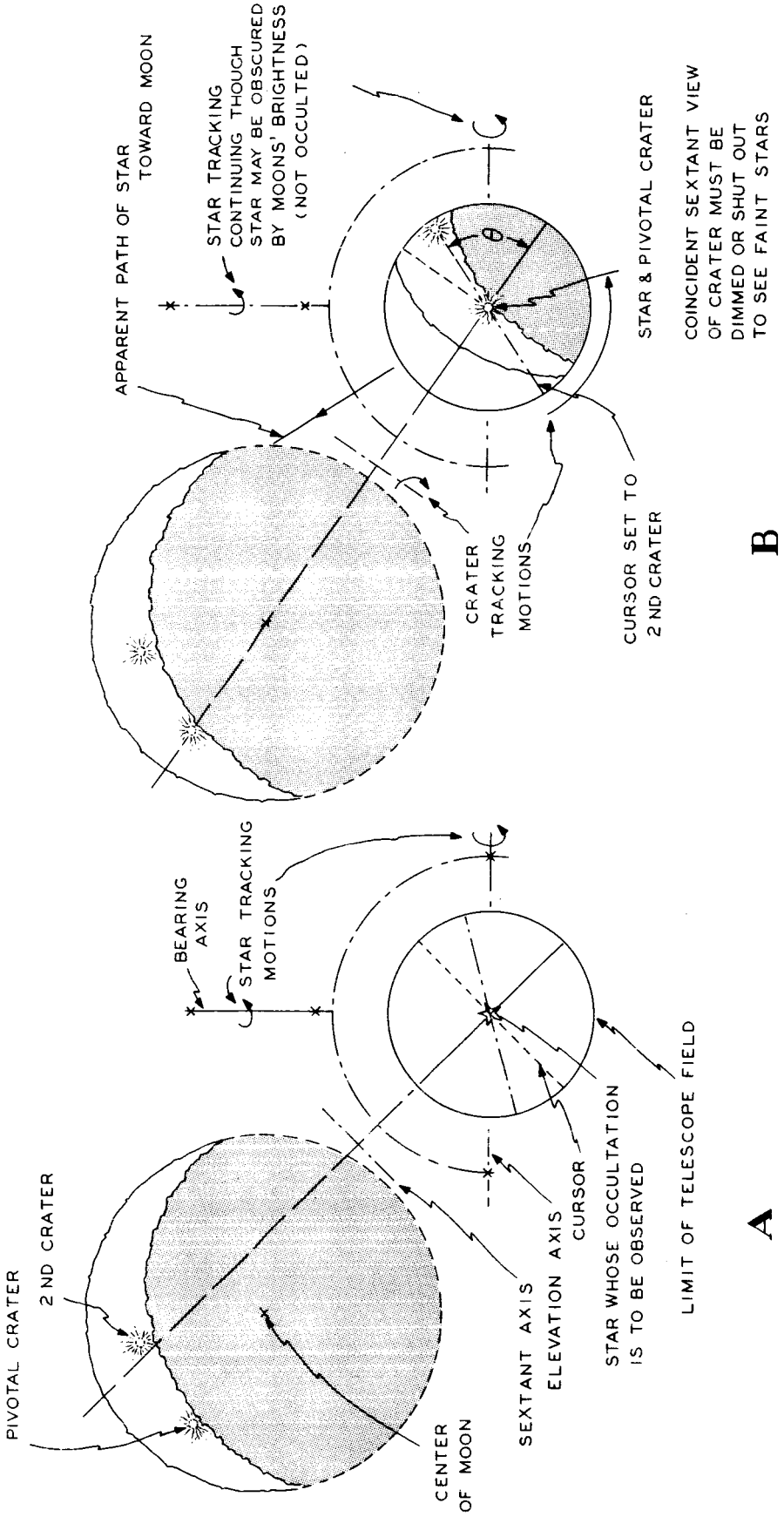

Fig. IV-23. Occultation Measurement

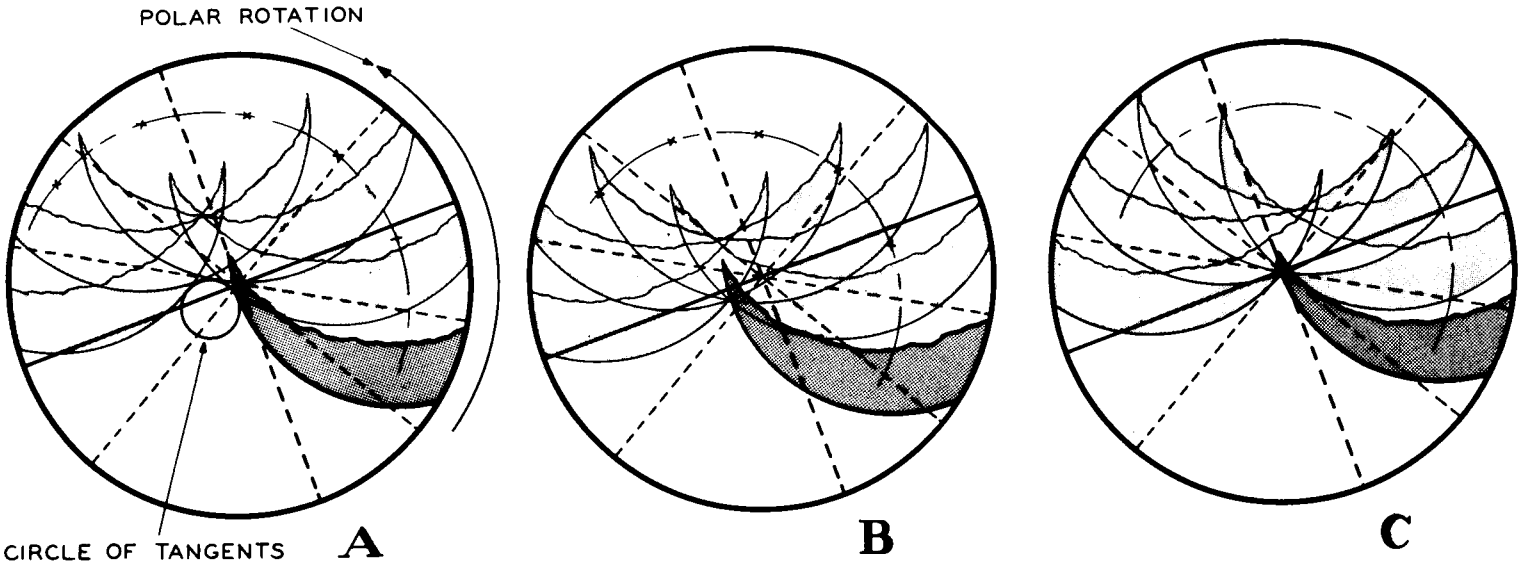

STEP 1 - THEODOLITE POINTED APPROXIMATELY TO TRACK CENTER OF MOON

STEP 2 - SEXTANT SET TO BRING EDGE TO CENTER OF FIELD WITH THEODOLITE VIEW DIMMED OUT.

STEP 3 - POLAR AXIS SET IN ROTATION. SITUATION AS SHOWN ABOVE

STEP 4 - REDUCTION OF THE CIRCLE OF TANGENTS TO A POINT BY ADJUSTMENT OF THE SEXTANT ANGLE. NOTE THAT THIS ADJUSTMENT ALONE IS SUFFICIENT FOR STADIA RANGING. TO PERFORM THE ADJUSTMENT PRECISELY, A REFERENCE POINT IS NEEDED. THIS IS PROVIDED IN STEP 5

STEP 5 - MOVING THE POINT OF TANGENCY TO THE RETICLE CENTER BY THEODOLITE ADJUSTMENT. REPEAT STEP 4 AS NEEDED. MOON'S RADIUS AS AN ANGULAR SUBTENSE IS READ ON THE SEXTANT ANGLE.

Fig. IV-24. Stadiametric Measurement

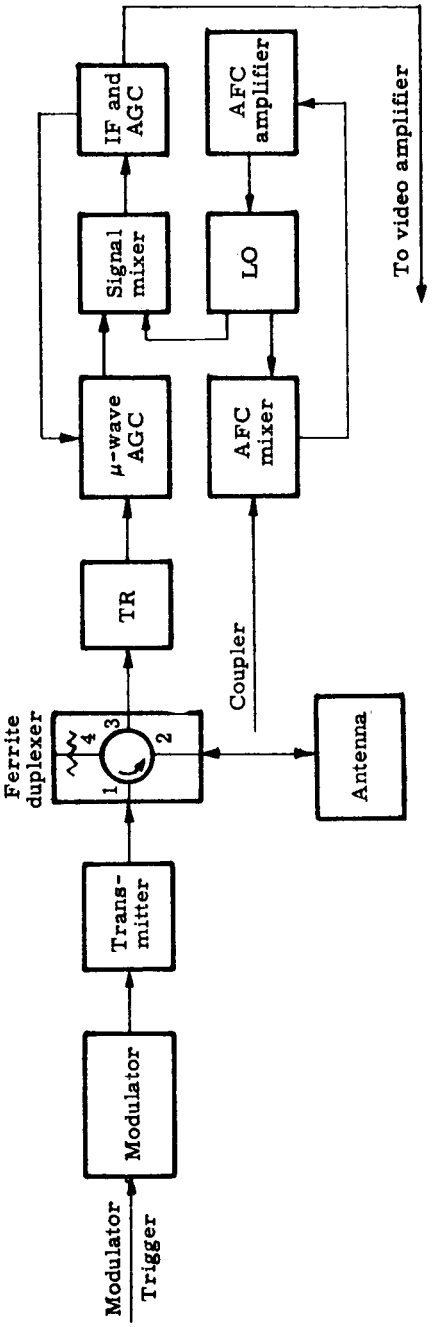

Fig. IV-25. Transmitter and Receiver Diagram

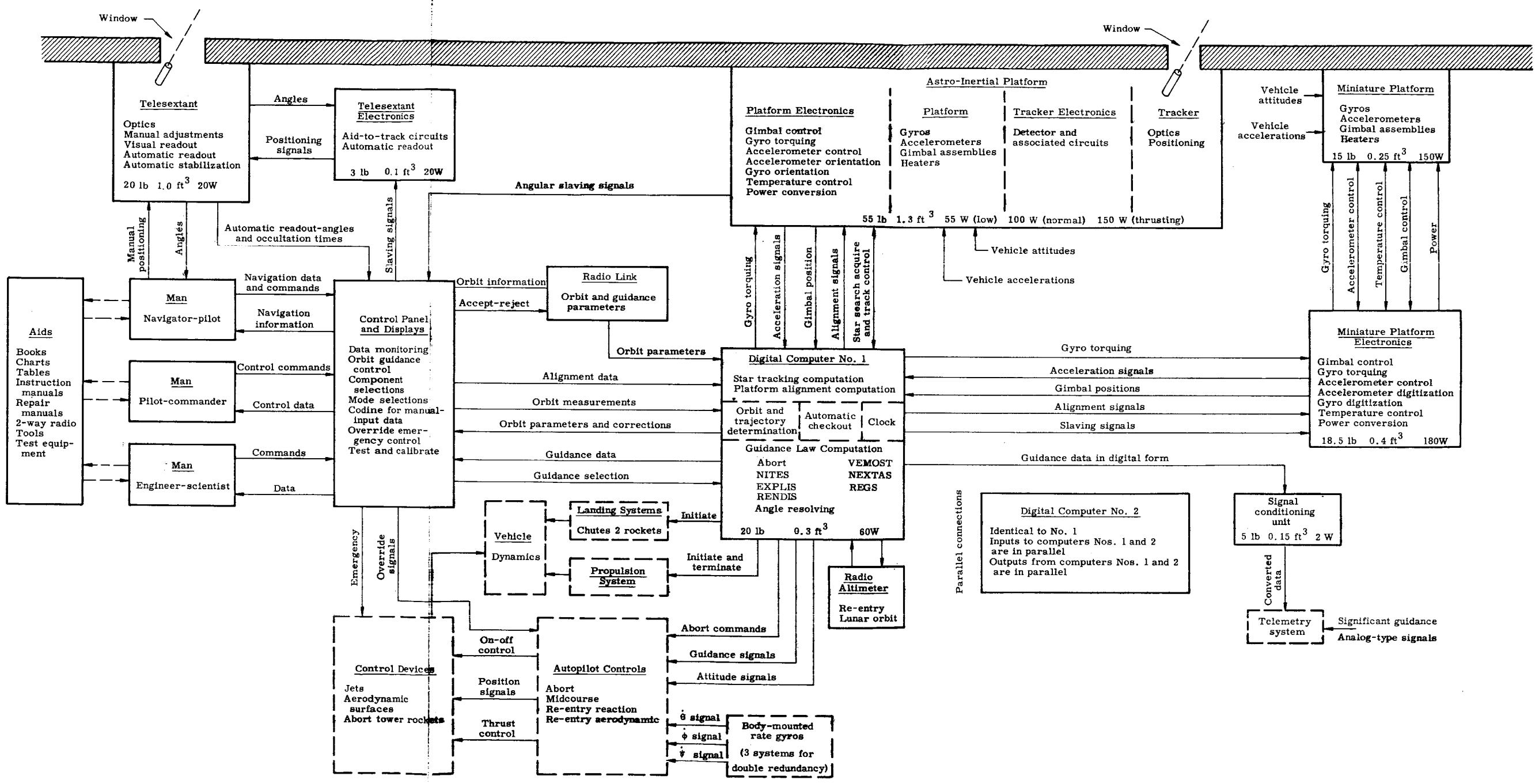

Fig. IV-26. Guidance System Block Diagram

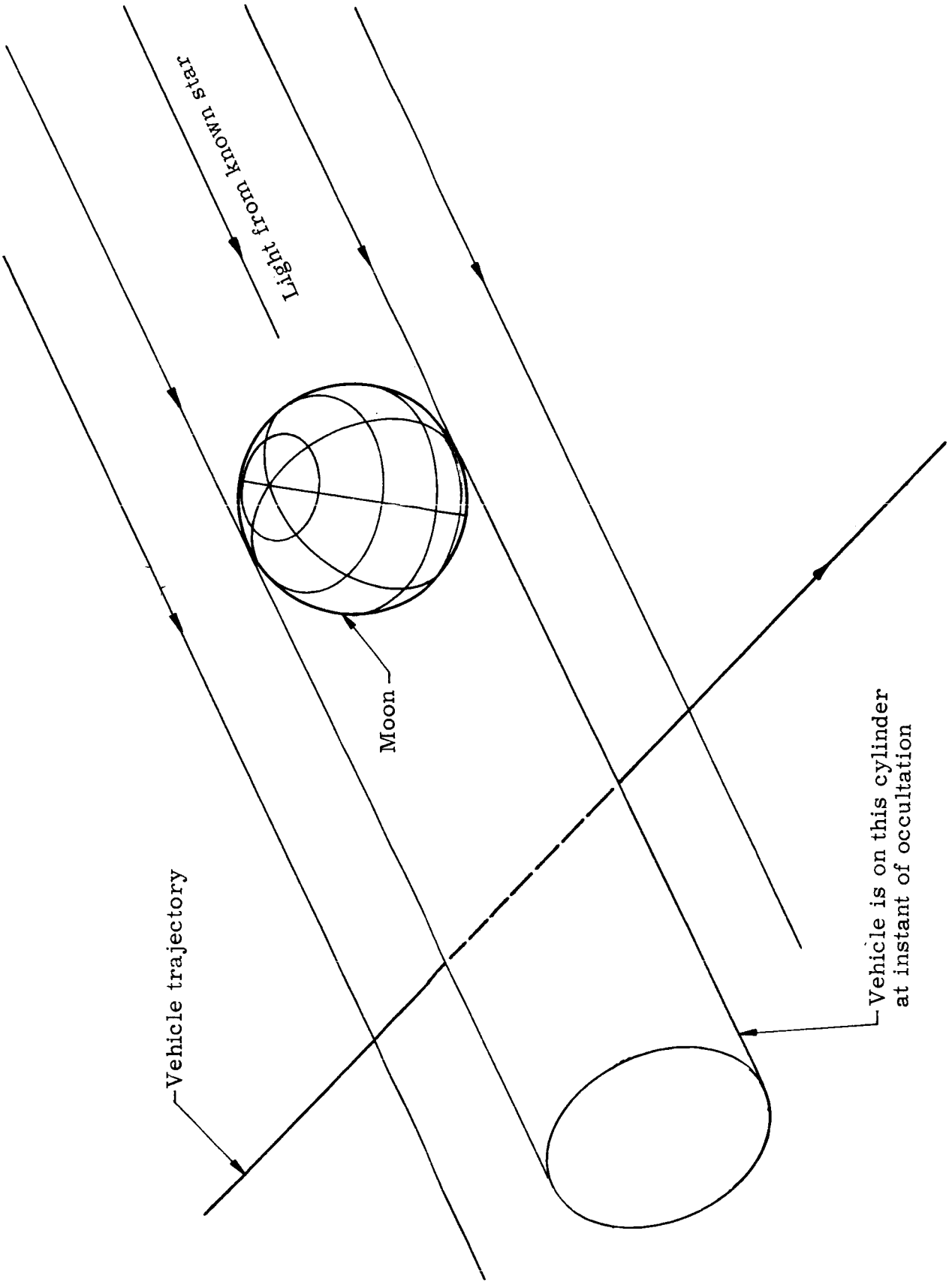

Fig. V-1. Occultation Geometry

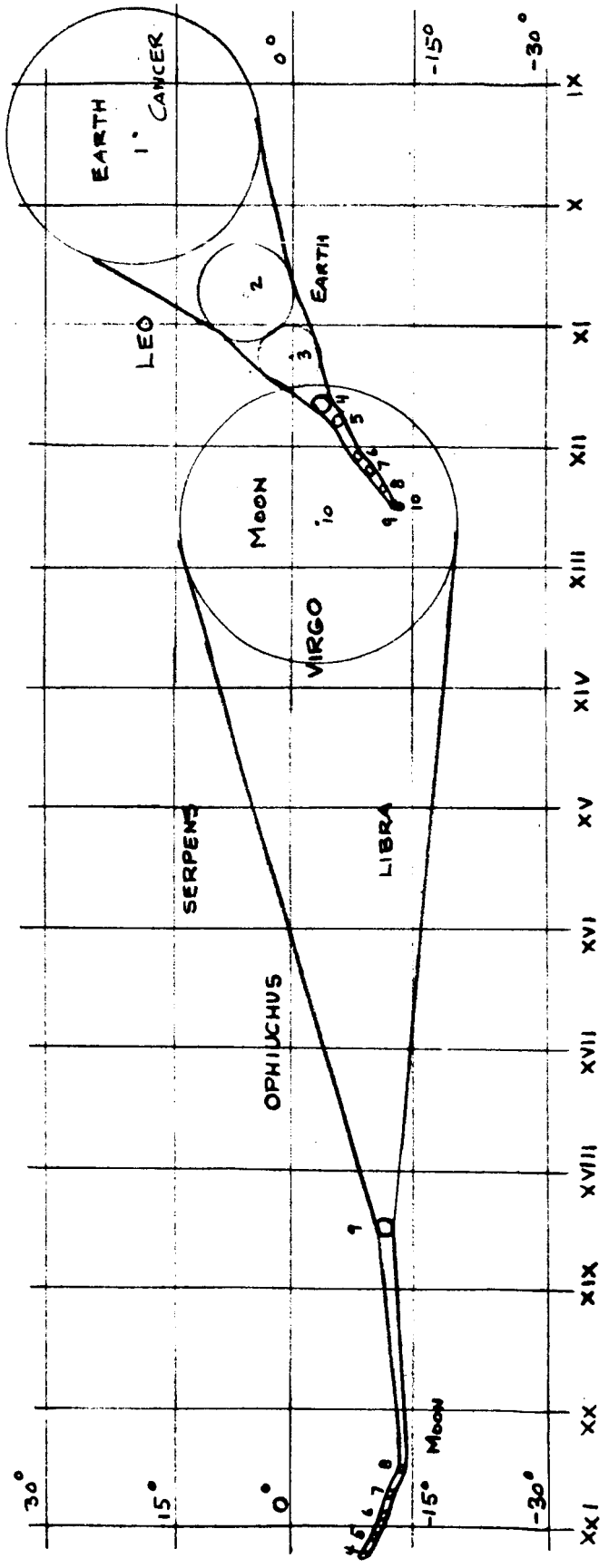

EARTH - MOON TRAJECTORY

INJECTION: OCT 29, 1960, 11h05m (GCT)			
POINT	FLIGHT TIME (HRS)	DISTANCE FROM EARTH (MI)	DISTANCE FROM MOON (MI)
1	1.03	14,300	
2	3.26	34,300	
3	6.16	53,000	193,000
4	11.95	82,500	171,000
5	17.67	104,600	154,000
6	26.93	136,000	131,000
7	36.11	158,000	111,000
8	52.33	192,000	75,200
9	72.76	223,000	27,700
10	84.66	235,000	3,500

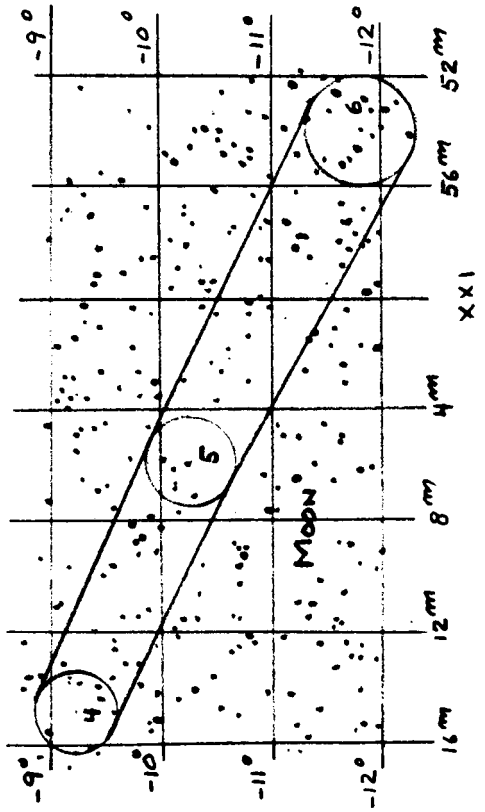

Fig. V-2. Moon and Earth Occultations--Stars up to 10th Magnitude

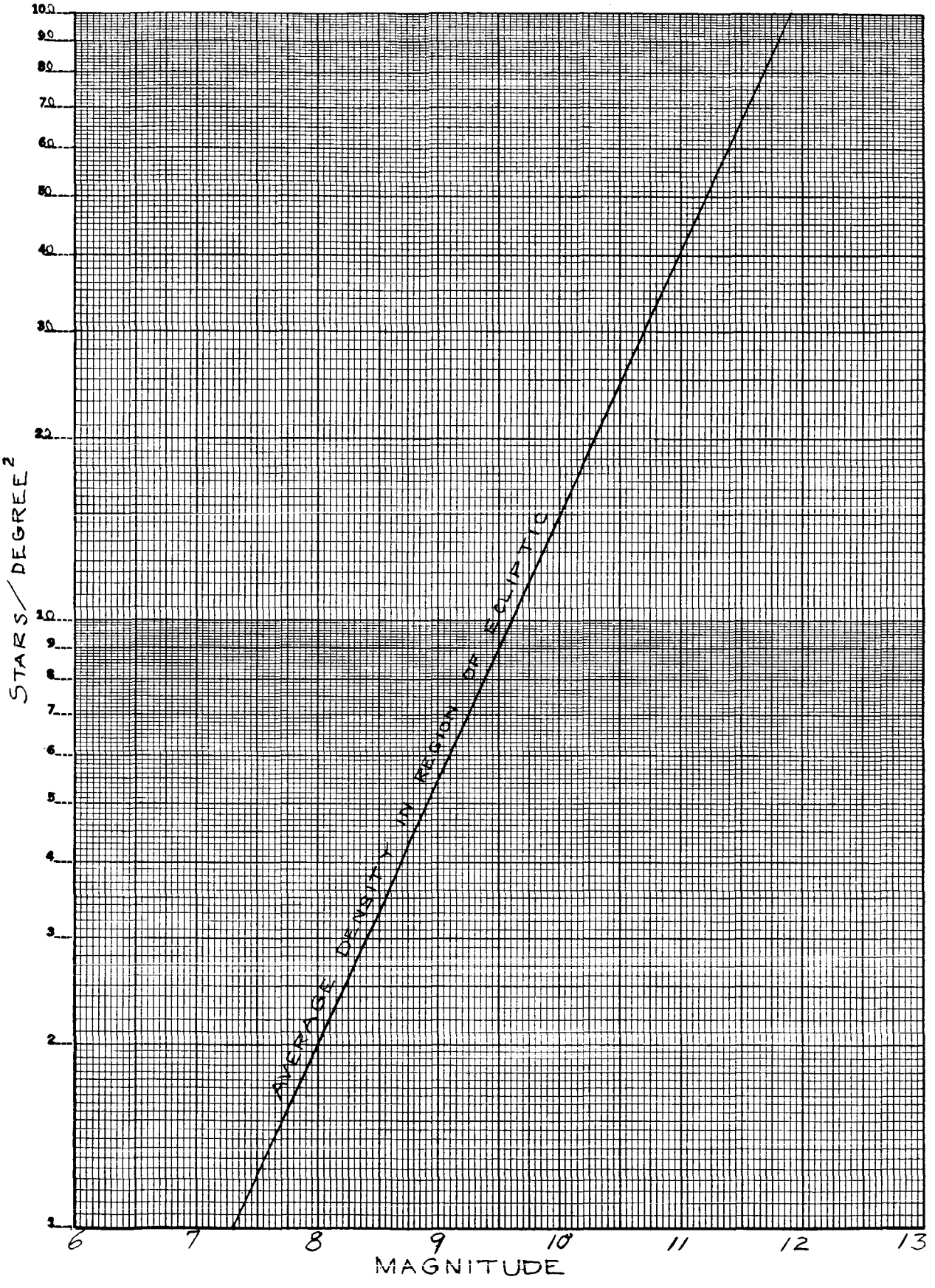

Fig. V-3. Visual Star Density

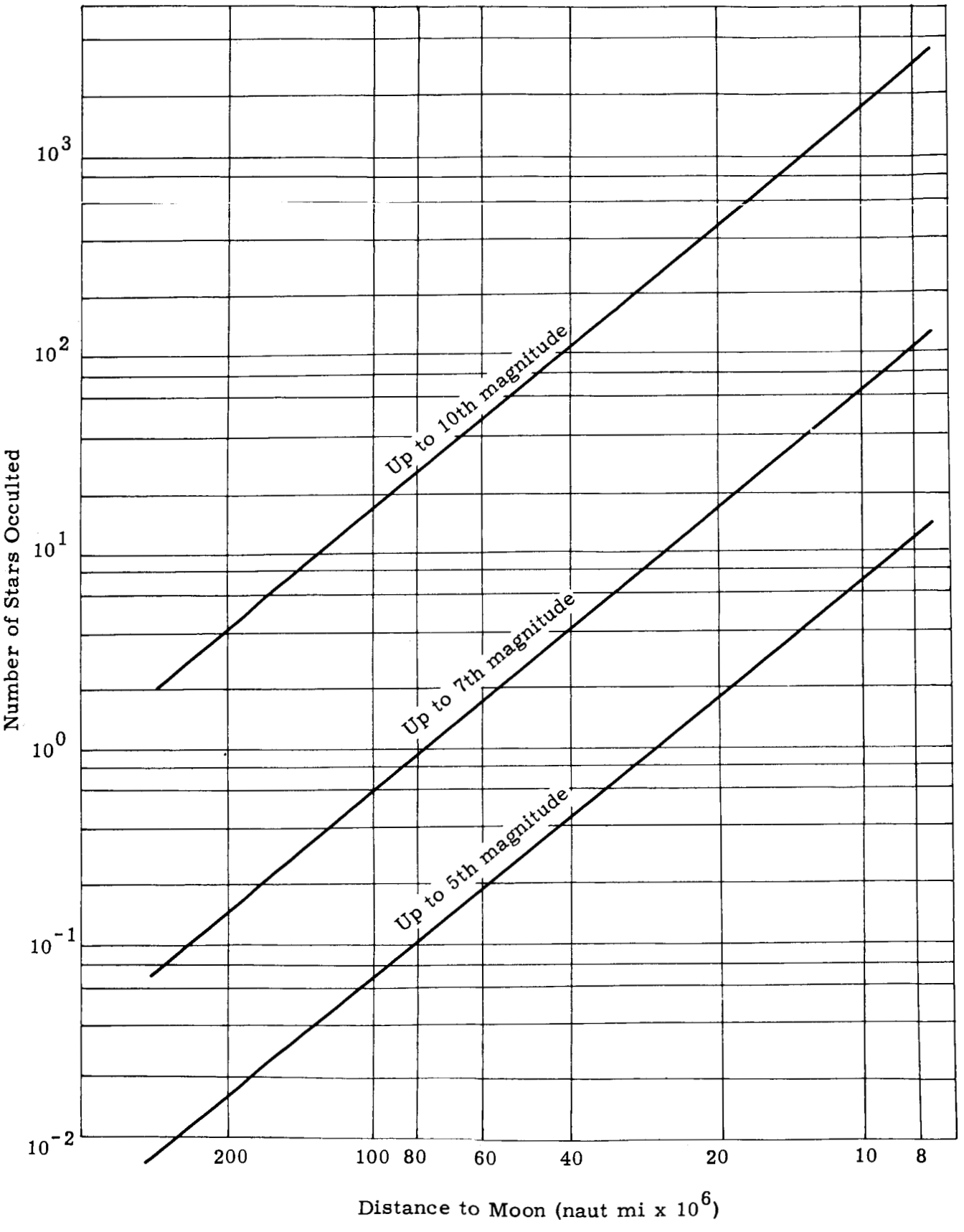

Fig. V-4. Number of Stars Occulted by the Moon

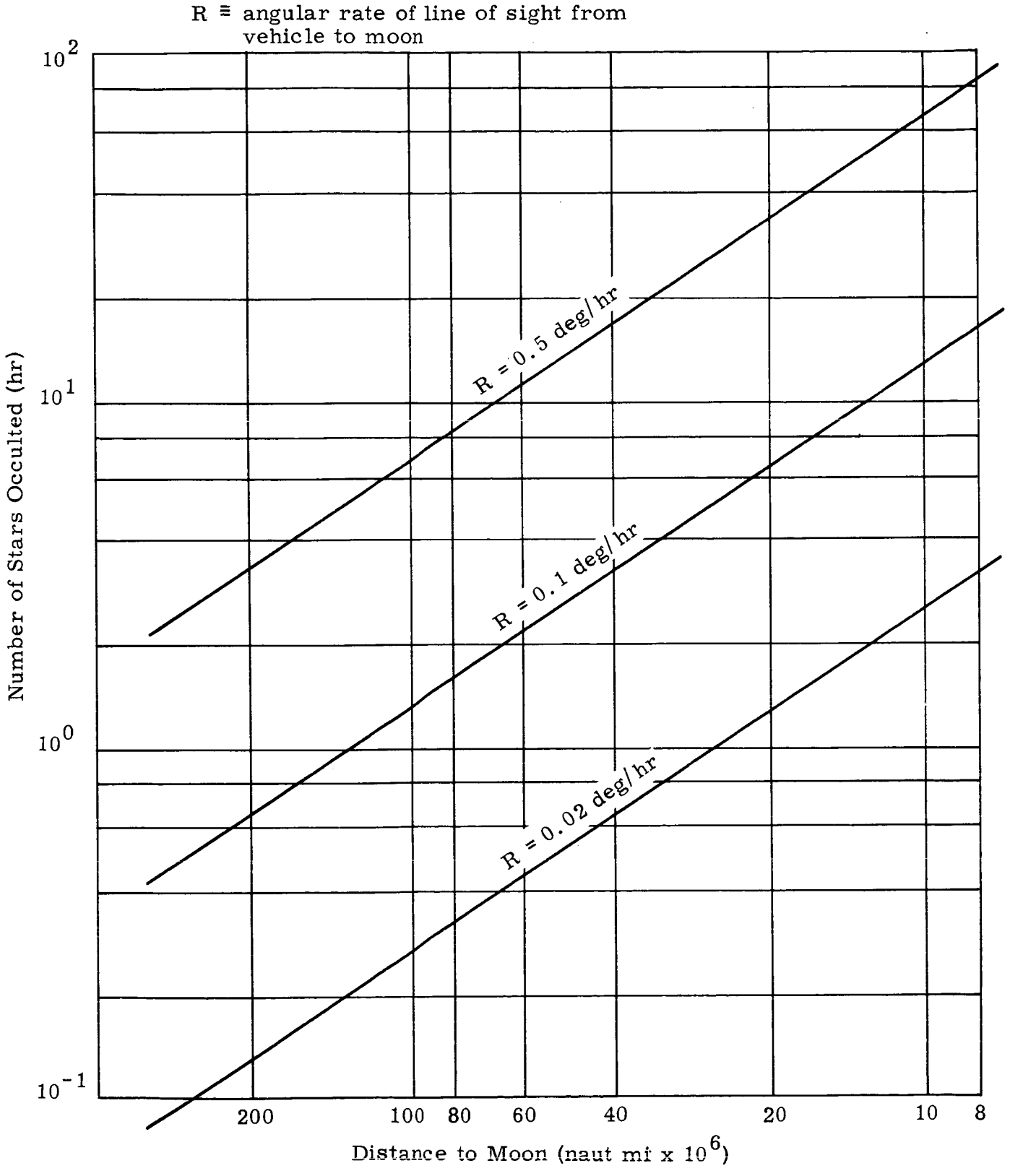

Fig. V-5. Star Occultation Rate by Moon for 10th Magnitude Stars

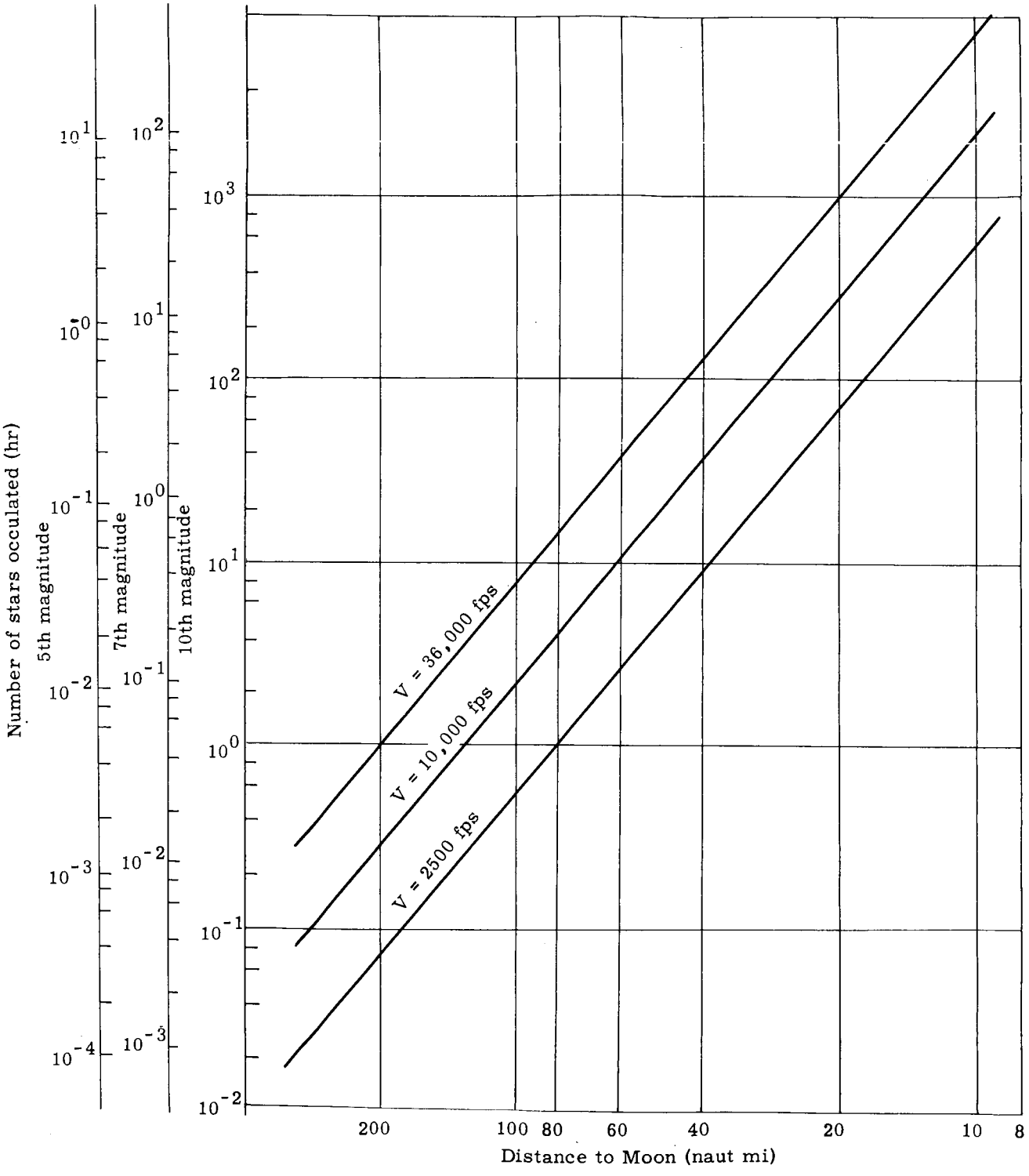

Fig. V-6. Star Occultation Rate When Approaching Moon with a Zero Angular Rate of Line of Sight to the Moon

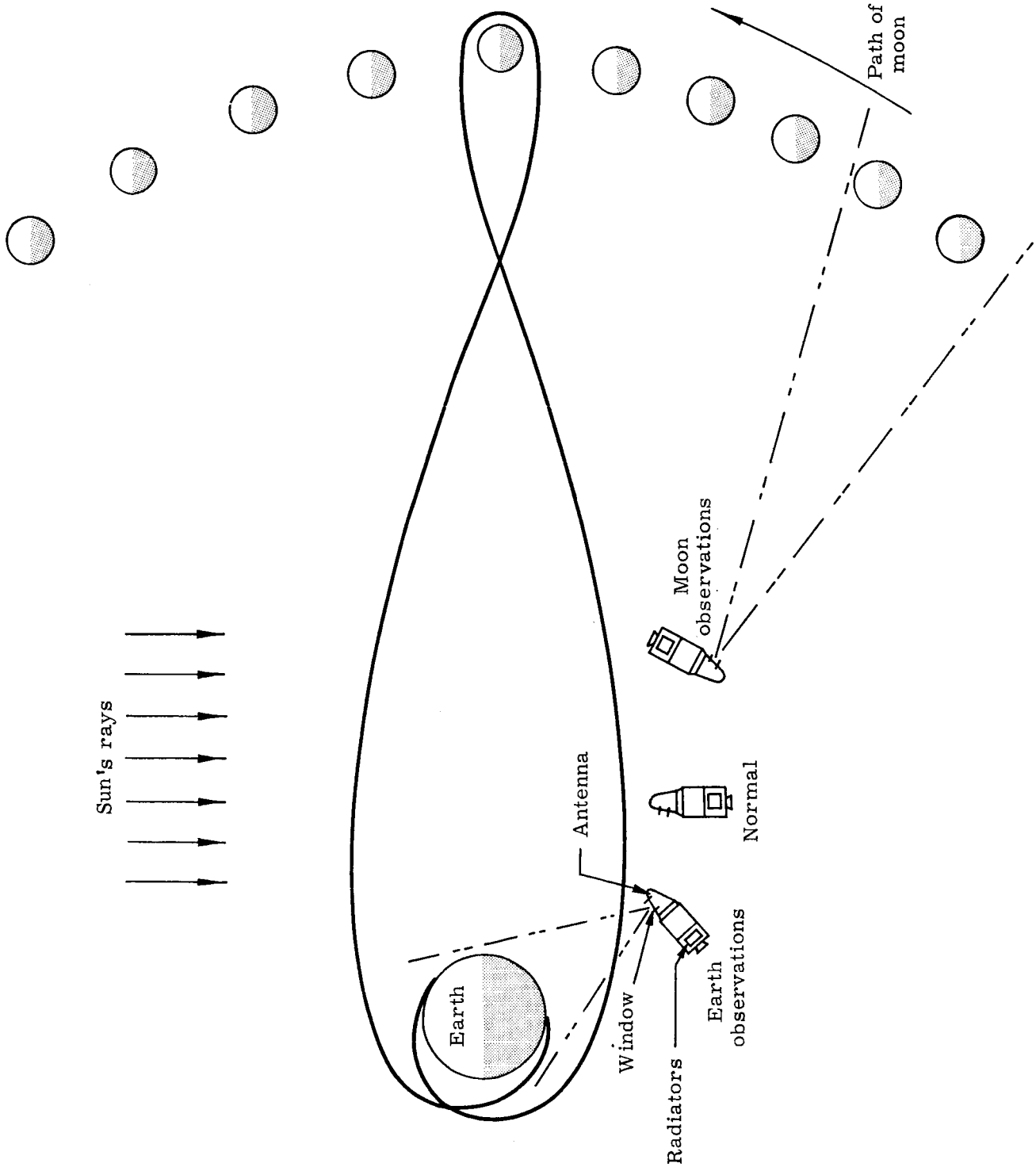

Fig. V-7. Attitude Changes in Midcourse

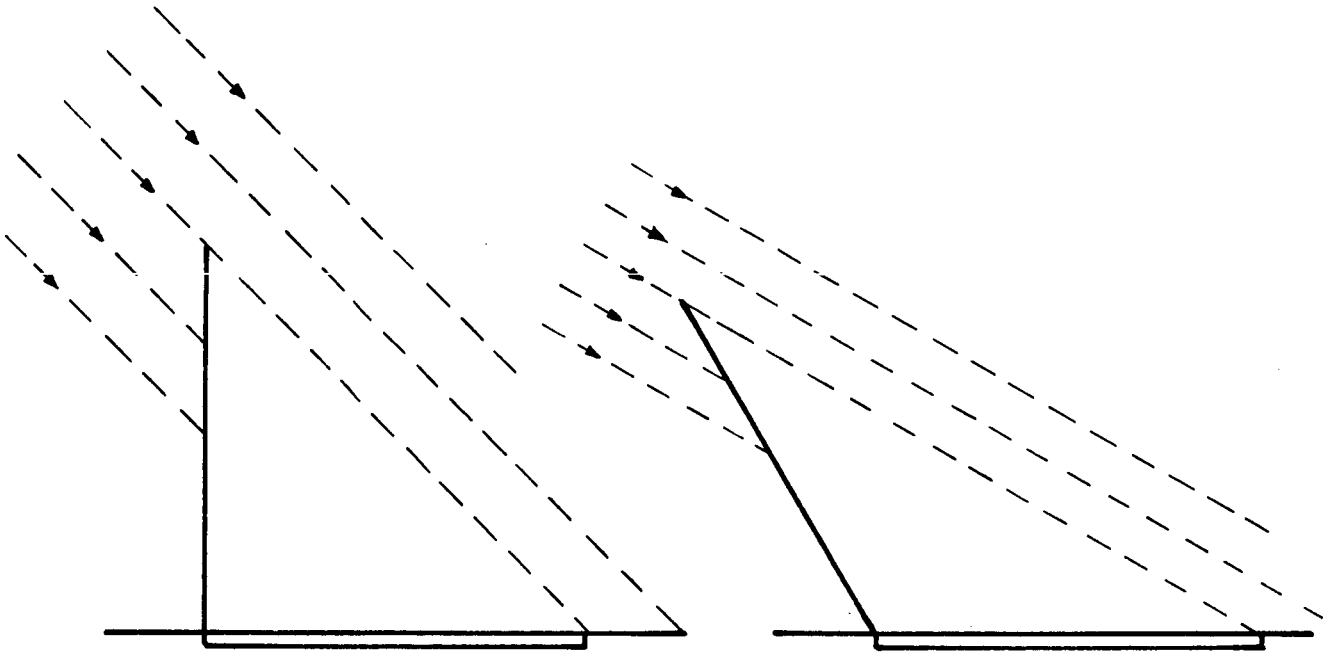

a. Sun 45° from normal to window

b. Sun 60° from normal to window

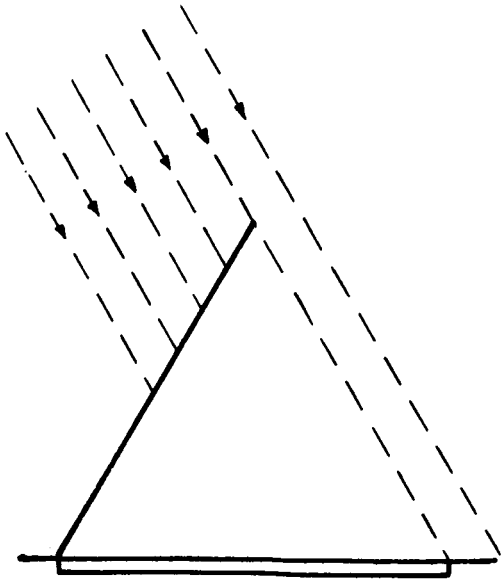

c. Sun 30° from normal to window

Fig. V-8. Window Shade Geometry

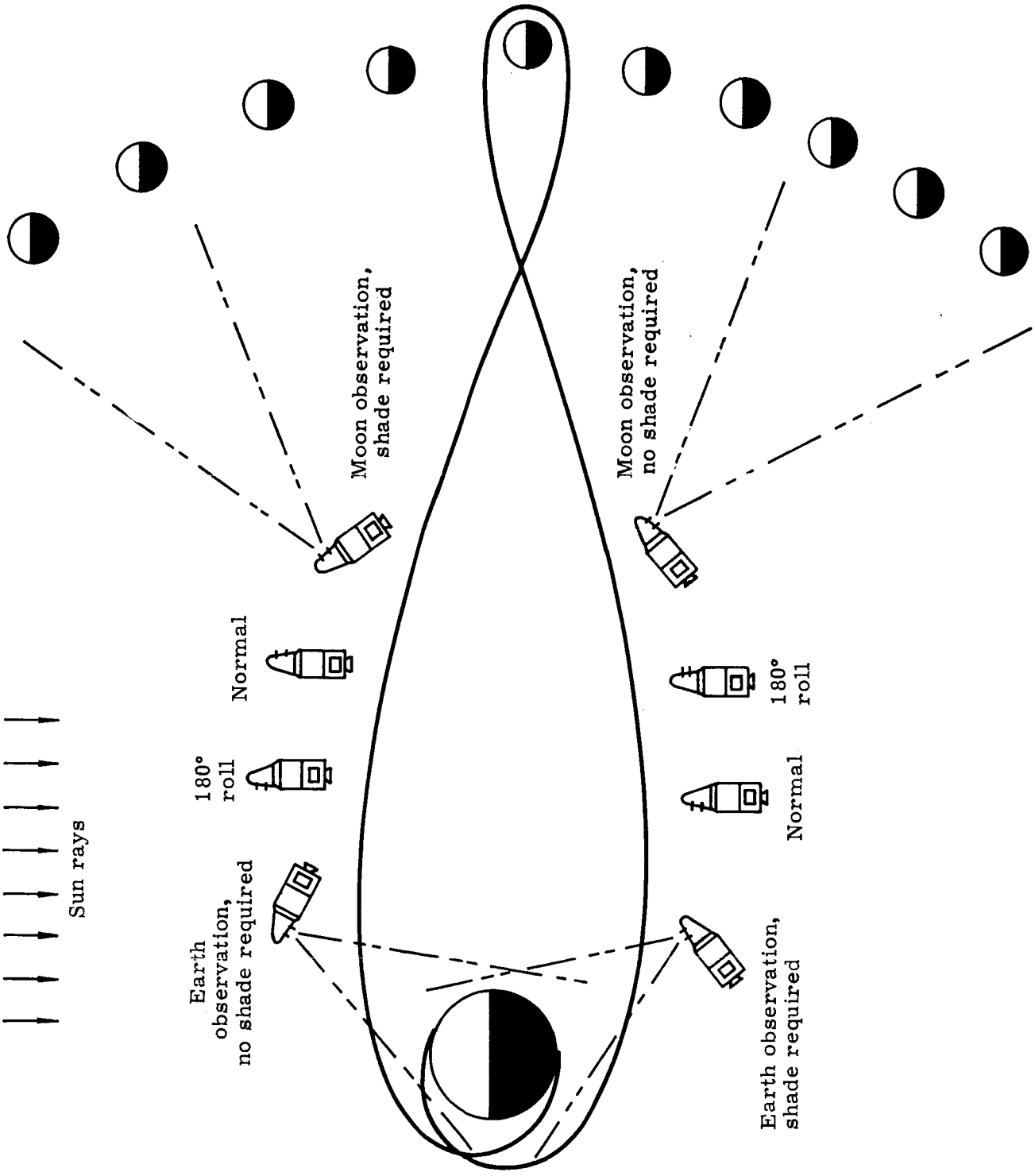

Fig. V-9. Shade Operation in Midcourse

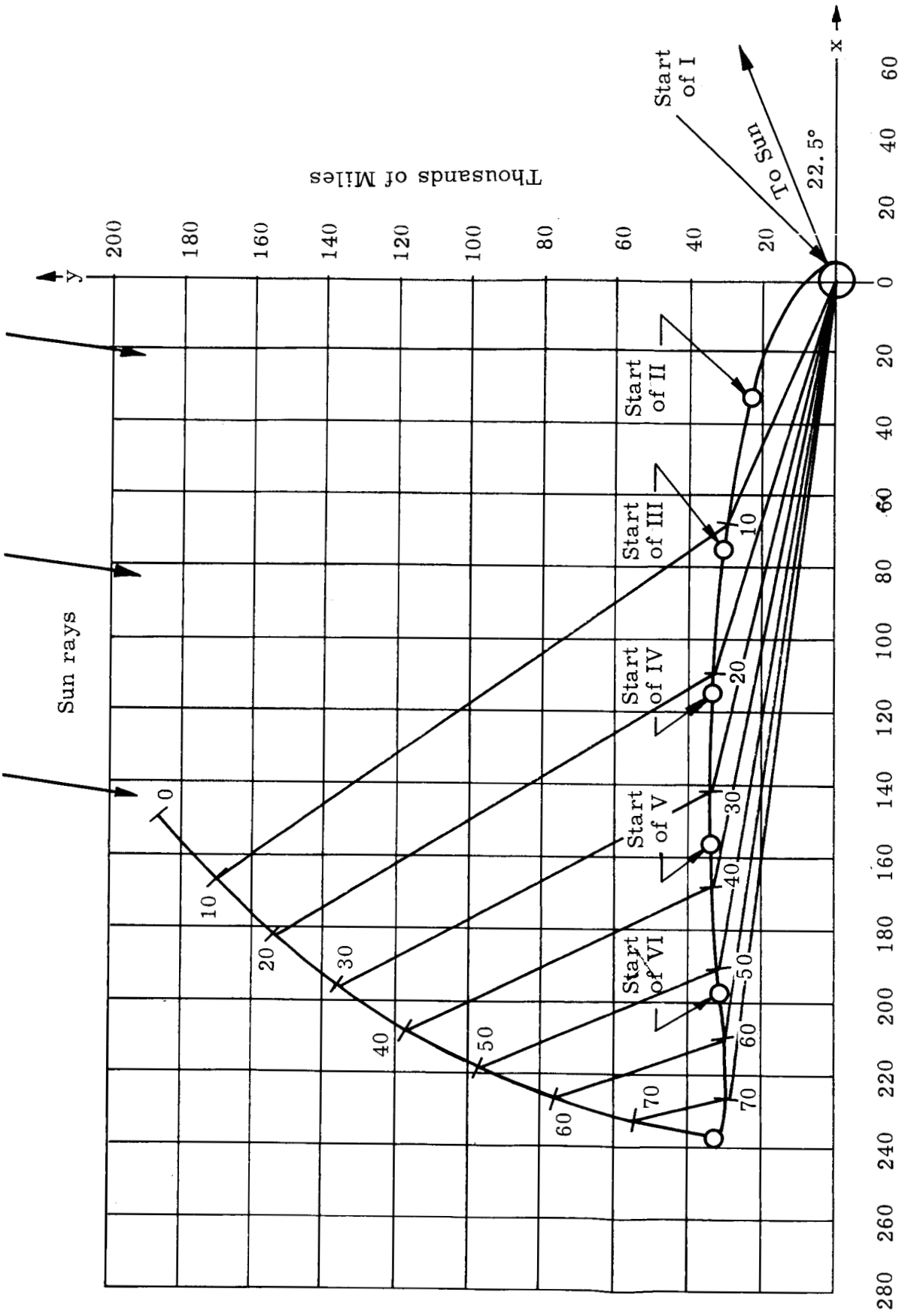

Fig. V-10. Translunar Trajectory

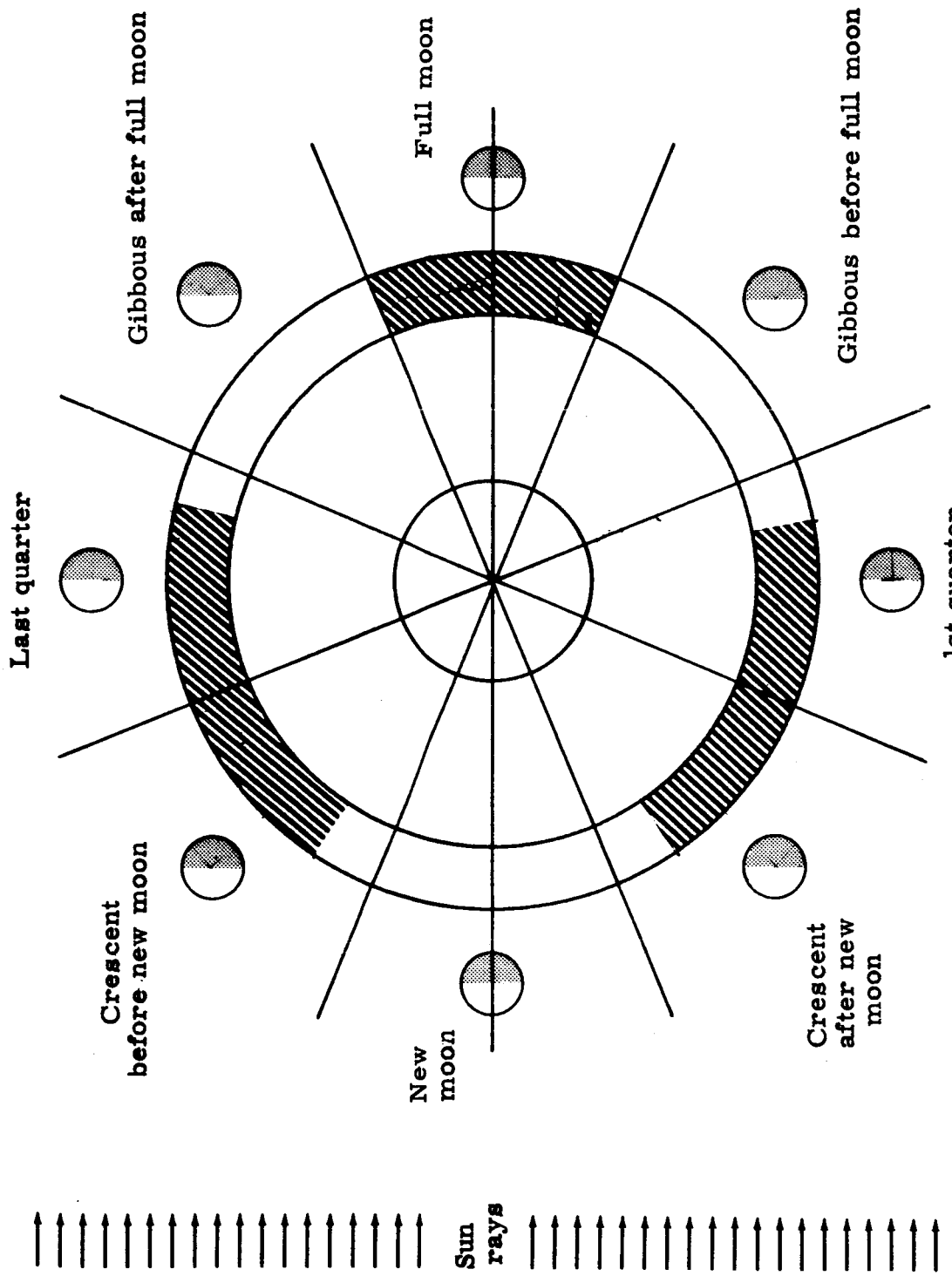

Fig. V-11. Lighting Conditions for Various Phases of the Moon at Perigelenium

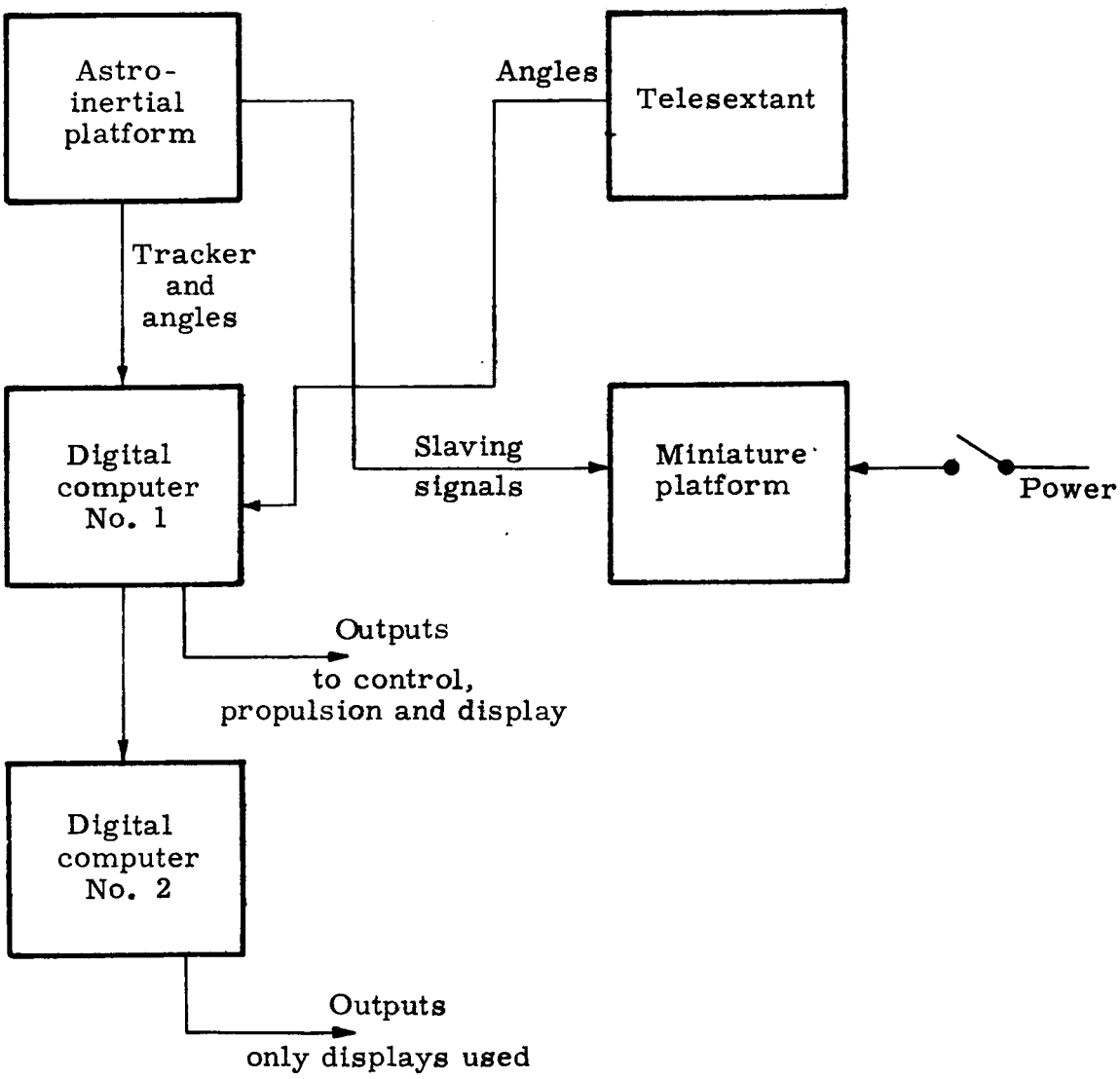

Fig. V-12. Normal Operation

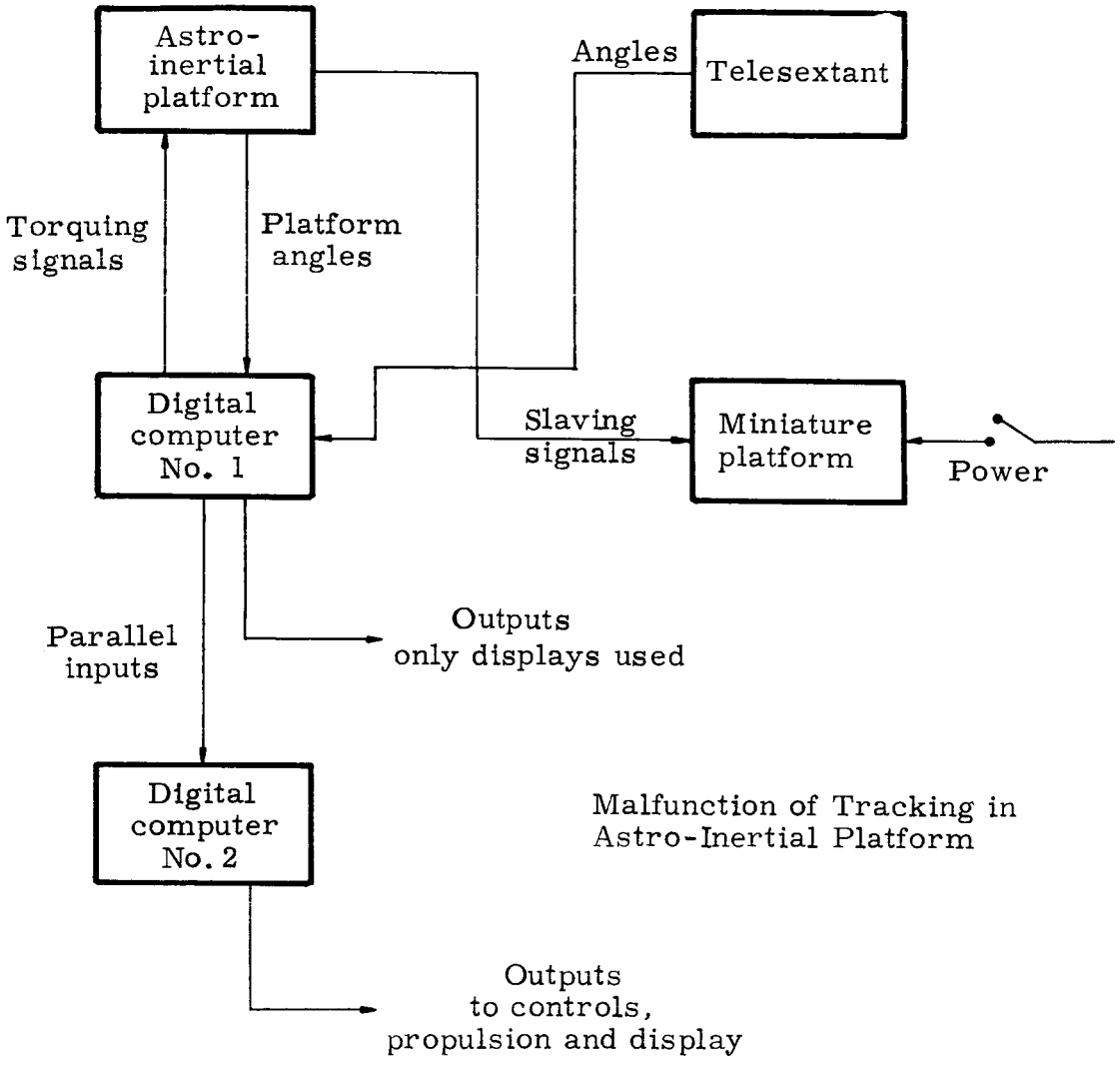

Fig. V-13. Emergency Mode

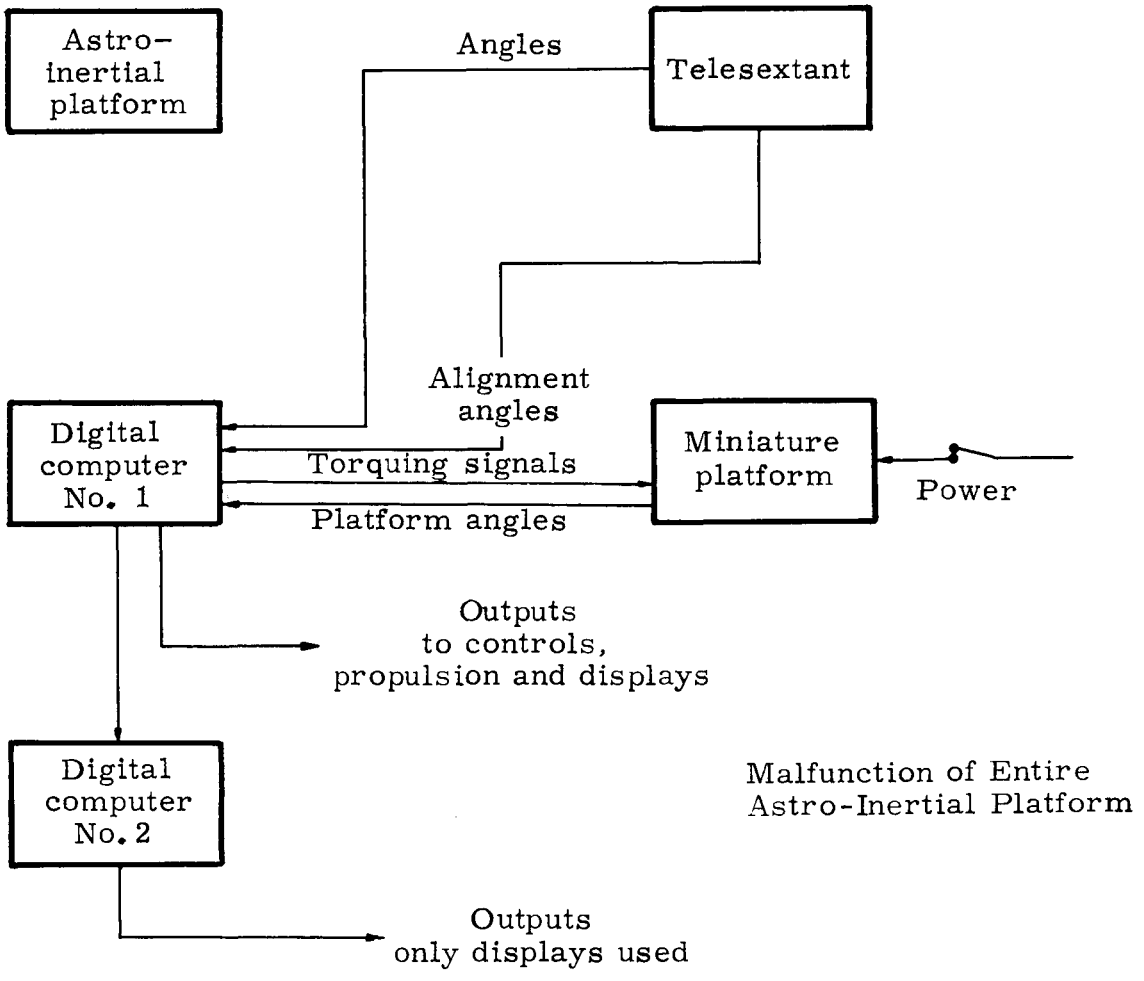

Fig. V-14. Emergency Mode

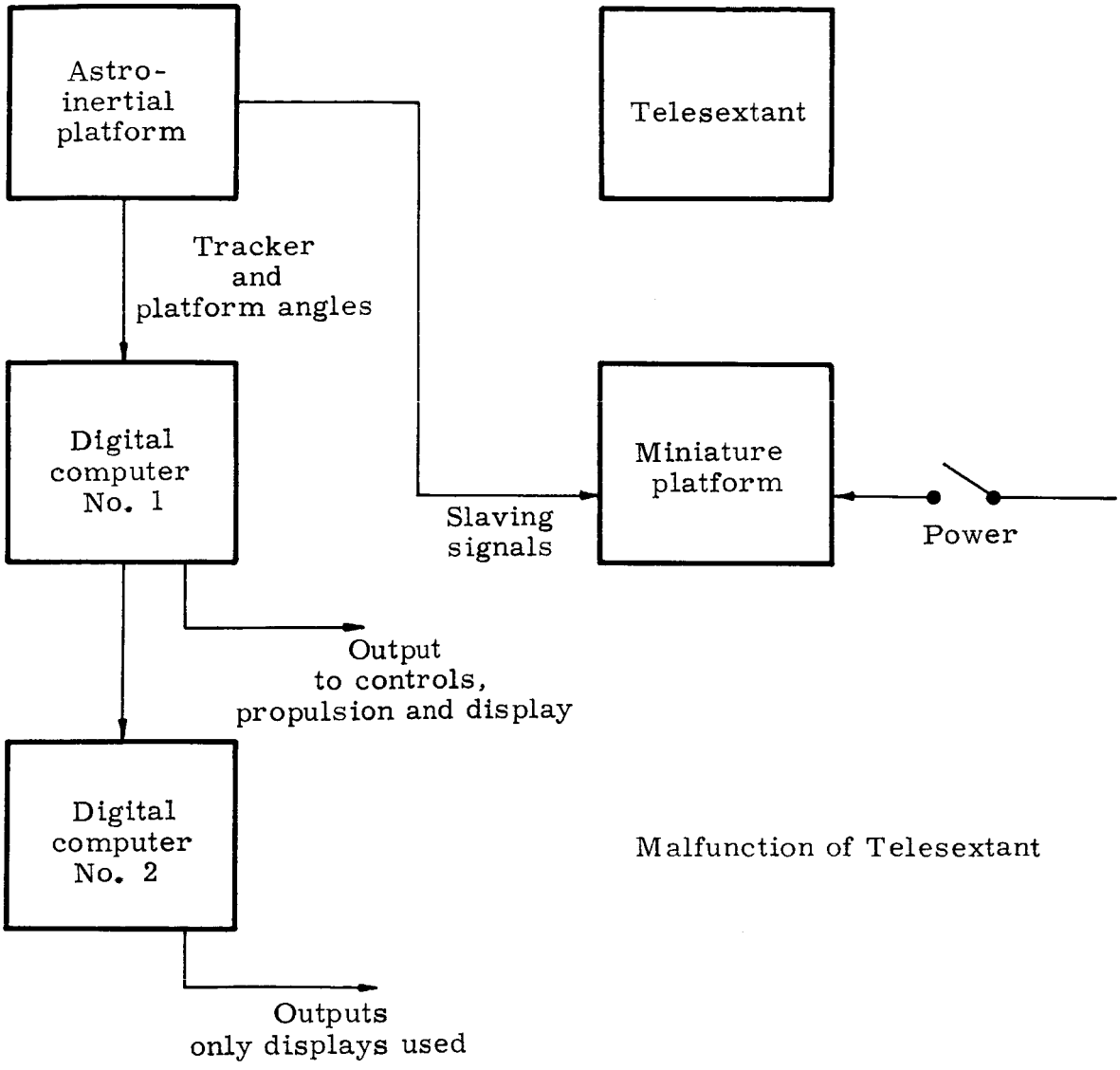

Fig. V-15. Emergency Mode

[redacted]

THE FINAL REPORT of The Martin Company's Apollo design feasibility study comprises the following publications:

System and Operation	ER 12001
Support	ER 12002
Trajectory Analysis	ER 12003
Configuration	ER 12004
Aerodynamics	ER 12017
Mechanical Systems	ER 12005
Aerodynamic Heating	ER 12006
Guidance and Control	ER 12007
Life Sciences	ER 12008
Onboard Propulsion	ER 12009
Structures and Materials	ER 12010
Instrumentation and Communications	ER 12011
Space Environment Factors	ER 12018
Test Program	ER 12012
Fabrication and Quality Assurance	ER 12013
Program Management	ER 12014
Business Plan	ER 12015
Preliminary Specifications	ER 12016

[redacted]